Angelo Peccerillo

Plio-Quaternary Volcanism in Italy

PETROLOGY · GEOCHEMISTRY · GEODYNAMICS

Springer

Angelo Peccerillo

Plio-Quaternary Volcanism in Italy

Petrology, Geochemistry, Geodynamics

Angelo Peccerillo

Plio-Quaternary Volcanism in Italy

Petrology, Geochemistry, Geodynamics

With 145 Figures and a CD-ROM

Springer

PROF. ANGELO PECCERILLO
DEPARTMENT OF EARTH SCIENCES
PIAZZA UNIVERSITÀ 1
06100 PERUGIA

ITALY

E-MAIL: PECCEANG@UNIPG.IT

ISBN 10 3-540-25885-x **Springer Berlin Heidelberg New York**
ISBN 13 978-3-540-25885-8 **Springer Berlin Heidelberg New York**

Library of Congress Control Number: 2005928988

Springer is a part of Springer Science+Business Media
springeronline.com

Printed in The Netherlands

Cover design: E. Kirchner, Heidelberg
Production: A. Oelschläger
Typesetting: Camera-ready by the Author

Printed on acid-free paper 32/2132/AO 5 4 3 2 1 0

Preface

Italian Plio-Quaternary magmatism exhibits a very wide petrological, geochemical and radiogenic-isotope variability, which makes magma genesis and geodynamic significance difficult issues. A large number of papers have been published on these rocks trying to explain the petrogenesis and evolution of single volcanoes or magmatic provinces. However, papers presenting a comprehensive review of the data and hypotheses on the magmatism of the region as a whole are few, if any. Synthesis of data at the local scale has definitely increased our degree of understanding of volcanism at that scale, but it has not resolved ambiguous issues such as the relationship among various magmatic provinces, the significance of regional compositional variations, and the geodynamic setting for this complex magmatism. The objective of this book is to fill this gap by providing an overview of the most prominent petrological and geochemical data and discussing currently held ideas on the petrogenesis and geodynamic significance of Italian Plio-Quaternary volcanic rocks. In summarising the intense debate on Italian magmatism, I have tried to report on, as objectively as possible, all the most significant ideas. The different weight given to the discussion of various points of view depends only marginally on the author's choice but is mostly an effect of the very different amounts of factual constraints which have been brought to supporting various hypotheses.

The book is subdivided into ten chapters. The first one provides an introduction to the main petrological and geochemical characteristics and gives the rationale for subdivision of the Italian Plio-Quaternary magmatism into several distinct magmatic provinces. The last chapter is a summary of the petrological, volcanological and structural characteristics of the volcanic provinces and of the most popular hypotheses that have been proposed to explain the relationship between geodynamics and volcanism. The other chapters are devoted to the volcanology, petrology and geochemistry of single magmatic provinces into which Recent Italian magmatism has been subdivided. The number of these provinces is slightly higher than recognised by most authors. However, the present subdivision is based on the bulk of compositional data, included a large number of trace

elements and radiogenic isotopes, which have provided the tools for setting new boundaries that were not obvious during early studies.

The data discussed in the text have been generally taken from the most recent literature; old analyses have not been considered in order to avoid analytical bias. In most diagrams, especially those showing major elements and the most commonly determined trace elements, a limited number of representative data have been plotted. Such a choice has been dictated by the need to avoid excessive crowding, which would have made diagrams difficult to read. In goes without saying that, in the choice of data points, care has been taken to select representative compositions, in order to preserve all necessary information. A few representative data for the single magmatic provinces have been reported in the tables attached to the end of each chapter. More data can be found in the CD attached to this book and at the Author's web-site (http://www.unipg.it/~pecceang).

For classification and nomenclature of volcanic rocks, the IUGS scheme of Le Maitre (1989) has been consistently adopted through the book. For rocks related to volcanic arcs, the classification scheme of Peccerillo and Taylor (1976) has been used. These classification schemes, together with a few notes on the petrogenesis of potassium-rich rocks, have been explained in the Appendix. Rocks names not reported in these schemes and eventually used through the book have been defined in footnotes. Explanations and comments reported in the Appendix, in footnotes and, sometimes, through the text are trivial for petrologists and geochemists, but may be useful for other potential readers who are not familiar with petrological-geochemical issues and jargon.

The bibliography on Italian volcanism and geodynamics is enormous and would deserve a book by itself. Therefore, the attached reference list is far from being comprehensive of the large quantity of the published papers and many important contributions, especially in the field of mineralogy, geophysics and geodynamics, have been omitted because of space constraints. Again, a more complete list of papers is reported in the attached CD and at the Author's web-site.

The various chapters of the book have been reviewed by several colleagues who made important suggestions, corrections and modifications which definitively improved the style of writing and quality of science. It is obvious, however, that the scientific responsibility for the contents of this book leans entirely on the author. I wish to express my gratitude to Russell Harmon, Gillian Foulger, Massimiliano Barchi, Michele Lustrino, Lucia Civetta, Sonia Esperança, Robert Ayuso, Elisabeth Widom, Carlo Doglioni, Giampiero Poli, Leonsevero Passeri, Alba Santo, Diego Perugini and Pamela Kempton for their help. Pamela Kempton, NERC, UK, also

co-authored Chapter 10. Very special thanks are due to Carmelita Donati who constructed the data files used in this book. My gratitude goes also to Christine Hardwick for correction of an early version of the text and for competent editing, and to Nicoletta Prosperini and Danilo Chiocchini for invaluable help with figure drawing and text formatting. Michele Lustrino, Giampiero Poli, Maria Luce Frezzotti and Gianfilippo De Astis generously allowed use of their data files and unpublished data on Sardinia, Capraia, Ernici and Mount Vulture. Luigi Carmignani furnished the DEM bases for volcanoes location maps. Giuseppe Vilardo and Giovanni Orsi provided DEM bases used for geological maps of active volcanoes. Giovanni Macedonio supplied the DEM base for Etna. The kindness of these colleagues is gratefully acknowledged. Altair Pirro and Giulio Castagnini assisted during drawing of geological maps and handling of DEM bases.

This effort is dedicated to my wife, my daughter and to the memory of my parents.

Table of Contents

1. Plio-Quaternary Magmatism in Italy: an Introductory Overview

1.1. Introduction

The Tyrrhenian Sea region is one of the most complex geodynamic settings on Earth (e.g. Mantovani et al. 1997; Doglioni et al. 1999; Vai and Martini 2001; Cavazza and Wezel 2003 and references therein). Its complexity is clearly expressed by the large variety of Plio-Quaternary volcanic rocks erupted in the area. These range from subalkaline (tholeiitic and calc-alkaline) to Na- or K-alkaline and ultra-alkaline, from mafic to silicic, and from oversaturated to strongly undersaturated in silica. Trace element contents and isotopic ratios are also variable, covering mantle and crustal values, and ranging from typical intra-plate to orogenic compositions.

In this chapter, an introductory overview of the geochronology, petrology and geochemistry of the Plio-Quaternary magmatism of Italy is given. Data will be presented with the aim of assessing the main compositional characteristics of the rocks, highlighting regional variations of magma compositions, and introducing major constraints for petrogenesis and geodynamic significance.

1.2. Geochronology and Petrology

Plio-Quaternary magmatism in Italy occurs along a NW-SE trending extensional zone on the Tyrrhenian border of the Italian peninsula, in western Sicily, in the Sicily Channel, on the Tyrrhenian Sea floor and in Sardinia. Geochronological data for the main magmatic centres (Fig. 1.1; Table 1.1) show that there is a general decrease in age from Tuscany and Sardinia towards the south-east, where volcanism is presently active.

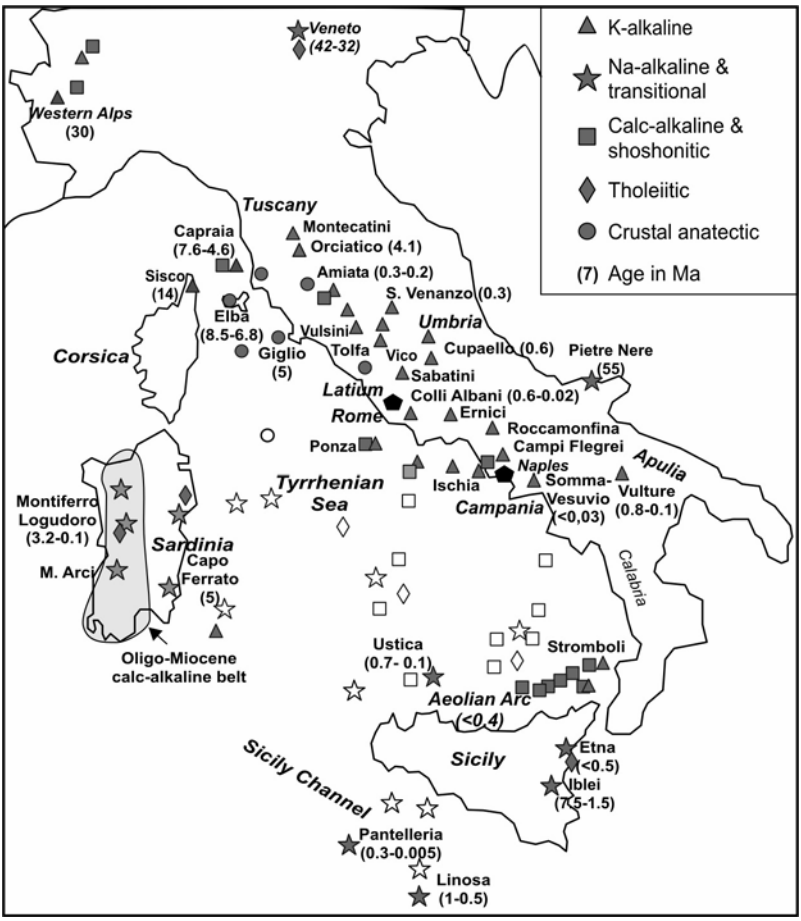

Fig. 1.1. Distribution, petrochemical affinity and ages of the main Plio-Quaternary magmatic centres in Italy. Location of the Eocene igneous body of Pietre Nere (Apulia) and of the Oligocene to Miocene magmatic provinces of Sardinia, Western Alps and Veneto is also indicated. Open symbols refer to outcrops below the sea level.

Volcanic and associated intrusive rocks in Tuscany range from about 8 Ma to 0.2 Ma, and generally young towards the east, from the Tuscan archipelago to the mainland. The age of this magmatism extends to about 14 Ma, if the ultrapotassic dyke from Sisco, Corsica, is included among the Tuscany rocks. Rocks cropping out from Vulsini to the Ernici Mountains and Roccamonfina appear almost coeval, covering a time span of about 0.8 to 0.02 Ma. Active volcanism starts in Campania (Vesuvio, Campi

Table 1.1. Petrological characteristics and ages of Plio-Quaternary volcanic provinces in Italy.

Magmatic Province	Main magmatic centers and ages (in Ma)	Volcanology and Petrology
Tuscany (14 to 0.2 Ma)	***Acid intrusions***: Elba (8.5-6.8), Montecristo (7.1), Giglio (5), Campiglia-Gavorrano (5.9-4.3) ***Acid volcanoes***: San Vincenzo (4.5), Roccastrada (2.5), Amiata (0.2), Cimini (1.3-0.9), Tolfa (3.5) ***Mafic centres***: Sisco (14), Capraia (7.6-4.6), Orciatico and Montecatini (4.1), Radicofani (1.3), Torre Alfina (0.9-0.8)	***- Crustal anatectic rocks***: Granitoid rocks, aplites, pegmatites. Monogenic lava flows and domes, and polygenetic cones (Amiata, Cimini.). ***- Mafic rocks***: monogenetic extrusive and subvolcanic bodies with potassic and ultrapotassic (*lamproites*) composition; calc-alkaline and shoshonitic rocks at Capraia.
Intra-Apennine (0.6 to 0.3 Ma)	San Venanzo (0.26), Cupaello (0.64), Polino (0.25), Acquasparta, Oricola (0.53) etc.	- Monogenic pyroclastic centres and rare lavas with an ultrapotassic melilititic (*kamafugite*) composition. Carbonatites (?).
Roman Province (Latium) (0.8 to 0.02 Ma)	Vulsini (0.6-0.15), Vico (0.4-0.1), Sabatini (0.8-0.04), Colli Albani (0.6-0.02)	- Large volcanic complexes formed of potassic (trachybasalt to trachyte) and ultrapotassic (leucite tephrite, to phonolite) pyroclastics and minor lavas.
Ernici - Roccamonfina (0.7 to 0.1 Ma)	Ernici: Pofi, Ceccano, Patrica, etc. (0.7-0.1) Roccamonfina (0.58-0.1)	- Monogenetic pyroclastic and lava centres (Ernici), and a stratovolcano (Roccamonfina) formed of mafic to felsic ultrapotassic and potassic rocks.
Campania and Pontine Islands (1 Ma to Present)	Somma-Vesuvio (0.03-1944 AD), Campi Flegrei (0.3-1538 AD), Ischia (0.15-1302 AD), Procida (0.05-0.01), Ventotene (0.8-0.1), younger Ponza (1).	- Shoshonitic, potassic (trachybasalt to trachyte) and ultrapotassic (leucite tephrite to phonolite) rocks forming stratovolcanoes and multi-centre complexes.
Vulture (0.8 to 0.1 Ma)	Vulture, Melfi	- Stratovolcano and a few parasitic centres formed by Na-K-rich tephrites, phonolites, foidites with haüyne. Possible carbonatite.
Aeolian arc (1 or 0.4 Ma to Present)	Alicudi (0.06-0.03), Filicudi (1(?)-0.04), Salina (0.4-0.013), Vulcano (0.12-1888 AD), Lipari (0.2-580 AD), Panarea (0.15-0.05), Stromboli (0.2 – Present)	- Stratovolcanoes with dominant calc-alkaline (basalt-andesite-rhyolite) and shoshonitic (basalt to rhyolite) compositions, with a few potassic alkaline products.
Sicily (7 Ma to Present)	Etna (0.5-Present), Iblei (7-1.5), Ustica (0.75-0.13), Pantelleria (0.3-0.005), Linosa (1-0.5), Sicily Channel seamounts	- Stratovolcanoes, diatremes, small plateaux, etc. formed of tholeiitic and Na-alkaline rocks (basanite, hawaiite, trachyte, peralkaline trachyte and rhyolite).
Sardinia (5.3 to 0.1)	Capo Ferrato (~5), Montiferro (4-2), Orosei-Dorgali (4-2), Monte Arci (3.7-2.3), Logudoro (3-0.1)	- Stratovolcanoes, basaltic plateaux and monogenetic centres composed of subalkaline and Na-alkaline rocks, sometimes with a K-affinity.
Tyrrhenian Sea Floor (12 Ma to Present)	Cornacya (12), Magnaghi (3), Marsili (1.8-0), Vavilov, Aceste, Anchise, Lametini, Palinuro, older Ponza, etc.	- Coexisting intraplate (oceanic tholeiites, Na-transitional and alkaline) and arc-type (arc-tholeiitic, calc-alkaline, potassic) rocks.

Flegrei and Ischia) and continues in the Aeolian islands, in eastern Sicily (Etna), and along the Sicily Channel. Young volcanism in Sardinia has ages of about 5 to 0.1 Ma. Several Pliocene to active seamounts occur on the Tyrrhenian Sea floor.

Plio-Quaternary magmatic rocks in Italy exhibit a large range of petrological characteristics (Fig. 1.2) and cover almost all the different compositional fields on Total Alkali vs. Silica diagram (TAS; Le Maitre 1989). They range from subalkaline to alkaline, and from mafic to silicic. In most areas, mafic rocks occur in subordinate amounts with respect to intermediate and silicic rocks and there is general agreement that most of the evolved rocks represent daughter magmas derived from mafic parents by complex evolutionary processes dominated by fractional crystallisation. Exceptions are represented by the silicic rocks in Tuscany, which were formed by crustal anatexis or by mixing between crustal anatectic and mantle-derived melts (Poli 1992).

Although present in small amounts, mafic rocks (here defined as those with MgO > 4 wt %[1]) are particularly interesting since they represent the closest relatives of primary melts generated in the upper mantle.

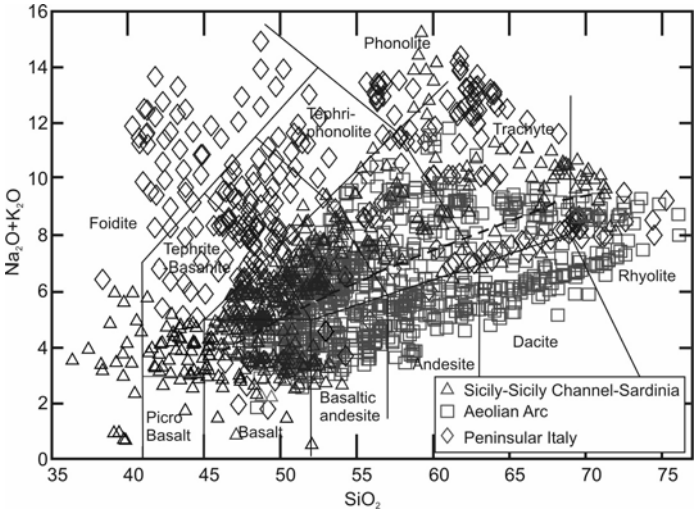

Fig. 1.2. Total alkali vs. silica (TAS) classification diagram of Le Maitre (1989) for representative Italian Plio-Quaternary volcanic rocks. The thick dashed line is the divide between the subalkaline and the alkaline fields of Irvine and Baragar (1971).

[1] A limit of MgO > 3 wt% has been chosen for provinces or volcanoes where mafic rocks are scarce.

Therefore, their composition gives the maximum information on the composition of mantle sources beneath the Italian region.

A classification diagram based on the ΔQ vs. K_2O/Na_2O relationship for mafic rocks is shown in Fig. 1.3 (Peccerillo 2002, 2003). ΔQ is the algebraic sum of normative quartz, minus undersaturated minerals (nepheline, leucite, kalsilite, and olivine). It quantifies the degree of silica saturation. Undersaturated magmas have $\Delta Q < 0$, whereas oversaturated magmas have $\Delta Q > 0$. The diagram shows that Italian Plio-Quaternary mafic rocks range from strongly undersaturated to oversaturated in silica. They cover the tholeiitic, calc-alkaline, shoshonitic, and the K-, Na-alkaline and ultra-alkaline fields, i.e. virtually the entire spectrum of the petrological compositions encountered worldwide. Among potassic and ultrapotassic rocks, various groups can be distinguished. These include lamproites, kamafugites, Roman-type potassic series (KS) and the high-potassium series (HKS). For classification of potassic rocks see Appendix.

1.3. Regional Distribution of Magma Types

There is a strong relationship between magma composition and the regional distribution of Plio-Quaternary magmatism in Italy (Fig. 1.1; Table 1.1). Tholeiitic rocks occur in western Sicily at Etna and Iblei, in Sicily Channel, Sardinia and on the Tyrrhenian Sea floor. Calc-alkaline and shoshonitic rocks are concentrated in the Aeolian arc, but also occur in the Naples area, in Tuscany (e.g. Capraia, Radicofani) and in the Tyrrhenian Sea basin, where they show an age increasing westward, up to the Oligo-Miocene calc-alkaline volcanic belt of Sardinia (Fig. 1.1). Na-alkaline rocks occur at Etna, Iblei, in the Sicily Channel, the Tyrrhenian Sea Basin (Ustica and some seamounts) and Sardinia. Potassic and ultrapotassic rocks represent the most typical compositions in central Italy. Some potassic rocks also occur in the Aeolian arc (e.g. Conticelli et al. 2002; Peccerillo 2002).

Ultrapotassic rocks from Tuscany have a lamproitic composition (see Appendix for nomenclature of potassic rocks). Older lamproites (14 Ma) occur at Sisco, Corsica. Kamafugitic rocks make up a few monogenetic centres in the internal zones of northern-central Apennines (Umbria, Latium, Abruzzi), and have been found at Vulsini and as ejected blocks in pyroclastic deposits at Colli Albani (Federico et al. 1994). Roman-type potassic and ultrapotassic rocks (KS and HKS) form the bulk of magma-

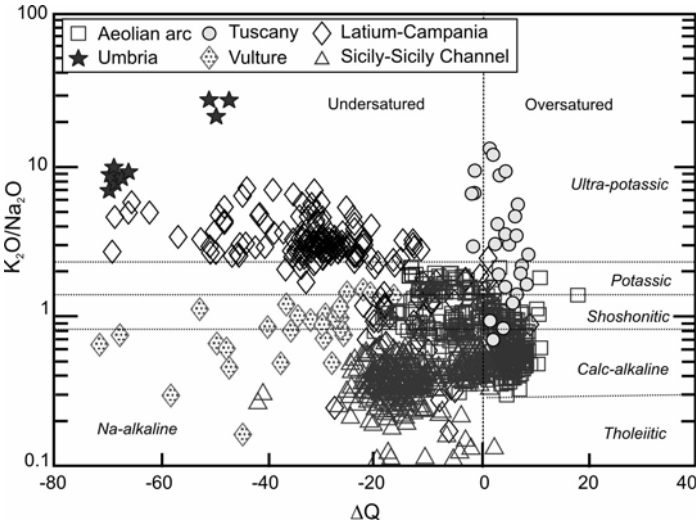

Fig. 1.3. ΔQ vs. K_2O/Na_2O classification diagram for mafic Plio-Quaternary volcanic rocks (MgO > 4 wt %) from Italy. For explanation see text.

tism in central Italy, extending from Vulsini to Vesuvio. Mount Vulture volcano, east of Vesuvio, is composed of undersaturated alkaline rocks that are rich in both K_2O and Na_2O (De Fino et al. 1986).

1.4. Regional Variation of Trace Element and Sr-Nd-Pb-O Isotopic Compositions

Mafic Plio-Quaternary rocks in Italy show very variable trace element and isotopic compositions. Incompatible[2] trace element abundances and ratios are best illustrated by mantle-normalised diagrams (spiderdiagrams), where concentrations of single elements in the rocks are divided by the abundances of the same elements in the mantle (Wood 1979).

[2] Incompatible elements are not hosted by common igneous rock-forming minerals. Their abundance in the mantle-derived magmas decreases with the increasing degree of partial melting. They also increase during fractional crystallisation. However, ratios of elements with comparable degrees of incompatibility normally remain constant or change very little during partial melting and fractional crystallisation. Therefore these ratios measured in mafic rocks give the most reliable information on the composition of mantle sources.

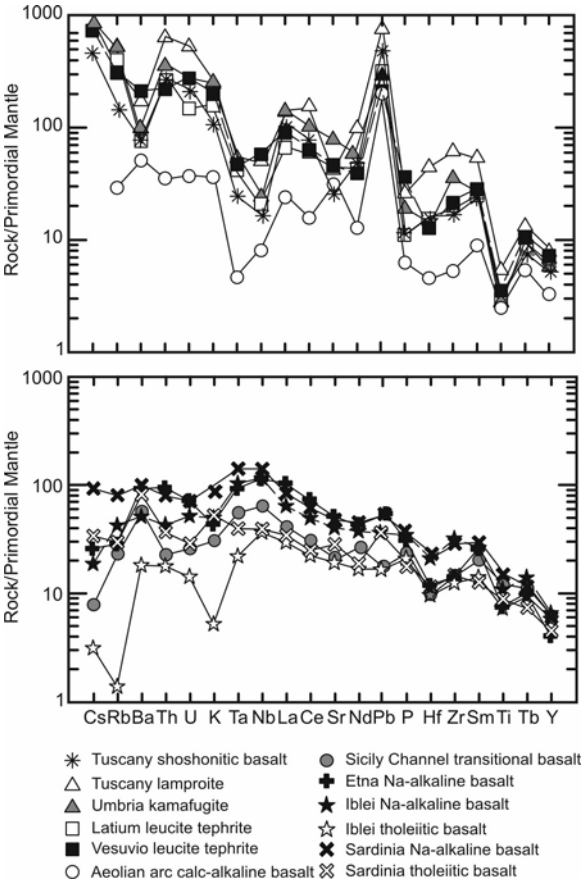

Fig. 1.4. Patterns of incompatible elements normalised against mantle compositions (Wood 1979; Sun and McDonough 1989) for some representative Italian Plio-Quaternary mafic rocks.

Spiderdiagrams of representative mafic rocks are shown in Fig. 1.4. Samples from Sicily, Sicily Channel and Sardinia mostly have bell-shaped patterns with a maximum at Ta and Nb, and negative anomalies of K and Rb. In contrast, the mafic rocks from the Aeolian arc are more enriched in Large Ion Lithophile Elements (LILE: Rb, Cs, Ba, U, Th, K, Light REE, and Pb) and display depletions of the High Field Strength Elements (HFSE: Ta, Nb, Zr, Hf and Ti showing high ratio between charge and ionic radius). The mafic potassic and ultrapotassic rocks from central-southern Italy exhibit very high enrichments in LILE and Pb, and are depleted in HFSE similar to Aeolian arc compositions. Note that negative anomalies

of HFSE and positive spikes of Pb are typical of rocks erupted along converging plate margins (Gill 1981).

Variation diagrams of incompatible element ratios can be used to discriminate between mafic magmas erupted in different tectonic settings, especially intraplate vs. subduction related volcanoes. Figure 1.5 shows a Th/Yb vs. Ta/Yb discriminant diagram (Pearce 1982). Italian Plio-Quaternary mafic rocks span intraplate and volcanic arc compositions. Volcanic rocks from Etna, Iblei, Ustica, Sardinia and Sicily Channel plot in the field of intraplate basalts (also indicated as anorogenic), whereas the Aeolian arc and central Italy plot in the field of arc basalts (orogenic).

Binary diagrams of LILE/LILE and LILE/HFSE ratios in mafic rocks define various trends (Fig. 1.6). These are closely related to the geographic position of volcanoes rather than to the main petrological characteristics of rocks. For instance, Tuscany mafic rocks plot as single trends on these diagrams, in spite of large difference in the main petrological characteristics, which range from calc-alkaline and shoshonitic to ultrapotassic.

Sr, Nd and Pb isotopic ratios of mafic rocks (Fig. 1.7) show large and continuous variations. However, various regions exhibit rather restricted and distinct isotopic signatures (Conticelli et al. 2002 and references therein). Oxygen isotopic data are also variable in the volcanic rocks from central-southern Italy. Data on whole rocks have brought to the conclusion

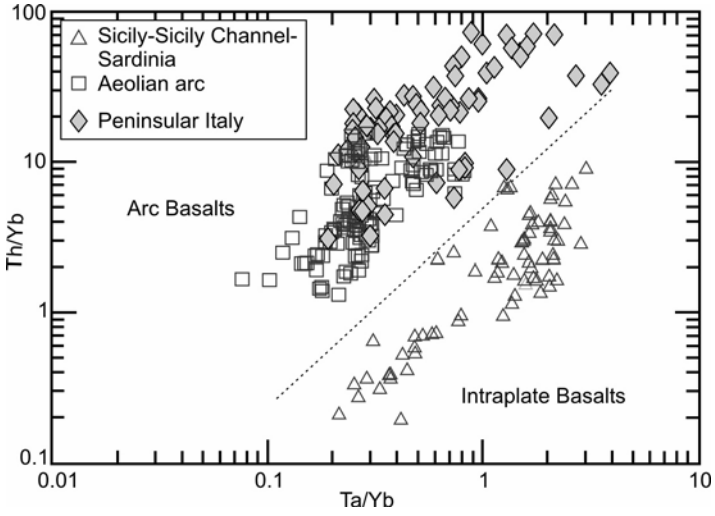

Fig. 1.5. Th/Yb vs. Ta/Yb discriminant diagram (Pearce 1982) for representative Plio-Quaternary mafic rocks (MgO > 4 wt %) from Italy.

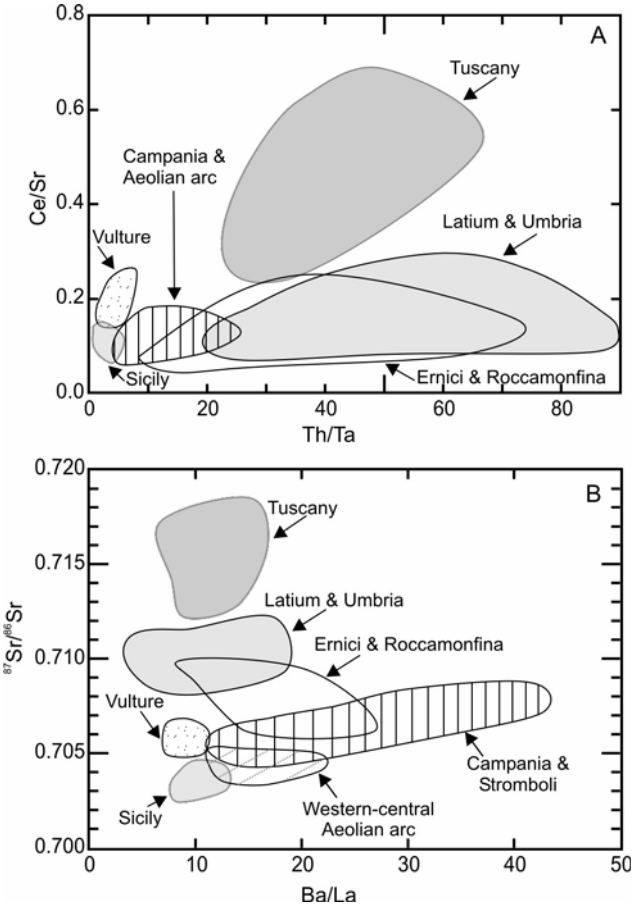

Fig. 1.6. Variation diagrams of incompatible trace element ratios and $^{87}Sr/^{86}Sr$ for mafic (MgO > 4 wt %) Plio-Quaternary volcanic rocks from Italy.

that the lowest $\delta^{18}O$ values are found in the south, whereas the highest oxygen isotopic ratios are observed in the potassic and ultrapotassic rocks from central Italy (e.g. Turi and Taylor 1976; Turi et al. 1986). However, new data on minerals separated from mafic rocks do not seem to substantiate this conclusion (Barnekow 2000; Dallai et al. 2004; Peccerillo et al. 2004).

1.5. Magmatic Provinces in Italy

The strong regionality for major, trace element and isotopic compositions of Italian Plio-Quaternary volcanism allows subdivision into several compositionally different magmatic provinces. For the purpose of this review, a "magmatic province" is defined as a relatively restricted zone within

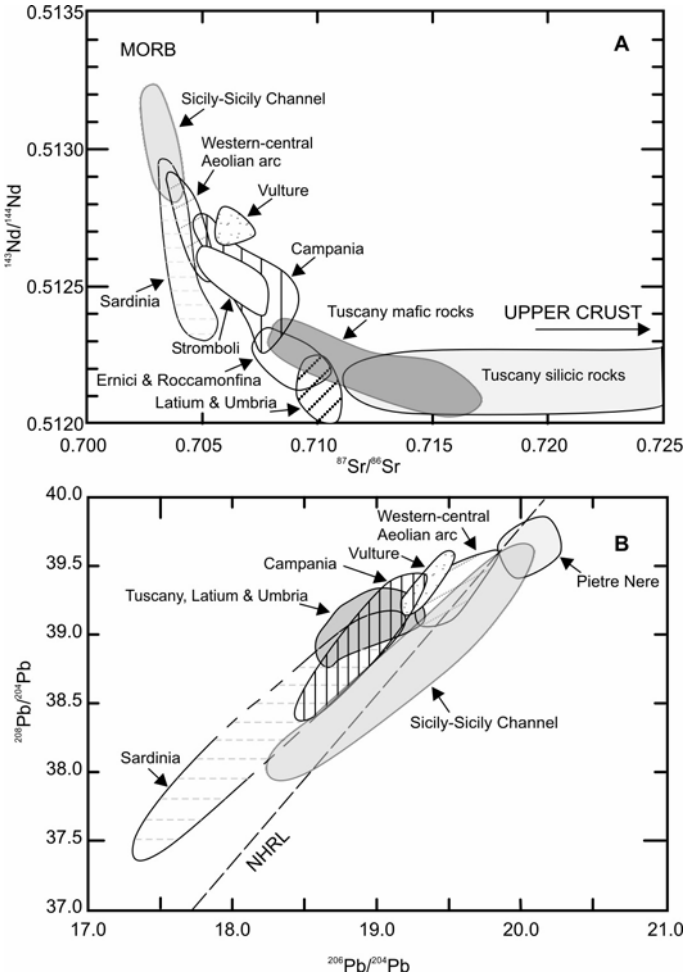

Fig. 1.7. $^{87}Sr/^{86}Sr$ vs. $^{143}Nd/^{144}Nd$ (A) and $^{206}Pb/^{204}Pb$ vs. $^{208}Pb/^{204}Pb$ (B) diagrams for Plio-Quaternary mafic volcanic rocks (MgO > 4 wt %) from Italy. The thick dashed line on Pb-isotope diagram is the Northern Hemisphere Reference Line (Hart 1984).

which igneous rocks have been emplaced over a relatively short period of time, of a few Ma or less. The rocks of each province show peculiar compositional characteristics, such as petrochemical affinity, geochemical signatures, or even a particular association of magma types, which make them different from rock associations occurring in other zones. However, rocks of a given province are not strictly comagmatic, i.e. do not necessarily derive from a single source or magma type, although in some cases they do. The underlying assumption of this definition is that magmas closely associated in space and time and showing specific compositional characteristics, are likely related to common geological events, which are somewhat different from those occurred in other areas. Based on the present definition, the Plio-Quaternary igneous activity in Italy has been grouped into the following magmatic provinces (Fig. 1.8, Table 1.1; Peccerillo 2002):

- **The Tuscany Province**

Both mafic and silicic rocks occur in this province. Silicic rocks are either of crustal anatectic origin or, in most cases, represent mixtures between crustal magmas and various amounts and types of mantle-derived melts. Mafic rocks range from calc-alkaline and shoshonitic to potassic and ultrapotassic. All the mafic rocks plot along single trends on incompatible element ratios and isotope diagrams. These trends connect typical upper mantle and upper crustal compositions and the geochemical and isotopic signatures of the Tuscany mafic rocks are much closer to upper crust than to mantle values (e.g. $^{87}Sr/^{86}Sr$ up to 0.717, $^{143}Nd/^{144}Nd$ and $^{206}Pb/^{204}Pb$ around 0.5122 and 18.80, respectively; Poli et al. 1984; Conticelli and Peccerillo 1992; Conticelli et al. 2002).

- **The Intra-Apennine Province**

This province comprises a number of small ultrapotassic monogenetic centres (e.g. San Venanzo and Cupaello) scattered through the internal zones of Apennines. The best known volcanic rocks consist of ultrapotassic kalsilite-pyroxene and olivine melilitites (kamafugites). Incompatible element ratios and isotopic signatures are similar to the Roman Province. However, the petrological characteristics are different, with the intra-Apennine kamafugites displaying lower Al_2O_3 and Na_2O, and higher CaO, K_2O/Na_2O and degree of silica undersaturation. Intra-Apennine volcanics also include some carbonate-rich pyroclastic rocks, which have been suggested represent carbonatitic magmas (Stoppa and Woolley 1997; but see discussion in Chap. 3).

- **The Roman Province or Latium Province**

This is part of the belt of potassic and ultrapotassic rocks running from northern Latium to the Neapolitan area, which was defined as the Roman Comagmatic Region by Washington (1906). The Roman Province (or

Latium Province) defined here only includes Vulsini, Vico, Sabatini and Colli Albani volcanoes. Potassic rocks (KS) basically consist of trachybasalts, latites and trachytes; ultrapotassic rocks (HKS) are represented by

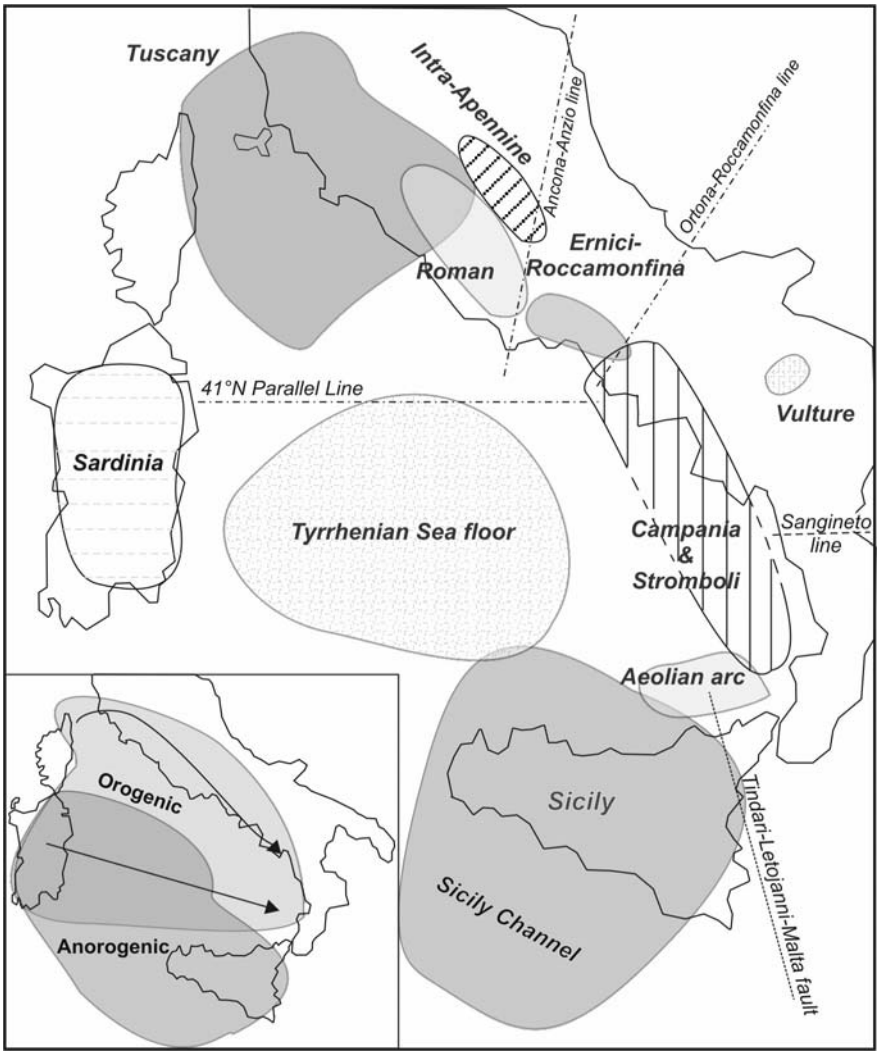

Fig. 1.8. Magmatic provinces in Italy, as identified from major, trace element and isotopic characteristics of mafic rocks. The Ancona-Anzio, Ortona-Roccamonfina, 41° Parallel, Tindari-Letojanni-Malta and the Sangineto tectonic lines are also indicated. Inset: distribution of volcanism with orogenic (i.e. high LILE/HFSE ratios) and anorogenic (i.e. low LILE/HFSE ratios) compositions. Arrows indicates migration of orogenic magmatism from Oligocene to present. See text for explanation.

leucite-tephrites, leucitites to leucite-phonolites. Evolved rocks largely prevail over mafic ones, and mainly occur as large ignimbritic sheets and fallout deposits. Isotope compositions are still close to crustal values, but are less extreme than in Tuscany (for example the $^{87}Sr/^{86}Sr$ ratio is around 0.7090-0.7110; Hawkesworth and Vollmer 1979; Conticelli et al. 2002 and references therein). Incompatible element ratios define distinct trends than those observed for mafic potassic and ultrapotassic rocks of Tuscany (Fig. 1.6).

- **The Ernici-Roccamonfina Province**

This province is characterised by the close association of KS and HKS rocks, showing diverse geochemical and isotopic signatures. Some low-potassium mafic rocks falling in the calc-alkaline compositional field have been also found. Potassic rocks display ratios of some incompatible trace elements such as Ba/La, and radiogenic isotope signatures that are close to those of the Neapolitan volcanoes (Vesuvio, Campi Flegrei, Ischia). On the contrary, ultrapotassic rocks resemble the Colle Albani and other Roman volcanoes. Therefore, the Ernici-Roccamonfina zone is characterised by the coexistence of Roman-type and Campanian-type rocks.

- **The Campania Province**

Somma-Vesuvio, Campi Flegrei and Ischia are the largest and best known volcanoes in this province. The composition of volcanic rocks is variable, from potassic to ultrapotassic; calc-alkaline rocks are also found by bore-hole drillings and among lithic ejecta. The mafic rocks with different enrichment in potassium have comparable concentrations for several incompatible elements and exhibit less extreme isotopic compositions than the equivalent rocks of the Roman Province (e.g. $^{87}Sr/^{86}Sr \sim 0.707$ to 0.708). Overall, trace element ratios and isotopes basically coincide with the rocks from Stromboli in the eastern Aeolian arc, a volcano consisting of calc-alkaline, shoshonitic and potassic rocks. This has led to the conclusion that Vesuvio and adjoining volcanoes do not represent the southern end of the Roman Province but rather the northern extension of the eastern Aeolian arc (Peccerillo 2001). The Pontine Islands are here considered as part of the Campania Province, although they contain, in addition to Quaternary potassic volcanics, older rocks (about 4 Ma-old rhyolites at Ponza) which are calc-alkaline in composition and probably related to a Pliocene volcanic arc along the Tyrrhenian Sea floor.

- **Mount Vulture**

This volcano is located east of the southern Apennines and is composed of alkaline rocks that are enriched in both Na_2O and K_2O (De Fino et al. 1986). Haüyne is common in these rocks. Vulture is petrologically and

geochemically different from any other Italian volcano. Such a diversity was early recognised by Washington (1906) who established a separate magmatic province for this volcano (Apulian Region). The latest activity at Vulture is characterised by explosive eruptions emitting carbonate-rich material (Stoppa and Woolley 1997).

- **The Aeolian arc Province**

This is divided into a western, a central and an eastern sector. The western Aeolian arc (Alicudi, Filicudi, Salina) consists of calc-alkaline rocks with typical island arc signatures. Mafic and intermediate rocks dominate the volcanic sequence, with minor silicic volcanics. The central islands (Vulcano and Lipari) are dominated by calc-alkaline to shoshonitic mafic to silicic rocks; mafic rocks from this sector show isotopic compositions and incompatible trace element ratios similar to the western islands. The eastern arc (Panarea and Stromboli) consists of calc-alkaline to potassic alkaline rocks. Stromboli shows geochemical and isotopic signatures akin to the Neapolitan volcanoes. The Island of Panarea, located between Stromboli and Lipari, has intermediate characteristics between these two volcanoes (Calanchi et al. 2002a).

- **The Sicily Province**

This includes several recent to active volcanoes (Etna, Iblei, Ustica, Linosa, Pantelleria and some seamounts) with an intraplate tholeiitic to Na-alkaline affinity. Rock types range from mafic to intermediate, but peralkaline rhyolites (pantellerites) are abundant at Pantelleria. All these volcanoes display intraplate geochemical signatures, although Etna and Ustica show some element abundances close to arc rocks (e.g. low TiO_2; Beccaluva et al. 1981; Cinque et al. 1988).

- **The Sardinia Province**

This province consists of central volcanoes, basaltic plateaux and monogenetic centres composed of tholeiitic to Na-alkaline rocks (basalt to rhyolite, basanite and trachybasalt to phonolite and trachyte). It overlies calc-alkaline rocks of Oligo-Miocene age.

- **The Tyrrhenian Sea floor**

Several volcanoes with calc-alkaline, tholeiitic (MORB and arc tholeiites) to Na-transitional and alkaline affinity coexist on the Tyrrhenian Sea floor. According to some authors (Savelli 1988; Locardi 1993), the calc-alkaline and shoshonitic seamounts developed along arcuate structures that become younger from west to south-east. The older volcanic cycle (4.5 Ma) of Ponza Island may represent the northern end of one of these arcs.

The magmatic provinces described above are often separated from each other by tectonic lines of lithospheric importance, such as the the Tindari-Letojanni-Malta Escarpment fault, dividing western and eastern Aeolian

arc, and the Ancona-Anzio line, separating the Roman and the Ernici-Roccamonfina provinces (Fig. 1.8). Peccerillo and Panza (1999) demonstrated that these provinces are also characterised by different geophysical features of the crust-mantle system, such as thickness of the crust, mechanical characteristics of the lid, and depth of earthquake foci (see Chap. 10).

1.6. Petrogenesis and Geodynamics: a Preliminary Perspective

The extreme variability of petrological and geochemical characteristics of Italian Plio-Quaternary volcanism calls for complex genetic and evolutionary processes for magma genesis. These will be discussed in the following chapters. Here, the main issues relevant to petrogenesis and geodynamics will be introduced.

As stated earlier, two broad groups of mafic magmas can be distinguished for the Plio-Quaternary volcanism in Italy. One group shows high LILE/HFSE ratios, typical of subduction-related magmas, whereas the other group has low LILE/HFSE ratios and shows affinities with intraplate volcanics (Fig. 1.5). Rock types with high LILE/HFSE ratios include those from the Aeolian arc, but also potassic and ultrapotassic volcanics from central Italy. However, while the Aeolian arc is associated with a zone of deep-focus earthquakes defining a steep Benioff zone (e.g. Falsaperla et al. 1999), such evidence is lacking along the Italian peninsula and the geodynamic significance (subduction-related vs. intra-plate origin) of potassic and ultrapotassic rocks is still debated. Rocks with intraplate geochemical affinities (i.e. low LILE/HFSE ratios) include those from Sicily, Sicily Channel and Sardinia and some rocks from the Tyrrhenian Sea floor.

Sr vs. Nd isotopic variation (Fig. 1.7a) suggests that magmatism in central-southern Italy broadly falls between extreme compositions resembling the upper crust and the upper mantle. This requires an interaction, or mixing, between mantle and crust. It is unlikely, however, that this interaction occurred during ascent of mantle-derived magmas to the surface (*magma contamination*). Many studies (e.g. Peccerillo 1995, 2002; Conticelli 1998) have shown that, although such a process has played an important role in Italian volcanism, it is unable to explain the large range of isotopic compositions encountered throughout Italy. Therefore, the trends shown by the isotopic data can be explained only by assuming that interaction between crustal and mantle end-members occurred in the mantle by the addition of upper crustal material to peridotite. This process is known as *mantle contamination* or also as *mantle metasomatism*. Mantle contamination by up-

per crust provides important evidence in favour of the hypothesis that all the magmatism from the Aeolian arc to Tuscany is related to subduction. In fact, subduction is the only process that is able to bring crustal material into the upper mantle. A key and still open problem is one of understanding the timing of mantle contamination processes.

However, variations of Pb isotopes and incompatible element ratios for both "orogenic" and "anorogenic" magmas (Figs. 1.6, 1.7b), reveal a more complex picture, which does not fit simple two-end-member mixing between mantle and crust. In general, these data suggest interaction between distinct types of mantle sources, as well as multiple events of mantle contamination by various types of crustal rocks (D'Antonio et al. 1995; Peccerillo 1999). These issues will be discussed in detail in later chapters.

1.7. Conclusions

Plio-Quaternary magmatism in Italy exhibits strong major, trace element and isotopic variations, which cover almost completely the compositional field displayed by worldwide igneous rocks. Single volcanic provinces, however, have relatively restricted variations for both age and petrological and/or geochemical signatures. Since most of the Italian volcanic rocks are of ultimate mantle origin, this extreme magmatic diversity requires a strongly heterogeneous upper mantle, which has distinct compositions in the various volcanic provinces. These complexities cannot be generated by any single geodynamic event and are likely a heritage of the intricate evolution history undergone by the circum-Tyrrhenian area.

In the following chapters, the most prominent petrological geochemical characteristics for each magmatic province will be reviewed and the various hypotheses for magma genesis and evolution will be discussed. Finally, the geodynamic significance of the entire circum-Tyrrhenian volcanism will be examined.

2. The Tuscany Province

2.1. Introduction

The Tuscany Magmatic Province (Fig. 2.1) comprises several mafic to silicic intrusive and extrusive centres scattered through southern Tuscany and the Tuscan archipelago. The silicic rocks of the Tolfa-Manziana-Cerite area, north-west of Rome, and a mafic ultrapotassic dyke from Sisco (Corsica) are also traditionally included into the Tuscany Province (Poli et al. 2003).

Magmatic rocks form stocks, dykes, necks, lava flows and domes, and the large volcanoes of Monte Amiata, Monti Cimini and Capraia island. Ages range from about 14 Ma for the Sisco dyke to about 0.2 Ma for Monte Amiata, and show a tendency to decrease from west to east. Magmatic centres, ages and a general description of rocks types are summarised in Table 2.1. Representative whole rock analyses are given in Table 2.2.

2.2. Regional Geology

The geology of Tuscany consists of stacked tectonic thrust units, mostly verging eastwards, overlain by Mio-Pleistocene post-orogenic neo-autochthonous sediments (e.g. Abbate et al. 1970; Boccaletti et al. 1971; Ciarapica and Passeri 1998; Decandia et al. 1998; Barchi et al. 2001; Carmignani et al. 2001). The main tectono-stratigraphic units include:

1. Paleozoic metamorphic rocks (quartz-metaconglomerates, quartzites, phyllites, metavolcanics and micaschists) that have been affected by Alpine metamorphism and are superimposed over a Paleozoic gneiss complex.

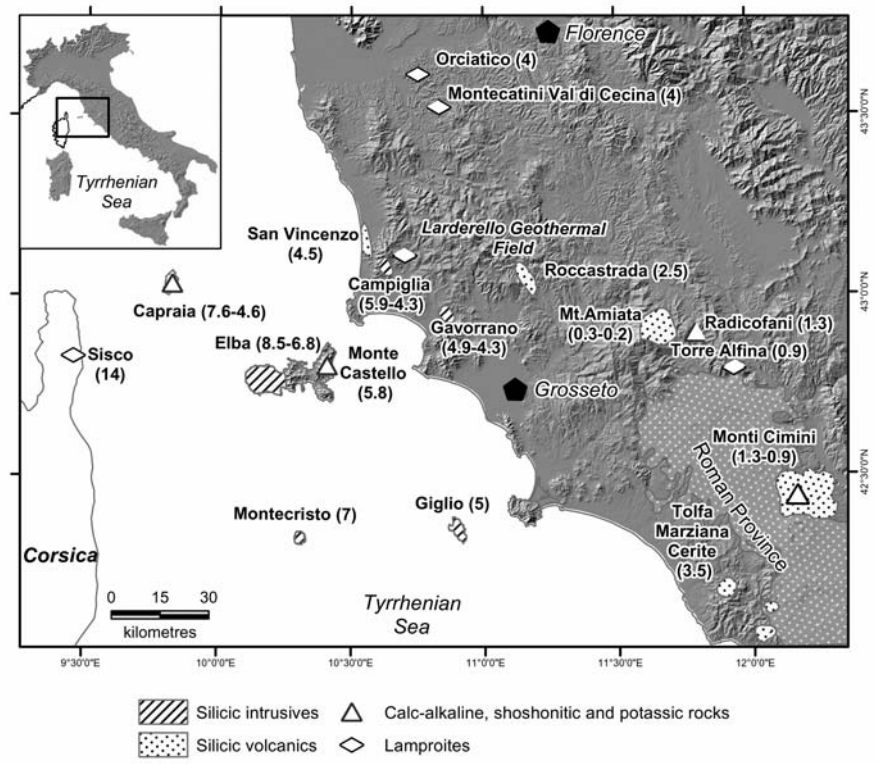

Fig. 2.1. Location of intrusive and extrusive rocks of the Tuscany Magmatic Province. Numbers in parentheses indicate ages (in Ma).

2. The Tuscan units consisting of Late Triassic to early Miocene sedimentary rocks (conglomerates, evaporites, limestones, marls and arenaceous flysch) overlying the metamorphic basement, and affected by Alpine metamorphism in some places (e.g. in the Alpi Apuane).
3. The Ligurian complex tectonically superimposed on the Tuscan units, consisting of middle to late Jurassic ophiolites and radiolarites plus Cretaceous to Eocene pelagic limestones and flysch sequences.
4. Oligo-Miocene clastic marine sediments resting unconformably over the Liguride sequences.
5. Neo-autochthonous Miocene to Pleistocene sediments (evaporites, lignite, fresh water limestones, conglomerates, clays, sands, etc.) infilling tectonic depressions formed during post-orogenic extension.

Table 2.1. Petrological characteristics and ages (in Ma) of magmatism in the Tuscany Province.

MAGMATIC CENTRES	AGE (in Ma)	VOLCANOLOGY and PETROLOGY
San Vincenzo	4.5	- Rhyolite lava flow and dome.
Roccastrada	2.5	- Rhyolite lava flow and dome.
Tolfa-Manziana-Cerite	3.5	- Multicentre complex made of trachydacite to rhyolite lava flows, domes and pyroclastic flows.
Monti Cimini	1.3-0.9	- Volcanic complex formed of trachydacite to latite lava flows, domes and ignimbrites, with a few late-erupted olivine-latite and shoshonite lavas.
Monte Amiata	0.3-0.2	- Central cone of prevailing trachydacite lava flows and domes, with a few late stage olivine-latite and shoshonite lavas.
Elba island	8.5-6.8	- Monzogranites and minor granodiorites, sienogranites, alkali feldspar granites, aplites and pegmatites forming stocks, laccoliths, dykes and sills. Late (5.8 Ma) calc-alkaline mafic dike.
Vercelli seamount	7.2	- Small intrusive body from which syenogranitic rocks have been dredged.
Montecristo island	7.1	- Monzogranite stock cut by aplite and pegmatite veins and porphyritic dikes.
Giglio island	5	- Monzogranite stock intruded by leucocratic monzogranite and by aplite-pegmatite dikes.
Campiglia-Gavorrano	5.9-4.3	- Leucocratic monzogranite, alkali-feldspar granite, monzogranite and tourmaline-bearing leucogranite forming large intrusion mostly hidden beneath surface. Altered mafic dykes with an apparently ultrapotassic composition also occur.
Sisco	14	- Minette dyke showing a high-silica lamproitic composition.
Capraia island	7.6-4.6	- Stratovolcano formed by high-K calc-alkaline andesites and dacites, and by late shoshonitic basalts.
Montecatini Val di Cecina	4.1	- Minette neck with high-silica lamproitic composition, permeated by leucocratic veins.
Orciatico	4.1	- Mafic hypabyssal body with high-silica lamproitic composition.
Radicofani	1.3	- Mafic neck and remnants of lava flow with shoshonitic to ultrapotassic composition.
Torre Alfina	0.9-0.8	- Mafic necks and lava flow with high-silica lamproitic composition.

These rock units were formed during a complex series of tectonic events, which include rifting, oceanic convergence, continental collision and post-orogenic extension. Early rifting occurred during Triassic-Jurassic times; continental to littoral clastic sediments, evaporitic deposits and carbonate rocks, as well as ophiolitic sequences of the Liguride units were formed during this phase. Compression started during Lower Creta-

ceous in the Liguride units and continued until the Lower Oligocene when the Tuscan units were tectonically emplaced over the Umbria sequences. Syn-tectonic terrigenous turbidite and pelagic sedimentation, thrusting and high-pressure metamorphism took place during the compressional tectonic phases. The compressive front shifted eastward from Oligocene to Pleistocene, involving progressively more external sectors of the Adriatic foreland. Contemporaneously, extension and magmatism affected the northern Tyrrhenian Sea, Tuscany and Umbria, migrating from west to east behind the shifting compressive front.

The thickness of the crust in Tuscany is moderate (about 20 to 30 km), and reaches a minimum beneath the Tyrrhenian border of southern Tuscany (see Chap. 10; Scarascia et al. 1994; Locardi and Nicolich 1988; Piromallo and Morelli 2003). A vertical zone of high S-wave velocity (up to 4.6 km/s) has been detected below a depth of about 70 km beneath the north-central Apennine area (e.g. Panza and Mueller 1979; Della Vedova et al. 1991). This has been interpreted as representing a relict lithospheric slab from the Adriatic plate (east of the Apennine chain), which is passively sinking into the upper mantle (Panza et al. 2003 and references therein). An important geophysical feature of the area is denoted by a layer in the uppermost mantle that exhibits crustal-like seismic wave velocities (V_P = 6.8 km/s). This layer may represent either the remnants of the Ligure-Piemontese slab, which was subducting beneath this area until Oligocene time, or partially molten mantle material (e.g. Finetti et al. 2001). Heat flow is high in the Tuscany area (around 100 to 200 mW/m^2 in some areas), as testified by the occurrence of well-known geothermal fields at Larderello and Amiata (Della Vedova et al. 2001 with references).

2.3. Compositional Characteristics of Tuscany Magmatism

The igneous rocks of the Tuscany Province consist of an association of mafic to silicic rocks (Fig. 2.2a) exhibiting contrasting compositions and genesis. Silicic rocks (here defined as those with SiO_2 > 65 wt %) consist of a large number of intrusive and extrusive bodies having a peraluminous character (Alumina Saturation Index, ASI > 1), and moderate variations of major and trace elements at a given silica level.

The mafic rocks (MgO > 3 wt %) range from calc-alkaline and shoshonitic to potassic and ultrapotassic (Fig. 2.2b). The Tuscan ultrapotassic

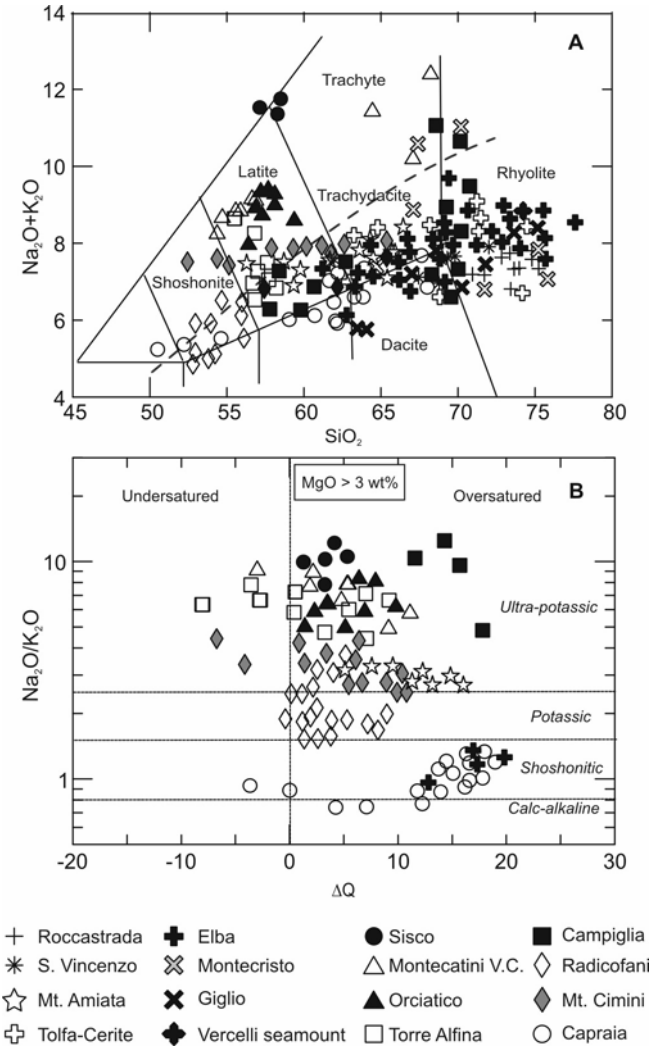

Fig. 2.2. A) TAS classification diagram of Tuscany magmatic rocks. Note that TAS nomenclature applies to volcanic rocks only. The dashed line divides the subalkaline and alkaline fields (Irvine and Baragar 1971). B) ΔQ vs. K_2O/Na_2O diagram for mafic rocks (MgO > 3 wt%) of the Tuscany Province. For definition of ΔQ see Chap. 1.

rocks are slightly undersaturated to oversaturated in silica, in contrast with the ultrapotassic rocks from the Roman Province, which are strongly undersaturated in silica (see Chap. 4). Tuscany rocks have high MgO

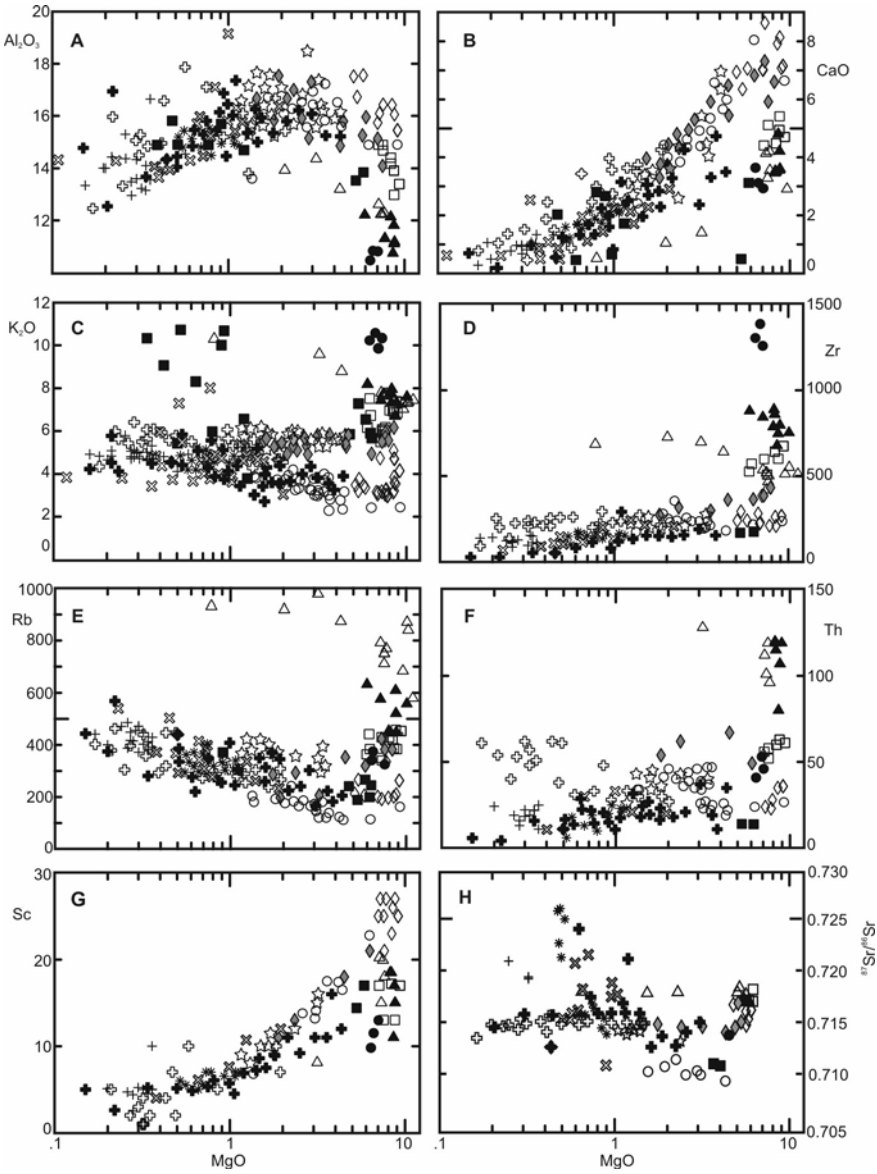

Fig. 2.3. Variation diagrams of MgO vs. selected major and trace elements and $^{87}Sr/^{86}Sr$ for magmatic rocks of the Tuscany Province. Symbols as in Fig. 2.2.

and SiO_2, low CaO, Al_2O_3, Na_2O, and FeO_{total} contents (Fig. 2.3; Table 2.2), and have been classified as high-silica lamproites (Peccerillo et al. 1988; Conticelli and Peccerillo 1992; see Appendix for classification of

potassic rocks). Other mafic rocks are less enriched in potassium and incompatible trace elements, and exhibit higher CaO and Al_2O_3 than lamproites, and fall in the calc-alkaline, shoshonitic and potassic fields (Fig. 2.2b).

Sr-Nd-Pb-Hf isotope ratios display comparable range of values in the silicic and mafic rocks and are closer to crustal than to mantle compositions (Fig. 2.4; Vollmer 1976; Hawkesworth and Vollmer 1979; Conticelli et al. 2002; Gasperini et al. 2002; author's unpublished data). These crustal-like isotopic signatures have led early authors to suggest a crustal

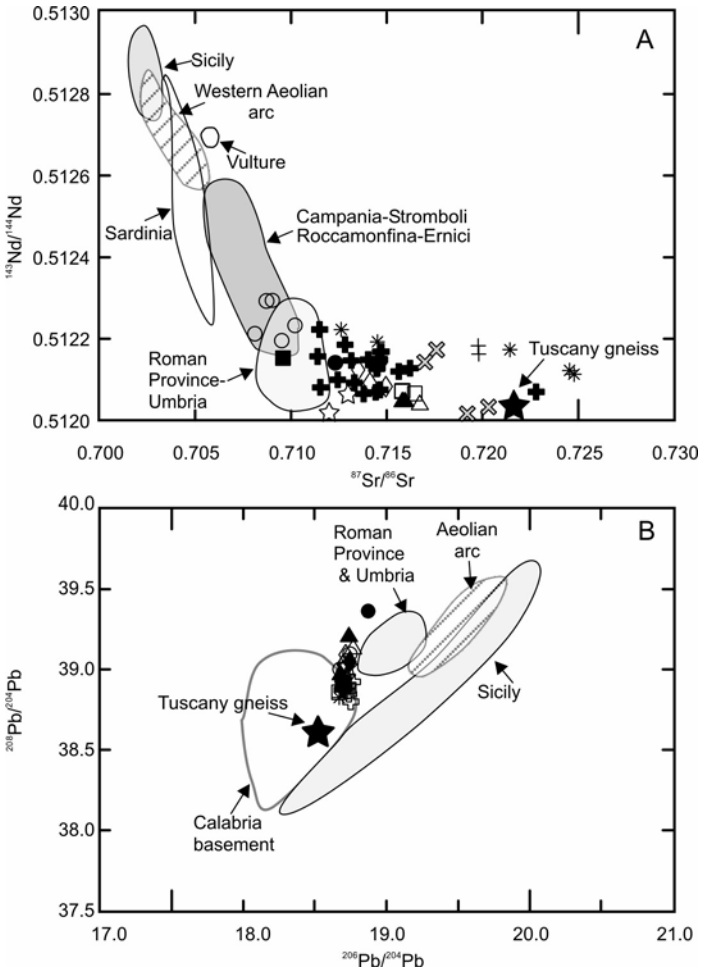

Fig. 2.4. Sr, Nd (A) and Pb (B) isotopic composition of Tuscany magmatic rocks. Symbols as in Fig. 2.2. Composition of other Italian magmatic provinces are shown or comparison.

anatectic origin for all Tuscany magmas without exceptions (Marinelli 1975).

2.4. Silicic Magmatism

Silicic volcanics occur as lavas at San Vincenzo, Roccastrada, Monte Amiata, Monti Cimini and Tolfa-Manziana-Cerite complex. Pyroclastic rocks are scarce or absent, and a few ignimbrites only occur at Monti Cimini and Cerite complex. Silicic intrusions crop out in the islands of Elba, Montecristo and Giglio, and at Campiglia and Gavorrano in southern Tuscany. Other granitoid bodies occur as seamounts in the northern Tyrrhenian Sea (e.g. Vercelli; Barbieri et al. 1986) and as hidden intrusions in several places of southern Tuscany (e.g. Franceschini et al. 2000; Poli et al. 2003).

2.4.1. Effusive Rocks

San Vincenzo. Rhyolitic lava flows and domes (4.5 Ma) crop out over an area of about 10 km^2 at San Vincenzo. Thin sections show porphyritic textures with phenocryst of K-feldspar, quartz, plagioclase and biotite, with minor cordierite. Zircon, apatite, epidote, monazite are present as accessories; the groundmass is glassy to microcrystalline. Some lavas contain clinopyroxene and orthopyroxene xenocrysts and latite enclaves. Petrological and geochemical data highlight a moderately peraluminous character (ASI = 1.1 to 1.3), high enrichment in some incompatible elements (e.g. Rb) and variable radiogenic isotope ratios ($^{87}Sr/^{86}Sr$ ~ 0.7133 to 0.7255; $^{143}Nd/^{144}Nd$ ~ 0.51214 to 0.51225; $^{206}Pb/^{204}Pb$ ~ 18.66 to 18.71; $^{207}Pb/^{204}Pb$ ~ 15.65 to 15.67; $^{208}Pb/^{204}Pb$ ~ 38.82 to 38.89; e.g. Vollmer 1976, 1977; Ferrara et al. 1989; Feldstein et al. 1994). REE are fractionated with negative Eu anomalies (Fig. 2.5a). Latitic enclaves have less radiogenic Sr isotopic compositions than host rhyolites. Radiogenic isotope disequilibrium has been demonstrated among various phenocrysts and the groundmass (Ferrara et al. 1989; Feldstein et al. 1994). $^{87}Sr/^{86}Sr$ ratios define a negative hyperbolic trend with Sr (Fig. 2.6), which has been interpreted to indicate that the San Vincenzo rhyolites experienced mixing with mafic magmas having a composition close to that of the latitic enclaves (Ferrara et al. 1989; Pinarelli et al. 1989; Feldstein et al. 1994). $\delta^{18}O_{SMOW}$ on whole rock and separated quartz and feldspars is about +13 to +14‰ (Turi and Taylor 1976).

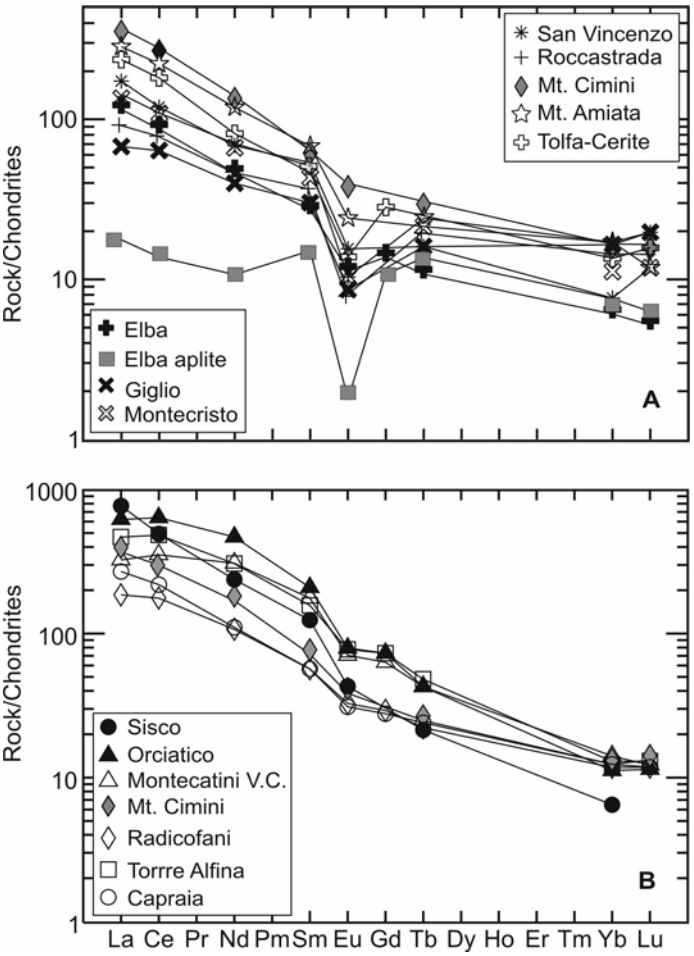

Fig. 2.5. REE patterns of selected Tuscany silicic (A) and mafic (B) rocks.

Roccastrada. Rhyolitic lava flows and domes with an age of about 2.5 Ma crop out over an area of about 100 km^2 at Roccastrada (Mazzuoli 1967; Pinarelli et al. 1989). These rocks exhibit porphyritic textures with phenocrysts and megacrysts of K-feldspar and quartz, plus minor plagioclase (An_{50-20}), biotite and cordierite. Accessory phases include zircon, apatite, magnetite, and rare garnet. Groundmass texture is generally massive, glassy to perlitic, sometimes microcrystalline. Small xenoliths of metasedimentary origin have been found, whereas there is no evidence for the

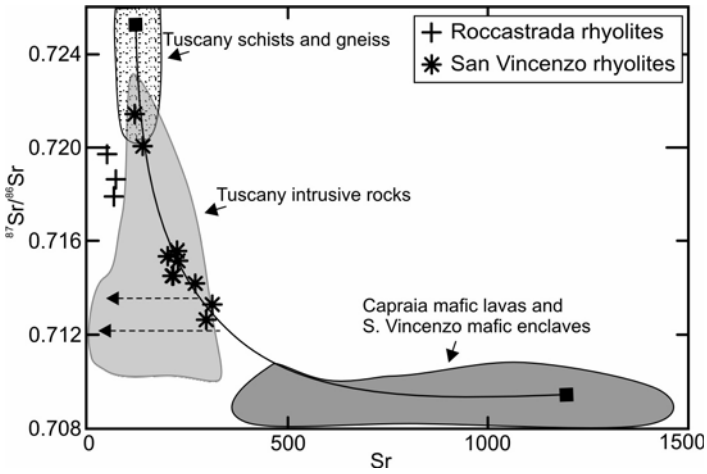

Fig. 2.6. $^{87}Sr/^{86}Sr$ vs. Sr for San Vincenzo and Roccastrada rhyolites. The curved line is a mixing trend between Tuscany metamorphic rocks and the calc-alkaline rocks from Capraia. Dashed lines are fractional crystallisation trends. For further explanation, see text.

occurrence of mafic enclaves. This suggests that the Roccastrada rhyolites experienced little or no interaction with mafic magmas (Pinarelli et al. 1989). The Roccastrada rhyolites are more strongly peraluminous (ASI ~ 1.2 to 1.5) and have less variable radiogenic-isotope composition than San Vincenzo lavas (e.g. $^{87}Sr/^{86}Sr$ ~ 0.718 to 0.720; $^{143}Nd/^{144}Nd$ ~ 0.51222; $^{206}Pb/^{204}Pb$ ~ 18.68; $^{207}Pb/^{204}Pb$ ~ 15.66; $^{208}Pb/^{204}Pb$ ~ 38.91 to 38.93; Vollmer 1976, 1977; Hawkesworth and Vollmer 1979). Oxygen isotopic composition is high with $\delta^{18}O_{SMOW}$ ~ +13‰ (Turi and Taylor 1976).

Tolfa-Manziana-Cerite. This volcanic complex is the most southerly exposure of the Tuscany Province. It mostly consists of a series of lava domes with some associated pyroclastic flow deposits strongly affected by secondary alteration. Rb/Sr, K/Ar and $^{40}Ar/^{39}Ar$ datings give probable age of about 3.5 Ma (Villa et al. 1989; Barberi et al. 1994a), although K/Ar ages of 3.7 to 1.8 Ma were reported by Clausen and Holm (1990).

The volcanic rocks range from trachydacite to rhyolite (Pinarelli 1991), and contain abundant mafic enclaves with variable potassium contents. Trachydacites have a porphyritic texture with phenocrysts of plagioclase (An_{60-50}), sanidine, orthopyroxene, clinopyroxene and biotite set in a glassy groundmass. Rhyolites are porphyritic with phenocrysts of reversely zoned (An_{35-70}) plagioclase, sanidine and some orthopyroxene and quartz set in a microcrystalline to glassy groundmass. Accessory minerals include zircon, apatite and Fe-Ti oxides. The Tolfa-Manziana-Cerite lavas display an increase in some incompatible elements (e.g. Rb, Th, LREE) from mafic en-

claves to rhyolites. Isotopic compositions are moderately variable ($^{87}Sr/^{86}Sr$ = 0.7123 to 0.7144; $^{206}Pb/^{204}Pb$ = 18.63 to 18.76; $^{207}Pb/^{204}Pb$ = 15.65 to 15.69; $^{208}Pb/^{204}Pb$ = 38.80 to 39.12; Clausen and Holm 1990; Pinarelli 1991). According to Clausen and Holm (1990) the compositional variation of Tolfa-Maziana-Cerite rocks reveals a genesis by fractional crystallisation starting from intermediate parents generated by melting of subducted upper crustal material. Pinarelli (1991) suggests fractional crystallisation and mixing between mafic and silicic melts as mechanisms of compositional evolution.

Monti Cimini is a 1.35 to 0.94 Ma volcano formed by dominant trachydacite lava flows, domes and ignimbrites, and by a few late-erupted latites and shoshonites (Puxeddu 1971; Lardini and Nappi 1987). Trachydacites display porphyritic textures with phenocrysts and megacrysts of sanidine plus plagioclase, biotite, othopyroxene and clinopyroxene set in a hypocrystalline groundmass containing the same phases plus accessory ilmenite, apatite and zircon. Latites and shoshonites have aphyric to porphyritic textures with phenocrysts of olivine and minor clinopyroxene set in a groundmass composed of the same phases plus sanidine and Fe-Ti oxides. The Monti Cimini rocks show a decrease in MgO, TiO_2, $FeO_{total,}$ CaO and ferromagnesian trace elements (i.e. Ni, Co, Cr, Sc, V) from shoshonites to trachydacites. Notably, several incompatible elements (e.g. Rb, Zr, Th, LREE) also show a similar trend. Sr- and Nd-isotope ratios are variable ($^{87}Sr/^{86}Sr$ ~ 0.7128 to 0.7156; $^{143}Nd/^{144}Nd$ ~ 0.51214 to 0.51209), the largest variation being observed in the mafic rocks (Poli et al. 1984; Conticelli et al. 2002; Perini et al. 2003 and references therein). These complex geochemical variations have made the genesis of Cimini rocks poorly understood. Trachytes probably derive from a mildly potassic parental magma by fractional crystallisation plus possible crustal assimilation. However, decrease of incompatible elements with increasing silica requires some additional explanation. Based on Sr-isotope variations in whole rocks and K-feldspar megacrysts, Perini et al. (2003) propose extensive mixing processes at Cimini. The isotopic variability in the mafic rocks is explained by mixing between lamproitic and high-K calc-alkaline mafic melts. Compositional variations in the evolved rocks would be the result of another mixing process between mafic potassic magmas and trachytes.

Monte Amiata is a 1738 m-high cone dominated by trachydacitic lava flows and domes with a few late-erupted shoshonites and latites. Magmatism is 0.3 to 0.2 Ma and is associated with well-known and long-exploited cinnabar mineralisations (Mazzuoli and Pratesi 1963; Barberi et al. 1971; van Bergen 1985; Ferrari et al. 1996 and references therein). The Monte Amiata trachydacites exhibit a porphyritic texture with abundant

phenocrysts and megacrysts of sanidine, plagioclase (An_{60-50}), orthopyroxene (En_{55-40}), high-TiO_2 biotite and diopside to augite clinopyroxene. These minerals are set in a glassy groundmass, containing microlites of clinopyroxene, rare orthopyroxene and some biotite. Xenocrysts of olivine have been observed. Accessory phases include apatite, zircon, ilmenite, magnetite and perrierite, a sorosilicate of Ti and REE (Ferrari et al. 1996; Cristiani and Mazzuoli 2003). Latites and shoshonites are porphyritic with phenocrysts of plagioclase, diopsidic clinopyroxene and olivine, set in a hypocrystaline groundmass containing the same phases plus sanidine and glass. Abundant magmatic and metamorphic xenoliths occur in the Monte Amiata lavas. Numerous magmatic mafic enclaves are found in the summit domes (Di Sabatino and Della Ventura 1982; van Bergen et al. 1983; Ferrari et al. 1996).

The Monte Amiata lavas display a moderate variations for many major and trace elements and for radiogenic isotope compositions (e.g. $K_2O \sim 5$ to 6 wt %; $^{87}Sr/^{86}Sr \sim 0.7112$ to 0.7131; $^{143}Nd/^{144}Nd \sim 0.51215$; $^{206}Pb/^{204}Pb \sim 18.68$ to 18.72; $^{207}Pb/^{204}Pb \sim 15.65$ to 15.67; $^{208}Pb/^{204}Pb \sim 38.91$ to 39.01; Vollmer 1977; Hawkesworth and Vollmer 1979; Poli et al. 1984; Giraud et al. 1986). Overall, there is an increase in incompatible elements and radiogenic Sr with decreasing MgO, which reveals an evolution by interaction between mafic magmas and rocks and/or melts of crustal origin (van Bergen and Barton 1984; Poli et al. 1984).

2.4.2. Intrusive Rocks

The **Elba Island** contains a large number of intrusive bodies of various sizes, ranging in composition from granodiorite to alkali-feldspar granite, aplite and pegmatite (Marinelli 1959; Barberi et al. 1971; Poli et al. 1989; Dini et al. 2002; Rocchi et al. 2002). K/Ar, $^{40}Ar/^{39}Ar$ and Rb/Sr ages range from about 8.5 to 6.8 Ma (Dini et al. 2002 and references therein). A 5.8 Ma old strongly altered calc-alkaline mafic dyke also has been found recently at Monte Castello, eastern Elba (Conticelli et al. 2001). Fe-Pb-Sn mineralisation is associated with intrusive magmatism at Elba and has been exploited since Etruscan times until a few years ago.

The largest intrusion is represented by the Monte Capanne monzogranitic stock (about 10 km in diameter), located in the western side of the island. It exhibit a porphyritic texture with centimetre- to decimetre-sized euhedral megacrysts of K-feldspar that are set in a medium- to coarse-grained matrix formed by variable amounts of plagioclase, quartz, K-feldspar and biotite with accessory apatite, zircon, monazite, ilmenite, and tourmaline. The intrusion contains abundant microgranular calc-alkaline

mafic enclaves and is cut by late aplitic and pegmatitic veins. Large euhedral crystals of quartz, K-feldspar, tourmaline, pollucite and other rare minerals have been recovered from pegmatites. Other minor intrusions (e.g. the Orano dyke, the Capo Bianco aplite, the Portoferraio porphyry etc.) include granodiorites, monzogranites, syenogranites, and alkali-feldspar granite (see Dini et al. 2002). These rocks are granular to porphyritic with megacrysts and phenocrysts of K-feldspar, plagioclase, quartz and biotite set in a quartz-feldspathic groundmass. Amphibole and relict clinopyroxenes are rarely observed. Accessory minerals include a wide variety of phases such as apatite, zircon, monazite, allanite, thorite and tourmaline.

Single igneous bodies at Elba exhibit moderate compositional variations, but important differences exist among various intrusions (Fig. 2.3). Overall, rocks are acid (SiO_2 = 62 to 75 wt %) and moderately peraluminous (ASI ~ 1.0-1.2). Trace elements are variable, although there is an overall increase in Rb and Nb, and a decrease in ferromagnesian trace elements (Ni, Cr, Sc, etc.), Sr and Light REE with decreasing MgO. Heavy REE and Y also decrease with decreasing MgO, but show a strong positive spike in some leucocratic dykes. REE patterns are fractionated with negative Eu anomalies that become stronger in some REE-depleted aplites (Fig. 2.5a). The Elba rocks exhibit a broad range of Sr- and Nd-isotope compositions ($^{87}Sr/^{86}Sr$ ~ 0.7114 to 0.7228; $^{143}Nd/^{144}Nd$ ~ 0.51210 to 0.51227). Pb-isotope ratios fall well inside the field of upper crustal compositions ($^{206}Pb/^{204}Pb$ ~ 18.68 to 18.73; $^{207}Pb/^{204}Pb$ ~ 15.66 to 15.69; $^{208}Pb/^{204}Pb$ ~ 38.87 to 38.95). Mafic microgranular enclaves have radiogenic isotope compositions lying within the field of host intrusive silicic rocks, probably indicating some isotopic re-equilibration with the enclosing magmas (Poli 1992; Dini et al. 2002). According to most authors, the Elba magmas were formed by mixing processes between mafic and silicic melts. However, important fractional crystallisation processes affected hybrid melts to produce evolved rocks such as aplites and pegmatites (Poli et al. 1989; Dini et al. 2002; Rocchi et al. 2002).

Montecristo is an island situated about 60 km south of Elba, along N-S trending extensional faults, parallel to the Corsica coast. It consists of a monzogranite stock cut by dykes that has a Rb/Sr age of 7.1 Ma (Innocenti et al. 1997). The Montecristo monzogranites have a porphyritic texture with phenocrysts and/or megacrysts of K-feldspar, quartz and plagioclase surrounded by a medium-grained matrix formed by the same phases, plus variable amounts of biotite. Accessory minerals include apatite, zircon, tourmaline, ilmenite, sphene, allanite, monazite and rutile. Cordierite has been also observed. Microgranular mafic enclaves are common.

The Montecristo monzogranites display moderate compositional variation (e.g. SiO_2 = 69 to 75 wt %). Sr-isotope ratios are around 0.7134 to 0.7150 (Innocenti et al. 1997). Some porphyritic dykes have a slightly lower silica content than monzogranites (SiO_2 ~ 66 to 70 wt %), but have a much higher K_2O (~ 5.5 to 8.1 wt %), and lower Sr isotopic ratios ($^{87}Sr/^{86}Sr$ = 0.7096 to 0.7123), suggesting a distinct origin with respect to the main intrusion. Enclaves show a broadly calc-alkaline composition (Poli 1992; Innocenti et al. 1997).

The **Island of Giglio** hosts a main monzogranitic stock cut by several dykes, and a small leucocratic monzogranitic body, with a Rb/Sr age of about 5 Ma (Westerman et al. 1993). The main monzogranite is isotropic to foliated in texture and consists of plagioclase, K-feldspar, quartz and variable amounts of biotite plus accessory muscovite, tourmaline, Fe-Ti oxides, apatite, monazite and zircon. K-feldspar megacrysts occur in some rocks. Xenocrystic cordierite, garnet, andalusite and sillimanite have been also observed. Metamorphic xenoliths and microgranular mafic enclaves are common. The leucocratic monzogranite contains megacrysts of K-feldspar set in a medium- to fine-grained matrix composed of quartz, plagioclase, alkali feldspar, biotite, tourmaline and cordierite. Dykes mostly consist of granites, tourmaline-rich aplites and pegmatites.

The Giglio rocks are moderately peraluminous (ASI ~ 1.1 to 1.3) and display variable major and trace element contents (Fig. 2.3). $^{87}Sr/^{86}Sr$ ranges from about 0.7159 to 0.7203 and increases from the main monzogranite to leucocratic rocks. $^{143}Nd/^{144}Nd$ ranges from 0.51205 to 0.51222, and shows an opposite tendency. The mafic enclaves have comparable and sometime more primitive Sr-Nd isotope compositions than the host rocks, indicating some equilibration during emplacement and cooling (Westerman et al. 1993).

The **Campiglia** intrusion crops out over a small area at Botro ai Marmi, the bulk of the body being hidden below the surface. The rock is a fine-grained leucocratic monzogranite cut by highly altered mafic to silicic porphyritic dykes, having K/Ar ages of 5.9 to 4.3 Ma (Barberi et al. 1967a; Poli et al. 1989). The Campiglia rocks are highly altered by late fluids coming from both the magma and the wall rocks. These processes generated dramatic geochemical modification of intrusive rocks and were responsible for the formation of long-exploited Cu-Pb-Zn-Ag mineralisation. Compositions of the least-altered intrusive rocks are moderately peraluminous (ASI around 1.2) and silicic (SiO_2 ~ 70 wt %). Altered silicic dykes are strongly enriched in potassium (up to K_2O ~ 10 wt %).

The **Gavorrano** intrusive rocks consist of 4.9 to 4.3 Ma syenogranites, alkali-feldspar granites and monzogranites that are mostly hidden below

the surface and encountered by deep borehole drilling. Their major and trace element compositions are rather variable (e.g. SiO_2 ~ 66 to 75 wt %; Rb = 250 to 700). Except for Rb, the incompatible trace element contents decrease with increasing silica (Poli et al. 1989). Sr-isotope ratios are in the range of other Tuscany silicic rocks ($^{87}Sr/^{86}Sr$ = 0.7138 to 0.7149; Ferrara and Tonarini 1985).

Hidden intrusive bodies and seamounts. There are several hidden intrusions in southern Tuscany, whose presence has been recognised by drilling and geophysical investigation (Zitellini et al. 1986; Franceschini et al. 2000; Gianelli and Laurenzi 2001). Northeast of Gavorrano (Castel di Pietra), borehole drilling encountered 4.3 Ma granodiorite to alkali-feldspar granites (Franceschini et al. 2000). At Monte Spinosa, a few kilometres south of Botro ai Marmi, drilling recovered syenogranites and monzogranites with SiO_2 = 66 to 71 wt %. At Larderello syenogranites to monzogranites have been encountered at about 2 km below the surface; these have ages of 3.8 to 1.3 Ma (Gianelli and Laurenzi 2001; Villa et al. 2001).

Several seamounts of likely granitoid composition occur between Corsica and Tuscany. These are aligned along a north-south trending ridge, south of Elba and Montecristo. A sample dredged from the Vercelli seamount, southeast of this alignment, consists of a leucocratic syenogranite with a K/Ar age of 7.2 Ma and $^{87}Sr/^{86}Sr$ = 0.71140 (Barbieri et al. 1986).

2.5. Mafic Magmatism

Mafic magmas (MgO higher than 3 wt %) mostly form small monogenetic intrusive and effusive bodies. High-silica lamproitic hypabyssal and volcanic rocks occur at Sisco, Montecatini Val di Cecina, Orciatico, Torre Alfina and Campiglia. Calc-alkaline, shoshonitic and potassic volcanics are found at Capraia island, Radicofani and among the latest eruped products of the prevailingly silicic volcanoes of Monti Cimini and Monte Amiata. Mafic rocks are also present as enclaves in several acid intrusive and extrusive rocks.

Sisco. A small sill that cuts through Alpine high-pressure metamorphic terrain occurs in Corsica, north of Sisco village. The rock has a microgranular to slightly porphyritic texture, and consists of altered olivine, sanidine, Al-poor diopside, phlogopite and K-richterite. Accessory minerals include sphene, chromite, ilmenite, priderite (K, Ba, Fe^{3+}, Ti oxide) and rutile (Wagner and Velde 1986). The age is about 14 Ma (Civetta et al. 1978). The Sisco rock is a peralkaline high-silica lamproite (normative

acmite around 4 to 5 wt%) exhibiting high concentrations MgO, Ni, Co and Cr and moderate Sc and V abundances. REE are fractionated with a small negative Eu anomaly (Fig. 2.5b). The mantle-normalised incompatible element pattern is fractionated, contains negative anomaly of HFSE, Ba and Sr (Fig. 2.7a). As illustrated in Fig. 2.4, the initial Sr isotope ratio of the Sisco minette is relatively high ($^{87}Sr/^{86}Sr \sim 0.7126$), whereas Nd and Pb isotope ratios are poorly to moderately radiogenic with $^{143}Nd/^{144}Nd \sim 0.51218$ and $^{206}Pb/^{204}Pb \sim 18.86$ (Table 2.2).

Montecatini Val di Cecina. The Montecatini lamproite consists of a 4.1 Ma old plug intruded into Miocene marine and lacustrine sediments and Liguride units. Petrographically, the rock is a medium- to fine-grained sometimes porphyritic minette consisting of abundant phlogopite, Al-poor diopside to augite clinopyroxene (Cellai et al. 1994), K-feldspar, minor altered olivine and accessory apatite, amphibole, Fe-Ti oxides, zircon, thorite, apatite and perrierite (Conticelli et al. 1992). The plug is pervasively intruded by a network of thin leucocratic veins, consisting of dominant sanidine with minor quartz and brown mica, plus accessory apatite. These veinlets probably represent residual felsic melts unmixed from the crystallising minette magma (Conticelli et al. 1992).

The Montecatini high-silica lamproite has lower alkali contents than that at Sisco. MgO, Ni, Co and Cr are high, in the range of mantle equilibrated melts, but Sc and V are lower than expected in normal, primitive mantle-derived rocks. The REE pattern is fractionated, with an upward convexity for light REE and a negative Eu anomaly (Fig. 2.5b). Incompatible element patters are highly fractionated and contain pronounced positive spikes of Rb, Th and Pb, and stronger negative anomalies of HFSE contents than at Sisco (Fig. 2.7a). Sr-Nd-Pb-Hf isotope ratios are close to crustal values ($^{87}Sr/^{86}Sr = 0.7169$; $^{143}Nd/^{144}Nd = 0.5121$; $^{206}Pb/^{204}Pb = 18.76$; $^{176}Hf/^{177}Hf = 0.28245$; Table 2.2). The leucocratic veins have much higher silica (SiO_2 = 64 to 66 wt %), K_2O (8 to 10 wt %) and incompatible element contents, and lower MgO and ferromagnesian concentrations than the host minette (Peccerillo et al. 1988; Conticelli et al. 1992). However, radiogenic isotopic signatures are similar, which is consistent with their derivation through magma unmixing.

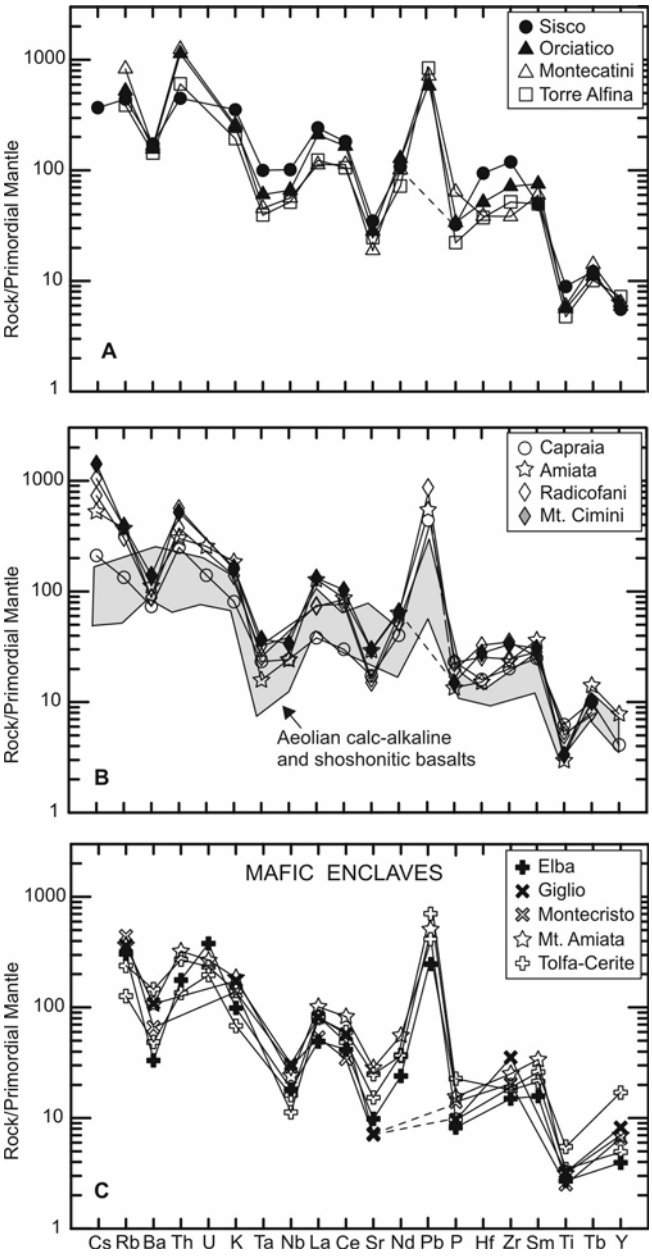

Fig. 2.7. Mantle normalised incompatible element patterns of representative Tuscany mafic rocks (A, B) and for mafic enclaves hosted by silicic rocks (C). The field of Aeolian arc calc-alkaline and shoshonitic mafic rocks is shown for comparison.

Fig. 2.8. Walls of the Torre Alfina castle showing large amounts of a wide variety of crustal and mantle xenoliths in the lamproitic lavas.

Orciatico. The Orciatico outcrop is a dark-coloured aphanitic dyke having a poorly porphyritic texture in this section, with microphenocrysts of olivine (Fo_{90-75}), phlogopite and Al-poor diopside ($Al_2O_3 \sim 0.5$ wt%; Cellai et al. 1994) set in a groundmass consisting of the same phases plus sanidine, glass, and accessory K-richterite, rutile, ilmenite and chromite. Some of the high-MgO olivine crystals show evidence of corrosion and kinking, and are probably xenocrysts resulting from disaggregation of high-pressure ultramafic xenoliths (Wagner and Velde 1986; Peccerillo et al. 1987, 1988; Conticelli and Peccerillo 1992; Conticelli et al. 1992). The age and composition of the Orciatico rock are very similar to the Montecatini lamproite. Oxygen-isotope ratios show large differences between phenocryst and groundmass minerals with $\delta^{18}O \sim +7.2‰$ in olivine phenocrysts and $\delta^{18}O \sim +11.1‰$ in groundmass sanidine (Barnekow 2000).

Torre Alfina. This is a monogenetic volcano (0.9 to 0.8 Ma) formed by a lava flow several hundred meters long, and two necks. Rocks have aphyric to poorly porphyritic textures and the only phenocryst phase is rare euhedral to skeletal olivine (Fo_{90-84}). Other phases include diopside, phlogopite, K-feldspar and glass (Conticelli and Peccerillo 1992; Conticelli 1998; Barnekow 2000). The Torre Alfina rocks contain a large number of xenoliths of both crustal and mantle origin, which document a rapid magma ascent on the order of few hours (Conticelli and Peccerillo 1990). The xenoliths, best observed on the walls of the castle dominating the vil-

lage of Torre Alfina (Fig. 2.8), include large amounts of crustal rocks (granulites, gneiss, schists, sandstones and marls) and a few cm-size ultramafic xenoliths (dunites, spinel harzburgites and lherzolites). Most of the crustal xenoliths and xenocrysts show evidence of partial melting and reaction with the host magma, exhibiting one of the most compelling cases of wall rock assimilation by a rapidly ascending magma (Conticelli 1998). The Torre Alfina lavas have similar composition as the Montecatini and Orciatico lamproites, although the latter have higher Th and Rb contents. There are small, but significant, variations within lava flow and necks, which have been suggested to derive from variable assimilation of crustal rocks by ascending mafic magma. Such a process generated minor modification of trace element ratios and isotopic characteristics, and a general dilution for several compatible and incompatible elements (e.g. Ni from 350 to 250; La from 100 to 85, $^{87}Sr/^{86}Sr$ increasing from about 0.7158 to 0.7165; Conticelli 1998).

Campiglia. Mafic dykes with an age of about 4.3 Ma occur in the Campiglia area, associated with silicic magmatism. These dykes have porphyritic textures with phenocrysts of clinopyroxene, plagioclase, biotite, alkali feldspar and some corroded quartz set in a groundmass of plagioclase, sanidine and pyroxene. The major element compositions of Campiglia mafic dykes resemble those of high-silica Tuscany lamproites. However, concentrations of several incompatible trace elements (e.g. Rb, Th, LREE, Zr) and Sr isotope ratio ($^{87}Sr/^{86}Sr = 0.7096$) are lower and Nd isotope ratio ($^{143}Nd/^{144}Nd = 0.51220$) is higher, falling close to Capraia calc-alkaline and shoshonitic rocks (Peccerillo et al. 1987; Conticelli and Peccerillo 1992; Conticelli et al. 2002). Therefore, it is likely that alteration may have changed the pristine geochemical compositions of these rocks, especially K_2O and other alkalis; note that several dykes at Campiglia show clear petrographic evidence of deuteric transformation with a sharp increase of K_2O/Na_2O up to 30-40 (Barberi et al. 1967a).

Radicofani. The volcano at Radicofani consists of a neck and a few remnants of lava flows with K/Ar and $^{40}Ar/^{39}Ar$ ages clustering around 1.3 Ma (D'Orazio et al. 1991, 1994). The rocks display a slight porphyritic texture with phenocrysts of olivine (Fo_{84-68}) and minor diopside to augite clinopyroxene; a few plagioclase (An_{91-76}) is found in some samples. The groundmass consists of the same phases plus K-feldspar, Fe-Ti oxides, minor brown mica, amphibole, and glass; orthopyroxene has rarely been observed. Resorbed xenocrysts of quartz, cordierite and other metamorphic minerals are also present. In spite of its small size, the Radicofani volcano shows variable composition. The neck consists of shoshonitic lavas, whereas some lava blocks scattered around the neck are ultrapotassic in

composition. All the rocks, however, have comparable silica (SiO_2 ~ 53 to 56 wt %) and MgO (8 wt %) contents. Incompatible elements (Rb, Th, Nb, Ta, REE, etc.) and some ferromagnesian elements (Ni, Cr) are positively correlated with K_2O, whereas V and Sc show a negative trend (D'Orazio et al. 1994). The incompatible element patterns resemble those of Tuscany lamproites, although absolute elemental enrichment is lower (Fig. 2.7b). $^{87}Sr/^{86}Sr$ ratios (0.7135 to 0.7164) increase with K_2O, whereas $^{143}Nd/^{144}Nd$ ratios (0.51213 to 0.51217) exhibit an opposite trend (Poli et al. 1984; D'Orazio et al. 1994; Conticelli et al. 2002). Pb- and Hf-isotope ratios ($^{206}Pb/^{204}Pb$ ~ 18.68; $^{207}Pb/^{204}Pb$ ~ 15.67; $^{208}Pb/^{204}Pb$ ~ 39.98; $^{176}Hf/^{177}Hf$ = 0.28255) fall in the field of the Tuscany ultrapotassic rocks (De Astis et al. 2000; Conticelli et al. 2002; Author's unpublished data). O-isotopes on clinopyroxene and olivine vary from $\delta^{18}O$ = +6.9‰ to + 7.8‰ (Barnekow 2000). Overall, the compositions of Radicofani magmas lie between moderately potassic rocks (e.g. Capraia shoshonites or Roman KS magmas) and lamproites (e.g. Torre Alfina), suggesting a genesis by mixing between these magmas.

Monti Cimini and **Monte Amiata**. Small lava flows having a mafic composition (shoshonite and latite) have been erupted during the latest stages of activity at the dominantly silicic volcanoes of Monti Cimini and Monte Amiata (Poli et al. 1984; Ferrari et al. 1996). The *Monti Cimini* mafic rocks have aphyric to porphyritic textures with dominant olivine and minor clinopyroxene phenocrysts set in a groundmass composed of the same phases as the phenocrysts plus sanidine and Fe-Ti oxides. Plagioclase is present in the groundmass of shoshonites. Some latites contain K-feldspar megacrysts, mica and accessory zircon and perrierite. Latites and shoshonites from *Monte Amiata* also exhibit porphyritic texture with phenocrysts of diopside, reversely zoned plagioclase (An_{50-85}) and minor forsterite-rich olivine set in a groundmass of sanidine, clinopyroxene, olivine, opaque minerals, apatite, and glass. These rocks show intermediate petrological and geochemical characteristics between Tuscany calc-alkaline and lamproitic mafic magmas, leading to the conclusion that they represent mixtures between these end-members.

Capraia is the only volcano in the Tuscany Province dominated by calc-alkaline rocks. The island was constructed during two distinct phases of activity at 7.6 and 4.6 Ma (Borelli et al. 2003). Porphyritic high-K calc-alkaline andesites and dacites were erupted during the older phase. These exhibit phenocrysts of plagioclase, clinopyroxene and minor orthopyroxene, olivine and biotite, K-feldspar and amphibole. Shoshonitic basalts comprise the younger activity and consist of mafic vesicular and slightly porphyritic rocks that form the southern promontory of Zenobito (Pros-

perini 1993; Poli and Perugini 2003). Andesites and dacites have variable concentrations of both LILE and HFSE (Fig. 2.3). Sr-isotope ratios vary from 0.7073 to 0.7102. The shoshonitic rocks have poorly variable major and trace element contents and Sr-isotope signatures ($^{87}Sr/^{86}Sr$ = 0.7074 to 0.7086). Nd-isotope ratios are comparable for calc-alkaline and shoshonitic rocks ($^{143}Nd/^{144}Nd$ = 0.51224 to 0.51227; Poli, personal communication). The incompatible element patterns of the Capraia rocks are characterised by strong fractionation and negative spikes of HFSE, Ba and Sr and positive anomaly of Pb (Fig. 2.7b).

Geochemical data suggest that the early high-K calc-alkaline andesites and dacites evolved from mafic calc-alkaline parents by combined fractional crystallisation and mixing with lamproitic magmas. Interaction with lamproites explains the large variation of trace element concentrations in andesites and dacites. The late shoshonites represent a distinct batch of magma with respect to calc-alkaline activity.

Mafic enclaves are found in most of the Tuscany silicic intrusive and extrusive rocks. They are generally ellipsoidal to rounded in shape and sometimes display crenulated and chilled margins, indicating that they were incorporated into the host magmas when they were still in a molten state (Poli 1992). Megacrysts and phenocrysts from the host silicic rocks are often enclosed within the enclaves. Textures range from microgranular to aphyric and porphyritic. The main minerals include biotite, plagioclase, K-feldspar, quartz, amphibole, and some clinopyroxene, orthopyroxene, olivine and sanidine. In most cases, especially in the intrusive rocks (e.g. at Elba and Giglio), the enclave mineralogy is the same as in the host silicic rocks, but the amounts of mafic phases are much greater. Major element compositions range from calc-alkaline to ultrapotassic. Calc-alkaline to shoshonitic enclaves occur at Elba, Giglio and San Vincenzo, whereas ultrapotassic compositions are observed at Monte Amiata and Monti Cimini. At Tolfa-Manziana-Cerite the enclaves vary from calc-alkaline to ultrapotassic and exhibit a granular to porphyritic texture (Pinarelli 1991; Bertagnini et al. 1995; Poli et al. 2002, 2003).

Trace element and radiogenic isotope signatures of the mafic xenoliths are quite variable. Incompatible elements patterns are fractionated and show negative spikes of Ba, Sr, and HFSE (Fig. 2.7c). REE patterns (not shown) are fractionated and display negative Eu anomalies. At San Vincenzo, mafic enclaves have $^{87}Sr/^{86}Sr$ around 0.708 to 0.709, close to the Capraia calc-alkaline rocks. At Tolfa, enclaves have radiogenic-isotope compositions defining two groups, with $^{87}Sr/^{86}Sr$ = 0.7079 to 0.7091 and 0.7117 to 0.7127, respectively. Pb-isotope ratios of Tolfa enclaves are less variable ($^{206}Pb/^{204}Pb$ = 18.72 to 18.79; $^{207}Pb/^{204}Pb$ = 15.67 to 15.79;

$^{208}Pb/^{204}Pb$ = 38.87 to 39.11), but the highest values are found in the high-radiogenic Sr group (Pinarelli 1991).

Petrological and geochemical signatures of mafic enclaves match quite closely those of the Tuscany mafic rocks. However, some of the observed geochemical characteristics may have been modified by interaction with host silicic magmas and could not represent pristine compositions of mafic melts.

2.6. Petrogenesis

2.6.1. Silicic Magmatism

A crustal anatectic origin is widely accepted for Tuscany silicic magmatism. This is strongly supported by a wealth of petrological and geochemical data, including the peraluminous nature of most rocks and their crustal-like geochemical and isotopic signatures (Poli 2004 and references therein). However, only a few silicic rocks actually represent pure anatectic melts. These include the Roccastrada rhyolites, some of the San Vincenzo lavas (the low Sr, high $^{87}Sr/^{86}Sr$ rocks) and some leucocratic granitoid bodies occurring, for example, at Elba and Giglio (e.g. Poli 1992; Westerman et al. 1993). Note that the Roccastrada rhyolites and most leucogranites do not contain mafic enclaves, supporting the hypothesis of little or no interaction with mafic melts (e.g. Pinarelli et al. 1989). Several studies have shown that the compositions of unmodified crustal anatectic magmas in Tuscany can be modelled by assuming large degrees (some 40-50%) of partial melting of metasediments. Garnet micaschists and gneiss, such as those found by drilling in Tuscany, have been successfully used as source rocks to model trace element and isotopic compositions of silicic magmas at Roccastrada and other localities in Tuscany (e.g. Pinarelli et al. 1989; Poli 1992). However, Poli et al. (2002) and Poli (2004) pointed out that CaO contents of most silicic rocks in Tuscany are exceedingly high for a pelite-derived melt and suggested that moderate degrees of partial melting of a plagioclase-rich rock (e.g. a metagreywake) would be a more suitable process. Petrological data and geochemical modelling suggest that melting of metasedimentary rocks occurred in fluid absent conditions at pressure of at least 0.4-0.6 GPa, leaving a garnet- and cordierite-bearing residue. This indicates that metasediments occur at great depths in the Tuscany Province.

The majority of the silicic rocks exhibit ample textural and geochemical evidence suggesting a more complex genesis than simple crustal anatexis. The occurrence of microgranular mafic enclaves and mafic xenocrysts in several granitoids and lavas is the most obvious indication of interaction (i.e. mixing or mingling) between felsic and mafic magmas. The variable radiogenic isotope signatures, observed both in the single silicic bodies and at the regional scale, and the hyperbolic trend of Sr vs. $^{87}Sr/^{86}Sr$ at San Vincenzo (Fig. 2.6) are considered as the most compelling geochemical evidence in favour of this process. Note that many granitoid rocks fall on this trend, suggesting that mixing operated at a regional scale.

The nature of the mantle end-member involved in the mixing processes is difficult to define, since several enclaves show clear evidence of being equilibrated with host rocks. However, Poli et al. (2002) noticed that the mafic enclaves from some plutons (e.g. Elba and Giglio) have patterns of incompatible elements that are similar to those of calc-alkaline rocks from Capraia island. This has led them to suggest that the mafic end-member of Tuscany plutonism was represented by a calc-alkaline melt. Such a hypothesis can be applied also to San Vincenzo, where the mafic enclaves contain orthopyroxene and have a relatively low Sr-isotope ratio, close to that of the Capraia rocks. However, in other cases (e.g. Monte Amiata, Tolfa-Manziana-Cerite complex), enclaves have much higher K_2O contents. Therefore, different types of mafic magma, from calc-alkaline to ultrapotassic, were involved in the mixing with crustal anatectic melts in Tuscany (Poli 2004).

Finally, several silicic bodies (e.g. at Elba) show variable major and trace element abundances at rather constant $^{87}Sr/^{86}Sr$ (Fig. 2.3h). This suggests that silicic magmas were also subjected to fractional crystallisation. Therefore, field, textural and geochemical evidence supports the hypothesis that the silicic rocks in Tuscany originated through a complex process of combined crustal melting, mixing-mingling with mafic melts and fractional crystallisation. The latter process mostly affected hybrid magmas, determining the formation of leucocratic rocks occurring as aplitic and pegmatitic veins in several intrusions. Therefore, the most leucocratic rocks in Tuscany represent either primary crustal anatectic melts or end-products of fractional crystallisation processes of less silicic hybrid parents.

2.6.2. Mafic Magmatism

The mafic rocks in Tuscany have highly variable compositions in terms of major elements, incompatible element abundances and isotopic signatures.

There is little doubt that the Tuscany mafic magmas have been subject to fractional crystallisation, mixing and crustal assimilation (e.g. Conticelli 1998). However, their high MgO, Ni and Cr concentrations, whose values are close to those of primary mantle melts, exclude that the mafic magmas with different enrichments in potassium and incompatible elements can be derived from each other by any common evolution process. Therefore, it has been concluded that the variable petrological and geochemical compositions of mafic rocks in Tuscany basically result from anomalous and heterogeneous mantle sources (Peccerillo et al. 1987).

The Tuscany lamproites are oversaturated in silica and contain low CaO, Na_2O, and Al_2O_3, and very high K_2O contents (Figs. 2.2, 2.3; Table 2.2). Therefore, an ultramafic rock containing a K-rich phase, most probably phlogopite or K-richterite (e.g. Harlow and Davies 2004), and little or no Ca-rich minerals such as clinopyroxene (e.g. a phlogopite-harzburgite) has been suggested as source for Tuscany lamproites (Peccerillo et al. 1988). The low V and Sc contents of lamproites support the scarcity of clinopyroxene in the source, since these elements are strongly partitioned into clinopyroxene. Experimental evidence demonstrates that melts derived from a phlogopite-bearing peridotite at 1.0-1.5 GPa are silica-saturated to oversaturated, whereas they become undersaturated in silica with increasing pressure of melting (e.g. Wendlandt and Eggler 1980a,b; Foley 1992; Melzer and Foley 2000). This has led to the conclusion that the silica-oversaturated high silica lamproites from Tuscany were formed in the uppermost mantle, probably in the lithosphere (e.g. Peccerillo et al. 1988; Conticelli et al. 2002). The occurrence of phlogopite in the upper mantle testifies to contamination or metasomatism by introduction of K-rich material.

Incompatible trace element and radiogenic isotope data have provided important evidence on the nature of the metasomatic modifications of lamproitic source. Peccerillo et al. (1988) noticed that incompatible element patterns of Tuscany lamproites (Fig. 2.9) resemble very closely the pattern for upper crustal rocks (e.g. Tuscany gneiss, Dora Maira metagranites, pelites, etc.), although lamproites show a more pronounced element enrichment (Cadoppi 1990; Conticelli et al. 2002). Sr-, Nd-, Pb- and

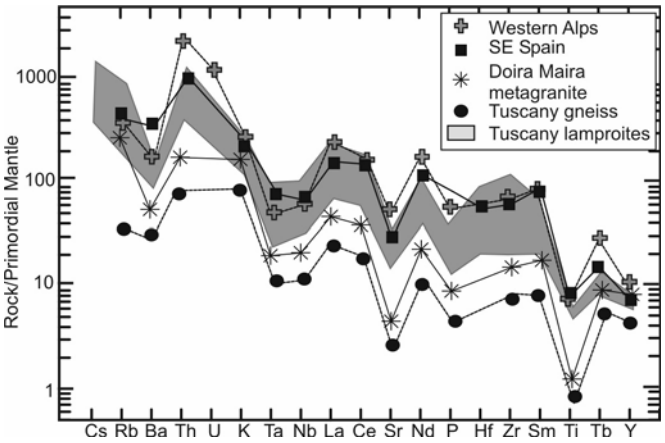

Fig. 2.9. Mantle-normalised incompatible element patterns for lamproites from Tuscany, Western Alps and south-eastern Spain. The Dora Maira metagranites and a Tuscany gneiss are also shown.

Hf-isotope ratios also fall close or within the field of crustal rocks (Fig. 2.4; Table 2.2). This has been interpreted as evidence that metasomatic modification of lamproitic mantle sources in Tuscany was provided by addition of crustal material (e.g. metapelites). Interestingly, the mantle-normalised incompatible element patterns of Tuscany lamproites are similar to those of gneisses and schists in almost every detail. This has been interpreted as evidence for addition of bulk upper crustal material to the mantle, with little element fractionation during metasomatism and the subsequent partial melting (Peccerillo 2002). This makes the Tuscany Province a zone where the upper mantle magmas look very much like the upper crust in terms of trace element and radiogenic isotope compositions.

Calc-alkaline and shoshonitic mafic rocks have lower enrichment in incompatible elements and radiogenic Sr than lamproites, but contents of CaO, Al_2O_3, and Na_2O are higher. However, the shapes of incompatible element patterns of these rocks are similar to that of the lamproites, and exhibit significant differences from those of typical calc-alkaline and shoshonitic rocks occurring in most island arcs, e.g. in the Aeolian arc (Fig. 2.7b). Therefore, trace element evidence suggests that calc-alkaline and shoshonitic magmas were generated in a source that had a similar, but perhaps less intense, enrichment than the lamproite mantle source. The higher CaO, Al_2O_3, and Na_2O contents of calc-alkaline and shoshonitic rocks have been interpreted to indicate melting of clinopyroxene, pointing to a lherzolitic rather than to a harzburgitic source (Conticelli and Peccerillo 1992). A somewhat alternative possibility is that the calc-alkaline primary melts were formed by higher degrees of partial melting of the same source

as the lamproites. Low degrees of partial melting would have generated ultrapotassic magmas by preferential melting of phlogopite. Increasing melting would have allowed significant amounts of clinopyroxene to enter into the liquid, determining an increase in CaO and a dilution of incompatible elements (Conticelli et al. 2004).

Finally, some mafic rocks, such as those from Cimini, Amiata and Radicofani have compositions that are intermediate between lamproites and calc-alkaline or shoshonitic rocks. As mentioned earlier, these magmas were formed by mixing between calc-alkaline (or shoshonitic) and lamproitic mafic magmas. Such a process is particularly evident at Radicofani. Obviously, mixing may have occurred in the source rather than, or in addition to, at shallow level (source mixing vs. magma mixing). However, additional studies are necessary to test this hypothesis.

2.6.3. Summary of Petrogenetic History

Petrological and geochemical data suggest a complex series of events in petrogenesis of the Tuscany Province. These can be summarised as follows:

1. Mantle contamination by addition of variable amounts of upper crustal material (e.g. metapelites) to peridotite, possibly represented by both harzburgite and lherzolite.
2. Melting of heterogeneously contaminated harzburgite-lherzolite mantle source to generate calc-alkaline to ultrapotassic magmas with variable enrichments in incompatible elements and radiogenic isotope signatures, but exhibiting very similar shapes of incompatible element patterns.
3. Mixing between different types of mantle-derived melts to form a variety of magmas with continuous compositional variations.
4. Moderate evolutionary modification of mafic melts during emplacement, with some fractional crystallisation, crustal assimilation (e.g. at Torre Alfina) and unmixing of felsic residual melts at Montecatini Val di Cecina.
5. Crustal melting, probably triggered by the emplacement of mafic melts, with generation of peraluminous, highly silicic magmas which were emplaced either as unmodified melts or mixed with different

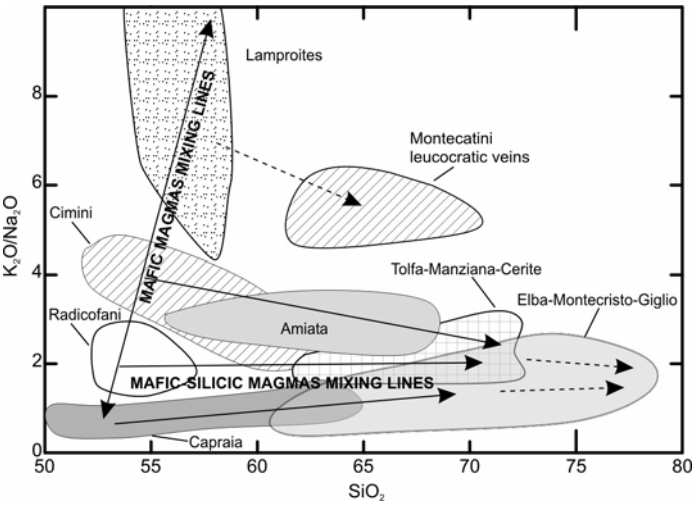

Fig. 2.10. SiO_2 vs. K_2O/Na_2O diagram for Tuscany magmatic rocks. Solid arrows indicate mixing between mafic magmas, and between these and crustal anatectic melts. Dashed arrows indicate fractional crystallisation and unmixing (Montecatini leucocratic veins).

types of mantle-derived magmas giving less strongly silicic hybrids products.

6. Fractional crystallisation of hybrid silicic melts to produce high-silica aplites and pegmatites.

The main steps of such a complex petrogenetic history are schematically shown in the SiO_2 vs. K_2O/Na_2O diagram reported in Fig. 2.10 (Poli 2004).

2.7. Geodynamic Implications

The conclusion that the trace element and isotopic characteristics of mafic Tuscan magmas require addition of crustal material to the upper mantle has led several authors to suggest a subduction-related origin for this magmatism (Peccerillo et al. 1988; Conticelli and Peccerillo 1992; Serri et al. 1993). However, the age of the subduction event(s) is discussed. Such a problem applies to Italian potassic magmatism in general, and will be discussed further in the next chapters.

It has been long established that there is a continuum of radiogenic isotope variation along the Italian peninsula, which requires a mixing between at least two end-members (e.g. Vollmer 1989). One end-member is represented by a relatively uncontaminated mantle reservoir best represented by

Etna, whereas the other end-member has a crustal-like character and is best represented by the Tuscany lamproitic magma. According to some authors, both components may have a deep mantle origin and were brought at relatively shallow depths by an upwelling plume (Bell et al. 2004). Mixing among deep and shallow mantle components would be responsible for the trends of increasing $^{87}Sr/^{86}Sr$ and decreasing Nd and Pb isotope ratios from southern Italy to Tuscany. This idea conflicts with a large variety of petrological and geophysical data (e.g. lack of abundant volcanism, strong subsidence of the Tyrrhenian Sea, etc.; for details see Peccerillo and Lustrino 2005). Moreover, the close affinity of trace element geochemistry between lamproites and upper crustal rocks would imply that the upper crustal material was brought deep into the mantle, stored and re-emplaced at shallow depth without undergoing any appreciable element fractionation over a time of 2 Ga.

Other authors suggest that isotopic trends along the Italian peninsula are the effects of mantle contamination by different types and amounts of crustal rocks, which were brought into the mantle by Late Mesozoic to Cenozoic subduction processes. Serri et al. (1993) suggested that delamination and westward subduction of the Adriatic continental plate beneath the Apennines provided large amount of crustal material to be incorporated into the mantle wedge, thus forming suitable sources for the generation of ultrapotassic magmatism in Tuscany. Peccerillo (1999, 2002) noticed that an association of lamproitic, calc-alkaline and shoshonitic rocks, such as observed in Tuscany, also occurs in the Western Alps (about 30 Ma) and in the Betic Cordillera of south-eastern Spain (from 23 to 6 Ma; Fuster et al. 1967; Venturelli et al. 1984a,b; Zeck 1998), and that there are close compositional affinities among all these occurrences (Fig. 2.9). It was also noted that the Western Alps, Tuscany and Spanish calc-alkaline to lamproitic rocks, although variable in age, are all situated east of the Alpine collision zone and cut through the African paleo-margin (Fig. 2.11). This was interpreted as evidence for similar, possibly coeval, contamination processes for mantle sources (Peccerillo 1999). However, the Western Alps and the Betic Cordillera were not affected by subduction of the Adriatic plate. Therefore, it was concluded that the association of calc-alkaline and lamproitic rocks in these localities of the Western Mediterranean records somewhat older mantle contamination events than envisaged by Serri et al. (1993).

According to several authors, Mesozoic to Oligocene convergence between Africa and Europe produced east-directed subduction of oceanic crust beneath the African continental margin until continent-continent collision generated the Alpine chain. There is evidence that upper crustal

rocks were subducted to great depths (more than 100 km) beneath the African margin during the Africa-Europe continental collision (Dora Maira Massif; Chopin 1984). After this event, a new subduction process with east and north-east dipping started, and successively migrated eastward to its present position in the southern Tyrrhenian Sea (e.g. Doglioni et al. 1999; see Chap. 10). This new subduction generated diachronous opening of backarc basins across the older Alpine collision zone, with consequent decompression of the mantle underlying the African paleomargin (Carminati et al 1998; Gueguen et al. 1997; Doglioni et al 1999). Decompression melting of the mantle rocks that had been contaminated during Alpine collision generated calc-alkaline to lamproitic melts whose isotopic and geochemical signatures reproduce those of the upper crustal contaminants (Peccerillo 1999, 2002). Therefore, magmatism is not coeval with source contamination events, but depends on setting up of extensional tectonic regime. This migrated eastward with time, which explains the migration of magmatism in the same direction. A schematic diagram illustrating the relations between contamination, subduction and post-collisional backarc extension and melting in Tuscany is shown in Fig. 2.12.

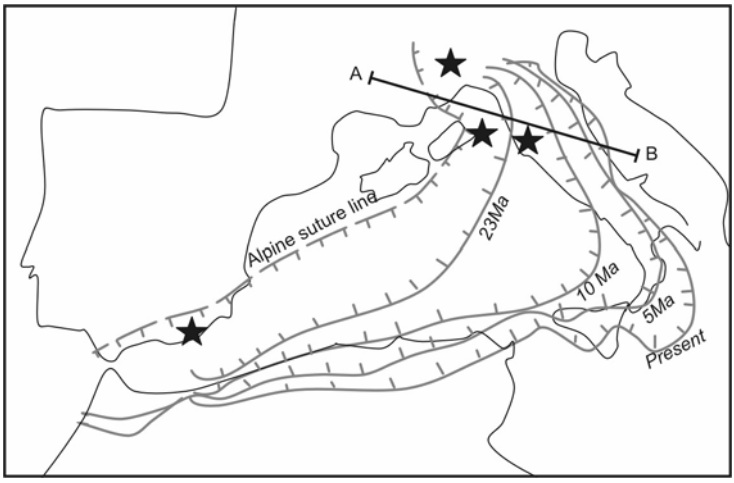

Fig. 2.11. Location of lamproitic magmatism in Western Alps, Tuscany and SE Spain. Thick dashed line indicates Alpine suture zone. Full lines indicate fronts of west-immerging subduction zone from Oligo-Miocene to Present. A-B line is the section of Fig. 2.12. Simplified after Doglioni et al. (1997).

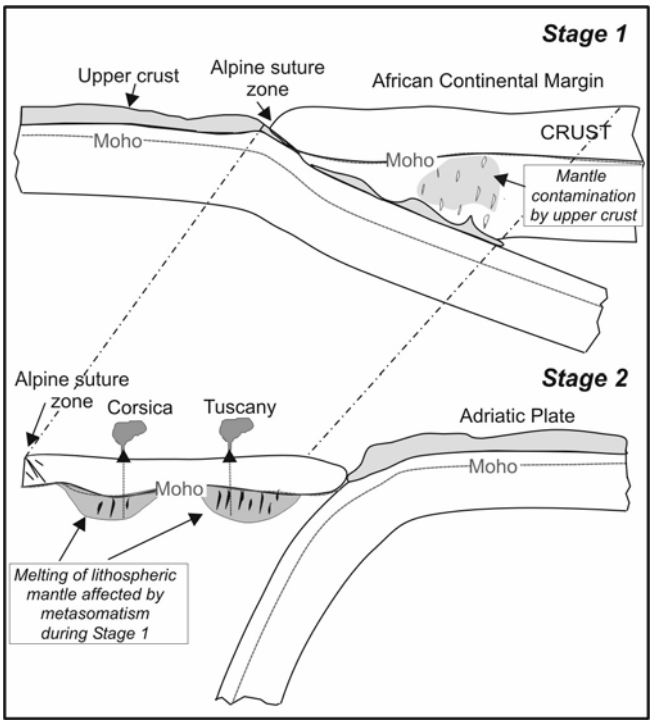

Fig. 2.12. Schematic diagram showing sequence of subduction, mantle contamination and calc-alkaline to lamproite magma formation in Tuscany. Stage 1: subduction processes during Alpine collision between Europe and Africa brought upper crustal material (e.g. Dora Maira metagranites) into the lithospheric mantle beneath the African margin. Stage 2: subduction inversion from Oligo-Miocene to present generated opening of backarc basins behind westerly dipping Adriatic plate, and triggered decompression melting of anomalous mantle contaminated during Alpine collision, to generate calc-alkaline to lamproitic magmatism. Location of section is reported in Fig. 2.11.

2.8. Conclusions

The Tuscany Magmatic Province consists of an association of calc-alkaline to lamproitic mafic to intermediate magmas and silicic intrusive and effusive rocks. Silicic melts have been formed by crustal melting, with an important role of mixing with mantle-derived magmas. Mafic melts are of mantle origin but resemble closely some upper crustal rocks, such as metapelites, in terms of incompatible trace elements and radiogenic isotope

compositions. The particular composition of mantle-derived magmas requires anomalous sources which underwent contamination by subduction of upper crustal rocks. However, the age of subduction processes is still debated.

Some authors invoke Late Cretaceous to Oligocene mantle contamination during Alpine, east-directed subduction process of European plate beneath the African margin. However, melting is much younger and took place from Miocene to present during opening of the northern Tyrrhenian Sea and the anticlockwise rotation of the Apennine chain. This was a consequence of backarc spreading above the west-dipping Adriatic subduction zone. Alternatively, an old metasomatic event has been envisaged for the Tuscany mantle. This implies aging of a discrete mantle mass, characterised by high Rb/Sr and low Sm/Nd, for long time before emplacement as a plume beneath the Tuscany Province.

Ascent of mafic magmas into the crust induced crustal anatexis with formation of peraluminous, highly silicic magmas. These were emplaced either as unmodified melts or mixed with different types of mantle-derived magmas giving less strongly silicic hybrid products. Fractional crystallisation of hybrid magmas produced high-silica aplites and pegmatites which are commonly found in many granitoid bodies in Tuscany.

Table 2.2. Representative compositions of Tuscany magmatic rocks. Numbers in parentheses refer to data obtained on distinct though similar rock samples from the same locality as those analysed for the other elements. Source of data: 1) Vollmer (1977); 2) Hawkesworth and Vollmer (1979); 3) Poli et al. (1984); 4) Giraud et al. (1986); 5) Peccerillo et al. (1988); 6) Pinarelli (1991); 7) Conticelli and Peccerillo (1992); 8) Poli (1992); 9) Prosperini (1993); 10) Westerman et al. (1993); 11) Innocenti et al. (1997); 12) De Astis et al. (2000); 13) Conticelli et al. (2002); 14) Dini et al. (2002); 15) Gasperini et al. (2002); 16) Author's unpublished data.

Magmatic centre	**Roccastrada**	**San Vincenzo**	**Tolfa**	**Manziana**	**Mt. Amiata**	**Mt. Cimini**
Rock type	Rhyolite	Rhyolite	Latite	Rhyolite	Trachydacite	Trachydacite
Data source	4,1,2	4,1,2	6	6	3,1	3,1
SiO_2 wt%	72.48	68.76	64.61	71.66	65.92	65.37
TiO_2	0.24	0.38	0.66	0.39	0.62	0.72
Al_2O_3	13.56	14.94	16.45	14.50	15.63	15.83
FeO_{total}	1.91	2.33	3.57	2.19	3.30	4.02
MnO	0.03	0.03	0.04	0.03	0.06	0.07
MgO	0.36	0.91	1.40	0.31	1.57	1.82
CaO	1.02	1.96	3.18	1.51	3.36	3.30
Na_2O	2.61	2.86	2.47	3.28	2.56	2.48
K_2O	4.86	4.63	5.23	4.99	5.20	5.16
P_2O_5	0.14	0.20	0.12	0.03	0.18	0.25
LOI	1.56	1.93	1.98	0.81	1.25	0.84
Sc ppm	5	6	-	-	9	11
V	12	36	-	-	70	73
Cr	10	28	-	-	29	33
Ni	19	21	-	-	11	
Rb	395	310	305	385	371	287
Sr	68	223	264	91	356	486
Y	33	24	28	35	-	-
Zr	113	149	275	214	264	276
Nb	14	13	19	10	-	-
Cs	-	-	-	-	41	33
Ba	172	400	567	231	377	991
La	30	43	51	71	74	84
Ce	68	91	97	133	156	164
Nd	29	43	36	50	66	63
Sm	6.8	8.9	6.7	9.4	10.6	9.4
Eu	0.6	1.3	1.2	0.82	1.2	2.2
Tb	1.1	1.0	-	-	0.9	1.1
Yb	3.1	1.8	2.4	3.4	2.8	2.67
Lu	0.3	0.2	0.5	0.63	0.5	0.44
Hf	3.8	4.1	-	-	5.4	7.9
Ta	-	-	-	-	1.5	1.7
Pb	45	50	56	75	(60)	-
Th	24	20	30	53	41	54
U	17	11	8.7	10	(13)	-
$^{87}Sr/^{86}Sr$	0.71799	0.71558	0.71383	0.71308	0.71310	0.7138
$^{143}Nd/^{144}Nd$	(0.51221)	(0.51225)	-	-	(0.51214)	-
$^{206}Pb/^{204}Pb$	(18.68)	(18.71)	18.74	18.723	(18.72)	(18.73)
$^{207}Pb/^{204}Pb$	(15.65)	(15.66)	15.70	15.663	(15.68)	(15.68)
$^{208}Pb/^{204}Pb$	(38.91)	(38.88)	38.79	38.859	(39.01)	(39.04)

Table 2.2 (continued)

Magmatic centre	**Elba**		**Montecristo**	**Giglio**		**Capraia**
Rock type	Monzo-granite	Leuco-granite	Monzo-granite	Monzogranite	Leucogranite	Shoshonitic basalt
Data source	14,1	14	8,11	8,10	8,10	9, 13
SiO_2 wt%	67.73	75.29	70.55	67.63	73.54	50.50
TiO_2	0.54	0.06	0.36	0.66	0.21	1.60
Al_2O_3	15.81	13.97	14.94	15.56	14.07	14.90
FeO	3.00	0.52	2.10	3.73	1.47	9.08
MnO	0.06	0.02	0.04	0.08	0.05	0.15
MgO_{total}	1.47	0.08	0.66	1.24	0.38	6.27
CaO	2.66	0.68	1.76	2.13	0.82	8.05
Na_2O	3.57	3.41	3.71	2.81	2.38	2.78
K_2O	3.86	5.40	4.77	4.79	6.04	2.46
P_2O_5	0.18	0.05	0.22	0.17	0.14	0.48
LOI	1.08	0.52	0.64	1.11	0.89	1.40
Sc ppm	8.6	2.8	6.1	10.7	4	23
V	34	2	-	-	-	166
Cr	24	3	28	44	4	400
Co	6.9	2.8	5	8.5	4	30
Ni	10.1	1.3	-	-	-	69
Rb	285	448	357	337	372	115
Sr	193	34	122	131	65	399
Y	18.3	17.2	22	30	21	20
Zr	160	45	116	223	92	221
Nb	12.8	5	6	12	11	15
Cs	45.2	38.2	-	0	-	4
Ba	279	62	293	318	74	556
La	36.2	10.8	30	44	16	27
Ce	73.9	24.3	61	96	39	57
Nd	31.3	10.9	27	41	18.6	51.9
Sm	6.12	3.02	5.8	8.8	4.6	9.6
Eu	0.87	0.13	0.7	1.1	0.48	2.1
Tb	0.65	0.42	0.6	1.0	0.55	1.0
Yb	1.38	1.57	1.7	2.7	2.8	2.3
Lu	0.19	0.21	0.30	0.45	0.46	0.4
Hf	-	-	-	5.5	2.8	5.6
Ta	2.37	2.17	-	2.5	1.1	1.0
Pb	47	53	-	-	-	20
Th	21.5	10.7	30	21	10	24
U	14.9	8.8	-	-	-	3.8
$^{87}Sr/^{86}Sr$	0.71471	0.71314	(0.71466)	(0.7173)	(0.7195)	0.70812
$^{143}Nd/^{144}Nd$	0.51222	0.512194	-	(0.5122)	(0.5121)	0.51226
$^{206}Pb/^{204}Pb$	(18.68)	-	-	-	-	18.667
$^{207}Pb/^{204}Pb$	(15.67)	-	-	-	-	15.664
$^{208}Pb/^{204}Pb$	(38.87)	-	-	-	-	38.993

Table 2.2 (continued)

Magmatic centre	Capraia	Mt. Cimini	Sisco	Monteca-tini v. C.	Orciatico	Torre Alfina	Radicofani
Rock type	Andesite	Latite	Lamproite	Lamproite	Lamproite	Lamproite	Shoshonite
Data source	9,13	3,13,15	5,16	12,16	12,16	12,16	12,16
SiO_2 wt%	60.70	57.43	58.50	56.62	57.79	55.47	53.05
TiO_2	0.70	0.85	2.27	1.57	1.51	1.36	0.96
Al_2O_3	15.60	15.99	10.84	12.2	11.79	13.39	16.87
FeO_{total}	4.66	4.55	3.14	6.17	5.14	5.78	6.90
MnO	0.09	0.09	0.06	0.07	0.08	0.10	0.11
MgO	4.38	6.30	6.63	7.46	8.23	9.36	8.17
CaO	5.99	6.82	3.12	3.52	3.46	4.70	8.06
Na_2O	2.90	1.81	1.02	1.40	1.31	1.18	1.75
K_2O	3.22	5.01	10.73	8.02	8.06	7.46	3.22
P_2O_5	0.23	0.31	0.67	1.18	0.85	0.54	0.22
LOI	1.15	0.51	2.09	2.13	1.55	0.58	0.39
Sc ppm	16	21	11	16	14	17	26
V	136	137	91	124	101	118	167
Cr	140	302	420	420	430	641	407
Co	7	-	23	24	27	29	33
Ni	11	108	264	152	288	349	97
Rb	113	336	380	776	601	453	201
Sr	966	688	803	461	604	726	355
Y	38	-	27	38	30	33	-
Zr	184	366	1309	519	859	674	211
Nb	9	21	63	32	42	31	(12)
Cs	9.0	27	7	15.3	15	25	13
Ba	742	1061	1310	1184	1210	1290	610
La	64	94	172	77	140	98	46
Ce	134	196	347	194	365	294	105
Nd	51.6	85	139	102	121	108	50
Sm	8.7	11.8	19	25	23.6	20.6	7.4
Eu	1.8	2.4	3.2	3.41	3.18	3.13	1.81
Tb	0.9	1.0	1.2	1.08	0.98	1.14	0.8
Yb	2.1	2.26	1.1	2.05	1.58	2.57	1.94
Lu	0.3	0.36	-	0.32	0.26	0.33	0.22
Hf	5.5	9.7	33	14	18.6	14.9	7.2
Ta	1.0	1.6	4.3	1.9	2.3	2.1	0.91
Pb	33	-	-	50	45	60	(27)
Th	22	50	43	109	87	57	35
U	6.6	-	-	23.6	15.3	15.3	4.8
$^{87}Sr/^{86}Sr$	0.70872	0.71284	0.71256	0.71691	0.71520	0.71625	0.713363
$^{143}Nd/^{144}Nd$	0.51234	0.51210	0.51218	0.51210	0.5121	0.51207	0.51218
$^{206}Pb/^{204}Pb$	18.735	(18.73)	18.863	18.757	18.729	18.661	18.686
$^{207}Pb/^{204}Pb$	15.702	(15.66)	15.705	15.675	15.715	15.658	15.674
$^{208}Pb/^{204}Pb$	39.086	(39.02)	39.352	39.116	39.192	38.855	39.984
$^{176}Hf/^{177}Hf$	-	-	-	0.28245	-	-	(0.28255)

3. The Intra-Apennine Province

3.1. Introduction

The Intra-Apennine Magmatic Province (IAP) consists of several small monogenetic centres of ultrapotassic pyroclastic rocks and minor lavas scattered along the axial zones of the Apennine chain, extending from Umbria to the nearby regions of Abruzzi and Lazio (Latium) in the south (Fig. 3.1). Pyroclastic rocks crop out at San Venanzo, Cupaello, Perugia, Pietrafitta, Acquasparta, Oricola and several other scattered localities. Lava flow and dyke rocks occur only at San Venanzo and Cupaello. The IAP has been also indicated as the Umbria Province by Washington (1906) and as the Intramontane Ultra-alkaline Province (IUP) or the Umbria-Lazio Ultra-alkaline District (ULUD) by Lavecchia and Stoppa (1996). Information on age, petrology and volcanology of the main centres of the IAP is given in Table 3.1.

3.2. Regional Geology

The internal zones of central Apennines are characterised by thick piles of sedimentary rocks, sitting on the metamorphic basement of the Adriatic plate (e.g. Keller et al. 1994; Ciarapica and Passeri 1998; Decandia et al. 1998; Barchi et al. 2001). Permian-Triassic phyllites and quartzites (Verrucano Group) encountered by borehole drillings represent the oldest rocks in the zone. These are overlain by sedimentary sequences that include Late Triassic evaporites, Late Triassic to Oligocene marls, limestones and dolostones, and Miocene mainly terrigenous turbiditic rocks. Messinian evaporites occur in the external (eastern) sector of the area. Plio-Pleistocene mainly continental sands, clay and conglomerates infill extensional basins.

The Intra-Apennine area was affected by late Triassic to Jurassic rifting, with sedimentation of both complete and reduced successions inside progressively deepening extensional basins. Starting in Cretaceous time,

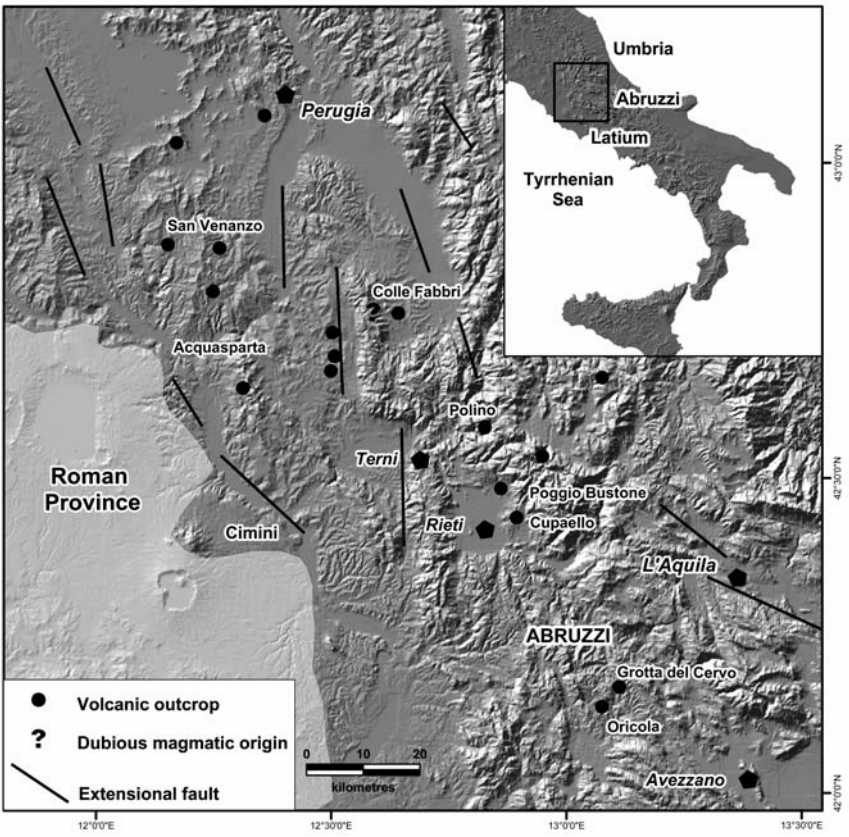

Fig. 3.1. Location of the main outcrops of the Intra-Apennine Magmatic Province.

sedimentation occurred in syn-orogenic basins. Compressional tectonics related to the formation of the Apennine chain began during the Miocene. The compression front progressively shifted eastward, contemporaneously with terrigenous foredeep sedimentation and with backarc extension. Compression was much less intensive than in Tuscany, and generated moderate thrusting and folding. Because of these processes, the overall thickness of sedimentary rocks in the internal zones of central Apennines reaches about 7000-8000 m (Barchi, personal communication). Post-orogenic continental rifting developed in the Plio-Pleistocene behind the eastward migrating compression front. Lacustrine to fluviatile sedimentation took place within these small subsiding basins, whose border faults were sites of volcanic activity of the IAP.

Crustal thickness in the IAP is slightly greater than in Tuscany, increasing across the Apennine chain up to about 35 km, and decreasing towards the Adriatic Sea (Scarascia et al. 1994; Piromallo and Morelli 2003). By

Table 3.1. Petrological characteristics and ages of the main centres of the Intra-Apennine Magmatic Province.

MAGMATIC CENTRES	AGE (in Ma)	VOLCANOLOGY and PETROLOGY
San Venanzo	0.26	- Three monogenetic centres formed by olivine melilitite lava and pyroclastic rocks.
Cupaello	0.64	- Kalsilite melilitite lava flow overlying pyroclastic rocks, some of which contain abundant carbonates.
Polino	0.25	- Two small diatremes filled with a chaotic breccia made of phlogopite- and calcite-rich blocks, lapilli and a fine matrix.
Acquasparta	0.39	- Pyroclastic fall, flow and surge deposit forming a small plateau.
Oricola-Carsoli	0.53	- A few monogenetic hydrovolcanic pyroclastic centres composed of altered ultrapotassic tuffs with a kamafugitic composition.
Grotta del Cervo	0.5 (?)	- Massive pyroclastic rocks containing kamafugitic juvenile material.
Colle Fabbri (?)	0.8	- Granular to vesicular igneous-like rock with variable composition. Magmatic origin is dubious.

contrast, there is a continuous increase of lithospheric thickness from about 40 km in Tuscany to about 80 km in the Adriatic Sea coast. The zone with low S-wave velocities ($V_S \sim 4.05$) occurring beneath Tuscany also extends in Umbria and overlies a vertical layer with high seismic wave velocities that has been suggested represents a remnant of a sinking lithospheric slab (see Chap. 2). The entire area is characterised by negative gravimetric anomalies and low heat flow (less than 70 mWm^{-2}; Della Vedova et al. 2001).

3.3. Compositional Characteristics of Intra-Apennine Magmatism

The IAP rocks have an ultrapotassic composition and some types show strong undersaturation in silica, containing melilite and kalsilite Overall, trace element and radiogenic isotope compositions are similar to the Roman Province. Lava flows and dyke rocks are mafic and strongly undersaturated in silica (see also Fig. 1.3), displaying major element characteristics typical of ultrapotassic rocks with a kamafugitic affinity (Sahama 1974; Gallo et al. 1984; Peccerillo et al. 1988; see Appendix). The pyroclastic rocks range from melilitite to trachyphonolite (Stoppa and Lavecchia 1992), although there are insufficient data to permit a satisfactory petrological and geochemical characterisation of these rocks.

3.3.1. San Venanzo

This volcano consists of three main centres (San Venanzo, Pian di Celle and Celli) whose explosive and effusive products cover an area of about 0.15 km^2 (Stoppa 1996). Lava flows and dykes occur at Pian di Celle. These are olivine melilitites that are known locally as venanzite. The juvenile pyroclastic material has an apparently less mafic composition than the lavas (Stoppa 1996). $^{40}Ar/^{39}Ar$ dating on minerals separated from Pian di Celle volcanics yields an age of 265 ka (Laurenzi et al. 1994).

The San Venanzo lava and dyke rocks have a poorly porphyritic holocrystalline texture and contain microphenocrysts of olivine (Fo_{90-65}) set in a groundmass composed of melilite, leucite, phlogopite, Al-poor clinopyroxene (Al_2O_3 ~ 0.5-1.3 wt%; Cellai et al. 1994), kalsilite, spinel, monticellite and calcite. Spinel, perovskite and apatite are present as accessory phases. The lava flow contains coarse-grained pegmatoid veins formed of leucite, melilite, spinel, olivine, clinopyroxene, phlogopite, kalsilite, calcite and apatite. Calcite is an important component of the San Venanzo rocks, particularly of the pyroclastic rocks. This carbonate material is considered to be of magmatic origin by Stoppa (1996) and Stoppa and Woolley (1997), which led these authors to suggest a carbonatitic affinity for the San Venanzo pyroclastic rocks. A large number of uncommon mineral phases, such as cuspidine, götzenite, and khibinskite have been found in the San Venanzo volcanics (e.g. Sharygin et al. 1996).

Compositions are characterised by a strong undersaturation in silica, yielding high levels of normative leucite and kalsilite (Peccerillo et al. 1988). Major elements exhibit high contents of MgO, CaO and K_2O, and moderate to low Na_2O and TiO_2 (Fig. 3.2; Table 3.2). Concentrations of Cr, Ni and Co are high, whereas V and Sc are lower than typical values for primitive basaltic rocks (Fig. 3.3a,b; Table 3.2). Boron contents are very high (B ~ 100 to 200 ppm; Vaselli and Conticelli 1990). REE patterns are fractionated and exhibit a significant negative Eu anomaly (Fig. 3.4a), which cannot be due to plagioclase separation as this phase is absent in the San Venanzo lavas. Mantle-normalised incompatible element patterns are fractionated, and contain positive spikes of Cs, Rb, Th and Pb, along with negative anomalies of Ba and HFSE (Fig. 3.4b). These patterns closely resemble those for the ultrapotassic mafic rocks from the nearby Roman Province (see Chap. 4). By contrast, they are strikingly different from patterns for ultrapotassic kamafugites from the Virunga region in east Africa. The latter are upward convex, with a maximum at Ta and Nb, and do not contain negative anomalies of Ba and HFSE (e.g. Rogers et al. 1992; Tappe et al. 2003). The pegmatoid veins cutting the Pian di Celle lava have lower silica, MgO, Cr and Rb contents, and much higher abun-

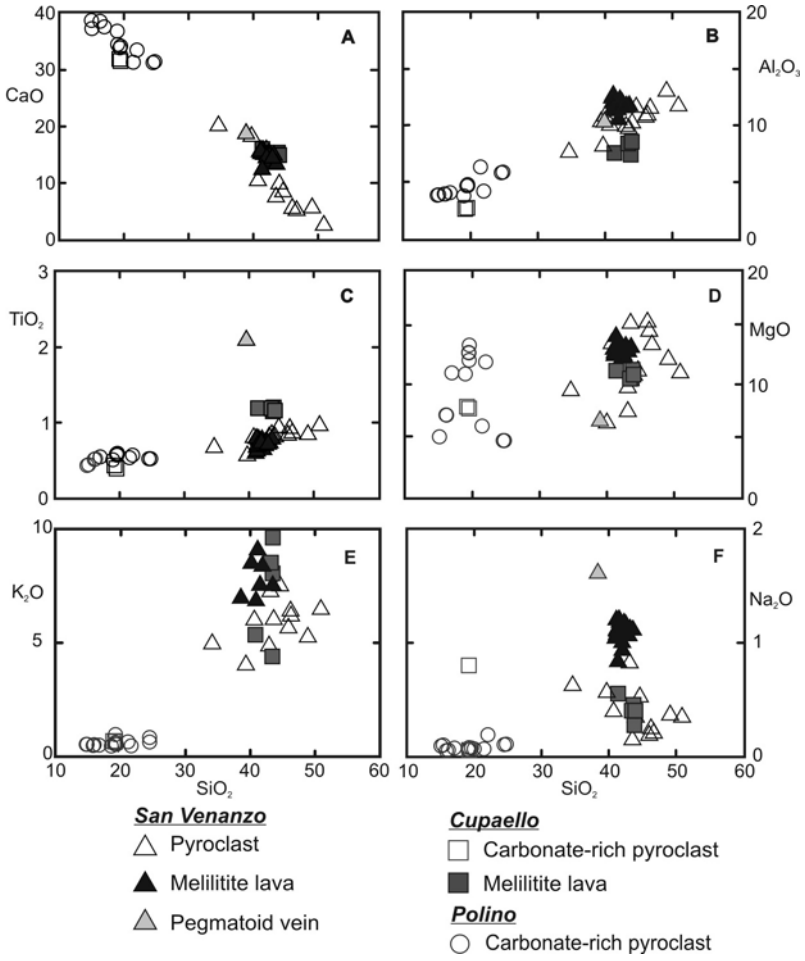

Fig. 3.2. Major element variations for most thoroughly studied of the Intra-Apennine volcanic rocks.

dances of TiO_2 and incompatible trace elements than the host lavas (Table 3.2). Their origin is not well understood and probably relates to fluid enrichment processes and/or magma unmixing. The carbonate-bearing rocks (containing about 10 wt% carbonate) have REE and incompatible element patterns that are similar to the associated lavas but show slight element depletion. The pyroclastic rocks have variable major and trace element abundances (Stoppa 1996), but detailed studies are necessary to understand the significance of these variations.

Radiogenic isotopic ratios for San Venanzo volcanics are close to values observed in the Roman Province ($^{87}Sr/^{86}Sr \sim 0.7104$; $^{143}Nd/^{144}Nd \sim 0.5121$; $^{206}Pb/^{204}Pb \sim 18.73$; $^{207}Pb/^{204}Pb \sim 15.66$; $^{208}Pb/^{204}Pb \sim 39.00$;

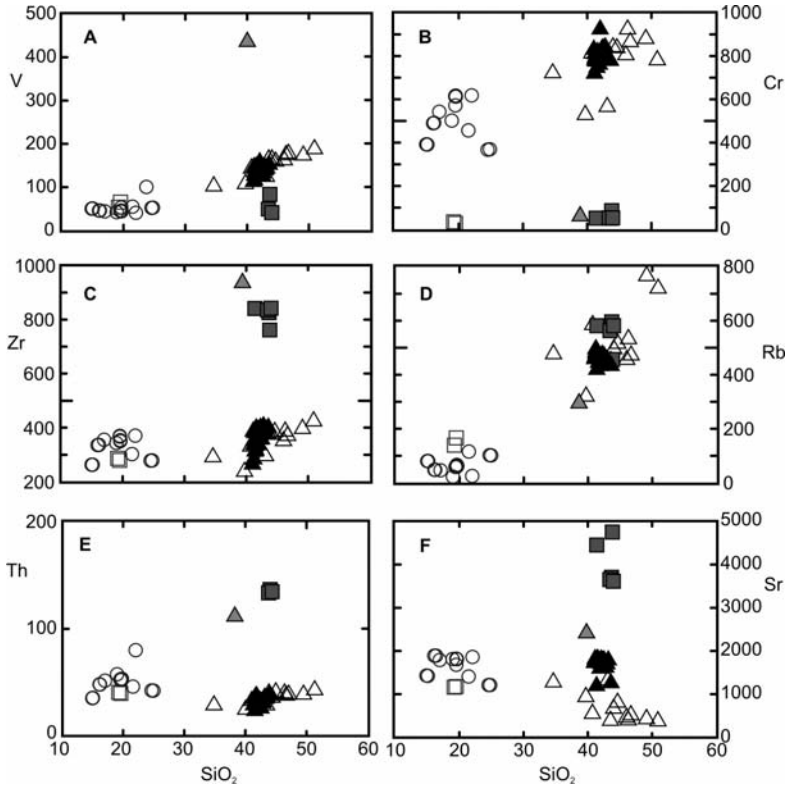

Fig. 3.3. Trace element variations for the Intra-Apennine volcanic rocks. Symbols as in Fig. 3.2.

$^{176}Hf/^{177}Hf$ ~ 0.28249; Conticelli et al. 2002; Author's unpublished data). Very high O-isotope ratios have been measured for lavas ($\delta^{18}O_{SMOW}$ ~ +11 to +12; Holm and Munksgaard 1982; Taylor et al. 1984) and for separated olivines ($\delta^{18}O_{SMOW}$ = + 13; Author's unpublished data).

3.3.2. Cupaello

The Cupaello volcanic centre consists of a single 750 m long lava flow overlying a sequence of pyroclastic material composed of altered ashes, breccias, lapilli and scoriae (Stoppa and Cundari 1995). $^{40}Ar/^{39}Ar$ dating on separated kalsilite and phlogopite yields an age of 639 ka (Laurenzi et al. 1994).

The lava has a poorly porphyritic hypocrystalline texture and contains phenocrysts of Al-poor diopside (Al_2O_3 ~ 0.3-0.4 wt%) and phlogopite set in a groundmass of kalsilite, melilite and glass. The rock has been petrographically classified as a pyroxene-kalsilite melilitite, and is also known by the local name of coppaellite. The Cupaello lava has been affected to

various extents by syn- to post-eruptive modification, which led to the formation of secondary phases such as zeolites and chlorite. The pyroclastic rocks consist of ashes and lapilli, the latter being mainly represented by fragmented melilite and crystal debris. Calcite is an important phase (up to more than 50% of total rock volume) of the Cupaello pyroclastic rocks. Some calcite crystals have been found to be enriched in Sr, Ba and REE, which has led some authors to suggest a magmatic origin for calcite and a carbonatitic nature for Cupaello pyroclastics (e.g. Stoppa and Woolley 1997). Accessory phases in the Cupaello rocks include magnetite, monticellite, apophyllite, spinel, khibinskite, götzenite, perovskite and apatite.

The Cupaello lava is peralkaline and strongly undersaturated in silica. As for typical kamafugitic rocks, Al_2O_3 and Na_2O are low and CaO is high (Fig. 3.2). K_2O is variable (~ 3-10 wt %), but the freshest samples have the highest concentration of K_2O, indicating secondary loss of potassium in the altered rocks (Peccerillo et al. 1988). Ferromagnesian trace elements (Cr, Ni, Co, V and Sc) have lower abundances than in the San Venanzo lavas, whereas LILE and HFSE are higher (Fig. 3.3). Incompatible element and REE patterns for Cupaello are similar to those of San Venanzo, although fractionation and element enrichment is stronger (Fig. 3.4). The carbonate-rich pyroclastic rocks have an incompatible element pattern that is similar to the associated kamafugitic lavas, but with much lower element concentrations (Fig. 3.4d).

Radiogenic isotopic composition for Cupaello volcanics are slightly but significantly different from those of San Venanzo ($^{87}Sr/^{86}Sr$ ~ 0.7113; $^{143}Nd/^{144}Nd$ ~ 0.51212; $^{206}Pb/^{204}Pb$ ~ 18.74; $^{207}Pb/^{204}Pb$ ~ 15.66; $^{208}Pb/^{204}Pb$ ~ 38.95). O-isotope ratios are very high, and values of $\delta^{18}O_{SMOW}$ = +11.9 to +14.4‰ have been determined for whole rock and separated diopside phenocrysts (Holm and Munksgaard 1982, 1986; Taylor et al. 1984).

3.3.3. Polino

The Polino centre consists of two small diatremes surrounded by layered lapilli tuffs and filled with a chaotic breccia containing massive blocks of a phlogopite- and carbonate-rich igneous rock, concentric carbonate-rich lapilli, country rock fragments and abundant fine-grained matrix; some lapilli consisting of olivine and phlogopite may represent mantle material (Stoppa and Lupini 1993). A $^{40}Ar/^{39}Ar$ age of 246 ka has been measured for phlogopites separated from the massive blocks (Laurenzi et al. 1994).

Massive carbonate-rich blocks contain phlogopite, olivine, perovskite, Zr-schorlomite and apatite set in a micro-cryptocrystalline groundmass (Stoppa and Lupini 1993). Olivine (Fo_{94-93}) occurs as anhedral to subhedral crystals, sometimes kinked and surrounded by a reaction rim of monticellite. Phlogopite is characterised by high contents of MgO and Cr. Calcite

occurs as vesicles, in veins and as groundmass material; according to Stoppa and Lupini (1993) the latter is enriched in Sr, Ba and REE.

As illustrated in Fig. 3.2, the Polino carbonate-rich blocks are depleted in silica (SiO_2 ~ 15-25 wt %) and rich in CaO (~ 30-40 wt %) and, to a lower extent, in MgO (~ 7-13 wt %). By contrast, K_2O (~ 0.2-0.7 wt %) and Na_2O (< 0.2 wt %) are low. Overall, the Polino rocks very closely resemble the carbonate-rich pyroclastics from Cupaello. However, concentrations of the ferromagnesian trace elements Ni and Cr are much higher at Polino. Radiogenic isotope ratios are similar to those of San Venanzo, with $^{87}Sr/^{86}Sr$ ~ 0.70104 and $^{143}Nd/^{144}Nd$ ~ 0.51203 (Castorina et al. 2000; Conticelli et al. 2002).

3.3.4. Intra-Apennine Pyroclastic Deposits

There are a large number of pyroclastic deposits scattered along the axial zone of the Apennines. Composition, grain size and depositional characteristics are variable and some of the finer-grained deposits may have a remote rather than local origin. The best-known occurrences in Umbria are those of Perugia, Acquasparta, Norcia, Pietrafitta and Poggio Bustone (Fig. 3.1). In the Lazio and Abruzzi regions, outcrops are found at Campo Imperatore, Grotta del Cervo, Oricola-Carsoli and several other localities (Bosi et al. 1991; Bosi and Locardi 1992; Lavecchia et al. 2002). Stratigraphic relationships and radiometric dating indicate an age of a few hundreds thousand years for all these outcrops.

In Perugia, a sequence of pumiceous lapilli makes up a small outcrop of a few tens of square metres at Pian di Massiano that is completely covered by a thick soil. At Acquasparta, phreatomagmatic deposits of ashes and lapilli have been erupted from monogenetic centres aligned along a N-S trend over a distance of about 10 km. $^{40}Ar/^{39}Ar$ dating on separated phases has yielded an age of 390 ka for this deposit. Mineral phases include diopside, olivine (up to Fo_{93}), sanidine, Ti-rich phlogopite, leucite, apatite, sphene and Fe-Ti oxides. Overall, this mineral assemblage is believed to reveal a kamafugitic affinity (Brozzetti and Stoppa 1995).

In the Lazio and Abruzzi regions, the pyroclastic rocks display variable depositional and structural characteristics. Some occurrences contain coarse-grained material (up to 10 cm in diameter), which supports the idea that vents were located close to the deposition area. Pyroclastic rocks containing juvenile material are present at Grotta del Cervo, a locality not far from L'Aquila in Abruzzo. Mineral phases present in this outcrop are olivine (up to Fo_{88}), diopside, phlogopite, garnet, haüyne, leucite, kalsilite,

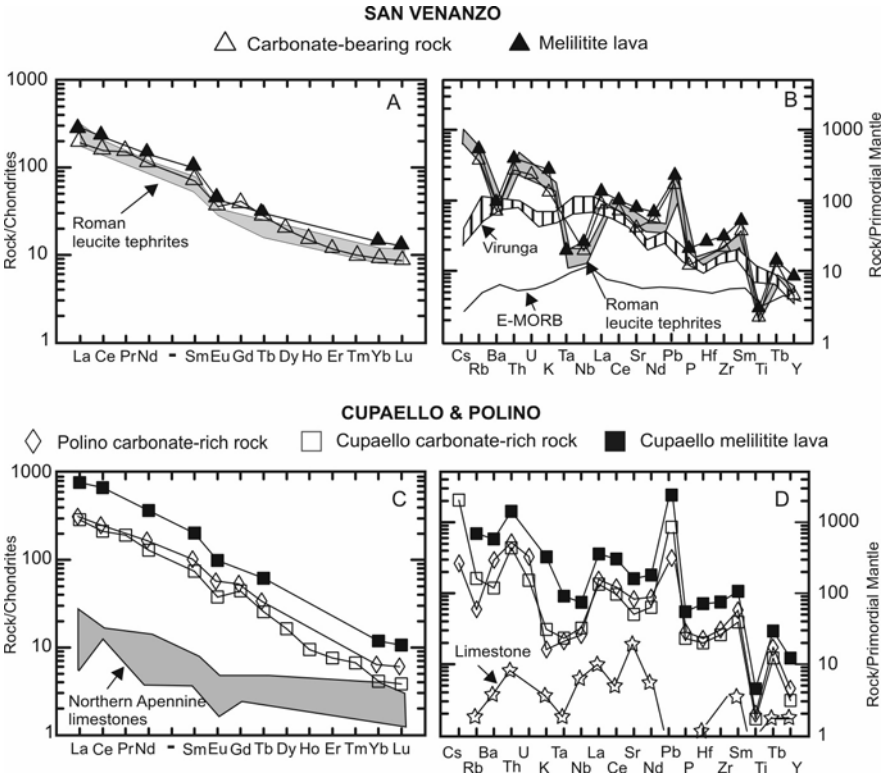

Fig. 3.4. Chondrite normalised REE patterns and mantle normalised incompatible element patterns of Intra-Apennine volcanic rocks. Patterns for mafic rocks from the Roman Province and the Virunga volcanoes (East Africa), for Enriched Mid Ocean Ridge Basalts (E-MORB) and for limestones from northern Apennines are also shown.

carbonate material, and accessory apatite and Ti-magnetite (Stoppa et al. 2002). Major and trace element composition is similar to San Venanzo kamafugitic lavas. Monogenetic pyroclastic centres (K/Ar age of 530 ka) composed of altered breccia, surge and fall deposits occur at Oricola-Carsoli, about 40 km southwest of L'Aquila (Bosi et al. 1991; Barbieri et al. 2002). Mineral phases of these rocks include olivine (Fo_{87}), diopside, leucite, phlogopite, alkali-feldspar, and accessory garnet, apatite and spinel. Trace element composition is characterised by a strong enrichment in LILE and a relative depletion in Nb. Sr isotopic ratios are around 0.710. Overall, the composition of Oricola-Carsoli rocks has been interpreted to indicate a kamafugitic affinity (Barbieri et al. 2002).

The geochemical composition of the volcanics at most localities in the internal zones of Abruzzi and Lazio is characterised by strongly fractionated REE patterns, with significant negative Eu anomalies. Incompatible element patterns are fractionated and contain negative spikes of Ba and

HFSE (Bosi and Locardi 1992). These characteristics are common to both the IAP and Roman Province, and do not allow the exclusion of a provenance from Roman volcanoes for the most fine-grained deposits.

3.3.5. Colle Fabbri

A small, metre-sized outcrop of melilite-bearing rocks with igneous-type textures is present at Colle Fabbri (Stoppa 1988). These rocks have medium- or fine-grained holocrystalline to glassy scoriaceous textures, passing from the centre to the border of the body. Modal mineralogy consists of various proportions of wollastonite, clinopyroxene, plagioclase and melilite. Accessory phases are leucite, perovskite and garnet. Ocelli filled with calcite are observed in the border rocks.

Major element compositions for the Colle Fabbri rocks are extremely variable for such a small outcrop (e.g. SiO_2 = 43–64 wt %; CaO = 4 to 37 wt %). Rare-earth elements (REE) are moderately enriched and fractionated, and contain an important negative Eu anomaly. $^{87}Sr/^{86}Sr$ ratios range from 0.7077 to 0.7119 and $^{143}Nd/^{144}Nd$ ratios vary from 0.71115 to 0.71192 (Melluso et al. 2003).

Colle Fabbri is thought to be member of the carbonatite-melilitite mantle-derived magmatic association that allegedly characterise the Intra-Apennine Magmatic Province (Stoppa and Woolley 1997). However, Melluso et al. (2003) point out that both the mineral paragenesis and the major and trace element geochemistry of Colle Fabbri rocks are unusual and even thermodynamically incompatible with any magmatic system. It was observed that abundances for several major and trace elements closely resemble those of marly sediments. Therefore, it was concluded that the Colle Fabbri rocks are not magmatic, but were generated by decarbonation and melting of marls (paralava). Burning of lignite, abundantly present in the recent sediments in the Colle Fabbri area, has been suggested to be responsible for marl melting. This same conclusion also was applied to another igneous-like rock cropping out at Ricetto, a few hundred km south of Colle Fabbri (Melluso et al. 2003).

3.4. Petrogenesis

The main questions concerning the volcanics of the IAP relate to the origin of the kamafugitic lavas at San Venanzo and Cupaello and the nature of carbonate-rich pyroclastic rocks present in several centres. Both issues have been much discussed in the literature, although the debate often has been based on preconceptions rather than on factual evidence.

3.4.1. Kamafugitic Rocks

There is a general consensus that the high MgO, Ni and Cr contents of the IAP kamafugites attest to a mantle origin (e.g. Peccerillo et al. 1988; Cundari and Ferguson 1991). However, modification of magma compositions during ascent has been suggested by a number of authors (e.g. Turi et al. 1986; Peccerillo 1995). Several lines of evidence support the idea of wall rock assimilation by kamafugitic magmas. The San Venanzo and Cupaello volcanoes are monogenetic centres developed on a thick sedimentary sequence composed mostly of limestones and marls. The scarcely porphyritic to aphyric texture of kamafugitic lavas indicate a near liquidus temperature during eruption (i.e. about 1250°C; Cundari and Ferguson 1991), which would make it likely the dissolution and incorporation of carbonate wall rocks into the kamafugitic magmas. Note that carbonate rocks can readily melt at a temperature of about 700°C in the presence of water at moderate to low pressure (e.g. Wyllie and Tuttle 1960).

An additional piece of evidence for wall rock assimilation comes from O-isotope data for whole rocks and separated minerals, which are characterised by $\delta^{18}O$ values ranging from +11 to +14‰. Holm and Munskgaard (1982) suggested that such high O-isotope values denoted an anomalous mantle source strongly modified by the addition of upper crustal material brought into the mantle by subduction processes. However, mantle contamination by subducted upper crust is readily able to modify $^{87}Sr/^{86}Sr$ and other radiogenic isotope ratios, but has less effect on O-isotope signatures (e.g. James 1981). This does not exclude mantle contamination, but mass balance calculations require exceedingly large amounts of crustal material to generate a sufficiently large ^{18}O shift in the mantle rocks to match compositions of the IAP lavas. Therefore, it was concluded that assimilation of wall rocks by ascending magma is the most likely explanation for the high O-isotope signatures of the IAP kamafugites (Turi et al. 1986).

However, wall rock assimilation may have not generated dramatic geochemical modification of kamafugitic magmas, at least for some incompatible element and radiogenic isotope ratios (Fig. 3.5; Peccerillo 1995). Such an effect is due to the low abundances of incompatible element in the limestone, compared to ultrapotassic magmas. The compositional contrast effectively buffers trace element ratios and radiogenic isotope signatures of magmas during carbonate assimilation, leaving these parameters basically unaffected (Fig. 3.5). The implication of this conclusion is that, whereas high O-isotope composition (and possibly CaO concentration) of kamafugites is an effect of magma assimilation processes, radiogenic iso-

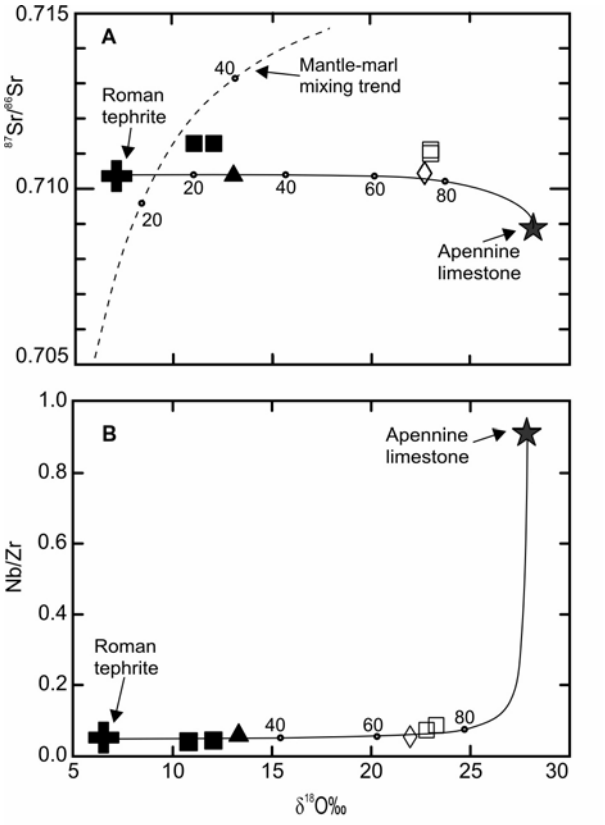

Fig. 3.5. $\delta^{18}O$ vs. $^{87}Sr/^{86}Sr$ (A) and Nb/Zr (B) diagrams for IAP rocks. Curved full lines are calculated mixing trends between Roman ultrapotassic magma and limestone (i.e. magma contamination trend). Dashed line is a mixing trend between mantle and marly sediments (source contamination). Numbers along lines indicate amounts of sediments involved in the mixing.

tope and trace element ratios reflect compositions of mantle sources (Peccerillo 1995).

Experimental investigations of kamafugitic rocks from both Umbria and other worldwide occurrences indicated that they are generated by melting of phlogopite-rich wherlite or clinopyroxenite mantle sources (Edgar 1987; Cundari and Ferguson 1991). These particular mantle compositions are anomalous and require metasomatic modification to generate abundant clinopyroxene and phlogopite. The strong degree of silica undersaturation reflects melting at high pressure, around 2 GPa (e.g. Wendland and Eggler 1980a,b; Green and Falloon 1998). Trace element and radiogenic isotope compositions of IAP kamafugites are intermediate between mantle and upper crust. This has led to the conclusion that the mantle modification was accomplished by addition of upper crustal material. However, radiogenic

isotope ratios are less close to upper crustal values than observed in the mafic rocks of the Tuscany Province, where a pelitic nature for mantle contaminant has been proposed. Therefore a mantle contamination by marly sediments was suggested (Peccerillo et al. 1988). Reaction between marls and peridotite could have generated abundant clinopyroxene and phlogopite, due to addition of K_2O and CaO. Marl addition to mantle rocks, however, does not explain the high LILE/HFSE ratios of the IAP kamafugites. For instance, the Th/Ta ratio ranges from about 35 to 50 in the San Venanzo and Cupaello lavas; these values are much higher than any common sediment (e.g. Taylor and McLennan 1985; Plank and Langmuir 1998). Therefore, it has been concluded that some element fractionation occurred either during mantle contamination or/and during melting to generate kamafugites (Conticelli and Peccerillo 1992). The low concentrations of HFSE, close to E-MORB composition (Sun and McDonough 1989; Fig. 3.4b), have been suggested to reflect a depleted pre-metasomatic composition for the mantle source (Serri 1990).

Alternative hypothesis for the genesis of kamafugitic magmas emphasises the strongly undersaturated and ultrapotassic composition of these magmas and their association with carbonate-rich pyroclastics, which are believed to represent carbonatites. According to this hypothesis, the compositional anomalies for the mantle sources of IAP magmas reflect addition of fluids or melts coming from the deep mantle (e.g. Cundari and Ferguson 1991; Castorina et al. 2000). The crustal-like Sr-Nd isotope signatures of the kamafugitic magmas would be related to the presence of discrete mantle reservoirs characterised by high Rb/Sr and low Sm/Nd ratios. These reservoirs were affected by ancient metasomatic episodes, and remained isolated for a long period of time (1-2 Ga) in order to acquire high Sr and low Nd isotopic ratios.

3.4.2. Carbonate-rich Rocks

The volcanic rocks from IAP commonly contain carbonates, essentially calcite, which occur in the lava groundmass but are particularly abundant in the pyroclastic rocks. As mentioned earlier, it has been suggested that these carbonates are of igneous origin, basically derived by unmixing from silicate magma (Stoppa and Cundari 1995; Stoppa and Wolley 1997). The hypothesis of a magmatic nature for carbonate material in the lava and pyroclastic rocks has gained a wide acceptance (e.g. Bailey and Collier 2000).

The core of the problem of carbonate-rich pyroclastic rocks form IAP relates to the question of whether they represent carbonatites or they are fragmented silicate rocks mixed with secondary calcite coming from the wall rocks. The main arguments that have been considered to be in favour

of a carbonatitic nature for these rocks include their high concentrations of Large Ion Lithophile Elements (LILE), similarity of REE patterns with carbonatites, the high contents of trace elements in calcite, the occurrence of exotic minerals (e.g. monticellite, Th-perovskite, Zr-schorlomite) typical of carbonatites, an alleged Sr-isotopic equilibrium between carbonates and associated silicate phases testifying to an origin by carbonate-silicate melt unmixing, and negative carbon isotopic compositions close to those of mantle-derived material ($\delta^{13}C_{PDB} < -5‰$; Stoppa and Woolley 1997).

However, it has been argued that none of these points represents a compelling piece of evidence in favour of the carbonatite hypothesis. In fact, the high contents of LILE are not exclusive to carbonatites, but are also typical of all ultrapotassic rocks from central Italy. REE patterns of IAP carbonate-rich rocks are closer to ultrapotassic rocks from central Italy than to carbonatites. As noted by Stoppa and Woolley (1997), carbonatites and related rocks do not normally display negative Eu anomalies in their REE patterns, although some do. The high trace element contents of some calcites and their mantle-like C-isotope composition are not exclusive to carbonatites, but have been observed in calcite from skarns, such as those enclosed in calc-alkaline dacites from Lascar volcano, northern Chile (LREE enrichments up to 70 x chondrites; Matthews et al. 1996), and those from the Colli Albani (Alban Hills) volcano in the Roman Province with up to SrO ~ 10 wt % (Federico and Peccerillo 2002). Exotic minerals such as baddeleyite, Zr-rich (ZrO_2 ~ 5%) garnet, cuspidine, Th-rich pyrochlore, REE-rich perovskite, all of which occur in carbonatites, have also been found in skarn xenoliths from the Alban Hills volcano (Federico et al. 1994; Federico and Peccerillo 2002). Finally, Sr- and Nd-isotope ratios reported for whole rocks and for coexisting carbonate and silicate fractions from some IAP carbonate-rich rocks show differences well outside analytical error (e.g. at Polino $^{87}Sr/^{86}Sr_{silicate} = 0.710793 \pm 9$, $^{87}Sr/^{86}Sr_{calcite} = 0.710343 \pm 30$; at Cupaello carbonate-rich rocks have $^{87}Sr/^{86}Sr_{whole\ rock} = 0.710075 \pm 14$, whereas silicate minerals have $^{87}Sr/^{86}Sr = 0.711436 \pm 12$ to 0.711267 ± 11; Castorina et al. 2000). These cannot be considered as equilibrium compositions.

Arguments invoked in favour of a secondary origin for carbonates are many and include the thick pile (several thousand meters) of carbonate sedimentary rocks occurring in IAP, the monogenetic nature of most volcanic centres which make interaction with carbonate wall rocks very likely, the high $\delta^{18}O$ values of calcite, in the range +21 to +26‰ (Stoppa and Woolley 1997) close to compositions of sedimentary carbonates, and the depletion of all major and trace elements (except CaO and CO_2) in the carbonate-rich rocks with respect to the silicate kamafugitic lava from the same volcano.

As for the last point, it has been pointed out that the carbonate-rich rocks from San Venanzo and Cupaello have similar REE and incompatible element patterns but lower absolute element abundances with respect to the kamafugitic lava from the same volcano (Fig. 3.4). Moreover, the element concentrations in the carbonate-rich rocks decrease linearly with increasing contents of calcite. Therefore, the depletion with respect to associated kamafugitic lava is much higher at Cupaello than at San Venanzo, reflecting the much higher calcite content in the former (about 50% calcite at Cupaello and 10% at San Venanzo). Depletion that is proportional to the calcite content of the rocks indicates a barren geochemical composition for carbonate fraction. This conflicts with a magmatic origin of calcite, given the extremely high concentrations of incompatible elements and REE in carbonatites (Woolley and Kempe 1989).

3.5. Geodynamic Implications

There is a general agreement that the magmatism from the internal zones of Apennines has been generated in anomalous mantle sources, which have been affected by metasomatic enrichment in incompatible elements. However, the nature and timing of mantle metasomatic processes are still debated. This issue has paramount geodynamic implications and applies to all ultrapotassic magmatic provinces in Italy.

As mentioned earlier, two conflicting hypotheses have been proposed for the genesis of IAP magmas. One suggests source contamination by marly sediments, whereas an alternative hypothesis invokes metasomatic modification by deep mantle material. Mantle contamination by marly sediments requires subduction processes. These could have occurred as a consequence of convergence between the Adriatic plate and the Apennine chain (e.g. Serri et al. 1993). Such a hypothesis is supported by the presence of a vertical body with high seismic wave velocities beneath the Northern Apennines (e.g. Panza et al. 2003). This body cuts the asthenosphere and has been interpreted as a relict slab of the Adriatic plate. Other hypotheses emphasise the coexistence of kamafugites and carbonate-rich rocks, suggesting that these represent a typical association of melilitites and carbonatites, of the same type as those observed in the Virunga province, East Africa. In the view of this hypothesis, the IAP rocks represent a magmatism emplaced in a intra-continental rifting zone (e.g. Lavecchia and Stoppa 1996; Stoppa et al. 2002). The origin of the magmatism could be related to the upwelling of deep mantle plume (Bell et al. 2004). These issues will be further discussed in Chaps. 4 and 10.

3.6. Conclusions

The volcanic centres of the IAP consist of pyroclastic deposits and a few lava flows and dyke rocks. Lavas have olivine melilitite and kalsilite melilitite composition and show an ultrapotassic kamafugitic affinity. Pyroclastic rocks range from melilitite to phonolite. Carbonate-rich pyroclastic rocks are also present.

Kamafugitic lavas have radiogenic isotope and incompatible trace element signatures similar to the mafic rocks of the nearby Roman Province, which suggest a close genetic relationship. These compositions are best explained by a genesis in an anomalous upper mantle enriched in incompatible elements. Mantle anomalies may be related to either contamination by subducted marly sediments, or to fluids or melts coming from the deep mantle. Interaction between kamafugitic magmas and crustal rocks (mostly sedimentary carbonates) occurred during magma ascent. This process generated an increase of $\delta^{18}O$ (up to + 14‰) and possibly in the CaO content of magmas, but affected the radiogenic isotope and incompatible element ratios to a much lower extent. Therefore, the composition of IAP magmas would be the result of the superimposition of two distinct contamination events, one occurred in the source of magmas, and one occurred in the volcanic system by magma-wall rock interaction.

The carbonate-rich rocks occurring in the IAP are mixtures of carbonate and silicate components. Evidence to discriminate between a primary (i.e. magmatic) or a secondary (i.e. from wall rocks) origin for these carbonates has been much debated. A magmatic origin has been invoked because of negative C-isotope compositions of calcite and the high concentrations of trace elements observed in some crystals. However, it has been observed that both characteristics occur in calcite from skarns. On the other hand, the high $\delta^{18}O$ values of carbonates and the depletion in several major (except CaO and CO_2) and trace elements of carbonate-rich rocks with respect to the associated kamafugitic lavas from the same centre, strongly supports a secondary origin for carbonates.

Table 3.2. Composition of selected Intra-Apennine rocks. Numbers in parentheses refer to data obtained on different, though similar rock samples from the same locality as those analysed for the other elements. Source of data: 1) Peccerillo et al. (1988); 2) Conticelli and Peccerillo (1992), 3) Stoppa and Woolley (1997), 4) Castorina et al. (2000); 5) Conticelli et al. (2002); 6) Stoppa et al. 2002; 7) Author's unpublished data.

Volcano	**San Venanzo**			**Cupaello**		**Polino**	**Grotta del Cervo**
Rock type	Melilitite lava	Pegmatoid vein	Calcite-bearing pyroclast	Lava	Calcite-rich pyroclast	Calcite-rich pyroclast	Pyroclastic bomb
Data source	2,5,7	1	3	2,5,7	3,4	3,4	6
SiO_2 wt%	41.88	38.96	39.70	44.49	19.20	16.00	42.50
TiO_2	0.69	2.14	0.56	1.11	0.43	0.51	0.89
Al_2O_3	12.28	10.44	8.16	7.92	2.60	3.90	12.60
FeO_{total}	2.21	9.89	5.12	7.13	2.33	4.60	7.36
MnO	0.11	0.18	0.10	0.11	0.06	0.07	0.13
MgO	12.78	7.30	7.39	10.38	8.03	7.31	7.28
CaO	15.21	18.85	18.20	14.68	32.02	38.30	15.40
Na_2O	1.06	1.65	0.56	0.32	0.80	0.05	2.49
K_2O	8.36	7.03	3.89	9.55	0.94	0.49	5.11
P_2O_5	0.39	1.49	0.23	1.34	0.48	0.59	0.46
CO_2	-	-	11.30	-	27.20	24.00	-
LOI	0.83	1.72	3.95	2.48	5.32	2.93	3.29
Sc ppm	21	58	-	17	5.3	10	27
V	110	430	107	72	53	47	260
Cr	880	75	528	65	33	490	61
Co	42	38	49	35	22	34	53
Ni	141	40	137	87	30	342	52
Rb	432	277	320	509	139	51	453
Sr	1706	2330	939	3758	1160	1897	1200
Y	27	95	22	44	15	22	25
Zr	319	952	237	848	286	337	267
Nb	15	39	12	47	20	16	16
Cs	33	-	-	74	39	5	39
Ba	501	2044	534	3980	895	2216	649
La	77	236	63	257	95	111	-
Ce	176	482	135	526	184	232	-
Nd	94	214	70	248	82	113	-
Sm	16.6	52	14.2	39	15.1	22.2	-
Eu	3.0	8.1	2.75	6.8	2.9	4.72	-
Tb	1.4	3.9	1.30	2.5	1.2	1.70	-
Yb	2.4	6.7	2.00	2.9	0.9	1.50	-
Lu	(0.33)	1.0	0.29	(0.36)	0.13	0.22	-
Hf	8.8	25	-	22.9	7.0	8.0	13.5
Ta	0.92	2.3	-	3.3	1.0	0.9	-
Pb	(25)	-	21	(133)	50	35	43
Th	30	112	26	124	42	50	25
U	9.5	-	6.3	27.9	4.1	8.8	7.0
$^{87}Sr/^{86}Sr$	0.71041	-	-	0.71128	(0.71007)	(0.71040)	-
$^{143}Nd/^{144}Nd$	0.51208	-	-	0.51212	(0.51188)	(0.51200)	-
$^{206}Pb/^{204}Pb$	18.735	-	-	18.740	-	-	-
$^{207}Pb/^{204}Pb$	15.658	-	-	15.663	-	-	-
$^{208}Pb/^{204}Pb$	38.931	-	-	38.953	-	-	-
$^{176}Hf/^{177}Hf$	0.28249	-	-	-	-	-	-
$\delta^{18}O$	(+13, ol)	-	-	(+11,cpx)	-	(+23, calc)	-

4. The Roman Province

4.1. Introduction

Early in the 20th century, the Roman Province was defined by Washington (1906) as the large region of potassium-rich volcanism, extending from southern Tuscany to the Campania area. The Roman Province described here is more restricted in extent, and only includes the belt of potassium-rich volcanoes running from southern Tuscany to the city of Rome, parallel to the border of the Tyrrhenian Sea. This is also called as the Latium Province (see Peccerillo and Turco 2004). The re-defined Roman Province is formed by the large volcanic complexes of Monti Vulsini, Vico, Monti Sabatini and Colli Albani (Alban Hills; Fig. 4.1), which together erupted about 900 km^3 of volcanic products over a time span from about 800 ka to less than 20 Ka. In the north, these volcanoes are superimposed over the Tuscany magmatic rocks and there is evidence of hybridism between these two provinces in some places (van Bergen et al. 1983; Conticelli and Peccerillo 1992). The southern border of the Roman Province is marked by the Ancona-Anzio line, an important NE-SW trending tectonic line that crosses the Italian peninsula and divides the northern Apennines from Abruzzi-Latium sequences (Castellarin et al. 1982; Locardi 1988). The prevalent volcanism has been explosive, with numerous plinian eruptions and associated caldera and volcano-tectonic collapses. The rocks consist of large-volume pyroclastic deposits and minor lava flows. Thick ignimbrite sheets are particularly abundant and interesting, from both a geological and historical viewpoint, as they tend to form small plateau surrounded by steep cliffs, upon which several historical towns have been constructed. Moreover, the moderate degree of welding makes these rocks an excellent building material, locally known as "peperino", which has been extensively used since Etruscan and ancient Roman times.

Petrologically, Roman Province volcanic rocks are mostly ultrapotassic and undersaturated in silica, but saturated to oversaturated potassic rocks

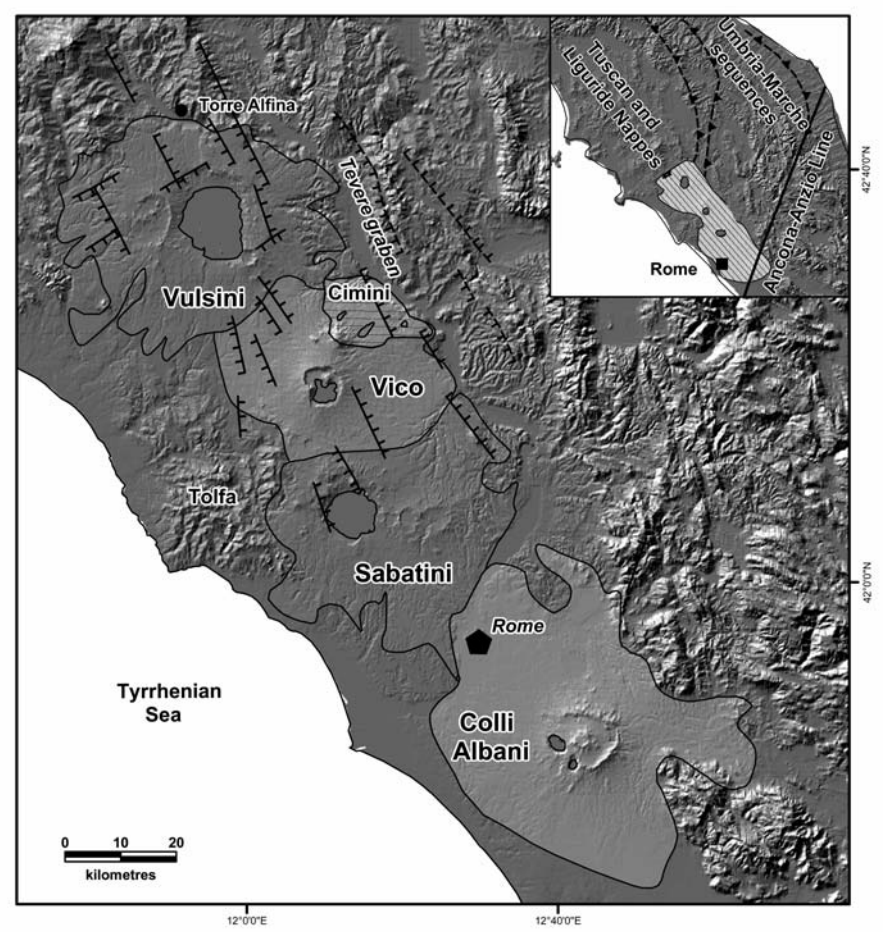

Fig. 4.1. 1 Location map of volcanoes of the Roman Province. Inset: schematic structural map of northern Apennines.

occur in some places, especially in the Vulsini district and, to a lower extent, at Vico volcano (Fig. 4.2). Evolved tephriphonolitic, phonolitic and trachytic rocks predominate over mafic types, except at Colli Albani where volcanic products range from tephrites and leucitites to phonotephrites. The main petrological, geochronological and volcanological features of Roman volcanoes are summarised in Table 4.1. Representative whole rock analyses are given in Table 4.2.

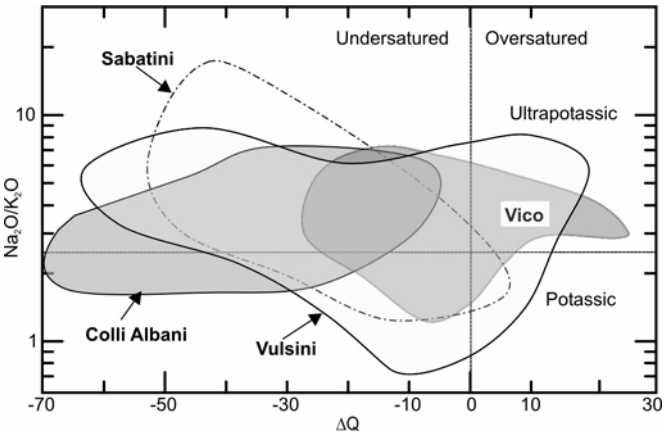

Fig. 4.2. K_2O/Na_2O vs. ΔQ plot for Roman volcanics. For definition of ΔQ, see Chap. 1.

4.2. Regional Geology

The volcanoes of the Roman Province developed in a region characterised by Late Miocene-Quaternary extensional tectonics related to the eastward migration of Apennine mountain range and to the contemporaneous opening of the Tyrrhenian Sea. The volcanic zone is characterised by a system of Upper Miocene to Pleistocene NW-SE basins, developed along normal faults and intersected by strike-slip NE-SW faults (Bartolini et al. 1982). Both fault systems represent zones of crustal weakness along which Roman potassic magmas were intruded.

The pre-volcanic rocks consist of Tuscany, Liguride and Umbria-Marche allochthonous sequences (see Chaps. 2 and 3), and of neo-autochthonous Miocene to Quaternary shallow marine to continental clays, sands, and conglomerates filling post-orogenic extensional basins (Buonasorte et al. 1987; Barberi et al. 1994a). The Umbria-Marche sequences, mainly consisting of carbonate rocks, define eastward convex regional structures in the northern Apennine and are cut by the Tyrrhenian Sea border in the southern end of Roman Province (Fig. 4.1, inset; e.g. Barchi et al. 2001).

The Roman Province is characterised by less than 25 km thick crust (Piromallo and Morelli 2003) and by anomalous heat flow of more than 100 mWm^{-2} at a regional scale (Mongelli and Zito 1991; Mongelli et al. 1991),

Table 4.1. Petrological-volcanological characteristics and ages of volcanoes in the Roman Province.

VOLCANO	AGE (in Ma)	VOLCANOLOGY and PETROLOGY
Vulsini	0.6 to 0.15	- Several multicentre volcanic complexes with calderas, developed around the volcano-tectonic depression of the Bolsena Lake. Dominant pyroclastic fall deposits and ignimbrites and minor lavas, showing KS (trachybasalt to trachyte) and HKS (leucitite and leucite tephrite to phonolite) compositions. Minor melilitite.
Vico	0.42 to 0.1	- Stratovolcano with a central caldera, an intra caldera cone and a few small circum-caldera centres. Dominant pyroclastic fall deposits and ignimbrites and minor lavas, mostly showing HKS (leucite tephrite to phonolite) composition. Minor trachybasalt, latite, trachyte and rhyolite.
Sabatini	0.8 to 0.04	- Two main multicentre complexes (Sacrofano and Bracciano) with several calderas, formed by pyroclastic fall deposits and ignimbrites and minor lavas, mostly showing HKS (leucite tephrite to phonolite) composition.
Colli Albani (Alban Hills)	0.6 to 0.02 possible historical activity	- Stratovolcano with central nested calderas and several post-caldera explosion craters and maars, consisting of HKS (leucitite, leucite tephrite and phonotephrite) pyroclastic fall, flow and hydromagmatic products, and minor lavas.

which is twice the average terrestrial value. Strong anomalies occur beneath most of the volcanoes and adjoining areas, where fluxes of 150 to 300 mWm^{-2} are found (Barberi et al. 1994a and references therein). The entire volcanic region is also characterised by a belt of positive gravity anomaly, which decreases going eastward up to a belt of negative anomaly along the external zones of Apennines (e.g. Scarascia et al. 1994). Shallow seismic activity has been registered in the Vulsini and Colli Albani areas (Montone et al. 1995).

4.3. Vulsini District

Monti Vulsini is a large district formed by various multi-center volcanic complexes, which developed in the northern sector of the Roman Province. Rocks consist of prevailing pyroclastic products and minor lava flows with a potassic to ultrapotassic composition, which cover an area of about 2200 km^2. Eruption occurred at over 100 different centres, including three calderas and the large volcano-tectonic depression of the Bolsena Lake. The volcanism developed along a Tortonian to Pleistocene horst and graben system (Siena-Radicofani and Paglia-Tevere grabens, Cetona and Razzano

horsts), from about 0.6 to 0.15 Ma. The pre-volcanic rocks include Liguride, Tuscan and Umbria sequences and the underlying metamorphic basement. Most of these rocks are found as xenoliths in several pyroclastic units, especially at Montefiascone and Latera.

4.3.1. Volcanology and Stratigraphy

According to Nappi et al. (1987, 1998) the Vulsini district consists of four distinct volcanic complexes: Paleo-Bolsena, Bolsena, Montefiascone and Latera. Several pyroclastic units and lava flows do not seem to belong to any of these complexes and have been attributed to a separate South Vulsini complex (Vezzoli et al. 1987; Palladino et al. 1994; Fig. 4.3). Paleo-Bolsena (about 0.6 to 0.45 Ma) is formed by latite, trachyte, tephriphonolite and phonolite lava flows, strombolian scoriae, plinian fallout and ignimbrites, which only outcrop at the margins of the Vulsini district, directly overlying the sedimentary bedrocks (Nappi et al. 1987, 1995). The Bolsena volcanic complex (about 0.49 to 0.32 Ma) consists of lava flows, strombolian scoriae, several plinian deposits, thick ignimbrite sheets, and hydrovolcanic products mostly displaying a leucite tephrite to trachyte and phonolite composition, with minor latite and shoshonite. These were mostly erupted from the Bolsena Lake depression and crop out extensively in the eastern sectors of the Vulsini district. Well known outcrops of pyroclastic rocks occur in the Orvieto and Bagnoregio areas where a thick ignimbrite layer forms small plateaux, bounded by steep cliffs, on which the towns of Orvieto and Civita di Bagnoregio are located. The Montefiascone volcano (about 0.3 to 0.2 Ma; Nappi et al. 1987, 1995; Brocchini et al. 2000) is formed by several coalescing eruptive centres developed around a 2.5 km wide caldera, and erupting lava flows, ignimbrites, hydrovolcanic products and strombolian scoriae, mostly with a leucite-tephrite and basanite composition. Melilite-bearing lavas and kalsilite-melilitolite ejecta have been also found (Di Battistini et al. 2001). The southern Vulsini complex consists of prevailing phonotephritic and phonolitic products with an age of 0.4 to 0.1 Ma (Palladino et al. 1994). The Latera volcano (about 0.38 to 0.15 Ma; Turbeville 1992a) consists of several pyroclastic units and some lava flows, cropping out around an 8 km wide polyphasic caldera. Compositions of the Latera rocks range from trachybasalt and phonotephrite to trachyte and phonolite (Nappi et al. 1987; Conticelli et al. 1987, 1991; Renzulli et al. 1995; Landi 1987; Turbeville 1993).

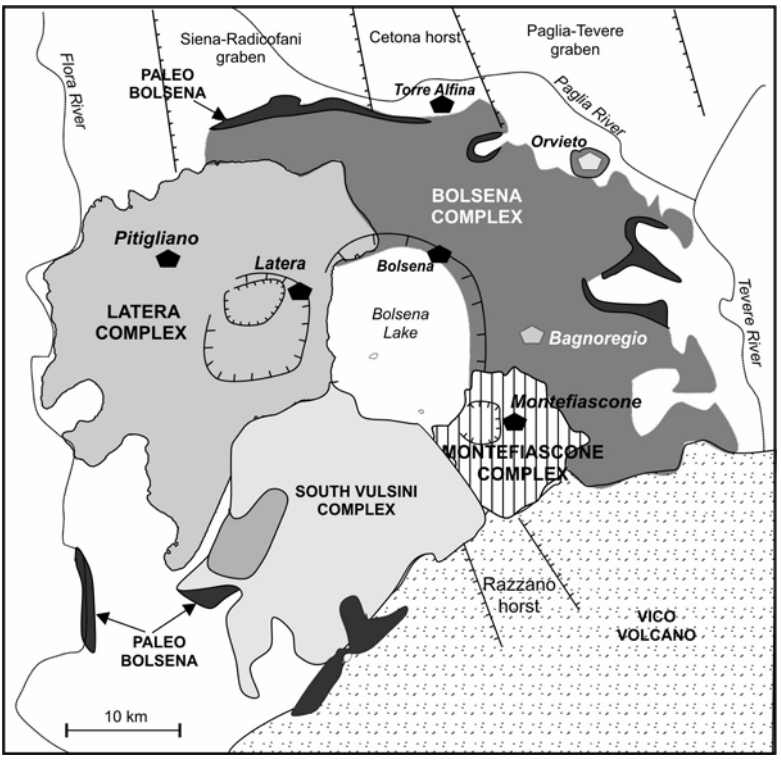

Fig. 4.3. Schematic geological map of Vulsini. Simplified after Vezzoli et al. (1987).

4.3.2. Petrography and Mineral Chemistry

The volcanic rocks from the Vulsini exhibit a wide range of compositions, from mafic to felsic, for rocks that are nearly saturated to undersaturated in silica (Figs. 4.2, 4.4). Although there is a continuum in potassium enrichments, two main series of rocks have been distinguished. One consists of moderately potassic and nearly saturated trachybasalts to trachytes, and is known as the Potassic Series (KS) or Saturated Series. Another rock series is ultrapotassic in composition and consists of leucitites, leucite tephrites, leucite basanites to leucite phonolites, and is known as the High Potassium Series (HKS). KS and HKS have been erupted through the entire evolution history of Vulsini districts; however, KS rocks appear to prevail during the latest stages of activity at Latera (e.g. the Lamone trachybasalt lava flow). A third minor group is formed by melilite-bearing rocks from Montefia-

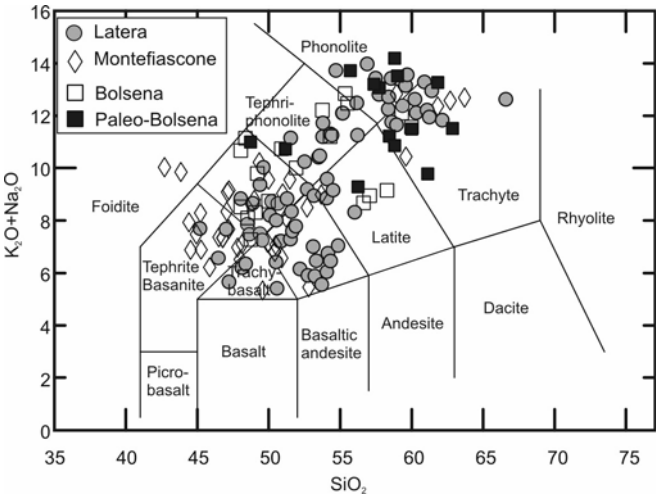

Fig. 4.4. Total alkali vs. silica (TAS) diagram for Vulsini volcanic rocks.

scone; these have major element compositions resembling ultrapotassic kamafugites and fall in the tephrite or in the foidite field on the TAS diagram (Di Battistini et al. 2001).

Lava textures range from almost aphyric to strongly porphyritic. Scoria and pumices are glassy with moderate to low phenocryst contents. Mafic KS rocks contain phenocrysts of clinopyroxene, olivine, and plagioclase set in a groundmass containing the same phases plus Fe-Ti oxides, some alkali-feldspar, and brown mica. Evolved KS rocks contain phenocrysts of sanidine, plagioclase, clinopyroxene and biotite set in a groundmass containing the same phases and Fe-Ti oxides. Leucite occurs as phenocrysts, xenocrysts and in the groundmass of several KS rocks, e.g. at Latera (Landi 1987). Apatite is the main accessory mineral.

The most mafic HKS rocks contain olivine and clinopyroxene phenocrysts; leucite and some plagioclase phenocrysts appear in the more evolved samples. The groundmass consists of clinopyroxene, plagioclase, leucite, some alkali-feldspar, and brown mica. Felsic rocks contain phenocrysts of clinopyroxene, leucite, plagioclase, sanidine and biotite, set in groundmass consisting of the same phases plus Fe-Ti oxides, sporadic haüyne, nepheline, amphibole, garnet, apatite, and sphene (e.g. Holm et al. 1982; Rogers et al. 1985 and references therein). Melilite-bearing lavas from Montefiascone have a poorly porphyritic texture with phenocrysts of leucite, clinopyroxene and melilite, and a groundmass of clinopyroxene, olivine, Fe-Ti oxides, pale brown mica, and carbonates (Di Battistini et al.

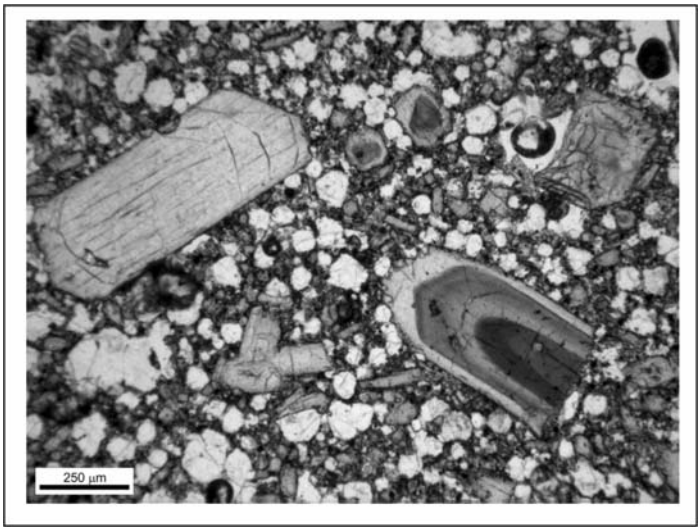

Fig. 4.5. Photomicrograph of a leucite tephrite from Vulsini showing color zoning (from deep green salite to colourless diopside) for clinopyroxene phenocrysts. Plane polarised light.

1998). Olivine (Fo_{92-60}), sometimes with inclusions of Cr-spinel, becomes progressively Mg-poor from mafic to intermediate rocks. Mg-rich olivine is found in some trachytes, where it coexist with Fe-rich (about Fo_{33}) crystals (Holm 1982); CaO is variable (0.3 to 1.5), the highest values occurring in olivine phenocrysts from Montefiascone melilite-bearing rocks (Di Battistini et al. 1998). Clinopyroxene ranges from Cr-diopside to salite. These compositional variations, often observed in single crystals, are revealed by strong colour modification in this section, from colourless diopside to green salite (Fig. 4.5). The coexistence of these two types of pyroxenes in single crystals is common in the ultrapotassic rocks from central Italy and has been explained as resulting from P_{H20} variations during crystallisation or from mixing between compositionally different potassic magmas (Thompson 1977; Brooks and Printzlau 1978; Dolfi and Trigila 1978; Barton et al. 1982; Varekamp and Kalamarides 1989). Leucite is often transformed to analcime. Brown mica ranges from phlogopite to biotite and is sometimes enriched in Ba and TiO_2.

Numerous xenoliths of magmatic, metamorphic and sedimentary origin occur in the Vulsini rocks, especially in the pyroclastic deposits. Most ejecta represent bedrocks; others are skarns, intrusive equivalents of erupted lavas, or cumulate lithologies (e.g. Turbeville 1992b; Di Battistini et al. 1998).

4.3.3. Petrology and Geochemistry

The Vulsini rocks are characterised by an overall decrease in CaO, and ferromagnesian element contents (Ni, Cr, Co, V, Sc) and an increase in K_2O and incompatible elements (e.g. Zr, Th, LREE, etc.) with decreasing MgO. TiO_2 and P_2O_5 show a bell-shaped trend (Fig. 4.6). In general, mafic rocks have high CaO and Al_2O_3, and moderately high Na_2O, showing a composition typical of the so-called Roman-type potassium-rich rocks (see Appendix). Note, however, that some mafic rocks from Latera have lower CaO and higher TiO_2 than rocks from other Vulsini volcanic centres with the same MgO contents. There is an overall increase in incompatible element concentration from KS to HKS rocks, which is particularly evident when only mafic rocks (MgO > 4 wt %) are considered (Fig. 4.7a). REE patterns of both KS and HKS mafic rocks are fractionated and display a small negative Eu anomaly, which increases slightly with decreasing MgO, but is also present in the most mafic rocks (Fig. 4.8a); note that most mafic rocks have no plagioclase on liquidus, suggesting that Eu anomalies are not due to plagioclase fractionation but are features of primary melts. Mantle normalised incompatible element patterns display strong fractionation with negative anomalies of Ba and HFSE (Fig. 4.8b), and positive spikes of Rb, Th, light REE and Pb. These resemble those for the IAP kamafugites, whereas are somewhat different than Tuscany mafic K-rich rocks, in which Nb and Ta negative anomalies are smaller and negative spikes of Sr are present. Note, however, that late-erupted Lamone trachybasalts have a significant Sr negative anomaly and more closely resemble the Tuscany rocks (Fig. 4.8b).

Sr isotope ratios cluster around 0.7100 to 0.7110, with a few values falling outside this interval (e.g. Holm and Munksgaard 1982; Rogers et al. 1985; Ferrara et al. 1986; Varekamp and Kalamarides 1989). These ratios are comparable to IAP kamafugites but are lower than for Tuscany K-rich rocks. There is a very rough increase of $^{87}Sr/^{86}Sr$ with decreasing CaO and MgO (Fig. 4.6f; Rogers et al. 1985), but there is no systematic isotopic difference among mafic rocks with different enrichments in potassium (Fig. 4.7b). $^{143}Nd/^{144}Nd$ ranges from about 0.5121 to 0.5123 (Fig. 4.9). Pb isotope ratios are moderately unradiogenic, falling close to Tuscany mafic rocks ($^{206}Pb/^{204}Pb$ ~ 18.73 to 18.77; $^{207}Pb/^{204}Pb$ ~ 15.65 to 15.71; $^{208}Pb/^{204}Pb$ ~ 38.93 to 39.15). $^{176}Hf/^{177}Hf$ determined on a few samples yielded values of about 0.28257 (Gasperini et al. 2002).

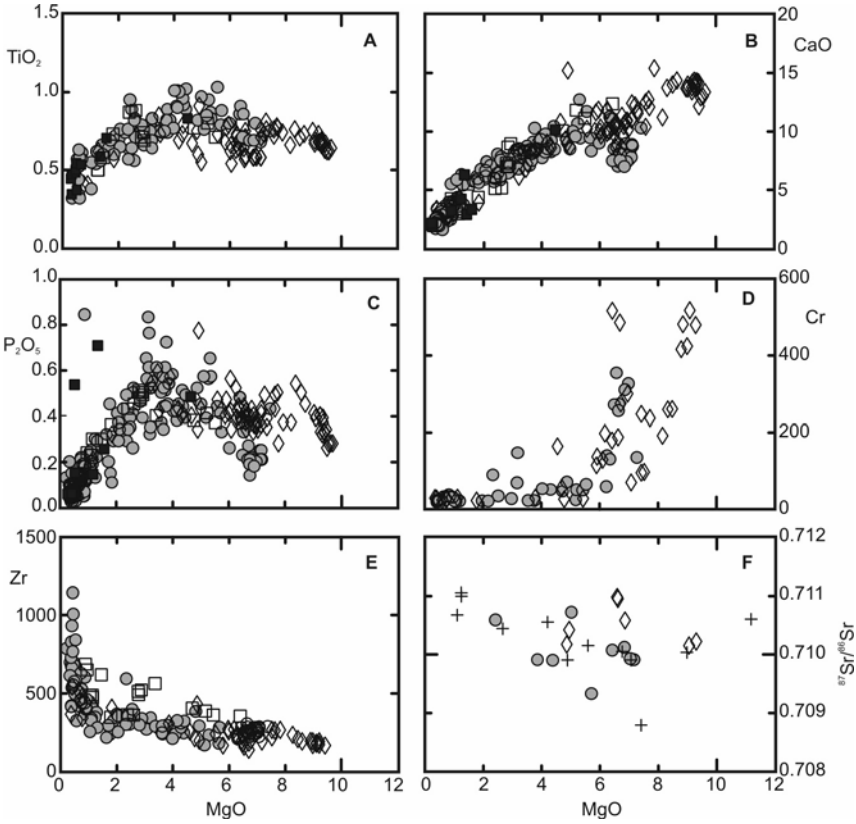

Fig. 4.6. Variation diagrams of selected major, trace elements and $^{87}Sr/^{86}Sr$ ratios vs. MgO for the Vulsini rocks. Symbols as in Fig. 4.4. Crosses indicate samples of uncertain location.

Oxygen isotope data for whole rocks range from $\delta^{18}O \sim +8$ to +12, and increase with increasing silica content (Holm and Munksgaards 1982; Rogers et al. 1985; Varekamp and Kalamarides 1989). Lower values of $\delta^{18}O \sim +6.5$ to +7.9 have been observed in clinopyroxene and MgO-rich olivine from Latera and Montefiascone by Varekamp and Kalamarides (1989) and Barnekow (2000).

Although scattered, major and trace element variations for the Vulsini rocks define overall trends that support an evolution dominated by fractional crystallisation starting from different types of parental melts. Holm et al. (1982) suggested that the evolution of HKS magmas was dominated by fractional crystallisation with separation of olivine and clinopyroxene in the mafic range, and of variable proportions of clinopyroxene, leucite, pla-

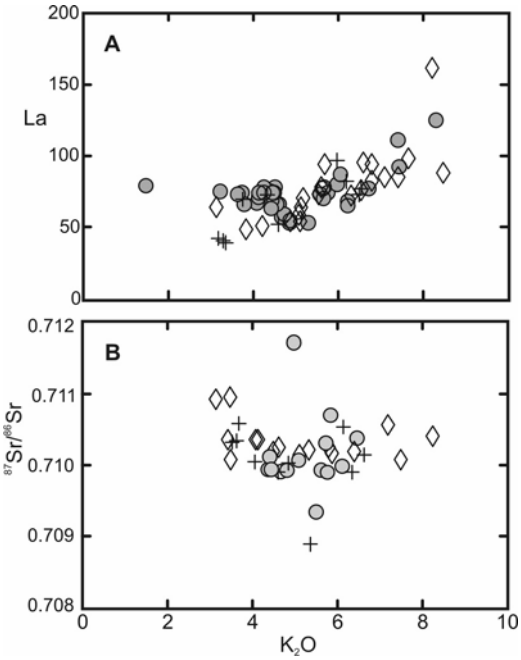

Fig. 4.7. K_2O vs. La (A) and K_2O vs. $^{87}Sr/^{86}Sr$ (B) diagrams for the Vulsini mafic rocks (MgO > 4 wt %). Symbols as in Fig. 4.4. Crosses indicate samples of uncertain location.

gioclase, sanidine, and some apatite in the evolved compositions. In contrast, KS magmas were suggested to have evolved from nearly saturated trachybasalts by separation of olivine, clinopyroxene, and feldspar. Variations of $\delta^{18}O$ and $^{87}Sr/^{86}Sr$ were interpreted as evidence for extensive crustal assimilation. Varekamp and Kalamarides (1989) also suggested that mixing between differently evolved melts was an additional first-order evolutionary process at Vulsini.

The variable compositions of mafic rocks at likely reflect the occurrence of different types of parental liquids, which are characterised by distinct enrichment in potassium and incompatible elements. The positive correlation of potassium vs. incompatible elements and the lack of systematic differences in isotopic compositions between potassic and ultrapotassic rocks are suggestive of a magma genesis by different degrees of partial melting in a broadly common mantle source. This is supported by the similar REE and incompatible element patterns of all the mafic rocks (Fig. 4.8). Also the melilite-bearing rocks from Montefiascone share these

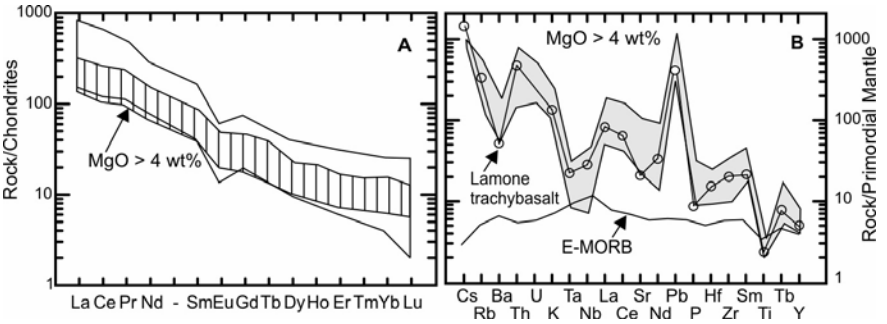

Fig. 4.8. (A). REE patterns of the Vulsini rocks. The ruled area encloses patterns of mafic rocks. (B) Incompatible element patterns of mafic rocks from Vulsini. The pattern of the late erupted Lamone trachybasalt lava is shown in detail. Composition of Enriched Mid Ocean Ridge Basalt (E-MORB; Sun and McDonough 1989) is reported for comparison.

characteristics, indicating a similar source. However, the latest erupted potassic products from Latera (e.g. the Lamone trachybasalt) exhibit negative spikes of Sr, positive spikes of Th and moderate LILE/HFSE ratios in their incompatible element patterns, resembling Tuscany rocks, such as the Radicofani shoshonites. This suggests that the latest Latera magmas have affinities with Tuscany magmatism, pointing to a somewhat different mantle source than for the other Vulsini mafic magmas. Such a conclusion is supported by the lower CaO and the higher TiO_2 contents of Latera lavas. It should be recalled that several ultrapotassic and potassic rocks from Tuscany have low CaO and relatively high TiO_2 (see Chap. 2).

4.4. Vico Volcano

The Vico volcano is located south of Monti Vulsini along the southern extension of the Siena-Radicofani, Paglia-Tevere and Monte Razzano graben-horst system (Locardi et al. 1977). It partially overlies the Monti Cimini rocks (1.3 to 0.9 Ma old), which belong to the Tuscany Magmatic Province. The volcano erupted silica-oversaturated to undersaturated potassic and ultrapotassic magmas over a time span of about 0.4 to 0.1 Ma. The pre-volcanic rocks of the Vico region consist of Tuscan allochthonous sequences (flysch, carbonates and low grade metamorphic rocks) and of neo-autochthonous sediments which crop out at the margins of the volcano and have been found by borehole drilling (Sollevanti 1983).

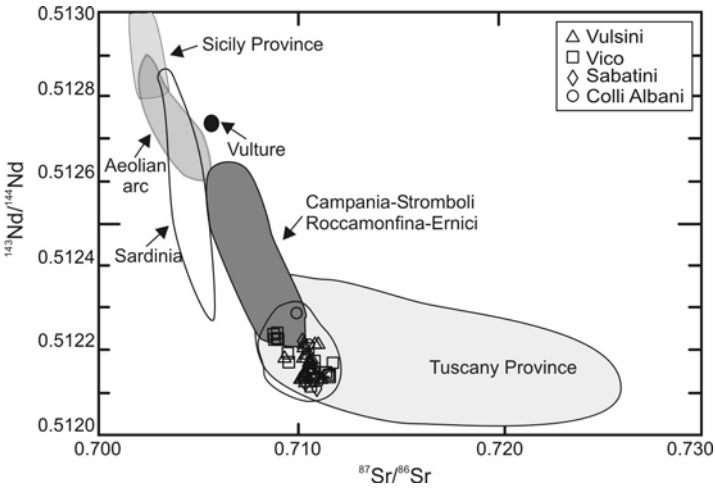

Fig. 4.9. Sr vs. Nd isotope diagram for the volcanic rocks of the Roman Province. Compositions of other provinces are reported for comparison.

4.4.1. Volcanology and Stratigraphy

Vico consists of a single large volcanic edifice with a central caldera and a small number of post-caldera mostly monogenetic centres, the largest being the intra-caldera cone of Monte Venere (Fig. 4.10). Volcanological and petrological data, as well as extensive $^{40}Ar/^{39}Ar$ and K/Ar dating on whole rocks and separated sanidine (Sollevanti 1983; Laurenzi and Villa 1987; Barberi et al. 1994a) allowed recognising three main periods for the Vico activity (Perini et al. 2000, 2004). The Period I (about 400 ka) is composed mainly of latite, trachyte, and rhyolite pyroclastic fall deposits and minor lava flows, which crop out mainly in the northern and eastern sector of the volcano. Period II (305 to 138 ka) was dominated by effusion of intermediate to felsic leucite-bearing lavas. These built up the main cone (305 to 258 ka), and were followed by eruptions of voluminous leucite-bearing pyroclastic flows and falls, which generated a progressive collapse of the central caldera (Locardi 1965). The post-caldera activity (Period III, about 138 to 95 ka) produced small volumes of both leucite-free and leucite-bearing mafic lavas, scoriae, and phreatomagmatic products, mostly scattered along the caldera rim and north of the caldera. The volcanism concluded with the formation of the intra-caldera leucite-bearing lava and scoria cone of Monte Venere (Bertagnini and Sbrana l986).

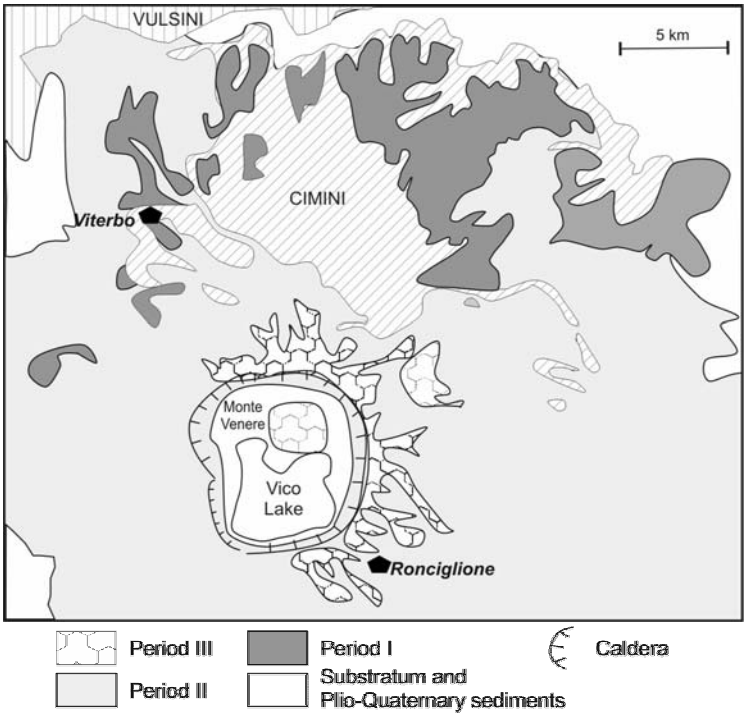

Fig. 4.10. Schematic geological map of Vico volcano. Simplified after Perini et al. (2004).

4.4.2. Petrography and Mineral Chemistry

According to the TAS classification diagram, the Vico rocks span the K-trachybasalt, phonotephrite, tephriphonolites, phonolite, latite and trachyte fields, reaching a rhyolitic composition for some rocks (Fig. 4.11; Cundari 1975; Barbieri et al. 1988; Perini et al. 2004). The trachybasalt to phonolite group is mildly to strongly undersaturated in silica and commonly contains leucite. The other rocks are leucite-free, saturated to oversaturated in silica.

All Vico rocks are porphyritic with phenocryst contents ranging from about 10 to 60 vol %. Groundmass is generally holocrystalline in the lavas, but is variably glassy in pyroclastics rocks. Zoned clinopyroxene (diopside to salite) is an ubiquitous phenocryst and groundmass phase. Plagioclase occurs in variable amounts as a phenocryst phase and in the groundmass of almost all the Vico volcanics. Olivine, sometimes with Mg-chromite

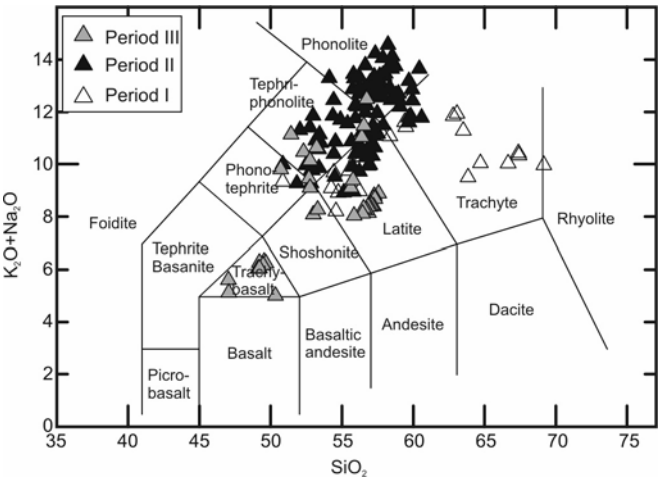

Fig. 4.11. Total alkali vs. silica (TAS) diagram for Vico volcanic rocks.

inclusions, is a common phenocryst of several mafic to intermediate leucite-bearing rocks and in the latites, which exhibit some of the highest forsterite contents (up to Fo_{91}). Leucite occurs as a phenocryst phase in the evolved undersaturated products and in the groundmass of potassic trachybasalts. Haüyne has been observed in some lavas. Sanidine is a phenocryst and megacryst phase in the trachytes and a groundmass mineral of phonolites and latites. Phlogopite is commonly present as a phenocryst phase in several leucite-free rocks. Magnesiohastingsite amphibole occurs in some trachytes. Accessory minerals include apatite, Fe-Ti oxides and sporadic zircon and titanite (Perini et al. 2004).

Like other Roman volcanoes, the Vico pyroclastic rocks contain xenoliths of various origin, including bedrock fragments, intrusive equivalents of lavas, and cumulate rocks. These xenoliths often contain exotic minerals, such as Zr-Ti-Th-U-REE rich phases (e.g. britholite, baddelyite, and pyrochlore), which have been interpreted to be the result of deposition from late-magmatic fluids rich in incompatible elements (e.g. Della Ventura et al. 1999).

4.4.3. Petrology and Geochemistry

Major elements of Vico rocks display scattered distributions on Harker diagrams (Fig. 4.12). However, rocks from different periods of activity define more coherent groups, which suggest the occurrence of different magma types in the volcanic systems at various stages of activity. For

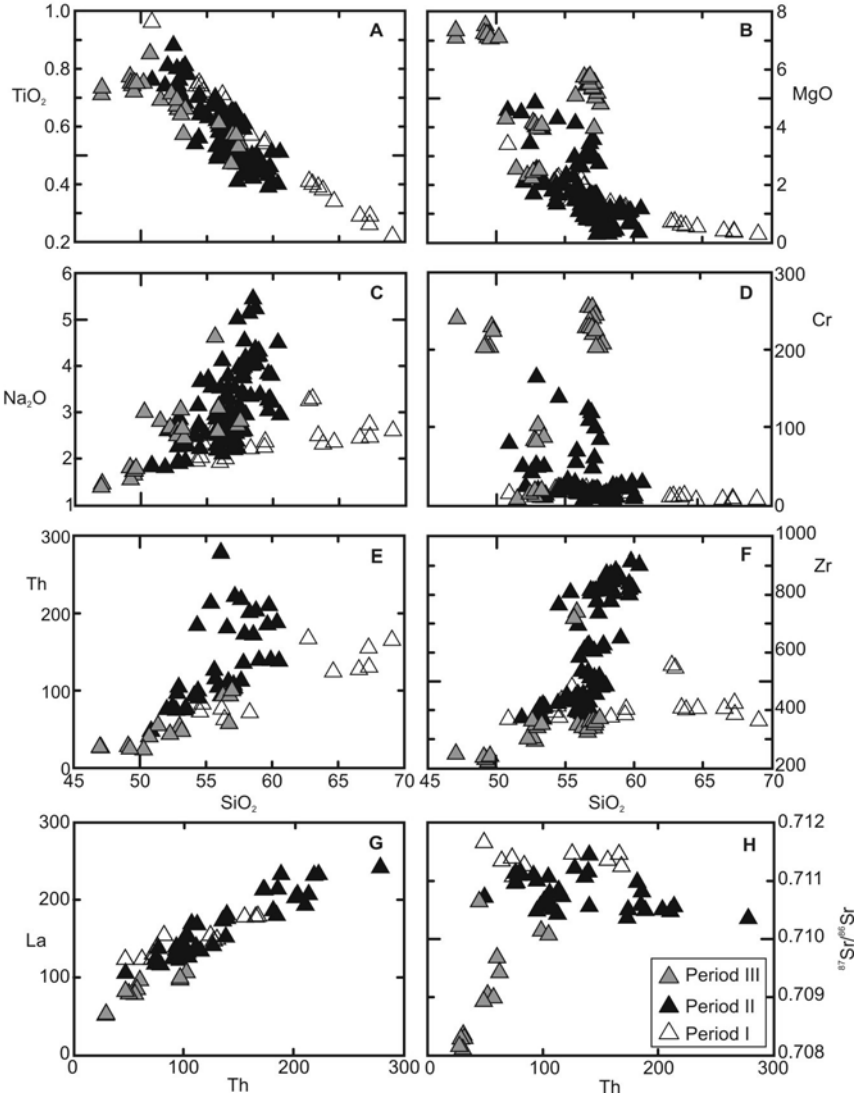

Fig. 4.12. Variation diagrams for the Vico volcano.

instance, rocks of Period I exhibit smooth correlation of CaO, MgO, Na_2O and other major oxides vs. SiO_2. The late-erupted latites and potassic trachybasalts have higher MgO and lower K_2O and incompatible element contents than rocks of other periods (Fig. 4.12a-c).

Trace elements also show scattering, with different levels of enrichment for rocks of different periods (Fig. 4.12d-f). However, incompatible ele-

ment vs. incompatible element diagrams show smooth positive trends (Fig. 4.12g). REE patterns (Fig. 4.13a) are fractionated with small negative Eu anomalies, which increase slightly with increasing silica contents. Incompatible element patterns of mafic rocks show enrichments in LILE and depletion in HFSE (Fig. 4.13b). Period III latites have strong positive spikes of U, Th, LREE and Pb, and negative anomalies of Sr, which are not observed in the coeval trachybasalts, and recall compositions of Tuscany mafic rocks.

The Vico rocks show a larger compositional range of radiogenic isotope ratios than other Roman volcanoes ($^{87}Sr/^{86}Sr$ ~ 0.7081 to 0.7117; $^{l43}Nd/^{l44}Nd$ ~ 0.51209 to 0.51223; Fig. 4.9). There is an overall decrease of Sr isotope ratios with time (Barbieri et al. 1988; Perini et al. 2004) and the youngest Vico rocks have the lowest $^{87}Sr/^{86}Sr$ values yet documented in the Roman Province (Fig. 4.12h). Pb-isotope compositions show moderate variability ($^{206}Pb/^{204}Pb$ ~ 18.70 to 18.82; $^{207}Pb/^{204}Pb$ ~ 15.60 to 15.70; $^{208}Pb/^{204}Pb$ ~ 38.80 to 39.10) and resemble closely those of other potassic rocks in central Italy (Vollmer 1976; Conticelli et al. 2002; Perini et al. 2004). $\delta^{18}O$ determined on whole rocks and separated leucite and sanidine by Turi and Taylor (1976) have high values, from about +9.0 to +10.2 ‰.

Early petrological studies (Cundari and Mattias 1974; Cundari 1975) interpreted the Vico volcanic suite as having formed from one parent magma by fractional crystallisation, with separation of plagioclase, clinopyroxene, leucite, phlogopite and Fe-Ti oxides. Villemant and Palacin (1987) accepted fractional crystallisation, but argued that the very high enrichments of incompatible elements (e.g. Th and Pb) in some phonolites required an additional evolutionary process such as element transfer by gaseous phases. Barbieri et al. (1988) noticed a wide Sr isotope variation in the Vico rocks and an overall decrease in radiogenic Sr and silica with time, suggesting that various batches of magmas were emplaced in the shallow level reservoir at different stages of volcanic activity; these magmas become more mafic and isotopically more primitive with time, until the late trachybasalts and latites were erupted. According to Barbieri et al. (1988), fractional crystallisation, crustal assimilation and magma mixing operated during evolution of various magma batches, with mixing being particularly evident at the transition between pre- and post-caldera activity. Perini et al. (2004) stated that the variable rock compositions at Vico provide evidence for complex shallow-level magmatic evolution starting from different types of parental magmas. Distinct evolutionary processes were envisaged for various activity periods. Transition from trachytes to rhyolites during Period I occurred primarily by fractional crystallisation, with separation of

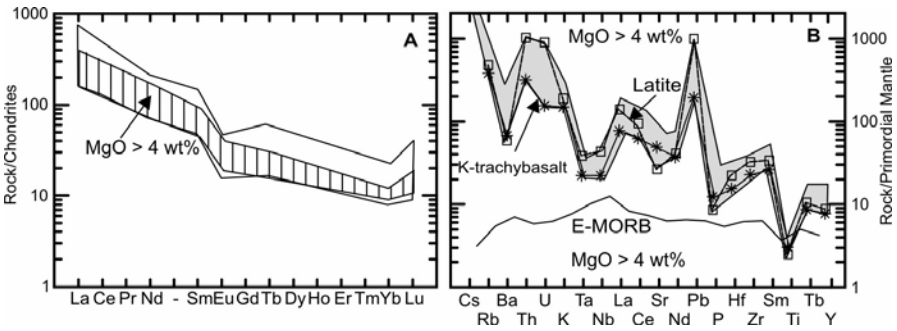

Fig. 4.13. (A). REE patterns of the Vico rocks. The ruled area encloses patterns of mafic rocks. (B) Incompatible element patterns of mafic rocks from Vico (grey area). Patterns of the late erupted trachybasalt (asterisks) and olivine latite (open squares) are shown in detail. E-MORB composition is reported for comparison.

plagioclase, sanidine, clinopyroxene, Fe-Ti oxides, apatite, titanite, and zircon. Period II was characterised by fractional crystallisation of clinopyroxene, plagioclase and alkali-feldspar, with generation of abundant phonolites with extreme enrichments in incompatible element. During Period III, two distinct types of magmas (latite and trachybasalts) were emplaced. These probably mixed shortly before eruption, as already suggested Barbieri et al. (1988) and as supported by mineral-host rock isotopic disequilibria (Perini et al. 2004). The variable compositions of mafic melts were not related to shallow level evolution but to source composition and/or processes (Barbieri et al. 1988; Perini et al. 2004).

4.5. Sabatini District

The Sabatini Volcanic District developed between about 0.8-0.6 Ma and 40 ka over a wide area located just to the north of Rome. Volcanism was predominantly explosive and generated widespread pyroclastic deposits with only minor lava flows, which were emitted from a large number of centres including several calderas (e.g. De Rita et al. 1983, 1993). The volcanism occurred along a zone of crosscutting NW-SE and NE-SW faults (Di Filippo 1993). The Sabatini rocks rest over the same type of sedimentary bedrocks as at Vico, as well over the acid volcanics of Tolfa-Manziana-Cerite complex of the Tuscany Province.

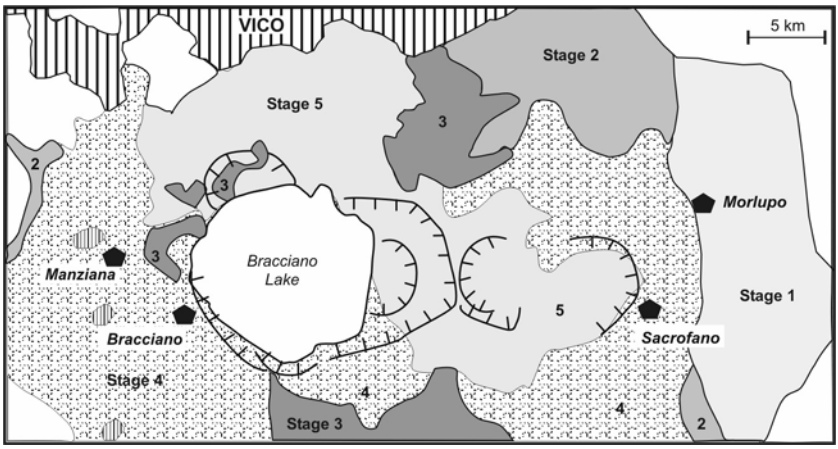

Fig. 4.14. Schematic geological map of Sabatini district. Simplified after Conticelli et al. (1997). Numbers indicate various activity phases. Vertically ruled areas west of the Bracciano Lake are Tolfa-Manziana-Cerite outcrops.

4.5.1. Volcanology and Stratigraphy

The Sabatini district consists of two main multicentre complexes, the Sacrofano volcano in the east and the Bracciano volcano in the west, both developed around a large E-W trending fracture zone affected by multiple caldera collapses (Fig. 4.14; Cioni et al. 1993). According to Conticelli et al. (1997), the activity of the entire Sabatini district can be divided into five main phases. The first phase was concentrated in the eastern centres of Sacrofano and Morlupo and occurred between 0.6 and 0.53 Ma, although rocks as old as 0.8 Ma have been dated by Karner et al. (2001). The second phase (from 0.51 to 0.43 Ma; Karner et al. 2001) was characterised by intense explosive activity at Sacrofano and at Bracciano where early caldera collapses occurred. The third phase (from about 0.41 to 0.28 Ma) produced large-magnitude explosive eruptions with the formation of the Sacrofano caldera (De Rita et al. 1983, 1993) and further subsidence of Bracciano caldera. The last phases took place from several circum-caldera and parasitic centres, and produced hydromagmatic pyroclastic rocks and some lavas. The youngest dated activity is 40 ka (Fornaseri 1985; De Rita et al. 1993; Villa 1993; Karner et al. 2001).

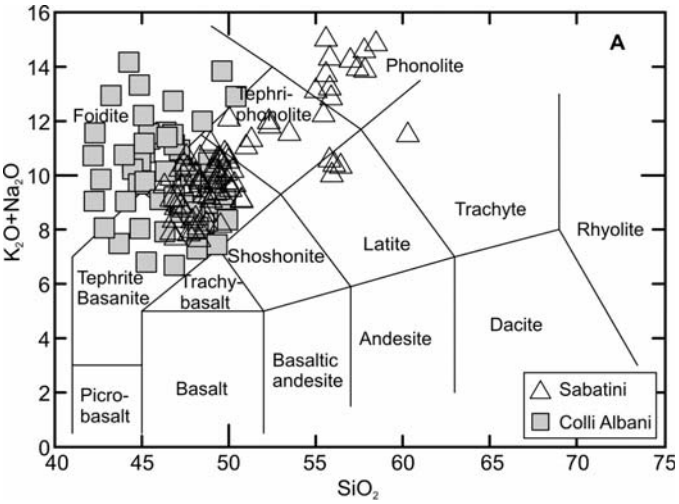

Fig. 4.15. Total alkali vs. silica diagrams for Sabatini and Colli Albani.

4.5.2. Petrography and Mineral Chemistry

Major element studies (Cundari 1979; Conticelli et al. 1997 and references therein) have shown that the Sabatini volcanics consist almost entirely of undersaturated ultrapotassic rocks, ranging from tephrite to phonolite (Figs. 4.2, 4.15), with dominant phonotephrites. A few trachytes and latites have been erupted locally (Morlupo and Vigna di Valle lava flows).

Rock textures are porphyritic with variable amounts of phenocrysts (about 5 to 40 vol %) set in holocrystalline to hypocrystalline groundmasses. Zoned diopside to salite clinopyroxene is an ubiquitous and abundant phenocryst phase. Leucite is a common groundmass mineral and occurs as a phenocryst in some phonotephrites and tephriphonolites. Olivine (Fo_{90-30}) is present as microphenocrysts, sometimes with euhedral chromite inclusions, and in the groundmass of leucite tephrites. Plagioclase (An_{93-53}) and Fe-Ti oxides are phenocryst and microphenocryst phases in tephriphonolites and phonotephrites; sanidine and haüyne occur in phonolites. Phlogopite phenocrysts are rare. Groundmass generally contains clinopyroxene, leucite and opaque minerals plus K-feldspar, plagioclase, some glass, and occasionally phlogopite and brown amphibole. Apatite is a common accessory mineral. Sphene is found in some leucite-haüyne phonolites. The rare latites have strongly porphyritic textures, with abundant phenocrysts of plagioclase and phlogopite, and minor clinopyroxene and K-feldspar set in a groundmass consisting of clinopyroxene, sanidine, hya-

lophane, plagioclase, opaque minerals, some nepheline, and apatite. Large leucite phenocrysts or xenocrysts are also present. Trachytes are characterised by a trachytic texture, with phenocrysts and microphenocrysts of sanidine and dark green zoned clinopyroxene surrounded by a groundmass of sanidine, clinopyroxene and opaque minerals (Cundari 1979; Conticelli et al. 1997).

4.5.3. Petrology and Geochemistry

Major element vs. MgO diagrams display rather smooth trends (Fig. 4.16). Incompatible trace elements display some scattering. Conticelli et al. (1997) recognised two groups of rocks, characterised by different enrichments in Ba, LREE and other incompatible elements. These are shown with open and full symbols in Fig. 4.16. The highly enriched rocks commonly have leucite phenocrysts, whereas the less enriched group contains plagioclase as phenocryst and leucite in the groundmass. Moreover, the group depleted in incompatible elements was mostly erupted by small post-caldera monogenetic centres, whereas the rocks enriched in incompatible elements were formed during pre- to syn-caldera activity. The two groups of rocks, however, do not show consistent differences for major elements and incompatible element ratios. All the rocks show fractionated REE with small negative Eu anomalies (Fig 4.17a). Incompatible element patterns of mafic rocks (Fig. 4.17b) resemble closely other mafic potassic volcanics from the Roman Province.

Sr-isotope ratios exhibit more radiogenic compositions in the highly enriched rock group. There is a rough increase of $^{87}Sr/^{86}Sr$ with decreasing MgO within each rock group (Fig. 4.16h). Nd-Pb-Hf isotope ratios fall within the field of other Roman volcanoes (Fig. 4.9; Table 4.2).

Trends of major element variation have been interpreted to indicate a fractional crystallisation evolutionary mechanism for the bulk of the Sabatini rocks (Cundari 1979). The separating mineral assemblage consisted of plagioclase, clinopyroxene, leucite, phlogopite and Fe-Ti oxides. Conticelli et al. (1997) suggested that all the rocks may be derived from one parent magma. However, the strongly enriched series was subjected to continuous fractional crystallisation and input of mafic magma. Such a process was able to generate strong enrichments in incompatible elements, leaving CaO and MgO at relatively high levels. In contrast, the less enriched group was subjected to a process in which continuous mixing of mafic magma played a minor role, but there was significant crustal assimilation. This generated an increase of Sr isotope ratios in the evolved magmas, with moderate incompatible element enrichment.

The latites and trachytes were probably derived from a different type of parent magma than the other Sabatini rocks. This magma was envisaged to have had lower enrichment in potassium than the parent of the tephrite-phonolite suites. However, no evidence for this mafic magma has been found at Sabatini.

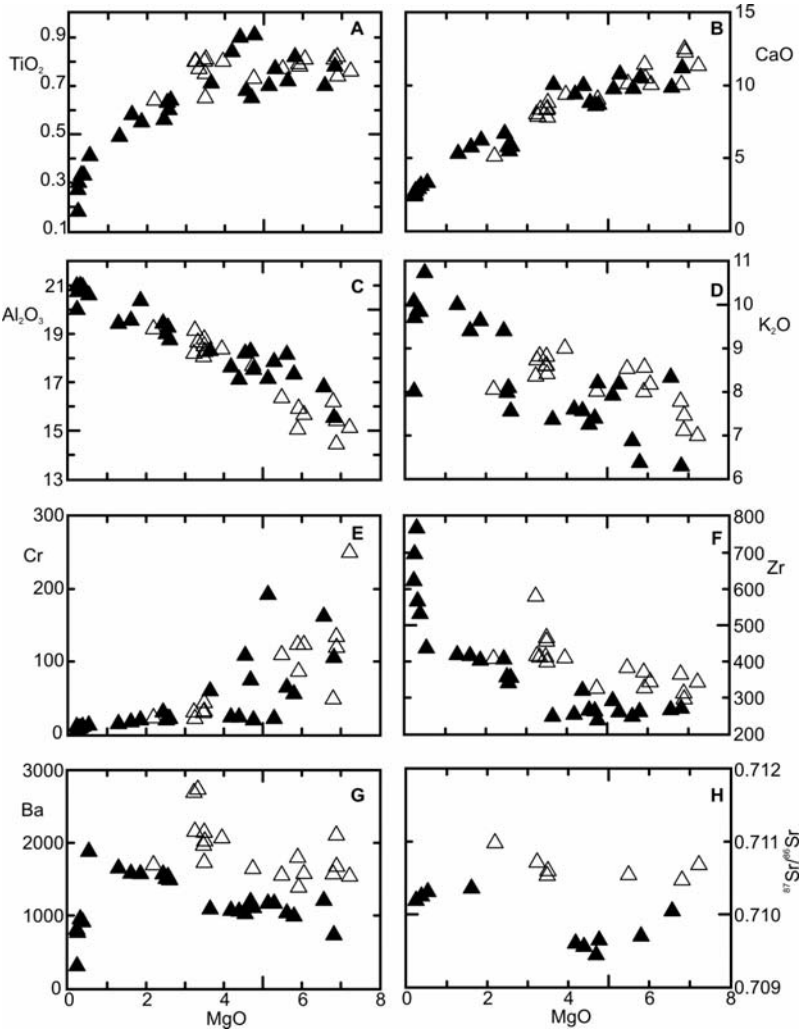

Fig. 4.16. Variation diagrams of MgO vs. selected major and trace elements and $^{87}Sr/^{86}Sr$ ratios for Sabatini volcanics. Open triangles and full triangles represent groups of rocks with different degrees of enrichments in incompatible elements (see text for explanation).

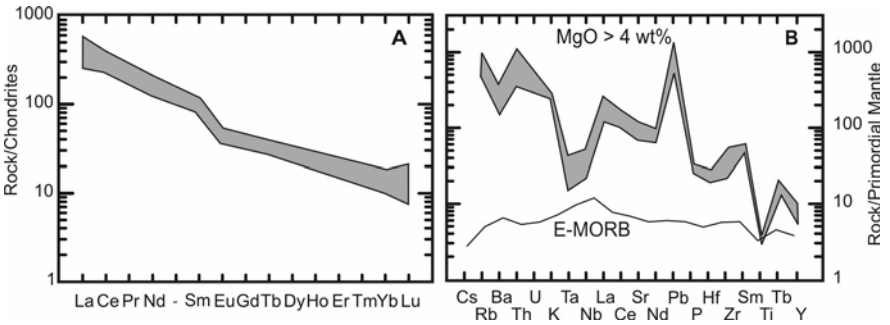

Fig. 4.17. REE (A) and incompatible element patterns (B), restricted to mafic rocks for Sabatini volcano. Composition of E-MORB is reported for comparison.

4.6. Colli Albani (Alban Hills)

The Colli Albani (Alban Hills), also known as Vulcano Laziale, is a large stratovolcano with a central multiple caldera, located about 20 km south-east of Rome (Fig. 4.18). It was constructed in an area affected by NW-SE, NE-SW, and N-S extensional and strike-slip faults. The edifice consists of dominant pyroclastic rocks and minor lavas flows, which were erupted from about 0.6 Ma until very recently, probably during early Roman times. The volcanic rocks crop out over an area of about 1000 km^2. They lie upon Plio-Pleistocene marine sands and clays that fill NW-SE trending extensional basins, developed over Tortonian pelitic-sandy flysch and thick Upper Triassic-Upper Miocene pelagic and platform carbonate units (Sabina facies and Umbria-Latium facies; De Rita et al. 1995 and references therein). The latter are believed to represent the wall rocks of the Colli Albani magma chamber (Funiciello and Parotto 1978). The volcano is located on the western side of the southern end of the Ancona-Anzio tectonic line, which cuts the Italian peninsula from NE to SW, and represents the southern boundary of northern Apennines (Fig. 4.1).

4.6.1. Volcanology and Stratigraphy

The Colli Albani volcano has long attracted the attention of scientists, who reported important field observations and clarified several first-order volcanological, petrological and morphological features of the volcano (e.g. Sabatini 1900). However, the extensive study by Fornaseri et al. (1963)

provided the basis for modern petrological and volcanological investigations and most of their findings are still valid today.

Volcanological and geochronological studies (Fornaseri et al. 1963; De Rita et al. 1995; Karner et al. 2001; Marra et al. 2003) have resulted in the recognition of three main phases of activity at Colli Albani:

1. The Tuscolano-Artemisio phase (about 0.6 to 0.3 Ma), which built up the main cone and was concluded by a caldera collapse.

2. The Faete phase (or Campi di Annibale phase; 0.3 to 0.2 Ma), during which activity was from the intra-caldera Faete cone and resulted in an intra-caldera collapse.

3. The hydromagmatic phase (0.20 to about 0.02 Ma), characterised by violent phreatomagmatic explosions.

The Tuscolano-Artemisio phase erupted about 280 km^3 of volcanic products, mostly consisting of ignimbrites and subordinate fall deposits. The biggest ignimbrite eruption of this phase (about 350 ka) formed a

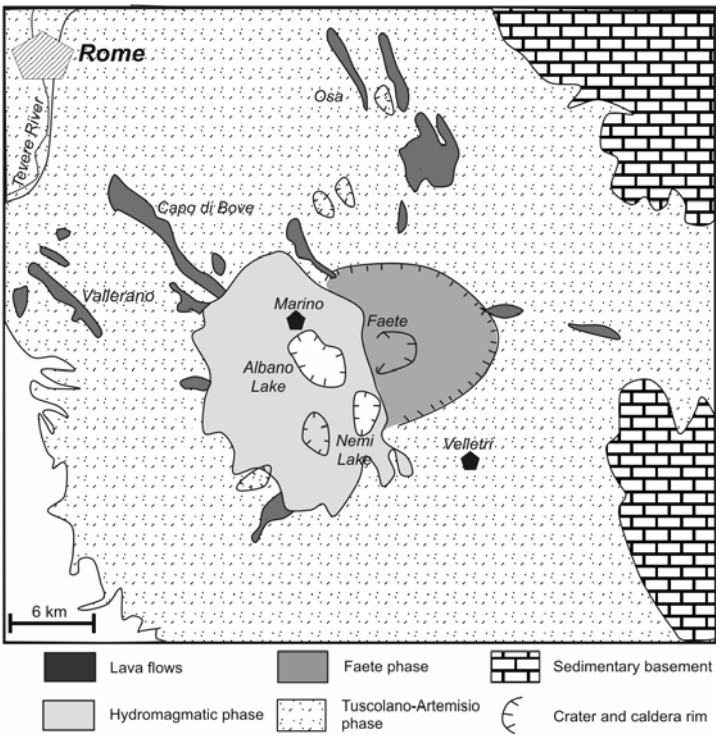

Fig. 4.18. Schematic geological map of Colli Albani volcano. Simplified after De Rita et al. (1995) and Trigila et al. (1995).

large unwelded massive pyroclastic flow (Villa Senni Tuff) and caused the caldera collapse. Syn- to post-caldera strombolian activity and lava effusions took place along the caldera fractures (De Rita et al. 1995; Marra et al. 2003).

The Faete phase erupted about 6 km^3 of volcanic products, which formed the Monte Faete lava and scoria cone, an intra-caldera massive pyroclastic flow deposit (Campi di Annibale pyroclastics), and some flank lava flows (Osa lava at 297 ka; Capo di Bove lava at 277 ka; Karner et al. 2001; Marra et al. 2003). The activity of the Faete phase was closed by the collapse of the Campi di Annibale nested caldera and by circum-caldera strombolian eruptions.

The final hydromagmatic phase occurred from several explosion craters mainly located in the western sector of the volcano, and produced about 1 km^3 of pyroclastic surge, flow and lahar deposits and very few lavas. The best known explosion craters include the maars of Nemi and Albano lakes. The youngest measured age, obtained by thermoluminescence methods on wet pyroclastic flow deposits from the Albano crater, yields a date of about 19 ka (Voltaggio and Barbieri 1995 and references therein).

There is considerable debate on the present condition of the Colli Albani volcano. As mentioned earlier, shallow seismicity has been repeatedly registered. Moreover, historical documents from Roman authors (e.g. Titus Livius, Pliny the Elder, etc.) report on phenomena, such as rain of stones, sudden explosions and fires, which can be ascribed to volcanic eruptions. Moreover, findings of pre-Roman pottery and other human artefacts beneath pyroclastic products are considered as an evidence of a volcanic activity which is much younger than the latest dated rock (see Voltaggio and Barbieri 1995 and references therein). Therefore, based on archaeological and historical records and on seismicity, the volcano is now considered in a quiescent state (Montone et al. 1995; Voltaggio and Barbieri 1995 and references therein).

4.6.2. Petrography and Mineral Chemistry

The Colli Albani rocks have a silica underaturated ultrapotassic composition, and range from tephrite to foidite (leucitite) and tephriphonolite (Fig. 4.2, 4.15). Lava flows are more mafic (i.e. contain higher MgO) than pyroclastic rocks from the same eruptive phase, but ranges in silica and alkalies are similar (Trigila et al. 1995).

Most lava flows exhibit poorly porphyritic textures. Main phenocryst phases include leucite and clinopyroxene; olivine and Fe-Ti oxides occur in minor amounts. Groundmass contains the same phases plus nepheline,

melilite, phlogopite and some calcite. Notably, plagioclase is virtually absent in the Colli Albani rocks, except for rare microcrysts observed in the groundmass of some lavas.

Pyroclastic rocks include scoria and pumices, which show variably porphyritic textures with dominant leucite phenocrysts and minor clinopyroxene, some mica, and rare olivine, set in a microcrystalline to glassy matrix that has been generally affected by strong secondary processes, with abundant zeolites and clay minerals (Fornaseri et al. 1963; Trigila et al. 1995). Accessory phases include Fe-Ti oxides, apatite and rare garnet.

Clinopyroxene is Ca-rich and ranges from diopside to hedenbergite in the lavas and scoriae (e.g. Aurisicchio et al. 1988; Trigila et al. 1995). Olivine exhibits a strong compositional variation (Fo_{92-50}), becoming enriched in FeO from phenocryst core to rims and to groundmass. Mica is generally phlogopite with variable Ti and Ba contents (Trigila et al. 1995). Leucite has a poorly variable nearly stoichiometric composition, nepheline is characterised by K/Na ratio around 2.7, and melilite has a fairly constant akermanite-rich composition.

The Colli Albani pyroclastic deposits contain abundant xenoliths of various compositions and origin. These include fragments of lava flows and several microgranular rocks that represent intrusive equivalents of erupted lavas, cumulate lithologies, and skarns. Some xenoliths are rich in kalsilite and have a composition resembling kamafugitic lavas of the Umbria volcanoes (Federico et al. 1994 and references therein). Xenoliths often contain exotic minerals such as uranpyrochlore, Th-rich britholite, cuspidine, baddeleyite, and perovskite (Washington 1906; Fornaseri et al. 1963; Federico et al. 1994; Federico 1995; Federico and Peccerillo 2002).

4.6.3. Petrology and Geochemistry

Variation diagrams of major and trace elements vs. MgO at Colli Albani (Fig. 4.19) show a positive correlation for CaO, TiO_2, FeO_{total} and ferromagnesian trace elements (Cr, Ni, Co, etc.), negative correlations for Na_2O, K_2O, Al_2O_3 and incompatible elements (Th, La, Ta, etc.), and a bell shaped trend for P_2O_5. Incompatible elements show smooth inter-element positive trends (Fig. 4.19g). The pre-caldera lavas seem to define different trends on some major and trace element variation diagrams, especially on plots of incompatible element vs. incompatible element ratios (Fig. 4.19h). REE and incompatible element patterns have shapes that are similar to those for other ultrapotassic rocks from the Roman Province (Fig. 4.20).

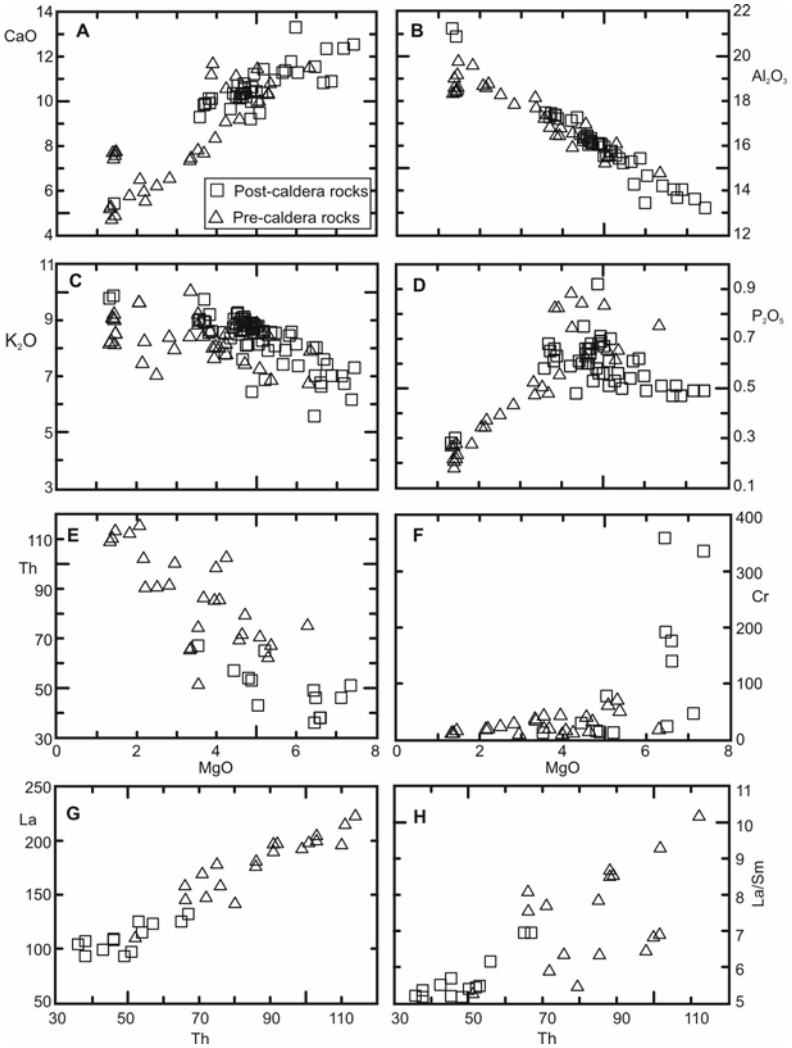

Fig. 4.19. Variation diagrams for the Colli Albani volcanic rocks.

Sr, Nd and Pb isotopic ratios for whole rocks are moderately variable (Fig. 4.9; $^{87}Sr/^{86}Sr$ ~ 0.7102 to 0.7109; $^{143}Nd/^{144}Nd$ ~ 0.51209 to 0.51229; $^{206}Pb/^{204}Pb$ ~ 18.76; $^{207}Pb/^{204}Pb$ ~ 15.70; $^{208}Pb/^{204}Pb$ ~ 39.03; Vollmer 1976; Hawkesworth and Vollmer 1979; Ferrara et al. 1985; D'Antonio et al. 1996; Conticelli et al. 2002). Sr-isotopes for separated clinopyroxenes show wider range of values with $^{87}Sr/^{86}Sr$ ratio mostly falling between 0.7094 to 0.7112 (Gaeta et al. 2005). O-isotope compositions for whole rocks and separated phenocrysts range from $\delta^{18}O$ ~ +5.4 to + 7.8‰, with

an overall positive trend observed between Sr- and O-isotope ratios and an increase of $\delta^{18}O$ values from early to late crystallised minerals in single rocks (Ferrara et al. 1985; Dallai et al. 2004).

Trigila et al. (1995) suggested that the entire rock suite from Colli Albani could be explained by about 60% fractional crystallisation of a mafic-tephrite, dominated by separation of clinopyroxene, and minor leucite and olivine. Such a clinopyroxene-dominated fractionating assemblage has high silica contents and prevented magma evolution to phonolitic compositions, which is typical for other Roman volcanoes. According to Gaeta et al. (2005) stabilisation of clinopyroxene was favoured by strong interaction between magma and the thick carbonate sequences underlying the Colli Albani volcano. Peccerillo et al. (1984) argued that distinct trace element trends for pre- and post-caldera rocks indicate the occurrence of two magma suites, possibly derived from slightly different parental magmas. In contrast, Trigila et al. (1995) report experimental and geochemical evidence in favour of the hypothesis that distinct trends may be related to variable chemical-physical conditions during fractionation. Whatever the case, the positive correlation between whole-rock O- and Sr-isotope ratios, and $\delta^{18}O$ variation in clinopyroxene require that interaction with wall rocks superimposed over fractional crystallisation. This could have been accomplished by bulk assimilation of carbonate rocks which are particularly abundant in the Colli Albani region and/or by input of CO_2-rich fluids into the magma chamber (Dallai et al. 2004). Parental melts of Colli Albani suite are likely to have been leucite tephrites.

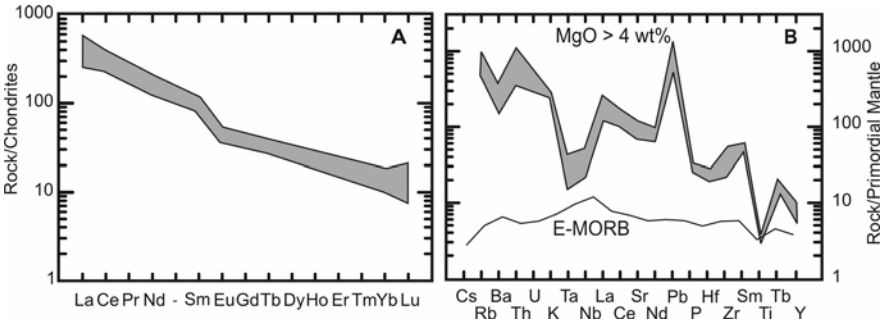

Fig. 4.20. REE (A) and incompatible element patterns (B) of the Colli Albani volcanic rocks.

4.7. Petrogenesis

The petrogenesis of ultrapotassic magmatism within the Roman Province is one of the most debated issues in igneous petrology. As for other Italian potassic rocks, controversial issue is the occurrence of lavas bearing mantle (e.g. high MgO, Ni, Cr contents and undersaturation in silica) and crustal (e.g. elevated K_2O, lithophile elements and radiogenic Sr) signatures. Some of these contrasting features were noticed by early scholars (e.g. Sabatini 1900; Washington 1906) and have prompted numerous studies over the last century.

According to Rittman (1933) the peculiar composition of potassic rocks from central Italy (and of the entire Mediterranean Series, as the potassic rock association was named in the past) was generated by assimilation of carbonate rocks by a trachytic magma. This hypothesis, first suggested by Daly (1918) for the undersaturated rocks in general, explained the high potassium contents of Roman rocks as inherited from the trachyte magma, whereas the characteristic silica undersaturation was related to carbonate syntexis. Such a process was rejected by Savelli (1967), who demonstrated that potassic rocks had higher incompatible element abundances than both limestones and any common magma, including trachytes.

Hypotheses suggesting potassium enrichment by gaseous transfer operating on normal basaltic magmas in shallow level reservoirs, became quite popular for some time, although it was not explained how this randomly operating process could generate potassic rocks which had very close compositional affinities at a regional scale. A genesis by interaction with silicate upper crustal rocks, such as metapelites, was also suggested by several authors (e.g. Turi and Taylor 1976). As will be discussed below, modern research has shown that all these processes actually have been working in Roman volcanic systems. However, they are unable to explain the first-order compositional characteristics of the Roman Province, implying that reasons for compositional peculiarities must be related to mantle rather than to intra-crustal processes.

4.7.1. Fractional Crystallisation and Magma Mixing

It has been noted in the previous sections that the most evolved rocks from the Roman volcanoes can be derived from mafic parents by evolution processes, including fractional crystallisation and mixing. These have affected most if not all the Roman volcanics including the most mafic ones, as demonstrated by the scarcity or absence of rocks showing mantle-

equilibrated Mg[1]# and ferromagnesian trace element (Ni, Co, Cr) contents, and by the common occurrence of strongly zoned clinopyroxenes often showing chemical and isotopic disequilibrium with the coexisting matrix.

Mass balance calculations have shown that some 50-60% fractionation is necessary to have felsic compositions (i.e. trachytes and phonolites) from mafic parents (i.e. K-trachybasalts and K-tephrites). Since the Roman Province mostly consists of evolved phonolites and trachytes, it is obvious that the largest fraction of the parental magmas has not been erupted at the surface. This implies that the amount of potassic magmatism produced in the Roman Province is much higher than the very huge volumes of rocks exposed at the surface.

Fractional crystallisation has been dominated by separation of various proportions of clinopyroxene and olivine in the mafic magmas, and of clinopyroxene and feldspars in the felsic melts. These generated decrease in ferromagnesian elements (FeO, MgO, Ni, Co, Cr, etc.) and increase in incompatible elements (e.g. Th, Ta, Nb, REE), with ongoing evolution. In contrast, ratios of incompatible trace elements were not affected by fractionation processes, and can be used to infer compositions of mantle-equilibrated melts.

Magma mixing has also been extensively working in the Roman Province. Mixing between differently evolved magma batches are the most easy to be recognised, due to the widespread occurrence of strongly zoned mineral phases, especially clinopyroxene (e.g. Thompson 1977; Varekamp and Kalamarides 1989). However, mixing also affected magmas with similar degree of evolution, a process which is much more difficult to constrain (Conticelli and Peccerillo 1992).

4.7.2. Magma Contamination by Crustal Rocks

Interaction between magma and wall rocks has been a common process in the Roman Province. However, the core problem is the question of how much this interaction has modified the pristine compositional characteristics of the mafic parent magmas. A particularly important issue is whether the crustal-like geochemical and isotopic signatures of Roman mafic volcanics can be explained solely by some form of crustal assimilation. These problems have been discussed at length not only for the Roman Province but for all the potassic volcanoes occurring across the Italian peninsula and in the Aeolian arc.

---

[1] Mg-number = $Mg/(Mg+Fe^{2+})$ atomic ratio calculated assuming a Fe^{3+}/Fe^{2+} = 0.85. Mg# of mantle-equilibrated melts is around 0.7 (Frey et al. 1978).

Geochemical studies have shown that assimilation of wall rocks by ultrapotassic magmas has a dilution effect on concentrations of most trace elements in the magmas (e.g. Conticelli 1998; Peccerillo 1998). This is not unexpected, since the most common crustal rocks have much lower degree of incompatible element enrichment than observed in some of the Roman mafic magmas. Such a compositional contrast also effectively buffers variations of incompatible element and radiogenic isotopic ratios, and it has been amply demonstrated that small to moderate degrees of assimilation do not affect to a significant degree these parameters for potassic magmas (e.g. Conticelli and Peccerillo 1992; Peccerillo 1995). Quantitative models of magma contamination by upper crustal rocks (Fig. 4.21) show that a minimum of 50-60% bulk assimilation would be necessary to produce Sr isotopic compositions as those of the Roman mafic magmas, starting from any of the less radiogenic Italian igneous rock. Such a large amount of assimilation would be accompanied by fractional crystallisation, with the production of melts strongly depleted in ferromagnesian elements and oversaturated in silica. Yet, the mafic Roman rocks contain high concentrations of ferromagnesian elements (Ni, Cr, Co, etc.), which exclude significant assimilation and fractionation. The undersaturation in silica and the relatively low values of $\delta^{18}O$ found in separated minerals by recent studies (e.g. Dallai et al. 2004) also point to the same conclusion. Therefore, it has been concluded that the first-order geochemical and radiogenic isotope characteristics of mafic Roman rocks must reflect source characteristics and processes (e.g. Conticelli and Peccerillo 1992; Peccerillo 2002 and references therein).

4.7.3. Genesis of Mafic Magmas

4.7.3.1. Evidence from Major Elements and Normative Compositions

As in the case of the Tuscany and Intra-Apennine magmatic provinces, the potassium-rich composition of Roman mafic rocks requires derivation from mantle sources containing phases rich in potassium, such as phlogopite or K-richterite. However, unlike in Tuscany K-rich rocks, concentrations of both CaO and Na_2O are high, suggesting participation to the melt of mineral phases containing these elements (i.e. clinopyroxene). Therefore, it has been concluded that the mafic magmas of the Roman Province derived from phlogopite-bearing lherzolites or clinopyroxenite,

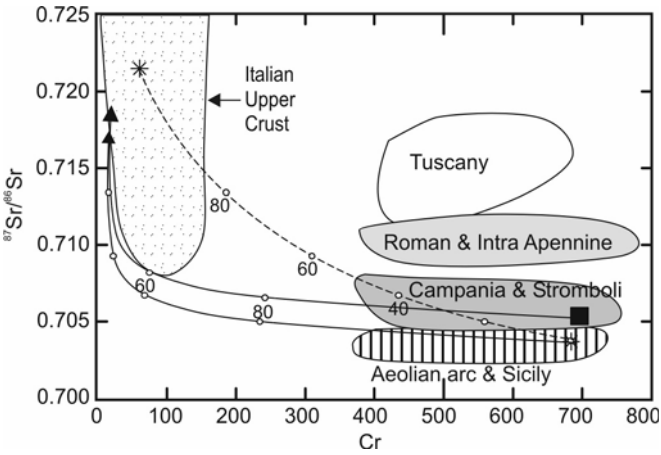

Fig. 4.21. Models of fractional crystallisation plus assimilation (AFC, solid lines) and bulk crust assimilation (dashed line) for mafic magmas from central-southern Italy. Numbers along assimilation line indicate amounts of assimilated crustal material. Numbers along AFC lines indicate amount of residual liquid. For further explanation, see text.

as also suggested for the IAP province (e.g. Conticelli and Peccerillo 1992). The variation in the enrichment in potassium and in the degree of silica saturation for mafic potassic magmas in the Roman Province has been attributed to the amount of phlogopite that entered into the melt and to the pressure conditions during melting. Experimental studies (Wendlandt and Eggler 1980b) have shown that low degrees of partial melting of a phlogopite-bearing peridotite under H_2O-poor conditions generate a potassic liquid that can range from oversaturated to strongly undersaturated in silica. According to these studies, silica saturated and oversaturated magmas are formed in the uppermost mantle at a pressure of about 1 GPa, whereas increasingly undersaturated potassic melts are formed with increasing pressure (i.e. at greater depth). Further studies have shown that melting of phlogopite-bearing peridotite under F-rich conditions gives silica-saturated to silica-undersaturated melts passing from moderate to high pressure (> 1.2 GPa for harzburgite and > 2.0 GPa for lherzolite; Melzer and Foley 2000 and references therein). These studies have led to conclusion that the Roman potassic and ultrapotassic magmas have been formed by different degrees of partial melting at variable pressures within a phlogopite-bearing mantle (e.g. Peccerillo and Manetti 1985). However, Conticelli et al. (2004) suggested that the variable degrees of incompatible element enrichments in the Roman mafic magmas could reflect different amounts of phlogopite entering into the melt. According to this hypothesis, metasomatic melts or fluids percolating through the mantle generated veins

rich in phlogopite, which permeate normal mantle rocks. Melting of these veins, triggered e.g. by an increase in temperature or decompression, generates potassic melts whose concentration in incompatible elements would be simply determined by the relative amounts of veins and wall rocks entering the melt.

The experimental evidence noted above, has produced a consensus that the potassic nature of Roman mafic rocks reflect a genesis in a metasomatically veined phlogopite-bearing upper mantle. Obviously, the high volumes of potassic magmas in this province require very extensive mantle veining. Thus, the debate has shifted in recent years to the problem of the very nature of the processes which produced phlogopite crystallisation in the mantle, i.e. the origin, age and intensity of mantle metasomatism. Trace element and isotopic data have helped to shed light on these issues.

4.7.3.2. Evidence from Trace Element and Radiogenic Isotope Geochemistry

The incompatible element patterns of mafic Roman rocks resemble those of schists and gneiss and of some granites (see Chap. 2). Negative anomalies of Eu in the chondritic patterns of REE also recall upper crustal rocks. Most likely, these features have been inherited from mantle sources, since evolution processes do not change significantly the ratios among incompatible elements and there is no plagioclase on liquidus for most mafic rocks, which could justify negative Eu anomalies. This has led to the conclusion that the mantle was affected by contamination of crustal material, as also envisaged for Tuscany and IAP provinces. Such a hypothesis was first reached by Thompson (1977), and was successively better constrained by trace element and isotopic studies (e.g. Peccerillo et al. 1984; Peccerillo 1985; Rogers et al. 1985). However, most of the Roman mafic rocks have lower LREE/Sr ratios than schists, gneiss and granites and do not show any Sr negative anomaly in their incompatible element patterns, a feature that is typical of these crustal rocks. Moreover, they have LILE/HFSE ratios (e.g. Th/Ta, La/Nb) that are higher than most crustal rocks. Therefore, incompatible element ratios in the Roman mafic rocks cannot be quantitatively explained by simple mixing between mantle and pelitic rocks or granites, as in the case of the Tuscany Province, and require some additional component or/and process. Radiogenic isotope ratios also point to the same conclusion. For instance, $^{87}Sr/^{86}Sr$ ratios of Roman mafic rocks, although close to upper crustal values, are lower than most pelites and their metamorphic equivalents (e.g. schists and gneiss from Tuscany metamorphic basement).

It has been suggested that poorly variable $^{87}Sr/^{86}Sr$ and relatively low LREE/Sr ratios of Roman mafic rocks reveal a mantle contamination by a sediment, which had higher Sr abundances than metapelites and rather constant $^{87}Sr/^{86}Sr$ buffered at around 0.709-0.710 (Peccerillo et al. 1988; Beccaluva et al. 1991; Conticelli and Peccerillo 1992). Such a composition is typical of marls. These rocks have similar incompatible element patterns as pelites, but have lower LREE/Sr and Sr isotope ratios as an effect of the presence of the carbonate component, which has very low LREE/Sr and $^{87}Sr/^{86}Sr$ around 0.707-0.708 (e.g. Melluso et al. 2003).

With regard to the very high values of LILE/HFSE, it has been noticed that these cannot derive from any common crustal rock and require element fractionation at some stage of the potassic magma generation or during mantle evolution (e.g. Conticelli and Peccerillo 1992; see Chap. 3). This fractionation could reflect the presence of a residual HFSE-rich phase during the formation of the potassic magmas (e.g. Foley and Wheller 1990) or may result from selective enrichments by a fluid or melt carrying higher amounts of mobile LILE relative to immobile HFSE (Conticelli and Peccerillo 1992). The high amounts of volatile elements (e.g. F, Cl, B) in the Roman rocks, support a role of fluid phases in mantle metasomatism (Vaselli and Conticelli, 1990; Turbeville 1992b, 1993). In any case, the Roman rocks have low amounts of HFSE, close to MORB values. This requires that the pre-metasomatic source rocks were depleted in HFSE, suggesting a MORB-type composition for the Roman mantle before metasomatism (e.g. Serri 1990).

As noted earlier, the Roman mafic rocks have similar REE and incompatible element patterns, as well as radiogenic isotopic signatures as the IAP kamafugites. This clearly indicates that the mantle metasomatic events and the pre-metasomatic mantle composition envisaged for the Roman Province also apply to the IAP magmas. The petrological differences observed between these two provinces may be related to differences in modal mineralogy of mantle sources and/or to different pressure conditions during partial melting (e.g. Peccerillo and Manetti 1985).

4.8. Age of Mantle Contamination and Geodynamic Implications

The age of mantle contamination in central Italy is a key issue for geodynamic interpretation. Some authors (e.g. Castorina et al. 2000) suggest that contamination by material with high Rb/Sr and low Sm/Nd took place

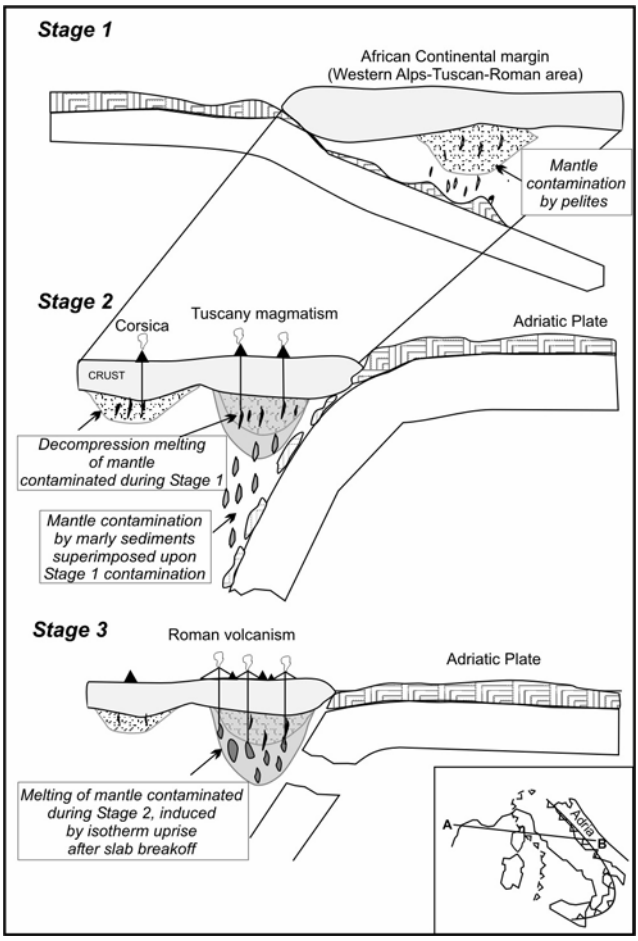

Fig. 4.22. Schematic model for multiple-stage contamination of the upper mantle beneath central Italy, along the section A-B indicated in the inset. Stage 1. Contamination by metapelites of mantle wedge above the east-dipping Alpine subduction zone (see Chap. 2). Stage 2. Oligocene to Quaternary backarc opening, formation of Tuscany magmas and mantle contamination by west-dipping subduction of the Adriatic plate beneath central Italy. The new contamination superimposed over older Stage-1 modification, generating extensive anomalies in the mantle. Stage 3. Increase in the upper mantle temperatures possibly after slab break-off and generation of Roman magmas. Inset: position of Alpine (pre-Oligocene, dashed line) and Plio-Quaternary (full line) collision zones. For further explanation, see text.

some 1.5 to 2.0 Ga ago, and the anomalous mantle remained isolated to develop the present day isotopic signatures. Conticelli et al. (2004) objected that this is unlikely in a tectonically unstable area such as the Mediterranean. However, storage of contaminated material in the deep mantle

and its emplacement as a plume overcomes this objection (Bell et al. 2004). Therefore, old contamination implies a plume mechanism.

Suggestion of very old ages for mantle contamination stems from the steep trend of Rb/Sr vs. $^{87}Sr/^{86}Sr$ defined by the volcanic rocks from central-southern Italy. If interpreted as an isochron, this trend would imply an aging of about 1.5 Ga within the mantle for material with variable Rb/Sr (Castorina et al. 2000). However, it has been noticed that, if considered in insulation, the Roman Province defines a flat trend of Rb/Sr vs. $^{87}Sr/^{86}Sr$ (Peccerillo 2002; see Chap. 10). Therefore, if this trend is considered as an isochron, it also implies a recent mantle contamination for the Roman Province. A young metasomatism has been also suggested by Villemant and Flehoc (1989) on the basis of Th-U disequilibrium studies of rocks from the Vico volcano.

Young metasomatism in the Roman Province has been related to input into the upper mantle of marly sediments by west-directed subduction of the continental-type Adriatic plate during Tertiary times (e.g. Serri, 1990; Doglioni et al. 1999). The occurrence of a steep vertical rigid body cutting the asthenosphere beneath central Italy has been interpreted as a relict slab (e.g. Panza 1984; Wortel and Spakman 2000; Panza et al. 2003). In the view of this hypothesis, the metasomatic contamination of the Roman Province would be younger than the one which affected the mantle source rocks of the Tuscany magmas. As discussed in Chap. 2, the Tuscany metasomatism took place during the Alpine phases of collision between Africa and Europe and was accomplished by introduction of upper crust into the mantle wedge above the east-directed subduction zone beneath the African margin. It is likely, however, that this old contamination event also affected the mantle underlying the Roman Province, as suggested by the superimposition between Tuscany and Roman magmatism in several areas, from Vulsini to Sabatini. Therefore, the mantle source of the Roman Province would be affected by two superimposed metasomatic events, one during Alpine orogenesis and another during subduction of Adriatic plate and formation of the Apennine chain. This twofold metasomatic contamination may represent an explanation for the huge amounts of potassic magmas in the Roman Province. The relatively young age for the Roman magmatism (less than 0.8 Ma) has been attributed to modification of thermal regime within the mantle wedge, possibly as a consequence of slab breakoff and consequent increase in temperature which triggered partial melting (Peccerillo 1990). This model is schematically shown in Fig. 4.22. Further discussion is reported in Chap. 10.

4.9. Conclusions

The Roman Magmatic Province is formed by about 900 km^3 of potassium-rich rocks, mostly consisting of felsic, generally phonolitic and trachytic, pyroclastic deposits. Mafic magmas occur in minor amounts, but are important because they represent the closest relatives of mantle-equilibrated parent melts. Petrological and geochemical studies suggest that the felsic magmas were derived from mafic ones by evolution processes dominated by extensive (some 50-60%) fractional crystallisation and mixing, with some crustal contamination and possibly gaseous transfer. This implies that the total amount of potassium-rich melts generated in the Roman Province is much higher than the huge volumes exposed at the surface.

Mafic magmas in the Roman Province range from saturated or oversaturated (potassic-trachybasalts) to undersaturated (potassic tephrites and foidites) in silica, and display variable degrees of enrichment in potassium and incompatible elements. These magmas were parental to potassic (KS) and ultrapotassic series (HKS). In contrast, radiogenic isotopic ratios are less variable, with most rocks clustering around $^{87}Sr/^{86}Sr \sim 0.7100$ to 7110, $^{143}Nd/^{144}Nd \sim 0.5121$, and $^{206}Pb/^{204}Pb \sim 18.80$; $^{176}Hf/^{177}Hf \sim 0.28258$.

The hypothesis that best explains the genesis of Roman mafic magmas suggests that they were generated by various degrees of partial melting at variable pressures of a lherzolitic mantle enriched in phlogopite by metasomatic processes. Geochemical data suggest that input of sedimentary material with a marly composition has been responsible for mantle metasomatism. The hypothesis of mantle contamination by sedimentary material inevitably implies a subduction-related origin for the Roman Province. The timing of this process is debated, and ages ranging from 2.0 Ga to very recent times have been suggested.

The Roman mafic rocks resemble closely the Intra-Apennine kamafugites for trace elements and radiogenic isotopes. This suggests that the same type and degree of metasomatic modifications affected the mantle sources of the IAP and Roman province. However, differences in the degrees of silica undersaturation, K_2O/Na_2O, CaO, Al_2O_3 and Na_2O abundances point to somewhat different modal mineralogy for mantle sources and/or to variable pressure of partial melting. In contrast, the Roman mafic volcanics exhibit significant petrological and geochemical differences than the Tuscany mafic rocks, for which distinct mantle mineralogy (phlogopite-harzburgite), age and nature of metasomatic event (i.e. mantle contamination by pelitic sediments during Alpine collision), as well as lower pressure of melting have been envisaged.

Table 4.2. Representative compositions of magmatic rocks from the Roman Province. Numbers in parentheses refer to data obtained on distinct though similar rock samples from the same locality as those analysed for the other elements. Source of data: 1) Fornaseri et al. (1963); 2) Peccerillo et al. (1984); 3) Rogers et al. (1985); 4) Conticelli et al. (1997); 5) Perini et al. (2000, 2004); 6) Di Battistini et al. (2001); 7) Conticelli et al. (2002); 8) Gasperini et al. (2002); 9) Author's unpublished data.

Volcano	**Vulsini**					**Vico**		
Rock type	Leucite tephrite	Trachy-basalt	Trachy-phonolite	Trachyte	Melilitite	Trachy-basalt	Latite	Phono-lite
Data source	8,9	8,9	3	3	6	5,8	5	5
SiO_2 wt%	46.14	53.95	56.54	57.72	41.70	49.21	57.07	57.09
TiO_2	0.83	0.71	0.63	0.56	0.91	0.76	0.62	0.61
Al_2O_3	17.82	16.99	18.67	18.66	14.90	15.96	16.66	18.50
FeO_{total}	8.09	5.53	4.83	4.32	8.03	8.03	4.70	4.19
MnO	0.15	0.11	0.13	0.12	0.16	0.15	0.10	0.15
MgO	5.69	7.44	1.18	1.17	4.90	7.60	5.67	0.84
CaO	11.54	7.40	4.55	3.98	15.20	11.02	6.05	3.72
Na_2O	1.89	2.58	2.75	2.55	1.67	1.59	2.71	3.51
K_2O	6.24	4.16	8.72	8.70	8.21	4.79	5.74	9.32
P_2O_5	0.50	0.22	0.31	0.26	0.77	0.22	0.16	0.08
LOI	0.73	0.84	0.62	0.62	2.30	0.64	0.30	1.72
Sc ppm	(32)	(17)	-	-	-	36	20	2
V	302	168	101	99	-	255	138	115
Cr	20	356	7	9	7	206	247	8
Ni	40	192	6	6	39	79	108	15
Co	37	99	-	-	32	33	21	5
Cs	26	15	-	-	-	-	-	-
Rb	402	312	494	342	635	348	423	509
Sr	1395	552	1160	1231	2547	1063	601	1595
Y	34	27	34	38	43	33	53	65
Zr	262	263	434	429	429	221	349	604
Nb	12	16	25	30	19	13	26	35
Ba	870	426	1776	1103	1628	576	425	896
La	71	66	112	137	161	51	105	167
Ce	155	123	251	276	336	115	186	309
Nd	70	49	95	108	152	45	58	96
Sm	12.7	8.2	14.6	15.2	27	9.6	14.2	21
Eu	2.67	1.59	2.92	3.36	21.6	2.05	1.65	3.15
Tb	1.24	0.85	1.65	1.70	-	0.9	1.2	1.6
Yb	2.42	2.29	3.17	3.23	3.19	2.1	2.6	3.6
Lu	0.34	0.36	0.41	0.42	0.37	0.39	0.43	0.57
Hf	5.98	6.23	9.6	9.7	9.8	5.6	8	12.2
Ta	0.59	0.96	1.68	1.49	1.0	0.83	1.8	2.6
Pb	38	42	-	-	89	24	101	142
Th	30	51	73	77	76	28.3	103	107
U	6.8	6.9	9.5	15.8	16.4	4.0	25	18
$^{87}Sr/^{86}Sr$	0.71020	0.70994	0.71099	0.71105	0.71042	0.70812	0.71013	0.71053
$^{143}Nd/^{144}Nd$	0.51213	0.51220	0.51210	-	0.51213	0.51223	0.51218	0.51211
$^{206}Pb/^{204}Pb$	18.779	18.740	-	-	-	18.81	18.73	18.74
$^{207}Pb/^{204}Pb$	15.653	15.663	-	-	-	15.68	15.67	15.68
$^{208}Pb/^{204}Pb$	39.015	39.039	-	-	-	39.05	39.01	39.01
$^{176}Hf/^{177}Hf$	0.28257	0.28260	-	-	-	(0.28260)	-	-

Table 4.2 (continued)

Volcano	**Vico**		**Sabatini**			**Colli Albani**		
Rock type	Phonotephrite	Rhyolite	Phono-tephrite	Tephri-phonolite	Phonolite	Leucite-tephrite	Phono-tefrite	Leucitite
Data source	5	5	8	4	4	1,2,7,9	1,2	1,2,9
SiO_2 wt%	50.80	69.10	49.52	53.48	56.99	42.84	47.37	42.51
TiO_2	0.99	0.20	0.67	0.58	0.41	1.22	1.10	0.61
Al_2O_3	18.15	14.30	16.55	19.55	20.6	13.79	20.13	16.88
FeO_{total}	8.55	1.63	6.97	5.84	3.14	9.04	4.51	10.21
MnO	0.14	0.09	0.13	0.12	0.12	0.11	0.10	0.13
MgO	3.40	0.29	6.73	1.61	0.53	6.30	5.21	2.95
CaO	7.40	1.58	10.03	5.73	3.29	9.93	9.86	10.21
Na_2O	1.85	2.6	1.43	2.13	3.35	1.38	3.40	2.75
K_2O	7.54	7.43	6.71	9.4	10.87	6.74	6.89	7.95
P_2O_5	0.56	0.02	0.62	0.36	0.1	0.70	0.34	0.34
LOI	0.58	2.7	0.64	1.2	0.6	4.89	0.60	1.22
Sc ppm	16.6	2.3	-	13.7	1.4	14	6	11
V	209	23	272	213	-	-	-	-
Cr	13	11	258	16	12	18	5	9
Ni	26	19	76	11	7	47	-	41
Co	27	2.2	33	20	7.2	32	20	33
Cs	-	-	31			36	46	18
Rb	497	730	524	658	393	390	410	280
Sr	1719	209	1728	2114	1989	1290	2450	2000
Y	56	69	30	43	54	-	-	-
Zr	368	363	299	415	436	-	-	-
Nb	17	37	13	17	29	-	-	-
Ba	2152	109	1013	1577	1879	1340	-	2680
La	121	176	90	134	156	159	125	199
Ce	230	297	182	274	295	352	267	437
Nd	86	80	88	103	92	130	-	-
Sm	19.6	15.4	17	19.5	17.8	25	18	29
Eu	3.62	1.18	3.27	3.3	3	4.6	3.4	5.3
Tb	1.6	1.1	1.28	1.6	1.8	2.2	1.8	2.6
Yb	1.8	3.9	2.14	2.7	3.1	2.5	2.7	2.9
Lu	0.29	0.63	0.28	0.58	0.49	0.55	0.58	0.73
Hf	7.9	11.3	7.1	7.4	7.7	15	7	18
Ta	0.99	3	0.66	1	1.3	1.70	1.30	2.21
Pb	222	261	45	-	-	-	-	-
Th	47	165	45	75	90	76	65	101
U	6	49	10	-	-	-	-	-
$^{87}Sr/^{86}Sr$	0.71168	0.71148	0.71009	0.71036	0.71031	(0.71063)	-	(0.7106)
$^{143}Nd/^{144}Nd$	0.51215	0.51211	0.51211	-	-	(0.51209)	-	-
$^{206}Pb/^{204}Pb$	18.70	-	18.797	-	-	(18.79)	-	-
$^{207}Pb/^{204}Pb$	15.66	-	15.674	-	-	(15.65)	-	-
$^{208}Pb/^{204}Pb$	38.91	-	39.090	-	-	(39.00)	-	-
$^{176}Hf^{177}Hf$	-	-	0.28256	-	-	-	-	-

5. The Ernici-Roccamonfina Province

5.1. Introduction

The Monti Ernici and Roccamonfina volcanoes are located south of the Roman Province, between the Ancona-Anzio and Ortona-Roccamonfina tectonic lines (Fig. 5.1). The Ernici volcanoes consist of a series of about twenty monogenetic pyroclastic and lava centres with an age of 0.7 to 0.1 Ma. The Roccamonfina volcano is a stratocone with a large central caldera, formed by lava flows, domes and pyroclastic deposits emplaced between about 0.6 and 0.1 Ma. Early studies (e.g. Appleton 1972; Civetta et al. 1981) recognised two distinct rock series in the Ernici and Roccamonfina volcanoes: a potassic series (KS) and a high-potassium series (HKS), showing distinct enrichments in potassium, incompatible elements and Sr-Nd isotopic signatures. However, subalkaline mafic rocks with low potassium contents (K_2O ~ 0.5 to 1 wt %), falling within the compositional range of calc-alkaline basalts, have been found both at Monti Ernici and Roccamonfina (Giannetti and Ellam 1994; Author's unpublished data). Unlike calc-alkaline basalts, however, these rocks are mostly undersaturated in silica and here will be called Low-Potassium Basalts (LKB). Therefore, a peculiarity of the Ernici-Roccamonfina Province is the close association of rocks with a very wide range of enrichment in potassium, incompatible trace element and radiogenic isotope compositions.

Information on age, volcanology and petrology for Ernici and Roccamonfina is summarised in Table 5.1. Major, trace elements and isotopic data for representative rocks are reported in Table 5.2.

5.2. Regional Geology

The volcanoes of Ernici and Roccamonfina occur on the Tyrrhenian side of the central Apennines, a sector of the Apennine orogen delimited by the Ancona-Anzio line in the north and by the Ortona-Roccamonfina line in the south (Locardi 1988). The pre-volcanic basement consists of various rock types belonging to distinct paleogeographic-structural units formed

during early Mesozoic to Quaternary times (e.g. Accordi et al. 1986). The Lazio-Abruzzi platform unit consists of several thousand meters of prevailing neritic carbonates that were deposited from Upper Triassic to Miocene. The Umbria-Marche basinal unit is formed by Upper Triassic to Upper Cretaceous pelagic carbonate sediments that pass into silico-clastic formations of Eocene to Miocene age; this is covered by east-verging allochthonous sequences of Miocene limestones, marly limestones and flysch sequences (Sicilides) intercalated with Messinian and Pliocene deposits. Foredeep sequences consist of Pliocene to Lower Pleistocene terrigenous sediments.

As other sectors of the Apennine chain, central Apennines have been affected by various tectonic phases. Compressional events dominated from Upper Cretaceous to Lower Pliocene and generated fragmentation of the carbonate platform and intensive thrusting and folding. Extensional tectonics dominated from Middle Pliocene to present. It initially affected the Tyrrhenian Sea border and successively shifted eastward, generating intensive NW-SE faulting with development of graben-horst systems.

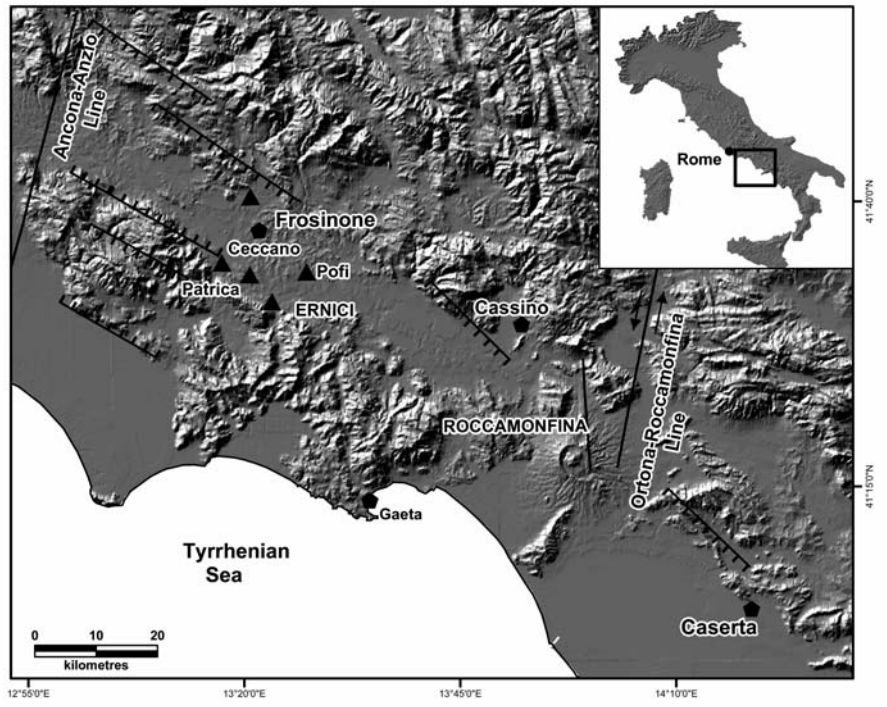

Fig. 5.1. Location map of Ernici (full triangles) and Roccamonfina volcanoes.

Table 5.1. Age, petrology and volcanology of Ernici and Roccamonfina volcanoes.

VOLCANO	AGE (in Ma)	VOLCANOLOGY and PETROLOGY
Monti Ernici	about 0.7 to 0.1 - HKS: 0.7 to 0.2 - KS: 0.2 to 0.1	- About twenty monogenetic cones formed of strombolian scoriae, hydrovolcanic surge and flow deposits and some lava flows displaying a mafic composition and a subalkaline (LKB) to alkaline potassic (KS) and ultrapotassic (HKS) petrochemical affinity (basalt, K-trachybasalt, tephrite, phonotephrite, leucitite).
Roccamonfina	0.58 to 0.1 Potassic rocks generally younger than ultrapotassic rocks	- Stravolcano with a main central caldera and eccentric cones, formed of alternating lava flows and pyroclastic products with a mafic to felsic subalkaline to alkaline potassic (KS) and ultrapotassic (HKS) composition.

Locardi (1988) suggested that the central Apennine chain represents a segment of the Apennine arc that developed as an independent sector in Middle Miocene times between the Ancona-Anzio and Ortona-Roccamonfina lines. According to this author, changes in the degree of anticlockwise rotation along the Apennine chain disrupted the orogenic arc and resulted in the formation of various segments bordered by dextral transcurrent faults. This hypothesis is supported by paleomagnetic data, which demonstrate different degrees of block rotation along the Apennine chain during Oligocene to Miocene evolution (Meloni et al. 1997).

The Ernici-Roccamonfina zone has a crustal thickness of about 30 km. The uppermost mantle is characterised by a thin layer of material with relatively low S-wave velocity (V_S = 3.95 km/sec), which passes into a thick lid that has higher S-wave velocities (V_S = 4.40-4.65 km/sec). This upper mantle structure is unique in the circum-Tyrrhenian area (Panza et al. 2004; Chap.10).

5.3. Monti Ernici

5.3.1. Volcanology and Stratigraphy

The Monti Ernici volcanoes consist of a series of about twenty small edifices spread over a small area (Mid Latina Valley) sited about 70 km SE of Rome. The volcanic activity has been characterised by moderately explo-

sive and effusive eruptions that generated strombolian scoriae, some pyroclastic flows and surges and a few lava flows. The volcanism developed between 0.7 and 0.1. The most K-rich products erupted first (about 0.7 to 0.2 Ma), followed by the less potassic volcanics (about 0.2 to 0.1 Ma; Basilone and Civetta 1975; Civetta et al. 1981).

The most important eruptive centres include the pyroclastic flows of Patrica and the cones of Tecchiena, Celletta, Colle Castellone, Borghetto, Pofi, Villa Santo Stefano and Giuliano di Roma. Most of these centres consist of mafic ultrapotassic rocks; potassic and low potassic basalts occur at Villa Santo Stefano and in a few places south of Ceccano (Fig. 5.2).

5.3.2. Petrography and Mineral Chemistry

The Ernici volcanics define a vertical trend on a TAS diagram, spanning the basalt, K-trachybasalt, shoshonite, leucite tephrite and foidite compositional fields, and straddling the boundary between subalkaline and alkaline fields of Irvine and Baragar (1971; Fig. 5.3a). The subalkaline rocks have K_2O and K_2O/Na_2O ratios within the range of calc-alkaline basalts (low-K basalts, LKB; Fig. 5.3b,c). However, in contrast to calc-alkaline mafic rocks, the Ernici samples are generally undersaturated in silica (Fig. 5.3c).

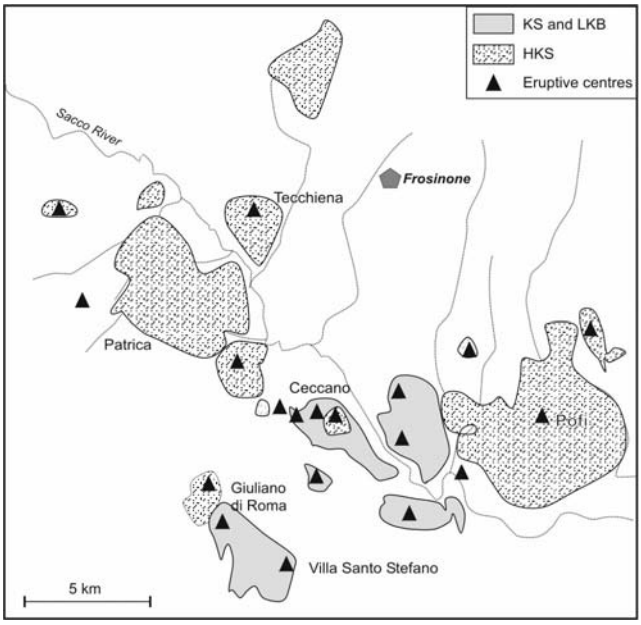

Fig. 5.2. Schematic geological map of Ernici volcanoes. Simplified after Civetta et al. (1981).

The alkaline rocks range from potassic (KS) to ultrapotassic (HKS) and are mildly to strongly undersaturated in silica.

The LKB have poorly porphyritic texture with sparse microphenocrysts of olivine and clinopyroxene set in a groundmass formed by the same phases, plus some plagioclase, phlogopite, Fe-Ti oxides and glass. The K-trachybasalts and shoshonites have aphyric to sparsely porphyritic textures with phenocrysts of zoned diopsidic to salitic clinopyroxene, some Mg-rich olivine (up to Fo_{90-85}) and rare microphenocrysts of plagioclase set in a groundmass consisting of strongly zoned plagioclase (An_{82-35}), salite, olivine (Fo_{75-60}), magnetite, rare leucite and alkali feldspar, and sporadic nepheline (Civetta et al. 1981; Author's unpublished data). The leucite-tephrites and leucitites generally exhibit moderately porphyritic textures with about 10 to 20 vol % phenocrysts of clinopyroxene, minor leucite and olivine (up to Fo_{90}) commonly rimmed by clinopyroxene, and sporadic microphenocrysts of andesine plagioclase. Clinopyroxene may also be present as 3 to 5 cm-long megacrysts and commonly shows strong compositional zoning from diopside to salite, which appears colourless to green in thin section. The groundmass consists of leucite, salitic clinopyroxene and opaque minerals. Nepheline, K-feldspar, brown mica and barkevikitic amphibole are commonly observed (Civetta et al. 1981; Author's unpublished data). Melilite has been found in some rocks (Colle Castellone; Conticelli, personal communication).

5.3.3. Petrology and Geochemistry

The Ernici rocks exhibit low SiO_2 contents and moderate to high MgO values, from about 4 to 9 wt%. Major element variation diagrams display positive correlations of CaO, FeO_{total}, and ferromagnesian trace elements (i.e. Cr, V, Ni, Co, Sc) vs. MgO (Fig. 5.4). In contrast, incompatible elements show steep negative trends, with some scattering. Overall, the LKB and KS rocks have higher MgO and ferromagnesian element abundances than HKS. Incompatible trace elements exhibit comparable abundances in the LKB and KS, whereas they increase sharply to HKS rocks. There is an erratic behaviour of some mobile trace elements (e.g. Cs and Rb; Author's unpublished data; Table 5.2) in the KS and LKB, which may derive from syn- or post-eruptive modification. REE are variably fractionated with LREE/HREE ratios increasing from LKB and KS to HKS. Most rocks exhibit a negative Eu anomaly, which is stronger in the HKS samples (Fig. 5.5a). Incompatible element patterns show strong fractionation, which in-

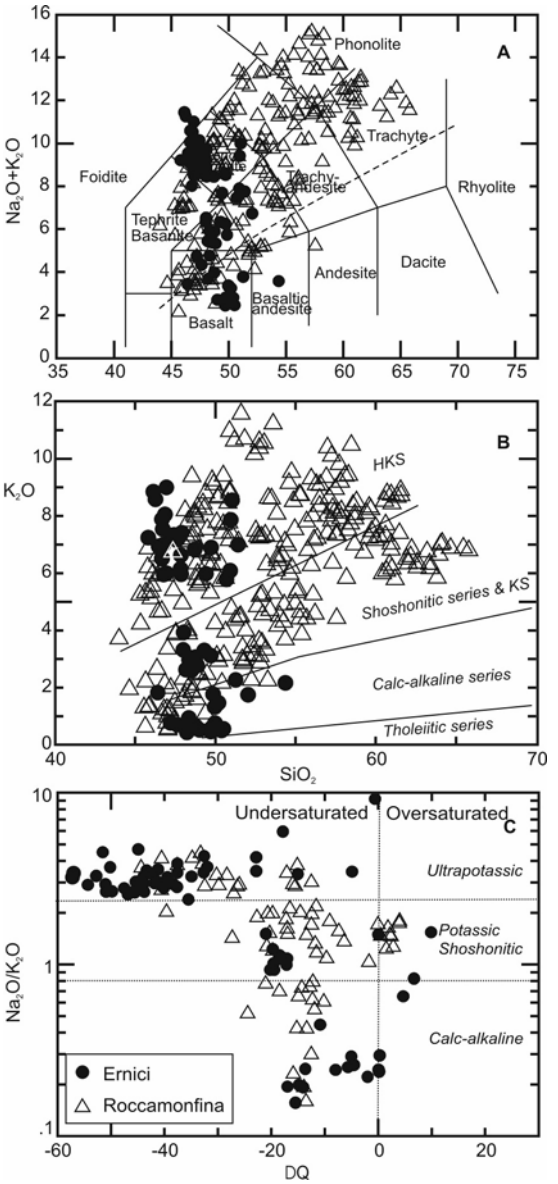

Fig. 5.3. A) TAS diagram for the Ernici and Roccamonfina volcanic rocks. The dashed line is the divide between alkaline and subalkaline fields of Irvine and Baragar (1971). B) K_2O vs. SiO_2 classification diagram (modified after Peccerillo and Taylor 1976). C) K_2O/Na_2O vs. ΔQ for the mafic rocks (MgO > 4 wt%). For definition of ΔQ see Chap. 1.

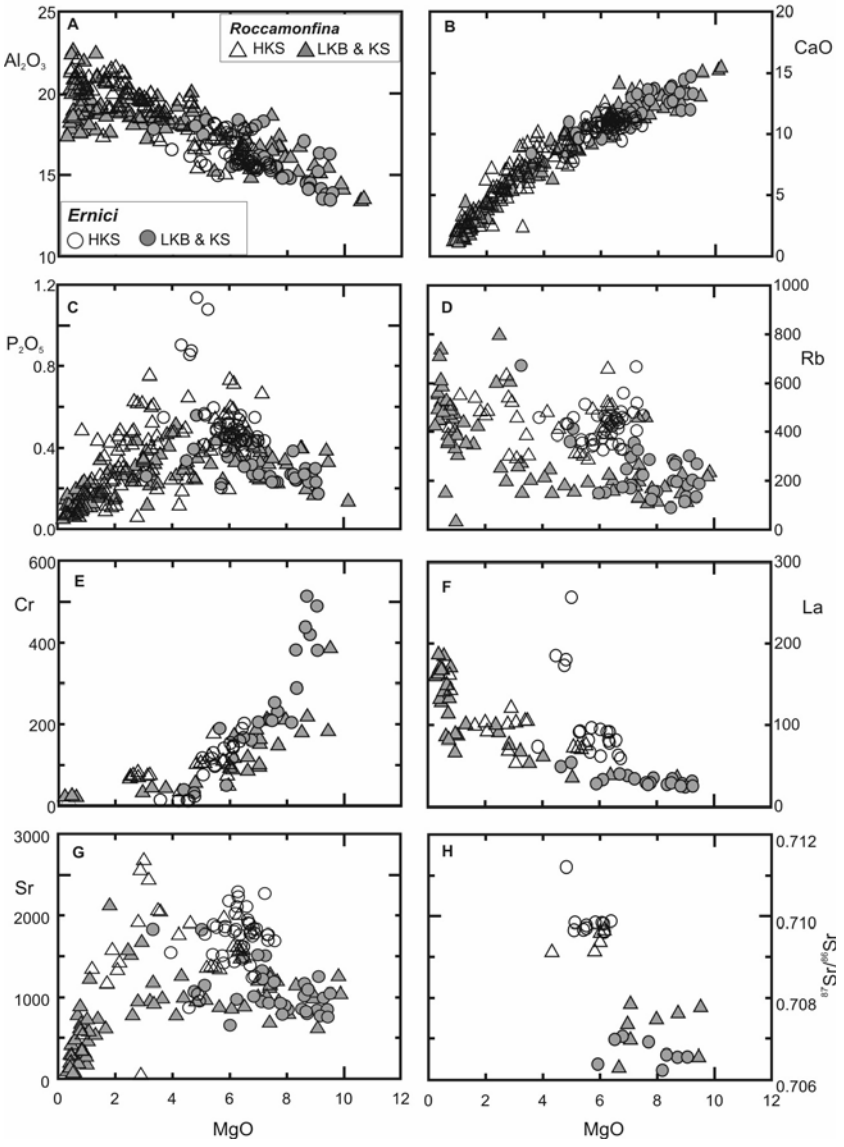

Fig. 5.4. Variation diagrams of selected major and trace elements and $^{87}Sr/^{86}Sr$ vs. MgO for Ernici and Roccamonfina volcanoes.

creases from LKB and KS to HKS rocks. All the rocks show relative depletions for HFSE and Ba, and positive spikes for LILE, LREE and Pb (Fig. 5.5b).

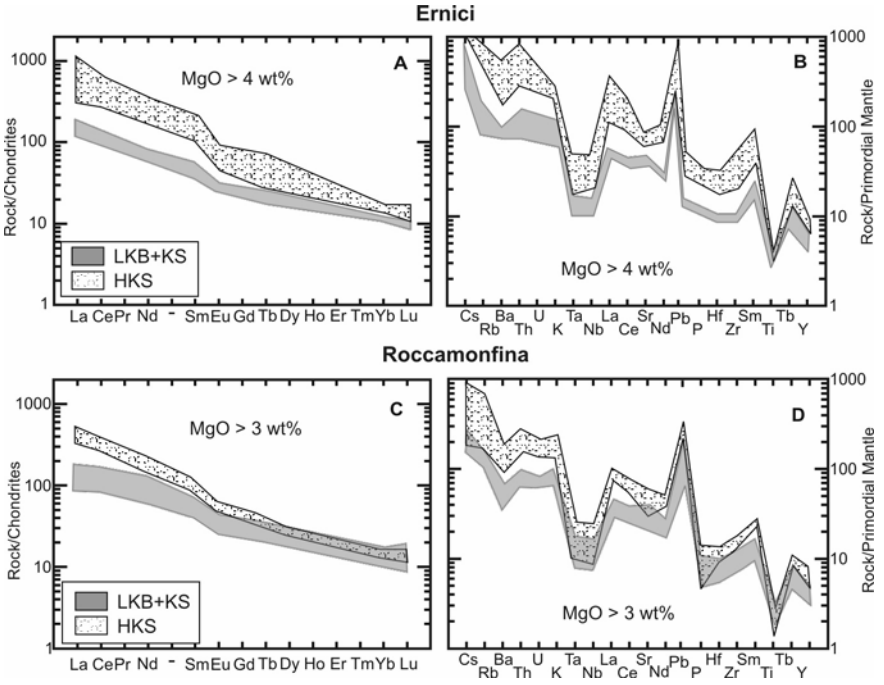

Fig. 5.5. REE and incompatible element patterns of mafic volcanics from Ernici (A, B) and Roccamonfina (C, D).

Sr-isotope ratios display a large variation from about 0.7062 to 0.7112. The lowest values ($^{87}Sr/^{86}Sr \sim 0.7062$ to 0.7070) are shown by the LKB and KS rocks, whereas the HKS rocks cluster around 0.7096-0.7099, with the single exception of a sample from Colle Castellone, which has an $^{87}Sr/^{86}Sr$ value of about 0.7112 (Civetta et al. 1981). Nd-isotope ratios show the opposite trend (Fig. 5.6a). Pb isotopic ratios exhibit moderate variation, with $^{206}Pb/^{204}Pb \sim 18.80$ to 18.90, $^{207}Pb/^{204}Pb \sim 15.67$ to 15.69 and $^{208}Pb/^{204}Pb \sim 39.00$ to 39.05 (Fig. 5.6b; Conticelli et al 2002). $^{176}Hf/^{177}Hf$ ratios determined on two samples yielded higher values for KS than for HKS (Table 5.2; Gasperini et al. 2002). Oxygen isotopic ratios determined by Turi et al. (1991) on whole rocks are variable ($\delta^{18}O \sim +5.8$ to +8.5), with most rocks clustering around $\delta^{18}O \sim +8.0$. Preliminary investigations on clinopyroxene separated from rocks with different potassium contents have shown lower values ($\delta^{18}O \sim +5.5$ to +6.0; Dallai, personal communication).

The mafic nature of all the Monti Ernici rocks, and the large differences in incompatible element abundances and isotopic signatures between rock

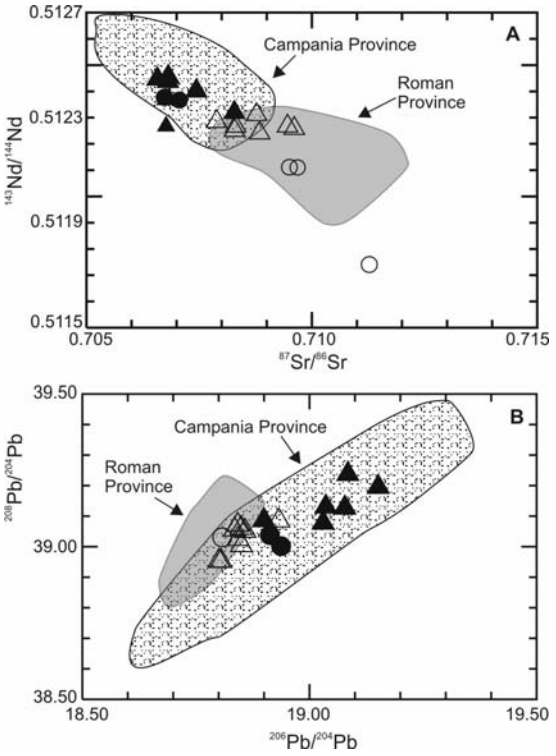

Fig. 5.6. Sr, Nd and Pb isotope variations for the Ernici and Roccamonfina volcanics. The fields of mafic rocks from the Campania and Roman provinces are also shown. Symbols as in Fig. 5.4.

groups with distinct enrichment in potassium, have led to the conclusion that the observed compositional variations cannot be the product of shallow level processes, such as fractional crystallisation or AFC (Civetta et al. 1981). In fact, assimilation of large volumes of crustal material (about 50 to 60%) would be necessary to drive isotopic compositions of LKB and KS rocks to those of HKS volcanics. This would produce an oversaturation in silica and much more dramatic decrease in MgO and compatible element contents than observed in the Ernici rocks. The monogenetic nature of the volcanic centres also supports rapid ascent of magmas from the mantle with little storage and evolution within the crust. Therefore, it has been concluded that most of the compositional variability shown by the Ernici rocks reveals the occurrence of compositionally different primary melts. However, the major and trace element variations within single series are likely the consequence of shallow level processes, including moderate degrees of fractional crystallisation and mixing between KS and HKS magma

(Civetta et al. 1981). Positive correlations between MgO and compatible trace elements, such as Cr, Ni and Sc, suggest separation of olivine and clinopyroxene. In contrast, negative correlations between MgO and Al_2O_3 and Sr rule out significant plagioclase fractionation. This agrees with petrographic evidence that the rocks contain few plagioclase phenocrysts, especially in the HKS rocks. The limited role for plagioclase fractionation means that the negative Eu anomalies observed in most samples, especially the HKS rocks, are not the product of fractional crystallisation processes and instead point to source characteristics and/or processes (see Chap. 4).

5.4. Roccamonfina

5.4.1. Volcanology and Stratigraphy

Roccamonfina is an asymmetric truncated composite cone, with a base diameter of about 20 km and a 6 km wide, NW-SE-elongated summit caldera that is breached on the east side (Fig. 5.7). The caldera floor, sited at about 600 m above sea level, hosts several lava flows and domes which reach a maximum altitude of about 1000 m. The volcano is composed of alternating lava flows, domes and pyroclastic deposits which were emitted both from central and parasitic vents between about 0.6 and 0.1 Ma. As shown in Fig. 5.3, rock compositions range from mafic to felsic, and from subalkaline to alkaline potassic and ultrapotassic (Appleton 1972; Giannetti and Ellam 1994). The volcanic activity took place in a zone of NW-SE trending extensional faults cut by younger N-S faulting (Chiesa et al. 1995; Fig. 5.1).

Most authors agree that the volcano developed in three main stages. A first stage dominated by emission of phonotephritic and tephriphonolitic lava flows and minor pyroclastics built up the main cone. Successively, large explosive eruptions formed several phonotephritic-phonolitic and trachytic pyroclastic deposits, the most prominent of which are known as the Brown Leucitic Tuff (BLT) and the White Trachytic Tuff (WTT; Giannetti and Luhr 1983; Luhr and Giannetti 1987). These rock units are associated with volcanic events that are believed to be responsible for caldera collapses, although it has been suggested that the caldera(s) may be formed as the result of rock removal by explosive eruptions (Chiesa et al. 1995). The final phases of activity were characterised by the emplacement of LKB and KS magmas forming lava flows, domes and some scoria cones both inside the caldera and along the flanks of the stratovolcano (e.g. Gian-

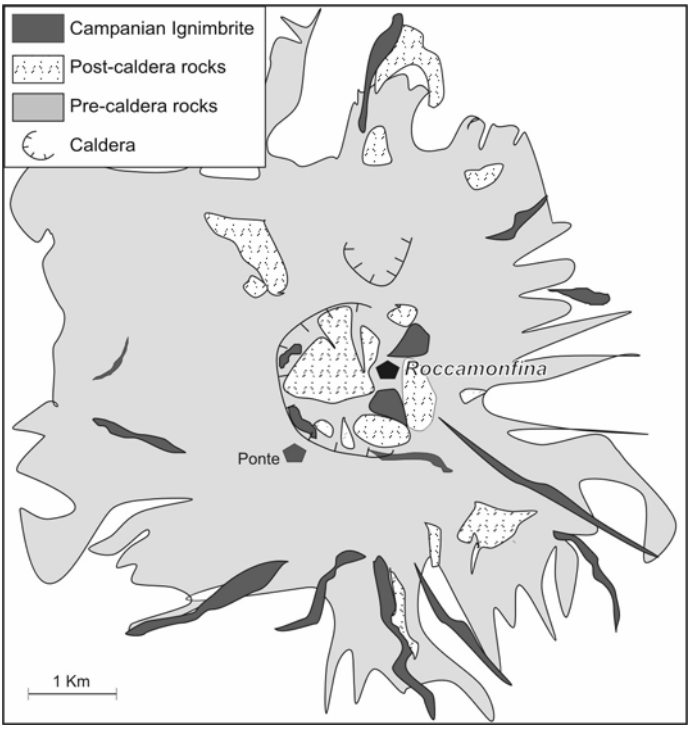

Fig. 5.7. Schematic geological map of the Roccamonfina volcano. Simplified after Giannetti and Luhr (1983).

netti and Luhr 1983; Luhr and Giannetti 1987; Cole et al. 1992; Chiesa et al. 1995). The Roccamonfina volcanics are covered discontinuously by product of the Campanian Ignimbrite (39 ka), a large pyroclastic deposit coming from Campi Flegrei (see Chap. 6).

The lowest exposed products of the cone have an age of about 550 ka. However, tephra recovered from the nearby areas have shown a somewhat older age of about 580 ka, which most probably represents the beginning of the volcanic activity at Roccamonfina. The youngest lava from the main cone has an age of about 370 ka. The BLT and WTT sequences result from various eruptions that occurred from about 380 to 230 ka. The activity inside the caldera and along the cone flanks developed between about 300 and 100 ka (Chiesa et al. 1995; Giannetti and De Casa 2000 and references therein).

5.4.2. Petrography and Mineral Chemistry

The Roccamonfina volcanic rocks range in composition from mafic to felsic. They exhibit a wide range of alkali contents and straddle the boundary between the subalkaline and alkaline fields of Irvine and Baragar (1971; Fig. 5.3a). The subalkaline rocks are silica undersaturated low-potassium basalts (LKB) whose K_2O and K_2O/Na_2O ratios plot within the field of calc-alkaline basalts (Fig. 5.3b, c). The KS rocks include K-trachybasalts, shoshonites, latites and trachytes. The ultrapotassic rocks range from leucite-tephrite to phonolite.

The LKB and KS basalts (potassic trachybasalts) are variably porphyritic with phenocrysts of olivine (up to Fo_{89-79}), diopside to salite clinopyroxene, which appears colourless to green in this section, and some plagioclase (about An_{90-80}) set in a groundmass composed of the same phases plus Fe-Ti oxides. Biotite is present in small amounts. The evolved KS rocks have porphyritic textures with phenocrysts of clinopyroxene, plagioclase, biotite and sanidine. Plagioclase is more abundant in the latites and decreases in the trachytes, where the phenocryst mineralogy is dominated by sanidine. Accessory phases include Fe-Ti oxides, apatite and in some cases amphibole, garnet and sphene (e. g. Giannetti 1964; Ghiara and Lirer 1977; Giannetti and Luhr 1983; Luhr and Giannetti 1987; Giannetti and Ellam 1994). The HKS mafic rocks are generally porphyritic with variable amounts of olivine, clinopyroxene and leucite phenocrysts set in a groundmass containing the same phases plus plagioclase, some nepheline and sanidine. The tephriphonolites and phonotephrites contain clinopyroxene, plagioclase, leucite and biotite phenocrysts, whereas phonolites are generally dominated by sanidine, some clinopyroxene, leucite and glass (Chiesa et al. 1995). Accessory phases include Fe-Ti oxides, apatite and sphene. Xenoliths of various origins, including metamorphic and sedimentary wall rocks and cumulate lithologies, are found at Roccamonfina (Appleton 1972; Giannetti and Luhr 1990).

In general, there is a strong compositional variability for single mineral phases in the Roccamonfina rocks. Plagioclase is generally zoned and ranges from bytownite to oligoclase. Diopside and salite clinopyroxenes coexist in many rocks and in single crystals. In contrast, olivine is generally rich in MgO, even in the evolved rocks, where crystals with Fo_{90-85} have been found. This has been interpreted as evidence of magma mixing (e.g. Giannetti and Luhr 1983; Luhr and Giannetti 1987).

5.4.3. Petrology and Geochemistry

The Roccamonfina rocks exhibit much larger variation of major elements than at Ernici (e.g. MgO ~ 10 to 0.1 wt%). Variation diagrams of major and trace elements vs. MgO (Fig. 5.4) show positive correlations for CaO, FeO_{total}, Cr and ferromagnesian elements. Incompatible elements increase sharply with decreasing MgO. The LKB and KS rocks show the highest MgO contents among the analysed samples, whereas the ultrapotassic rocks have less primitive compositions. An overall positive correlation is observed between incompatible elements and K_2O for rocks with similar MgO contents. However, Giannetti and Ellam (1994) recognised a decrease in incompatible elements from LKB to KS mafic rocks.

The REE patterns of mafic rocks are fractionated, with increasing LREE abundances and La/Yb ratios going from LKB and KS to the HKS. Negative Eu anomalies are observed in several mafic rocks, especially the HKS (Fig. 5.5c). REE patterns of some trachytes (not shown) have an upward concave pattern with strong depletion in intermediate REE. Incompatible element patterns of mafic rocks are strongly fractionated, and this increases with increasing K_2O. All of the rocks show relative depletions in the HFSE and Ba, and positive spikes for LILE, LREE and Pb (5.5d).

Sr-isotope ratios range from about 0.7062 to 0.7099. As in the case of Monti Ernici, the ultrapotassic rocks have higher Sr isotopic ratios than KS and LKB. However, there is no significant isotopic difference between LKB and mafic KS rocks. Nd-isotope ratios range from about 0.5122 to 0.5125 and decrease from KS to HKS (Fig. 5.6a). Pb-isotope ratios displaying slightly more radiogenic compositions in the LKB and KS than in the HKS rocks (Fig. 5.6b; Hawkesworth and Vollmer 1979; Vollmer and Hawkesworth 1980). Oxygen isotopic ratios determined by Taylor et al. (1979) on whole rocks are variable ($\delta^{18}O$ ~ +6.6 to +10.3) with most rocks clustering around $\delta^{18}O$ ~ +8.0.

The magmas from the Roccamonfina volcano record a more complex evolutionary pattern than the Ernici monogenetic centres. Major, trace element and isotopic variation suggests that the evolution of KS and HKS magmas at Roccamonfina was dominated by fractional crystallisation, with some magma mixing and assimilation of wall rocks. These processes generated rock suites that have evolved toward trachytic and phonolitic compositions, staring from K-trachybasalt and tephrite parental melts. HKS magmas evolved by separation of leucite, clinopyroxene and some plagioclase and magnetite, followed by fractionation of plagioclase and K-feldspar in the felsic compositions. The KS magmas underwent low-pressure separation of a clinopyroxene-plagioclase-biotite-magnetite as-

semblage and, finally, separation of plagioclase and K-feldspar (Appleton 1972).

There is abundant geochemical and petrographic evidence that the Roccamonfina magmas also underwent mixing and interaction with wall rocks. Mixing gave rise to a large number of hybrid magmas resulting from interaction between differently evolved melts of single series and between KS and HKS magmas (Giannetti and Luhr 1983; Luhr and Giannetti 1987). Mixing processes are supported by the common coexistence of pyroxenes with different compositions in the same rocks, as well as by the presence of juvenile material with contrasting major and trace element contents in single pyroclastic deposits. Assimilation of crustal rocks is indicated by the increase in Sr and O isotopic ratios from mafic to felsic rocks (Taylor et al. 1979).

As in the case of Ernici, the wide compositional variation of mafic magmas cannot be due to evolution processes and points to the occurrence of distinct parental melts generated in a heterogeneous source. Appleton (1972) has suggested that mafic melts were not necessarily independent magmas but may be related to each other by high pressure separation of eclogite from KS basalts to give HKS mafic magmas. Successively, mafic KS and HKS magmas underwent low-pressure fractionation. However, separation of eclogite conflicts with the sharp variation of radiogenic isotope compositions observed in the mafic KS and HKS rocks.

5.5. Petrogenesis

As for all K-rich Italian volcanoes, the Ernici and Roccamonfina mafic magmas contain mantle and crustal signatures, given by the coexistence in the same rocks of high MgO, Ni, Cr contents and elevated concentrations of K_2O, LILE and radiogenic Sr. Therefore, they require contributions from both mantle and crustal components in their magma genesis, similar to the Roman and Intra-Apennine provinces (see Chaps. 3 and 4). As demonstrated by several studies, evolution processes did not modify the first-order pristine compositional characteristics of the mafic magmas (e.g. Civetta et al., 1981; Giannetti and Ellam 1994). Therefore, there is a wide consensus on the hypothesis that the potassic nature of mafic magmas denote anomalous mantle sources that contained crustal components (e.g. Civetta et al. 1981; Giannetti and Ellam 1994 and references therein). Most authors suggest a subduction related origin for crustal components (e.g. Civetta et al. 1991; Beccaluva et al. 1991).

A peculiarity of Ernici and Roccamonfina volcanoes is given by the distinct, almost bimodal geochemical and isotopic compositions for mafic rocks. The variable degrees of enrichment in potassium, incompatible elements and radiogenic isotopes have been interpreted as evidence for variable chemical-physical conditions of melting within the mantle. Civetta et al. (1981) suggested that the KS and HKS parental magmas were generated by small degrees of partial melting (from about 1% to 5%) of a compositionally anomalous and heterogeneous phlogopite-bearing garnet peridotite. The KS mafic magmas were formed by higher degrees of partial melting than HKS. However, the observed isotopic differences led these authors to suggest a compositional heterogeneity of the source or disequilibrium melting. Giannetti and Ellam (1994) also suggest that the primary LKB, KS and HKS melts at Roccamonfina formed by variable degrees of partial melting of garnet peridotite. However, whereas the HKS parental melts were generated in a phlogopite-rich mantle, the KS and LKB magmas formed in an amphibole-bearing garnet peridotite. According to these authors, the decrease in several incompatible elements passing from LKB to KS (i.e. the reverse relation between K_2O and incompatible elements), indicates that the degree of partial melting increased from LKS to KS. However, the erratic behaviour of some trace elements (e.g. Rb and Cs; Giannetti and Ellam 1994) in these rocks casts doubts on this hypothesis, suggesting that syn- or post-eruptive processes may be responsible for compositional variations. Peccerillo and Manetti (1985) proposed that KS and HKS mafic melts are derived from different depths within the mantle. The KS magmas would be generated at relatively shallow depth where phlogopite melting produced saturated or slightly undersaturated liquids. In contrast, the HKS primary magmas would be formed at higher pressure where undersaturated compositions are favoured (Wendlandt and Eggler 1980b). Different degrees of partial melting also played a role, with the KS basalts being formed by higher amounts of melting than HKS. According to this hypothesis, the variable isotopic signatures of mafic KS and HKS magmas indicate a strong vertical compositional zoning within the upper mantle beneath Ernici and Roccamonfina. Such a zoning was an effect of percolation through the mantle of metasomatic agents released by subducted upper crustal material. Finally, Conticelli et al. (2004) suggest that all K-rich primary melts are generated in a single mantle source containing veins of phlogopite. The compositional differences between mafic KS and HKS would be controlled by the amount of phlogopite entering into the melt. Therefore, low degrees of partial melting would favour the formation of ultrapotassic magmas, whereas higher degrees of melting would result in dilution of incompatible element contents by virtue of melting significantly less enriched peridotite. Isotopic variations may also depend on this proc-

ess, providing that (i) there was strong isotopic disequilibrium between veins and mantle wall rocks and (ii) magmas were extracted very rapidly to avoid re-equilibration.

5.6. Nature of Mantle Metasomatism and Geodynamic Implications

The Ernici and Roccamonfina magmas exhibit peculiar compositional characteristics in terms of their very variable geochemical and isotopic signatures for potassic to ultrapotassic mafic rocks. These are not encountered in other potassic volcanoes of central Italy (i.e. Roman and Campanian provinces, with the possible exception of Vico volcano), where coexisting KS and HKS rocks have different potassium and incompatible trace element abundances but exhibit similar incompatible element ratios and radiogenic isotope signatures (Peccerillo 1999, 2002).

It has been recently pointed out that the HKS rocks at Ernici and Roccamonfina have incompatible element ratios and radiogenic isotope compositions very similar to Roman magmas, whereas the KS and LKB rocks resemble more closely Campanian magmas (Peccerillo and Panza 1999; Figs. 5.6, 5.8). This has led to the hypothesis that at least two distinct episodes of mantle metasomatism, respectively similar to those affecting the Roman and the Campanian provinces, took place in the Ernici-Roccamonfina area. As discussed in Chap. 4, the compositional modifications of the upper mantle beneath the Roman Province were produced by introduction of marly sediments into a lherzolitic mantle. In contrast, the metasomatic event affecting the mantle beneath the Campania Province is thought to have been generated by fluids and melts coming from an oceanic slab, with some contributions from pelagic sediments (Peccerillo 2002; see Chap. 6). Since the LKB and KS rocks are younger that the HKS volcanics both at Monti Ernici and Roccamonfina, it has been concluded that the Roman-type preceded the Campanian-type metasomatism (Peccerillo 1999; Peccerillo and Panza 1999). The superimposition of two distinct types of metasomatism would have generated a zoned mantle which was parental to potassic and ultrapotassic magmas.

The hypothesis for the occurrence of two distinct types of metasomatic events in a restricted area has important geodynamic implications. It has been suggested that the metasomatic modifications of the upper mantle beneath the Roman Province was produced by upper crustal material from the

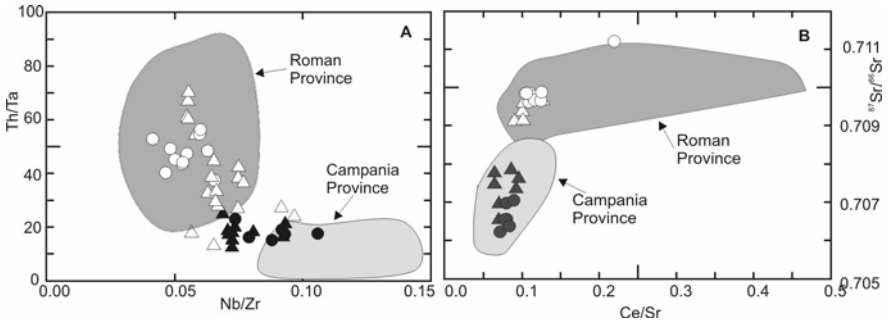

Fig. 5.8. Plots of incompatible element ratios for the mafic rocks (MgO > 3%) of Ernici and Roccamonfina volcanoes, compared with the mafic rocks from the Campania and Roman provinces. Symbols as in Fig. 5.4.

subducting Adriatic plate (e.g. Peccerillo et al. 1988; Serri 1990). In contrast, the common geochemical characteristics between some Campanian volcanoes and the eastern Aeolian arc have been interpreted as evidence that the metasomatism in the two regions was provided by the introduction of fluids and sediments from the oceanic Ionian plate (Peccerillo 2001). The occurrence of both Roman-type and Campanian-type metasomatism in the Ernici-Roccamonfina area suggests contributions from both the Adriatic and Ionian plates.

According to several authors, geodynamic evolution of the Tyrrhenian Sea and of the Apennines has been characterised by eastward migration of the subduction zone from Oligocene to present (e.g. Doglioni et al. 1999 with references). This caused eastward migration of the compression front, the locus of backarc extension, and the sites of orogenic magmatism across the Tyrrhenian basin from Miocene to present time (see Chaps. 9 and 10). However, the Tyrrhenian basin extended in an E-W direction until Pliocene times and successively turned to a NW-SE direction (e.g. Sartori 2003). This modification in the direction of the backarc spreading has been related to the different resistance opposed to slab retreat by the Adriatic continental plate and by the Ionian oceanic plate. These became decoupled from each other during the Pliocene, resulting in an independent evolution with different dipping direction and degrees of rollback (e.g. Carminati et al. 1998). Consequently, an early process of west-directed subduction of the joined Adriatic-Ionian plates would have been followed by a double process of west-directed subduction for the Adriatic plate and northwest-directed subduction for a clockwise rotated Ionian plate. The latter is presently highlighted by an active Benioff zone extending from the Aeolian arc to the Campania area. In this context, the westward directed subduction of the Adriatic plate could have been responsible for an early mantle contami-

nation event beneath the Roman and the Ernici-Roccamonfina zones. Successively, the Ionian subduction zone would have generated a new type of metasomatism beneath the Ernici-Roccamonfina area, as well as in Campania and in the eastern Aeolian arc.

5.7. Conclusions

Volcanism in the Ernici-Roccamonfina area is characterised by rocks with variable contents in potassium, from Low-K basalts to KS and HKS. At Ernici several monogenetic volcanoes were formed by eruption of mafic magmas. At Roccamonfina, effusive and explosive activity formed a stratocone with a large central caldera and various intra-caldera and flank cones and domes. The magmas again show large variations of potassium contents, but mafic types are subordinate to evolved rocks. At Ernici mafic magmas were erupted at the surface after moderate evolution dominated by fractional crystallisation and mixing. At Roccamonfina, the mafic KS and HKS magmas underwent strong fractional crystallisation, which generated evolved potassic and ultrapotassic series ranging from K-trachybasalt to latite and trachyte and from leucite-tephrite to phonolite, respectively. Low-potassic basalts are restricted to mafic compositions, both at Ernici and Roccamonfina.

The mafic magmas from Ernici and Roccamonfina volcanoes display variable abundances and ratios of incompatible elements as well as very distinct isotopic signatures. These were probably generated in a vertically zoned heterogeneous mantle source which was modified by two temporally and compositionally distinct metasomatic events. These episodes of mantle metasomatism may be related to subduction of the Adriatic plate beneath central Italy, followed by the arrival of new subduction-related material from the Ionian plate.

Table 5.2. Composition of selected Ernici and Roccamonfina rocks. Numbers in parentheses refer to data obtained on distinct though similar rock samples from the same locality as those analysed for the other elements. Source of data: 1) Civetta et al. (1981); 2) Hawkesworth and Vollmer (1979); 3) Vollmer and Hawkesworth (1980); 4) Giannetti and Ellam (1994); 5) D'Antonio et al. (1996); 6) Conticelli et al. (2002); 7) Gasperini et al (2002); 8) Frezzotti ML unpublished data; 9) Author's unpublished data.

Ernici volcanoes				
Rock type	Low-K basalt	K-trachy-basalt	Leucite-tephrite	Leucitite
Data source	8,9	1,5,6,7	1,5,6,7	1,6,8
SiO_2 wt%	48.84	48.18	47.39	46.13
TiO_2	0.87	0.77	0.72	1.00
Al_2O_3	14.63	16.41	17.85	16.92
FeO_{total}	8.49	7.20	5.85	6.49
MnO	0.16	0.15	0.13	0.14
MgO	8.35	8.68	6.36	4.80
CaO	13.24	11.98	10.53	9.67
Na_2O	2.68	2.82	2.51	2.60
K_2O	0.50	2.63	7.36	8.85
P_2O_5	0.22	0.27	0.54	1.14
LOI	1.39	0.66	0.57	1.83
Sc ppm	-	37	27	23
V	264	238	233	242
Cr	297	515	151	11
Co	41	38	32	30
Ni	65	89	58	30
Rb	153	112	335	451
Sr	987	841	1412	1815
Y	24	19	31	44
Zr	111	91	218	443
Nb	7.0	8	9	29
Cs	11.5	-	(23)	(63)
Ba	504	539	892	4057
La	35.7	30	83	257
Ce	69.3	65	177	398
Nd	34.2	26	81	166
Sm	6.84	5.8	14.5	35
Eu	1.73	1.42	3	5.3
Tb	0.81	0.8	1.5	2.5
Yb	2.00	1.9	2.5	2.2
Lu	0.31	0.23	0.41	0.41
Hf	2.83	2.7	6.1	11.3
Ta	0.49	0.53	0.53	2.3
Pb	17.8	15.2	33	(126)
Th	10.1	8.9	28	86
U	2.67	3.0	5.8	-
$^{87}Sr/^{86}Sr$	0.70659	0.70654	0.70974	0.71120
$^{143}Nd/^{144}Nd$	-	0.51237	0.51212	0.51173
$^{206}Pb/^{204}Pb$	-	18.929	18.831	-
$^{207}Pb/^{204}Pb$	-	15.665	15.690	-
$^{208}Pb/^{204}Pb$	-	38.997	39.048	-
$^{176}Hf/^{177}Hf$	-	(0.28276)	(0.28259)	-

Table 5.2 (continued)

Roccamonfina Volcano						
Rock type	Low-K basalt	K-trachy-basalt	Latite	Trachyte	Leucite-tephrite	Phonolite
Data source	4,2, 3	9	9	9	9	9
SiO_2 wt%	47.03	51.09	55.55	58.63	46.53	56.66
TiO_2	1.01	0.73	0.71	0.39	1.00	0.46
Al_2O_3	16.89	19.17	19.00	19.05	17.05	20.99
FeO_{total}	9.41	8.55	6.23	2.53	8.45	2.91
MnO	0.17	0.13	0.14	0.10	0.15	0.15
MgO	7.04	4.03	2.43	0.57	5.61	0.50
CaO	12.53	9.43	6.70	2.79	11.99	2.39
Na_2O	2.38	2.24	3.15	3.79	1.47	4.00
K_2O	1.00	2.95	5.09	8.19	5.03	9.32
P_2O_5	0.37	0.23	0.40	0.09	0.56	0.60
LOI	1.40	1.25	0.20	3.50	1.50	1.77
Sc ppm	33	31	20	13	21	15
V	287	200	134	72	259	86
Cr	85	30	35	6.5	123	23
Co	-	23	15	6.5	36	2
Ni	41	13	15	4	133	1
Rb	448	121	173	253	365	351
Sr	1120	930	1070	611	1764	1058
Y	-	25	38	34	39	42
Zr	109	133	170	300	211	384
Nb	6	11	16	33	12	23
Cs	-	8.2	8.1	21	25	-
Ba	706	550	756	189	987	1262
La	-	35	63	111	75	157
Ce	78.1	73	117	201	155	271
Nd	40.8	33	51	68	77	97
Sm	8.6	6.7	9.6	10.7	14.6	14.6
Eu	2.13	1.59	2.10	1.92	2.88	2.80
Tb	-	0.79	1.20	1.21	1.37	1.37
Yb	2.07	2.3	2.80	3.3	2.4	3.06
Lu	-	0.33	0.43	0.52	0.37	0.50
Hf	-	3.75	3.3	7.3	4.3	6.1
Ta	-	0.72	1.11	1.9	0.73	1.70
Pb	-	19	25	56	32	129
Th	-	9.3	21	39	26.3	39
U	-	2.5	4.9	8.6	6.1	9.1
$^{87}Sr/^{86}Sr$	0.70695	0.70691	0.70982	-	0.70931	-
$^{143}Nd/^{144}Nd$	(0.51245)	0.51241	0.51227	-	0.51224	-
$^{206}Pb/^{204}Pb$	(19.076)	19.081	19.123	-	18.830	-
$^{207}Pb/^{204}Pb$	(15.669)	15.672	15.682	-	15.688	-
$^{208}Pb/^{204}Pb$	(39.128)	39.133	39.169	-	39.041	-

6. The Campania Province, Pontine Islands and Mount Vulture

6.1. Introduction

The Campania Province (Fig. 6.1) represents the southernmost sector of the Plio-Quaternary volcanic belt along the Italian peninsula. It is formed by the active volcanoes of Somma-Vesuvio, Ischia and Campi Flegrei (Phlegraean Fields), and by the islands of Procida and Vivara. The Pontine Islands (Ponza, Palmarola, Zannone, Ventotene and Santo Stefano) are also sometimes included in the Campania Province, although petrological data suggest that only the eastern islands (Ventotene and Santo Stefano) and the younger rocks from Ponza (about 1 Ma) have compositions that resemble those of some Campanian volcanoes.

Volcanic rocks in Campania and Pontine Islands range from mafic to felsic and mostly have silica undersaturated potassic to ultrapotassic compositions (Fig. 6.2). Mafic rocks with K_2O contents close to calc-alkaline basalts have been found both as lavas and as lithic ejecta at Ventotene and Procida-Vivara. Pliocene (about 4.5 Ma) calc-alkaline rhyolites occur at Ponza, and 2 Ma old calc-alkaline basalts to andesites have been found by borehole drilling beneath the Campanian Plain north of Campi Flegrei.

Mount Vulture is a 0.8 to 0.1 Ma old stratovolcano rising as an isolated cone about 100 km east of Vesuvio. Although the Vulture rocks are alkaline and undersaturated in silica, they are enriched in both sodium and potassium, and show distinct composition with respect to other alkaline volcanoes in central-southern Italy. This led Washington (1906) to propose a separate magmatic province for Mount Vulture (Apulian Province). This suggestion is maintained in this review, although Vulture is described with Campanian volcanoes not only because of their geographic contiguity but also for some significant geochemical affinities. Vulture is also unique because of its tectonic position, located east of the Apennine chain on the western border of the Apulia foreland, a promontory of the African-Adriatic plate.

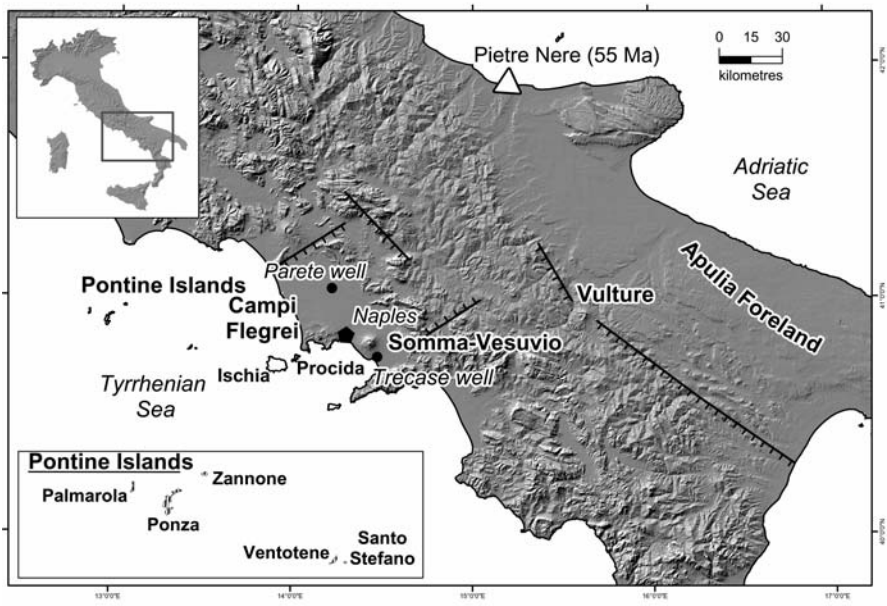

Fig. 6.1. Location map of the Campanian volcanoes, Pontine Islands and Mount Vulture.

A summary of the ages and compositional characteristics of volcanism in Campania, the Pontine Island and Vulture is given in Table 6.1. Data on representative rocks are reported in Table 6.2.

6.2. Regional Geology

The Campania Province, Pontine Islands and Mount Vulture are located along a transect that stretches from the Tyrrhenian Sea to the Apulia foreland, across the southern Apennine chain (Fig. 6.1). Southern Apennines consist of a number of thrusts, locally covered by Plio-Quaternary autochthonous shallow marine and continental sediments. Overthrusting of tectonic units occurred during Upper Oligocene to Lower Pleistocene compressional phases. These were followed by intensive extension, which generated fault systems both parallel and normal to the Apennine chain (Cello and Mazzoli 1999). Tectonic units (Sicilide, Liguride, Verbicaro-San Donato, Alburno-Cervati, Lagonegro, etc.) (Ippolito et al. 1975; Grasso 2001) consist of a wide variety of rock types (limestones, dolostones, flysch sequences, sandstones, marls, ophiolitic rocks, etc.) ranging

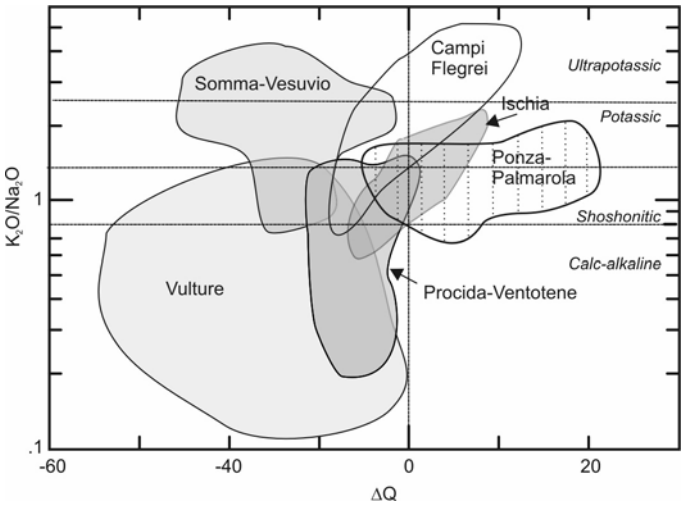

Fig. 6.2. K_2O/Na_2O vs. ΔQ diagram for the volcanic rocks from Campania Province, Pontine Islands and Mount Vulture. For definition of ΔQ, see Chap. 1.

in age from Upper Triassic to Miocene. They mostly represent basinal sequences formed on the border of the African plate, which were delaminated and superimposed over the Apulia foreland. The latter is located east of the Apennine chain and consists of Mesozoic to Tertiary platform carbonates (e.g. Ogniben et al. 1975; Grasso 2001; Patacca and Scandone 2001; Vai and Martini 2001).

The volcanic centers of the Campania Province developed inside Quaternary extensional basins along the Tyrrhenian Sea border at the intersection between NE-SW and NW-SE fault systems. The Pontine Islands form a row of volcanoes with a W-E trend, offshore the Campania Province, and along the so-called 41st Parallel Tectonic Line (Serri 1990; Bruno et al. 2000). Vulture is located at the eastern border of the Apennine compression front, in an extensional tectonic setting affecting the border of the Apulia foreland.

The thickness of the lithosphere along the Pontine-Campania-Vulture transect increases from about 50 km along the Tyrrhenian Sea border to more than 110 km in the Apulia foreland (Calcagnile and Panza 1981). The depth of the Moho increases from about 20-25 km offshore the Tyrrhenian Sea coast to 40 km beneath the internal zones of the Apennines, to decrease to about 30 km beneath the Apulia foreland (e.g. Locardi and Nicolich 1988; Piromallo and Morelli 2003). In contrast with other zones of the Apennine chain, the sector running from the Campania Province to

Table 6.1. Age and composition of volcanism in Campania, the Pontine Islands, and Mount Vulture.

VOLCANO	AGE	VOLCANOLOGY and PETROLOGY
Somma-Vesuvio	30 ka to 1944 AD	- Stratovolcano (Mount Somma) with multiple caldera and an intracaldera cone (Vesuvio) formed of slightly to strongly silica undersaturated trachybasalt and leucite-tephrite to trachyte and phonolite.
Campi Flegrei	About 0.2 Ma to 1538 AD. Buried volcanism 2 Ma old	- Multicentre volcanic complex with two nested calderas and several monogenetic cones and maars, formed of prevailingly pyroclastic rocks with trachybasalt to trachyte-phonolite composition.
Ischia island	150 ka to 1302 AD	- Volcano-tectonic horst formed of prevailing pyroclastic rocks with trachybasaltic to dominant trachytic composition.
Procida-Vivara islands	55 to 17 ka	- Coalescing explosive centres formed of basalt, K-trachybasalt to trachyte pyroclastics.
Pliocene buried volcanism	2 Ma	- About 1300 m thick sequence of calc-alkaline basalt to andesite underlying Campi Flegrei potassic rocks.
Ponza, Palmarola, Zannone, La Botte	4.2 to 1 Ma	- Lava flows, domes, breccias and hydrovolcanic products formed of Pliocene calc-alkaline rhyolites and Pleistocene peralkaline rhyolites and potassic trachytes.
Ventotene and Santo Stefano islands	0.8 Ma to < 130 ka	- Stratovolcano with a caldera formed of basalt, K-trachybasalt to trachyte lava flows, domes (Santo Stefano) and pyroclastics.
Vulture	0.8 to 0.13 Ma	- Stratovolcano with a summit caldera, intracaldera explosion craters and some parasitic centres formed of lavas and pyroclastics with Na-K-alkaline tephrite, foidite, melilitite, haüynophyre, and phonolite compositions. Late carbonate-rich pyroclasts.

the Vulture area is characterised by a moderate elevation and by a positive Bouguer anomaly, which crosses the Apennines connecting the positive anomalies of Tyrrhenian Sea and Apulia (Turco and Zuppetta 1998). Such a lineament is sited along the continuation of the 41° Parallel line, which represents a divide between northern and southern Tyrrhenian basins (Bruno et al. 2000)

6.3. Campania Province

6.3.1. Somma-Vesuvio

6.3.1.1. Volcanology and Stratigraphy

Somma-Vesuvio is a 1279 m high composite volcano consisting of an older dissected cone (Somma) with a summit polyphasic asymmetrical caldera (Fig. 6.3), and an intra-caldera cone (Vesuvio). The onset of the Somma-Vesuvio activity post-dates the Campanian Ignimbrite eruption of Campi Flegrei (39 ka) and is probably younger than 30 ka, although a much older volcanic activity (some 0.4 Ma; Brocchini et al. 2001) has been indicated by deep borehole drillings in the Somma-Vesuvio area. Vesuvio is younger than the 79 AD eruption that destroyed Pompeii and Herculaneum, and probably started to grow after the 472 AD eruption, inside the amphitheatre shaped depression of the Somma caldera (Santacroce 1987; Rolandi et al. 1998; Santacroce et al. 2003). The lowest exposed rocks of Somma volcano consist of alternating mafic lava flows and scoriae with a trachybasalt to potassic tephrite composition. Starting from about 18 ka up to 79 AD, the style of volcanic activity became more explosive, and plinian eruptions took place, affecting evolved potassic magmas ranging from latite and trachyte to phonolite and tephriphonolite. Plinian activity was preceded by long periods of volcanic quiescence, and was accompanied by volcano collapses that formed the Somma caldera; emissions of lavas and pyroclastics by strombolian, vulcanian and subplinian eruptions also occurred during inter-plinian phases. After the 79 AD eruption, Vesuvio has been characterised by strombolian and effusive activity alternating with periods of 200-500 years of volcanic quiescence (e.g. 472 AD and 1631 AD), each closed by large explosive eruptions.

The plumbing system of the Somma-Vesuvio volcano has been the subject of much research and debate. According to some authors (e.g. Joron et al. 1987; Cioni et al. 1997; Santacroce et al. 2003 and references therein) a shallow magma chamber has been operating in conditions of alternated periods of open or obstructed conduit. This reservoir was periodically replenished by mafic magmas coming from depth. When the conduit was obstructed, magma injection generated expansion of magma chamber and extensive fractional crystallisation, with generation of felsic melts. These

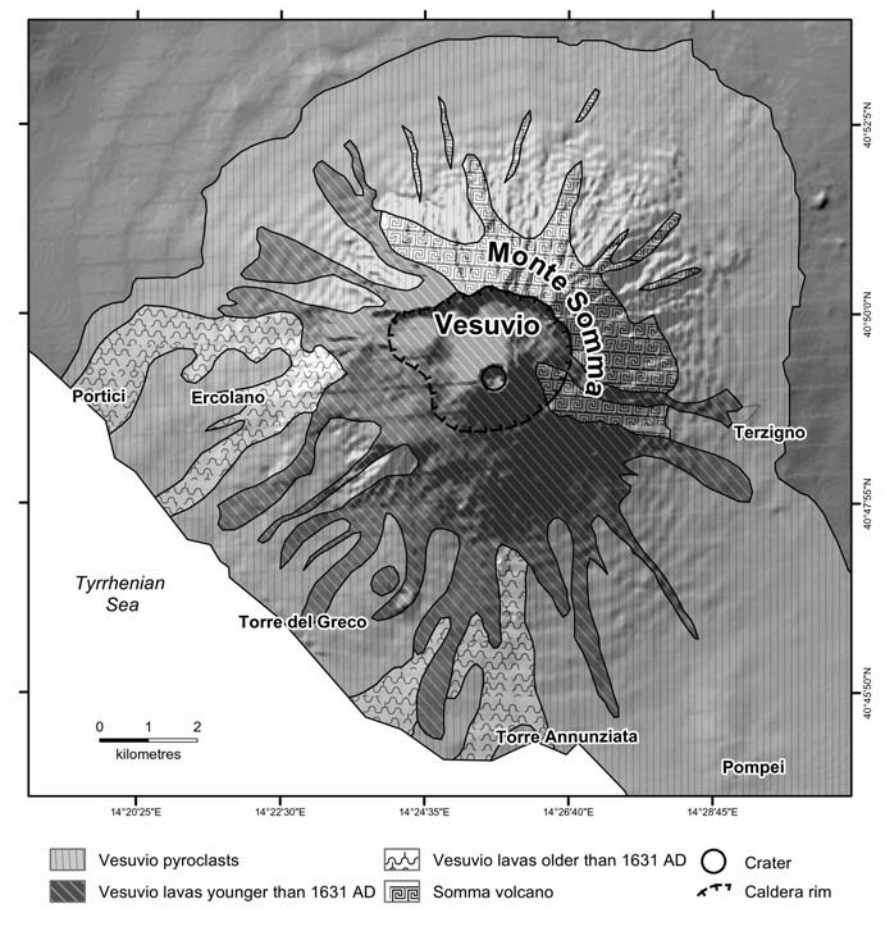

Fig. 6.3. Sketch map of Somma-Vesuvio volcano. Simplified after Civetta et al. (2004).

accumulated at the top of the reservoir which became chemically zoned (Cioni et al. 1995). Stronger explosions occurred after quiescent periods reflecting the recharge of the system. In these cases the magnitude of explosions correlates very significantly, though not exclusively, with the duration of repose time (Santacroce et al. 2003). During periods of open conduit, the magma chamber was smaller and the arrival of fresh magma resulted in either quiet lava effusions or moderately explosive eruptions. The 1944 eruption marks the transition from open to obstructed conduit conditions.

Other authors argue that geophysical studies have been unable to reveal a shallow level reservoir of significant size (Zollo et al. 1998; Auger et al. 2001). Therefore, it has been suggested that the plumbing system of Somma-Vesuvio consists of a complex feeding column connecting several small magma chambers sited at different depths beneath the volcano. These are believed to represent sites of magma ponding and crystallisation and of fluid entrapment in magmatic minerals and in xenoliths. Belkin et al. (1985) and Belkin and De Vivo (1993) found a distribution of CO_2 fluid inclusion densities suggesting an entrapment at about 4-5 km, at 8-10 km and at 12 km. These were interpreted to reveal the occurrence of various magma reservoirs beneath the volcano. Two deep magma chambers were also suggested by Cortini and Scandone (1982), on the basis of Sr-isotope and xenolith compositional variations.

6.3.1.2. Petrography and Mineral Chemistry

Joron et al. (1987) distinguished three main rock series at Somma-Vesuvio. These are characterised by different ages, degrees of silica undersaturation and enrichment in potassium. Except for a few outliers, the rocks of the first series (older than about 8 ka) consist of slightly silica undersaturated potassic trachybasalt to trachyte (Fig. 6.4). A second series (about 8 ka to 79 AD) consists of phonotephrites, tephriphonolites and phonolites with intermediate degrees of silica undersaturation. Finally, a third series (younger than 79 AD) shows a strongly undersaturated leucite

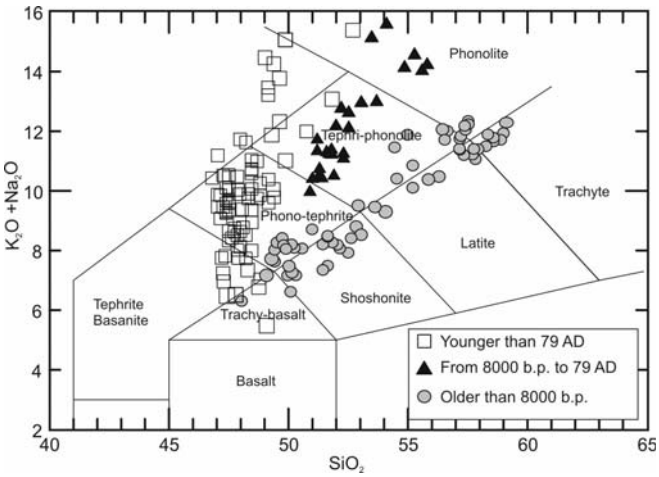

Fig. 6.4. TAS classification diagram for Somma-Vesuvio volcanics. Note different trends for groups of rocks with different ages.

tephrite, leucitite, phonotephrite, tephriphonolite and phonolite composition. However, trachybasalts are also found among the products of the 1906 eruption (Santacroce et al. 1993). Ayuso et al. (1998) also recognised three series on the basis of trace element concentrations, although time limits among series were somewhat different than those of Joron et al. (1987).

The rocks belonging to the slightly undersaturated older series display moderately to poorly porphyritic textures, with decreasing phenocryst contents from mafic to felsic rocks. Plagioclase and clinopyroxene are ubiquitous phenocrysts; olivine and leucite occur in the mafic rocks, whereas biotite, K-feldspar and some amphibole are observed in the latites and trachytes. Groundmasses range from holocrystalline to hypocrystalline and contain the same phases as the phenocrysts plus Fe-Ti oxides, accessory garnet, apatite and variable amounts of glass. Trachytic pumices are strongly vesicular and range from aphyric to poorly porphyritic with a few phenocrysts of sanidine, plagioclase, green clinopyroxene and Fe-Ti oxides.

Phonotephrites of the mildly undersaturated series are strongly porphyritic with phenocrysts of plagioclase, clinopyroxene and leucite set in a groundmass formed by the same phases and glass. Tephriphonolites include lavas and pumices exhibiting variably porphyritic textures in thin section, with phenocrysts of clinopyroxene (green to colourless in thin section), plagioclase, leucite, alkali-feldspar, biotite and Fe-Ti oxides, set in a glassy groundmass. Melanite garnet and amphibole have been sometimes observed. Phonolites consists of pumices with a poorly porphyritic to aphyric vesicular texture; phenocrysts are represented by clinopyroxene, sanidine, some biotite and leucite set in a glassy groundmass; minor phases include garnet, olivine and calcic plagioclase; nepheline is observed in some rocks.

Tephrites, leucitites and phonotephrites of the highly undersaturated younger series are more strongly porphyritic than older rocks. Phenocrysts consist of dominant clinopyroxene, and minor leucite and olivine; groundmass is holocrystalline to hypocrystalline and contains the same phases as the phenocrysts plus plagioclase, opaques and some brown mica. Tephriphonolites are strongly porphyritic with phenocrysts of leucite, clinopyroxene and plagioclase, and sporadic olivine and biotite set in holocrystalline to hypocrystalline groundmass formed by the same phases, Fe-Ti oxides and accessory apatite. Phonolites consist of vesicular porphyritic pumices made of leucite and clinopyroxene phenocrysts and of a glassy matrix containing plagioclase, sanidine, garnet, amphibole, Fe-Ti oxides and sporadic haüyne.

Clinopyroxene shows mainly a diopsidic composition with common occurrence of zoned crystals showing salitic rims. Olivine is scarce and exhibits a large compositional variation both in the phenocrysts (up to about Fo_{90}) and in the groundmass (about $Fo_{70\text{-}45}$). Some highly forsteritic crystals (up to Fo_{94}) probably represent xenocrysts from disaggregated skarns. Plagioclase is strongly zoned and exhibits a wide range of compositions ($An_{90\text{-}50}$). Sanidine is more sodic in the slightly undersaturated latites and trachytes than in the highly undersaturated tephriphonolites and phonolites. Leucite shows an almost stoichiometric composition. Mica is rich in fluorine and ranges from phlogopite to biotite, the latter being confined to felsic products. Amphibole has potassic ferropargasite composition (Cioni et al. 1997).

Several ejected blocks are found in the Somma-Vesuvio pyroclastics. These include lavas, sedimentary carbonate rocks, skarns, and mafic and ultramafic xenoliths (e.g. Joron et al. 1987). The latter have been suggested

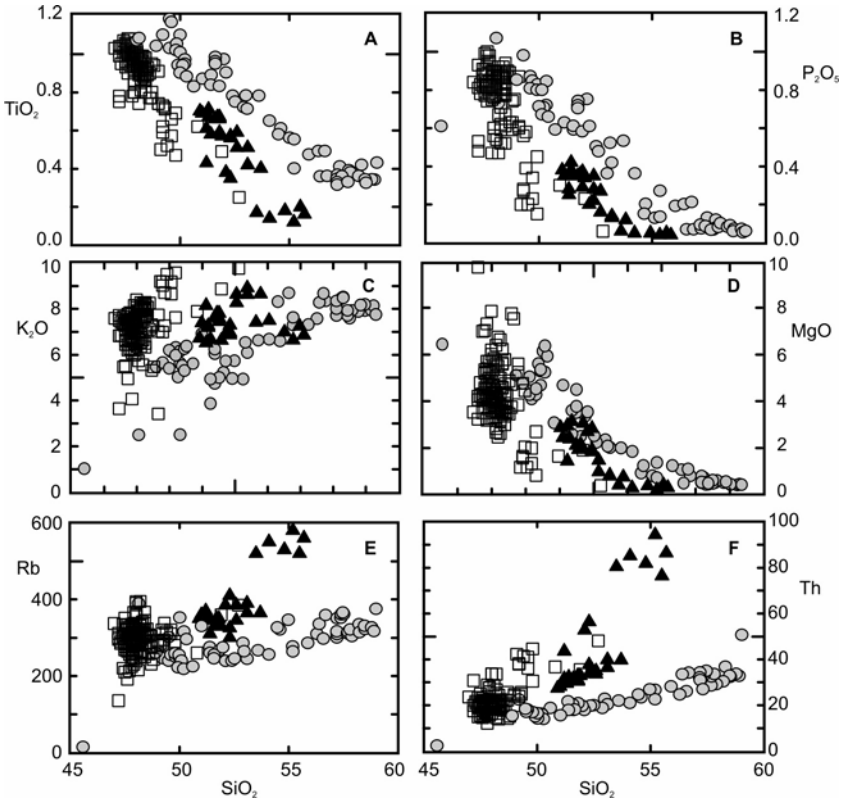

Fig. 6.5. Variation diagrams of selected major and trace elements vs. SiO_2 for Somma-Vesuvio rocks. For symbols see Fig. 6.4.

to represent either cumulates, sometimes affected by post-crystallisation deformation, or possibly mantle material that partially survived magma chamber processes (Cigolini 1999).

6.3.1.3. Petrology and Geochemistry

Variation diagrams of selected major and trace elements for Somma-Vesuvio rocks are shown in Fig. 6.5. There is an overall decrease in TiO_2, P_2O_5, MgO, CaO, and FeO_{total} with increasing silica, and an increase in K_2O, Na_2O and incompatible elements (e.g. Th, Rb, LREE etc.). Most elements display different trends in the three rock series. Distinct trends are also shown by several inter-element diagrams (Fig. 6.6), as pointed out by Ayuso et al. (1998). However, all trends seem to originate from a single starting composition. Volatile elements (F, Cl, B) show high concentrations, of several thousand ppm for all the rocks (e.g. Somma et al. 2001).

REE patterns show variable fractionation, with small negative Eu anomalies, which increase in trachytes and phonolites (Fig. 6.7a). HREE depletion is observed is some phonolites. Patterns of incompatible elements normalised to primordial mantle compositions for mafic rocks (Fig. 6.7b) are fractionated and contain positive spike of Pb and negative anomalies of HFSE. However, these are less sharp than in other Italian ultrapotassic rocks, such as those of the Roman Province, and HFSE abundances are much higher than observed in MORBs (Sun and McDounough 1989).

Sr, Nd and Pb isotopic compositions show moderate variations and similar range of values for the three rock series ($^{87}Sr/^{86}Sr$ ~ 0.7063 to 0.7080; $^{143}Nd/^{144}Nd$ ~ 0.5124 to 0.5125; $^{206}Pb/^{204}Pb$ ~ 18.90 to 19.10; $^{207}Pb/^{204}Pb$ ~ 15.61 to 15.71; $^{208}Pb/^{204}Pb$ ~ 38.90 to 39.30 (Fig. 6.8; Hawkesworth and Vollmer 1979; Civetta et al. 1991a; Civetta and Santa-

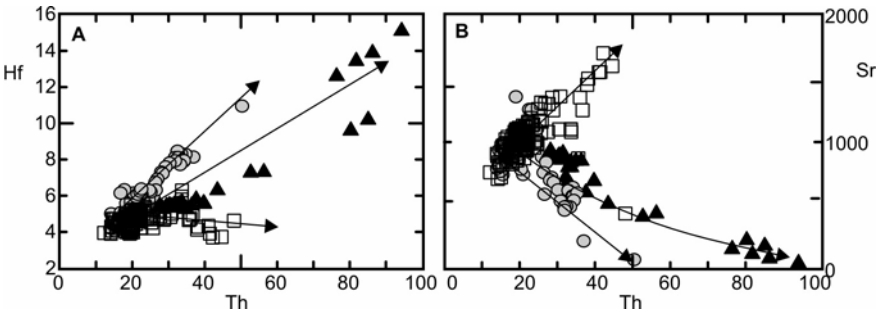

Fig. 6.6. Inter-element variation diagrams for the Somma-Vesuvio rocks. For symbols see Fig. 6.4.

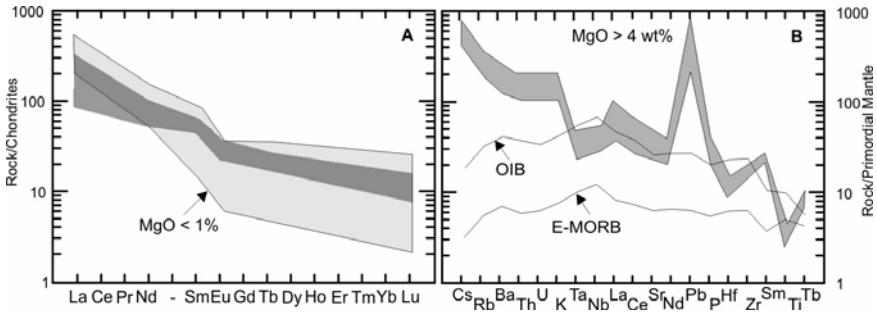

Fig. 6.7. REE (A) and incompatible element (B) patterns (restricted to mafic compositions) for Somma-Vesuvio rocks. Patterns of average E-MORB and OIB (Sun and McDonough 1989) are also shown.

croce 1992; Cioni et al. 1995; Ayuso et al. 1998; Somma et al. 2001). Significant isotopic variations have been observed within single cycles of volcanic activity, possibly indicating continuous variations of magmas feeding the erupting system (Cortini and Hermes 1981; Civetta and Santacroce 1992; Somma et al. 2001). $^{176}Hf/^{177}Hf$ isotopic ratios determined on two samples gave values of about 0.28278 (Gasperini et al. 2002).

Oxygen isotope signatures of Vesuvio rocks show wide variations ($\delta^{18}O$ ~ +7.0 to +10.0) and are negatively correlated with MgO (Ayuso et al. 1998). Helium isotope studies on clinopyroxene and olivine from historical lavas gave values of R/R_A ~ 2.2 to 2.7, close to ratios found in the fumaroles of Campanian volcanoes (Tedesco et al. 1990; Graham et al. 1993).

Variation of many major and trace elements in the Somma-Vesuvio rocks suggest that fractional crystallisation was a main mechanism in magma evolution. Different trends shown by the various rock series for both major and trace elements have been interpreted either to reveal the presence of different types of parental magma and/or to indicate fractionation dominated by different relative amounts of clinopyroxene and feldspar, possibly as a consequence of variable pressure during fractionation (Joron et al. 1987; Trigila and De Benedetti 1993).

A large number of data (e.g. compositionally zoned phenocrysts, contrasting types of clinopyroxenes coexisting in the same rocks, geochemical and isotopic variations within juvenile clasts from single eruption, etc.) suggest that mixing was also a main evolutionary process of the Somma-Vesuvio magmas (e.g. Civetta et al. 1991a). Assimilation of the wall rocks is also demonstrated by a wealth of data, including the presence of abundant skarn xenoliths, which testify to interaction with carbonate wall rocks. Civetta et al. (2004) proposed a process of magma contamination at mid

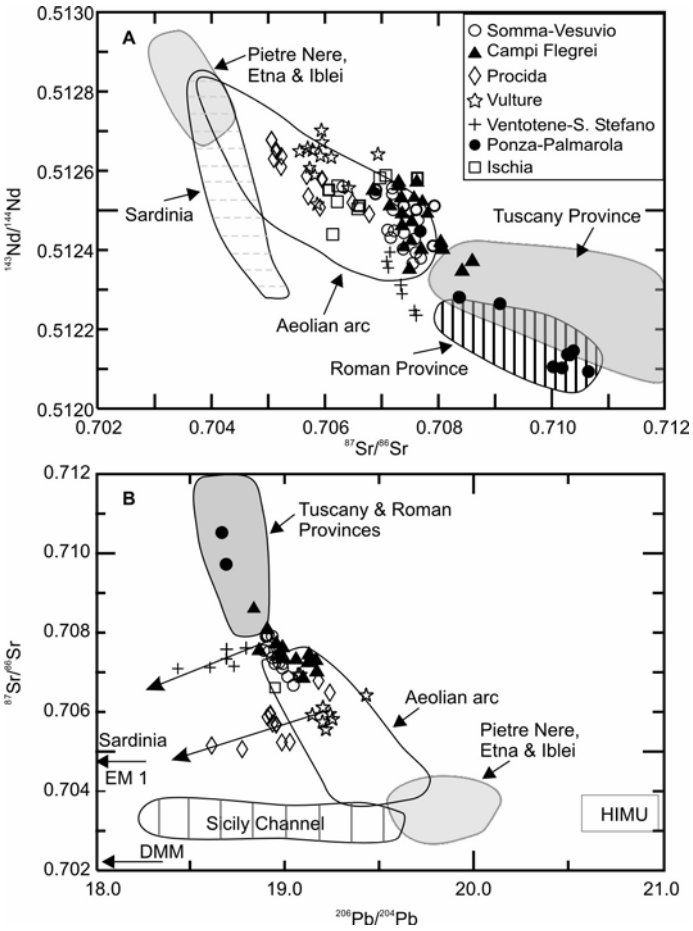

Fig. 6.8. Sr-Nd-Pb isotopic variation of Campania, Pontine Islands and Vulture volcanoes. The fields of other Italian magmatic provinces and HIMU, EM1 and DMM mantle compositions are also shown.

crustal depth (10-20 km), mostly based on the results of a thermal model of the deep magma chamber. The increase of $\delta^{18}O$ with decreasing MgO could represent an evidence for this process, although Ayuso et al. (1998) suggest that oxygen isotope variation may have been influenced by other processes, such as fluid flux through the volcanic system. Also, differences for radiogenic isotope ratios may partially result from wall rock assimilation, although it is not clear how much of this variation depends on heterogeneities of primary melts or on shallow level processes.

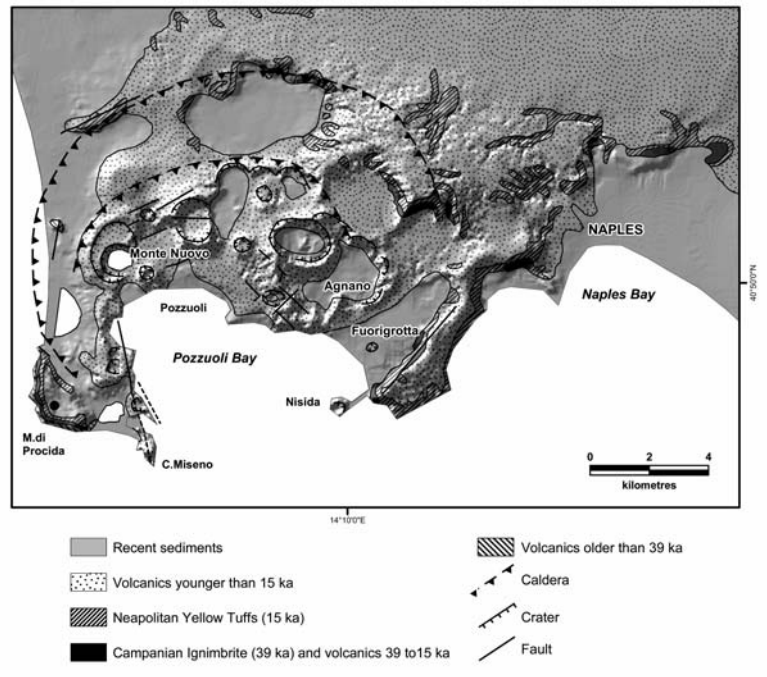

Fig. 6.9. Sketch geological map of Campi Flegrei volcanic complex. Simplified after Orsi et al. (1996).

6.3.2. Campi Flegrei (Phlegraean Fields)

6.3.2.1. Volcanology and Stratigraphy

The Campi Flegrei volcanic complex is formed by two nested calderas and by several monogenetic cones and craters (Fig. 6.9). The calderas are related to gigantic explosive eruptions which deposited the Campanian Ignimbrite and Neapolitan Yellow Tuff (Orsi et al. 1995). Campanian Ignimbrite eruption (39 ka) (De Vivo et al. 2001), is a phreatoplinian event that outpoured some 200 km^3 of phonolitic-trachytic pyroclastics. The Neapolitan Yellow Tuff eruption (15 ka), discharged some 40 km^3 of latite to trachyte-phonolite pyroclastics, forming an internal caldera (Orsi et al. 1995). The pyroclastic rocks of these eruptions rest over older products, some of which have been dated between about 157 ka to 205 ka (De Vivo

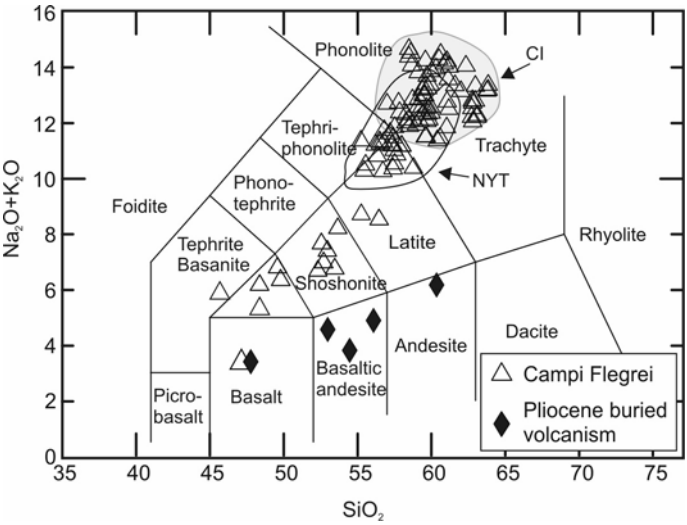

Fig. 6.10. TAS classification diagram for Campi Flegrei and for buried Pliocene rocks beneath Campi Flegrei (Parete-2 well). Circled fields indicate compositions of the Campanian Ignimbrite (CI) and Neapolitan Yellow Tuff (NYT) pumices.

et al. 2001). The volcanism younger than 15 ka concentrated inside the caldera and has been characterised by several explosive events. These generated a large number of craters and cones, which pockmark Campi Flegrei caldera and represent a main morphological feature of the area (e.g. Orsi et al. 1996; Santacroce et al. 2003 and references therein). The latest eruption dates back to 1538 AD when the Monte Nuovo phonolitic cone was formed. After this eruption, Campi Flegrei has been subjected to a number of volcanic crises characterised by strong soil uplift and intense shallow seismicity, but no eruptions have occurred. The main unrest events in the past 40 years, took place in 1969-72 and 1982-84, and generated uplifts of 170 and 180 cm, respectively (e.g. Orsi et al. 1996).

The magmatic system of the Campi Flegrei volcano is believed to consist of a shallow-level trachytic reservoir, which has been periodically refilled by a deep magma chamber located at depths of 10-15 km. The shallow reservoir would be hosted by sedimentary arenaceous rocks, and has been the site of complex processes dominated by extensive fractional crystallisation and mixing. The deeper chamber developed within the Hercynian basement. Here, magmas experienced complex evolutionary processes including significant assimilation of wall rocks before ascending to shallow levels or being erupted at the surface directly through lateral fractures (Pappalardo et al. 2002).

6.3.2.2. Petrography and Mineral Chemistry

The Campi Flegrei rocks consist of dominant pyroclastic deposits and minor lavas (Armienti et al. 1983; Rosi and Sbrana 1987). Compositions are slightly undersaturated to oversaturated in silica and range from trachybasalt to trachyte and phonolite on the TAS diagram (Figs. 6.2, 6.10). Some phonolites are peralkaline. Overall mafic and intermediate rocks show moderate enrichment in potassium. The rocks older than 39 ka and the Campanian Ignimbrite have a composition straddling the limit between trachyte and phonolite; the Neapolitan Yellow Tuff ranges from latite to trachyte and phonolite (Fig. 6.10; Pappalardo et al. 1999; Signorelli et al. 1999). Rocks younger than 12 ka have a wider compositional range, from trachybasalt-shoshonite to trachyte and phonolite (D'Antonio et al. 1999a).

Rock textures range from porphyritic to sub-aphyric, with phenocryst contents decreasing from trachybasalts to trachytes and phonolites (Armienti et al. 1983). The least-evolved rocks have abundant clinopyroxene and plagioclase, minor olivine and rare biotite and magnetite phenocrysts set in a groundmass formed by the same phases. Latites contain clinopyroxene, plagioclase and biotite phenocrysts, set in a hypocrystalline groundmass made of abundant sanidine, Fe-Ti oxides and glass. Trachytes and phonolites range from holocrystalline to almost glassy, with phenocrysts of alkali-feldspar, minor clinopyroxene, biotite, plagioclase, Fe-Ti oxides and rare amphibole and sodalite-group minerals. Accessory phases include apatite, zircon and sphene (Armienti et al. 1983; Rosi and Sbrana 1987).

Clinopyroxene composition ranges from diopside in the mafic rocks to ferrosalite in the felsic rocks. Single crystals often show colour and compositional zoning in thin section. Olivine (about Fo_{80}) is commonly altered to iddingsite. Plagioclase (about $An_{90\text{-}35}$) is generally zoned and is mantled by sanidine in the most evolved rocks (Armienti et al. 1983).

6.3.2.3. Petrology and Geochemistry

Major elements variation diagrams for Campi Flegrei rocks (Fig. 6.11) show decrease in TiO_2, MgO, CaO, FeO_{total} and P_2O_5, and increase in Na_2O, K_2O and Al_2O_3 from trachybasalt to trachytes, but with large scattering. Ferromagnesian trace elements (Ni, Co, Cr, Sc) and Sr show an overall decrease with increasing silica; in contrast, incompatible trace elements (Rb, Th, Y, Ta, Nb, Zr and LREE) increase sharply from mafic to

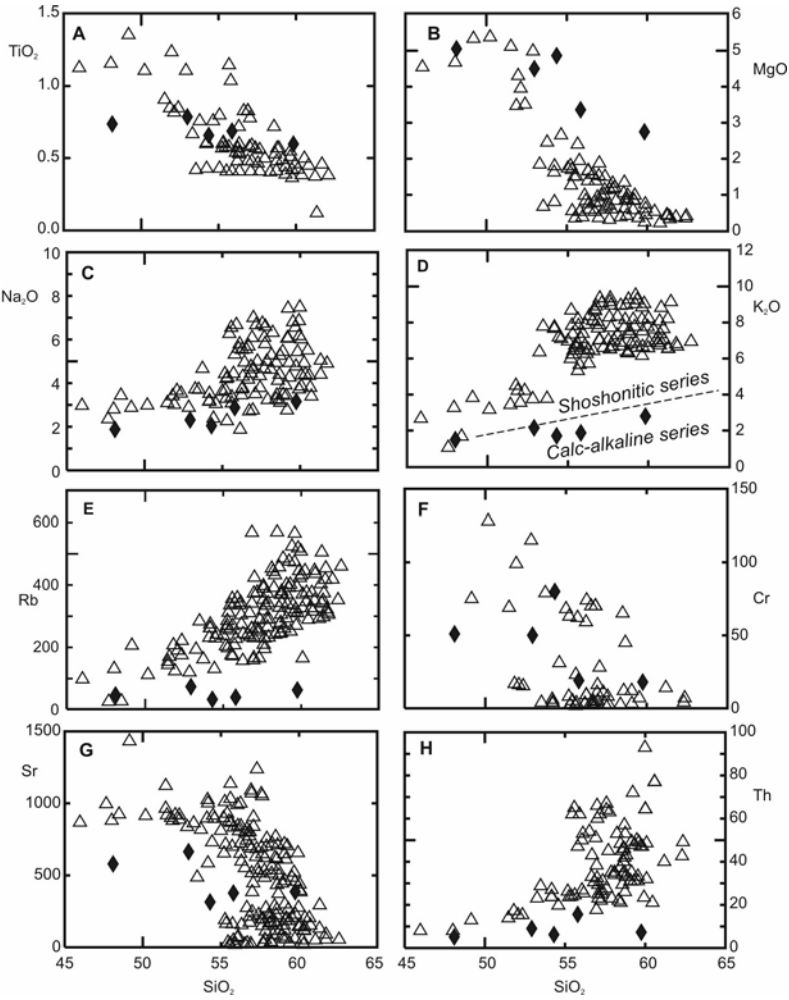

Fig. 6.11. Variation diagrams for Campi Flegrei rocks and for Pliocene buried volcanics from Parete-2 well. Symbols as in Fig. 6.10.

felsic rocks. Most incompatible elements show similar concentrations to the Somma-Vesuvio rocks, which, however, contain higher contents of Rb. Volatile elements (Cl, F) show high concentrations, from several hundred to several thousand ppm, and increase from mafic to felsic rocks (Villemant 1988).

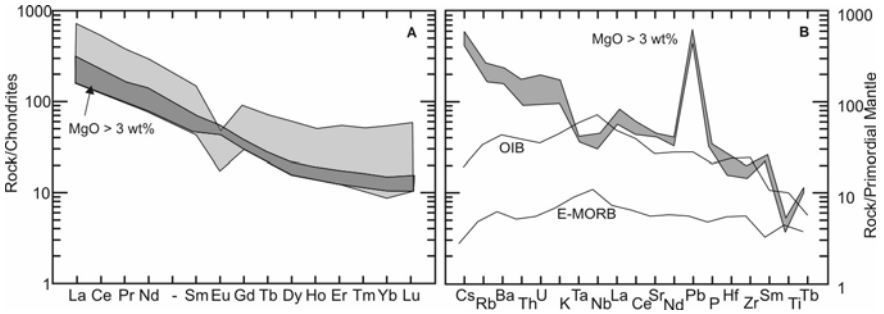

Fig. 6.12. REE (A) and incompatible element (B) patterns (restricted to mafic compositions) for Campi Flegrei volcanic rocks. Patters of E-MORB and OIB (Sun and McDonough 1989) are also shown.

REE patterns are fractionated, with evolved rocks showing negative Eu anomalies (Fig. 6.12a). Incompatible element patterns of mafic rocks normalised to primordial mantle composition (Fig. 6.12b) show Pb spikes and relatively high concentration and moderate negative anomalies of HFSE.

Sr isotopic ratios are variable ($^{87}Sr/^{86}Sr$ ~ 0.7065 to 0.7086; $^{143}Nd/^{144}Nd$ ~ 0.5124 to 0.5128; $^{206}Pb/^{204}Pb$ ~ 18.90 to 19.25; $^{207}Pb/^{204}Pb$ ~ 15.65 to 15.77; $^{208}Pb/^{204}Pb$ ~ 38.95 to 39.38; e.g. Vollmer 1976; Cortini and Hermes 1981; D'Antonio et al. 1996; De Vita et al. 1999; Pappalardo et al. 1999, 2002). There is a general increase of $^{87}Sr/^{86}Sr$ and a decrease of Nd and Pb isotopic ratios from older to younger rocks. However, the rocks younger than 12 ka show an increase in $^{87}Sr/^{86}Sr$ (and a decrease in $^{206}Pb/^{204}Pb$ and $^{143}Nd/^{144}Nd$) with increasing MgO (Fig. 6.13). Boron isotopic compositions display negative $\delta^{11}B$ values (about -4.5 to -9.9), which decrease with increasing $^{87}Sr/^{86}Sr$ (Tonarini et al. 2004).

Major and trace element variations at Campi Flegrei have been suggested to reveal fractional crystallisation and mixing as main magma evolution mechanisms (e.g. Armienti et al. 1983). However, Villemant (1988) pointed out that contents of some elements such as K, Sb, Cl and F are very high in the felsic rocks, and their concentrations exceed those predicted by fractional crystallisation. Therefore, a selective enrichment by fluids percolating through magma chambers was suggested. The variable isotopic ratios also exclude simple fractional crystallisation, and may be ascribed to crustal contamination (Pappalardo et al. 2002). The mafic rocks with the highest Sr and the lowest Nd and Pb isotopic signatures erupted during the final activity of Campi Flegrei revealing that these magmas were the most contaminated. Pappalardo et al. (2002) suggested that

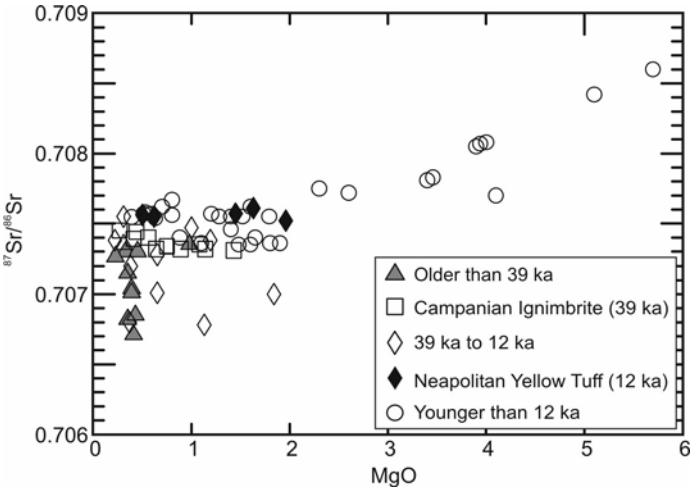

Fig. 6.13. MgO vs. $^{87}Sr/^{86}Sr$ diagram for Campi Flegrei rocks. Note positive trend for rocks younger than 12 ka.

this was a result of the longer time spent by magmas in the deep chamber. However, increasing Sr and decreasing Nd-Pb isotopic ratios with increasing MgO point to variable contamination as a function of the degree of magma evolution. Similar behaviour has been observed at Alicudi, in the western Aeolian arc, and has been suggested to reveal a higher degree of assimilation for the most mafic (i.e. hotter and more fluid) magmas than for the evolved (cooler and more viscous) ones (see Peccerillo and Wu 1992; Peccerillo et al. 2004; Chap. 7).

6.3.3. Ischia

6.3.3.1. Volcanology and Stratigraphy

The Island of Ischia (Fig. 6.14) represents the remnants of a larger volcano, located 35 km west of Naples, at the intersection of NE-SW and NW-SE regional fault systems. The morphology of Ischia is dominated by the central volcano-tectonic horst of Monte Epomeo, by the Ischia graben in the north-eastern sector of the island, and by numerous gravitationally collapsed areas (e.g. Rittmann 1930; Vezzoli 1988a). Stratigraphic studies and radiometric dating indicate several phases of activity (e.g. Gillot et al.

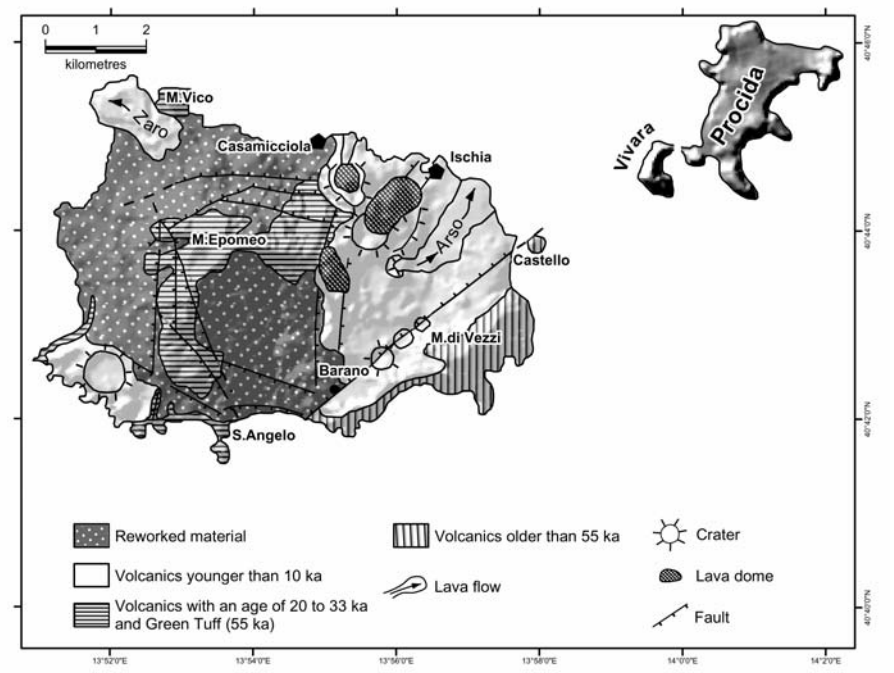

Fig. 6.14. Sketch map of Ischia, Procida and Vivara islands. Simplified after Gillot et al. (1982).

1982; Poli et al. 1987; Civetta et al. 1991c). The lowest exposed rocks are older than 150 ka, and consist of pyroclastic products with intercalated lava flows and paleosols. A second phase of activity (150 ka to 75 ka) is represented by several lava domes emplaced along a semicircular structure, probably a caldera rim. A third phase (55-20 ka) was opened by a caldera-forming ignimbritic eruption (Monte Epomeo Green Tuff) and was followed by explosive and effusive eruptions at different centres. The fourth phase (10 ka to 1302 AD) erupted lavas and some pyroclastics from monogenetic centres along extensional faults of the Ischia graben.

6.3.3.2. Petrography and Mineral Chemistry

The Ischia rocks are mildly undersaturated to oversaturated in silica and contain slightly lower alkalies and K_2O/Na_2O ratios than Campi Flegrei (Figs. 6.2 and 6.15). The rocks of the first two stages are mainly trachytic lavas and pyroclastics. The Monte Epomeo Green Tuff and the following activity of the third phase are trachytic to phonolitic in composition with a few trachybasalts and shoshonites. During the last period of activity, latitic

to trachytic lava and pyroclastics were erupted (Poli et al. 1987; Civetta et al. 1991c).

The Ischia rocks are generally porphyritic with plagioclase, clinopyroxene, alkali-feldspar, biotite, olivine, and Fe-Ti oxides as main phenocryst phases. Sodalite-group minerals occur in some trachytes and trachyphonolites. Apatite and sphene are common accessories. The groundmass is generally hypocrystalline and contains the same phases as the phenocrysts, with an increase in alkali-feldspar and a decrease of clinopyroxene from trachybasalt to trachytes; amphibole is also sometimes present, and alkali pyroxene has been found in the groundmass of some trachytes. Plagioclase is a main phenocryst phase. It shows large compositional variation (about An_{95-25}), zoning and is often surrounded by a rim of alkali-feldspar. Clinopyroxene is a main phenocryst of the mafic to intermediate rocks, whereas it occurs in small amounts in the phonolites; its composition is mainly salite with minor diopside; crystal zoning is common. Olivine is highly forsteritic (Fo_{90-80}), revealing a xenocrystic origin (Rittmann 1930; Chiesa and Poli 1988; Crisci et al. 1989).

6.3.3.3. Petrology and Geochemistry

Major and trace elements of the Ischia rocks define continuous trends on variation diagrams, although with scattering (Fig. 6.16). TiO_2, MgO, FeO_{total}, CaO, P_2O_5, ferromagnesian trace elements, Sr and Ba decrease with in-

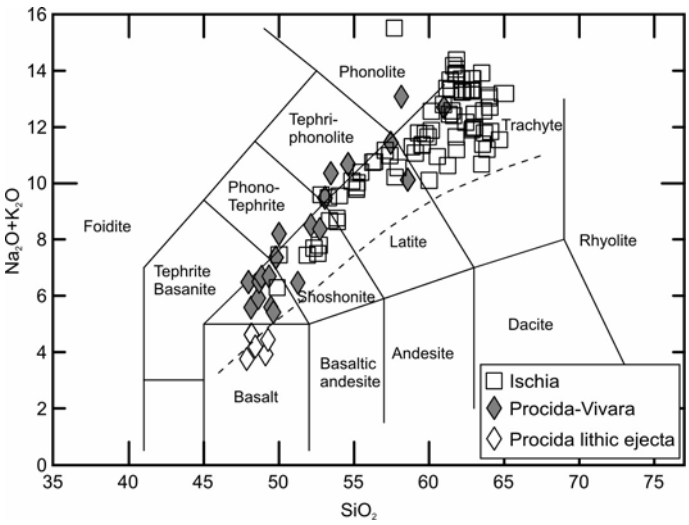

Fig. 6.15. TAS classification diagram for Ischia and Procida-Vivara volcanics.

creasing silica, whereas Na_2O, K_2O and Al_2O_3 have an opposite trend. Incompatible trace elements (Rb, Th, Nb, REE) increase strongly from mafic to felsic rocks (Fig. 6.16).

REE patterns are variably fractionated, with negative Eu anomalies in the evolved rocks (Fig. 6.17a). Patterns of incompatible elements of mafic rocks exhibit moderate negative anomalies in HFSE and Sr (Fig. 6.17b), resembling those of the Campi Flegrei. Sr isotopic ratios range from about 0.7061 to 0.7076, whereas $^{143}Nd/^{144}Nd$ ranges from 0.51246 to 0.51261 (Cortini and Hermes 1981; Hawkesworth and Vollmer 1979; Civetta et al. 1991c). Pb isotopic ratios are close to those of Somma-Vesuvio ($^{206}Pb/^{204}Pb \sim 19.01$-$19.21$; $^{207}Pb/^{204}Pb \sim 15.66$-$15.71$; $^{208}Pb/^{204}Pb \sim 39.06$-$39.34$; Vezzoli 1988a). Oxygen isotopic data on clinopyroxenes and alkali-feldspars range from $\delta^{18}O \sim +5.5$ to $+7.7$ (Turi et al. 1991).

The Ischia rocks are mostly evolved compositions from potassic parental magmas, whereas primitive mafic rocks are rare or absent. Plots of rock composition against eruption ages have shown distinct trends for different eruptive phases. These data have been interpreted as evidence that different styles and degrees of evolution affected potassic magmas during various stages of activity. However, strong though continuous compositional variations for magmas have been detected at the transition from one phase to the next. This has been suggested to indicate that at the and of single phases new types of magmas entered the magma chamber, mixed with the resident melts, triggered volcanic eruptions and generated sharp compositional modifications in the erupted volcanic products (Poli et al. 1987; Civetta et al. 1991c). Therefore, Ischia represents an important example showing how geochemical composition of the magmas can help elucidating magma chamber processes and volcano eruptive behavior.

6.3.4. Procida and Vivara

The Island of Procida and the nearby islet of Vivara are sited between Campi Flegrei and Ischia. Procida consists of a number of coalescing explosive monogenetic cones, whereas Vivara is the remnant of a tuff cone (Rosi et al. 1988). Ages range from older than 55 ka to 17 ka (D'Antonio and Di Girolamo 1994; D'Antonio et al. 1999b and references therein). The erupted material consists of scoriae, hyaloclastites, accessory lithics and pumices, which are interfingered with and sometimes hardly distinguishable from pyroclastic deposits from Ischia and Campi Flegrei. Compositions range from basalt to trachyte (Di Girolamo and Stanzione 1973).

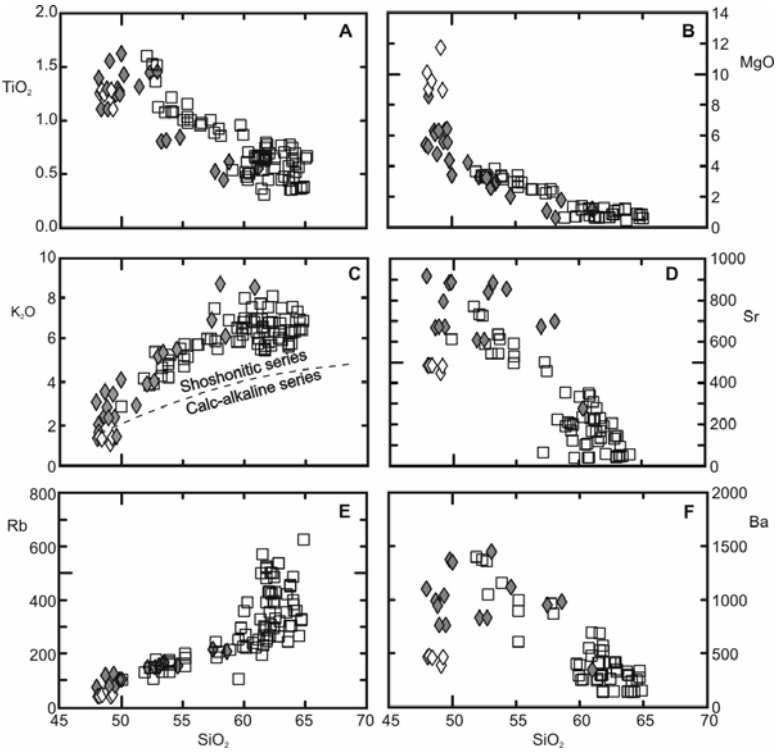

Fig. 6.16. Variation diagrams for Ischia and Procida-Vivara volcanics. Symbols as in Fig. 6.15.

The most mafic lithologies are encountered among lithic ejecta (Fig. 6.16).

Rock textures are porphyritic and variably vesicular. Mafic lithics and scoriae contain phenocrysts of olivine (Fo_{88-80}), diopside, and plagioclase (An_{80-50}) in a matrix made of the same phases plus Ti-magnetite, rare alkali-feldspar and some glass. Trachytes contain dominant sanidine phenocrysts, with minor diopside to salite clinopyroxene and an-desine plagioclase (Di Girolamo and Stanzione 1973; D'Antonio and Di Girolamo 1994).

Major elements show a vertical trend for potassium in the mafic rocks (Fig. 6.16c). These have moderate enrichments in incompatible elements, which are lower than in other Campanian volcanoes; ferromagnesian trace element contents are high in the mafic rocks (Ni up to 230 ppm, Cr up to 600 ppm). REE are fractionated, with small or no Eu anomalies (Fig. 6.17a). Incompatible element patterns of mafic rocks are fractionated and contain small negative anomalies of HFSE and positive spikes of Pb (Fig. 6.17b). Sr and Nd isotopic ratios respectively display lower and higher

values than other Campanian volcanoes; Pb isotope compositions are variable (Fig. 6.8; $^{87}Sr/^{86}Sr$ = 0.7051 to 0.7065; $^{143}Nd/^{144}Nd$ = 0.5125 to 0.5126; $^{206}Pb/^{204}Pb$ ~ 18.68 to 19.30; $^{206}Pb/^{204}Pb$ ~ 38.68 to 39.99). Oxygen isotopic compositions measured on clinopyroxenes and alkali-feldspars have variable values with $\delta^{18}O$ increasing from about +5.5 to +8.1 passing from basalts to felsic rocks (Turi et al. 1991).

Overall, the rocks at Procida and Vivara closely resemble the potassic series from Ischia, although mafic compositions are much better represented at Procida. Some basaltic scoriae and xenoliths have K_2O contents plotting within the field of calc-alkaline series and display lower enrichments in incompatible elements than potassic rocks. However, unlike typical calc-alkaline basalts, the Procida rocks are slightly undersaturated in silica. Such a feature has been also observed for the low-potassic basalts at Ernici and Roccamonfina (see Chap. 5). Major element trends suggest fractional crystallisation as a main evolutionary process; however, variable incompatible element contents and O-Sr-Nd isotopic clearly indicate that assimilation of wall rocks and magma mixing have been important evolutionary processes Procida and Vivara (D'Antonio et al. 1999b). Procida contains the most mafic rocks in the Campania Province. These rocks have more primitive isotope compositions, but display very similar incompatible element patterns as the mafic rocks from other Campanian mafic volcanics. Such a geochemical resemblance likely indicates that incompatible element patterns of mafic rocks in the Campania volcanoes are rather uniform. Their shape does not appear to depend on shallow level processes and, most likely, represents reasonable approximation of mantle-equilibrated melts.

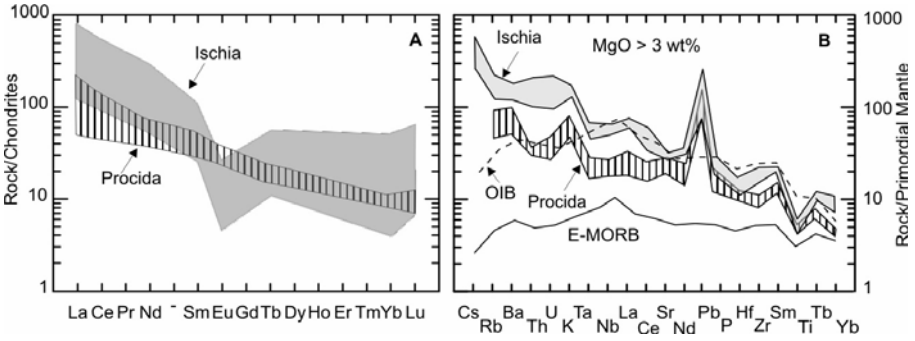

Fig. 6.17. REE (A) and incompatible element patterns (B; restricted to mafic compostions) for Ischia and Procida-Vivara volcanics.

6.4. Buried Volcanism beneath the Campanian Plain

The volcanic activity in Campania is much older than indicated by the outcropping products. Deep borehole drilling south of Vesuvius (Trecase well, Fig. 6.1) reached the sedimentary basement after crossing several levels of tuffs and lavas ranging in composition from leucite-tephrite to phonolite. The deepest recovered volcanic products are 0.4 Ma old leucite-tephritic lavas that indicate ultrapotassic magmatism has long been a characteristic of the Somma-Vesuvio area.

Drilling in the Campanian Plain, north of the Campi Flegrei caldera (Parete-2 well; Fig. 6.1), encountered a huge complex of calc-alkaline basalts to andesites at depths of 300 to 1900 m, beneath a sequence of potassic alkaline volcanics belonging to Campi Flegrei (Di Girolamo et al. 1976; Barbieri et al. 1979; Albini et al. 1980). The lowest recovered lavas have an age around 2 Ma. These rocks show porphyritic textures with phenocrysts of zoned plagioclase, clino- and orthopyroxene and sparse biotite set in a groundmass consisting of the same phases and Fe-Ti oxides. The available data (Figs. 6.10, 6.11) show moderate enrichments in incompatible elements. Sr isotopic ratio varies considerably and overlaps values of the Campania Province ($^{87}Sr/^{86}Sr$ = 0.7060-0.7081; Barbieri et al. 1979; Albini et al. 1980). The importance of these volcanic rocks is high because their occurrence testifies to a temporal transition from calc-alkaline to potassic and ultrapotassic magmatism in the Campanian area (Di Girolamo 1978).

6.5. Pontine Islands

The Pontine archipelago consists of five islands and a number of islets, aligned almost in an EW direction offshore the Campania Province (Fig. 6.1). The volcanoes rise on the margin of the Tyrrhenian abyssal plain (De Rita et al. 1986), basically along the 41° Parallel tectonic line (Bruno et al. 2000). Rocks show variable ages and compositions from western islands (Ponza, Palmarola, Zannone and La Botte islet, located midway between Ponza and Ventotene) to eastern islands (Ventotene and Santo Stefano). The western islands have an age of 4.2 to 1.0 Ma and basically consist of Pliocene rhyolites and Pleistocene trachytes and alkaline to peralkaline rhyolites (Barberi et al. 1967b; Vezzoli 1988b; Conte and Dolfi 2002; Cadoux et al. 2005). The eastern group has an age of 0.8 to less than

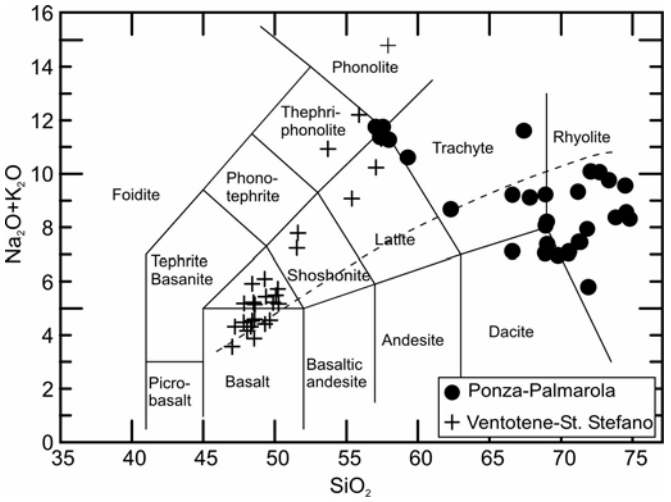

Fig. 6.18. TAS and K_2O vs. SiO_2 classification diagrams for the Pontine Islands volcanic rocks. The dashed line is the divide between subalkaline and alkaline fields of Irvine and Baragar (1971).

0.13 Ma (Metrich 1985; Metrich et al. 1988) and consists of basalt, trachybasalt, shoshonite, latite and phonolite (Fig. 6.18). The Pontine Islands are formed entirely of volcanic rocks, except for Zannone, where the sedimentary and metamorphic basement (phyllites, quartzites and Mesozoic to Miocene limestones, dolostones, marls and siltstones) crops out.

6.5.1. Ponza, Palmarola and Zannone

Volcanism in the western Pontine Islands include obsidian lava flows and domes, dykes, breccias, and hydromagmatic products showing rhyolitic to trachytic compositions. K/Ar dating on sanidines for a large number of samples indicates that rhyolitic volcanism at Ponza took place between 4.2 and 3.0 Ma; Palmarola activity has been dated at about 1.6 Ma; trachytes at Ponza were erupted at about 1.0 Ma (Cadoux et al. 2005). Rhyolites are calc-alkaline in composition, although some late-erupted acidic rocks at Ponza are peralkaline (Conte and Dolfi 2002). Trachytes resemble those from Campanian volcanoes and Roccamonfina. Therefore, the western Pontine Islands is another site where potassic alkaline magmatism follows

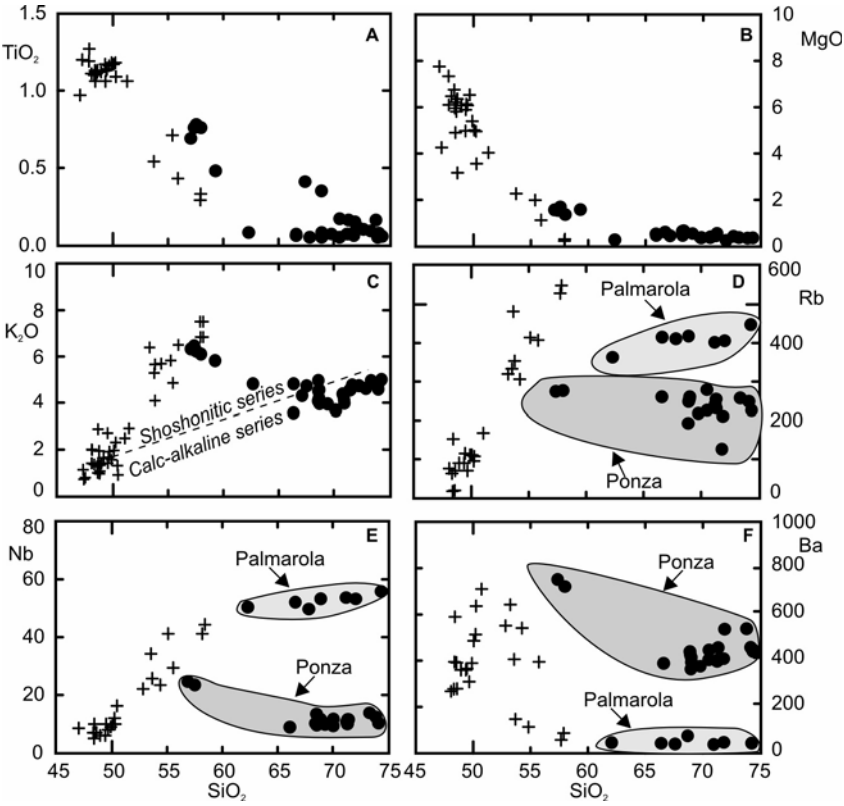

Fig. 6.19. Variation diagrams for the Pontine Islands.

calc-alkaline activity. Rhyolites show poorly porphyritic textures with phenocrysts of plagioclase (about An_{60-30}), sanidine, biotite, orthopyroxene and salitic clinopyroxene set in a glassy to microgranular groundmass. Peralkaline rhyolites are also scarcely porphyritic with microphenocrysts of anorthoclase set in a groundmass containing alkali-feldspar, alkali-amphibole, mica and zircon. Trachytes are poorly porphyritic with phenocrysts of plagioclase (about An_{65-30}), alkali-feldspar, salitic clinopyroxene and biotite and a microcrystalline groundmass mostly formed of alkali-feldspar, some clinopyroxene and Fe-Ti oxides (Conte and Dolfi 2002).

Rhyolites exhibit variable concentrations of major and trace elements, with Palmarola showing higher incompatible trace element and lower Sr contents than Ponza (Fig. 6.19). Peralkaline rhyolites are strongly enriched in Rb, Th and other incompatible elements. REE patterns are fractionated, with rhyolites showing negative Eu anomalies, which are stronger at Palmarola (Fig. 6.20a). Incompatible element patterns (not shown) have mod-

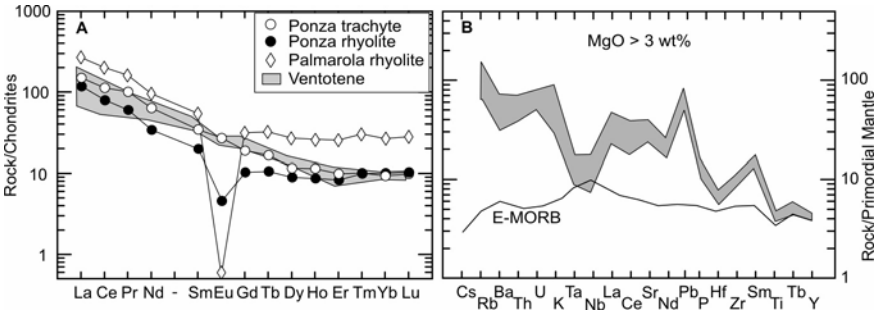

Fig. 6.20. A) REE patterns for rocks from the Pontine Islands; B) Incompatible element patterns for mafic rocks from Ventotene.

erate depletion in HFSE, and strong negative spikes of Ba and Sr. Volatile elements (F, Cl) show variable concentrations, from several hundreds to several thousand ppm (Conte and Dolfi 2002). $^{87}Sr/^{86}Sr$ ranges from about 0.7085 to 0.7104 in the trachytes and clusters around 0.7105 in most rhyolites. Nd isotopic ratio is higher in the trachytes ($^{143}Nd/^{144}Nd \sim 0.51240$) than in the rhyolites ($^{143}Nd/^{144}Nd \sim 0.51225$; Conte and Dolfi 2002). Pb isotopic ratios are fairly homogeneous at $^{206}Pb/^{204}Pb$ around 18.80, $^{207}Pb/^{204}Pb$ around 16.80, and $^{208}Pb/^{204}Pb$ around 39.00 (Cadoux, personal communication). Oxygen isotope composition from whole rocks and separated feldspars ranges from $\delta^{18}O \sim +7.3$ to + 11.1, showing an increase from trachytes to rhyolites (Turi et al. 1991).

The Pliocene calc-alkaline rhyolites from the western Pontine Islands have a composition suggesting a derivation from a basalt or andesite parent by fractional crystallisation plus assimilation. The Pleistocene trachytes have been suggested to be derived by assimilation and fractional crystallisation (AFC) from mildly potassic alkaline parents akin to trachybasalts and latites of the Campania or Ernici-Roccamonfina provinces (Conte and Dolfi 2002; Cadoux et al. 2005).

6.5.2. Ventotene and Santo Stefano

The Island of Ventotene consists of a basal series of thin mafic lava flows cut by a caldera rim and covered by intermediate to felsic pyroclastic products. Santo Stefano is an eccentric lava dome covered by pyroclastic products. Pyroclastic rocks include fall, flow and surge magmatic and hydrovolcanic products, and contain lava lithics, cumulate xenoliths and skarns (Perrotta et al. 1996). Rock compositions range from basalt and trachybasalt to phonolite (Fig. 6.18). Basalts and trachybasalts have a porphyritic texture with phenocrysts of olivine (about Fo_{85-65}), diopside to

salite clinopyroxene and plagioclase (An_{90-50}), set in holocrystalline groundmass formed by the same phases plus Fe-Ti oxides and alkali-feldspars. Latites have similar phenocryst assemblage as trachybasalts but also contain biotite and sometimes are characterised by the coexistence of two distinct types of clinopyroxene (Cr-diopside and salite). Phonolites have phenocrysts of sanidine, plagioclase (An_{85-35}), potassic ferropargasitic amphibole and Fe-Ti oxides. Haüyne and nepheline are found in some latites and trachytes (Metrich 1985; Metrich et al. 1988; D'Antonio and Di Girolamo 1994; D'Antonio et al. 1999b). Major elements show continuous variation from basalt to phonolite, with an increase in Al_2O_3 and alkalies, and a decrease in MgO, CaO, FeO_{total} and TiO_2; there is a steep increase in K_2O in the mafic range (Fig. 6.19). Mafic rocks exhibit a low to moderate enrichment in potassium, with some of the basalts having K_2O and K_2O/Na_2O ratios that plot in the field for calc-alkaline basalts (Figs. 6.2, 6.19c); however, the Ventotene rocks are undersaturated in silica, a feature which has been also observed for the low-potassic basalts at Ernici-Roccamonfina. Incompatible trace elements also increase from basalts to phonolites, displaying smooth inter-element variations (Metrich 1985). REE are fractionated with small negative Eu anomalies (Fig. 6.20a). Incompatible element patterns of mafic rocks (Fig. 6.20b) have negative anomaly of Ba and large negative anomalies of HFSE, resembling closer Ernici-Roccamonfina than Campania potassic rocks. Radiogenic isotope compositions mostly fall in the field of Campanian volcanoes but also of the Ernici-Roccamonfina potassic series ($^{87}Sr/^{86}Sr$ ~ 0.7070 to 0.7077; $^{143}Nd/^{144}Nd$ ~ 0.51228 to 0.51244; $^{206}Pb/^{204}Pb$ ~ 18.50 to 18.86; $^{207}Pb/^{204}Pb$ ~ 15.64 to 15.68; $^{208}Pb/^{204}Pb$ ~ 38.45 to 38.99; D'Antonio et al. 1996, 1999b). Oxygen isotopic compositions measured on whole rocks range from $\delta^{18}O$ ~ +5.9 to +7.6, showing and increase from basalts to felsic rocks (Turi et al. 1991).

Overall, major and trace element data suggest an evolution in an open system for the eastern Pontine Islands. Fractional crystallisation was a dominant process, but mixing with latitic magma enriched in incompatible elements and radiogenic Sr has been invoked to explain trace element and isotopic variations (D'Antonio and Di Girolamo 1994; D'Antonio et al. 1999b).

6.6. Mount Vulture

6.6.1. Volcanology and Stratigraphy

Mount Vulture (Fig. 6.21) is a 1326 m high isolated composite cone with a few eccentric domes and craters. It is constructed at the intersection between NE-SW and NW-SE trending faults, on the eastern side of the Apennine chain, where Apennine thrust front overlaps the Apulia carbonate platform. The contact between the Apulia carbonate platform and the overlying sediments occurs at about 5 km depth (Boenzi et al. 1987), where the magma chamber of Vulture volcano probably developed.

The volcanic sequence consists of dominant pyroclastic deposits and minor lava flows, which cover an area of about 150 km^2. Activity took place between about 0.8 and 0.1 Ma (La Volpe et al. 1984; Guest et al. 1988; La Volpe and Principe 1991). The oldest activity (0.8-0.7 Ma) was characterised by phonolitic to trachytic ignimbritic eruptions and emplacement of some lava domes. The following activity was dominated by

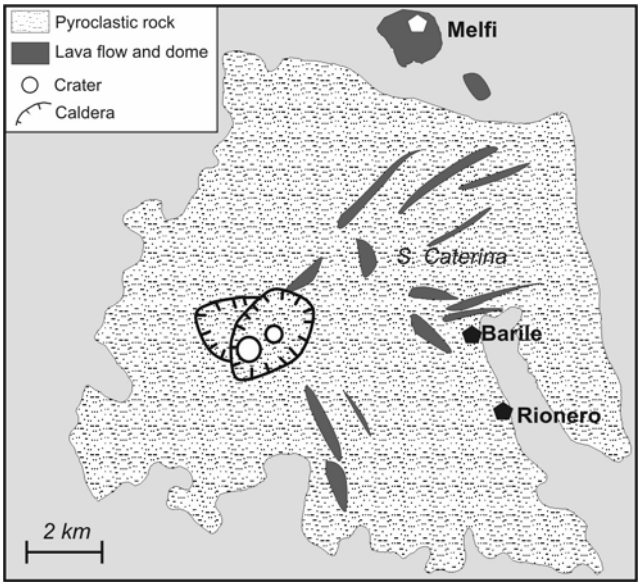

Fig. 6.21. Schematic geological map of Vulture volcano. Simplified after Beccaluva et al. (2002) and references therein.

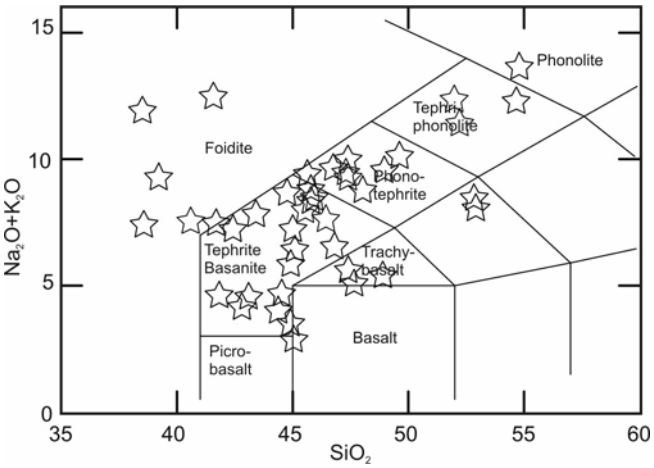

Fig. 6.22. TAS diagram for the Vulture rocks

pyroclastic eruptions and minor lava flows that formed the main cone and summit caldera collapses; rock compositions of this phase range from tephrite and basanite to phonotephrites, and include a few melilitites, haüynophyres (at Melfi, 0.56 Ma) and melafoidites. The most recent activity (0.13 Ma) occurred after a quiescence period of about 200 ka and produced two intra-caldera maars occupied by the Monticchio Lakes, and a tuff sequence reported, more convincingly than in the case of Intra-Apennine Province, to have a carbonatite-melilitite composition (Brocchini et al. 1994; Stoppa & Principe 1997). Ultramafic nodules and megacrysts of clinopyroxene, amphibole, and phlogopite are found in these deposits. Some nodules are believed to represent fragments of upper mantle rocks (Stoppa and Principe 1997; Jones et al. 2002) and have shown subduction-related geochemical signatures (Downes 2001).

6.6.2. Petrography and Mineral Chemistry

The Vulture rocks range from foidite, tephrite and basanite to tephriphonolites and phonolite (Fig. 6.22), with a few melafoidites and melilitites. Rock textures are generally porphyritic. Basanites contain phenocrysts of MgO-rich olivine (Fo_{89-85}) with Cr-spinel inclusions, diopside to salite clinopyroxene (colourless to pale green in thin section), and haüyne set in a glassy to microcrystalline groundmass containing magnetite, plagioclase, Sr-Ba-rich anorthoclase and rare phlogopite. Phenocrysts in the tephrites and phonolitic tephrites consist of complexly zoned clinopyroxene, haüyne, and leucite with some plagioclase, amphibole and biotite, set in a

groundmass of plagioclase, anorthoclase, clinopyroxene, feldspathoids and accessory apatite; corroded olivine crystals have been also observed. Phonolites show phenocrysts of Ba-Sr-rich alkali feldspar, haüyne, green clinopyroxene, leucite and some melanite garnet, magnetite and apatite. Melilitite is characterised by phenocrysts of MgO-rich melilite, Ti-rich salitic clinopyroxene and Fe-Ti oxides, set in a holocrystalline groundmass composed of the same phases plus nepheline, leucite, haüyne, apatite, perovskite and schorlomite garnet; calcite, clinopyroxene, nepheline and magnetite are present. Melafoidite (Santa Caterina locality) shows clinopyroxene phenocrysts surrounded by a matrix made of clinopyroxene, nepheline, leucite, haüyne, Fe-Ti oxides, gehlenite-rich melilite and apatite. The Melfi haüynophyre consists of clinopyroxene, abundant haüyne, leucite, and apatite phenocrysts set in a holocrystalline groundmass of the same phases plus nepheline, Na-Fe-Sr-rich melilite and magnetite (De Fino et al. 1986; Melluso et al. 1996; Beccaluva et al. 2002).. Late erupted melilite-carbonatite tuff sequences consist of a mixture of silicate and carbonate material. Main minerals include melilite, phlogopite, Sr, Ba, REE-rich calcite, apatite, perovskite and haüyne (Stoppa and Principe 1997).

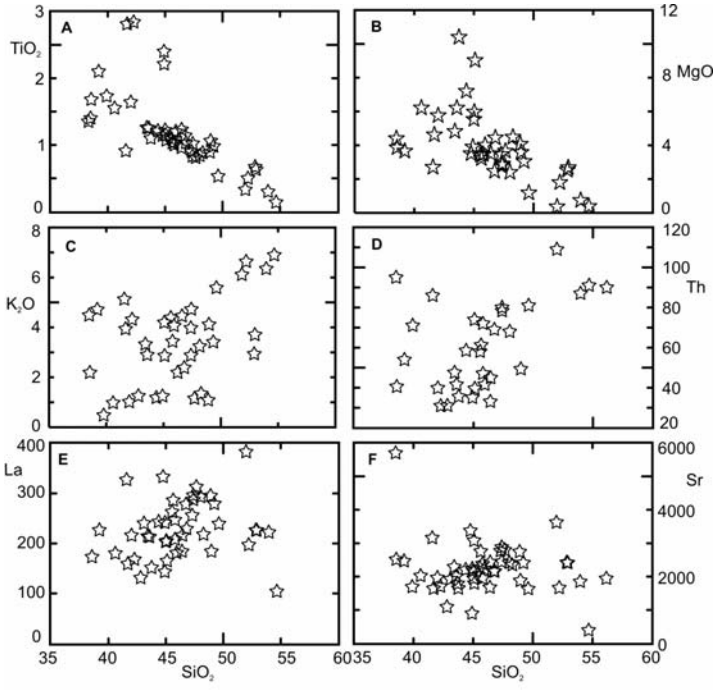

Fig. 6.23. Variation diagram for selected major and trace elements of Mount Vulture rocks.

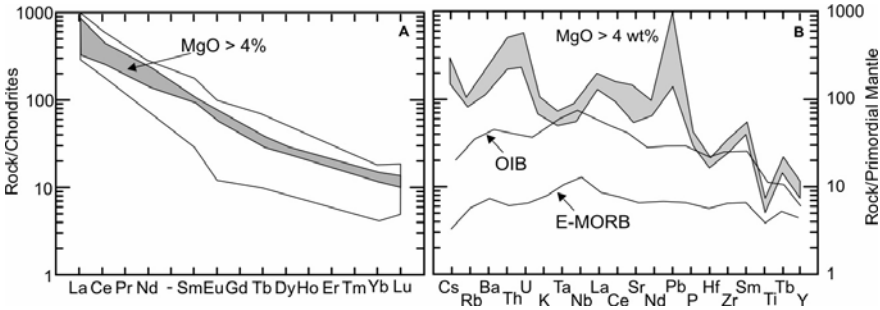

Fig. 6.24. REE (A) and incompatible element (B) patterns (restricted to mafic compositions) for the Vulture volcanics.

6.6.3. Petrology and geochemistry

Major element variation diagrams for Vulture rocks exhibit an overall decrease in TiO_2, P_2O_5, MgO, FeO_{total} and Cao, and an increase in Na_2O, K_2O and Al_2O_3 with increasing silica, but with strong scattering especially in the silica-poor rocks (Fig. 6.23). Trace elements are also scattered although some incompatible elements (e.g. Th, Sr, Ta) show a poorly defined positive correlation with silica. REE are fractionated, with extreme values of La/Yb ratios (up to 300) in some phonolites (Fig. 6.24a). Incompatible element patterns are also fractionated and show the typical HFSE negative anomalies of all the alkaline rocks from central Italy (Fig. 6.24b). However, the Vulture rocks also display negative spikes in Rb and K, which are not found in other potassic alkaline rocks from the Italian peninsula, and are typical of OIB-like Na-alkaline rocks from Etna and Iblei (see Chap. 8). One of the most striking compositional characteristics of the Vulture rocks is their enrichment in volatile elements, especially sulfur and chlorine, which show concentrations from several thousands ppm to about one percent level. These two volatiles show smooth positive correlations with Na_2O (see De Fino et al. 1986), which contrasts with the scattering observed on other inter-element diagrams.

Sr isotope ratios cluster around 0.7055-0.7060, although some samples show significantly higher values (up to 0.7070). $^{143}Nd/^{144}Nd$ values are around 0.5126-0.5128 and do not show any significant correlation with $^{87}Sr/^{86}Sr$ (Fig. 6.8). Lead isotopic ratios ($^{206}Pb/^{204}Pb$ = 19.13-19.48; $^{207}Pb/^{204}Pb$ = 15.68-15.72; $^{208}Pb/^{204}Pb$ = 39.16-39.55) show comparable to slightly more radiogenic compositions than other volcanic rocks from the Italian peninsula (De Astis et al. 2005). Stable isotope studies are scanty. Cavarretta and Lombardi (1990) found $\delta^{34}S$ = +6.1 to +6.6. Preliminary

oxygen isotopic investigation on clinopyroxenes from some mafic rocks yielded values of $\delta^{18}O$ around +5.8 (Dallai, personal communication).

The genesis, evolution and geodynamic significance of the Vulture magmatism are still poorly understood. De Fino et al. (1986) suggested that the rock series from foidite to phonolite could be derived by combined fractional crystallisation and mixing processes, mainly with separation of clinopyroxene, biotite, Fe-Ti oxides and accessory apatite. Melluso et al. (1996) and Beccaluva et al. (2002) accepted fractional crystallisation as a main evolutionary mechanism, but suggested different types of parental

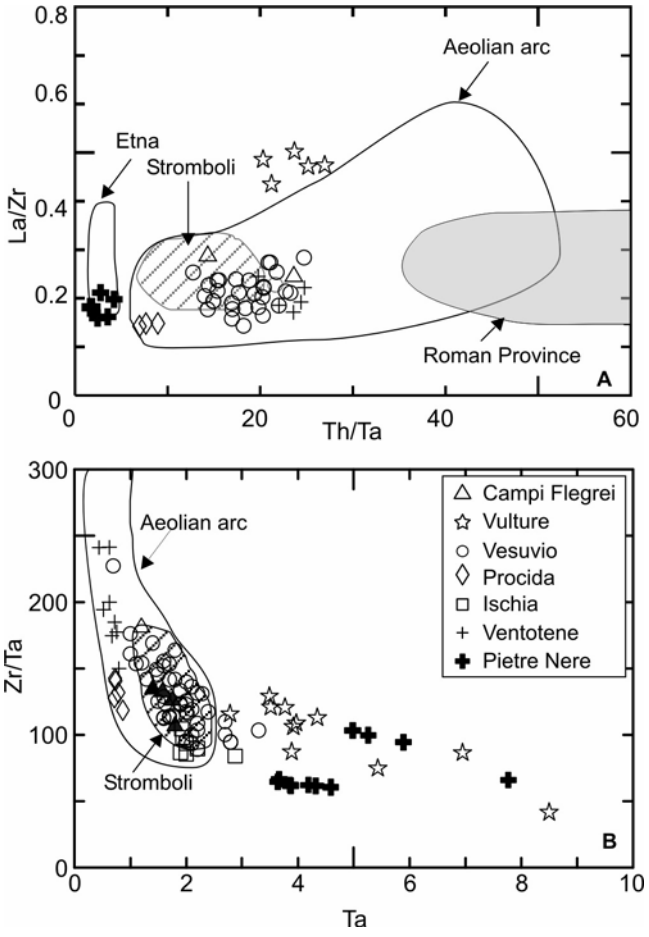

Fig. 6.25. Variation of incompatible element ratios for the Vulture, Campania and Pontine mafic volcanic rocks (MgO > 3 wt%). Compositions for the intraplate Eocene Pietre Nere rocks (Fig. 6.1) and for other Italian magmatic provinces are shown for comparison.

magmas. This is supported by variable Sr isotopic ratios (e.g. $^{87}Sr/^{86}Sr$ ranging from 0.7055 to 0.7070) for rocks displaying high MgO (De Astis et al. 2005). Finally, the positive correlations of Na_2O vs. SO_3 and Cl highlighted by De Fino et al. (1986) are also problematic. These were suggested to reveal interaction between magma and evaporitic rocks from the basement, a hypothesis that does not conflict with sulfur isotope data (Cavarretta and Lombardi 1990), but still needs testing by integrated stable and radiogenic isotope studies.

6.7. Petrogenesis of Campania, Pontine and Vulture magmas

The volcanoes in the Campania Province, Pontine Islands and Vulture are composed of a wide variety of magma types. Silica undersaturated ultrapotassic volcanism is restricted to Somma-Vesuvio, whereas mildly undersaturated to oversaturated potassic rocks occur at Campi Flegrei, Ischia, Procida and Ventotene. In the latter two islands, low potassium compositions close to calc-alkaline basalts are found among lavas and lithic ejecta. Pliocene calc-alkaline rocks are found as rhyolites at Ponza and as basalts and basaltic andesites beneath the Campanian Plain. At Vulture, volcanism is highly enriched in both Na and K, a composition that is distinct from any other volcano in the Italian peninsula.

An important feature of magmatism in Campania is that the Campi Flegrei mafic rocks are moderately potassic in composition but have very similar concentrations and ratios of several incompatible elements as the ultrapotassic rocks from Somma-Vesuvio; these, however, contain higher concentrations of K and Rb (e.g. Peccerillo 2001). In other words, the positive correlation between potassium and incompatible elements observed in other Italian volcanic districts (e.g. Ernici and Roccamonfina) is not so evident in Campania.

In spite of the large variations of petrological characteristics, all the rocks from Pontine Islands, Campania and Vulture show island-arc geochemical signatures given by negative anomalies of HFSE in their incompatible element patterns, and by high LILE/HFSE ratios that are comparable to those of the Aeolian arc (Fig. 6.25). However, most of these volcanoes show relatively high contents of HFSE, with lower LILE/HFSE ratios than observed in other potassic provinces of central Italy such as in the Roman and Ernici-Roccamonfina volcanoes (Beccaluva et al. 1991). High concentrations of HFSE and low LILE/HFSE ratios are typical of OIB, and, therefore, it has been suggested that the rocks from Campania and Vulture have intermediate compositions between OIB and arc rocks

(e.g. Beccaluva et al. 1991, 2002). De Astis et al. (2005) noticed that, although OIB and arc-type signatures are present both at Vulture and in the Campanian volcanoes, Vulture rocks exhibit negative spikes of K and Rb, which are typical of several OIBs. These features are not surprising, since Vulture is located on the Apulia foreland, i.e. basically in an intraplate setting.

Campi Flegrei, Somma-Vesuvio and, to a lower extent, Ischia have similar ranges of Sr-Nd-Pb isotope compositions. They plot along a trend connecting OIB-type volcanoes of Etna, Iblei and Pietre Nere, and the Tuscany Province (Fig. 6.8). Pietre Nere is an Eocene subvolcanic body located on the Apulia foreland (Fig. 6.1) and may be considered to have compositions representative of Adriatic intraplate mantle (e.g. Vollmer 1976). Vulture also plots on the same trend, although it is slightly displaced from the field for the Campanian volcanoes. The rocks from Procida have lower Sr isotopic compositions as the majority of the Campanian rocks. When plotted on Pb-Sr-Nd diagrams, the Procida and Ventotene rocks depart from the main Italian trend and point towards low $^{206}Pb/^{204}Pb$ compositions (Fig. 6.8b). Note that rocks with low values of $^{206}Pb/^{204}Pb$, displaying compositions akin to EM1 and DMM[1] mantle reservoirs, are found in Sardinia and in the Tyrrhenian Sea (e.g. Gasperini et al. 2000, 2002; Lustrino et al. 2000).

These varied compositional characteristics have been long debated and many aspects concerning magma genesis and related geodynamic setting are still controversial. There is now a general agreement that mafic magmas in the Campania, Pontine Islands and Vulture volcanoes derive by different degrees of partial melting of upper mantle rocks characterised by variable modal mineralogy and anomalous enrichments in potassium, incompatible elements and radiogenic isotopes (e.g. Beccaluva et al. 1991). The main petrological characteristics, and in particular the variable enrichment in alkalis indicate that different proportions and amounts of K- and Na-rich phases (e.g. phlogopite, amphibole) participated into the melt during generation of primary magmas (see discussion in Chaps. 2 to 5).

[1] EM1 (Enriched Mantle 1) and DMM (Depleted MORB Mantle) are two extreme compositions of OIBs and MORBs, measured in intraoceanic volcanoes and representing distinct mantle isotopic signatures. EM1 is characterised by unradiogenic Pb (low Pb isotopic ratios) and moderately unradiogenic Sr. DMM exhibits unradiogenic Sr (low Sr isotopic ratio) and Pb, and high $^{143}Nd/^{144}Nd$. Other mantle end-member compositions include HIMU (high μ, where μ is U/Pb ratio) characterised by radiogenic Pb and unradiogenic Sr, EM2 (Enriched Mantle 2) containing highly radiogenic Sr and intermediate Pb isotopic compositions between HIMU and EM1, and FOZO (Focus Zone) showing intermediate Sr-Nd-Pb isotopic compositions between HIMU and EM1.

Phlogopite likely played a stronger role at Somma-Vesuvio than for Campi Flegrei and Ischia, generating variable enrichments in K and Rb, but not so much for other incompatible elements. In contrast, the sodic and potassic nature of the Vulture rocks probably reflect a source mineralogy characterised by the occurrence of both phlogopite and a Na-rich phase such as amphibole. The variable degrees of silica undersaturation have been related either to different depths and/or fluid pressure during magma genesis (e.g. Peccerillo and Manetti 1985) or to variable participation of metasomatic phases in the melting (Conticelli et al. 2004).

As for trace elements, much debated problems are the origin of incompatible element enrichments and the coexistence of OIB- and arc-type signatures. Morris et al. (1993) suggested that the Be and B contents and Be/B ratios of Somma-Vesuvio are different from those found in arc rocks, arguing against a subduction-related enrichment for mantle sources. Such a hypothesis was shared by other authors (e.g. Ayuso et al. 1998). However, Di Girolamo (1978), Serri (1990), Beccaluva et al. (1991), Peccerillo (1999, 2001), De Astis et al. (2000) and many others underscored the arc signatures of Campania mafic rocks and their association with older calc-alkaline volcanism, suggesting that enrichment in LILE resulted from subduction processes. Beccaluva et al. (1991) advocated marly sediments and fluids as metasomatic agents. The close similarity between Campanian volcanoes and Stromboli has been considered an important evidence for a subduction-related origin for the Campanian rocks (Peccerillo 2001). In the frame of this hypothesis, the high concentrations of HFSE contents and low LILE/HFSE ratios have been interpreted to indicate that the pre-metasomatic mantle did not have a MORB-type composition as in the Roman Province, but had, instead, an OIB-type composition (e.g. Serri 1990; Beccaluva et al. 1991). In contrast, the lower HFSE concentrations and higher LILE/HFSE ratios of Ventotene volcanics reveal moderate degrees of metasomatism of a MORB-type mantle (D'Antonio et al. 1999b). The hypothesis of a subduction-related contamination of an OIB-type mantle also applies to Vulture that shares hybrid geochemical characteristics between OIB and arc-type with the Campanian volcanoes. Vulture exhibits stronger OIB-like signatures, which have been related to the particular tectonic position of this volcano that sits on the margin of the Apulia foreland, basically in an intraplate setting (De Fino et al. 1986). Therefore, the problem with this volcano is the one of explaining the origin of its island-arc geochemical signatures.

Radiogenic isotope data have added important information on evolution of mantle sources. The continuous trends of Sr-Nd-Pb isotope ratios along the Italian peninsula, from Etna-Iblei to Tuscany, have been interpreted as a result of contamination of upper mantle by different types of upper

crustal material (e.g. Peccerillo 1999 with references). The intermediate position of Campania, Vulture and Pontine Islands along this trend has been suggested as an evidence for contamination of OIB-type source by sall amounts of sediments plus fluids (e.g. Beccaluva et al. 1991; D'Antonio et al. 1999b). Sediment contamination is also supported by $\delta^{11}B$ values for Campanian volcanic rocks (Tonarini et al. 2004). However, Pb isotopic data have shown that Procida and Ventotene divert from the main trend, shifting toward less radiogenic Pb compositions (Fig. 6.8b). This reveals a role for some additional components in the genesis of these islands. An interaction with EM1 and/or DMM mantle components, such as those occurring in Sardinia ad in the Tyrrhenian Sea (Gasperini et al. 2000, 2002; Lustrino et al. 2000) could explain these isotopic peculiarities.

6.8. Geodynamic Setting

The continuous compositional variation from Pietre Nere and Vulture to Campania and Pontine Islands supports the idea that the upper mantle beneath this transect is a hybrid between OIB-type and subduction-type material, with variable proportions between these two end-members. The origin of these components has important bearing on geodynamic significance of magmatism along the Vulture-Pontine Islands transect.

The arc component sampled by the Campania volcanoes and Pontine Islands has been attributed to the presence of a subducting slab beneath this region (Beccaluva et al. 1991). The close compositional similarity between Campanian volcanoes and Stromboli (Fig. 6.25) has been interpreted as an evidence for a common source and tectonic setting for these volcanoes. Stromboli is clearly related to subduction of Ionian plate, which has led to conclude that the Campanian magmas have also been generated in an upper mantle contaminated by the Ionian plate (Peccerillo 2001). However, Campanian volcanoes are closer to the Apulian than to the Ionian foreland, which would support that the mantle source of Campanian volcanoes was contaminated by material coming from the Apulian rather than the Ionian plate. Distinct compositions would be expected for the Campanian and Stromboli magmas, if contaminants with different histories modified their sources. A proposed solution to this problem is that the subducting slab was initially continuous and homogeneous from Apulia to the Ionian Sea, but that, subsequently, there was slab breakoff in the Apulian sector because of its collision with southern Apennines (De Astis et al. 2000; Peccerillo 2001). Slab break-off in Apulia caused a narrow slab to remain joined to the Ionian plate; this underwent sinking, some clockwise rotation

and rollback toward the southeast. Fluids and sediments coming from the sinking and retreating slab contaminated the upper mantle, both beneath Campania and Stromboli, leading to the similarity in the arc signatures for these volcanoes (Peccerillo 2001). The slab detachment could have occurred at about 0.8 Ma, when compression phases in the Vulture area ended and distension tectonics generated fractures along which Vulture magmas ascended to the surface (Patacca and Scandone 2001). A general sketch in Fig. 6.26 shows such a geodynamic evolution model.

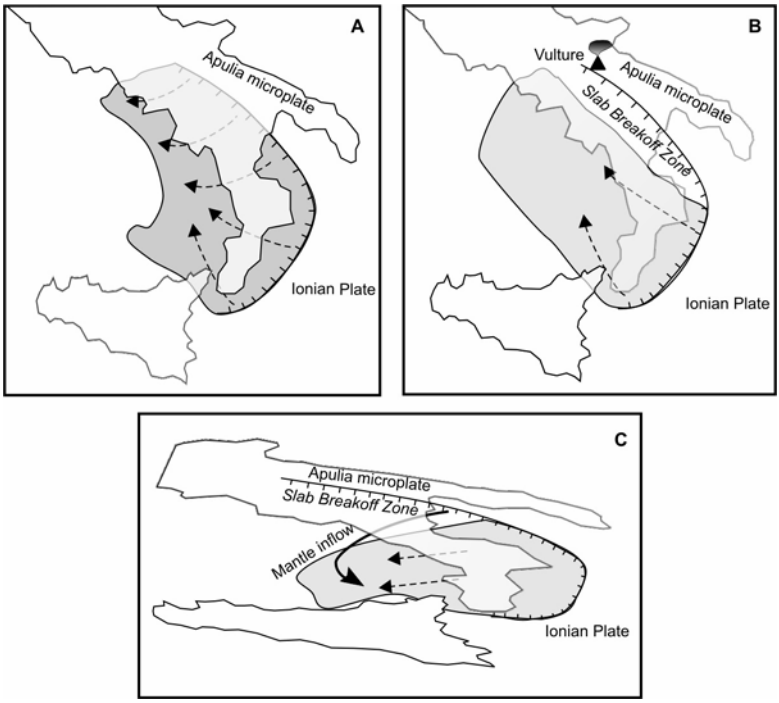

Fig. 6.26. Geodynamic evolution model for the southern Italian Peninsula. A) A continuous subduction zone of the Apulian-Ionian plate was active until about 0.8 Ma. B) Slab breakoff in the Apulian sector generated distension regime at the contact between Apulia and the southern Apennines, mantle contamination by subduction components beneath the edge of the Apulian plate and the formation of Vulture volcano; active subduction continued in the Ionian sector. C) Sinking and rollback of the narrow Ionian slab generated suctioning of intraplate asthenosphere from the Apulia foreland; this was contaminated by sedimentary material and fluids from the subduction zone and generated a hybrid OIB-arc mantle wedge, whose melting gave the Campanian volcanoes and Stromboli.

According to slab break-off model, the arc signatures of Mount Vulture would derive from melts and fluids released by the detached and sinking

slab, which contaminated the mantle beneath the edge of the Apulia plate, where Mount Vulture magmas were formed. Speculatively, the OIB component in the Campania Province as well as in the Stromboli area could be related to a mantle inflow from the Apulian plate through the widow opened by slab breakoff, onto the sinking and retreating Ionian slab. According to this hypothesis, the OIB component would be allochthonous in origin.

Alternative hypothesis on the origin of hybrid geochemical signatures of Campania, Pontine Islands and Vulture magmatism invokes a mantle plume rising beneath the southern Tyrrhenian Sea and contamination by subducting Ionian plate (Gasperini et al. 2002). According to this hypothesis a deep plume would have been emplaced at shallow level through a slab window formed as a consequence of differential slab retreat during the opening of the Tyrrhenian Sea. Plume material was contaminated by slab components, acquiring hybrid characteristics. The magmatism of Etna, Iblei and Ustica has a composition close to HIMU mantle component and would represent almost pure plume material.

6.9. Conclusions

The Vulture, Campania and Pontine volcanoes are characterised by magmas that vary from calc-alkaline to ultrapotassic compositions. Calc-alkaline rocks occur as rhyolites at onza and as basalt to basaltic andesites beneath the Campanian plain. Both these occurrences are older than the potassic and ultrapotassic magmas, indicating an overall time-related increase in potassium on a regional basis.

The mafic rocks from the Campania Province, Pontine Islands and Mount Vulture have intermediate geochemical signatures between OIB and arc-type rocks that indicate melt generation in a hybrid mantle source, formed by the interaction of various amounts of OIB- and arc-type components. OIB-type signatures are stronger in the Vulture volcano and decrease in the Pontine island of Ventotene. The large compositional overlap for several incompatible trace element and radiogenic isotopic ratios among rocks from Campi Flegrei, Ischia and Vesuvio and between these and Stromboli suggests genesis in a common source for all these magmas. The strong enrichment in potassium found at Vesuvio probably reflects a more significnt role of a K-rich phase (e.g. phlogopite) during melting, which was not as important in the case of Campi Flegrei, Ischia and Stromboli. This affected concentration of potassium and rubidium in the magmas but had less dramatic effects on other incompatible elements and

on radiogenic isotope compositions. The intermediate signatures between OIBs and arc basalts for these volcanoes can be explained by the input of asthenospheric mantle from the Apulia foreland and contemporaneous contamination by sedimentary material and fluids coming from the Ionian-Apulia slab. Migration of asthenospheric mantle from Apulia to the Campania region was favoured by the opening of a slab window generated by slab breakoff of the Apulian plate. Alternative hypotheses suggest that the OIB component derives from a deep mantle plume rising beneath the Tyrrhenian Sea area.

Table 6.2. Selected compositions for rocks from the Campania Province, Pontine Islands and Mount Vulture. Numbers in parentheses refer to compositions determined on distinct, though compositionally similar samples from the same locality as those analysed for the other elements. Source of data: 1) Albini et al. (1980) ; 2) Metrich (1985); 3) De Fino et al. (1986) ; 4) Joron et al. (1987); 5) Poli et al. (1987); 6) Vezzoli (1988a) ; 7) Civetta et al. (1991c); 8) Belkin et al. (1993) ; 9) D'Antonio et al. (1996); 10) Ayuso et al. (1998); 11) D'Antonio et al. (1999a); 12) D'Antonio et al. (1999b); 13) Conte and Dolfi (2002); 14) Pappalardo et al. (2002); 15) Cadoux et al. (2005); 16) De Astis et al. (2005).

Volcano	**Somma-Vesuvio**				**Campi Flegrei**			
Rock type	Leucitite	Tephrite	Tephri-phonolite	Phonolite	Trachyte	Shosho-nite	Latite	Trachy-phonolite
Data source	4,9	8,10	10	10	4	11,14	11,14	11,14
SiO_2 wt%	47.33	47.90	51.80	57.50	60.15	50.94	53.35	58.94
TiO_2	0.88	0.90	0.67	0.37	0.44	0.84	0.84	0.42
Al_2O_3	17.40	18.00	19.50	18.40	17.43	16.20	17.87	17.88
FeO_{total}	6.76	7.54	5.50	3.73	2.92	7.30	7.11	3.63
MgO	6.14	3.77	1.88	0.39	0.45	5.67	2.56	0.64
CaO	11.32	8.94	6.38	3.45	2.11	10.66	6.18	2.56
Na_2O	2.22	2.62	3.59	3.89	4.33	2.14	5.22	4.29
K_2O	6.13	7.48	7.66	8.38	8.27	3.89	3.33	8.00
P_2O_5	0.92	0.88	0.38	0.08	0.06	0.54	0.58	0.15
LOI	0.46	0.33	1.62	2.20	3.51	0.40	1.53	2.81
Sc ppm	21	14	6.3	1	2.4	21	10	3.9
V	-	-	-	-	-	219	206	51
Cr	-	26	<20	<20	-	78	8	1.8
Co	26	29	15	2.3	1.7	26	15	2.6
Ni	48	27	<10	2.5	3.6	35	5	-
Rb	254	295	350	365	303	158	315	350
Sr	780	1060	890	580	202	913	919	348
Y	27	17	34	45	-	27	31	35
Zr	243	191	290	390	360	169	240	382
Nb	26	24	44	53	-	17	30	53
Cs	15.0	16.6	23	23.9	18	7	12.7	18
Ba	1705	2270	1450	540	106	1823	1651	269
La	45	52	73	73	76	48	58	85
Ce	96	101	125	135	154	98	114	160
Nd	-	44	44	49	-	48	51	60
Sm	9.0	9.7	8.9	9.9	9.5	10.1	10.1	10.9
Eu	2.48	2.2	1.86	1.93	2.1	2.7	2.6	2.0
Tb	0.91	1.1	0.85	1.05	1.0	1.0	1.1	1.2
Yb	2.00	2.1	2.25	3.18	4.6	2.3	2.4	3.4
Lu	0.22	0.3	0.30	0.45	-	0.3	0.4	0.5
Hf	4.7	4.3	5.3	7.9	8.0	4.1	5.0	9.0
Ta	1.56	2.0	2.3	3.6	3.4	1.1	1.9	3.1
Pb	-	-	59	52	-	32	30	59
Th	17.6	19.2	30	34	33.1	13.6	20.5	35.7
U	6.2	5.7	9.2	9.6	10.2	3.5	6.0	11.7
$^{87}Sr/^{86}Sr$	(0.70760)	0.70719	(0.70705)	(0.70769)	-	0.70860	0.70772	0.70762
$^{143}Nd/^{144}Nd$	(0.51243)	0.51261	(0.51247)	(0.51243)	-	0.51242	0.51257	0.51243
$^{206}Pb/^{204}Pb$	(19.00)	(19.12)	(18.982)	(18.990)	-	18.898	19.016	19.049
$^{207}Pb/^{204}Pb$	(15.69)	(15.71)	(15.666)	(15.693)	-	15.657	15.680	15.702
$^{208}Pb/^{204}Pb$	(39.17)	(39.25)	(39.076)	(39.168)	-	38.959	39.126	39.209

Table 6.2 (continued)

Volcano	**Ischia**		**Procida**		**Parete-2 well**	**Ponza**	
Rock type	Latite	Trachyte	K-trachybasalt	Basalt	Basaltic andesite	Trachyte	Rhyolite
Data source	5,6,7	5,7	9,12	9,12	1	15,13	15,13
SiO_2 wt%	54.67	61.71	48.65	47.98	52.93	57.98	71.32
TiO_2	1.03	0.63	1.22	1.23	0.78	0.76	0.07
Al_2O_3	17.25	19.39	18.05	15.37	17.80	18.92	12.37
FeO_{total}	6.01	2.83	7.30	8.40	7.18	4.64	1.16
MnO	0.13	0.13	0.15	0.14	0.09	0.11	0.04
MgO	3.41	0.53	5.51	9.47	4.49	1.36	0.13
CaO	5.84	1.27	10.52	11.92	9.79	3.53	0.98
Na_2O	4.65	5.73	3.12	2.83	2.31	4.74	3.04
K_2O	5.13	6.79	3.47	1.46	2.21	6.53	4.41
P_2O_5	0.30	0.03	0.58	0.28	-	0.28	-
LOI	0.55	0.53	1.25	0.77	1.00	0.55	6.14
Sc ppm	16.6	3.2	25.5	37.2	24	-	-
V	104	23	228	206	-	63	2
Cr	48	2.5	83	444	50	-	-
Co	18	5.2	29	39	27	6.5	0.5
Ni	-	-	53	154	18	-	-
Rb	201	300	123	45	74	277	255
Sr	486	91	780	476	664	591	103
Y	49	57	27	21	23	23	19
Zr	242	363	130	102	54	255	96
Nb	41	67	18	12	7	24	10
Cs	11	14.1	-	-	5.2	18.7	22.1
Ba	893	175	1040	458	465	706	390
La	50	70	29	15	23	50	35
Ce	115	134	60	30	45	98	62
Nd	51	-	33	18	-	40.9	18.5
Sm	8.9	9.4	7.7	4.7	3.8	7.2	3.6
Eu	2.1	0.59	2.19	1.52	1.2	1.96	0.45
Tb	0.8	1.2	-	-	0.61	0.73	0.46
Yb	2.8	1.5	1.93	1.77	3.2	2.32	2.3
Lu	0.46	0.3	0.28	0.23	0.49	0.31	0.34
Hf	6.1	8.8	-	2.7	3.2	5.59	3.46
Ta	2.88	5.0	-	0.86	-	1.66	1.51
Pb	(10)	-	14	10	-	32	49
Th	20	33	-	3.0	9.0	17.9	28
U	5.9	8.2	-	0.7	-	5.04	7.8
$^{87}Sr/^{86}Sr$	0.70658	0.70622	0.70595	0.70515	0.7060	(0.7085)	(0.7105)
$^{143}Nd/^{144}Nd$	0.51255	0.51257	0.512627	0.512698	-	(0.5124)	(0.5123)
$^{206}Pb/^{204}Pb$	(19.07)	-	18.985	18.675	-	-	-
$^{207}Pb/^{204}Pb$	(15.66)	-	15.647	15.637	-	-	-
$^{208}Pb/^{204}Pb$	(39.06)	-	39.988	38.682	-	-	-

Table 6.2 (continued)

Volcano	**Ventotene**			**Vulture**			
Rock type	Basalt	K-trachy basalt	Phono-lite	Melilitite	Haüynophyre	Basanite	Tephri-phonolite
Data source	9,12	9,12	2	16	16	16	3
SiO_2 wt%	48.83	49.25	58.21	39.21	41.57	45.10	54.67
TiO_2	1.14	1.15	0.33	2.10	0.91	1.07	0.14
Al_2O_3	17.07	17.99	21.46	13.73	18.54	15.27	21.10
FeO_{total}	8.43	8.60	2.28	10.53	7.36	8.03	1.74
MnO	0.15	0.15	0.18	0.25	0.23	0.16	0.12
MgO	6.42	4.93	0.29	3.65	2.70	9.02	0.24
CaO	11.59	10.57	1.14	16.52	11.54	11.97	1.92
Na_2O	2.80	2.94	7.39	4.54	7.33	3.53	5.37
K_2O	1.67	2.45	7.31	4.73	5.14	2.88	6.91
P_2O_5	0.23	0.3	0.33	0.90	0.68	0.96	0.02
LOI	1.04	1.04	0.51	3.11	3.43	1.49	7.65
Sc ppm	31	24	0.99	12.6	5.2	28.1	1
V	203	218	-	250	199	194	-
Cr	190	35	10	6.6	9	483.3	-
Co	35	32	1.06	28.1	-	61	-
Ni	57	34	6	18	10	157	-
Rb	70	111	525	122	135	118	246
Sr	612	816	-	2463	3156	1794	388
Y	25	24	-	70	51	37	15
Zr	101	120	817	601	513	339	571
Nb	8	10	-	121	155	51	149
Cs	-	-	57	6.5	22	9.9	-
Ba	295	472	24	1754	1872	1383	201
La	21	28	160	226	327	165	104
Ce	44	56	310	432	554	291	189
Nd	27	31	-	182.4	166	114.7	48
Sm	6.4	6.7	15.2	37.8	28.6	23.4	6.4
Eu	1.72	1.83	0.91	8.11	6.2	5.06	1
Tb	-	-	1.08	3.38	2.3	1.83	0.5
Yb	1.95	1.93	5.0	4.34	4.3	2.48	1
Lu	0.31	0.28	-	0.41	0.54	0.3	0.21
Hf	2.2	2.7	17.7	11.3	6.89	6.46	9
Ta	0.52	0.8	3.02	6.95	9.1	3.89	5.7
Pb	13	10	-	(73)	(95)	(33)	-
Th	4.9	7.7	133	53	86	39	91
U	1.1	-	29	11.7	21	10.5	-
$^{87}Sr/^{86}Sr$	0.70709	0.70758	-	0.70642	0.70574	0.70693	-
$^{143}Nd/^{144}Nd$	0.51242	0.512296	-	0.51260	0.51270	0.51269	-
$^{206}Pb/^{204}Pb$	18.496	18.759	-	19.492	19.256	19.142	-
$^{207}Pb/^{204}Pb$	15.638	15.659	-	15.714	15.686	15.685	-
$^{208}Pb/^{204}Pb$	38.451	38.903	-	39.558	39.264	39.170	-

7. The Aeolian arc

7.1. Introduction

The Aeolian archipelago is an active volcanic arc in the southern Tyrrhenian Sea (Keller 1982). It consists of several stratovolcanoes forming seven main islands and several seamounts, which extend to the west and northeast of the emergent portion of the arc, around the Marsili basin (Fig. 7.1). The volcanic activity exposed above the sea level took place entirely during the Quaternary, most probably from about 400 ka to the present (Gillot 1987).

Rock compositions range from mafic to silicic, and show a calc-alkaline (CA), high-potassium calc-alkaline (HKCA) to shoshonitic (SHO) affinity. A few potassic alkaline rocks with a composition close to the Roman potassic series (KS) occur at Vulcano and Stromboli (e.g. Keller 1982; Francalanci et al. 2004). Arc tholeiites have been dredged along some seamounts (Beccaluva et al. 1982).

There are important variations of structural, volcanic and magmatic features along the arc (e.g. Cortini 1981). This makes the Aeolian volcanism an interesting example of a complex subduction-related magmatism, strongly correlated and probably dependent on local features of the lithosphere and related tectonic regime. A summary of age, petrological and volcanological characteristics of Aeolian islands is given in Table 7.1. Analyses for representative rocks are reported in Table 7.2.

7.2. Regional Geology

The Aeolian Arc has developed over a continental crust along the northern and western margins of the Calabro-Peloritano basement. This is a fragment of the European plate which was affected by complex structural and metamorphic evolution during pre-Hercynian, Hercynian and Alpine oro-

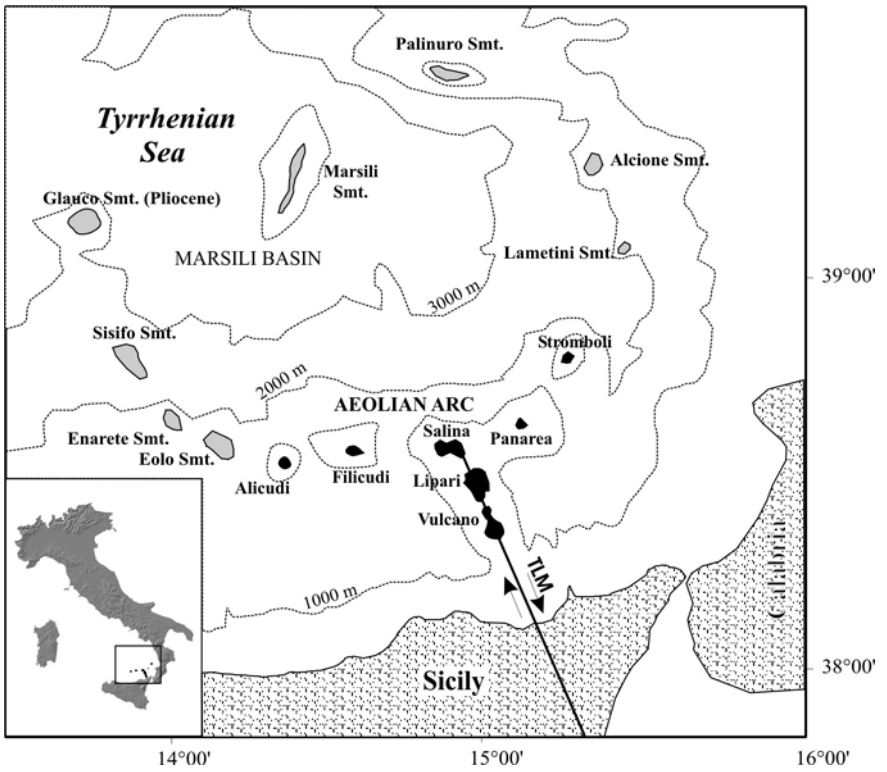

Fig. 7.1. Location of Aeolian islands and seamounts. TML: Tindari-Letojanni-Malta trectonic line

genies, and migrated away from the Corsica-Sardinia block to its present position during the Miocene to Quaternary opening of the Tyrrhenian Sea. The Calabro-Peloritano basement runs from northern Calabria to eastern Sicily, and connects the southern Apennine and the Sicily-Maghrebian chains (Bonardi et al. 2001). It is bounded by the Sangineto tectonic line in the north and the Tindari-Letojanni-Malta line in the south. The structure of the Calabro-Peloritano belt consists of a stack of various nappes composed of pre-Alpine metamorphic and granitoid rocks, often with Alpine metamorphic overprint, Mesozoic to Tertiary sedimentary rocks, ophiolitic sequences, and Quaternary sediments. Metamorphic rocks comprise a wide array of lithologies, including metavolcanics, phyllites, micaschists, gneiss, amphibolites, granulites, eclogites, marbles, and quartzites. Granitoid intrusions are Permo-Carboniferous in age and consist of dominant calc-alkaline granodiorites and tonalites and minor metaluminous to per-

Table 7.1. Summary of chronology, volcanology and petrology for the Aeolian arc volcanoes.

VOLCANO	AGE	VOLCANOLOGY and PETROLOGY
Alicudi	60 ka to 28 ka	- Calc-alkaline basalt to andesite stratovolcano with small summit calderas, intracaldera domes and lava flows.
Filicudi	400 to 40 ka	- Several coalescing calc-alkaline basalt to andesite composite cones, and dacite domes.
Salina	430 to 13 ka	- Eroded calc-alkaline basalt to andesite stratovolcanoes overlain by twin andesite cones and by a rhyolite explosion crater.
Lipari	220 ka to 580 AD	- Multicenter volcano formed of calc-alkaline and high-K calc-alkaline basaltic andesite and andesite, followed by latite and abundant rhyolite lava flows, domes and pyroclastic rocks.
Vulcano	120 ka to 1888-1890 AD	- Composite volcano with two calderas and a small eccentric basaltic shield (Vulcanello) formed of high-K calc-alkaline and shoshonitic basalt to andesite (Primordial Vulcano), latite to rhyolite (Lentia), potassic alkaline shoshonite-trachyte (Vulcanello), and of rhyolite pyroclastics and lavas (Cono della Fossa active cone).
Panarea	150 ka to 45 ka	- Mostly submerged stratovolcano with a flat top at about 100-150 m below sea level, formed by domes and minor lava flows and pyroclastics with a dominant calc-alkaline dacite to rhyolite composition. Minor shoshonites.
Stromboli	200 ka to present	- Stratovolcano with summit caldera and flank collapses, and a satellite neck (Strombolicchio) formed of mafic to intermediate lavas and pyroclastic rocks with calc-alkaline, shoshonitic and potassic alkaline petrochemical affinities.

aluminous granites and silicic dykes. The ophiolitic sequences consist of the typical association of metabasalts, radiolarites, limestones and pelites. Sedimentary rocks include evaporites, shales, sandstones, carbonate rocks, and continental to shallow marine clastic sediments (Bonardi et al. 2001 and references therein).

Seismic studies reveal a thin crust of about 15-20 km beneath the Aeolian arc (Piromallo and Morelli 2003). This becomes thicker beneath the Calabria peninsula (about 25 km), but thins going westward, reaching typical oceanic values of about 10 km in the Marsili basin. There is a belt of low-gravity anomalies east of the Calabria peninsula where values of 20 to 30 mGal have been measured. These contrast with the 130-250 mGal values for the Ionian Sea floor and with the values of about 100 to 200 mGal for the southern Tyrrhenian Sea and Aeolian arc area. This belt of gravimetric lows is likely related to formation of an accretionary wedge of

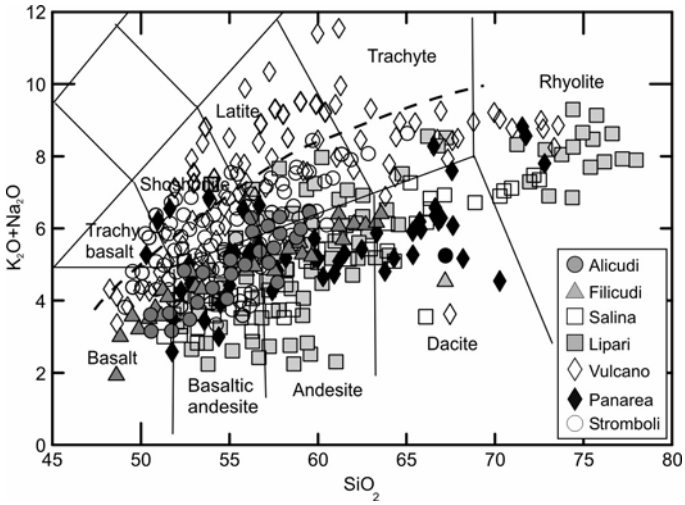

Fig. 7.2. TAS classification diagram for the Aeolian arc rocks. The dashed line is the limit between the alkaline and subalkaline field of Irvine and Baragar (1971)

subducting Ionian crust against the Calabria peninsula (Catalano et al. 2001).

The Aeolian arc consists of three main sectors, each of which shows distinct magmatic, volcanic and structural features. The western sector includes the islands of Alicudi, Filicudi and Salina, where the exposed volcanism developed along a W-E trending fault system, between approximately 0.4 Ma and 13 ka (Keller 1980a; Gillot 1987). Seismic activity is restricted to the upper 20 km. The composition of volcanic rocks is typically calc-alkaline with dominance of mafic and intermediate rocks (Fig. 7.2, 7.3). The central sector includes the islands of Lipari and Vulcano, which developed along the NNW-SSE striking Tindari-Letojanni-Malta line (Fig. 7.1), a dextral strike-slip fault running from the Salina island to the mainland Sicily and to the Malta escarpment. The exposed activity in the central arc has an age younger than about 0.2 Ma, and is characterised by lava flows and pyroclastic rocks that have constructed large stratovolcanoes with calderas. Rock composition is much more variable than in the west, with the presence of mafic to silicic calc-alkaline, shoshonitic and potassic alkaline products. Seismicity is confined to the crust and is concentrated along the Tindari-Letojanni-Malta fault system. The eastern sector develops prevailing along NE-SW faults and includes Panarea and Stromboli. The exposed rocks have ages younger than 0.2 Ma. Rock compositions range from mafic to silicic, with calc-alkaline, shoshonitic to potassic alkaline affinity. The seismic activity is both at crustal

and mantle levels, with earthquake foci defining a narrow and steep Benioff plane dipping NNW and reaching a depth of more than 500 km (e.g. Falsaperla et al. 1999; Panza et al. 2003, 2004).

Active volcanism is restricted to the central and eastern sectors (e.g. Mercalli 1907). At Lipari, the last eruption occurred at about 580 AD, whereas at Vulcano it dates to 1888-1890 AD (Faraone 2002). At Stromboli, there is continuous mildly explosive strombolian volcanism. Fumaroles and hot springs characterize the submarine zone at Panarea.

7.3. Alicudi

7.3.1. Volcanology and Stratigraphy

The Island of Alicudi is located at the western end of the Aeolian archipelago (Fig. 7.1). It rises about 2000 m above the sea floor and 675 m above sea level. According to Villari (1980a), the emergent part of the island was constructed during three main stages of activity, each separated by a summit collapse. Calc-alkaline basalt and basaltic andesite lavas plus minor pyroclastics were erupted during the first two stages; andesite lava flows and domes were emplaced during the third phase in the summit crater and along the south-eastern flank of the cone. K/Ar measurements performed by Gillot (1987) give ages younger than 60 ka for the lowest exposed rocks, and about 28 ka for the latest andesitic lava flows and domes.

7.3.2. Petrography and Mineral Chemistry

All rocks display a holocrystalline to hypocrystalline porphyritic texture, and contain phenocrysts of plagioclase (An_{82-67}), olivine (Fo_{79-68}), and diopside to salite clinopyroxene that are set in a groundmass consisting of the same phases plus Ti-magnetite and glass. Orthopyroxene and brown hornblende are present in basaltic andesites and andesites, where olivine is scarce and strongly resorbed; accessory phases include Fe-Ti oxides and apatite (Peccerillo and Wu 1992; Peccerillo et al. 1993).

Alicudi rocks, like other Aeolian volcanics, contain a variety of metamorphic and magmatic xenoliths. Metamorphic xenoliths are represented by predominant quartz-rich rocks displaying evidence of partial melting along grain boundaries, and by a few biotite gneiss and granulite

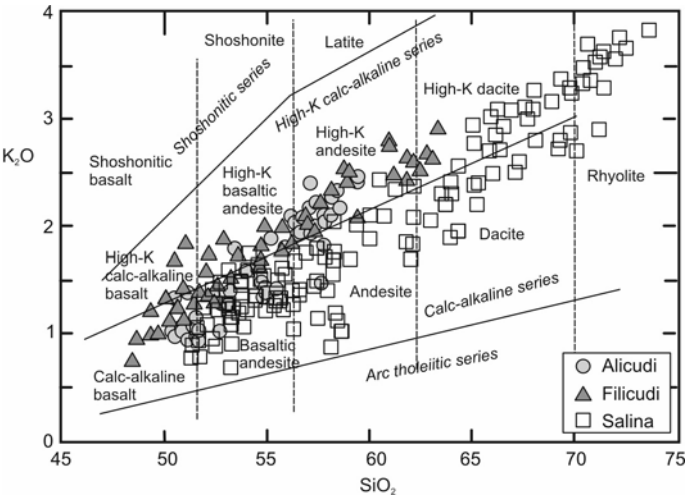

Fig. 7.3. K_2O vs. SiO_2 classification diagram for the islands of Alicudi, Filicudi and Salina.

lithologies. Metamorphic xenoliths are more abundant in the mafic rocks than in the andesites (e.g. Peccerillo and Wu 1992; Peccerillo et al. 1993; Frezzotti et al. 2003). Igneous xenoliths include gabbros, diorites, and a few ultramafic inclusions made up of clinopyroxene and olivine. Some of the ultramafic xenoliths are cumulate in origin, whereas others display a typical granoblastic texture with kinked olivine (~ Fo_{90}), Cr-diopside, and accessory Cr-spinel, which probably denote an upper mantle origin (Peccerillo et al. 2004).

7.3.3. Petrology and Geochemistry

Alicudi rocks range in composition from calc-alkaline basalts to high-K andesites (Fig. 7.3). Basalts exhibit the most primitive compositions over the Aeolian arc (Table 7.2). Mg# (up to 0.72), Ni (up to 150 ppm), and Cr (up to 750 ppm) fall close to values of mantle equilibrated melts (Frey et al. 1978). There is an increase in K_2O, P_2O_5 and incompatible trace elements with increasing silica contents that is mirrored by a decrease in CaO, MgO, TiO_2 and ferromagnesian trace elements (Fig. 7.4). REE are fractionated with flat HREE patterns (Fig. 7.5a). Incompatible element patterns of mafic rocks have negative anomalies of HFSE, and positive spikes

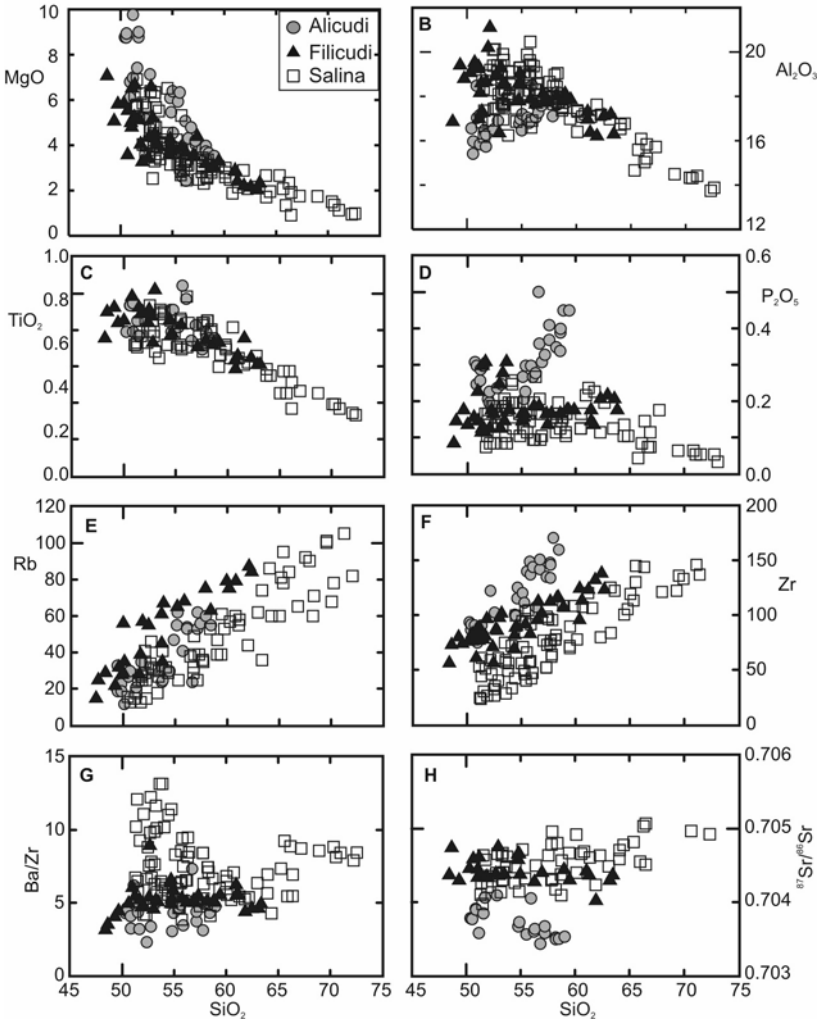

Fig. 7.4. Variation diagrams for the islands of Alicudi, Filicudi and Salina.

of Sr and Pb (Peccerillo et al. 2003; Fig. 7.5b). LILE/HFSE (e.g. Ba/Zr) are somewhat lower than for the other western Aeolian islands (Fig. 7.4g).

The Alicudi rocks have the least radiogenic Sr isotope and the most radiogenic Nd isotope compositions over the entire Aeolian arc ($^{87}Sr/^{86}Sr$ = 0.70343 to 0.70406; $^{143}Nd/^{144}Nd$ = 0.51280 to 0.51290; Fig. 7.6a). However, an important feature of the Alicudi volcanics is that the evolved andesites have lower $^{87}Sr/^{86}Sr$ ratios and higher $^{143}Nd/^{144}Nd$ ratios than basal-

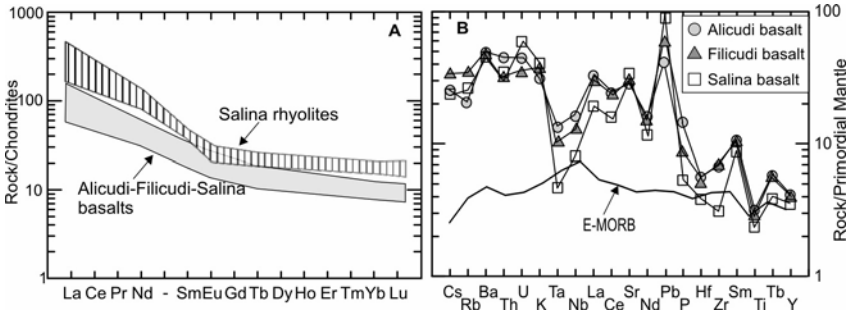

Fig. 7.5. REE (A) and incompatible element (B) patterns for the islands of Alicudi, Filicudi and Salina.

tic andesites and basalts (Peccerillo and Wu 1992). Therefore, there is an overall decrease of $^{87}Sr/^{86}Sr$ and an increase of $^{143}Nd/^{144}Nd$ with increasing degree of evolution (i.e. increasing SiO_2 and decreasing MgO; Fig. 7.4h). Pb-isotope ratios are moderately radiogenic ($^{206}Pb/^{204}Pb$ ~ 19.19 to 19.67; $^{207}Pb/^{204}Pb$ ~ 15.62 to 15.67; $^{208}Pb/^{204}Pb$ ~ 39.07 to 39.36; Fig. 7.6b), and show a tendency to increase from basalts to andesites. Sr-Nd-Pb isotopic disequilibrium between phenocrysts and groundmass has been observed (Peccerillo et al. 2004). Hf isotope composition determined on a basaltic andesite sample yielded a value of $^{176}Hf/^{177}Hf = 0.283096$ ($\varepsilon Hf = 11.45$; Gasperini et al. 2002). He-isotope composition measured on olivine and pyroxene phenocrysts has R/R_A around 6.5 to 7.1 (Di Liberto 2003).

Whole-rock oxygen isotope ratios range between $\delta^{18}O$ ~ +5.6 to +7.3 ‰ (Peccerillo et al. 1993), but values on separated clinopyroxenes show a more restricted range ($\delta^{18}O$ = +5.1 to +5.6), indicating $\delta^{18}O$ values of coexisting liquid between +5.4 ‰ and +5.7 ‰. A positive correlation is observed between clinopyroxene $\delta^{18}O$ and whole rock $^{87}Sr/^{86}Sr$ (Peccerillo et al. 2004).

Variations of several major and trace elements point to a derivation of the whole Alicudi series from a single magma by fractional crystallisation. However, variable isotopic signatures call for the involvement of some additional process in magma evolution. It has been suggested that the negative correlation between silica and Sr isotope ratios found at Alicudi is the effect of a combined early fractional crystallisation process, followed by bulk assimilation of wall rocks. Fractional crystallisation of olivine, pyroxene and plagioclase produced a suite of basalt to andesite magmas, which underwent assimilation of wall rocks during their rise to the surface. The more fluid and hotter mafic magmas dissolved higher amounts of crustal rocks than the andesitic liquids, due to their higher temperature and to turbulent flow through volcanic conduits. This generated stronger isotopic

modifications in the mafic lavas compared to the evolved melts (Peccerillo and Wu 1992). The high abundance of quartz-rich xenoliths in the basalts, but not in the andesites, supports such a hypothesis.

7.4. Filicudi

7.4.1. Volcanology and Stratigraphy

The Island of Filicudi represents the emergent part of a NW-SE elongated volcanic complex that was formed by several partially-overlapping eruptive centres, some of which (La Canna and Banco di Filicudi in the west) are partially or completely submerged (Villari 1980b; Calanchi et al. 1995). The exposed volcanic products consist of early erupted calc-alkaline basalts to andesites, followed by andesite and dacite lava flows, domes, and pyroclastic products. The age of the lowest exposed rocks is still a matter of debate. Santo et al. (1995) determined a $^{40}Ar/^{39}Ar$ age of 1.02 Ma, whereas De Rosa et al. (2003) measured K/Ar ages of 0.2 Ma. Gillot (1987) report an age of 0.4 Ma for some of the lowest exposed rocks. The basalt to basaltic andesite neck of La Canna and the nearby islets, sited offshore west of the main island, is considered as the final products of Alicudi activity (about 40 ka) by Santo et al. (1995), although this conclusion is questioned by Tranne et al. (2002).

7.4.2. Petrography and Mineral Chemistry

The Filicudi rocks range in composition from calc-alkaline basalts to high-K andesites and dacites (Figs. 7.2, 7.3). Textures are holocrystalline to hypocrystalline porphyritic, with phenocryst content ranging from 30 to 50 vol %. Phenocryst mineralogy of mafic rocks consists of zoned plagioclase (An_{95-50}), diopside to augite clinopyroxene, and minor olivine (Fo_{86-60}) and orthopyroxene (En_{72-64}) set in a groundmass formed by the same phases plus Fe-Ti oxides and glass (Santo 1998). Intermediate rocks have plagioclase as the dominant phase, with minor augitic clinopyroxene and orthopyroxene; biotite and brown hornblende are present in some rocks. Ti-magnetite, ilmenite and apatite are found in accessory amounts.

As at Alicudi, the Filicudi rocks contain both magmatic and metamorphic xenoliths. Igneous xenoliths consist of gabbros, granodiorites, and lavas. Metamorphic xenoliths, particularly abundant in rocks from La

Canna neck, generally exhibit a granoblastic texture and have a quartz-rich composition with minor K-feldspar and plagioclase.

7.4.3. Petrology and Geochemistry

Major element variations for Filicudi rocks are characterised by negative correlation of silica vs. Al_2O_3, MgO, CaO, TiO_2 and FeO_{total} and positive trends for K_2O, Na_2O and P_2O_5 (Figs. 7.3, 7.4). LILE and HFSE increase with silica, whereas ferromagnesian trace elements decrease, although

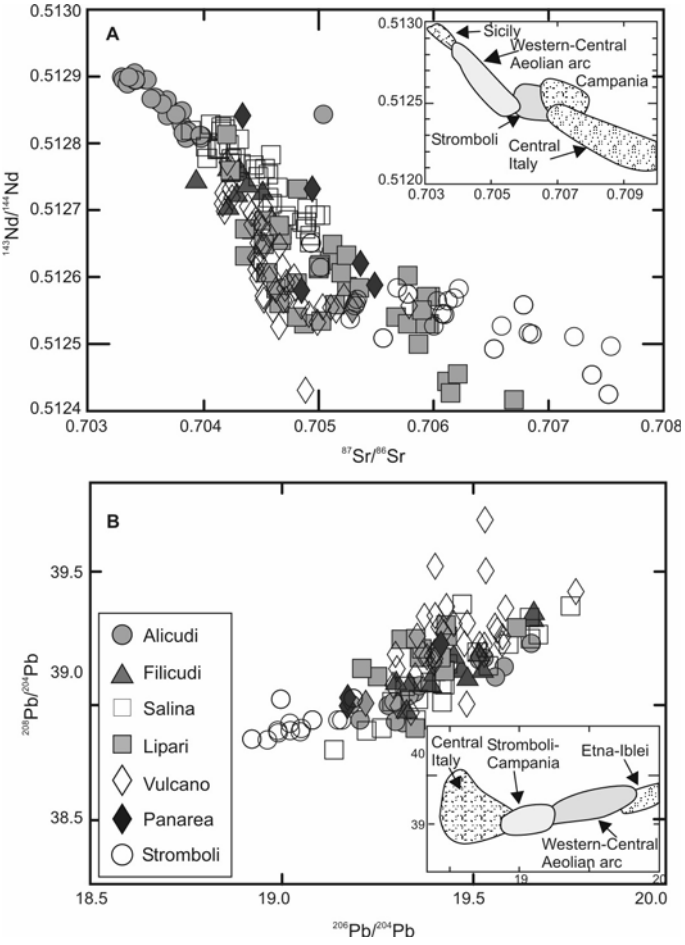

Fig. 7.6. Sr-Nd-Pb isotopic variations of Aeolian arc rocks. Inset diagrams indicate isotopic compositions for mafic rocks of other Italian volcanic provinces.

with scattering. The rocks from La Canna neck have higher K_2O, P_2O_5 and Rb contents than other rocks with comparable SiO_2 and MgO contents. REE patterns at Filicudi are moderately fractionated, with almost flat HREE (Fig. 7.5a); mantle-normalised incompatible trace element patterns of mafic rocks are characterised by slight fractionation, with negative anomalies of HFSE and positive spikes of Sr and Pb (Fig. 7.5b).

Sr-isotope ratios range from 0.70401 to 0.70474, and exhibit a poorly defined negative correlation with silica (Fig. 7.4h). Nd-isotope ratios range from 0.51267 to 0.51276; Pb-isotope ratios exhibit low variations (Fig. 7.6b; $^{206}Pb/^{204}Pb$ ~19.31 to 19.67; $^{207}Pb/^{204}Pb$ ~ 15.64 to 15.69; $^{208}Pb/^{204}Pb$ ~ 39.11 to 39.47; Santo et al. 2004). Hf-isotope ratio for a basalt sample has a value of $^{176}/Hf/^{177}Hf = 0.283096$ ($\varepsilon Hf = 10.69$), close to the composition of Alicudi (Gasperini et al. 2002). He-isotope composition has slightly lower R/R_A values than Alicudi (Di Liberto 2003).

Geochemical modelling by Santo et al. (2004) indicates that various degrees of fractional crystallisation, mixing, and assimilation affected individual batches of magmas in small-size magma chambers sited at various depths. Such a model agrees with the particular structure of the Filicudi island, which consists of several distinct magmatic centres of moderate size. Basaltic melts underwent larger amounts of crustal assimilation than andesites and dacites, although such a process is less well-defined than at Alicudi. Clinopyroxene crystal chemistry and fluid inclusion studies support polybaric magma ponding and crystallisation (Nazzareni et al. 2001; Frezzotti et al. 2003). Geochemical and isotopic variability, however, also reveals some variations in primary melts. In particular, the more K-rich character of La Canna neck is believed to represent a pristine compositional feature of parental melts, possibly derived from a different source as the rest of the Filicudi magmas (Santo et al. 2004).

7.5. Salina

7.5.1. Volcanology and Stratigraphy

The island of Salina (27 km^2) lies at the intersection between the Alicudi-Filicudi alignment and the Tindari-Letojanni-Malta fault system. It represents the emergent part of a structure that rises 1500 meters above the sea floor and 962 m above sea level. The island is characterised by the well-preserved cones of Monte Felci and Monte Porri, which have been constructed upon the eroded volcanoes of Rivi, Capo and Corvo. The age of

the exposed volcanic products ranges between 430 to 13 ka (Keller 1980a; Gillot 1987), although a much younger age of 168 ka has been found for the lowest exposed products by De Rosa et al. (2003).

Stratigraphic and volcanological studies have recognised various stages of volcanic activity (Keller 1980a; Gillot 1987; Mazzuoli et al. 1995; Calanchi et al. 1993). Early eruptions built up a row of basaltic to andesitic stratovolcanoes (Rivi-Capo, Corvo and Fossa Felci). Successively, the Monte Porri andesite-dacite cone (about 67 ka) was constructed in the western part of Salina. Final activity (30 to 13 ka) produced a few basaltic-andesite lava flows and the rhyolitic explosion crater of Pollara, at the northwestern end of the island.

7.5.2. Petrography and Mineral Chemistry

Mafic and intermediate products from Salina exhibit porphyritic textures with microcrystalline intergranular to hypocrystalline groundmass. Strongly zoned plagioclase (An_{90-56}), diopside to augite clinopyroxene, partially resorbed olivine (Fo_{75-65}) and Fe-Ti oxides are the dominant phenocrysts of basalts; orthopyroxene and pigeonite occur in the groundmass (Gertisser and Keller 2000). Andesites and dacites have porphyritic textures dominated by zoned plagioclase phenocrysts (An_{90-40}), with minor diopside to augite clinopyroxene, orthopyroxene and amphibole, the latter increasing in abundance from andesites to dacites. Rare rounded crystals of olivine are found in some andesites. Rhyolites consist of poorly porphyritic pumices containing less than 10 vol % phenocrysts of plagioclase, salitic clinopyroxene, amphibole and biotite, and bearing evidence of commingling with mafic melts. The Salina lavas and pyroclastics contain xenoliths of magmatic and metamorphic origin, which are similar to those observed at Filicudi.

7.5.3. Petrology and geochemistry

Variation diagrams of SiO_2 vs. major and trace elements exhibit a decrease in CaO, Al_2O_3, FeO_{total}, MgO, P_2O_5, and ferromagnesian trace elements, and an increase in LILE and HFSE with increasing silica (Fig. 7.4). LILE/HFSE ratios (e.g. Ba/Zr, La/Nb, Th/Ta) are variable, but are generally higher than observed at Filicudi and Alicudi. REE and incompatible element patterns resemble those of Alicudi and Filicudi rocks, but have stronger negative spikes of HFSE and higher positive anomalies of Sr (Fig. 7.5).

Sr-isotope ratios range between 0.70397 and 0.70507, and slightly increase with increasing silica (Gertisser and Keller 2000; Fig. 7.4h). Nd-isotope ratios range from 0.51265 to 0.512815. Pb isotopes are moderately radiogenic, with $^{206}Pb/^{204}Pb \sim 19.30$ to 19.66, $^{207}Pb/^{204}Pb \sim 15.61$ to 15.77, $^{208}Pb/^{204}Pb \sim 39.15$ to 39.51. Oxygen isotope ratios on whole rocks range from $\delta^{18}O = +6.4$ to +8.5 and increase with Sr isotope ratio and silica (Ellam et al. 1988; Ellam and Harmon 1990; Gertisser and Keller 2000).

Major and trace element variations indicate that fractional crystallisation of mafic phases and plagioclase was a first-order evolutionary process at Salina. However, Sr- and O-isotope ratios of mafic and intermediate rocks are variable, indicating assimilation processes concomitant with fractional crystallisation. Basalts and basaltic andesites have large variations of LILE/LILE and LILE/HFSE ratios (author's unpublished data), which are difficult to explain by fractional crystallization or assimilation, and indicate the occurrence of geochemically different primary melts. Therefore, the overall petrogenetic history of Salina seems to be related to combined fractional crystallisation, mixing and assimilation processes, starting from compositionally different mafic melts (Ellam and Harmon 1990; Gertisser and Keller 2000). Polybaric evolution processes are suggested by clinopyroxene crystal chemistry and fluid inclusion studies, with the older magmas crystallising in deeper magma chambers than younger ones (Nazzareni et al. 2001; Zanon and Nikogossian 2004).

7.6. Lipari

7.6.1. Volcanology and Stratigraphy

Lipari covers an area of about 38 km^2 and is the largest of the Aeolian islands. Detailed volcanological investigations and geological mapping recognised various cycles of activity (e.g. Pichler 1980; Sheridan et al. 1985; Crisci et al. 1991; Tranne et al. 2000; Calanchi et al. 2002a; Fig. 7.7). Early exposed products (223 to 127 ka) consist of sub-aqueous and subaerial basaltic andesitic and andesitic lavas and pyroclastic rocks. These are followed by high-K andesites and minor dacites and shoshonites with an age of about 120 to 80 ka. Successively, strongly explosive eruptions (70 to 13 ka) formed several large brown-coloured high-K calc-alkaline to shoshonitic pyroclastic deposits (the so-called Brown Tuffs), alternating with silicic lava flows and domes. Brown Tuffs probably originated from

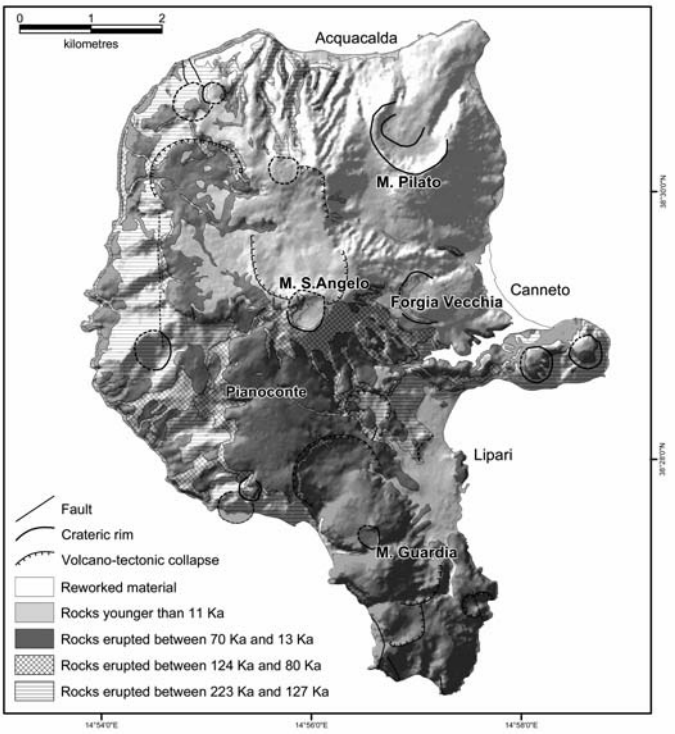

Fig. 7.7. Simplified geological map of Lipari island. Modified after Tranne et al. (2000) and Calanchi et al. (2002a).

eruptive centres located between Lipari and Vulcano (Gioncada et al. 2003), and are found in many of the Aeolian islands (Salina, Filicudi, Vulcano and Panarea) as well as along the coast of Sicily and Calabria (Lucchi 2000). The final activity at Lipari (11 ka to 580 AD) gave rhyolitic obsidian lava flows, domes and pumices. The oldest and more mafic activity appears to be associated with the E-W fracture system, whereas younger shoshonitic and rhyolitic magmas were erupted primarily along the NW-SE tectonic alignment of the Tindari-Letojanni-Malta fault system (Crisci et al. 1991 and references therein).

7.6.2. Petrography and Mineral Chemistry

The SiO_2 vs. K_2O plot (Fig. 7.8) shows that the Lipari volcanics define a steep increase in K_2O from mafic to intermediate rocks, straddling the limits between arc tholeiitic, calc-alkaline and shoshonitic series. Basaltic andesites and andesites have porphyritic textures with phenocrysts of zoned

plagioclase (An_{80-50}), augite and orthopyroxene set in a groundmass composed of the same phases, plus Fe-Ti oxides and glass (Pichler 1980). Hornblende and biotite are rare; corroded olivine xenocrysts occur in some lavas. Abundant xenocrystic phases, including cordierite, garnet, andalusite, K-feldspar, sillimanite, corundum, and quartz occur in some andesites, testifying to entrapment of the basement rocks (Maccarrone 1963; Barker 1987). The rhyolitic lava and pyroclastic rocks from the younger activity range from poorly porphyritic to aphyric and sometimes show evidence of mingling with latitic magmas. Rocks of latest activity consist almost entirely of glass with a few phenocrysts of K-feldspar (Or_{66-73}), plagioclase (An_{24-20}), rare amphibole and biotite, and accessory apatite and zircon (Gioncada et al. 2003).

7.6.3. Petrology and Geochemistry

Major and trace element variations for the Lipari rocks show scattering and a bimodal distribution of compositions (Fig. 7.9). However, detailed studies highlighted distinct trends for several trace elements, especially Zr vs. Sr (see Crisci et al. 1991). Rhyolites display variable abundances for several trace elements such as Zr, Th, and Rb. REE of mafic rocks are fractionated and have flat HREE patterns; silicic rocks contain strong negative Eu anomalies (Fig. 7.10a). Incompatible element patterns of mafic rocks are fractionated with negative anomalies of HFSE and positive spikes of Sr and Pb (Fig. 7.10b).

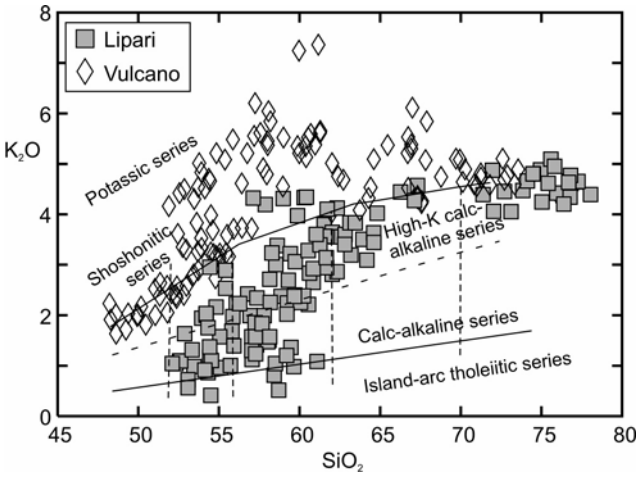

Fig. 7.8. K_2O vs. SiO_2 classification diagram for the islands of Lipari and Vulcano.

Radiogenic isotope data show wide variations ($^{87}Sr/^{86}Sr$ = 0.7043 to 0.7067; $^{143}Nd/^{144}Nd$ = 0.51276 to 0.51242; $^{206}Pb/^{204}Pb$ = 18.46 to 19.63; $^{207}Pb/^{204}Pb$ = 15.61 to 15.71; $^{208}Pb/^{204}Pb$ = 39.05 to 39.43; Fig. 7.6). There is a rough increase of $^{87}Sr/^{86}Sr$ with increasing silica, although the most radiogenic compositions are observed in some cordierite-bearing andesites (Esperança et al. 1992; Gioncada et al. 2003).

The time-related variation of rock compositions, the steep increase in K_2O passing from mafic to intermediate and silicic rocks, and the distinct

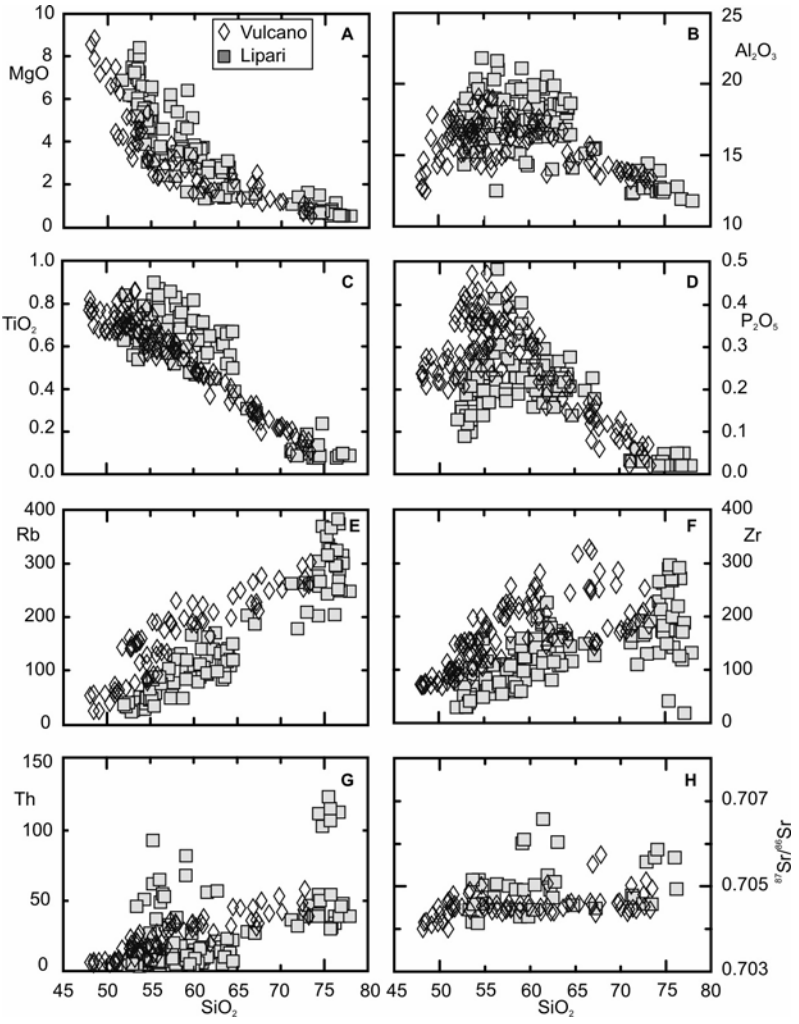

Fig. 7.9. Variation diagrams of selected major and trace elements for the islands of Vulcano and Lipari.

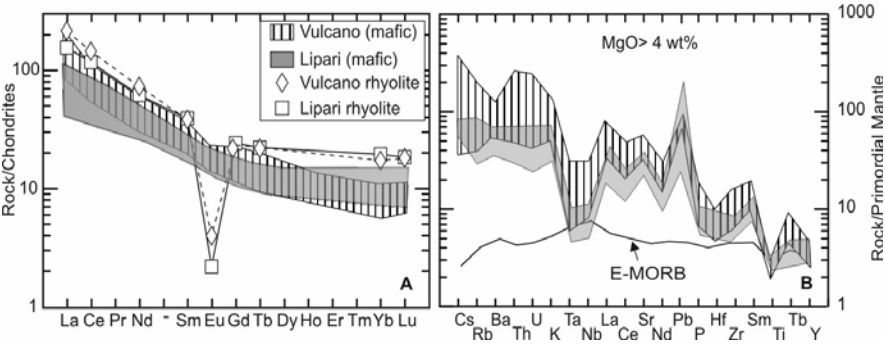

Fig. 7.10. REE (A) and incompatible element (B) patterns (restricted to mafic rocks) for the islands of Vulcano and Lipari.

trends shown by several incompatible elements make the petrogenesis of Lipari rocks a complex problem. Crisci et al. (1991) suggested that fractional crystallisation was a main magma evolution process. However, magma contamination plus mixing among various types of melts have also played important roles in the petrogenesis of the Lipari magmas. Crustal contamination was particularly strong in cordierite-bearing andesites, as indicated by petrographic and radiogenic isotope data. According to these authors, subalkaline to K-rich melts were generated in a stratified mantle, characterised by decreasing degree of metasomatism with increasing depth; early large degrees of partial melting of depleted deeper mantle generated tholeiitic magma, whereas late melting of uppermost anomaous lithospheric mantle produced K-alkaline melts. Potassic mafic melts intruded into the volcanic system and mixed with tholeiitic magmas, causing the steep increase in potassium which is observed in the Lipari rocks. Upward migration of mantle melting processes was related to increase of isotherms within the upper mantle, as a consequence of doming beneath Lipari. Magma emplacement in the crust also generated anatexis, with formation of rhyolitic melts. However, Gioncada et al. (2003) noticed that isotopic compositions (especially Pb) of rhyolites are different from those of the Calabro-Peloritano basement, concluding that a generation of acid melts by crustal anatexis is unlikely. Therefore, it has been suggested that rhyolitic magmas formed by fractional crystallisation, starting from parental andesitic to latitic melts, accompanied by crustal assimilation and mixing with latitic magmas.

7.7. Vulcano

7.7.1. Volcanology and Stratigraphy

The Island of Vulcano is exposed over an area of about 22 km^2, and likely represents the southern sector of a larger volcanic complex, which includes both Vulcano and Lipari (Gioncada et al. 2003). The timing of the volcanic activity for the exposed rocks ranges between 120 ka and the present; the latest eruption dates back to 1888-1890 and the description made by Mercalli and Silvestri (1891) has been adopted as a basis to define vulcanian-type eruptions in the volcanological literature (see Faraone 2002). Rock compositions range from mafic to silicic, with high-K calc-alkaline to shoshonitic and potassic alkaline (KS) affinities (Figs. 7.8).

Volcanological and stratigraphic studies (e.g. Keller 1980b; De Astis et al. 1997) allowed identification of various stages of volcanic activity (Fig. 7.11). Primordial Vulcano (120 to 100 ka) and Piano Caldera (100 and 20 ka) are a composite cone and a filled caldera, mostly formed by HKCA mafic to intermediate lava flows, pyroclastic rocks and dikes. The Lentia

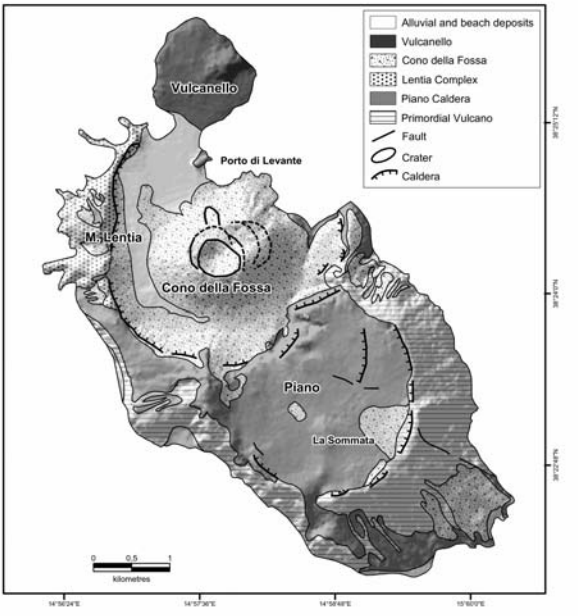

Fig. 7.11. Schematic geological map of Vulcano. Simplified after Keller (1980b).

Complex (20 and 15 ka), sited north of Primordial Vulcano, is the remnant of a stratovolcano with a central caldera (Fossa Caldera), mainly formed by latitic, trachytic and rhyolitic lava flows, domes, and pyroclastic rocks. Fossa Caldera products were erupted between 15 and 8 ka by pyroclastic and effusive eruptions of shoshonitic intermediate to silicic magmas. Cono della Fossa is a 391 m high active edifice that rises at the center of the Fossa Caldera; it was formed in the last 6000 years by several silicic pyroclastic eruptions and a few lava effusions. Vulcanello is a shield made of mafic potassic lavas showing a KS affinity, with central trachytic pyroclastic cones. Vulcanello was formed as a new island probably about one thousand years ago (magnetostratigrafic age by Tanguy, personal communication); sand accumulation in the isthmus area finally connected Vulcanello with the main island.

7.7.2. Petrography and Mineral Chemistry

The rocks from Primordial Vulcano and Piano Caldera are porphyritic with phenocrysts of plagioclase (An_{75-55}), salitic to augitic clinopyroxene, olivine (Fo_{88-57}), magnetite and some biotite set in a microcrystalline groundmass that is formed of the same phases as the phenocrysts; microphenocrysts of leucite, often transformed to analcite, are sometimes observed. The Lentia rocks have textures ranging from porphyritic to subaphyric; phenocryst mineralogy is represented by clinopyroxene, plagioclase, minor sanidine, biotite, and magnetite, and rare resorbed olivine. The Fossa Caldera rocks have porphyritic textures with phenocrysts of labradoritic plagioclase, clinopyroxene, and magnetite set in a microcrystalline to hypocrystalline groundmass; olivine and K-feldspar are present in some samples.

The rhyolites from Cono della Fossa are subaphyric to poorly porphyritic with phenocrysts of plagioclase (An_{56-43}), sanidine, biotite, brown amphibole, and opaque minerals set in a glassy matrix; olivine (Fo_{70-65}) and diopsidic pyroxene are also present. Clear evidence of mixing-mingling with mafic melts (e.g. resorbed olivine and pyroxene crystals with reaction rims, very variable and sometimes bimodal mineral compositions, mafic inclusions with irregular crenulated margins) characterise the Cono della Fossa rhyolites. The mafic lavas from Vulcanello are porphyritic with phenocrysts of clinopyroxene, subordinate large plagioclase laths (An_{65-49}), and opaques. Leucite, often transformed to analcite, and rare olivine occur as microphenocrysts and in the groundmass. The trachytic lavas and pyroclastics are porphyritic and contain phenocrysts of plagioclase (An_{54-20}), diopsidic to augitic pyroxenes, sanidine, opaques and subordinate olivine

(Fo_{71-56}), set in a microcrystalline groundmass; rare biotite and brown amphibole are also observed.

7.7.3. Petrology and Geochemistry

The Vulcano rocks define scattered plots on element variation diagrams. However, when single stages of activity are considered separately, element variations become much smoother (De Astis et al. 1997). There is an overall negative correlation of MgO, FeO, CaO, and ferromagnesian trace elements, and positive correlation of K_2O, Na_2O, Rb and other incompatible elements with SiO_2 (Fig. 7.9). Al_2O_3 and P_2O_5 have a bell-shaped variation pattern, with maximum concentrations observed in the intermediate compositions (Fig. 7.9b,d). K_2O and some incompatible elements (e.g. Zr) show a decrease in the most silicic rocks (Figs. 7.8, 7.9f). Chondrite-normalised REE patterns are fractionated and exhibit small negative Eu anomalies, which become stronger in the silicic rocks (Fig. 7.10a). Incompatible element diagrams of mafic rocks contain negative anomalies of HFSE and positive spikes of Pb (Fig. 7.10b). The HKCA rocks from Primordial Vulcano and Piano Caldera have lower incompatible element abundances than younger shoshonitic and KS products at comparable degree of evolution (De Astis et al. 1997). Overall, incompatible elements exhibit stronger fractionation and higher enrichments than at Lipari.

Sr-isotope ratios range from 0.7042 to 0.7059. The largest variations are observed in the older HKCA rocks, whose $^{87}Sr/^{86}Sr$ ratios (= 0.7042 to 0.7052) show a negative correlation with MgO and a positive correlation with silica. The Lentia rocks ($^{87}Sr/^{86}Sr \sim 0.7046$-$0.7047$) and Cono della Fossa and Vulcanello ($^{87}Sr/^{86}Sr \sim 0.7046$-$0.7048$) show modest Sr-isotope variation, although a few rhyolites reach higher values ($^{87}Sr/^{86}Sr$ = 0.70565-0.70588; De Astis et al. 1997; Del Moro et al. 1998). Overall, the most primitive HKCA rocks from Primordial Vulcano have lower Sr isotopic ratios than the mafic SHO and KS rocks. Hf-isotope ratio for a high-K calc-alkaline basalt ($^{176}Hf/^{177}Hf = 0.282916$; $\varepsilon Hf = 5.1$) has a lower value than at Alicudi and Filicudi (Gasperini et al. 2002). He-isotope composition measured on olivine and pyroxene phenocrysts yielded values of $R/R_A \sim 2.3$ to 4.9 (Di Liberto 2003).

The geochemical and petrological data for the Vulcano rocks imply complex magma evolution processes, which occurred in an open system (De Astis et al. 1997; Del Moro et al. 1998). The positive correlation of $^{87}Sr/^{86}Sr$ vs. silica for Primordial Vulcano and Piano Caldera indicates interaction between mafic magmas and continental crust. However, these rocks basically have a mafic composition despite the large amount of AFC

that is needed to generate the observed Sr-isotope variations. This feature has been interpreted to reflect continuous mixing with mafic melts during AFC; such a process would preserve the mafic composition of magma, whereas Sr-isotopes would become more radiogenic (De Astis et al. 1997).

The poorly variable isotopic composition of the Lentia rocks favours a derivation of rhyolites from mafic-intermediate parents by dominant fractional crystallisation. However, there are linear relationships for many inter-element variations, which suggest mixing between acid and mafic magmas (De Astis et al. 1997).

Finally, element variation for Cono della Fossa and Vulcanello is consistent with dominant fractional crystallization starting from shoshonitic to KS mafic parents. The decrease in K_2O and some incompatible elements in the most evolved products indicates separation of K-feldspar and of accessory phases such as zircon. Feldspar fractionation generated strong negative Eu anomalies in the REE patterns of Vulcano rhyolites. However, the rhyolitic rocks from Cono della Fossa were also affected by mixing-mingling with mafic melts, as demonstrated by the occurrence of mafic enclaves and of xenocrystic olivine with high-MgO in the lavas. The increase of $^{87}Sr/^{86}Sr$ ratios in some of the most acidic rocks indicates modest crustal assimilation (Del Moro et al. 1998).

Overall, the magmatism at Vulcano is characterised by an increase in the degree of rock chemical evolution with time. Potassium and incompatible elements also increase in the mafic magmas from older to younger activity. The time-related increase in the proportions of silicic vs. mafic magmas has been attributed to an enhanced role of fractional crystallisation with respect to mafic magma input into the volcanic system. These effects are considered as related to an overall migration of magma chambers toward shallow levels (De Astis et al. 1997; Zanon et al. 2003; Frezzotti and Peccerillo 2004). The variable enrichment in potassium and incompatible elements in mafic melts has been interpreted to indicate a heterogeneous mantle source (De Astis et al. 1997), with early activity tapping deeper and less metasomatised mantle rocks than younger shoshonitic and KS volcanism. Melting at various levels in a stratified mantle would depend on isotherm upraise, which triggered melting at progressively shallower depth with time.

7.8. Panarea

7.8.1. Volcanology and Stratigraphy

Panarea is a composite cone situated midway between Lipari and Stromboli (Fig. 7.1). It rises about 1700 m above sea floor and forms a flat surface of about 50 km^2 at an average depth of 100-150 m below seal level. The emergent section of the volcano forms the main island of Panarea and a number of islets including Basiluzzo, Formiche, and Lisca Bianca (Gabbianelli et al. 1990; Calanchi et al. 1999; Calanchi et al. 2002b). Exposed rocks consist mostly of andesitic and dacitic lava domes and minor flows and pyroclastics. They were emplaced between about 150 and 45 ka, but the bulk of the activity was concentrated between 150 to 125 Ka. Successively, mafic calc-alkaline strombolian scoriae were erupted and the rhyolitic dome of the Basiluzzo islet (about 54 ka; Gabbianelli et al. 1990) formed. This activity occurred after a long hiatus in volcanism, which resulted in formation of various marine terraces. A deposit of Brown Tuff, originating outside Panarea, comprises the youngest rocks on the island (Calanchi et al. 1999). Many lavas and pyroclastic rocks at Panarea contain igneous and metamorphic xenoliths, sometimes reaching about 20% of the total rock mass. Magmatic enclaves include some high-K calc-alkaline and shoshonitic mafic lavas with irregular crenulated edges, which suggest incorporation while in a plastic state.

7.8.2. Petrography and Mineral Chemistry

The Panarea lavas have a variably porphyritic texture. Zoned plagioclase (An_{90-35}) is the dominant and ubiquitous phenocrystic phase; diopside-augite and orthopyroxene are also abundant in basaltic andesites; hornblende phenocrysts appear in the andesites and dacites; olivine (Fo_{78-76}) is found in small amounts in the mafic rocks; biotite phenocrysts are present in the Basiluzzo rhyolite. Groundmass is generally hypocrystalline to holohyaline and contains plagioclase, opaque minerals, pyroxene and, sometimes, biotite.

Xenoliths of both magmatic and metamorphic origin are found in the Panarea lavas. Quartz-rich rocks are the most common metamorphic enclaves. Some lava xenoliths have crenulated margins which reveal incorporation when were still in a plastic state (Calanchi et al. 2002).

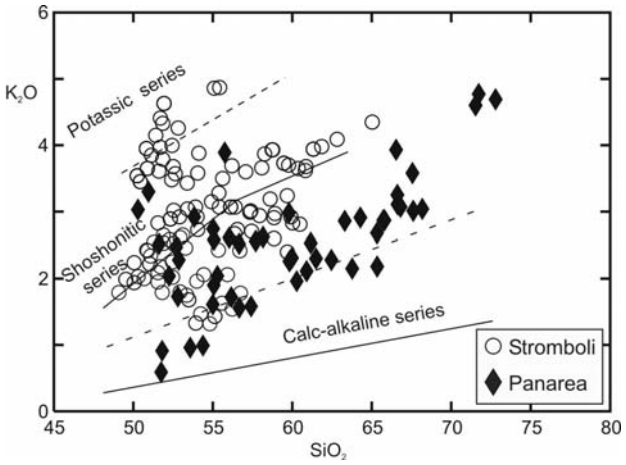

Fig. 7.12. K_2O vs. SiO_2 classification diagram for Panarea and Stromboli.

7.8.3. Petrology and Geochemistry

The SiO_2 vs. K_2O classification diagram (Fig. 7.12) indicates that Panarea rocks mostly plot in the compositional field of HKCA series, from basalt to rhyolites, with some shoshonites and a few calc-alkaline basaltic andesites. The latter, represented by the final stage strombolian scoriae, exhibit distinct geochemical and isotopic signatures with respect to the older rocks. Intermediate and acid rocks largely dominate over mafic lithologies, which are mostly found as enclaves within silicic products.

Variation diagrams of major element vs. SiO_2 show a decrease for TiO_2, Al_2O_3, CaO, FeO_{total} and MgO with increasing silica, with scattering (Fig. 7.13). Trace elements exhibit a decrease in V, Sc, Ni and Sr, and an increase in Rb, Zr, and Light Rare Earth Elements (LREE) with increasing silica. The calc-alkaline rocks have lower contents of incompatible elements than HKCA and SHO rocks at comparable degree of evolution (Calanchi et al. 2002b).

REE patterns are fractionated; silicic rocks contain negative Eu anomalies (Fig. 7.14a), which are much smaller than observed for the Lipari and Vulcano rhyolites. Mantle normalised incompatible element patterns of mafic rocks show high LILE/HFSE ratios and a positive anomaly of Pb; a small positive Sr spike is observed in the calc-alkaline basaltic andesites (Fig. 7.14b). HKCA and shoshonitic rocks have higher incompatible element abundances than the associated CA products.

Sr isotope composition ranges from 0.7040 to 0.7057; the least radiogenic composition is observed for the late calc-alkaline scoriae (Fig. 7.13h). Nd isotopic ratios range from 0.51284 to 0.51257. Pb isotopic composition is also variable (e.g. $^{206}Pb/^{204}Pb$ = 18.18 to 19.43; $^{207}Pb/^{204}Pb$ = 15.67-15.71; $^{208}Pb/^{204}Pb$ = 39.13-39.36).

The very discontinuous and limited nature of the outcrops makes it difficult to understand magma genesis and evolution at Panarea. Calanchi et al. (2002b) suggested that the variable incompatible element contents for calc-alkaline to shoshonitic mafic rocks indicate the occurrence of distinct

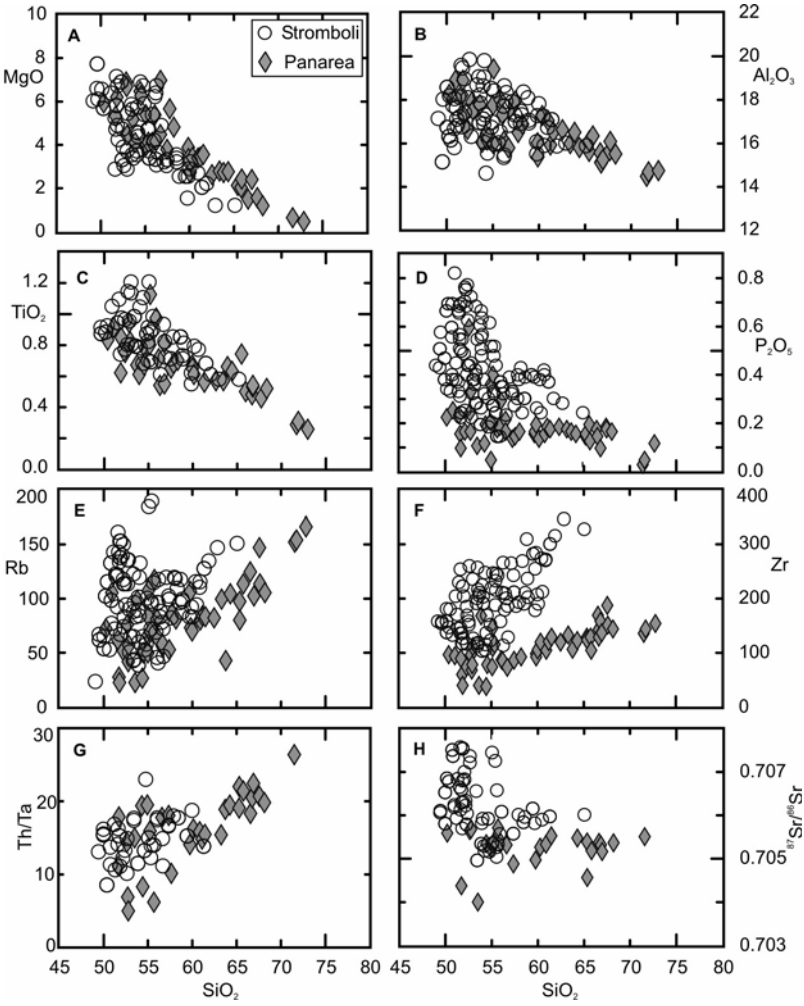

Fig. 7.13. Variation diagrams of selected major and trace elements for the islands of Panarea and Stromboli.

types of primary magmas. These underwent an evolution dominated by fractional crystallisation, magma mixing and moderate interaction with wall rocks in some cases, to produce intermediate and acidic products. The rhyolites from Basiluzzo show geochemical and isotopic evidence of a derivation from a shoshonitic mafic parent, probably represented by the mafic enclaves occurring in the rhyolite. Fractional crystallisation was less extreme and involved lower amounts of alkali-feldspar than at Lipari and Vulcano, which explains the less strong negative Eu anomalies of Panarea rhyolites.

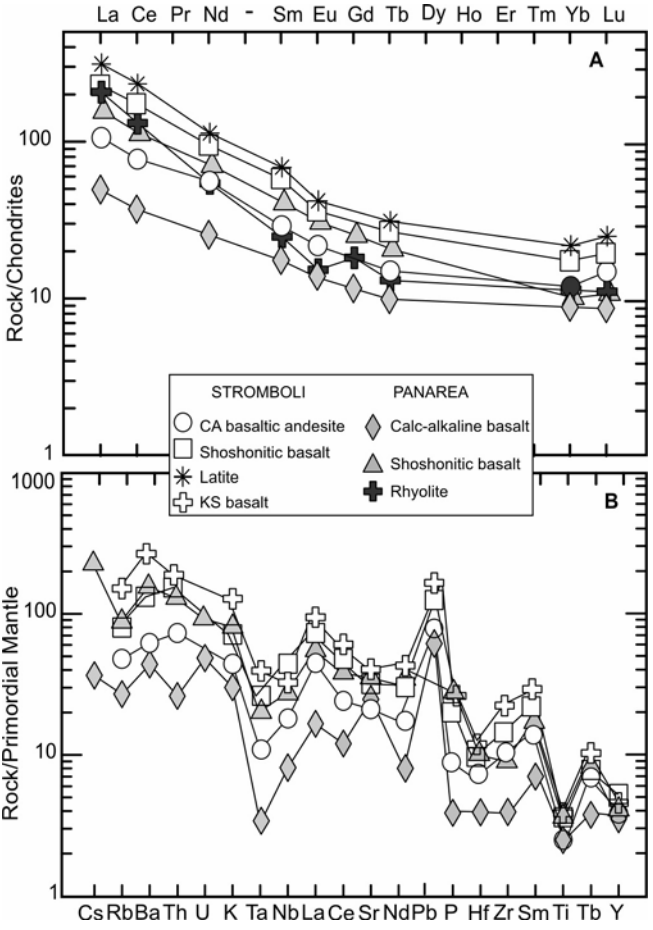

Fig. 7.14. REE (A) and incompatible element (B) patterns for selected rocks from Panarea and Stromboli.

The Panarea mafic calc-alkaline rocks have Sr-, Nd-, and Pb-isotope compositions similar to those of the western Aeolian arc. In contrast, HKCA and shoshonitic rocks have higher Sr-isotope and lower Nd- and Pb-isotope ratios and fall midway between the western Aeolian arc and Stromboli. This is also observed for some trace element ratios (e.g. Ba/La, La/Ta, Ce/Sr; Calanchi et al. 2002b). Therefore, geochemical and isotopic data suggest that two types of mantle sources have contributed to Panarea volcanic activity. One source is similar to western arc and produced the calc-alkaline magmas, whereas the other is a mixture between the western and eastern arc and generated the high-K calc-alkaline to shoshonitic melts.

7.9. Stromboli

7.9.1. Volcanology and Stratigraphy

The Stromboli volcano consists of a NE-SW elongated structure that forms the main island of Stromboli (12 km^2) and the nearby islet of Strombolicchio. Stromboli rises about 2000 m above the sea floor, reaching an altitude of 924 m above sea level. The age of the outcropping rocks is about 200 ka at Strombolicchio and younger than 100 ka at Stromboli (Condomines and Allegre 1980; Gillot 1987; Gillot and Keller 1993). Rock compositions display a large range of potassium contents, from calc-alkaline and high-K calc-alkaline to shoshonitic and potassic alkaline (Fig. 7.12). The present-day activity emits HKCA to shoshonitic basaltic lavas and scoriae (Rosi 1980; Francalanci et al. 1989; Bertagnini et al. 2003). Calc-alkaline rocks are restricted to basaltic andesites; KS show mafic compositions, whereas shoshonites and HKCA rocks range from basalt to high-K dacite and latite.

Since historical times, Stromboli has been characterised by continuous degassing and persistent discrete mildly strombolian explosions emitting scoriae and ashes every few minutes; random larger explosions and effusion of lava flows have occurred every few years. The active craters are located at an altitude of about 750 m, on a terrace sited at the top of the Sciara del Fuoco. This is a large depression bounded by parallel faults, developed along the NW flank of the volcano and continuing under the sea level almost to the foot of the cone.

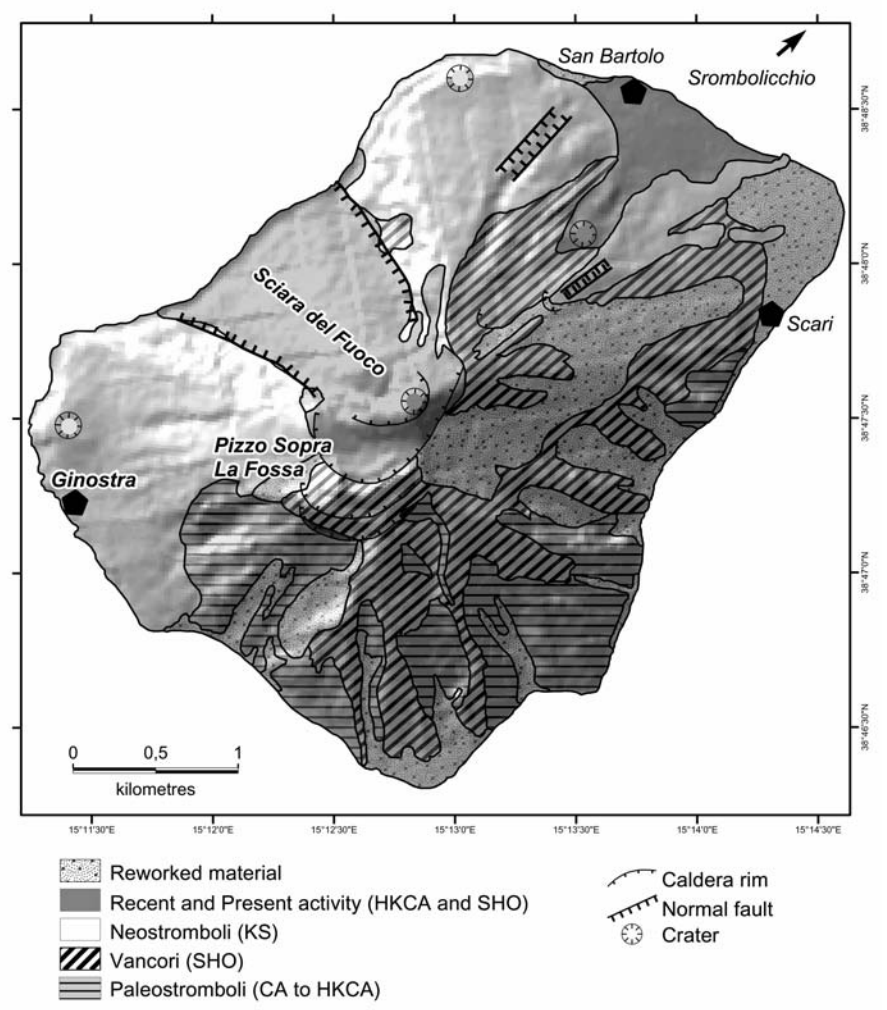

Fig. 7.15. Schematic geological map of Stromboli. Simplified after Hornig-Kjarsgaard et al. (1993).

Volcanological studies (Hornig-Kjarsgaard et al. 1993) have recognised various stages of activity (Paleostromboli, Vancori, Neostromboli, Recent and Present Activity; Fig. 7.15). A caldera formation marks the transition from Palaeostromboli to Vancori and a collapse of the entire western sector of the island divides Vancori and Neostromboli. The transition from Neostromboli to Recent Activity is associated with the formation of the Sciara del Fuoco. Flank instability is one of the main morphogenetic proc-

esses affecting the volcano, and represents a main hazard, as demonstrated by the landslide and associate tsunami that occurred in December 2002.

Compositionally, there is a tendency for potassium to increase and then to decrease with time at Stromboli. Calc-alkaline and high-K calc-alkaline basaltic andesites and andesites comprise the early activity of Strombolicchio and of older Paleostromboli. This is followed by HKCA and SHO mafic to intermediate products (younger Paleostromboli). The overlying Vancori series is a sequence of shoshonitic basalt to trachyte lavas and pyroclastics, which is followed by potassic alkaline lavas (KS) that form a large part of the western sector of the island (Neostromboli). The youngest activity includes a HKCA mafic lava flow along the northern flank of the volcano and the HKCA-shoshonitic basaltic scoriae and lavas of the present activity along the Sciara del Fuoco (Francalanci et al. 1989, 1993a; Hornig-Kjarsgaard et al. 1993; Bertagnini et al. 2003).

7.9.2. Petrography and Mineral Chemistry

All Stromboli lavas display seriate porphyritic holocrystalline to hypocrystalline textures, with phenocryst contents varying between about 10 to 50 vol % (Francalanci et al. 1993a; Bertagnini et al. 2003). Strongly zoned plagioclase (An_{90-45}) is the dominant phenocryst in all the rocks, followed by diopside to salite clinopyroxene. Olivine phenocrysts (Fo_{91-60}), often corroded and altered to iddingsite, occur in the mafic rocks. Orthopyroxene is present as microphenocryst in the CA and HKCA rocks and in the most evolved shoshonites. Leucite occurs as microphenocrysts and in the groundmass of the Neostromboli KS rocks. Rare biotite and amphibole occur in some andesites and latites; biotite is also found in the KS rocks as a groundmass phase. Small amounts of Ti-magnetite and ilmenite occur as a microphenocryst and groundmass phase. Apatite is a common accessory mineral.

7.9.3. Petrology and Geochemistry

Calc-alkaline rocks at Stromboli have lower K_2O, P_2O_5 and incompatible trace element contents than the associated shoshonitic and KS rocks. However, REE and the mantle-normalised incompatible element patterns have similar shapes for all rocks, with positive spikes of Ba and negative anomalies of HFSE (Fig. 7.14). Glass inclusions with primitive compositions (MgO ~ 7.8 wt %) contained in olivine (Fo_{91-84}) from basaltic scoriae of the present-day activity, have the same type of incompatible element patterns as the whole rocks (Bertagnini et al. 2003). Sr-isotope ratios are

higher than in the other Aeolian islands and increase from calc-alkaline ($^{87}Sr/^{86}Sr$ = 0.70500 to 0.70538) to KS rocks ($^{87}Sr/^{86}Sr$ = 0.70660-0.70757), whereas $^{143}Nd/^{144}Nd$ ratios decrease from 0.51265 to 0.51243. Sr and Nd isotopic ratios are negatively correlated, but display distinct values and a flatter trend than in the western-central Aeolian islands (Fig. 7.6a; Ellam et al. 1988, 1989; Francalanci et al. 1993b). Pb isotopic compositions are slightly less radiogenic than for the other Aeolian volcanoes ($^{206}Pb/^{204}Pb$ = 18.93 to 19.09; $^{207}Pb/^{204}Pb$ = 15.64 to 15.70; $^{208}Pb/^{204}Pb$ = 39.01 to 39.16; Fig. 7.6b). Whole rock O-isotope ratios cluster around $\delta^{18}O$ = +6.6 to +7.0‰, with little variation observed from calc-alkaline to potassic rocks (Ellam and Harmon 1990). He-isotope compositions exhibit the lowest values in the Aeolian arc with R/R_A ratios determined on olivine that range from about 2.4 to 4.6 (Di Liberto 2003).

Stromboli has been the subject of a large number of volcanological, petrological and geochemical studies aimed at understanding the genesis and evolution of various types of magmas, the relationship between magma compositional variations and timing of volcanic activity, and the structure of the magma plumbing system (e.g. Ellam et al. 1988; Luais 1988; Francalanci et al. 1989; Ellam and Harmon 1990; Hornig-Kjarsgaard et al. 1993; Renzulli et al. 2001; Bertagnini et al. 2003; Vaggelli et al. 2003). Many studies suggested that wide variation of major, trace element and isotopic compositions for rocks with a comparable degree of evolution may be the effect of complex fractional crystallisation, mixing and assimilation processes (Dupuy et al. 1981; Luais 1988). Francalanci et al. (1989, 1993a) have shown that when rock samples are separated according to their stratigraphic position, the geochemical variability becomes smaller and Sr isotope ratios change very little within single rocks series. This was interpreted as evidence that different batches of mafic parental magmas (CA, HKCA, SHO, and KS) underwent various degrees of fractional crystallisation to generate distinct suites of derivative liquids with broadly homogeneous isotopic signatures. Exceptions to this general scenario are the KS rocks of Neostromboli and the magmas erupted at the transition from Vancori (SHO) to Neostromboli (KS) activity that have variable isotopic compositions clearly indicative of mixing and/or assimilation processes. Calc-alkaline basalt and potassic magmas, which show poorly evolved mafic compositions, have been probably affected by a lower extent of fractional crystallisation than the HKCA and shoshonitic melts, which evolved to silica-rich and MgO-poor compositions.

However, the primary petrologic problem at Stromboli is the origin of the variable compositions of mafic magmas, which are parental to calc-alkaline, HKCA, shoshonitic and potassic suites. Dupuy et al. (1981) suggested that the parent magmas of various rock suites were generated in a

heterogeneous mantle wedge affected by various degree of metasomatism. Such a view was shared by several authors (e.g. Ellam et al. 1988; Luais 1988). Francalanci et al. (1993b) proposed that, in addition to source heterogeneity, geochemical and isotopic variations in the mafic magmas could be also created by a process of continuous mixing, fractionation, and assimilation of calc-alkaline parent magmas in a deep reservoir. Such a process would be able to produce a suite of mafic melts characterised by a wide range of incompatible element abundances and isotopic compositions. Fractional crystallisation at shallow level of these melts would generate various suites of rocks.

Peccerillo (2001) noticed that the Stromboli KS rocks, have concentrations and ratios of incompatible elements (e.g. Ta, Zr, Th, Sr, Ba, REE, Th/La, Ba/Nb, Zr/Nb) and radiogenic isotope signatures that closely resemble those at Somma-Vesuvio, except for K and Rb which are higher at Vesuvio. Moreover, the compositions of calc-alkaline and shoshonitic rocks from Stromboli also exhibit close compositional affinities to the rocks from the Campi Flegrei and Procida. This compositional similarity argues against the idea that geochemical variation in the Stromboli mafic rocks could derive from any kind of process occurring in the volcanic system, given the different type of basement and magmatic plumbing system at Stromboli, Vesuvio and Campi Flegrei. Therefore, compositionally similar mantle sources were invoked for the Stromboli and Campanian magmas.

7.10. Aeolian Seamounts

There are several seamounts located to the northwest (Sisifo, Enarete, Eolo) and to the northeast (Lametini, Alcione, Palinuro) of the Aeolian archipelago that define a horseshoe-type pattern around the Marsili basin. Ages range from 1.3 to less than 0.1 Ma. Compositions range from arctholeiitic (Lametini and southern Marsili basin), calc-alkaline and HKCA (Marsili, Sisifo, Eolo, Panarea slope, Palinuro, Stromboli canyon and Alcione) to shoshonitic (Enarete, Eolo, Sisifo, and northern Stromboli slope). Description of rocks from Aeolian seamounts is given in Chap. 9.

7.11. Petrogenesis

The Aeolian magmas are characterised by complex major, trace element and isotopic variations, which are observed both within the single islands

and at the regional scale. Petrological, crystal chemistry and fluid inclusion studies on rocks from several islands have shown that magmas have undergone polybaric evolution processes (e.g. Nazzareni et al. 2001; Zanon et al. 2003, Frezzotti et al. 2003). These were dominated by fractional crystallisation, but crustal assimilation and mixing also played an important role in most centres. Fractional crystallisation was more active in the central islands than in the external volcanoes. Therefore, abundant rhyolitic rocks are observed at Lipari and Vulcano.

In general terms, the Aeolian calc-alkaline rocks have lower degrees of incompatible element enrichment and $^{87}Sr/^{86}Sr$ ratios at a given silica and MgO content than the associated shoshonitic and potassium alkaline volcanics in the single islands or arc sectors. However, there are significant trace element and isotopic variations along the arc, which are best observed if single magmatic suites are considered in insulation. For instance, mafic calc-alkaline rocks from western-central islands have much lower

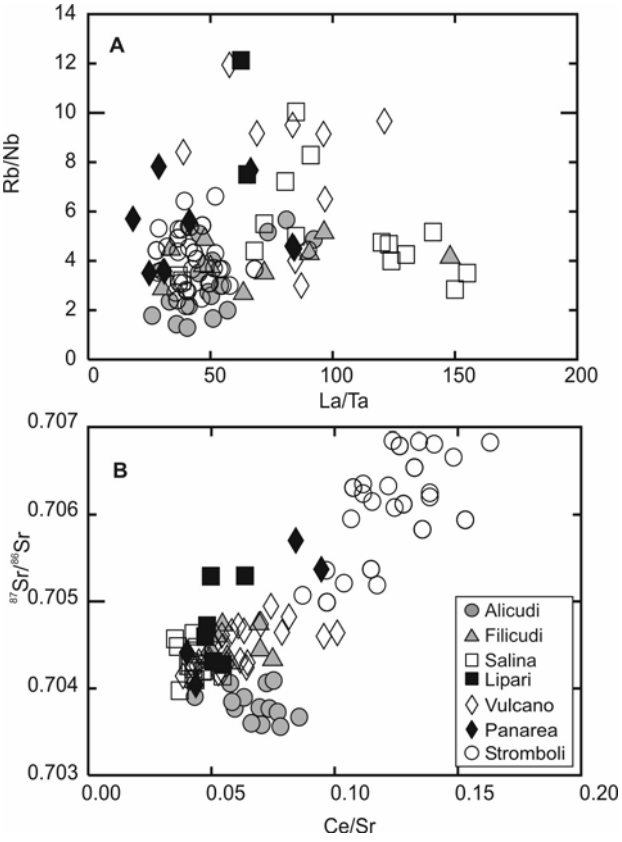

Fig. 7.16. Variation of LILE/HFSE element ratios and $^{87}Sr/^{86}Sr$ in the Aeolian arc.

$^{87}Sr/^{86}Sr$ than at Stromboli; the same holds for KS rocks from Vulcanello and Stromboli. Moreover, an overall increase of LILE/HFSE ratios has been observed from the external islands of Alicudi and Stromboli to the central sector of the arc (Francalanci et al. 1993b, 2004; Fig. 7.16).

Based on compositional characteristics summarised above, major petrological problems for the Aeolian arc magmatism include:

1. The genetic relations among various types of mafic magmas characterised by different enrichment in potassium;
2. The reasons of the along-arc petrological and geochemical variations;
3. The relations between compositional variations of volcanism and regional tectonics.

7.11.1. Genesis of Mafic Magmas

A much debated issue in the petrogenesis of Aeolian arc magmatism has been whether mafic magmas with different enrichments in potassium, incompatible elements and radiogenic isotopes are related to each other by some type of shallow level evolution process, or they reflect the occurrence of different types of primary melts, possibly derived from compositionally variable mantle sources.

7.11.1.1. Role of Shallow-Level Processes

The increase of $^{87}Sr/^{86}Sr$ and the decrease of $^{143}Nd/^{144}Nd$ from mafic calc-alkaline to potassic rocks in the Aeolian arc, along with the increase in incompatible element contents have been suggested to reveal a stronger crustal component in the potassic rocks than in the associated calc-alkaline magmas (e.g. Ellam et al. 1988; Esperança et al. 1992; De Astis et al. 2000). In principle, these compositions could have been imparted to magmas during their ascent through the crust by various degrees of wall rock assimilation (magma contamination). Alternatively, different amounts and/or types of upper crustal materials may have been added to the mantle (mantle contamination), whose melting generated a range of geochemically and petrologically different magmas.

There is ample evidence that the Aeolian magmas underwent interaction with crustal rocks during their ascent to the surface. Metamorphic xenoliths occur in all the islands, and some appear to have been melted extensively by contact with the enclosing magma (e.g. Barker 1987; Peccerillo et al. 1993; Frezzotti et al. 2004). Isotopic studies of single volcanic suites highlighted crustal contamination processes, which in some cases (e.g. at Alicudi) have affected more heavily mafic than evolved magmas. This has

lead some authors to propose that crustal assimilation, possibly combined with fractional crystallisation and continuous mixing, might have generated a range of mafic magmas with different levels of enrichment in incompatible elements (e.g. Esperança et al. 1992).

De Astis et al. (2000) and Calanchi et al. (2002b) noticed that calc-alkaline and HKCA basalts at Vulcano and Panarea have distinct trace element ratios (e.g. La/U, Rb/Zr, Zr/Nb) compared to the associated shoshonitic and KS mafic volcanics. However, the rocks of the Calabro-Peloritano basement underlying the Aeolian volcanoes show compositions that resemble the calc-alkaline rather than shoshonitic and KS rocks; this was interpreted to exclude a derivation of potassic rocks from calc-alkaline parents via crustal assimilation. The same conclusion was drawn by Frezzotti et al. (2004), who modelled magma contamination processes using melt inclusions entrapped in metamorphic xenoliths as contaminants.

At Stromboli, the increase in incompatible element abundances and Sr isotopic ratios from calc-alkaline to potassic suites was suggested by Francalanci et al. (1989) to have been generated by a process of continuous fractional crystallisation, assimilation and mixing. However, although this process can be modelled numerically, it fails to explain the geochemical similarity of Stromboli and Campanian volcanoes, as discussed earlier.

Isotopic and geochemical variations at the regional scale are also difficult to explain by magma assimilation processes. De Astis et al. (2002) calculated that at least 40% of average Calabrian crust should be assimilated to drive isotopic composition of Alicudi magmas to those typical of the Stromboli basalts. However, Ellam and Harmon (1990) found only modest O-isotope variations at a regional scale, for rocks displaying different $^{87}Sr/^{86}Sr$ signatures. Since magma contamination by crustal rocks generally produces strong ^{18}O enrichment accompanied by a moderate increase of $^{87}Sr/^{86}Sr$ ratios, it is unlikely that such a process is responsible for the wide range of mafic magma compositions observed along the Aeolian arc.

In conclusion, although crustal contamination has been an important evolutionary process at most of the Aeolian volcanoes, it seems inadequate to explain the geochemical and isotopic variations observed from calc-alkaline to potassic mafic melts at both local and regional scales. Therefore, many studies concluded that the mafic magmas with different enrichment in potassium reflect primary compositions which were generated in a heterogeneous mantle source (e.g. Ellam et al. 1988; Ellam and Harmon 1990; De Astis et al. 1997, 2000; Francalanci et al. 2004).

7.11.1.2. Role of Mantle Processes

The coexistence in the Aeolian arc of calc-alkaline, shoshonitic and potassic primary melts showing variable geochemical signatures has been interpreted as an effect of compositional heterogeneities in the mantle wedge and of different degrees of partial melting, decreasing from CA to KS magmas (e.g. Ellam et al. 1988; Francalanci et al. 1993b; De Astis et al. 2000). Isotopic modifications from calc-alkaline to potassic mafic rocks in single islands (e.g. at Vulcano and Stromboli) have brought to suggest vertical compositional heterogeneities within the upper mantle (e.g. Ellam et al. 1989; Francalanci et al. 1989, 1993a; De Astis et al. 1997, 2000). Alternatively, the mantle source of Aeolian magmas could be permeated by phlogopite-rich veins. Therefore, a variable degree of partial melting of veined peridotite would involve different proportions of veins and host rock, leading to generations of melts with different K_2O, incompatible element contents and isotopic signatures (Francalanci et al. 2004).

Whatever model is assumed for the mantle source of Aeolian magmas, Sr-Nd-Pb-He isotope variations call for the involvement of upper crustal components in magma genesis. It can be calculated that less than 10% of upper crust added to a pyrolite mantle could explain the entire range of radiogenic isotopic compositions encountered in the Aeolian mafic rocks. Sediments transported by the Ionian subducting plate represent the most likely candidates for such a mantle source contaminant (e.g. Ellam et al. 1988; Francalanci et al. 1993b).

7.11.2. Along-arc Compositional Variations

The variable relative abundances of calc-alkaline and shoshonitic magmatism in the various sectors of the Aeolian arc, along with trace element and isotopic variations require important regional modifications in the physicochemical conditions of magma genesis (i.e. fluid activity, degrees of partial melting, nature of mantle mineralogy, nature and degree of mantle metasomatism). Fluid activity has important effects on phase stability during mantle melting and, therefore, heavily controls the petrological characteristics of magmas. In particular, hydrated conditions determine an increase of peridotite partial melting and favour calc-alkaline with respect to potassic magmatism (e.g. Wendlandt and Eggler 1980a,b; Ulmer 2001). Accordingly, variable activity of hydrous fluids is a likely explanation for along arc petrological variability.

Different roles for fluids and silicate melts were suggested by Francalanci et al. (1993b) on the basis of trace element data. These authors argued that an increased fluid/melt ratio in the metasomatic modifications

for mantle source was responsible for the increase of LILE/HFSE ratios towards central islands. Note that fluids preferentially transport LILE with respect to HFSE (e.g. Becker et al. 2000; Scambelluri et al. 2001). Variable contribution of slab-derived fluid to arc petrogenesis is supported by positive correlation of $\delta^{11}B$ (-6.1 to +2.3‰) vs. mobile/immobile element ratios in mafic rocks (Tonarini et al. 2001a).

Alternative explanation for regional variations of LILE/HFSE ratios suggests that the pre-metasomatic source beneath Stromboli and Alicudi was an OIB-type mantle enriched in HFSE, whereas there was a depleted MORB-type mantle beneath central arc (Ellam et al. 1988; Gertisser and Keller 2000; De Astis et al. 2000). OIB-type rocks, such as those from Etna, exhibit high contents of HFSE and low LILE/HFSE ratios (Ellam et al. 1988). The origin of such an OIB source is debated. Recent views suggest a derivation from an upwelling deep mantle plume (Gasperini et al. 2002). Other authors propose mantle inflow from the side plates of Apulia and Africa during rollback of the Ionian plate (Peccerillo 2001, 2002; Trua et al. 2004). Note, however, that the few available Hf isotopic data indicate that Alicudi has a composition close to central Tyrrhenian volcanoes, eventually indicating a mantle inflow from the Tyrrhenian basin.

Sr-Nd-Pb isotope variation along the Aeolian arc represents a part of a larger hyperbolic array connecting the Na-alkaline rocks of Etna-Iblei-Ustica and Tuscany (Figs. 7.6, 7.17). Most of the western and central Aeolian islands plot near to the low-Sr, high-Nd-Pb end-member, whereas the Stromboli volcanics plot away from Etna together with Campanian volcanoes and Ernici-Roccamonfina KS rocks. However, the isotopically most primitive rocks from Alicudi have low Sr-isotopic ratios that fall outside the trend (Fig. 7.17).

Radiogenic isotopic trends along the Italian peninsula have been interpreted as an evidence for interaction between mantle and upper crustal materials (e.g. Hawkesworth and Vollmer 1979; Peccerillo 1985; De Astis et al. 2000; see discussion in previous chapters). Similarly, the increase of $^{87}Sr/^{86}Sr$ and the decrease of Nd-Pb-He isotope ratios going from east to the west along the Aeolian arc suggest an increasing amount of mantle contamination by crustal material, such as subducted sediments. The low Sr-isotope compositions of Alicudi require that little if any sediments were added to the source. Therefore, fluids or melts derived from a subducting oceanic slab has to be assumed as the only contaminant for this volcano (e.g. Ellam et al. 1988; De Astis et al. 2000).

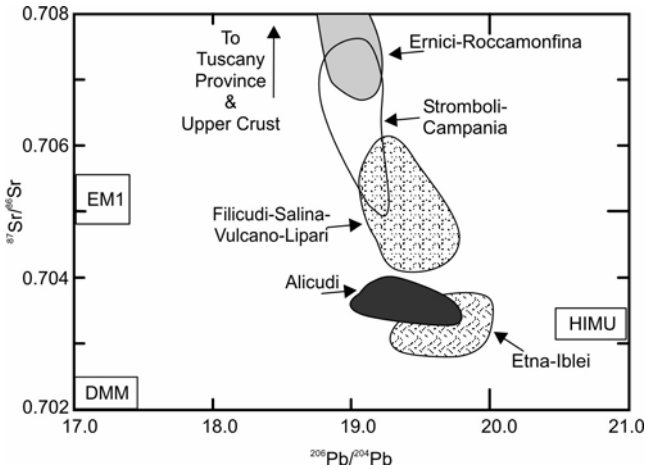

Fig. 7.17. $^{206}Pb/^{204}Pb$ vs. $^{87}Sr/^{86}Sr$ for the Aeolian arc and other volcanic provinces in central and southern Italy. Composition of HIMU, DMM and EM1 mantle reservoirs is also show.

7.12. Geodynamic Setting

The occurrence of abundant calc-alkaline andesites and the high LILE/HFSE ratios of rocks have brought to a general, though not unanimous consensus that the Aeolian arc is genetically related to subduction processes. Such a hypothesis is strongly supported by the occurrence of deep-focus earthquakes beneath the eastern sector of the arc.

However, there are important along-arc structural and geophysical variations that parallel compositional modifications of magmas and make the Aeolian arc an intriguing case where magmatism and geodynamics are closely related. The Tindari-Letojanni-Malta strike-slip fault system represents a primary divide for both magmatism and structural setting. Deep seismicity affects only the eastern sector, continuing almost until the Campania volcanoes. Moreover, there is a strong variation of the attitude of the foreland monocline west and east of the Tindari-Letojanni-Malta fault, the dip angles passing from some 4-6° in northern Sicily to more than 20° offshore southern Calabria. Doglioni et al. (2001) suggested that subduction is active both west and east of the Tindari-Letojanni-Malta fault system, but subduction rate is higher in the east than in the west. Such a difference in the subduction behaviour would be related to a variable nature of the undergoing crust, which would be of oceanic-type in Calabria and of continental-type in Sicily. The subduction of a high-density oceanic slab off-

shore Calabria would generate a steeper dip angle and a faster rate of slab rollback compared to northern Sicily. The lack of deep seismicity in the west is explained by the plastic behaviour of the easily fusible continental crust as opposed to the more rigid characteristics of the oceanic or transitional Ionian plate. In such a model, the Tindari-Letojanni-Malta fault is viewed as a zone of accommodation of differential slab retreat rates (Doglioni et al. 2001). Gvirtzman and Nur (1999) proposed a somewhat different model, which hypothesizes southeastward retreat of the Ionian plate, but no active subduction beneath the western Aeolian arc. The subduction of the narrow Ionian plate would provide sediments to the upper mantle, whereas its southeastward rollback would generate inflow of OIB-like mantle material from the side plates of Apulia and Africa.

The occurrence of rocks with relatively primitive isotopic signatures in the western Aeolian arc argues against the presence of a subducting continental-type slab. Moreover, the prevailing calc-alkaline nature of the western arc suggests abundant hydrous fluid percolation through the mantle wedge. This is more easily accomplished by oceanic rather than continental-type crust. Therefore, petrological and geochemical data apparently support the hypothesis of subduction of oceanic crust beneath the western arc. The absence of deep seismicity in the west would indicate that active subduction has ceased. In this view, the low dip angle of the foreland monocline in Sicily, could result from slab break-off.

Finally, the increase in the volume of silicic rocks progressing from the external to central islands is related to modification of the crustal structural setting along the arc. Barberi et al. (1994b) report geophysical and field evidence indicating extensive development of host and graben structures along the Tindari-Letojanni-Malta strike-slip fault system, where Lipari and Vulcano are located. Such a geological setting would favour the formation of large shallow-level magma chambers, where extensive fractional crystallisation processes generated abundant silicic melts.

7.13. Conclusions

The Aeolian islands consist of calc-alkaline to shoshonitic lavas and pyroclastics, with minor potassic alkaline rocks, which were generated in a subduction environments developed between the converging African and Eurasian plates. There are strong variations of rock compositions, both at local and regional scales. Regional variations consist of an increase in the amounts of potassic relative to calc-alkaline volcanics from western to eastern islands, parallel to an increase of $^{87}Sr/^{86}Sr$ and a decrease of Nd, Pb

and He isotope ratios. The eastern island of Stromboli resembles closely the volcanoes of the Campania Province. These variation patterns do not seem to extend to the Aeolian seamounts, on which, however, very small amount of data are available. Range of silica contents in the single Aeolian volcanoes is also very variable and increases from external to central islands.

Petrological and geochemical variations along the arc are considered to result from variable relative amounts of slab-released fluids and melts added to the mantle wedge, as well as from higher amounts of subducted sediments added to the mantle beneath eastern islands. Variation of pre-metasomatic mantle composition, from MORB-type in the central arc to OIB-type in the external islands, is also considered as an important factor for compositional diversity along the arc.

The range of rock compositions occurring within single islands reflects both the variable characteristics of parental magmas and the shallow-level evolution history. In particular, the presence of abundant silicic rocks in the central Aeolian islands has been suggested to depend on extensive fractional crystallisation processes in large magma chambers developed along the horst-graben system associated with the Tindari-Letojanni-Malta strike-slip fault. This fault represents an important structural divide in the Aeolian arc, separating arc sectors characterised by distinct petrological, structural and volcanological settings. Active volcanism and deep seismicity are restricted to central and eastern sectors, whereas they are absent in the west. This has been related to active subduction of the oceanic or thinned continental Ionian plate beneath eastern arc, whose effects are observed until the Campania Province.

Table 7.2 Composition of selected Aeolian arc volcanics. Source of data: 1) Francalanci et al. (1989, 1993a); 2) Peccerillo et al. (1993); 3) De Astis et al. (1997, 2000); 4) Del Moro et al. (1998); 5) Gertisser and Keller (2000); 6) Calanchi et al. (2002b); 7) Gasperini et al. (2002); 8) Gioncada et al. (2003); 9) Santo et al. (2004); 10) Author's unpublished data. Numbers in parentheses indicate data on different, though compositionally similar samples from the same locality as those analysed for the other elements.

Volcano	**Alicudi**		**Filicudi**		**Salina**		
Rock type	Basalt	Andesite	Basalt	Dacite	Basalt	Andesite	Rhyolite
Data source	2,7,10	2,10	9,1,7	9	5	5	10
SiO_2 wt%	50.89	56.80	50.03	63.20	51.35	60.12	70.63
TiO_2	0.79	0.63	0.72	0.56	0.61	0.59	0.33
Al_2O_3	18.48	17.58	18.95	16.23	16.82	17.31	14.39
FeO_{total}	8.13	6.15	8.43	4.64	8.81	6.42	3.23
MnO	0.16	0.14	0.17	0.11	0.18	0.14	0.12
MgO	6.11	4.79	5.80	2.31	6.24	2.99	1.29
CaO	10.61	7.54	11.39	5.86	11.05	6.89	3.00
Na_2O	2.68	3.32	2.31	3.43	2.24	3.39	3.22
K_2O	1.06	2.08	1.10	2.89	1.09	1.97	3.57
P_2O_5	0.26	0.33	0.16	0.18	0.17	0.17	0.08
LOI	0.52	0.30	0.59	0.36	0.56	0.18	0.22
Sc ppm	32.9	27.3	30	17	-	-	16
V	-	-	-	-	313	204	77
Cr	172	124	68	12	61	6	18
Co	31	23	30	13	31	15	19
Ni	48	25	23	2	36	7	7
Rb	24	42	23	85	26	48	99
Sr	814	886	687	608	778	576	333
Y	14	25	17	15	16	21	15
Zr	84	107	75	123	52	90	136
Nb	6	13	7	10	3.14	5.35	19
Cs	0.61	0.80	0.26	-	0.99	0.97	2.6
Ba	347	787	352	646	351	496	1099
La	17	39	16	33	17	22	22
Ce	35	69	34	54	34	42	52
Nd	15	29	17	25	16	19	20
Sm	3.2	4.8	3.6	5.4	3.6	4.2	4.0
Eu	1.1	1.5	1.0	1.1	1.1	1.2	0.91
Tb	0.56	0.59	0.48	0.49	0.47	0.64	0.49
Yb	1.86	1.92	2.00	1.80	1.63	2.44	1.90
Lu	0.32	0.29	-	0.30	0.27	0.38	0.30
Hf	1.69	2.77	2.00	2.60	1.52	2.60	2.80
Ta	0.34	0.72	-	0.49	0.19	0.35	0.55
Pb	(5)	(4)	(6)	-	6.3	6.8	-
Th	2.93	8.7	3.0	8.7	3.4	5.1	9.0
U	3.71	2.84	1.02	2.80	1.08	1.97	2.60
$^{87}Sr/^{86}Sr$	0.70391	0.70343	0.70445	0.70436	0.70410	0.70439	0.70496
$^{143}Nd/^{144}Nd$	0.51281	0.51288	0.51273	0.51272	0.51279	0.51277	0.51272
$^{206}Pb/^{204}Pb$	19.326	19.667	19.500	19.464	19.398	19.336	-
$^{207}Pb/^{204}Pb$	15.638	15.648	15.650	15.661	15.686	15.688	-
$^{208}Pb/^{204}Pb$	39.114	39.363	39.230	39.263	39.243	39.204	-
$^{176}Hf/^{177}Hf$	(0.283096)	-	(0.283074)	-	-	-	-

Table 7.2 (cont.)

Volcano	**Lipari**			**Vulcano**			
Rock type	Basaltic andesite	Andesite	Rhyolite	Shoshonitic basalt	Shoshonite	Trachyte	Rhyolite
Data source	1	10	8	4,7	3,8	3	8
SiO_2 wt%	53.76	54.23	73.35	48.10	53.35	60.28	72.76
TiO_2	0.61	0.62	0.10	0.82	0.67	0.49	0.13
Al_2O_3	16.27	18.23	12.70	12.75	16.36	16.36	13.24
FeO_{total}	8.26	9.03	2.00	11.12	8.13	5.81	2.62
MnO	0.16	0.13	0.11	0.22	0.16	0.11	0.11
MgO	6.25	4.33	0.34	8.34	3.61	1.72	0.34
CaO	9.86	8.05	0.92	12.69	7.25	4.52	0.99
Na_2O	2.14	2.33	4.02	2.20	4.17	4.20	4.25
K_2O	1.15	1.91	4.60	2.29	4.36	5.19	4.83
P_2O_5	0.17	0.18	0.02	0.24	0.36	0.32	0.04
LOI	1.03	0.31	1.67	0.03	1.14	0.59	0.68
Sc ppm	42	23	3	39.1	20.8	12.8	4
V	-	255	10	-	167	105	13
Cr	128	17	10	239	53	30	4
Co	32	33	2	22	28.18	20.7	2
Ni	33	19	3	50	21	12	2
Rb	27	38	267	53.7	153	190	280
Sr	580	506	52	1110	1212	887	81
Y	18	13	14	-	22	28	44
Zr	58	51	202	81	166	208	264
Nb	3.6	6	32	-	18	25	36
Cs	1.1	2.21	17	1.5	5.65	4.2	18.6
Ba	319	493	42	556	904	672	85
La	13	30	50	28	65	69.7	77
Ce	28	55	97	49	117	115	136
Nd	14.7	19	39	-	48.5	43	49
Sm	3.2	5.5	8.1	5.6	8.75	7.58	9.3
Eu	0.90	1.61	0.17	1.70	1.65	1.25	0.26
Tb	0.48	0.7	1.12	0.60	0.67	0.8	1.16
Yb	1.7	2.4	4.46	1.5	2.05	2.38	4.50
Lu	-	0.32	0.63	-	0.26	0.37	0.67
Hf	1.8	2.3	6.2	2.3	3.75	4.7	7.6
Ta	0.2	0.63	2.4	0.4	1.13	1.3	3.0
Pb	6.8	12	27	-	(20)	-	29
Th	3.4	6.25	46.7	6.1	21.8	31.6	58
U	0.91	1.91	13.5	1.9	6.7	8.5	16.6
$^{87}Sr/^{86}Sr$	0.70472	0.70431	0.70472	0.70425	0.704578	0.704616	0.70527
$^{143}Nd/^{144}Nd$	0.51267	0.51283	0.51256	0.51269	0.512671	0.512615	0.51257
$^{206}Pb/^{204}Pb$	19.44	19.633	19.380	19.528	19.412	19.375	19.379
$^{207}Pb/^{204}Pb$	15.66	15.655	15.701	15.656	15.676	15.658	15.694
$^{208}Pb/^{204}Pb$	39.26	39.421	39.343	39.314	39.291	39.221	39.321
$^{176}Hf/^{177}Hf$	-	-	-	0.282916	-	-	-

Table 7.2 (cont.)

Volcano	**Panarea**			**Stromboli**			
Rock type	Basalt	Andesite	Rhyolite	HKCA basalt	CA Basaltic andesite	Shoshonitic basalt	KS Shoshonite
Data source	6	6	6	1,3	1	1,3	1,3
SiO_2 wt%	51.16	55.33	69.36	51.08	55.58	52.72	51.93
TiO_2	0.62	0.62	0.27	0.92	0.67	0.94	0.90
Al_2O_3	17.11	17.33	14.11	17.16	16.08	16.65	17.45
FeO	9.69	8.13	1.82	7.64	7.03	7.41	7.16
MnO	0.16	0.13	0.09	0.15	0.15	0.15	0.14
MgO	6.25	3.58	0.56	6.30	6.47	5.64	5.93
CaO	10.24	7.05	2.20	10.62	9.02	9.01	8.76
Na_2O	2.54	2.58	4.08	2.31	2.35	2.36	2.18
K_2O	0.90	1.52	4.46	2.34	1.63	3.61	4.63
P_2O_5	0.08	0.12	0.01	0.48	0.23	0.56	0.50
LOI	1.26	3.62	3.03	0.66	0.54	0.50	0.23
Sc	41	29	4	33	36	29	28
V	287	228	26	-	-	-	-
Cr	115	23	2.3	162	271	78	140
Co	33	21.5	2.5	34	33	30	30
Ni	27	13	1	52	53	36	34
Rb	23	53	151	68	40	113	152
Sr	566	441	289	750	540	708	773
Y	17	22	17	27	21	32	27
Zr	43	89	138	177	111	198	188
Nb	5	7	17	25	7	21	28
Cs	0.69	2.54	8.88	-	1.30	-	-
Ba	329	409	885	1095	517	1538	1782
La	12	20	47	50	23	50	56
Ce	23	38	77	102	47	103	99
Nd	12	19	24	50	22	42	45
Sm	2.7	3. 9	3.6	8.8	4.6	8.8	10.8
Eu	0.85	1.05	0.85	2.10	1.20	2.10	2.2
Tb	0.37	0.56	0.47	1.0	0.53	1.0	0.95
Yb	1.50	1.97	1.85	2.50	1.90	2.50	2.2
Lu	0.22	0.31	0.27	0.40	-	0.42	0.5
Hf	1.36	2.62	4.47	3.90	2.80	4.00	4.2
Ta	0.14	0.36	1.13	1.40	0.50	1.20	1.2
Pb	-	-	-	(18)	6.5	-	-
Th	2.5	6.5	30	16	8.2	18	18.1
U	1.3	4.0	9.3	-	1.9	-	-
$^{87}Sr/^{86}Sr$	0.70441	0.70491	0.70553	(0.70660)	0.70507	0.70683	0.70753
$^{143}Nd/^{144}Nd$	0.51284	0.51258	0.51259	(0.51253)	0.51261	0.51252	0.51250
$^{206}Pb/^{204}Pb$	19.43	19.233	19.186	(19.01)	19.17	19.002	18.975
$^{207}Pb/^{204}Pb$	15.71	15.680	15.682	(15.65)	15.66	15.658	15.654
$^{208}Pb/^{204}Pb$	39.36	39.142	39.163	(39.03)	39.08	39.041	39.007

8. The Sicily Province

8.1. Introduction

The Sicily Province consists of several young to active volcanoes occurring in eastern Sicily, in the Sicily Channel and in the southern Tyrrhenian Sea. Etna is by far the best known among these volcanoes; other centres include Iblei, Pantelleria, Linosa, several seamounts in the Sicily Channel, the Island of Ustica and the Prometeo submarine lava field in the southern Tyrrhenian Sea (Fig. 8.1). The rocks have a variable petrochemical affinity, from tholeiitic to Na-alkaline, but all show typical intraplate trace element signatures (i.e. low LILE/HFSE ratios) and isotope compositions characterised by unradiogenic Sr, and radiogenic Nd. Ages range from about 7 Ma to present. A synthesis of ages, volcanological and petrological characteristics of Sicily volcanoes is given in Table 8.1. Geochemical analyses for representative rock types can be found in Table 8.2.

8.2. Regional Geology

The Sicily volcanoes are located in a variety of structural settings and on different types of bedrocks. Mount Etna (about 0.6 Ma to present) occurs on the accretionary prism of the Africa-Europe subducting system, at the contact between the Ionian lithosphere, the northern margin of the African plate (Pelagian Block, a promontory of the African foreland) and the corrugated Sicilian-Maghrebian chain (Fig. 8.1; Behncke 2001).

The Iblei volcanoes (about 7-1.5 Ma) are sited on the Iblean Plateau, an area of the Pelagian Block which has been intermittently affected by volcanism since Triassic times. Plio-Quaternary volcanism developed along NE-SW trending faults at graben margins cutting Oligocene to Miocene platform carbonates and foredeep sequences.

The volcanoes of the Sicily Channel (Linosa and Pantelleria and a number of seamounts; Miocene to present in age) are mainly located along ex-

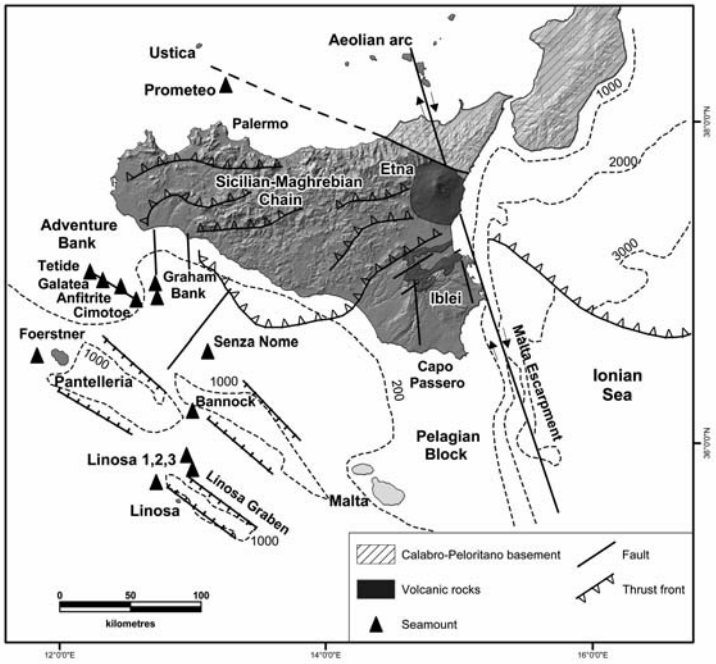

Fig. 8.1. Location map of Sicily volcanoes.

tensional NW-SE trending faults bordering the continental rift systems that affected the northern African continental lithosphere or along N-S strike-slip faults (e.g. Calanchi et al. 1989). Three main rift zones are recognized in the Sicily channel: the Malta, Linosa and Pantelleria grabens (e.g. Boccaletti et al. 1984). The processes that generated rifting in this zone are not fully understood.

The Ustica island (0.75-0.13 Ma) occurs in the southern Tyrrhenian Sea, west of the Aeolian volcanic arc, along the southern margin of the Tyrrhenian abyssal plain, probably at the intersection between E-W and NW-SE trending faults (e.g. Boccaletti et al. 1984). The recently discovered Prometeo submarine lava field is located a few km southeast of Ustica (Trua et al. 2003).

Crustal thickness in the Sicily volcanic province is about 20 to 25 km (Boccaletti et al. 1984; Hirn et al. 1997; Nicolich 2001, and references therein). The lithosphere shows variable thickness from about 50 km beneath the Ustica island, to 60 km beneath the Sicily Channel and some 70 km in the Etna and Iblei area (Calcagnile et al. 1982). Heath flow is about 50 to 70 mW/m^2 at the regional scale but is higher than 80-100 mW/m^2 in the areas affected by recent magmatism (Della Vedova et al. 2001).

Table 8.1. Summary of geochronological, volcanological and petrological characteristics of the Sicily volcanoes.

VOLCANO	AGE	VOLCANOLOGY and PETROLOGY
Etna	About 0.6 Ma to present	- Several coalescing and superimposed stratovolcanoes mostly formed of lavas, spotted with hundreds of cinder cones, cut by three rift zones and by the Valle del Bove depression. Rocks include tholeiitic basalts followed by Na-alkaline rocks (trachybasalts, hawaiites and minor benmoreites and trachytes).
Iblei	7 to 1.5 Ma	- Multicentre district with several monogenetic cones, maars and lava flows formed by both submarine and subaerial activity. Rocks range from tholeiitic basalt to hawaiite, basanite and nephelinite.
Linosa	1.06 to 0.53 Ma	- Several monogenetic hydrovolcanic, strombolian and effusive centres and two larger cones formed of mildly alkaline basalts and hawaiites. Benmoreite-trachyte lithics occur in early pyroclastic deposits.
Pantelleria	320 to less than 10 ka	- Stratovolcano with central nested calderas formed of peralkaline rhyolitic (pantellerites) and trachytic ignimbrites and lava domes, with minor weakly Na-alkaline basaltic lava flows and cinder cones.
Sicily Channel seamounts	Miocene to Present	- Several cones (Cimotoe, Tetide, Anfitrite, Graham, Senza Nome, Foestner, etc.) rising along NW-SE and N-S trending faults, formed of tholeiitic basalt, hawaiite and basanite.
Ustica and Prometeo	750 to 130 ka	- Multicentre complex formed of dominant hawaiite and mugearite with minor benmoreite and trachyte lava flows and minor hydrovolcanic products and pumices. Prometeo is a benmoreite submarine lava flow.

8.3. Etna

Etna is an active volcano reaching an altitude of about 3315 m, and covering an area of about 1260 km^2 (Fig. 8.2). It has developed at the intersection between various tectonic lineaments, the most important being the NNW-SSE trending Tindari-Letojanni-Malta and the NNE-SSW trending Messina-Giardini fault systems (e.g. Boccaletti et al. 1984; Chester et al. 1985; Lanzafame and Bousquet 1997). Etna shows an asymmetrical conical shape. The flank inclination is low (5-10 degrees) up to 1800 m altitude, but increases sharply (about 25 degrees) in the upper part of the volcano. This morphology results from the coalescence and superimposition of several distinct cones, and from flank eruptions which built up a large

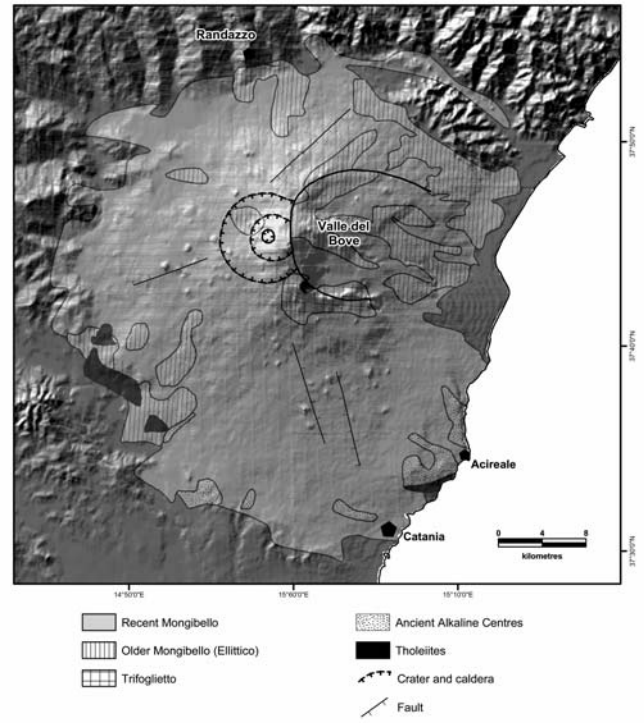

Fig. 8.2. Schematic geological map of Etna volcano. Modified after Gillot et al. (1994).

number of monogenetic cones concentrated along zones of weakness, especially in the NE sector. The pre-volcanic sequence consists of Triassic to Tertiary carbonate rocks of the Iblean foreland that gently dip northward and attain a depth of 6-7 km beneath Etna, and a stack of southward-verging tectonic units of the Sicily-Maghrebian chain. These are mostly formed by flysch sequences, marls, and conglomerates of various ages (e.g. Grasso 2001).

8.3.1. Volcanology and Stratigraphy

Four main evolution stages have been distinguished for Mount Etna activity (Gillot et al. 1994; Branca et al. 2004). The first stage (580 to 225 ka) was characterised by emplacement of tholeiitic basalts, which were erupted over a wide area from the Iblean Plateau in the south to the Peloritani mountains in the north, and presently crop out as pillow-lavas**,** hyaloclastites and sills along the Ionian Sea coast north of Catania, between

Acicastello and Acitrezza, and along the south-western margin of the volcano (Fig. 8.2; Corsaro and Cristofolini 2000). Starting from about 220 ka, the volcanic activity concentrated in the Ionian coast and changed from tholeiitic to Na-alkaline (Branca et al. 2004). A number of central volcanoes (Ancient Alkaline Centres or Timpe Volcanoes) were constructed over a time span of about 100 ka (172 to 96 ka), and their remnants mainly crop out along the present-day margin of Etna. Successively, various cones (Tifoglietto, Cavigghiuni, Vavalaci etc.) making up the so-called Trifoglietto unit (Chester et al. 1985) were built up by effusive and explosive eruptions between about 80 to 60 ka (Gillot et al. 1994). Finally, the Mongibello stratovolcano was constructed between about 60 ka (80 ka according to Branca et al. 2004) to present. Older Mongibello activity built up the so-called Ellittico volcano, consisting of prevailing benmoreitic to trachytic lavas and pyroclastics, and was closed by a caldera collapse (at about 15 ka). Recent Mongibello activity (14 ka to present) has been characterised by dominant effusive eruptions and strombolian explosions, giving lava flows and scoria cones, which cover extensively the flanks of the Etna volcano. Minor collapses (e.g. the summit Piano caldera, about 2000 years before present) occurred during recent Mongibello activity.

Etna is marked by several important volcano-tectonic structural features, in addition to the calderas mentioned above. The Valle del Bove is one of the largest and best known. It is a horse-shoe shaped depression occurring on the eastern flank of the volcano. It formed about 8000-5000 years before present, but its origin is controversial. Some authors suggest it is related to coalescing collapses widened by rapid erosion; others propose flank sliding along fault planes (e.g. Chester et al. 1985; Borgia et al. 1992; Santacroce et al. 2003). Other important volcano-tectonic features are represented by fractures radiating from the central crater area and forming three main rift zones along the flanks. Rift zones have been preferential sites of flank eruptions and are marked by a large number of cinder cones, a few meters to more than 200 m high. The relations between these structures and the regional stress field are debated, although most authors agree that the structural features and extensional stress regime of the eastern flank of Etna are related to proximity of the Tindari-Letojanni-Malta strike-slip fault system (e.g. Bousquet and Lanzafame 2004).

The eruptive style of Etna has varied, although effusive activity and strombolian explosions have dominated (e.g. Chester et al. 1985; Branca and Del Carlo 2004). High energy explosive eruptions have also occurred, especially during the activity of older Mongibello, when magma evolution produced benmoreitic-trachytic melts which were erupted as pumice fall and ignimbrites. Historical eruptions have occurred both at the summit vents and along the flanks. Activity at summit vents has consisted of quiet

steam emission, strombolian to vulcanian and subplinian explosions and lava fountaining, sometimes accompanied by lava effusions, lasting from a few hours to months or sometimes years. As a consequence, the morphology of the summit crater area has been continuously modified. At present it consists of a slightly N-S elongated circular platform representing a small collapsed area (Caldera del Piano), containing a major cone with two summit large craters (Bocca Nuova and Voragine) and two lateral cones (NE Crater, SE Crater). Flank activity has been prevailingly effusive and strombolian; it has often taken place at low elevations (down to 300 m a.s.l.) close to inhabited areas, raising severe problems for civil defence. The eruptions that occurred in 1669 and from 1991 to 1993 represent the most dramatic events of the recent history of Etna. The 1669 eruption started on 11 March along a 12 km-long fissure which opened on the southern flank of the volcano. By April 12 a lava flow, originating from the main cones of Monti Rossi at 948 m altitude, reached Catania, where it knocked down about 40 meters of the city walls, destroyed part the town, and reached the sea on April 23. The eruption stopped on 15 July (Chester et al. 1985; Faraone 2002). The 1991-1993 eruption started on 14 December 1991 on the eastern flank of the volcano, along a radial fracture extending between 2400 m above sea level and the central crater area. The eruption lasted fifteen months, giving rise to voluminous lava flows that threatened the village of Zafferana Etnea (Calvari et al. 1994).

8.3.2. Petrography and Mineral Chemistry

The Etna rocks have tholeiitic to Na-alkaline affinity, with a few products exhibiting a potassic alkaline tendency (e.g. Monte Maletto). Compositions range from basalt to hawaiite, mugearite, benmoreite and trachyte on the TAS diagram (Fig. 8.3). Ol-hy normative tholeiites are the lowest exposed products. They show ophitic to poorly porphyritic textures. Phenocrysts phases include MgO-rich olivine (up to about Fo_{86-83}), plagioclase (An_{95-65}) and diopside to augite pyroxene set in a groundmass formed of the same phases plus Fe-Ti oxides and glass. Olivine phenocrysts include chromite and rare orthopyroxene, and are slightly more enriched in MgO than olivine crystals in the groundmass (about Fo_{84-81}; Kamenetsky and Clocchiatti 1996). Clinopyroxene ranges from diopside to salite and pigeonite. Ca-rich plagioclase occurs as phenocrysts (mostly around An_{70-60}), whereas oligoclase to anorthoclase are found in the groundmass (Tanguy et al 1997; Corsaro and Cristofolini 1997; Armienti et al. 2004; Corsaro and Pompilio 2004).

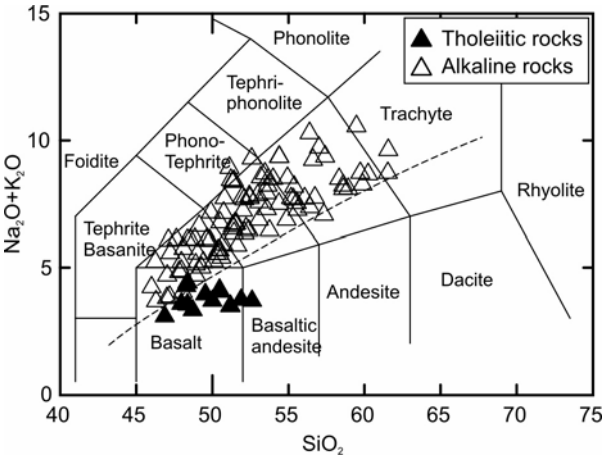

Fig. 8.3. TAS classification diagrams of Etna volcanic rocks. The dashed line is the boundary between subalkaline and alkaline fields of Irvine and Baragar (1971).

Alkali basalt[1] are aphyric to weakly porphyritic with phenocrysts of clinopyroxene, plagioclase and olivine (sometimes with chromite inclusions) set in a groundmass of the same phases plus glass. Hawaiites (trachybasalts) are porphyritic with phenocrysts of plagioclase (An_{90-55}), MgO-rich olivine (up to Fo_{90}), clinopyroxene (Cr-diopside to salite and augite), Fe-Ti oxides and sometimes kaersutite. Groundmass contains the same phases and in some cases nepheline, sodalite, and phlogopite. Hawaiitic lavas of the historic activity show strong differences in modal composition. Most products older than the 1669 eruption are dominated by plagioclase phenocrysts with very few clinopyroxene and rare or absent olivine. Younger hawaiites have a typical phenocryst paragenesis consisting of plagioclase, clinopyroxene and olivine with some Fe-Ti oxides (Armienti et al. 1997). Locally, these rocks are referred to as etnaites. Mugearites and benmoreites are porphyritic with phenocrysts of dominant plagioclase (An_{80-40}), salite to augite clinopyroxene, olivine (Fo_{77-73}), and some amphibole and Ti-magnetite set in a groundmass containing the same minerals, plus some alkali-feldspar, nepheline, sodalite, phlogopite and apatite. Trachytes are aphyric to weakly porphyritic with microphenocrysts of plagioclase (An_{40}), augitic clinopyroxene, Fe-Ti oxides, and some olivine (~ Fo_{75}) and kaersutite, set in a groundmass containing alkali-feldspar (anor-

[1] Alkali basalts are here defined as nepheline- and olivine-normative basaltic rocks with moderate enrichment in alkalis, which fall in the basalt field on the TAS diagram above the divide between alkaline and subalkaline fields of Irvine and Baragar (1971).

thoclase to Na-sanidine), clinopyroxene, olivine, Ti-magnetite, biotite and sporadic sodalite and nepheline (Tanguy 1978; Kamenetshy and Clocchiatti 1996; Tanguy et al. 1997; Corsaro and Pompilio 2004).

8.3.3. Petrology and Geochemistry

Variation diagrams of major and trace elements against silica show continuous and moderately scattered trends (Fig. 8.4). Tholeiitic rocks display higher MgO, Ni and Cr and lower K_2O and other incompatible elements than alkaline mafic rocks with the same silica content. Among alkaline rocks, those younger than the 1669 eruption and, in particular, lavas erupted during the last thirty years, display higher contents of fluid-mobile elements (e.g. K, Rb and Cs) as older rocks with the same degree of evolution (i.e. similar MgO; Armienti et al. 2004 and references therein; Fig. 8.4).

REE patterns are fractionated for all the rocks, but tholeiites show lower La/Yb ratios than alkaline products (Fig. 8.5a). Incompatible element patterns normalised to primordial mantle compositions for mafic rocks are very different from the Aeolian arc and central-southern Italian peninsula. Both tholeiitic and alkaline basalts show a marked upward convexity, with negative spikes of K (Fig. 8.5b). Note, however, that there are also negative anomalies for Hf and Ti, which are uncommon in most Na-alkaline basalts from intraplate settings (e.g. Wilson 1989). Overall, the Etna magmas have been found to be more enriched in volatile components than common intraplate magmas, and water contents up to 3-4 wt % have been found by melt inclusion studies (Corsaro and Pompilio 2004; Pompilio, personal communication).

$^{87}Sr/^{86}Sr$ (~ 0.7030 to 0.7040) and $^{143}Nd/^{144}Nd$ (~ 0.51285 to 0.51298) ratios display moderate variation (Fig. 8.6a; Carter and Civetta 1977; Marty et al. 1994; Tonarini *et al.* 1995; Armienti *et al.* 1996; D'Orazio *et al.* 1997; Tanguy et al. 1997; Tonarini *et al.* 2001b; Armienti et al. 2004). There is a slight increase of Sr and a decrease of Nd isotopic ratios from early tholeiites and alkaline basalts to recent activity (e.g. Marty et al. 1994; Armienti et al. 2004). Detailed studies have shown the occurrence of small but significant isotopic variations both among different eruptions and within single lava flows (Armienti et al. 1984; Tonarini et al. 2001b). Data on separated clinopyroxenes have often shown Sr isotopic disequilibrium with surrounding matrix. These are more common in the lavas erupted during the last 30 years (e.g. D'Orazio et al. 1997; Armienti et al. 2004). Pb-

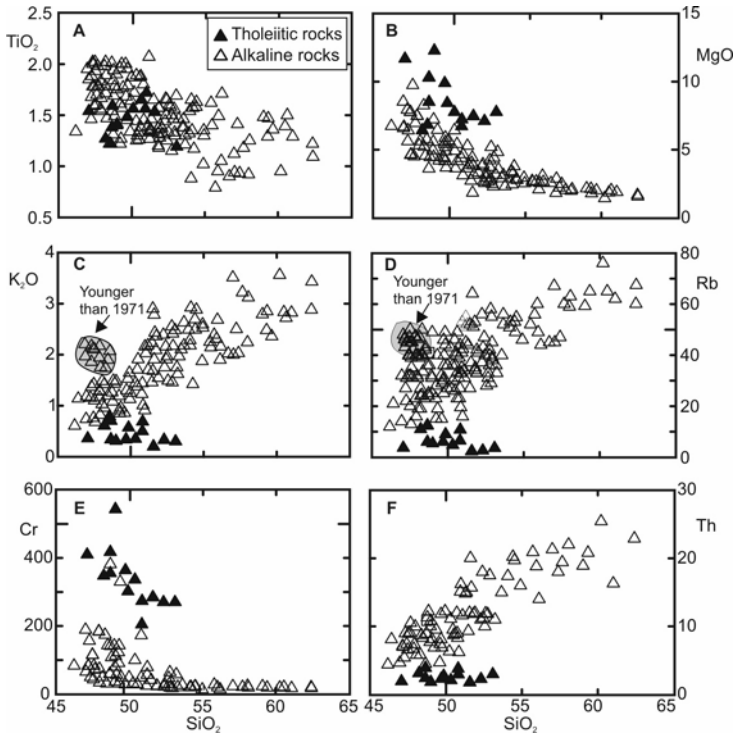

Fig. 8.4. Variation diagrams of silica vs. selected major and trace elements for Etna volcanic rocks.

isotope ratios (Fig. 8.6b) show the most radiogenic compositions among recent Italian volcanic rocks (e.g. $^{206}Pb/^{204}Pb$ ~ 19.47 to 20.01; $^{207}Pb/^{204}Pb$ ~ 15.62 to 15.66; $^{208}Pb/^{204}Pb$ ~ 39.11 to 39.59; Carter and Civetta 1977). $^{176}Hf/^{177}Hf$ is around 0.28297 ($\varepsilon Hf = +7.10$; Gasperini et al. 2002).

Oxygen isotopic data on whole rocks show $\delta^{18}O$ in the range + 5.0 to +5.9 (Marty et al. 1994). Boron isotopic compositions have small but significant variations ($\delta^{11}B$ ~ -8‰ to -3‰), probably derived from both deep (i.e. source contamination) and shallow (i.e. magma contamination) processes (Tonarini et al. 2001b).

Noble gas isotope compositions are within the range of MORB (Nakai et al. 1997). $^{3}He/^{4}He$ ratios measured on clinopyroxene and olivine phenocrysts show little variation, and compositions normalised to atmospheric values cluster around R/R_A ~ 6.5 (Marty et al. 1994). Similar values have been found in fumarolic gases (Nakai et al. 1997).

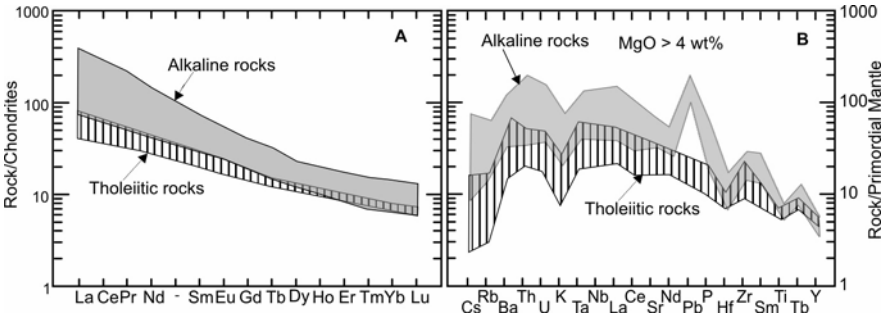

Fig. 8.5. REE (A) and incompatible element (B; restricted to mafic rocks) patterns of Etna volcanic rocks.

Major and trace element data for mafic rocks and melt inclusions in olivine phenocrysts suggest that distinct magmas were parental to Etna rocks (e.g. Clocchiatti et al. 1992: Corsaro and Cristofolini 1996; Kamenetshy and Clocchiatti 1996). Parental magmas underwent polybaric evolution dominated by fractional crystallisation. According to Tanguy et al. (1997), a deep magma chamber sited at the boundary between the crust and mantle has been active throughout the entire history of Etna volcano. Occasionally, however, magmas have ponded in shallow reservoirs and have given rise to evolved benmoreitic and trachytic products. Fluid inclusions in olivine phenocrysts indicate pressures of at least 0.2 GPa for the shallower crystallisation site. Seismological studies identified a high-velocity body below Mt. Etna between 12 and 3-5 km (e.g. Murru et al. 1999; Patanè et al. 2003), which has been interpreted as a solidified intrusion separating two regions of magma ponding.

Fractional crystallisation was dominated by early separation of olivine, joined by variable amounts of plagioclase and clinopyroxene. The relative amounts of these phases were a function of the pressure conditions of crystallisation, with the plagioclase/clinopyroxene ratio increasing during low-pressure crystallisation. Polybaric evolution may represent an explanation for the variable textures and phenocryst assemblages of Etna rocks (Armienti et al. 2004), although experimental data reported by Metrich and Rutherford (1998) suggest that the main control on the sequence of mineral crystallisation and amount of crystals in the Etna rocks would be related to the amount of water present in the magma and on modalities of degassing at very shallow depth.

Sr-Nd-B isotopic studies, however, show significant variations, which require other processes in addition to fractional crystallisation. There is a debate on how much of this variation is due to source modification and

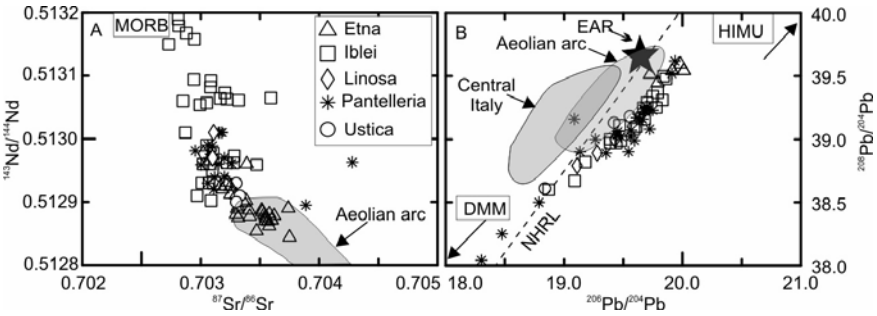

Fig. 8.6. Sr-Nd (A) and Pb (B) isotope diagrams for the Sicily Province. Compositions of HIMU, DMM, MORB and European Asthenospheric Reservoir (EAR) are also shown. See text for explanation.

how much depends on shallow-level bulk or selective assimilation of crustal rocks (e.g. Clocchiattti et al. 1988; Condomines et al. 1995; Tonarini et al. 2001b). Most probably, the long term geochemical and isotopic variations from early tholeiites to present-day activity are related to source modification, whereas some deviation from the main trend may depend on local assimilation processes (e.g. Armienti et al. 2004).

8.4. Iblei

The Iblean Plateau has been affected by volcanism from Triassic to Quaternary times. In this review, older volcanism will briefly discussed, and emphasis will be given to Plio-Quaternary rocks on which detailed studies have been carried out. The oldest volcanic rocks in the Iblean Plateau are Triassic and Jurassic in age and have been recovered by drilling (Patacca et al. 1979, Longaretti and Rocchi 1990). These consist of alkali basalts, hawaiites and basanites containing Ti-clinopyroxene, olivine, plagioclase, Fe-Ti oxides and sporadic kaersutite, biotite and apatite. The oldest oucropping volcanics are Cretaceous to Paleocene in age (84 to 54 Ma; Barberi et al. 1974; Carveni et al. 1991a,b) and are found in the Capo Passero area. These rocks consist of almost aphyric to strongly porphyritic alkali basalts and basanites containing variable amounts of olivine, Ti-clinopyroxene, plagioclase. and secondary minerals (e.g. Longaretti et al. 1991; Di Grande et al. 2002; Groppelli and Pasquarè 2004).

The youngest volcanic activity in this area ranges from Upper Miocene (Tortonian) to Lower Pleistocene and occurs along NE-SW extensional

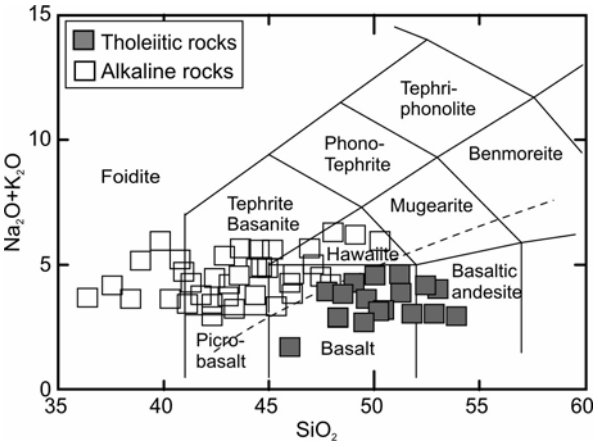

Fig. 8.7. TAS diagram for Iblei Plio-Quaternary volcanic rocks. The dashed line is the boundary between subalkaline and alkaline fields (Irvine and Baragar 1971).

faults bordering graben zones in the northernmost sector of the Iblean Plateau (e.g. Grasso et al. 1983). The volcanism was dominated by fissure-type eruptions, which formed monogenetic centres and lava flows of variable size. Overall, Miocene to Quaternary volcanic rocks cover an area of about 250 km^2 and have an estimated volume of about 30-40 km^3. The volcanic products rest over a sedimentary substratum of Upper Cretaceous and Early Tertiary reef and marly limestones and Oligo-Miocene calcarenites, and are interfingered with Mio-Pleistocene calcarenites, evaporitic rocks and silicoclastic sediments.

8.4.1. Volcanology, Stratigraphy and Petrography

Miocene volcanic cycle (about 7 to 4.9 Ma) was prevailingly submarine and erupted volcanoclastites from maar-type centres, along with volumetrically less significant lavas (Schmincke et al. 1997; Di Grande et al. 2002). Rocks have compositions similar to the younger Plio-Pleistocene activity (see next section), but Na-alkaline rock (alkalibasalt, basanite, nephelinite and ankaratrite[2]) prevail over subalkaline volcanics. Miocene alkaline rocks are variably porphyritic with phenocrysts of olivine and clinopyroxene set in a groundmass consisting of the same phases, plus nepheline, Fe-Ti oxides, apatite and some plagioclase and glass. Tholeiites

[2] Ankaratrite is a melanocratic variety of nephelinite, rich in olivine phenocrysts and/or xenocrysts, and containing phlogopite.

are aphyric to poorly porphyritic with olivine, clinopyroxene, some orthopyroxene and plagioclase microphenocrysts set in a matrix containing the same phases plus Fe-Ti oxides and sporadic glass (Di Grande et al. 2002). Xenoliths of both crustal and mantle origin occur in some tuff-breccias around diatremes. Ultramafic xenoliths consist mainly of spinel-harzburgites and lherzolites, plus minor websterites, and clinopyroxenites. Crustal xenoliths are predominantly basic granulites and minor gabbros, diorites and anorthosites (Sapienza and Scribano 2000 with references).

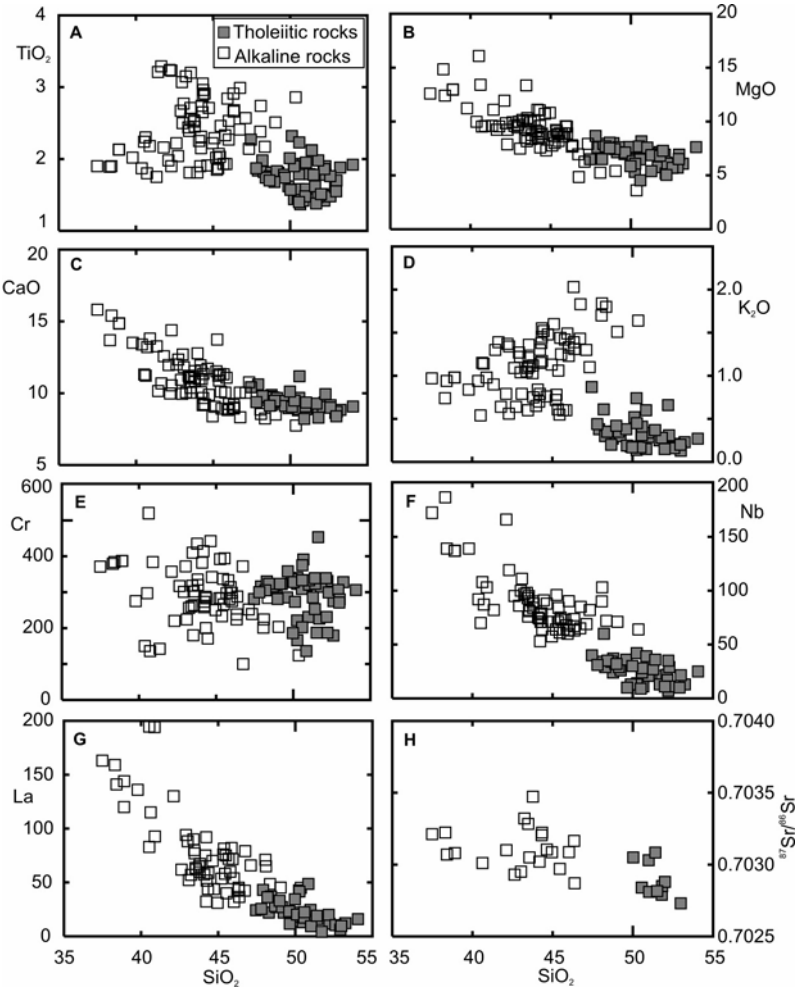

Fig. 8.8. Variation diagrams of selected major and trace elements against SiO_2 for Iblei Plio-Quaternary volcanic rocks.

The Plio-Peistocene activity is by far the best studied (Beccaluva et al. 1998; Trua et al. 1998). It took place during Lower-Middle Pliocene (4.9 to 3.5 Ma) and Upper Pliocene-Lower Pleistocene (2.4 to 1.5 Ma). The earlier products are principally submarine and are represented by volcanoclastic products, pillow lavas and minor subaerial lava flows. The Upper Pliocene-Lower Pleistocene activity erupted lava in subaerial to shallow marine environments (Di Grande et al. 2002).

Iblean Plio-Quaternary magmas range from basalts and basaltic andesites to nephelinites, and straddle the boundary between the alkaline and subalkaline fields of Irvine and Baragar (1971; Fig. 8.7). Subalkaline basalts are the dominant rock types and range from slightly oversaturated (qz-tholeiites) to slightly undersaturated (ol-tholeiites) in silica. Alkaline rocks have a sodic affinity and include alkali basalts, hawaiites, basanites, and nephelinites.

The tholeiitic basalts and basaltic andesites are aphyric to poorly porphyritic holocrystalline to hypocrystalline. Qz-normative rocks contain microphenocrysts of olivine (Fo_{81-76}), orthopyroxene (En_{85}), augite and plagioclase, with pigeonite in the groundmass. Ol-normative tholeiites contain olivine, augite clinopyroxene and plagioclase phenocrysts. Alkaline rocks have porphyritic textures with dominant MgO-rich olivine (Fo_{89-75}), augite and plagioclase phenocrysts set in a groundmass containing the same phases plus Fe-Ti oxides. Nepheline occurs in the groundmass of basanites and nephelinites. In the latter, haüyne, rare amphibole and primary carbonate have been also found. Some basanites contain abundant phenocrysts and xenocrysts of olivine and clinopyroxene and have been classified as ankaratrites (Beccaluva et al. 1998; Bianchini et al. 1998; Trua et al. 1998 and references therein).

Small (normally up to about 10 cm) xenoliths are found in some Quaternary basanitic and nephelinitic lavas (e.g. Sapienza and Scribano 2000 and references therein). These include both mantle-derived and crustal lithologies.

8.4.2. Petrology and Geochemistry

Variation diagrams of major and trace elements show an increase in SiO_2 and a decrease in MgO, CaO, TiO_2, K_2O and incompatible trace elements from alkaline to tholeiitic rocks. In contrast, Ni and Cr do not show systematic variations between the two rock groups and have high concentrations in most samples (Fig. 8.8). REE patterns exhibit variable degrees of fractionation, which increases from subalkaline to alkaline samples (Fig. 8.9a). Incompatible element patterns normalised against primordial mantle

compositions for the most mafic rocks (MgO > 4 wt %) invariably have upward convex shapes and negative anomalies of potassium. Negative spikes of Hf and Ti are observed in some rocks, especially in the alkaline volcanics (Fig. 8.9b; Tonarini et al. 1996).

$^{87}Sr/^{86}Sr$ ratios (~0.7027 to 0.7036) are relatively low (Fig. 8.6a) and increase slightly from subalkaline to alkaline rocks (Fig. 8.8h); $^{143}Nd/^{144}Nd$ (0.5129 to 0.5130) shows the opposite tendency. Pb isotopic ratios (Fig. 8.6b; $^{206}Pb/^{204}Pb$ ~ 18.87 to 19.86; $^{207}Pb/^{204}Pb$ ~ 15.59 to 15.69; $^{208}Pb/^{204}Pb$ ~ 38.50 to 39.50) become more radiogenic from tholeiites to alkaline rocks (Carter and Civetta 1977; Beccaluva et al. 1998; Trua et al. 1998). Sr and Nd isotopic compositions of ultramafic xenoliths from both Miocene and Plio-Quaternary volcanics ($^{87}Sr/^{86}Sr$ = 0.70298 to 0.70334; $^{143}Nd/^{144}Nd$ = 0.51289 to 0.51299) fall in the field of the alkaline lavas (Tonarini et al. 1996).

The high concentrations of MgO (~ 3 to 15 wt %), Ni (~ 100 to 300 ppm) and Cr (~ 100 to 500 ppm) of Iblean lavas suggest that magmas underwent little evolution during ascent to the surface, a conclusion supported by the monogenetic nature of volcanic centres and by the occurrence of mantle xenoliths and xenocrysts in several alkaline rocks. The decrease in MgO from alkaline rocks to tholeiites is not related to evolutionary processes, since Ni and Cr remain constant and incompatible elements decrease instead of increasing. Therefore, there is a general agreement that the Iblean magmatism consists of various batches of magmas, whose petrological and geochemical variation is related to source compositions and processes.

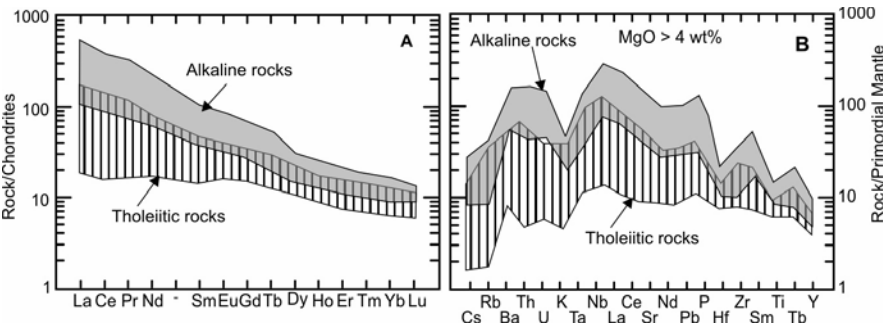

Fig. 8.9. REE (A) and incompatible element patterns (B; restricted to mafic rocks) of Iblei Plio-Quaternary volcanic rocks.

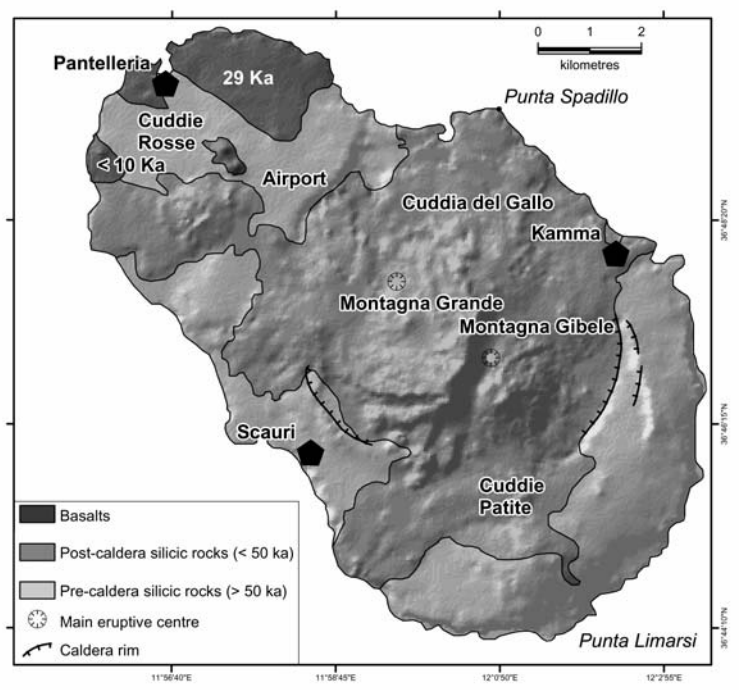

Fig. 8.10. Schematic geological map of the Pantelleria island. Simplified after Civetta et al. (1998).

8.5. Pantelleria

The Island of Pantelleria is located in the NW-SE trending rift zone affecting the Pelagian block (Pantelleria rift; Fig. 8.1). The volcano rises about 1000 m above the sea floor and reaches an altitude of 836 m above sea level. The structural setting is dominated by NW-SE and N-S trending fractures. A NE-SW tensile fault system divides the island into two sectors. The northwestern sector contains most of the exposed basaltic rocks, whereas the southeastern sector is constructed entirely by silicic peralkaline rocks (Fig. 8.10).

8.5.1. Volcanology and Stratigraphy

The Island of Pantelleria is a NW-SE elongated stratovolcano with two nested calderas, built up by dominant peralkaline trachytes and rhyolites (pantellerites) and minor Na-transitional to mildly alkaline basalts. The oldest dated rocks are 324 and 220 ka old, whereas the youngest dated activity on the island is about 4 ka-old (e.g. Civetta et al. 1984, 1988, 1998; Mahood and Hildreth 1986). However, volcanism in the area is still active, and a submarine eruption occurred on 1891 a few km NE of Pantelleria (Foerstner volcano) has been described by Washington (1909).

Most of the volcanism at Pantelleria was explosive and emitted silicic peralkaline pyroclastic products and some lavas. Basaltic magmas have been erupted episodically (at 118, 83, 29 and less than 10 ka; Civetta et al. 1984, 1998; Mahood and Hildreth 1986) by effusive and strombolian activity. Large explosive eruptions occurred at about 114 ka and 50 ka, and generated caldera collapses in the southeastern sector of the island (Orsi and Sheridan 1984; Mahood and Hildreth 1986). The younger collapse is associated with the deposition of the so-called Green Tuff, a complex pyroclastic trachytic to pantelleritic deposit, formed of ignimbrite, fall and surge beds (Orsi and Sheridan 1984). Resurgence has taken place inside the younger caldera. Post-caldera silicic activity has occurred both inside and outside the caldera, whereas basaltic eruptions took place outside the calderas, in the north-western sector of the island.

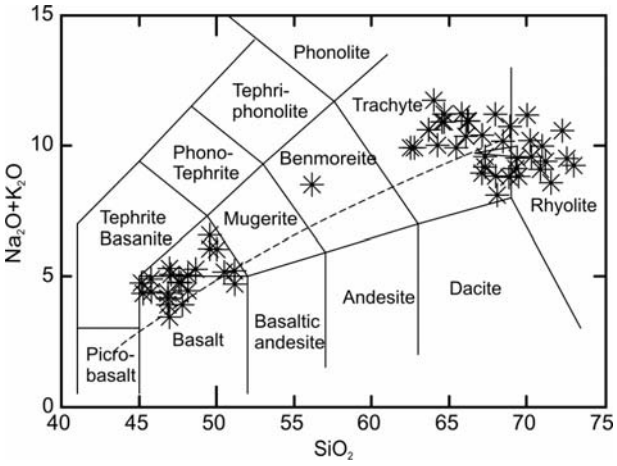

Fig. 8.11. TAS classification diagrams of Pantelleria volcanic rocks. The dashed line is the boundary between subalkaline and alkaline fields of Irvine and Baragar (1971).

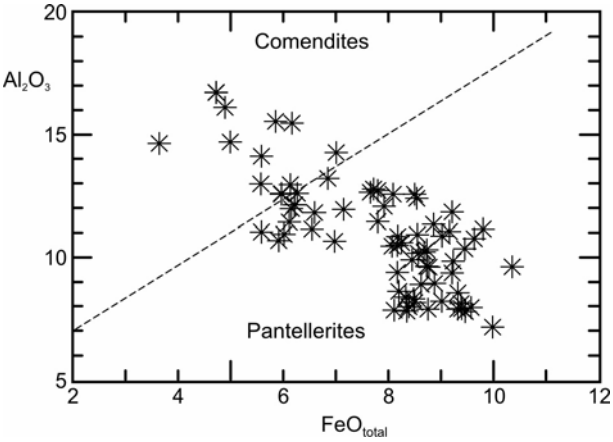

Fig. 8.12. Classification of Pantelleria peralkaline acid rocks (SiO_2 > 63 wt %; after Le Maitre 1989).

8.5.2. Petrography and Mineral chemistry

Based on the TAS diagram, the mafic volcanic rocks from Pantelleria are classified as basalt and hawaiite, whereas the silicic products fall in the trachyte and rhyolite fields (Fig. 8.11). Mafic rocks show transitional to weakly alkaline petrochemical affinity (Civetta et al. 1984; Mahood and Baker 1986). Transitional basalts are generally hyperstene-normative, whereas alkaline basalts contain small amounts of normative nepheline. The felsic volcanic rocks are generally peralkaline, and are classified as comendites (comenditic trachyte and comenditic rhyolite) and pantellerites (pantelleritic trachyte and pantelleritic rhyolite) according to the Al_2O_3 vs. FeO_{total} grid reproted in Fig. 8.12 (Macdonald 1974; Le Maitre 1989).

Basalts and hawaiites are variably porphyritic, with 5-20 vol % of plagioclase, olivine, clinopyroxene and magnetite phenocrysts, set in a microcrystalline groundmass consisting of the same phases plus accessory apatite and sporadic analcite. Comendites are hypocrystalline porphyritic, with variable modal abundances of alkali-feldspar, clinopyroxene, fayalitic olivine, Fe-Ti-oxides and rare aenigmatite phenocrysts, set in a glassy groundmass containing microlites of alkali-feldspar, clinopyroxene, alkali-amphibole and Fe-Ti oxides. Pantellerites are porphyritic, with phenocrysts of alkali-feldspar, clinopyroxene, aenigmatite, olivine, Fe-Ti-oxides, and some corroded quartz, set in a glassy, sometimes vesicular, groundmass containing scarce microlites of the same phases that occur as phenocrysts.

Clinopyroxene in the mafic rocks is generally zoned and ranges from diopside to augite. Olivine shows a wide compositional variation both in the mafic (Fo_{86-45}) and in the silicic rocks (Fo_{20-5}; Mahood and Baker 1986; Civetta et al. 1998). Plagioclase (about An_{80-40}) occurs in the mafic rocks both as a phenocryst and in the groundmass. Feldspars in the silicic rocks are mostly anorthoclase.

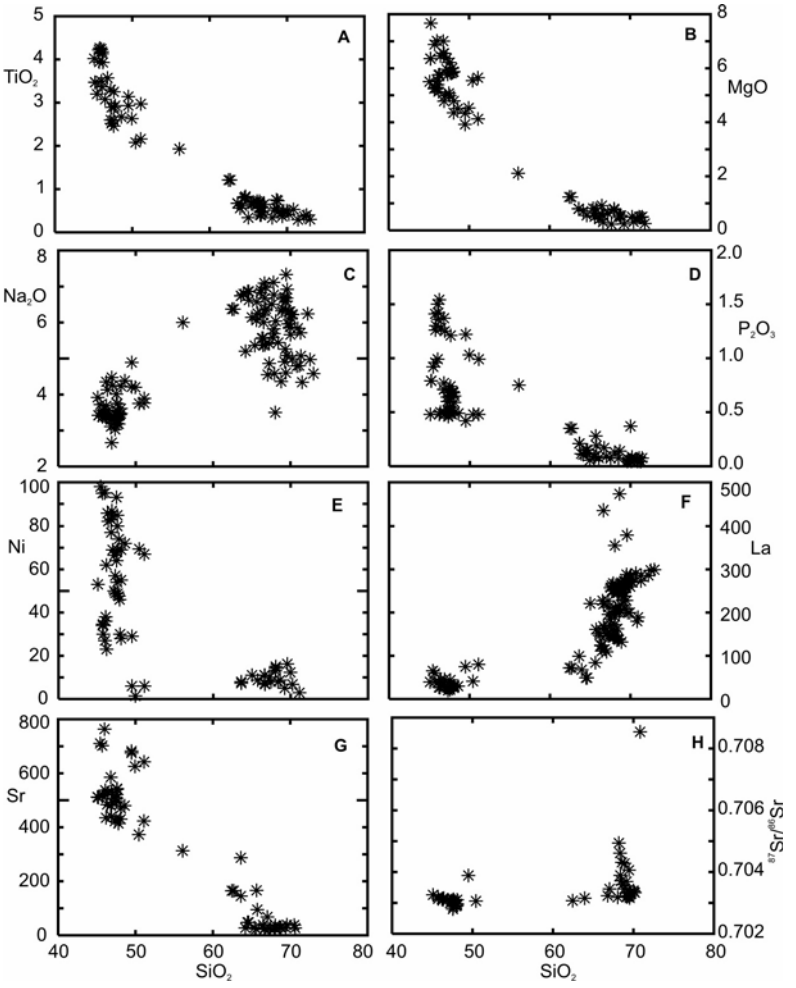

Fig. 8.13. Variation diagrams of selected major and trace elements and of $^{87}Sr/^{86}Sr$ against SiO_2 for Pantelleria volcanic rocks.

8.5.3. Petrology and Geochemistry

Variation diagrams of major and trace elements vs. SiO_2 (Fig. 8.13) show a bimodal distribution between basalts and rhyolites, with a gap for intermediate compositions (Daly gap). Such a distribution of rock types is typical of volcanoes from continental rift settings (see Peccerillo et al. 2003 and references therein). A few intermediate samples have been found as xenoliths, and these have been suggested to represent hybrids between mafic and felsic magmas (e.g. Mahood and Baker 1986).

There is an overall decrease in TiO_2, MgO, FeO_{total}, CaO and P_2O_5 with increasing silica contents, whereas K_2O shows the opposite trend. Al_2O_3 and Na_2O have a tendency to increase in the mafic compositions and decrease in the silicic rocks, but with considerable scatter. Ferromagnesian trace elements (i.e. Ni, Cr, Co, Sc, V) and Sr decrease with increasing silica, whereas incompatible elements (e.g. La, Th, Rb, Nb, Ta, Zr) show positive trends (Fig. 8.13). Incompatible elements define smooth positive correlations on inter-element diagrams (Fig. 8.14).

REE patterns for basalts show moderate fractionation and a slightly positive Eu anomaly. The silicic rocks have much higher REE contents than basalts and display negative Eu anomalies (Fig. 8.15a). Extended incompatible element diagrams of mafic rocks show an upward convex pattern with a maximum at Ta and Nb, and a positive spike of Ba, but negative Sr, Hf and, to a lesser extent, Ti (Fig. 8.15b).

$^{87}Sr/^{86}Sr$ ratios cluster around 0.7029 to 0.7032 in the mafic rocks, whereas in the silicic rocks they show comparable to higher values ($^{87}Sr/^{86}Sr \sim 0.7031$ to 0.7042), with a few samples falling outside this range (Figs. 8.6a, 8.13h; Civetta et al. 1984, 1998; Esperança and Crisci 1995). The higher values of silicic rocks probably represent contamination by foreign material, which produced strong effects on Sr isotopic ratios due to the very low Sr absolute abundances in the silicic magmas. Nd isotopic ratios show a restricted range for both mafic and felsic rocks ($^{143}Nd/^{144}Nd = 0.5129$-$0.5130$). Pb isotopic ratios are variable (Fig. 8.6b) with most samples falling in the ranges $^{206}Pb/^{204}Pb \sim 18.48$ to 19.94; $^{207}Pb/^{204}Pb \sim 15.55$ to 15.67; $^{208}Pb/^{204}Pb \sim 38.25$ to 39.61 (Esperança and Crisci 1995; Civetta et al. 1998).

The Island of Pantelleria shows many characteristics that are commonly found in volcanoes from continental rift settings, such as the abundance of acid peralkaline rocks, the compositional gap between mafic and silicic compositions and the smooth inter-element trends. Therefore, its petrogenesis shares the same problems as magmatism from continental rifts (see Peccerillo et al. 2003 for discussion). The similar isotopic compositions of

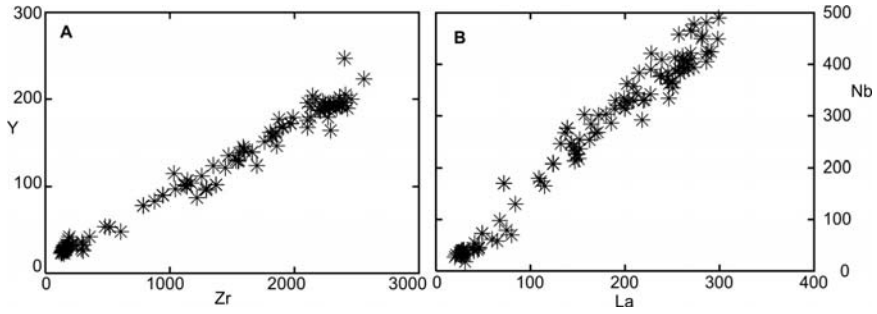

Fig. 8.14. Inter-element variation diagrams for Pantelleria volcanic rocks.

mafic and the majority of felsic rocks have been interpreted as evidence for a close genetic relationship between basalts and rhyolites. Two classes of hypotheses have been proposed to explain these similarities. One advocates continuous fractional crystallisation starting from transitional basaltic parents, possibly with a small role for crustal contamination. The other suggests that peralkaline silicic rocks and the associated basalts represent two genetically independent melts. The basalts were formed in the mantle, whereas the silicic liquids were generated by melting of alkali gabbros in the crust. This generated trachytic magma, which underwent fractional crystallisation giving pantelleritic compositions. Civetta et al. (1998) performed mass balance calculations and trace element modelling, which demonstrated that the silicic rocks could be derived from weakly alkaline or transitional basaltic parents by 80% to 95% fractional crystallisation. Separation of a solid made of plagioclase, clinopyroxene and subordinate olivine, apatite and Fe-Ti oxides would be necessary to pass from mafic melts to comenditic trachytes. Additional fractionation dominated by alkali feldspar would drive comenditic trachytes to pantelleritic rhyolite compositions. However, as stated by the same authors, these models do not demonstrate that silicic magmas derive from mafic ones by fractional crystallisation, but simply that such a process is possible. In fact, experimental evidence shows that partial melting of a basalt followed by fractional crystallisation can also give rise to silicic peralkaline melts (e.g. Mahood and Baker 1986; Lowestern and Mahood 1991). However, the fractional crystallisation hypothesis better explains several geochemical features of silicic rocks, especially their low contents of compatible elements (Sr, Cr, V). Nonetheless, it introduces the problem that large volumes of basaltic magma must be present in the volcanic system to produce the silicic rocks, an idea which conflicts with the scarcity of mafic rocks at the surface. Finally, the lack of intermediate rocks is also a problem for fractional crystallisation, whereas it is better explained by the crustal melting hypothesis.

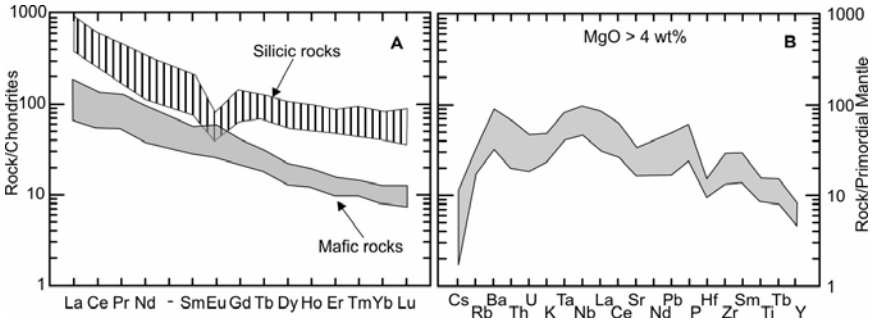

Fig. 8.15. REE (A) and incompatible element patterns (B; restricted to mafic compositions) of Pantelleria volcanic rocks.

8.6. Linosa

8.6.1. Volcanology and Stratigraphy

The Island of Linosa is the emergent summit of a large submarine cone located at the south-western margin of the Linosa graben (Fig. 8.1). The exposed volcanism has been both explosive and effusive and developed during three main phases of activity between about 1.06 to 0.53 Ma (Rossi et al. 1996). The lowest exposed products consist of a few scoria cones and tuff rings formed of basaltic to hawaiitic juvenile clasts and a few benmoreitic to trachytic lithic ejecta. The second phase was both effusive and explosive and gave hydromagmatic products, strombolian scoriae and some lava with basalt to hawaiite compositions. Finally, the third phase erupted abundant basalt to hawaiite lavas, scoriae and minor hydromagmatic products, which built up some of the largest cones in the island.

8.6.2. Petrography and Mineral Chemistry

Linosa rocks range in composition from mildly alkaline basalts to hawaiite (Fig. 8.16). A few benmoreites and trachytes are found as lithic clasts in some of the lowest exposed pyroclastic deposits. All the rocks display a texture ranging from poorly to strongly porphyritic. Basalts contain a phenocryst assemblage made of variable relative amounts of olivine (Fo_{85-75}) and plagioclase (An_{70-40}), and minor diopsidic clinopyroxene. Groundmass consists of the same phases plus opaque oxides and rare apatite and

nepheline. Hawaiites contain phenocrysts of colourless to green clinopyroxene, olivine (Fo_{80-72}), plagioclase (An_{75-60}), and sometimes amphibole surrounded by a microcrystalline to hypocrystalline groundmass containing the same minerals and opaque oxides. The benmoreite and trachyte lithics found in pyroclastic units are porphyritic, with abundant plagioclase (An_{55-35}) and anorthoclase phenocrysts, minor clinopyroxene and kaersutitic amphibole, and some biotite set in a microcrystalline groundmass of plagioclase, clinopyroxene and opaques. Accessory phases include apatite, magnetite and perovskite (Rossi et al. 1996; Bindi et al. 2002).

8.6.3. Petrology and Geochemistry

Major and trace element variation diagrams (Fig. 8.17) show an increase in Al_2O_3, Na_2O, K_2O and incompatible trace elements (Th, Nb, Zr, REE) and a decrease in TiO_2, MgO, Cr and Ni from basalt to trachyte (Rossi et al. 1996; Bindi et al. 2002). Incompatible elements plotted against SiO_2 are rather scattered in the mafic rocks, but diagrams involving pairs of incompatible elements exhibit smooth trends (Fig. 8.17g, h).

REE patterns of all the rocks are moderately fractionated, and most samples show a small positive Eu anomaly (Fig. 8.18a). Mantle normalised

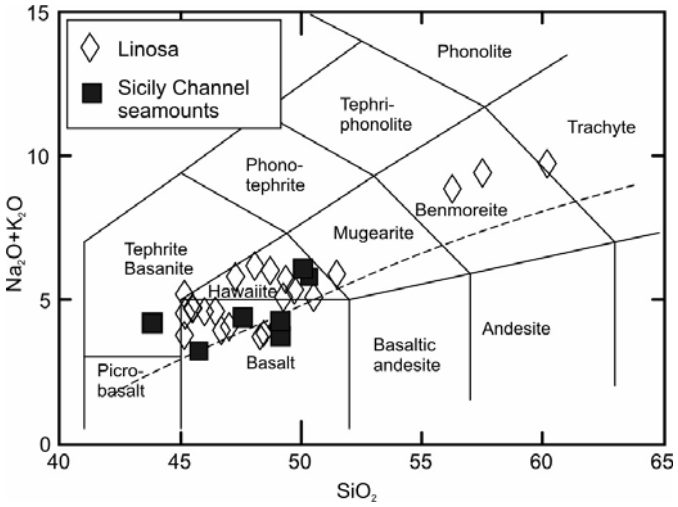

Fig. 8.16. TAS classification diagrams of Linosa and Sicily Channel seamounts. The dashed line is the boundary between subalkaline and alkaline fields of Irvine and Baragar (1971). Data on seamounts have been recalculated on water-free basis.

incompatible element diagrams show a bell-shaped pattern with positive anomaly at Nb (Fig. 8.18b).

Few Sr, Nd and Pb isotopic analyses have been published (Fig. 8.6). The available data show unradiogenic Sr isotopic compositions ($^{87}Sr/^{86}Sr$ around 0.7030) and radiogenic Nd and Pb ($^{143}Nd/^{144}Nd$ ~ 0.51296; $^{206}Pb/^{204}Pb$ ~ 19.11 to 19.43; $^{207}Pb/^{204}Pb$ ~ 15.60 to 15.63; $^{208}Pb/^{204}Pb$ ~ 39.79 to 39.02; Civetta et al. 1998).

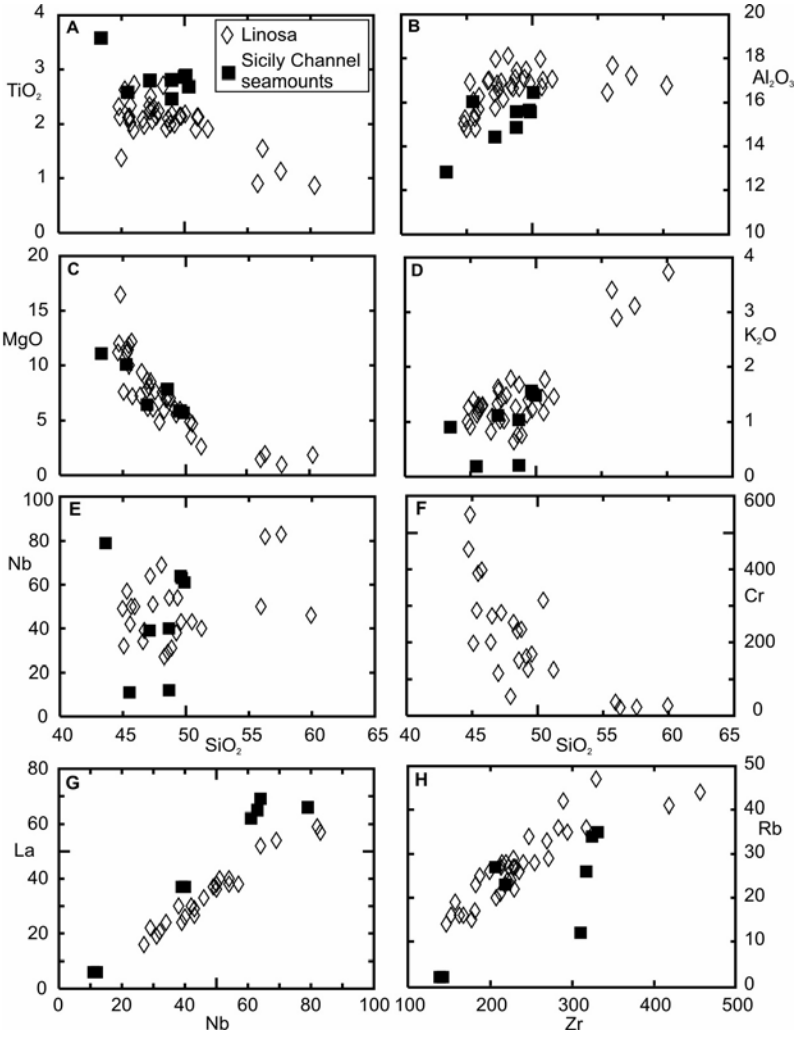

Fig. 8.17. Variation diagrams of selected major and trace elements for Linosa island and Sicily Channel seamounts. Major elements of seamounts have been recalculated on water-free basis.

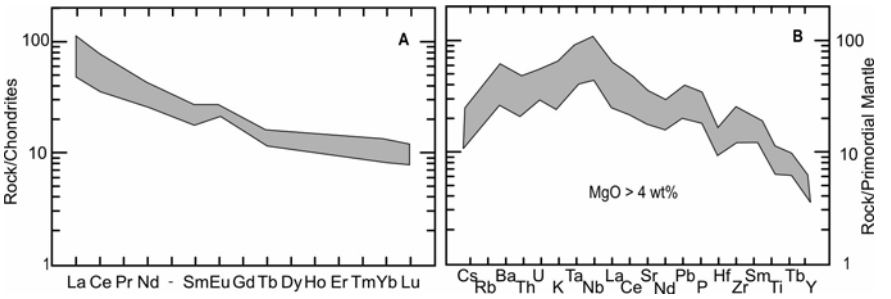

Fig. 8.18. REE (A) and incompatible element patterns (B; restricted to mafic rocks) for Linosa volcanics.

Various lines of evidence point to polybaric evolution history for Linosa magmas. Bindi et al. (2002) investigated crystal chemistry of clinopyroxenes from various activity stages of Linosa and found a decrease of cell volume, passing from early to late erupted basalts. This was interpreted as an evidence of increasing pressure of crystallisation with time. Therefore, it was suggested that early stages of activity were fed by a shallow magma chamber where dominant fractionation gave trachytic melts. In contrast, the younger activity was fed by a deeper magma chamber where fractional crystallisation was accompanied by continuous input of mafic magmas from the source. This kept the magma composition in the mafic range, preventing evolution toward benmoreite-trachyte. Increase in CaO, Sr and decrease in Cr and Co with decreasing MgO in the basalts and hawaiites (not shown) indicate that fractionation in the mafic magmas was dominated by separation of olivine with some clinopyroxene. The decrease in CaO, Sr, TiO_2, Fe_2O_3 and P_2O_5 in benmoreites and trachytes implies that plagioclase, Fe-Ti oxides and apatite had a significant role during evolution to felsic compositions.

8.7. Sicily Channel Seamounts

Numerous volcanic centres occur on the seafloor of the Sicily Channel (Fig. 8.1). Calanchi et al. (1989) recognised at least ten recent submarine volcanoes of various dimensions, mostly located along NW-SE regional faults. Some of these volcanoes have erupted during historical times; others are covered by undisturbed Pliocene-Quaternary sediments and have been detected by seismic profiles and magnetic survey (Allan and Morelli 1971).

Tetide, Anfitrite, Galatea and *Cimotoe* define a row of centres aligned in a NW-SE direction on the eastern margin of the Banco Avventura (Adventure Bank), a large erosional sedimentary plateau located off the southwestern Sicily coast. The Tetide volcanic cone is about 3 km in diameter and rises from a seafloor about 70 m deep, reaching a depth of about 18 m below sea level. Anfitrite is about 1 km in diameter and reaches a minimum depth of about 40 m. Galatea is a cone with a diameter of 2 km, reaching a depth of about 74 m. Cimotoe consists of a series of conical peaks sited on the southeastern margin of Banco Avventura.

The *Graham Bank* is located east of Banco Avventura, about 50 km south of the Sicily coast. It is sited on a plateau about 200 m deep, shows a N-S elongated shape and a summit area formed by a 25-30 m oval-shaped terrace from which a fractured neck of massive lava rises up to a depth of about 9 m below sea level. This represents the feeder neck of the 1831 eruption (Washington 1909) that formed the ephemeral Isola Ferdinandea (Graham Island), rapidly dismantled by marine erosion. Another volcanic cone is located a few km south of the Graham seamount and reaches a minimum depth of 76 m. The N-S alignment of these twin volcanoes and the elongated shape of Graham seamount highlight magma emplacement along a N-S fault system.

The *Banco Senza Nome* (*Nameless Bank*) is a pinnacle rising to about 80 m below sea level from a high probably made of sedimentary rocks (Beccaluva et al. 1981). K/Ar isochrone dating on dredged samples gave an age of 9.5 Ma (Beccaluva et al. 1981).

The *Bannock* seamount is located between the Island of Malta and the Pantelleria graben. It rises from a depth of about 1 km reaching 230 m below sea level. In spite of its conical shape, there are doubts about the volcanic nature of this seamount, since no magnetic anomalies have been detected.

Three seamounts (*Linosa 1, Linosa 2 and Linosa 3*) have been found north of Linosa island. Little is known about these cones and the volcanic nature of the northernmost centre (Linosa 3) is dubious.

Finally, the most recent centre in the Sicily Channel is the *Foerstner* volcano sited about 5 km north-west of Pantelleria. This is reported to have erupted in October 1881. The eruption lasted about a week, but was not observed by any scientist and descriptions are based on fishermen accounts (Washington 1909).

Petrological and geochemical data are available for a few dredged samples from some seamounts. Rock compositions range from tholeiitic basalt to alkali basalt, hawaiite and basanite (Calanchi et al. 1989 and references therein; Fig. 8.16). Tholeiites have been found at Tetide volcano. These rocks are sparsely porphyritic, with phenocrysts of orthopyroxene rimmed

by pigeonite and olivine microphenocryst set in a groundmass containing Ca-rich clinopyroxene, pigeonite, plagioclase and secondary calcite and Fe-hydroxides. Transitional basalts are found at Anfitrite. These are porphyritic with phenocrysts of olivine, clinopyroxene and plagioclase set in a groundmass containing the same phases, along with Fe-Ti oxides alkali feldspar and secondary minerals. Hawaiites were recovered from the Graham seamount. They exhibit porphyritic texture with phenocrysts of plagioclase, clinopyroxene and olivine surrounded by a matrix made up by the same phases plus glass, Fe-Ti oxides, alkali feldspar, apatite, amphibole and secondary minerals. Alkali basalt to basanite have been found at Banco Senza Nome. These rocks show plagioclase, olivine and clinopyroxene phenocrysts in a groundmass composed of the same phases, some alkali-feldpspar, nepheline, accessory apatite and secondary minerals. Bombs erupted by Foerstner volcano have alkali-basalt compositions. Textures are porphyritic with phenocrysts of plagioclase, olivine and minor clinopyroxene set in a highly glassy matrix (Washington 1909).

Trace element abundances of rocks dredged from the Sicily Channel seamounts are scarce (Beccaluva et al. 1981; Calanchi et al. 1989). They show variable concentrations, with incompatible element abundances increasing from tholeiitic to alkaline basalts and basanites (Fig. 8.17). Mantle normalised incompatible elements define bell-shaped patterns (not shown), which resemble those for the exposed rocks in the Sicily Channel.

8.8. Ustica

The Island of Ustica is located in the southern Tyrrhenian Sea about 60 km north of the Sicily coast. The island represents the summit of a wide submerged complex, which rises more than 2000 m above the sea floor and reaches an altitude of 244 above sea level. Southeast of Ustica, a submarine mugearitic lava field (Prometeo) has been recently discovered, and data indicate a close compositional affinity with Ustica (Trua et al. 2003; see Chap. 9). The island is strongly affected by tectonism and erosion. Faults are mostly normal, sometimes with a sinistral horizontal component, and show a prevailing ENE-WSW trend. Ustica shows evidence of at least five relative sea-level stands, with marine terraces located at elevations from 5 m to 120 m above sea level, and ages ranging from 350 ka to 80 ka (De Vita et al. 1998).

8.8.1. Volcanology and Stratigraphy

Structural and stratigraphic studies have shown that the exposed volcanism developed between 750 and 130 ka (De Vita et al. 1998). The activity occurred below sea level until about 500 ka and consists of pillow lavas and pillow breccias presently exposed along the southern border of the island. Successively, both effusive and explosive activity took place, the latter being mainly related to water-magma interaction during eruption. The best preserved hydrovolcanic tuff cone is the Capo Falconiera centre, sited on the eastern tip of the island, where steep erosion cliffs expose a section of this centre. The magmatism has been predominantly mafic, with a single trachytic eruption and dome emplacement at about 424 ka (Romano and Sturiale 1971; Cinque et al. 1988; De Vita et al. 1998).

8.8.2. Petrography and Mineral Chemistry

The Ustica rocks range from mildly Na-alkaline basalt to trachyte on the TAS classification diagram, with a gap in intermediate compositions between about 55-60 wt % SiO_2 (Fig. 8.19). The mafic rocks straddle the boundary between the subalkaline and the alkaline fields, displaying a transitional to mildly alkaline affinity.

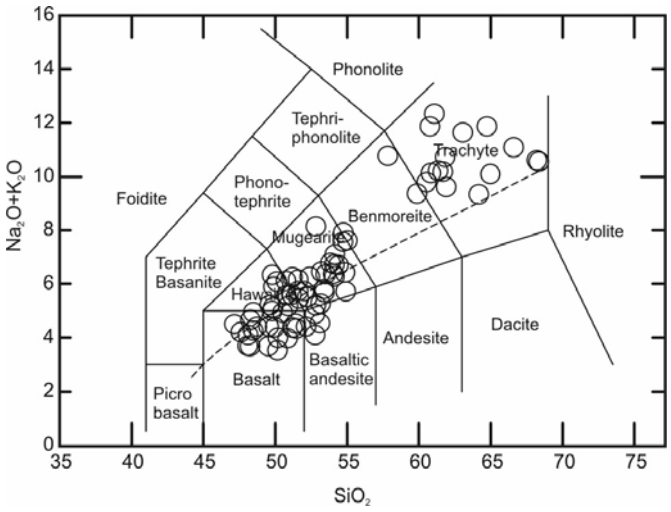

Fig. 8.19. TAS classification diagrams of Ustica island volcanic rocks. The dashed line is the boundary between subalkaline and alkaline fields of Irvine and Baragar (1971).

Textures of mafic rocks are variably porphyritic with phenocrysts of plagioclase and olivine and sporadic clinopyroxene. Fe-Ti oxides are generally found as microphenocrysts in the most differentiated rocks. Plagioclase crystals are generally weakly zoned. Olivine (Fo_{83-76}) is the most abundant mafic phase. Clinopyroxene ranges from diopside to salite. Trachytic pumices contain a few phenocrysts of alkali feldspar, plagioclase and a few biotite and Fe-Ti oxides set in a vesicular glassy matrix.

8.8.3. Petrology and Geochemistry

Variation diagrams of major and trace elements show a decrease in TiO_2, FeO_{total}, MgO, CaO, Cr, Ni and Sc, and an increase in K_2O and incompatible elements with increasing silica. P_2O_5 shows a wide scattering in the mafic rocks (Fig. 8.20). REE patterns exhibit variable degrees of fractionation, sometimes with a small positive anomaly of Eu (Fig. 8.21a). Mantle-normalised incompatible element plots of mafic rocks show an upward convex shape and negative anomalies of K, Hf and Ti (Fig. 8.21b).

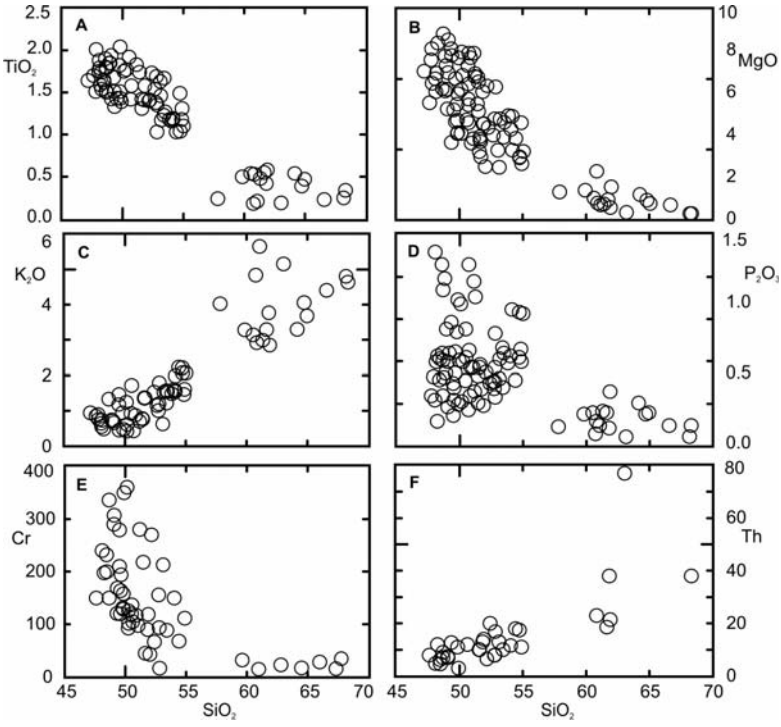

Fig. 8.20. Variation diagrams of selected major and trace elements against SiO_2 for volcanic rocks from Ustica island and Prometeo seamount.

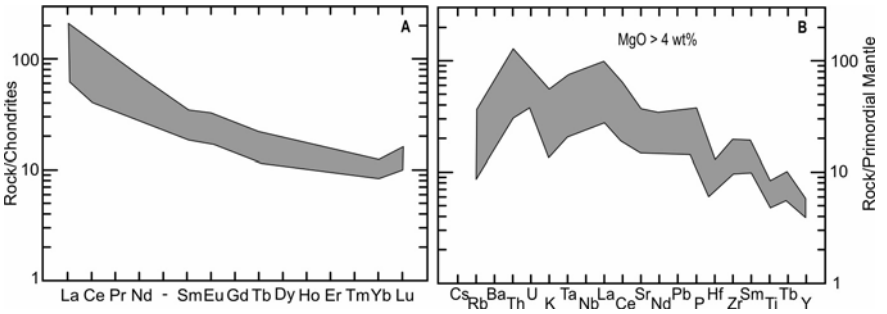

Fig. 8.21. REE (A) and incompatible element patterns (B; restricted to mafic rocks) for the Ustica volcano.

The few available data on Sr-Nd-Pb isotope compositions show limited variations (Fig. 8.6; $^{87}Sr/^{86}Sr$ = 0.70306 to 0.70343; $^{143}Nd/^{144}Nd$ = 0.51290 to 0.51300; $^{206}Pb/^{204}Pb$ = 18.84 to 19.56; $^{207}Pb/^{204}Pb$ = 15.62 to 15.66; $^{208}Pb/^{204}Pb$ = 38.61 to 39.18; Cinque et al. 1988; Trua et al. 2003; Author's unpublished data). Overall these values are close to those for Etna volcano, except for the presence of some less radiogenic Pb isotope compositions at Ustica. Sr isotope ratios show a positive correlation with P_2O_5 and LILE/HFSE ratios in the mafic rocks (see Cinque et al. 1988), but do not define any correlation with silica or other evolutionary geochemical parameters.

Based on major and trace element variations, it has been argued that fractional crystallisation was the dominant evolutionary mechanism for Ustica magmas (Cinque et al. 1988). The lack of correlation between silica and Sr isotopic ratios has been interpreted as evidence that assimilation of crustal rocks played a minor role during magma evolution. The variable contents of K_2O, P_2O_5, incompatible elements and radiogenic Sr in the mafic rocks most likely reflect the occurrence of various types of primary melts at Ustica.

8.9. Petrogenesis

The mafic rocks of the Sicily Province range from silica oversaturated quartz tholeiites to undersaturated nephelinites (Fig. 8.22), which display variable enrichment in incompatible elements and radiogenic isotopes. At Etna there is an apparent increase in alkalinity with time, from early tholeiites to late alkali basalts and hawaiites, although tholeiitic to Na-alkaline compositions coexist as melt inclusions in mineral phases of single rocks, demonstrating the contemporaneous production of the two types of magmas (Kamenetsky and Clocchiatti 1996). At Iblei, mafic rocks show

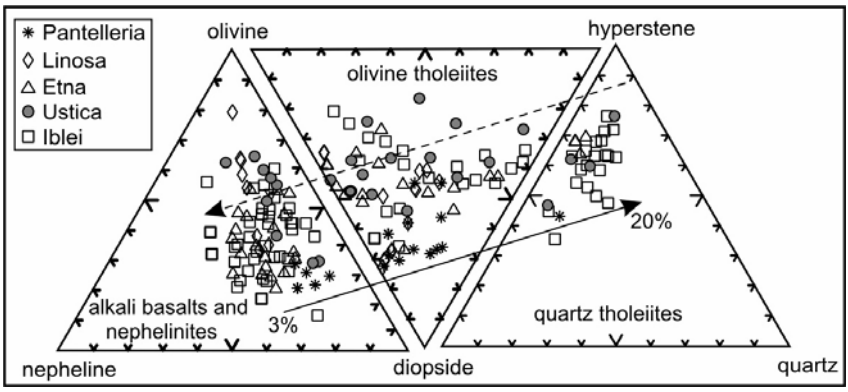

Fig. 8.22. Normative compositions of basaltic rocks (SiO_2 < 52 wt %; MgO > 4 wt %) from the Sicily Province. Dashed arrow indicates increasing depth of magma genesis and degree of source metasomatism. Full arrow indicates degree of partial melting, increasing from about 3% to 20% for nephelinitic to tholeiitic magmas.

a wider compositional range from quartz-tholeiites to nephelinites. At Pantelleria, Linosa and Ustica the mafic rocks are mostly transitional to Na-alkaline, ranging from hyperstene- to nepheline-normative.

There is a general agreement that the variable petrochemical affinity, degree of silica saturation and incompatible element enrichment of mafic rocks in Sicily are the effect of the variation in the degrees of partial melting, depth of magma generation and intensity of source metasomatism within the upper mantle (e.g. Tanguy 1978; Tanguy et al. 1997; Beccaluva et al. 1998; Trua et al. 1998). This is schematically shown in Fig. 8.22. However, the variable isotopic signatures found in the mafic rocks, both at local and regional scales, require that sources were compositionally heterogeneous. In general, tholeiitic rocks have more primitive (less radiogenic Sr and more radiogenic Nd) isotopic compositions than alkaline rocks, suggesting a lower degree of incompatible element enrichment for their sources.

Major and trace element geochemistry of melt inclusions indicate that the primary alkaline and tholeiitic magmas at Etna had compositions much more mafic than the outcropping rocks. They were also more compositionally variable, indicating that a large range of primitive magmas were formed. Geochemical modelling has shown that magmas parental to the alkaline suite were generated by less than 5% of mantle melting, whereas primary tholeiitic magmas were formed by much more extensive mantle melting of about 15-20% (e.g. Corsaro and Cristofolini 1996). Armienti et al. (2004) indicated a pressure of 1.5-1.8 GPa for the last equilibration

within the upper mantle for the parental magmas of Etna rocks. This represents a minimum depth of partial melting, and Corsaro and Cristofolini (1996) and Corsaro and Pompilio (2004) suggest derivation of alkaline magmatism from somewhat deeper sources (1.5 to 3.0 GPa), within the stability field of garnet lherzolite. Geochemical and isotopic investigations have shown significant time-related variation of magma composition at Etna, with an overall increase in radiogenic Sr, volatiles and fluid-mobile elements (e.g. Rb, Cs, B and K) and a decrease of Nd isotopic ratios from early tholeiites and alkaline rocks to recent activity. Although wall rock assimilation has occurred during the evolution of Etna volcano, the secular variations of magma compositions have been attributed to modification of the mantle sources. The most recent views propose that the increase in volatile contents and fluid-mobile elements with time is the result of fluids derived from the nearby subducting Ionian slab, progressively metasomatising mantle that is either upwelling asthenosphere or deep plume material (e.g. Schiano et al. 2001; Tonarini et al. 2001b).

The Island of Ustica and the nearby Prometeo lava field have been less extensively studied than Etna. However, the available data have shown close compositional similarities among these volcanoes. Cinque et al. 1988) found that the Ustica basalts have incompatible element and Sr-isotope ratios that are intermediate between the intraplate basalts from the African plate (e.g. Pantelleria) and the calc-alkaline mafic rocks from Alicudi (Aeolian arc). This has led to the conclusion that the source of Ustica magmas is an intraplate-type mantle contaminated by subduction fluids or melts. A similar conclusion has been reached by Trua et al. (2003).

The wide variety of petrological and trace element compositions found in the Iblei Plio-Quaternary volcanoes requires more complex sources than at Etna and Ustica. Beccaluva et al. (1998) used an integrated thermodynamic, geochemical and isotopic approach to reach the conclusion that tholeiitic to nephelinitic lavas were generated by variable degrees of lithospheric mantle melting (about 20% for tholeiites and about 3% for nephelinites) at various pressures (from 1.0 to 2.5 GPa passing from tholeiites to nephelinites). The mantle rocks were lherzolites containing some amphibole at shallow depth and amphibole plus phlogopite and carbonates at greater depth. These exotic mantle minerals were formed by reaction between depleted lithospheric mantle and percolating fluids or melts. Metasomatism was stronger at the base of the lithosphere, where alkaline melts were generated, with respect to the intermediate and upper lithospheric mantle, which generated tholeiitic magmas.

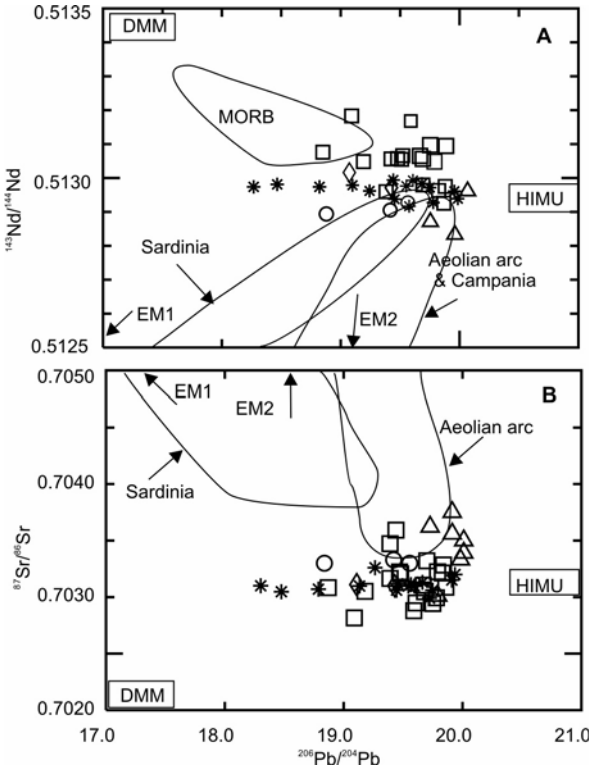

Fig. 8.23. Isotopic variations for Sicily mafic rocks (MgO > 4 wt %). Compositions of HIMU, DMM, EM1 and EM2 are shown. For explanation, see text.

Trua et al. (1998) noticed that there are variable incompatible ratios (e.g. Sm/Nd, Rb/Sr, Th/Pb, La/Yb, etc.) but not so variable Sr-Nd-Pb isotope composition in the Iblean magmas. It was suggested that trace element variability was basically the result of source metasomatism by Si-K-rich silicate and carbonatitic melts. The contrast between the primitive, MORB-like Sr-Nd isotopic signatures of Iblean mafic magmas and their high Sm/Nd and Rb/Sr ratios was explained by assuming that the metasomatic event responsible for element enrichment was very young. Therefore, in spite of the high elemental enrichment and fractionation, there was insufficient time available to develop high $^{87}Sr/^{86}Sr$ and low $^{143}Nd/^{144}Nd$ ratios. According to Trua et al. (1998), metasomatism could have occurred during the Triassic extensional event, which affected the north African plate.

The mafic rocks from Linosa are mildly enriched in alkalies and range from saturated to slightly undersaturated in silica. These characteristics indicate intermediate degrees of partial melting between those of tholeiites

and nephelinitic magmas. The few available data have also shown that the Linosa mafic rocks have incompatible element abundances and ratios and isotopic signatures that are less variable than other rocks from the Sicily Province (Civetta et al. 1998; Bindi et al. 2002). Assuming this observation is not an artefact of the small number of available data, it could indicate derivation from a relatively homogeneous mantle source. The moderate degree of REE fractionation and the low and constant La/Y ratios suggest that melting occurred in the stability field of spinel peridotite and that the source was not heavily contaminated by metasomatism, as is the case for Iblei volcanoes.

The mafic rocks at Pantelleria show a much larger range of values than other Sicily volcanoes, and define a trend for Pb isotopes that extends from radiogenic compositions like those of Etna, to unradiogenic signatures close to DMM mantle end-member (Fig. 8.23). This has been interpreted as evidence that the source of the Pantelleria basalts is isotopically heterogeneous and basically consists of a mixture of HIMU- and DMM-type mantle material, possibly with some contribution by EM1 (e.g. Mahood and Baker 1986; Esperança and Crisci 1995; Civetta et al. 1998). The nature and origin of these compositions are debated, however, and will be discussed in the next section.

8.10. Geodynamic Setting

Overall, the mafic magmas of the Sicily Province display typical intraplate trace element compositions, with low LILE/HFSE ratios, depletion in some LILE (e.g. K, Rb) and enrichments in Ta and Nb (see also Chap. 1). Sr and Nd isotopic compositions show moderate variation, when compared with rocks from other Italian volcanic provinces (Fig. 8.23). In contrast, Pb isotopic ratios are variable. Most rocks (i.e. Iblei, Etna and some rocks from the other volcanoes) show Sr-Nd-Pb isotope values close to HIMU-type OIBs mantle compositions (Zindler and Hart 1986; see also Chap. 6). Some authors also suggested an affinity with the FOZO mantle source (Hoernle et al. 1996; Bell et al. 2004), although such a hypothesis is ruled out by Gasperini et al. (2002). Other rocks plot along a trend which crosses the Northern Hemisphere Reference Line (NHRL, Hart 1984) on Pb isotope diagrams (Figs. 8.6b), pointing to an unradiogenic end-member composition intermediate between DMM and EM1-type mantle (Fig. 8.23; Carter and Civetta 1977; Esperança and Crisci 1995; Civetta et al. 1998). Much of this trend is formed by the Pantelleria basalts and may be less extended if only data from leached samples are considered (Civetta et al.

1998). Overall, isotope and trace element data have led to the conclusion that the mantle sources beneath the Sicily Province are heterogeneous and result from the interaction between various mantle compositions or reservoirs. There is a lively debate on the origin and physical nature of these mantle compositions, not only in Sicily, but at a global scale (e.g. Hofmann 1997; Meibom and Anderson 2003).

Most authors agree that DMM compositions represent mantle material containing low concentrations of incompatible elements, low Rb/Sr, Th/Pb and U/Pb, and high Sm/Nd, a condition that was generated by extraction of basaltic magmas during previous melting events that occurred at various stages of Earth's evolution. In contrast, HIMU, EM1 and EM2 compositions reflect enriched mantle materials characterised by variable trace element ratios, basically derived by recycling of different types of crustal rocks. According to some authors these enriched mantle rocks remained as isolated reservoirs in the deep mantle for a long time (of the orders of a few billion years) in order to develop peculiar isotopic signatures. These discrete deep mantle masses are emplaced as plumes into the shallow mantle.

Other authors are against the idea of more or less isolated regions of the mantle with peculiar trace element and isotopic features. They argue that the HIMU, EM1 and EM2 compositions may not represent discrete mantle reservoirs and do not imply the presence of active mantle plumes (e.g. Meibom and Anderson 2003). Therefore, an alternative model to the plume hypothesis is that the upper mantle is strongly heterogeneous and consists of more and less fusible portions, which show a wide range of trace element and isotopic compositions (e.g. Kellog et al. 2002; Meibom and Anderson 2003). The relative compositional homogeneity of MORBs, compared to OIBs, would be simply related to the higher degree of melting and to the larger region sampled during melting of the MORBs. These smooth out compositional heterogeneity and produce melts that show little variable geochemical and isotopic compositions (see discussion in Foulger et al. 2005).

The debate on global-scale mantle compositions is echoed by the discussion on the Sicily magmatism. Based on HIMU-type compositions, a plume origin has been suggested by a number of authors for Etna and Iblei (e.g. Carter and Civetta 1977; Condomines et al. 1982; Clocchiatti et al. 1998; Gasperini et al. 2002). At Pantelleria, HIMU-type, DMM-type and possibly EM1 mantle components have been invoked to explain Pb-isotope variability. Civetta et al. (1998) proposed that DMM composition would represent the uppermost portion of the asthenosphere, whereas the HIMU-type component would be derived from deep mantle plume emplaced beneath the entire Sicily area. At Pantelleria, HIMU-type material interacted

with the shallower DMM asthenospheric mantle to give rise to a range of isotopic compositions. The plume could be either an independent deep mantle body or may be linked to the large homogeneous layer occurring at a continental scale beneath Europe (European Asthenospheric Reservoir, EAR; Fig. 8.6b), which is believed to represent an expanded plume head (Wilson and Downes 1991; Granet et al. 1995). It has been suggested that this layer is the source for many Miocene to Quaternary volcanoes in Europe, including the Eifel region (Germany), the French Massif Central and Central Spain. The close isotopic similarity between some Sicily volcanics and EAR would indicate a common single source for all these volcanoes (see also Chap. 10).

In contrast, Esperança and Crisci (1995) and Trua et al. (1998) propose that magmatism in the Sicily Province is derived from young lithosphere that was enriched by addition of asthenosphere-derived melts. As recalled earlier, this is a relatively young process, which occurred during Permian-Triassic times. The young age of metasomatism is supported by Sr-Nd isotopic studies on the Iblei xenoliths, which give a pseudo-isochron of about 200 Ma (Tonarini et al. 1996).

As for Etna, alternative models to plume advocate passive ascent of asthenopheric material through a slab window that opened between the Ionian plate and the Pelagian Block. Whatever the case, the relatively low Ti and HFSE contents, combined with LILE/HFSE (e.g. Rb/Nb) ratios that are slightly higher than other HIMU-type magmas, require a role of components and/or processes similar to those affecting the mantle source of arc basalts (Beccaluva et al. 1982; Armienti et al. 2004). It has been suggested that these components are derived from the side Ionian plate, as discussed earlier in this Chapter. A similar hypothesis has been also assumed for Ustica (Cinque et al. 1988; Trua et al. 2003). The coexistence of both subduction-type and HIMU-type signatures in the Etna and Ustica volcanoes is related to their particular position on the boundary of the African foreland. According to recent views, faster rollback of the Ionian plate with respect to the African plate generated a slab window through which deep asthenospheric material was intruded and underwent small degrees (2-3%) of contamination by slab material. Melting of this hybrid mantle gave rise to Etna and Ustica volcanoes (Gvirtzman and Nur 1999; Doglioni et al. 2001; Trua et al. 2003).

8.11. Conclusions

The Sicily Province consists of tholeiitic to Na-alkaline magmas. Most rocks are mafic in composition, ranging from basalt to hawaiite and nephelinite, except at Pantelleria where peralkaline acid volcanics (pantellerites) dominate. A few trachytic rocks occur at Etna, Ustica and as lithic ejecta at Linosa.

Intermediate and acid rocks were formed by evolutionary processes dominated by fractional crystallisation, although a genesis by melting of basaltic crust has been suggested for Pantelleria rhyolites by some authors. Fractional crystallisation and other evolutionary processes occurred during magma ponding in shallow-depth reservoirs. These have been active episodically at Etna, Ustica and Linosa, whereas they could have been a permanent feature of Pantelleria volcano where peralkaline acid magmas have been erupted almost continuously. At Iblei the dominance of mafic rocks is related to the fissural nature of the volcanism, which favoured rapid magma ascent to the surface.

Mafic rocks from the Sicily Province display variable abundances of incompatible elements, which increase from tholeiites to alkali basalts and nephelinites. However, all the rocks show low LILE/HFSE ratios, typical of intraplate basalts, in contrast with the high LILE/HFSE compositions of volcanism from the Aeolian arc and the Italian peninsula. They have a relatively restricted range of Sr-Nd isotopic compositions, but variable Pb isotopic ratios, which fall along a trend connecting HIMU and intermediate compositions between DMM and EM1 mantle.

The variable petrogenetic affinity and incompatible element contents of the Sicily mafic magmas are mainly related to different degrees of partial melting at different depths within the mantle. Based on experimental and geochemical constraints, about 20% to 3% melting is required to generate the tholeiitic to nephelinitic magmas.

The variable isotopic compositions (especially for Pb) reveal geochemically heterogeneous sources. The origin of this heterogeneity is debated and may derive either from shallow mantle processes, such as variable metasomatic modifications of the lithosphere by asthenospheric melts, or from mixing between a deep-mantle plume and asthenosphere-lithosphere material. Etna and Ustica show some trace element and isotopic characteristics (e.g. Rb/Nb, Ce/Pb, and boron isotopes), indicative of a contribution from subduction-derived components.

Table 8.2. Selected major, trace element and isotopic compositions of Sicily volcanic rocks. Numbers in parentheses refer to data obtained on different, though compositionally similar samples as those analysed for the other elements. Source of data: 1) Carter and Civetta (1977); 2) Cinque et al. (1988); 3) Calanchi et al. (1989); 4) Esperança and Crisci (1995); 5) D'Orazio et al. (1997); 6) Beccaluva et al. (1998); 7) Civetta et al. (1998); 8) Trua et al. (1998); 9) Trua et al. (2003); 10) Armienti et al. (2004); 11) Author's unpublished data.

Volcano	**Tetide seamount**	**Anfitrite seamount**	**Graham Bank**	**Banco Senza Nome**
Rock type	Tholeiitic basalt	Alkali-basalt	Hawaiite	Basanite
Data source	3	3	3	3
SiO_2 wt%	47.02	48.00	49.32	41.14
TiO_2	2.43	2.78	2.68	3.31
Al_2O_3	15.09	14.74	16.26	12.28
FeO_{total}	11.37	10.83	10.25	12.28
MnO	0.17	0.16	0.15	0.22
MgO	7.62	7.80	5.75	10.35
CaO	9.10	9.77	7.87	10.06
Na_2O	3.22	3.02	4.29	2.95
K_2O	0.23	1.03	1.45	0.86
P_2O_5	0.38	0.53	0.85	0.86
LOI	2.77	1.02	0.81	4.79
Rb ppm	2	23	26	12
Sr	236	527	749	773
Y	28	27	29	27
Zr	142	218	317	310
Nb	12	40	61	79
Ba	69	315	468	587
La	6	37	62	66

Table 8.2 (continued)

Volcano	**Etna**					**Iblei**	
Rock type	Tholeiitic basalt	Hawaiite	Mugearite	Benmoreite	Trachyte	Tholeiitic basalt	Nepheli-nite
Data source	10,1	5,1	5	5	5	8	8
SiO_2 wt%	49.18	51.09	52.74	57.66	61.02	50.03	38.31
TiO_2	1.47	1.68	1.23	1.18	1.29	1.57	1.89
Al_2O_3	17.20	18.74	17.44	18.36	16.94	16.91	11.15
FeO_{total}	9.58	8.15	7.44	5.27	5.32	10.60	10.77
MnO	0.15	0.14	0.13	0.16	0.17	0.16	0.21
MgO	8.73	4.37	5.20	2.04	1.88	7.38	14.84
CaO	9.27	7.76	7.76	4.12	3.43	8.56	13.69
Na_2O	3.20	4.15	4.28	6.64	5.95	2.89	2.88
K_2O	0.35	1.74	1.76	3.22	2.82	0.21	0.74
P_2O_5	0.38	0.65	0.50	0.50	0.45	0.32	2.18
LOI	0.39	1.08	1.00	0.72	0.52	1.04	2.77
Sc ppm	25	18	20	-	14	28	33
V	169	226	228	108	85	187	279
Cr	363	23	64	8	5	328	379
Co	45	33	32	14	13	51.5	58.8
Ni	144	25	40	3	3	234	311
Rb	5.5	34	36	60	62	6.4	16.1
Sr	455	1449	942	1041	857	319	1685
Y	22	20	17	26	30	32.7	41.1
Zr	99	178	162	333	408	118	297
Nb	17	71	53	94	102	15.8	186
Cs	0.17	0.63	0.30	1.75	2.56	0.24	0.39
Ba	142	851	644	1372	1335	247	1087
La	19.6	81	64	125	111	15.6	159
Ce	40	154	121	223	210	28.4	311
Nd	20	60	45	82	79	17	131
Sm	4.7	10.0	7.3	12.3	12.9	4.3	20.4
Eu	1.59	2.82	2.09	3.46	3.58	1.79	6.58
Tb	0.74	1.06	0.77	1.15	1.33	0.78	2.5
Yb	1.75	1.89	1.53	3.12	2.51	2.06	2.97
Lu	0.25	0.24	0.21	0.45	0.37	0.29	0.44
Hf	2.48	4.50	3.90	7.40	-	2.85	5.13
Ta	0.88	3.40	2.70	5.80	5.20	0.75	6.52
Pb	1.3	7.5	7.5	13.3	13.7	1.45	8.58
Th	2.22	11.6	11.8	19.4	16.3	1.0	11.1
U	0.49	3.50	3.50	4.90	3.50	0.35	4.18
$^{87}Sr/^{86}Sr$	0.703147	0.703251	0.703367	0.703409	-	0.70305	0.703223
$^{143}Nd/^{144}Nd$	0.512924	0.512912	0.512899	0.512887	-	0.51306	0.512962
$^{206}Pb/^{204}Pb$	(19.47)	(19.80)	-	-	-	19.18	19.79
$^{207}Pb/^{204}Pb$	(15.65)	(15.65)	-	-	-	15.61	15.62
$^{208}Pb/^{204}Pb$	(39.11)	(39.45)	-	-	-	38.82	39.37

Table 8.2 (continued)

Volcano	**Iblei**		**Linosa**			**Pantelleria**
Rock type	Basalt	Basanite	Hawaiite	Basalt	Trachyte	Basalt
Data source	6	8	11,7	11,7	11	7
SiO_2 wt%	46.37	43.24	50.48	45.67	63.02	46.90
TiO_2	2.68	3.15	2.21	2.21	0.39	3.38
Al_2O_3	16.62	14.02	16.67	15.35	18.95	14.20
FeO_{total}	9.80	11.74	8.69	10.46	3.05	11.93
MnO	0.16	0.19	0.15	0.21	0.08	0.18
MgO	7.70	10.14	3.75	11.31	0.80	6.55
CaO	9.00	10.05	9.76	8.43	1.75	10.49
Na_2O	2.98	2.89	3.82	3.14	4.40	2.66
K_2O	1.31	1.23	1.17	1.19	6.76	0.88
P_2O_5	0.73	0.99	0.47	0.52	0.12	1.25
LOI	2.37	1.99	1.87	0.35	0.65	-0.06
Sc ppm	-	33	27	24	4.1	22
V	233	279	222	214	15	269
Cr	288	256	315	389	35	162
Co	45	52	29	55	4.5	36.5
Ni	197	188	46	238	9	87
Rb	23	28	27	26	48	16
Sr	648	994	470	580	124	532
Y	25	37	34	24	8	33
Zr	261	369	213	235	505	214
Nb	63	97	43	50	28	44
Cs	-	0.44	0.9	1.0	0.26	-
Ba	549	420	290	379	327	620
La	36.5	57	27	36	20	45
Ce	76.3	115	51	67	39	97
Nd	38.2	57	23	27	13	53
Sm	8.3	10.8	4.9	5.4	2.34	10.8
Eu	2.61	3.6	2.0	2.1	0.87	4.53
Tb	-	1.71	0.72	0.77	0.28	1.30
Yb	1.81	2.65	2.8	2.9	0.91	2.18
Lu	0.31	0.37	0.41	0.38	0.13	0.30
Hf	-	6.94	5.0	5.1	1.58	-
Ta	-	4.48	3.3	2.3	1.96	-
Pb	-	3.14	3	7	2.9	-
Th	7	5.62	3.7	4.1	2.24	4.09
U	-	1.6	1.0	0.8	0.86	-
$^{87}Sr/^{86}Sr$	0.70287	0.703321	(0.70303)	(0.70311)	-	0.7031
$^{143}Nd/^{144}Nd$	0.51301	0.513061	(0.51297)	(0.51301)	-	0.51297
$^{206}Pb/^{204}Pb$	-	19.70	(19.28)	(19.11)	-	18.302
$^{207}Pb/^{204}Pb$	-	15.64	(15.60)	(15.63)	-	15.571
$^{208}Pb/^{204}Pb$	-	39.29	(38.89)	(38.79)	-	38.040

Table 8.2 (continued)

Volcano	Pantelleria			Ustica		
Rock type	Hawaiite	Trachyte	Pantellerite	Hawaiite	Benmore-ite	Trachyte
Data source	4	7	7	9,11	9,11	2,11
SiO_2 wt%	49.50	63.95	69.53	47.44	52.21	61.65
TiO_2	2.93	0.56	0.36	1.47	1.45	0.55
Al_2O_3	16.90	14.30	8.01	16.77	16.71	19.47
FeO_{total}	10.16	6.94	9.07	9.44	9.89	4.36
MnO	0.18	0.24	0.29	0.16	0.14	0.18
MgO	3.92	0.25	0.25	7.68	5.74	0.80
CaO	7.79	1.10	0.54	9.17	9.22	2.35
Na_2O	4.89	6.79	5.08	4.16	3.93	6.89
K_2O	1.80	5.08	4.33	1.40	0.97	3.29
P_2O_5	0.42	0.08	0.03	0.88	0.38	0.23
LOI	1.32	0.47	2.05	0.12	-0.25	1.69
Sc ppm	21	5.5	2.5	23	23	-
V	264	-	7	177	180	-
Cr	-	-	-	199	186	-
Ni	29	-	-	168	104	-
Rb	43	74	217	27	20	61
Sr	675	16	14	1050	496	333
Y	42	53	202	25	23	26
Zr	356	480	2363	185	120	320
Nb	79	98	425	50	32	82
Cs	0.17	-	-	0.3	-	-
Ba	686	413	30	723	454	-
La	75	67.6	288	85	40	97
Ce	145	125	520	142	67	-
Nd	63	58	187	50	26	37
Sm	11.8	12.51	40.86	7.9	4.9	5.5
Eu	3.72	3.0	4.89	2.56	1.74	-
Tb	1.55	-	-	0.93	0.80	-
Yb	2.86	4.82	17.9	2.22	2.10	1.9
Lu	0.43	0.87	3.04	0.32	0.29	-
Hf	6.74	-	-	3.7	3.2	5.3
Ta	4.34	-	-	3.03	1.79	3.6
Pb	6.8	4.6	13	12.1	11.6	-
Th	7.34	7	52	11.1	6.4	18.6
U	1.04	-	-	2.4	0.85	-
$^{87}Sr/^{86}Sr$	0.703888	0.70315	0.70316	0.70312	0.70322	0.70321
$^{143}Nd/^{144}Nd$	0.512895	0.51301	0.51301	0.51291	0.51294	-
$^{206}Pb/^{204}Pb$	19.086	19.481	19.612	(19.56)	(18.83)	-
$^{207}Pb/^{204}Pb$	15.672	15.591	15.641	(15.64)	(15.62)	-
$^{208}Pb/^{204}Pb$	39.160	39.020	39.170	(39.19)	(38.62)	-

9. Sardinia and the Southern Tyrrhenian Sea

9.1. Introduction

Sardinia and the Tyrrhenian Sea have been affected by magmatic activity from the Eocene to the present. Two main distinct cycles of igneous activity have occurred in Sardinia: an Oligo-Miocene cycle (about 32 to 15 Ma) that generated dominant calc-alkaline products and minor tholleiites with arc-type petrological and geochemical characteristics, and a Plio-Quaternary cycle (about 5 to 0.1 Ma), during which tholeiitic to alkaline products with intraplate-like geochemical signatures were erupted (e.g. Savelli 1988; Morra et al. 1994; Downes et al. 2001; Lustrino et al. 1996, 2000, 2002, 2004a; Gasperini et al. 2000). A very limited and still poorly known Eocene (~ 62 to 61 Ma) igneous activity with emplacement of a few lamprophyric dikes has been discovered by borehole drillings in southwest Sardinia (Maccioni and Marchi 1994).

Magmatism within the Tyrrhenian Sea basin is characterized by the emplacement of a wide variety of magmatic products, ranging in age from approximately 12 Ma to the Present. Igneous activity in the northern Tyrrhenian Sea has been dominated by granitoid plutonism and by minor mafic to felsic volcanism belonging to the Tuscany Magmatic Province. The bulk of the magmatism represents crustal anatectic melts or hybrids between crust- and mantle-derived magmas (see Chap. 2). The southern Tyrrhenian Sea contains a wide variety of volcanic rocks, ranging in composition from MORB- and OIB-type to arc-type. All these magmas are of ultimately mantle origin and their genesis and tectonic setting will be discussed in the following paragraphs. An important fault system, the so-called 41° Parellel Line, divides the northern and the southern Tyrrhenian basins.

Information on ages and on petrological and volcanological characteristics of Plio-Quaternary Sardinian and southern Tyrrhenian Sea volcanoes is given in Tables 9.1 and 9.2. Selected analyses are given in Tables 9.3 and 9.4. The locations of the main eruptive centres are shown in Fig. 9.1.

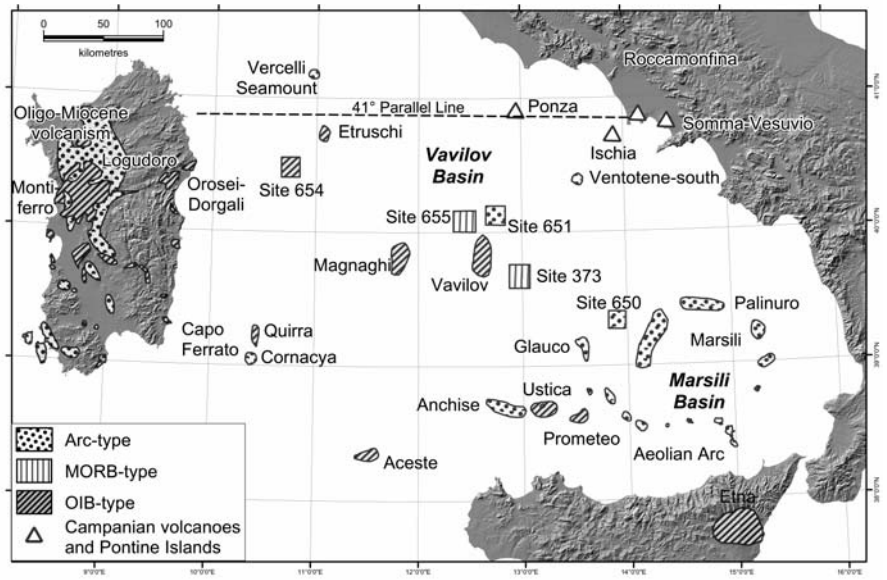

Fig. 9.1. Distribution of Plio-Quaternary volcanism in the southern Tyrrhenian Sea and Sardinia. The Oligo-Miocene arc-type magmatism of Sardinia is also reported.

9.2. Sardinia

9.2.1. Regional Geology

The Island of Sardinia, together with Corsica, forms a microplate characterised by a crustal thickness of approximately 30 km and a lithospheric thickness of 70 km (Panza 1984; Scarascia et al. 1994). The rocks outcropping in Sardinia consist of a wide variety of Precambrian to Palaeozoic igneous and metamorphic terrains, Mesozoic carbonates, Oligo-Miocene tholeiitic to calc-alkaline volcanics, Cenozoic sediments and Plio-Quaternary volcanics. The Oligo-Miocene magmatism is concentrated in western Sardinia along a graben structure known as Fossa Sarda, whereas Plio-Quaternary volcanism is scattered across the island (Fig. 9.2).

Sardinia was constructed during a long and complex geodynamic evolutionary history. One of the most important geological events is the Her cynian orogeny, which occurred during Carboniferous-Early Permian time

by consumption of the proto-Tethys ocean floor and collision between the Gondwana and Laurussia plates (e.g. Tait et al. 1997). This event generated metamorphism, deformation and widespread late- to post-collisional intrusive magmatism represented by monzogranites, granodiorites, minor tonalites and gabbros, and late lamprophyric dykes (e.g. Carmignani et al. 1994a; Tommasini et al. 1995). Sedimentation of dominant neritic and pelagic carbonates occurred during the Mesozoic and early Tertiary. From the Upper Oligocene to Miocene (32 to 15 Ma), Sardinia was affected by arc-type magmatism, coeval with opening of the Balearic-Provençal basin and the consequent counter-clockwise rotation of the Corsica-Sardinia block. According to most authors, magmatism and back-arc extension were related to a NW-dipping subduction of Mesogea oceanic crust beneath the southern European margin (e.g. Gueguen et al. 1998; Doglioni et al. 1999; Speranza et al. 2002). The Oligo-Miocene igneous rocks are mostly calc-alkaline in composition with minor arc tholeiites. Dacitic to rhyolitic lavas and ignimbrites are more abundant than andesites and basalts. Porphyry copper and epithermal gold mineralisation are associated with subvolcanic and volcanic rocks in some areas (e.g. Osilo and Sulcis).

Table 9.1. Petrological characteristics and ages of the main centres of the Sardinia Plio-Quaternary Magmatic Province.

MAIN VOLCANIC CENTRES	AGE (in Ma)	VOLCANOLOGY and PETROLOGY
Capo Ferrato	5.3 to 4.9	- Lava flows, dykes and domes with a trachyandesitic to trachytic composition.
Central Sardinia	3.5 to 2.1	- Several small centres of basaltic andesite, hawaiite to mugearite lavas.
Monte Arci	3.2	- Volcanic ridge formed of dacite and rhyolite lavas with minor basalts, trachybasalts and andesites.
Orosei-Dorgali	3.9 to 2.0	- Subaerial and submarine lavas composed predominantly of hawaiites and mugearites and minor tholeiitic basaltic andesites.
Campeda-Planargia	3.2 to 2.0	- Lava plateaux composed of basaltic andesites, hawaiites and mugearites.
Montiferro	3.8 to 2.3	- Multicentre volcanic complex formed of basanite and hawaiite to trachyte and phonolite.
Logudoro	3.2 to 0.1	- Cinder and spatter cones and associated lava fields formed predominantly of alkaline mafic rocks with both Na and K affinity, and of minor tholeiites.

Mildly peralkaline rhyolites (comendites) were erupted during the final stages of the Oligo-Miocene volcanic cycle in the S. Pietro and S. Antioco islands, and in the Sulcis district, SW Sardinia (Araña et al. 1974; Morra et al. 1994). The Oligo-Miocene rocks have typical arc signatures with low TiO_2 contents and high LILE/HFSE ratios. Radiogenic isotope ratios are in the range of 0.70399 to 0.71127 for $^{87}Sr/^{86}Sr$, and 0.51270 to 0.51218 for $^{143}Nd/^{144}Nd$. Pb isotopic ratios are moderately radiogenic ($^{206}Pb/^{204}Pb$ = 18.52 to 18.71; $^{207}Pb/^{206}Pb$ = 15.62 to 15.68; $^{208}Pb/^{204}Pb$ = 38.41 to 39.11; Lustrino et al. 2004a).

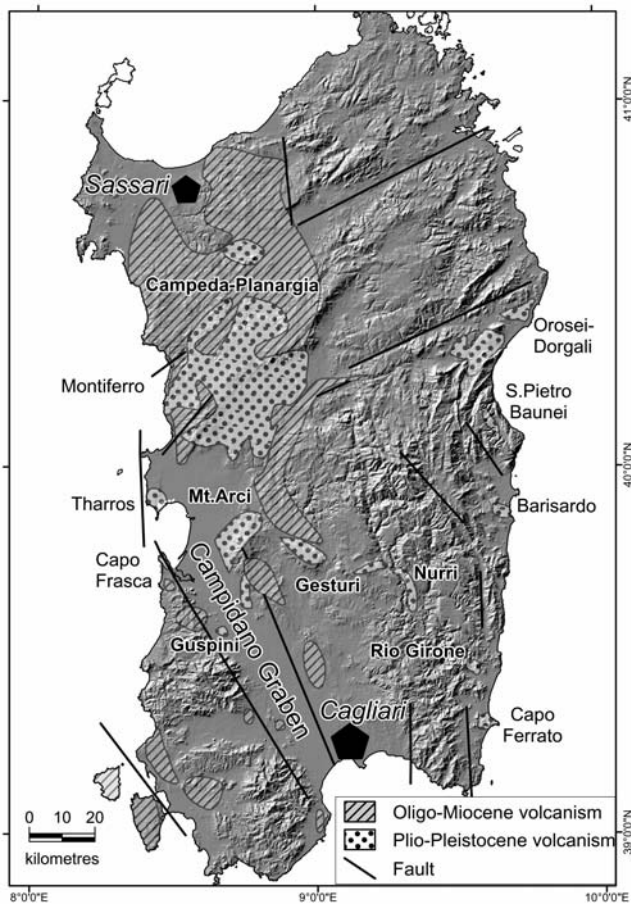

Fig. 9.2. Schematic distribution of Oligo-Miocene and Plio-Quaternary volcanism in Sardinia.

The orogenic magmatic cycles ended at about 15 Ma, when the Tyrrhenian Sea started to open. Successively, Sardinia was subjected to a late Miocene to Pliocene tectonic uplift, followed by a Plio-Quaternary extensional phase and by a new cycle of volcanic activity from about 5 to 0.1 Ma that exhibits intraplate signatures (Beccaluva et al. 1985a; Lustrino et al. 2004a). New $^{40}Ar/^{39}Ar$ data, however, shift the end of Oligo-Miocene cycle at about 11 Ma and the beginning of the Plio-Quaternary magmatism at about 6.4 Ma (Lustrino, personal communication).

9.2.2. Plio-Quaternary Volcanism

9.2.2.1. Regional Distribution and Age

Plio-Quaternary volcanism in Sardinia consists of a wide variety of rock types, ranging from mafic to silicic and from subalkaline to alkaline (Fig. 9.3), which cover an area of about 2200 km^2. Mafic rocks are the most abundant and range from compositions that are oversaturated to strongly undersaturated in silica (Fig. 9.4).

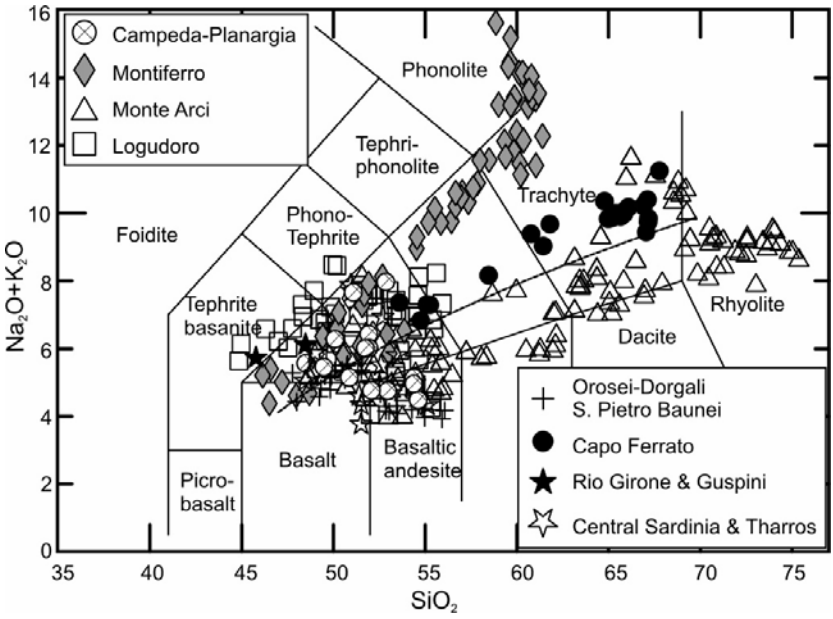

Fig. 9.3. TAS classification diagram for the Sardinia Plio-Quaternary volcanic rocks.

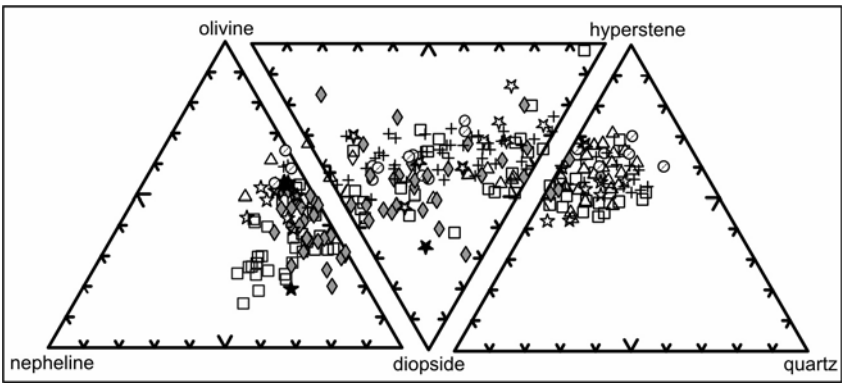

Fig. 9.4. Normative compositions of mafic Plio-Quaternary volcanic rocks (MgO > 4%) from Sardinia. Symbols as in Fig. 9.3.

The volcanoes in southern Sardinia are represented by the small outcrops of Capo Ferrato, Guspini and Rio Girone (Fig. 9.2). *Capo Ferrato* contains the oldest exposed rocks of the Plio-Quaternary volcanic cycle (~ 5.3 to 4.9 Ma). It is a small volcano constructed over the Hercynian basement by emplacement of a few lava flows, dykes and dome. Rock composition ranges from mugearite to trachyte, with a mildly alkaline affinity. *Rio Girone* and *Guspini* are two necks that have a basanitic and hawaiitic composition, respectively (Lustrino et al. 2000, 2004a,b).

The volcanic outcrops in central-northern Sardinia include both small centres (Barisardo, San Pietro Baunei, Tharros, Gergei, Gesturi, Siddi, etc.) and large volcanic complexes and plateaux (Orosei-Dorgali, Monte Arci, Logudoro, Montiferro and Campeda-Planargia). *Barisardo* is a small volcano formed of hawaiite, mugearite and a few basaltic andesite lava flows. A single basaltic lava flow approximately 5 km in length occurs at *S. Pietro Baunei*. *Capo Frasca* and *Tharros* are small outcrops of basaltic andesite lavas (Lustrino et al. 2000). The *central Sardinian* volcanic area (Gesturi, Nurri, Siddi, Serri, Monte Guzzini, etc.), which developed from about 3.5 to 2.1 Ma, is formed by several small scattered centres of basaltic andesite, hawaiite and mugearite lavas that overlie Hercynian and pre-Hercynian basement and Mesozoic sediments (Lustrino et al. 1996, 2000). *Monte Arci* (about 3.2 Ma) is a 20 km long N-S trending volcanic ridge located on the eastern margin of the Campidano graben. It consists predominantly of dacitic to rhyolitic lava flows and minor basalts, trachybasalts and basaltic andesites. These volcanic rocks crop over an area of about 150 km^2 and rest upon Oligo-Miocene volcanic rocks and Miocene marine sediments (Cioni et al. 1982; Montanini et al. 1994). The *Orosei-Dorgali* volcanism (about 3.9 to 2.0 Ma) extends over an area of about 150 km^2.

Activity took place along NE-SW trending faults cutting the Hercynian and pre-Hercynian basement and Mesozoic sedimentary rocks, and consists of lava cones and flows, sometimes with a pillow structure. Compositions are dominated by hawaiites and mugearites with minor basaltic andesites with a tholeiitic affinity (Lustrino et al. 2002). The *Campeda-Planargia-Abbasanta-Paulilatino* basaltic plateaux (about 3.2-2.0 Ma) are constructed of tholeiitic (basaltic andesite) to Na-alkaline mafic to intermediate lava flows (hawaiites, mugearites) covering an area of about 850 km^2 (Beccaluva et al. 1977; Lustrino et al. 2004a). The *Montiferro* volcanic complex (approximately 3.8 to 2.3 Ma) covers an area of about 400 km^2 in northern Sardinia, located in an uplifted region at the intersection between NE-SW faults and the Campidano graben. Montiferro volcanics exhibit a wide compositional variation from analcime-bearing mafic rocks (basanite, hawaiite, mugearite) to trachyte and phonolite, mainly forming lava flows, dykes and domes (Di Battistini et al. 1990; Lustrino et al. 2004a). The *Logudoro* volcanic field (3.2 to 0.1 Ma) represents the northernmost activity and contains the youngest rocks. Eruptive centres consist of several monogenetic spatter cones, cinder cones and lava flows, associated with minor pyroclastic deposits erupted along N-S and NE-SW faults, and covering an area of about 500 km^2. The volcanic rocks rest on Miocene sediments and calc-alkaline rocks of Oligo-Miocene age. Compositions are mafic and prevailingly alkaline, with a sodic to mildly potassic affinity; subalkaline rocks occur in minor amounts. Rock types include basanites, trachybasalts, basaltic trachyandesites and basaltic andesites (Beccaluva et al. 1976, 1977, 1985a; Savelli 1988; Gasperini et al. 2000).

9.2.2.2. Petrography and Mineral Chemistry

The Plio-Quaternary mafic tholeiitic rocks from Sardinia (basalts and basaltic andesites) exhibit aphyric to porphyritic textures. Olivine (Fo_{85-45}) and plagioclase (An_{70-50}) are common phenocrysts and microphenocrysts. Orthopyroxene, augitic-pigeonitic clinopyroxene and Fe-Ti oxides crystallised later and frequently are confined to the matrix. The groundmass of these rocks mostly contains the same phases and some glass (Beccaluva et al. 1975; Lustrino et al. 2000). Andesites, dacites and rhyolites from Monte Arci have porphyritic textures with variable absolute and relative abundances of plagioclase, orthopyroxene, clinopyroxene and opaques. Sanidine, biotite, and quartz phenocrysts occur in the rhyolites. The groundmass ranges from strongly to totally glassy, sometimes with perlitic texture. Apatite and zircon are found as accessory phases (Cioni et al. 1982; Montanini et al. 1994).

Basanites are porphyritic, with a phenocryst mineralogy characterized by variable amounts of olivine (generally Fo_{85-75}), clinopyroxene (mostly Ti-augite), biotite, and Fe-Ti oxides; globular analcime occurs in Montiferro basanites. Clinopyroxene and biotite sometimes occur as megacrysts. Plagioclase is more common in the groundmass but is also present as a phenocryst phase in the less mafic basanites. The matrix of these lavas contains the same minerals plus some glass. Hawaiites (trachybasalts) and mugearites (basaltic trachyandesites) range from subaphyritic to porphyritic with phenocrysts of olivine (up to Fo_{88}), labradoritic plagioclase (about An_{60-50}), diopside to augite clinopyroxene and rare amphibole set in a groundmass containing the same phases. Analcime is sometimes observed in the groundmass of the most alkali-rich hawaiites. Sanidine is also present in some trachybasalts having a potassic affinity. Trachytes are porphyritic, containing abundant phenocrysts of sanidine plus minor clinopyroxene, biotite, plagioclase and amphibole. Orthopyroxene has been occasionally observed. Zircon, apatite and opaque minerals are common accessory phases. The groundmass of trachytes is hypocrystalline to glassy.

Various types of xenoliths occur in the Plio-Quaternary volcanic rocks in Sardinia. These include high-pressure ultramafic nodules and a variety of crustal rocks. Ultramafic xenoliths consist of spinel harzburgites, lherzolites and minor wherlites and pyroxenites, which have been found in alkaline basalts from several centres from Orosei-Dorgali, Montiferro, Logudoro, Rio Girone, central Sardinia and Monte Arci (e.g. Beccaluva et al. 2001; Lustrino et al. 2004b).

9.2.2.3. Petrology and Geochemistry

The Sardinian Plio-Quaternary rocks define at least three main evolutionary series that are clearly defined on several major and trace element diagrams (Figs. 9.3, 9.5, 9.6):

- A strongly silica undersaturated Na-alkaline series ranging in composition from basanite-tephrite to phonolite, with some of the most evolved rocks reaching a peralkaline composition. This is best represented by volcanic rocks from Montiferro.
- A mildly silica undersaturated to saturated series (trachybasalt to trachyte) with a moderate alkali content and a Na- to mildly K-alkaline affinity. This comprises most of the Plio-Quaternary rocks, including some lavas from Monte Arci.
- A silica oversaturated series (basalt-dacite-trachyte-rhyolite) having a tholeiitic affinity. The large majority of Monte Arci rocks fall along this trend.

The alkaline mafic volcanics are less enriched in silica and more enriched in incompatible trace elements than oversaturated tholeiitic rocks with similar MgO contents. REE show smooth and fractionated patterns (Fig. 9.7). Mantle normalised incompatible element patterns of mafic rocks generally display a small upward convexity with moderate enrichments in Ta and Nb. The large majority of the mafic volcanic rocks exhibit positive spikes of Ba and Pb, which are small or absent in the southern outcrops of Capo Ferrato, Guspini and Rio Girone (Fig. 9.7). Silicic volcanics exhibit a large range of incompatible element concentrations. Sr- and Nd-isotopic

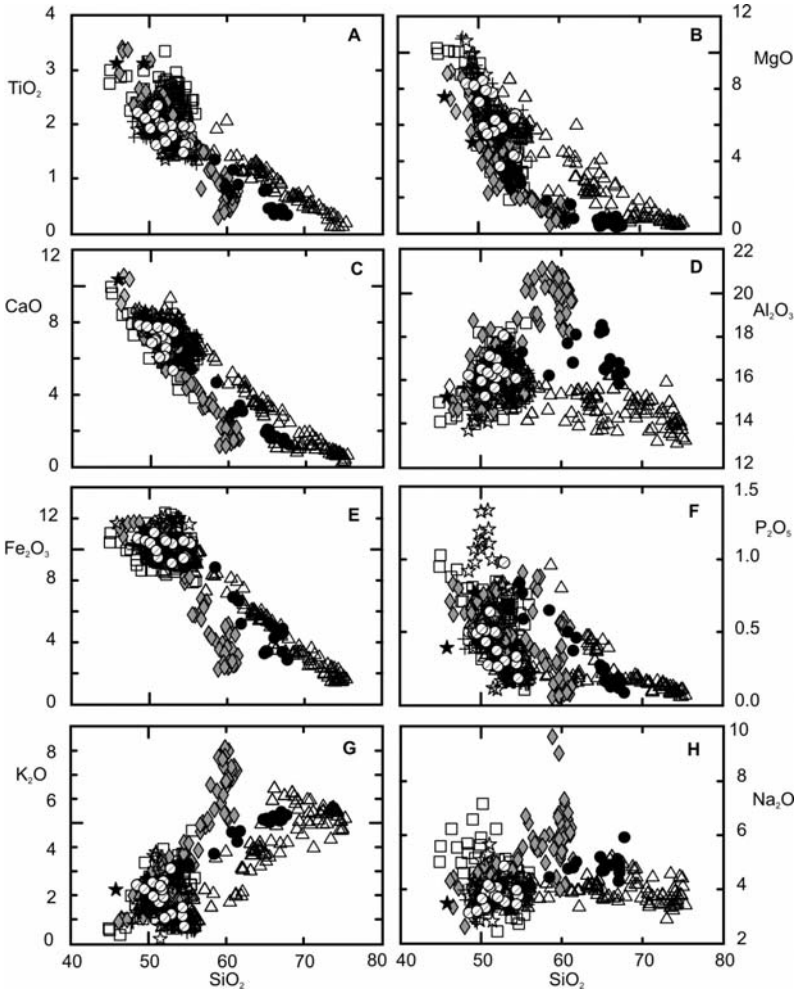

Fig. 9.5. Major element variation diagram for Plio-Quaternary volcanic rocks from Sardinia. Symbols as in Fig. 9.3.

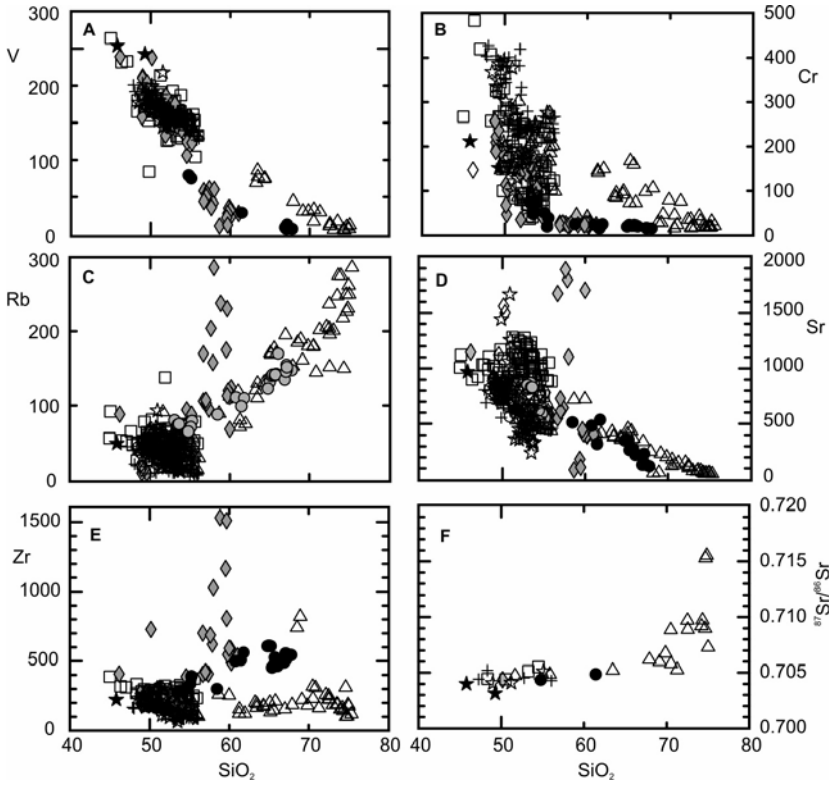

Fig. 9.6. Variation diagrams of selected trace elements and $^{87}Sr/^{86}Sr$ vs. SiO_2 for Plio-Quaternary volcanic rocks from Sardinia. Symbols as in Fig. 9.3.

compositions are highly variable with $^{87}Sr/^{86}Sr$ and $^{143}Nd/^{144}Nd$ ranging from about 0.7042 to 0.7153 and from 0.5122 to 0.5129, respectively (Fig. 9.8a). The mafic rocks define a vertical trend in the Sr-Nd space. The rocks from southern outcrops of Guspini, Rio Girone and Capo Ferrato plot on the mantle array, close to fields of the Sicily and Aeolian arc volcanoes. The other rocks display comparable Sr-isotope compositions to these centres, but have much lower Nd-isotope ratios, defining a trend toward the EM1 mantle end-member (Lustrino and Dallai 2003). However, there is no systematic difference between alkaline and subalkaline rocks. The Monte Arci silicic rocks have variable $^{87}Sr/^{86}Sr$ ratios, which increase with silica (Fig. 9.6f), whereas $^{143}Nd/^{144}Nd$ ratios are low (Fig. 9.8a). Pb-isotope ratios are also variable: the southern centres of Capo Ferrato, Guspini and Rio Girone have relatively radiogenic Pb-isotope compositions ($^{206}Pb/^{204}Pb$ ~ 18.84 to 19.42; $^{207}Pb/^{204}Pb$ ~ 15.64 to 15.66; $^{208}Pb/^{204}Pb$ ~ 38.98 to 39.16), whereas the other centres display unradiogenic Pb isotope ratios

($^{206}Pb/^{204}Pb$ ~ 17.34 to 18.07; $^{207}Pb/^{204}Pb$ ~ 15.53 to 15.62; $^{208}Pb/^{204}Pb$ ~ 37.44 to 38.23) and plot close to EM1 mantle end-member (Lustrino et al. 2004a, and references therein; Fig. 9.8b). Hf isotopic compositions range from = $^{176}Hf/^{177}Hf$ ~ 0.28258 to 0.28269 (Gasperini et al. 2000). O-isotope data are scarce. Analyses of plagioclase, clinopyroxene and olivine give $\delta^{18}O_{SMOW}$ values of +6.46 to +7.56‰ (Lustrino et al. 2003).

Radiogenic isotopic variations for Sardinia Plio-Quaternary volcanics are accompanied by systematic modifications of trace element ratios (Lustrino et al. 2004a). For instance, Ba/Nb is higher in the northern than in the southern outcrops, whereas Ce/Pb is lower (Fig. 9.9). In general terms, the rocks from the southern occurrences have incompatible element ratios close to typical anorogenic magmas such as those of the Sicily Province,

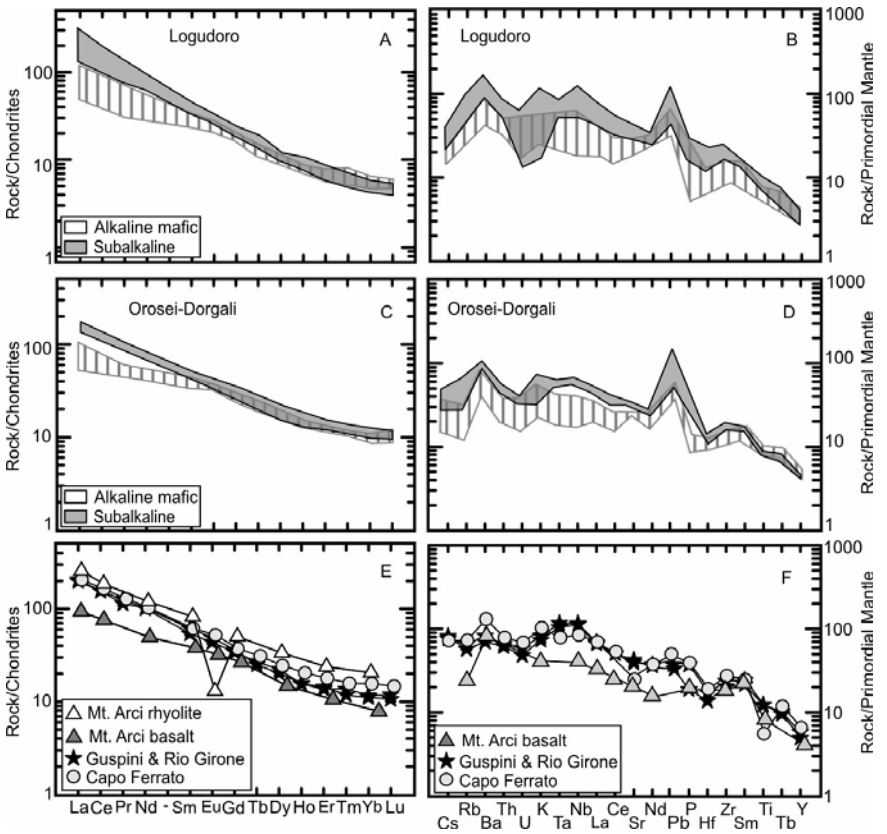

Fig. 9.7. REE patterns and mantle-normalised incompatible element patterns (restricted to mafic rocks for most centres) for Plio-Quaternary volcanic rocks from Sardinia.

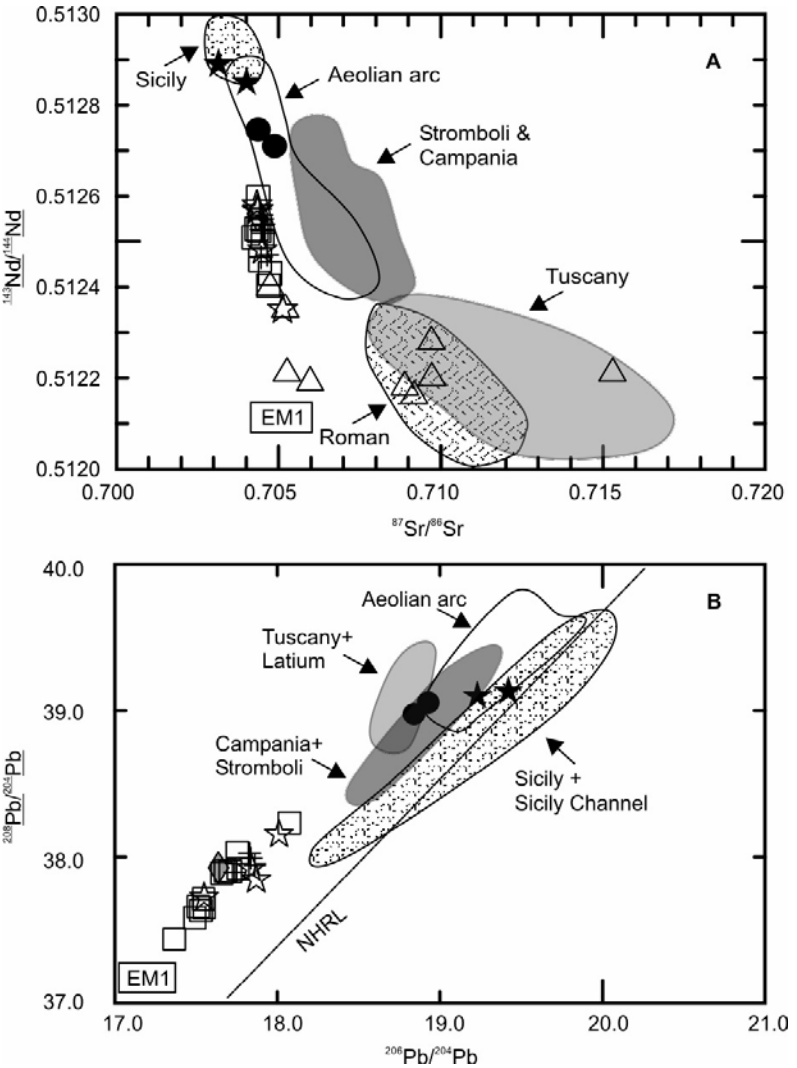

Fig. 9.8. Sr-Nd-Pb isotopic composition of Sardinian Plio-Quaternary volcanic rocks. Compositions of EM1 mantle end-member and of other Italian volcanic provinces are also shown. Symbols as in Fig. 9.3.

although they have a slightly more K-rich character than Sicilian volcanic rocks. In contrast, the rocks from central and northern Sardinia have intermediate compositions between these and the arc-type rocks, such as the Oligo-Miocene calc-alkaline volcanics occuring in western Sardinia (Fig. 9.9).

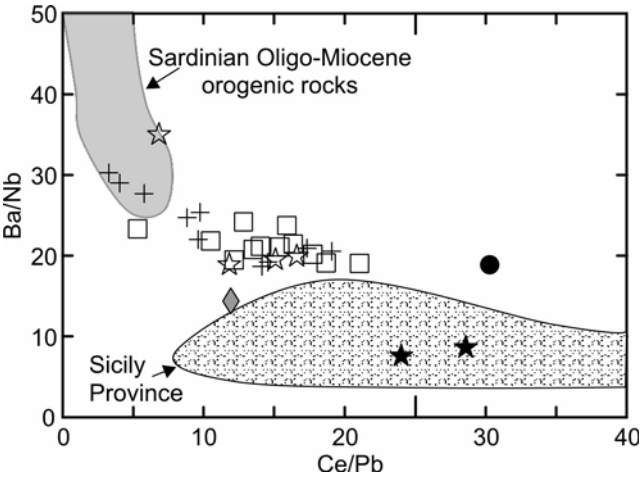

Fig. 9.9. Ba/Nb vs. Ce/Pb variation diagram for Sardinian Plio-Quaternary volcanic rocks (MgO > 4 wt %). The composition of the Sardinian Oligo-Miocene orogenic volcanism and of the anorogenic rocks from Sicily are shown for comparison. Symbols as in Fig. 9.3.

9.2.3. Petrogenesis

9.2.3.1. Shallow Level Processes

Trends of major, trace elements and isotopic ratios vs. silica indicate that different types of evolutionary processes occurred in the various volcanic centres of Sardinia (e.g. Beccaluva et al. 1977 and references therein). Field, petrological and geochemical data indicate that the strongly undersaturated Montiferro series evolved by fractional crystallisation, starting from a basanitic-tephritic parental magma. Early stages of fractionation were dominated by separation of olivine, clinopyroxene and some Ti-magnetite, which determined a sharp increase in Al_2O_3 and decrease in CaO, TiO_2, MgO and Fe_2O_3. The decrease in Al_2O_3 (plus Sr and Ba) in the phonolitic compositions records a late separation of alkali-feldspar. The mildly alkaline suite (Capo Ferrato) shows element variation consistent with a process of fractionation of mafic phases, Fe-Ti oxides and feldspar. The decrease in Al_2O_3 observed in the trachytic rocks suggests that alkali-feldspar was a dominant separating phase during the final stages of fractionation. However, alkali-feldspar started to crystallise at a later stage than in the alkaline series of Montiferro. The decrease in P_2O_5 also indi-

cates separation of apatite. Finally, the Monte Arci subalkaline suite appears to have undergone both fractional crystallisation and interaction with the crust, as denoted by the increase of Sr-isotope ratios with silica and by the occurrence of partially digested crustal xenoliths in some rocks (Montanini et al. 1994). The low concentrations of several incompatible elements such as LREE, Zr and Th highlight an important role for accessory phases (e.g. zircon) in the genesis of acid melts. According to some authors, the most silica-rich rocks from Monte Arci were generated by crustal melting rather than by fractionation from mafic parents, whereas the intermediate magmas were derived from mixing between mantle- and crustal-derived melts (Cioni et al. 1982; Montanini et al. 1994). Although a crustal anatectic origin for the most evolved rhyolites is questionable, the linear trends between mafic and silicic compositions at Monte Arci support mixing as a potentially important process of magma evolution.

9.2.3.2. Genesis of Mafic Melts and Composition of Mantle Sources

The variation of major and trace elements for the Plio-Quaternary mafic rocks from Sardinia likely reflect distinct compositions of primary melts. The increase in silica from alkaline to tholeiitic rocks cannot be generated by fractional crystallisation or other evolutionary mechanisms, since there is a parallel decrease in incompatible element contents. Moreover, the lack of any significant variation of isotopic composition between alkaline and subalkaline mafic rocks excludes a transition from one type of magma to the other via crustal assimilation. Therefore, the different incompatible trace element abundances and the similar radiogenic isotope compositions of mafic alkaline and subalkaline magmas have led to the conclusion that they represent distinct mantle-derived magmas which were generated by different degrees of partial melting of sources, which were homogeneous on a local scale. Lustino et al. (2002, 2004a) suggested about 3 to 6% melting for the alkaline magmas and about 8-12% for the tholeiites. However, the dramatic isotopic and trace element differences on a regional scale between the majority of outcrops and the southern centres of Capo Ferrato, Guspini and Rio Girone require distinct mantle sources for the two groups (Lustrino et al. 2004a).

The bulk of Sardinian Plio-Quaternary rocks have radiogenic isotope ratios resembling EM1-type composition. There is an ongoing debate concerning the origin of the EM1-type mantle in Sardinia. Gasperini et al. (2000) noticed that the unradiogenic Pb-isotope signatures of Logudoro basalts are accompanied by high Ba/La and Eu/Eu* and Sr/Eu* values (where Eu* is the concentration of Eu estimated by interpolation between the nearby elements Sm and Gd on chondritic patterns), and relatively

higher Ce/Pb values in comparison with uncontaminated oceanic basalts. In contrast, the Nb/U ratio is close to average for uncontaminated oceanic basalt. These features were interpreted to indicate that the mantle source of the Logudoro magmas was an ancient basaltic plateau that had been recycled into the mantle over a long time and was recently sampled by a plume. In particular, the excess Ba and Eu was considered to indicate a plagioclase component in the source, which was explained by assuming that the basaltic plateau material was composed of a high proportion of gabbros formed originally by plagioclase accumulation. Lustrino et al. (2004a) argued that the volcanic rocks from north-central Sardinia do not show a significant correlation of Eu/Eu* vs. Sr/Nd and Sr/Eu*, as expected for plagioclase-dominated compositions, and suggested that the unique EM1 signature of the Sardinian basalts could be related to local lithospheric mantle processes. It was postulated that strong syn-collisional crustal shortening and thickening during the Hercynian continental collision generated delamination and passive sinking of a dense, granulitic to eclogitic mafic lower crustal keel. This underwent partial melting during sinking, giving silicic liquids which reacted with the surrounding mantle. The lower crust is depleted in U and Rb and enriched in Ba and Sr. Therefore, liquids formed by melting of the delaminated lower crust would have inherited these characteristics, thus providing a selective enrichment to the lithospheric mantle. Viewed in this light, the EM1 composition in Sardinia would result from the aging of a metasomatised lithosphere (Lustrino and Dallai 2003). Finally, it cannot be excluded that the particular isotopic compositions of the north-central Plio-Quaternary Sardinian rocks may record a modification of lithospheric mantle occurred during the Oligo-Miocene volcanic cycle. Note that the northern-central Plio-Quaternary volcanics have intermediate composition between intraplate and arc-type rocks, which support a role of subduction-related components.

9.3. Southern Tyrrhenian Sea

9.3.1. Regional Geology

The Tyrrhenian Sea is an extensional basin developed behind the Apennine-Maghrebide collisional chain. It started to open at about 15 Ma and is still expanding at present. The rate of opening has been much stronger in the south than in the north. This has resulted in a triangular shape for the Tyrrhenian basin and produced a major lithospheric structural discontinu-

ity, known as the 41st Parallel Line, which divides the northern and southern Tyrrhenian Sea (e.g. Serri 1990; Bruno et al. 2000). In the northern sector, extension caused lithospheric boudinage and led to emplacement of small amounts of igneous rocks, mostly belonging to the Tuscany Province, which has been described in Chap. 2. In the south, stronger lithospheric extension (up to about 5 cm/year) resulted in the diachronous formation of the Vavilov and Marsili oceanic basins, opened between about 6 or 4.5 to 2.5 Ma and from about 1.8 Ma to the Present, respectively (Kastens et al. 1988; Sartori 1990, 2001, 2003). This was accompanied by the emplacement of a wide variety of magma types.

The Tyrrhenian Sea (Fig. 9.1) has a crustal thickness which decreases from approximately 20 to 25 km along its borders to less than 10 km in the Marsili and Vavilov basins. The lithosphere is about 50 km thick along the borders and reaches a minimum of 20 km beneath the Marsili basin. There is a high positive Bouguer gravity anomaly (> 250 Mgal) and high heat flow (more than 100 mW/m^2, and reaching more than 220 mW/m^2 in some areas) in the central Tyrrhenian basin (Della Vedova et al. 2001; Zito et al. 2003). These features are consistent with the occurrence of high-density hot material at shallow depth (Panza 1984; Doglioni et al. 2004 and references therein). The upper mantle beneath the Marsili and Vavilov basins is characterised by relatively low values of S-wave velocity, which reach a minimum of approximately 3.05 km/sec beneath the Moho of the Vavilov basin (Panza et al. 2003, 2004). This suggests mantle melting and magma underplating beneath the crust. A layer of seismic fast material has been detected at a depth of about 650 km and has been interpreted as the accumulation of subducted slab material (e.g. Lucente et al. 1999).

The rock types forming the Tyrrhenian Sea floor include Messinian evaporitic deposits and Plio-Quaternary pelagic sediments that overlie various types of rocks, including the same lithologies that occur on the mainland along the margins of the Tyrrhenian Sea and an oceanic-type crust in the Vavilov and Marsili basins (e.g. Kastens and Mascle 1990; Sartori 2003; Doglioni et al. 2004).

Igneous activity in the southern Tyrrhenian Sea basin produced a wide variety of magmas. Volcanic centres exposed at the surface (Aeolian arc, Ustica and Pontine Islands) have been already discussed (Chaps. 6, 7 and 8). In this chapter, the submarine volcanism will be described. The large majority of the sampled rocks from the southern Tyrrhenian basin have a basaltic composition and often exhibit severe alteration, which has significantly modified the major and trace element compositions. Therefore, combined major and immobile trace element criteria have been adopted to classify these rocks (Barberi et al. 1978; Beccaluva et al. 1982, 1990). Three broad groups of volcanic rocks are recognised, which exhibit

MORB, OIB and island-arc geochemical signatures, respectively. The distribution of various rock types are schematically shown in Fig. 9.1. Compositional characteristics and ages are given in Tables 9.2. Compositions for selected rocks are reported in Table 9.4. The TAS diagram based on oxide concentrations recalculated on a water-free basis is shown in Fig. 9.10. Variation diagrams of some major and trace elements and mantle-normalised incompatible element patterns for selected samples are shown in Figs. 9.11 and 9.12.

9.3.2. MORB-type Rocks

Rocks with a composition similar to the Mid-Ocean Ridge Basalts have been recovered from the Vavilov basin (ODP Site 655 and DSDP Site 373)

Table 9.2. Petrological characteristics and ages of the main volcanic centres of the Tyrrhenian Sea floor.

MAGMA TYPES	MAIN VOLCANIC CENTRES	AGE (in Ma)	VOLCANOLOGY and PETROLOGY
MORB-type	**DSDP Site 373** **ODP Site 655**	7.3 to 4.1 4.3	- Basaltic lavas forming the Vavilov basin.
OIB-type	**ODP Site 654 and Etruschi Seamount**	Plio-Quaternary	- Tholeiitic lavas (site 654) and hawaiite (Etruschi) similar to Sardinia Plio-Quaternary volcanics.
	Magnaghi Seamount	3.0 to 2.7	- N-S elongated, about 1400 m high, cone containing Na-transitional basalts.
	Vavilov Seamount	Late Pliocene to 0.1	- N-S elongated, about 2000 m high, cone contaning tholeiitic to Na-transitional basalts.
	Aceste Seamount	Pliocene	- E-W elongated volcano with an intraplate hawaiitic to trachytic composition.
	Prometeo	Quaternary	- Benmoreitic lava field.
ARC-Type	**Cornacya**	12	- Altered shoshonitic lavas with lamproitic enclaves
	Anchise	5.2 to 3.6	- Mafic high-K calc-alkaline to shoshonitic lavas.
	ODP sites 650 and 651	3.0 to 2.6 1.9 to 1.7	- Lavas with a calc-alkaline to HKCA mafic composition.
	Marsili Seamount	0.8 to < 0.1	- A 50 km by 16 km NNE-SSW ridge rising about 3000 above sea floor, consisting of calc-alkaline basalts to high-K andesites.
	Aeolian Seamounts (Sisifo, Enarete, Eolo, Lametini, Alcione, Palinuro)	1.3 to < 0.1	- Arc tholeiites (Lametini and southern Marsili basin) to calc-alkaline and shoshonitic mafic to intermediate rocks.

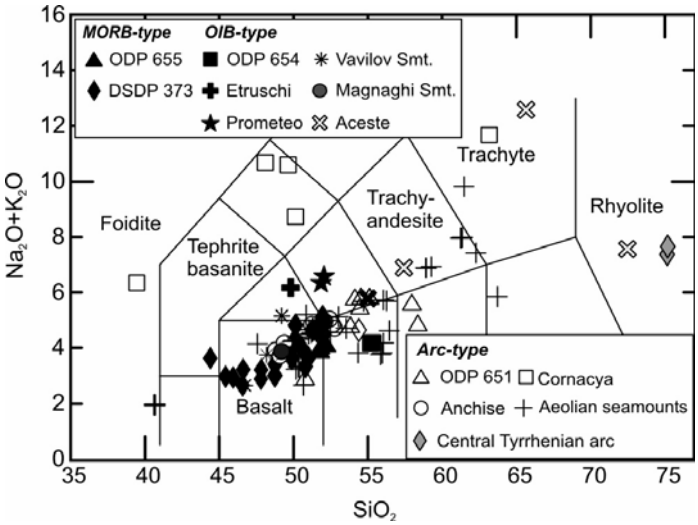

Fig. 9.10. TAS diagram for submarine volcanism from the Tyrrhenian Sea. Compositions have been recalculated on a water-free basis.

1. ODP Site 655. Basaltic pillow lavas, beneath Upper Pliocene sediments, were drilled at this site. $^{40}Ar/^{39}Ar$ dating indicates an age of about 4.3 Ma (Feraud 1990). Rock textures vary from aphyric to porphyritic with phenocrysts and glomerophyric aggregates of olivine (Fo_{87-82}), plagioclase (An_{85-60}) and some augitic clinopyroxene set in a groundmass containing the same phases, Fe-Ti oxides, secondary carbonates, zeolites and altered glass (Bertand et al. 1990). Major and trace element compositions are characterised by low silica contents (SiO_2 ~ 47.0-50.5 wt %), moderate enrichment in TiO_2 (~ 1.2-1.7 wt %), MgO (~ 4.1-7.3 wt %), Ni (~ 80-100 ppm) and Cr (~ 100-200 ppm) and low concentrations of incompatible elements. Isotopic compositions (Fig. 9.13) show relatively unradiogenic Sr and Pb, and radiogenic Nd and Hf ($^{87}Sr/^{86}Sr$ = 0.70375 to 0.70451; $^{143}Nd/^{144}Nd$ ~ 0.51331; $^{206}Pb/^{204}Pb$ ~ 18.70; $^{207}Pb/^{204}Pb$ ~ 15.575; $^{208}Pb/^{204}Pb$ ~ 38.68; $^{176}Hf/^{177}Hf$ ~ 0.28314 to 0.28321, i.e. εHf = 12.09 to 15.38; Beccaluva et al. 1990; Gasperini et al. 2002).

2. DSDP Site 373. Basalts recovered at this site show aphyric to porphyritic textures with plagioclase (about An_{80}) and olivine phenocrysts set in a strongly altered groundmass containing clinopyroxene, opaques and various secondary minerals such as chlorite, amphibole, smectite and carbonates (Kreuzer et al. 1978). K/Ar ages of about 7.3 Ma have been obtained for these rocks (Barberi et al. 1978; Savelli and Lipparini 1978). However, the oldest sediments overlying the basalt lava are about 3.5 Ma old, which suggest younger ages at least for the uppermost lavas (4.1 Ma according to

Sartori 1990). Based on abundance of TiO_2, two groups of lavas have been distinguished. The high-Ti group (TiO_2 > 1.4 wt %) has higher K, P, Zr, Hf and REE, and lower MgO and Cr than the low-Ti group (TiO_2 < 1.1) (Dietrich et al. 1977; Barberi et al. 1978).

Overall, the rocks from the Vavilov basin have MgO, Ni and Cr contents, which are lower than expected for mantle equilibrated magmas. This excludes a direct derivation from the mantle and, instead, suggests an origin through variable degrees of fractional crystallisation, mainly with removal of olivine. Incompatible element abundances are relatively low and mantle-normalised patterns are poorly fractionated with modest positive spikes of Ta and Nb and sometimes of Ba, Rb and Pb (Fig. 9.12). REE patterns are poorly fractionated (not shown), with low values of chondrite normalised La/Sm ratios (generally La/Sm_N = 1.0 to 1.5), and positive spikes of Eu in some samples (Dietrich et al. 1977). Immobile incompatible element contents and ratios mostly resemble Transitional-type MORB. However, $^{87}Sr/^{86}Sr$ and $^{208}Pb/^{204}Pb$ ratios are somewhat higher than typical MORB values (Beccaluva et al. 1990; Gasperini et al. 2002).

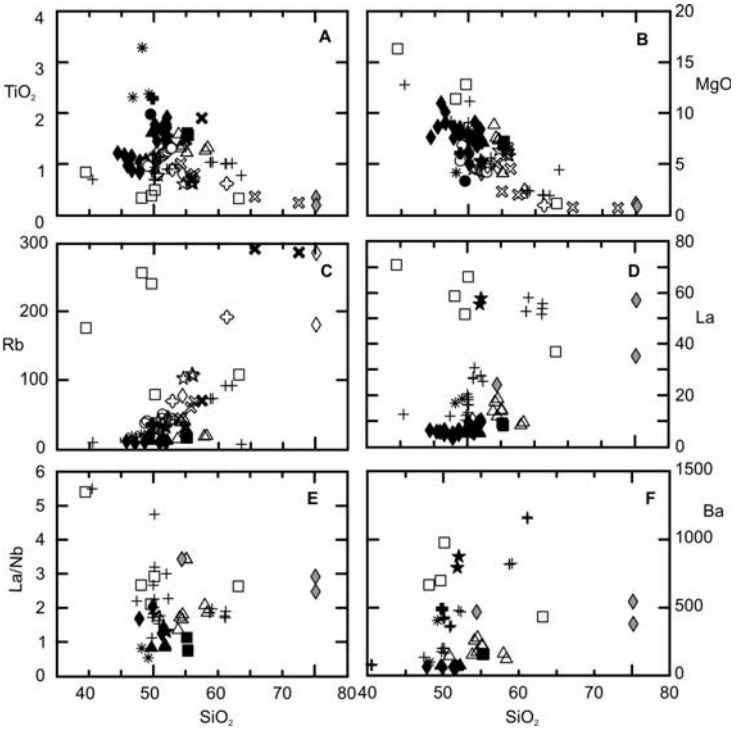

Fig. 9.11. Variation diagrams of selected major and trace elements vs. SiO_2 for volcanic rocks from Tyrrhenian Sea. Symbols as in Fig. 9.10.

9.3.3. OIB-type Rocks

Rocks akin to the Ocean Island Basalts have been found at the Vavilov and Managhi seamounts, off the eastern Sardinian coast (Quirra and Etruschi seamounts and rocks drilled at ODP Site 654), and north and northwest of the western Sicily coast (Aceste seamount, Promoteo lava field and Ustica island; Fig. 9.1). Ustica has been described in Chap. 8.

1. ODP Site 654. A block of lava (possibly a re-sedimented boulder) was drilled from the Upper Pliocene volcano-sedimentary sequence overlying a tilted block of the eastern Sardinian margin (Beccaluva et al. 1990). These lavas exhibit almost aphyric textures and contain a few microphenocrysts of olivine (about Fo_{83}) and labradoritic plagioclase set in groundmass containing clinopyroxene, glass and secondary minerals. Some chromite is included in the olivine. Composition is basaltic andesitic, according to TAS diagram. Trace element composition is characterised by relatively high Ni and Cr (about 170-180 and 250-270 ppm, respectively), and modest enrichment in several incompatible elements (Fig. 9.11). The $^{87}Sr/^{86}Sr$ ratio is 0.70488 and $^{143}Nd/^{144}Nd$ is 0.51244 (Beccaluva et al. 1990; Fig. 9.13). Overall, this rock has a composition close to continental tholeiites occurring in Sardinia, and can be considered as belonging to the Plio-Quaternary magmatic cycle of this island.

2. Etruschi seamount. Basaltic fragments about 0.1 Ma old have been recovered from this site (Keller 1981). The rock is mostly glassy with a few small grains of olivine and acicular plagioclase crystals.

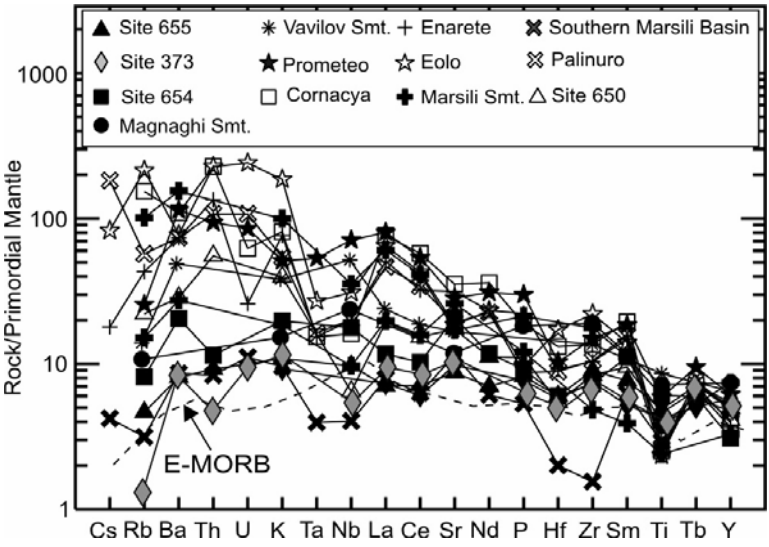

Fig. 9.12. Incompatible element patterns for selected Tyrrhenian Sea volcanoes.

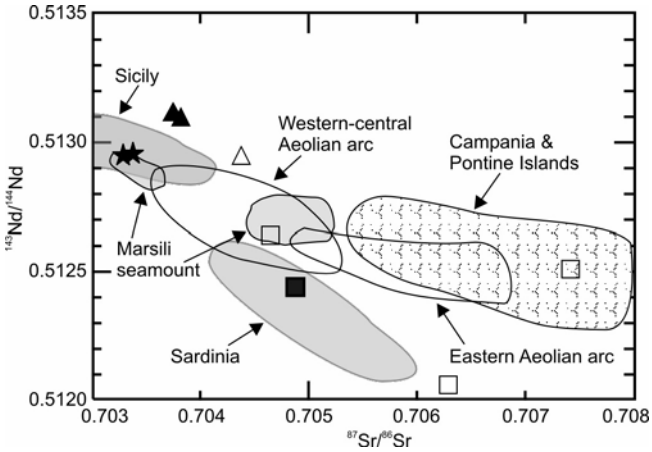

Fig. 9.13. Sr vs. Nd isotope diagrams for the Tyrrhenian Sea volcanics. Symbols as in Fig. 9.10.

It is undersaturated in silica and displays a hawaiitic composition, similar to the analogous rocks from Sardinia.

3. Magnaghi and Vavilov seamounts. Magnaghi (3.0 to 2.7 Ma) and Vavilov (Late Pliocene to 0.1 Ma) seamounts are two N-S elongated volcanoes. The few rocks recovered to date have a basaltic composition with moderate to high TiO_2 (1.9 to 3.2 wt %), variable Ni (about 30 to 180 ppm) and Cr (about 30 to 350 ppm; Selli et al. 1977; Beccaluva et al. 1982; Robin et al. 1987; Kastens et al. 1988, 1990; Savelli 1988). Incompatible elements are moderately enriched and mantle-normalised patterns show a small upward convexity, a moderate spike of Nb, and no LILE spikes or HFSE depletion (Fig. 9.12).

4. Aceste seamount and Quirra. The Aceste seamount and the volcanic rocks collected near Quirra seamount are Pliocene in age and show Na-alkaline affinity. Aceste has a composition ranging from hawaiite to trachyte (Beccaluva et al. 1984). These rocks are slightly porphyritic to microgranular, with microphenocrysts of plagioclase and clinopyroxene in the mafic rocks and sanidine in the trachytes. The groundmass consists of the same phases plus opaques, glass and secondary phases such as clay minerals. Alkali-olivine basalts have been found south of the Quirra seamount (Colantoni et al. 1981).

5. Prometeo. This lava field site is located southeast of Island of Ustica. The recovered lavas have mafic to intermediate Na-alkaline composition, close to the equivalent rocks from Ustica.

9.3.4. Arc-type Rocks

Rocks displaying an arc affinity with high LILE/HFSE ratios are widespread in the southern Tyrrhenian Sea. According to several authors (e.g. Savelli 1988; Locardi 1993; Argnani and Savelli 1999), these volcanic centres are arranged along arcuate structures becoming younger from west to east. One of these arcs (Central Tyrrhenian Arc; Argnani and Savelli 1999) has a Pliocene age (5 to 2 Ma) and runs from the Anchise seamount in the south to Ponza island in the north, and includes the Glauco and Ventotene-south seamounts and the buried calc-alkaline rocks of the Campanian Plain (Argnani and Savelli 1999). According to this view, the rhyolitic phase of magmatism occurred from about 4 to 3 Ma on the Island of Ponza would represent the northern end of the Pliocene Central Tyrrhenian Arc. K_2O vs. SiO_2 diagram for arc-type rocks is reported in Fig. 9.14.

1. Cornacya Seamount. This seamount recently was discovered, named and studied by Mascle et al. (2001). It is an about 12 Ma old volcano located SE of the southern Sardinian coast. Samples from Cornacya consist of strongly altered lavas that contain enclaves of mica-rich lamprophyres. The lavas have varied porphyritic textures with ubiquitous phenocrysts of zoned plagioclase and biotite plus some amphibole and clinopyroxene that are surrounded by a glass-rich matrix containing minor Na-rich plagioclase, anorthoclase, biotite and secondary products. Accessory minerals include Fe-Ti oxides, apatite and zircon. The lamprophyric enclaves are por-

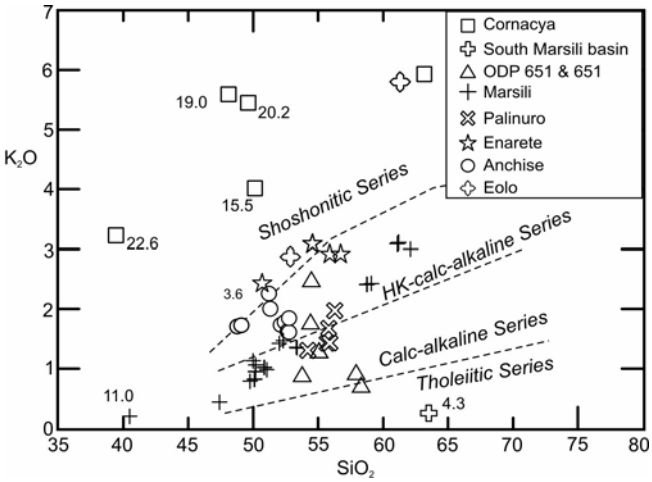

Fig. 9.14. K_2O vs. SiO_2 diagram for submarine arc-type volcanics from the Tyrrhenian Sea. Compositions have been recalculated on a water-free basis. Numbers refer to the highest measured LOI values.

phyritic with phenocrysts of altered olivine, amphibole and phlogopite that are set in a fine-grained groundmass of the same phases plus plagioclase. All the Cornacya samples have high to extreme LOI (up to about 23 wt %), which indicates severe secondary alteration. Nevertheless, mineral chemical data and immobile element distributions indicate a shoshonitic to ultrapotassic lamproitic affinity for lavas and enclaves, respectively. These rocks have fractionated REE patterns (not shown) generally with a small negative Eu anomaly. Patterns of primordial mantle normalised incompatible elements show strong fractionation, positive spikes of Th, U and Pb and negative anomalies of Ba, Sr, Ti and HFSE (Fig. 9.12). The Cornacya rocks resemble lamproites and shoshonites from Tuscany (see Chapter 2). Sr- and Nd-isotope ratios are variable ($^{87}Sr/^{86}Sr$ = 0.70465 to 0.70742; $^{143}Nd/^{144}Nd$ = 0.51206 to 0.51265; Fig. 9.13), with the lamprophyric enclaves showing the most primitive compositions.

2. Anchise seamount. This volcano is a W-E elongated irregular cone situated west of Ustica island. It consists of several coalescing eruptive centres, which reach a minimum depth of 532 m below sea level. K/Ar ages on whole rocks have yielded values of 5.2 to 3.6 Ma (Savelli 1988). Lavas from Anchise have a vesicular porphyritic texture, with phenocrysts of plagioclase, clinopyroxene and minor olivine set in a groundmass of the same phases plus Fe-Ti oxides, sanidine and minor biotite and glass. Secondary phases include calcite, Fe-hydroxides and clay minerals (Calanchi et al. 1984). Major element data indicate mafic high-K calc-alkaline to shoshonitic compositions on the K_2O vs. SiO_2 classification diagram of Peccerillo and Taylor (1976; Fig. 9.14). Mantle-normalised trace element pattern (not sown) exhibits enrichment in Rb and depletion in Ti, Nb and Zr.

3. ODP 651 Site. Drilling in the northern Vavilov basin revealed the occurrence of two thick basaltic lava series separated by a doleritic sill and sediments. Serpentinised peridotites were found beneath the lava units (Bonatti et al. 1990). The igneous sequence is covered by Pliocene-Pleistocene sediments. $^{40}Ar/^{39}Ar$ dating on three basalt samples indicates an age of approximately 3.0 to 2.6 Ma (Feraud 1990). Volcanic rocks have a microcrystalline to moderately porphyritic texture with microphenocrysts of strongly altered olivine (Fo_{89-81}), zoned plagioclase (An_{72-50}) and augite to salite clinopyroxene and some biotite set in a groundmass containing clinopyroxene, opaque minerals and glass (Bertrand et al. 1990). Clay minerals, zeolites, Fe-hydroxides and carbonates are common secondary phases. Chlorite, talc and minor actinolite have been observed in some basalts, indicating low-grade metamorphism for these rocks (Beccaluva et al. 1990). Data on the least altered samples indicate the occurrence of two types of magmas with different alkali contents, progressively decreasing

from the older to younger flows. Incompatible element patterns for both groups (not shown) resemble the calc-alkaline and high-K calc-alkaline rocks from Stromboli. Isotopic compositions are variable, with $^{87}Sr/^{86}Sr \sim 0.7044$ to 0.7073; $^{143}Nd/^{144}Nd \sim 0.5129$; $^{176}Hf/^{177}Hf \sim 0.28297$ to 0.28307; $^{206}Pb/^{204}Pb \sim 18.83$ to 18.92; $^{207}Pb/^{204}Pb \sim 15.64$ to 17.78; $^{208}Pb/^{204}Pb \sim 38.97$ to 39.18 (Beccaluva et al. 1990; Gasperini et al. 2002).

4. ODP 650 Site. This site in the Marsili basin is characterised by the occurrence of basaltic rocks beneath an approximately 600 m thick pile of sediments. Magnetostratigraphic and biostratigraphic age for the base of sedimentary pile is 1.9 to 1.7 Ma. Recovered volcanic rocks are vesicular altered basalts, displaying a texture that is characterised by a network of skeletal plagioclase and altered olivine and some clinopyroxene surrounded by an altered glass mesostasis. Petrogenetic affinity of these rocks is hampered by severe alteration. However, a composition not far from some Stromboli calc-alkaline basaltic andesites has been suggested by Beccaluva et al. (1990) on the basis of incompatible element ratios.

5. Central Tyrrhenian arc. Very little information is available on these volcanoes, except for Anchise (see previous paragraphs), the buried andesitic rocks of the Campanian plain (Parete-2 well) and Ponza rhyolites (see Chap. 6).

6. Marsili and Aeolian seamounts. Several seamounts with an arc-type composition occur in the area of the Aeolian arc, mostly situated around the Marsili basin (see Chap. 7, Fig. 7.1). Data on dredged and cored samples (Beccaluva et al. 1985b; Trua et al. 2002; 2004 and references therein) indicate ages from 1.3 to less than 0.1 Ma. The oldest rocks are observed at Sisifo (1.3 to 0.9 Ma), whereas the samples from Eolo (0.85 to 0.66 Ma), Enarete (0.78 to 0.67 Ma), Palinuro (0.35 Ma) and submarine Stromboli (0.53 to 0.18 Ma) are younger. Compositions are mostly calc-alkaline to shoshonitic, with a few arc tholeiitic basalts present at Lametini and along the southern margin of the Marsili basin. Calc-alkaline and high-potassium calc-alkaline (HKCA) rocks are present at Sisifo, Eolo, Palinuro and Alcione seamounts, and along the slopes of Panarea and Stromboli volcanoes. Shoshonitic rocks were found at Enarete, Eolo, Sisifo, and on the northern slope of Stromboli. Rocks recovered from the Marsili seamount have a wide compositional variation from basalt to HKCA andesites. Basalts display variable enrichment in incompatible elements, LILE/HFSE and radiogenic isotope ratios, suggesting the occurrence of different types of primary magmas (Trua et al. 2002, 2004 and references therein). Overall, textural and compositional features of rocks from the Aeolian seamounts are not very different from equivalent rock types of the Aeolian islands, although arc tholeiites have not been found in the emergent volcanoes, with the possible exception of Lipari. Textures are generally

porphyritic, with phenocrysts of plagioclase, clinopyroxene, and Ti-Fe oxides set in a matrix of the same phases plus some glass. Olivine is present in the mafic rocks at Marsili, Eolo, Palinuro and along the southern margin of the Marsili basin. Orthopyroxene appears in intermediate calc-alkaline, HKCA and shoshonitic rocks, whereas biotite and hornblende generally occur in the evolved rocks (Trua et al. 2004). Incompatible trace elements display variable concentrations, with an increase from tholeiitic to shoshonitic rocks. Incompatible element patterns are fractionated, contain negative anomalies of HFSE, and closely resemble the emergent rocks. Available Sr- and Nd-isotope ratios (Marsili seamount) exhibit a wide range in values ($^{87}Sr/^{86}Sr$ ~ 0.7032 to 0.7052; $^{143}Nd/^{144}Nd$ ~ 0.5127 to 0.5129; Trua et al. 2004; Fig. 9.13). Although a reliable picture of the submarine volcanism in the Aeolian area cannot be drawn from the available data, it seems that the distribution of rock types does not follow the pattern defined by the exposed activity. The western seamounts contain both calc-alkaline and shoshonitic rocks, the latter being absent in the western Aeolian islands. By contrast, the only dredged tholeiitic basalt comes from Lametini, located in the east where the emergent volcanoes are dominated by potassium-rich compositions.

9.3.5. Petrogenesis

The occurrence of MORB, OIB and arc-type volcanic rocks in the southern Tyrrhenian Sea is interpreted as an evidence for variable composition for their mantle source. MORB-type rocks display the lowest incompatible element concentrations. Their genesis can be included within the problem of the origin of oceanic ridge basalts world-wide. Presnall et al. (2002) suggest a generation for MORB magmas at the transition between the plagioclase- to the spinel-lherzolite stability fields. This indicates a depth of about 30 to 35 km, although some contribution by small fractions of melts coming from the deeper mantle has been envisaged. Seismic data beneath the Tyrrhenian Sea basin indicate the occurrence of a body with relatively low S-wave velocities, ranging from about 4.15 km/sec to around 3.0 km/sec in the depth interval between 70 km to the Moho (Panza et al. 2003, 2004). This agrees with the hypothesis of an increasing degree of mantle melting with decreasing depth, although the layer with S-wave velocity of 3.15 to 2.9 km/sec beneath the Moho of the Vavilov basins probably represents a zone of magma accumulation rather than a main site of partial melting (Panza et al. 2004).

The OIB-type rocks have variable isotopic and trace element characteristics, which appear to be related to different processes and/or sources.

Some rocks from the central Tyrrhenian basin have isotopic signatures and incompatible trace element ratios that are very similar to associated MORB-type rocks, but exhibit higher concentrations of incompatible elements. This indicates a genesis by lower degrees of partial melting of the same source that generated the tholeiitic basalts. Other OIB-type rocks from the western Tyrrhenian Sea floor (Quirra, Etruschi and ODP Site 654) have compositions, and most likely a genesis, similar to the alkaline volcanic rocks of the Plio-Quaternary cycle of Sardinia. Finally, the Na-alkaline rocks from the southern Tyrrhenian Sea (Prometeo and Ustica) have compositions which closely resemble the Etna lavas. These have HIMU-like geochemical and radiogenic isotopic signatures, with a small depletion in some HFSE (e.g. TiO_2), which have been interpreted as suggestive of a genesis in an HIMU-type source, with some contamination by subduction components (e.g. Beccaluva et al. 1982; Cinque et al. 1998; Schiano et al. 2001; Marani and Trua 2002; Trua et al. 2003; see Chap. 8).

The variable compositions of arc-type volcanics also indicate different types of mantle sources. The 12 Ma Cornacya volcanics and enclosed lamprophiric xenoliths resemble the shoshonitic and lamproitic rocks from the Tuscany Province (Mascle et al. 2001). It has been postulated that these derive from lithospheric mantle sources that had been affected by contamination of upper crustal material during the Alpine subduction processes and successively melted during the opening of the Tyrrhenian Sea basin (see Chap. 2). The similar compositions of the Cornacya rocks and Tuscany lamproites suggest a common origin and lead to the conclusion that the contaminated lithosphere occurring in Tuscany extends southward to zones offshore the coast of western Sardinian. The other arc-type rocks range from calc-alkaline to shoshonitic in character. These magmas may be the products of melting of various types of mantle rocks, which had been contaminated by fluids or melts of subduction origin. The ratios of some incompatible elements, which are not modified by subduction processes (e.g. Zr/Nb; Pearce and Parkinson 1993; Pearce and Peate 1995), have been used to infer the composition of arc-type mantle sources prior to metasomatism by subduction-related components**.** Trua et al. (2004) found that the great majority of arc-type rocks in the southern Tyrrhenian Sea plot within the MORB array in the Zr/Yb vs. Nb/Yb diagram, suggesting a derivation from sources which had a transitional-type MORB pre-metasomatic composition. As previously noted, however, some volcanics resemble those at Stromboli, which may imply interaction between OIB- and arc-type components (e.g. Ellam et al. 1988; see Chap. 7).

9.4. Geodynamic Setting

The Cenozoic-Quaternary volcanism in the southern Tyrrhenian Sea area is characterised by the coexistence of intraplate and arc-type compositions. The latter is older in the west (Oligo-Miocene activity in Sardinia) and becomes progressively younger toward the east-southeast, up to the presently active Aeolian arc. The Oligo-Miocene volcanism in Sardinia is mostly calc-alkaline in composition but contains a few arc-tholeiites. Calc-alkaline, shoshonitic to potassic rocks represent the bulk of the exposed arc-type Plio-Quaternary activity in the south-eastern Tyrrhenian Sea. Therefore, there is an increase in potassium contents of lavas with time and from west to east for arc-type rocks, which becomes much more striking if the magmatism from central-southern Italy is also considered. Intraplate tholeiitic to alkaline volcanics in Sardinia are much younger than arc-type rocks from the same area, whereas age relations in the Tyrrhenian Sea basin are less clear. Na-alkaline volcanics are younger than arc-type rocks at Ustica and Anchise whereas a decrease in alkali content with time has been detected at ODP Site 651.

Most authors agree that the compositional and temporal variation of magmatism through the Tyrrhenian Sea basin is better explained by a process of eastward and south-eastward discontinuous migration of the Ionian-Adriatic subducting plates from Oligo-Miocene time to the Present, accompanied by asymmetric back-arc spreading, anticlockwise rotation of the Apennine chain and a passive ascent and melting of the asthenospheric mantle during several discrete rifting episodes (Fig. 9.15; see Beccaluva et al. 1989; Sartori 2001, 2003; Doglioni et al. 2004). According to this hypothesis, Oligo-Miocene subduction of an oceanic-type crust beneath the Sardinia block generated arc-tholeiitic to calc-alkaline magmatism in the island and back-arc spreading in the Balearic-Provençal basin, concomitant with the detachment of the Sardinia-Corsica block from the southern European margin. Successively, slab rollback caused an eastward migration of the compression front, followed by back-arc extension and orogenic magmatism migrating in the same direction. Therefore, arc-type volcanic rocks with a decreasing age from the central to the eastern and south-eastern Tyrrhenian Sea were formed. Back-arc spreading migrated from west to east from the Miocene until the late Pliocene time. Starting from the end of the Pliocene, however, there was a rapid change in stretching direction which became NW-SE and caused the opening of the Marsili basin (e.g. Sartori 2003). This change in the direction of back-arc extension has

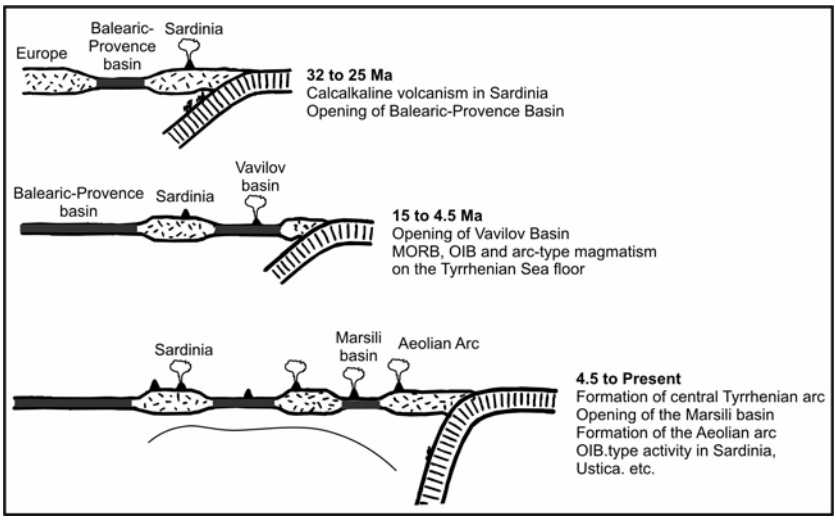

Fig. 9.15. Schematic evolution of the Tyrrhenian Sea and Sardinia from Oligocene to present (simplified after Argnani and Savelli 1999). See text for explanation.

been related to the different resistance opposed to slab retreat by the Adriatic and Ionian plates, which had variable thickness and compositions (i.e. continental and oceanic). The increase in potassium content for arc-type magmas from the Oligo-Miocene to the Present could be related to modifications in the nature of the undergoing slab, which involved an increasing amount of upper crustal material during its eastward shifting. According to this hypothesis, the wide variety of anorogenic magma types in the Tyrrhenian Sea and Sardinia is the result of decompression melting of passively uprising asthenospheric, and/or of mantle material suctioned from the African plate during back-arc extension (e.g. Trua et al. 2002). According to some authors, the lithospheric mantle also participated in the melting and contributed significantly to both arc-type and anorogenic magmatism. For instance, the Cornacya volcano could represent arc-type melts coming from a lithosphere that had been contaminated during the Alpine subduction (Mascle et al. 2001). The processes responsible for migration of subduction zones and related events remain a matter of debate. Some authors suggest passive sinking of the lithosphere and slab rollback (e.g. Kastens and Mascle 1990), whereas others emphasise the role of global eastward flux of the asthenospheric mantle (Doglioni et al. 2004), or lateral expulsion of lithospheric blocks between colliding major continents (e.g. Mantovani et al. 1997).

Alternative hypotheses about the geodynamic evolution of the Tyrrhenian basin advocate convective movements of the modified upper mantle

material or an active upwelling of deep-mantle plumes. Locardi and Nicolich (1988) and Locardi (1993) suggested that both the orogenic and anorogenic magmatism in the Tyrrhenian region is the result of uprising and melting of a large body of mantle material, which had been softened by fluids of deep origin. Bell et al. (2004) advocate the ascent of a large and heterogeneous mantle plume at 400 to 670 km beneath the Tyrrhenian Sea. Its emplacement generated basin opening and the wide variety of magmas in the entire area. Finally, Gasperini et al. (2002) hypothesised that, although subduction was a main geodynamic process, the active upwelling of a mantle plume ascending through a window generated by slab break-off provided an important contribution to Tyrrhenian Sea magmatism. However, a role for active mantle upraise has been questioned based, among others, on both the scarcity of volcanism on the Tyrrhenian Sea floor and on the very sharp subsidence of the Tyrrhenian basin, which has reached a depth of more than 3600 meters in a time interval of a few million years (Peccerillo and Lustrino 2005; see Chap. 10 for further discussion).

9.5. Conclusions

A wide variety of magmatic activity affected the Sardinia island and the Tyrrhenian Sea from Oligocene to Quaternary times. Oligocene-Miocene (32-15 Ma) volcanism in Sardinia produced arc-tholeiitic to calc-alkaline rocks. Orogenic magmatism successively shifted towards the eastern and south-eastern Tyrrhenian Sea, parallel to the opening of the Tyrrhenian basin, the eastward shifting of the compression front and the anticlockwise rotation of the Apennine chain. The opening of the southern Tyrrhenian basin was also accompanied by MORB- to OIB-type magmatism. Extensive anorogenic Pliocene to Quaternary tholeiitic to alkaline volcanism also occurred in Sardinia (~ 5 to 0.1 Ma).

Geochemical and radiogenic isotopic data for the Plio-Quaternary volcanic rocks from Sardinia and the Tyrrhenian Sea suggest a derivation from various types of mantle sources. One composition, best represented by the Ustica and Prometeo rocks, is close to the HIMU-like mantle component. The Plio-Quaternary centres of Guspini, Rio Girone and Capo Ferrato in southern Sardinia have affinities with this group. Another OIB-type composition is represented by the bulk of the Plio-Pleistocene volcanism from central-northern Sardinia. These rocks, which find no counterparts in the entire circum-Mediterranean Cenozoic-Quaternary magmatism, have unradiogenic Pb and Nd and moderately radiogenic Sr isotopic ratios, re-

sembling the EM1 mantle composition. Other rocks from the Vavilov basin are depleted in incompatible elements and were generated in a MORB-type source. Finally, several rocks have island-arc geochemical signatures, which can be related to the addition of different types of subduction components to mantle sources mostly with a MORB-type composition.

The reasons for this upper mantle heterogeneity in the Tyrrhenian Sea and Sardinia are debated. Most authors agree that the age and compositional characteristics of arc-type magmatism are related to an eastward and south-eastward migration of the Adriatic-Ionian subduction zones taking place from the Oligocene to the Present. The Tyrrhenian Sea would represent a back-arc basin where passive ascent of the asthenospheric mantle triggered partial melting and generation of MORB- and OIB-type magmas. Other views propose a role of actively uprising mantle plumes that would be responsible for at least the OIB-type rocks in the Tyrrhenian basin and surrounding areas.

Table 9.3. Representative compositions of Sardinia Plio-Quaternary rocks. Source of data: 1) Beccaluva et al. (1973); 2) Cioni et al. (1982); 3) Montanini et al. (1994); 4) Gasperini et al. (2000); 5) Lustrino et al. (2000); 6) Lustrino et al. (2002); 7) Author's unpublished data.

Volcanic centre	**Monte Arci**		**Capo Ferrato**	**Rio Girone**	**Logudoro**	**Montiferro**		**Orosei-Dorgali**	
Rock type	Andesite	Rhyolite	Trachy-andesite	Basanite	Hawaiite	Hawaiite	Tephri-phono-lite	Alkali basalt	Ande-site
Data source	2	3	5	5	4	4	1,7	6	6
SiO_2 wt%	60.49	70.40	60.34	45.80	48.52	50.13	57.67	47.60	52.22
TiO_2	1.16	0.29	0.87	3.13	2.31	3.18	1.03	1.75	1.84
Al_2O_3	15.27	14.20	16.51	15.20	16.19	14.62	20.08	15.53	16.69
$FeO_{totaò}$	6.16	1.73	6.56	10.53	10.16	11.5	3.66	9.38	11.00
MnO	0.11	0.03	0.12	0.16	0.14	0.14	0.13	0.14	0.14
MgO	4.36	0.33	1.24	7.55	7.82	4.85	0.95	10.82	3.56
CaO	4.66	0.88	3.35	10.40	7.30	8.49	3.01	8.42	8.69
Na_2O	3.82	3.64	4.72	3.49	3.24	4.32	5.94	3.58	3.39
K_2O	1.93	5.28	4.15	2.23	2.40	1.61	5.48	0.81	1.30
P_2O_5	0.14	0.13	0.36	0.39	0.55	1.11	0.26	0.38	0.30
LOI	1.77	2.98	2.18	1.22	1.41	-	1.89	1.59	1.46
Sc ppm	10	4	-	20	-	19	3.8	-	-
V	-	11	29	254	165	238	-	192	165
Cr	146	3	1	212	195	54	6	427	279
Co	27	-	-	44.3	44	-	3.3	51.7	39
Ni	83	5	6	126	125	52	4	298	168
Rb	71	204	99	49	52	67	51	21.2	21
Sr	386	105	321	970	870	1561	1305	690	536
Y	-	26	46	28	17	19	33	17. -	18
Zr	122	225	508	223	242	728	565	159	134
Nb	-	26	74	70	51	107	110	31.2	20
Cs	1.7	-	-	1.55	0.71	-	-	0.82	0.53
Ba	357	669	1022	528	1037	1537	629	648	507
La	26	43.9	67	47	46	110	114	27	20
Ce	47	87.6	130	96	87	216	244	52	39
Pr	-	-	15	12.1	9.96	23.3	-	6.16	4.71
Nd	-	35.5	58	47	40	86	96	25.2	20
Sm	-	7.23	10.7	8.27	8.1	13.6	12.4	4.87	4
Eu	1.5	1.01	2.81	2.53	2.44	4.11	3.8	1.63	1.57
Tb	0.63	-	1.43	1.01	0.79	1.35	1.10	0.60	0.6
Yb	-	1.63	3.97	1.97	1.36	2.51	2.8	1.16	1.36
Lu	-	-	0.61	0.3	0.21	0.36	0.37	0.18	0.22
Hf	3.4	-	11.8	4.8	5.32	15.5	12.9	3.46	3.31
Ta	0.81	-	-	4.51	3.57	7.7	8.2	2.10	1.4
Pb	-	22	11.8	4	4.9	18.1	-	3. 0	4
Th	7.9	25	14.9	5.9	7.55	13.5	12.3	3.4	2.9
U	1.9	-	3.5	1.3	1.25	3.4	-	0.79	0.64
$^{87}Sr/^{86}Sr$	0.70534	0.7097	0.70487	0.70401	0.70423	0.70435	-	0.70442	0.70453
$^{143}Nd/^{144}Nd$	(0.51235)	0.51228	0.51271	0.51285	0.51251	0.512561	-	0.51257	0.51253
$^{206}Pb/^{204}Pb$	-	-	18.840	19.23	17.757	17.638	-	17.860	17.738
$^{207}Pb/^{204}Pb$	-	-	15.657	15.64	15.601	15.569	-	15.596	15.531
$^{208}Pb/^{204}Pb$	-	-	38.977	39.1	37.917	37.923	-	37.942	37.894
$^{176}Hf/^{177}Hf$	-	-	-	-	-	-	-	0.28268	-

Table 9.4. Representative compositions of Tyrrhenian Sea volcanic rocks. Source of data: 1) Dietrich et al. (1977); 2) Beccaluva et al. (1982 and references therein); 3) Calanchi et al. (1984); 4) Beccaluva et al. (1990); 5) Mascle et al. (2001); 6) Gasperini et al. (2002); 7) Trua et al. (2002); 8) Trua et al. (2003); 9) Trua et al. (2004).

Volcanic centre	**ODP-655**	**DSDP-373**	**Magnaghi Seamount**	**Vavilov Seamount**	**Prometeo**	**Cornacya**
Rock type	MORB-type basalt	MORB-type basalt	OIB-type basalt	OIB-type basalt	Mugearite	Lamproite
Data source	4, 6	1	2	2	8	5
SiO_2 wt%	50.43	48.00	48.57	45.73	51.37	39.34
TiO_2	1.24	0.92	1.94	2.26	1.53	0.30
Al_2O_3	16.34	18.30	19.60	15.51	17.08	17.91
FeO_{total}	8.19	7.32	9.81	10.85	8.50	2.08
MnO	0.13	0.10	0.16	0.17	0.16	-
MgO	7.33	7.66	3.29	8.65	5.28	10.15
CaO	9.83	10.3	10.58	11.86	8.23	0.98
Na_2O	3.40	3.16	3.29	2.23	4.84	4.08
K_2O	0.33	0.33	0.49	0.36	1.44	4.32
P_2O_5	0.17	0.12	0.40	0.25	0.64	0.11
LOI	1.70	3.39	1.34	1.81	0.34	20.24
Sc ppm	28	29	-	-	16	2.3
V	203	-	236	321	161	13
Cr	222	227	79	357	151	1.1
Co	32	30	-	-	-	-
Ni	101	-	30	184	87	67
Rb	3.3	1	10	9	22.8	188
Sr	180	232	295	311	655	156
Y	22	23	39	24	29.5	11
Zr	88	77	228	139	157	237
Nb	6	3.1	-	-	42	19
Ba	45	59	-	-	787	554
La	5.5	6.3	-	-	55	41
Ce	14	15	-	-	98	92
Nd	9.8	-	-	-	39	26
Sm	3.05	1.9	-	-	7.2	3.8
Eu	1.05	0.9	-	-	2.26	0.65
Tb	0.56	0.63	-	-	0.91	0.38
Yb	2.37	2.2	-	-	2.64	1.36
Lu	0.36	0.29	-	-	0.38	0.18
Hf	2.25	1.6	-	-	3.5	6.47
Ta	0.32	-	-	-	2.23	1.51
Pb	1.6	2.2	-	-	4.3	31
Th	0.75	0.42	-	-	8.3	25
U	0.2	0.24	-	-	1.9	7.8
$^{87}Sr/^{86}Sr$	0.70375	-	-	-	0.70327	0.70742
$^{143}Nd/^{144}Nd$	0.51311	-	-	-	0.51294	0.51251
$^{206}Pb/^{204}Pb$	18.698	-	-	-	-	-
$^{207}Pb/^{204}Pb$	15.573	-	-	-	-	-
$^{208}Pb/^{204}Pb$	38.666	-	-	-	-	-
$^{176}Hf/^{177}Hf$	0.28317	-	-	-	-	-

Table 9.4 (continued)

Volcanic centre	Enarete	Eolo	Palinuro	Marsili Seamount	ODP-651	Anchise
Rock type	Shoshonitic basalt	Latite	Andesite	Calc-alkaline basalt	Calc-alkaline basalt	Andesi-te
Data source	9	9	9	7	6,4	3
SiO_2 wt%	48.48	59.62	54.83	49.20	52.75	51.50
TiO_2	0.74	0.60	0.67	1.19	1.32	1.28
Al_2O_3	19.98	18.92	15.55	17.50	15.39	17.52
FeO_{total}	7.80	4.56	7.32	8.46	7.68	7.78
MnO	0.13	0.03	0.15	0.14	0.12	0.11
MgO	4.31	0.93	6.15	7.35	7.10	4.12
CaO	8.76	2.82	9.64	9.91	7.06	9.93
Na_2O	2.66	3.92	2.12	3.50	3.56	3.30
K_2O	2.32	5.64	1.64	0.76	1.68	1.80
P_2O_5	0.46	0.20	0.18	0.20	0.20	0.29
LOI	3.57	2.48	1.19	0.65	2.29	1.69
Sc ppm	25	14	34	-	-	-
V	253	149	228	184	209	-
Cr	69	3.3	126	214	173	-
Co	-	-	-	37	35	-
Ni	34	5.7	33	118	125	-
Rb	37	184	49	14	18	40
Sr	723	425	444	354	225	457
Y	17.9	25.2	23.5	20	23	30
Zr	114	242	116	94	84	119
Nb	12.4	19.2	12.5	7	5.1	17
Cs	0.34	1.57	3.46	-	1.0	-
Ba	556	584	558	198	131	-
La	36	46	33	13	8.6	-
Ce	61	81	65	27	18.9	-
Nd	30	30	29		12.1	-
Sm	5.7	5.4	6	-	2.9	-
Eu	1.68	1.44	1.34	-	1.05	-
Tb	0.65	0.7	0.76	-	0.57	-
Yb	1.77	2.84	2.06	-	2.20	-
Lu	0.25	0.41	0.3	-	0.33	-
Hf	3.2	6	3.1	-	2.1	-
Ta	0.66	1.16	0.7	-	0.41	-
Pb	14.8	47	12.1	-	2.7	-
Th	12.9	21.8	10.3	-	1.76	-
U	0.7	6.5	2.9	-	0.56	-
$^{87}Sr/^{86}Sr$	-	-	-	-	0.70438	-
$^{143}Nd/^{144}Nd$	-	-	-	-	0.51294	-
$^{206}Pb/^{204}Pb$	-	-	-	-	18.834	-
$^{207}Pb/^{204}Pb$	-	-	-	-	15.644	-
$^{208}Pb/^{204}Pb$	-	-	-	-	38.967	-
$^{176}Hf/^{177}Hf$	-	-	-	-	0.28307	-

10. Petrogenesis and Geodynamics in Italy

10.1. Introduction

The geodynamic setting of the Tyrrhenian Sea and surrounding regions has been a matter of debate for decades, and there is still disagreement on the processes that generated first order structural features, such as the Tyrrhenian Sea and the Apennine chain (e.g. Boccaletti and Guazzone 1974; Boccaletti et al. 1971, 1984, 1990a,b; Lavecchia and Stoppa 1990; Mantovani et al. 1997; Cello and Mazzoli 1999; Doglioni et al. 1999; Lustrino 2000; Faccenna et al. 2004 and references therein). Consequently, the relationship between the complex Plio-Quaternary magmatism in the circum-Tyrrhenian area and the tectonic context of its generation and emplacement are still not well established.

The magmatic provinces discussed in the previous chapters exhibit exceedingly large compositional variations and almost entirely cover the compositional range of magmatic rocks occurring worldwide. Since magmatism reflects closely the characteristics of the mantle sources, the wide variety of magmas occurring around the Tyrrhenian Sea area reveals an extremely heterogeneous upper mantle. This is likely the result of a complex evolution history suffered by the Tyrrhenian Sea and Western Mediterranean during the least 300 Ma.

In this chapter, the main petrological, geochemical and structural characteristics of the individual magmatic provinces will be summarised, and the most widely accepted hypotheses on the geodynamic processes responsible for magmatism will be discussed.

10.2. Compositional and Structural Characteristics of Volcanism in Italy

The wealth of data on Plio-Quaternary magmatism in Italy highlight the existence of two broad groups. One shows geochemical characteristics typical of rocks emplaced along converging plate margins (i.e. high ratios of Large Ion Lithophile Elements -LILE- to High Field Strength Elements

-HFSE- and radiogenic isotope signatures intermediate between mantle and crust) and has been defined as "orogenic". The other group has compositions within the range of magmas emplaced in intraplate settings or along passive plate margins (i.e. low LILE/HFSE and isotopic ratios close to mantle values) and has been referred to as “anorogenic” or “intraplate”.

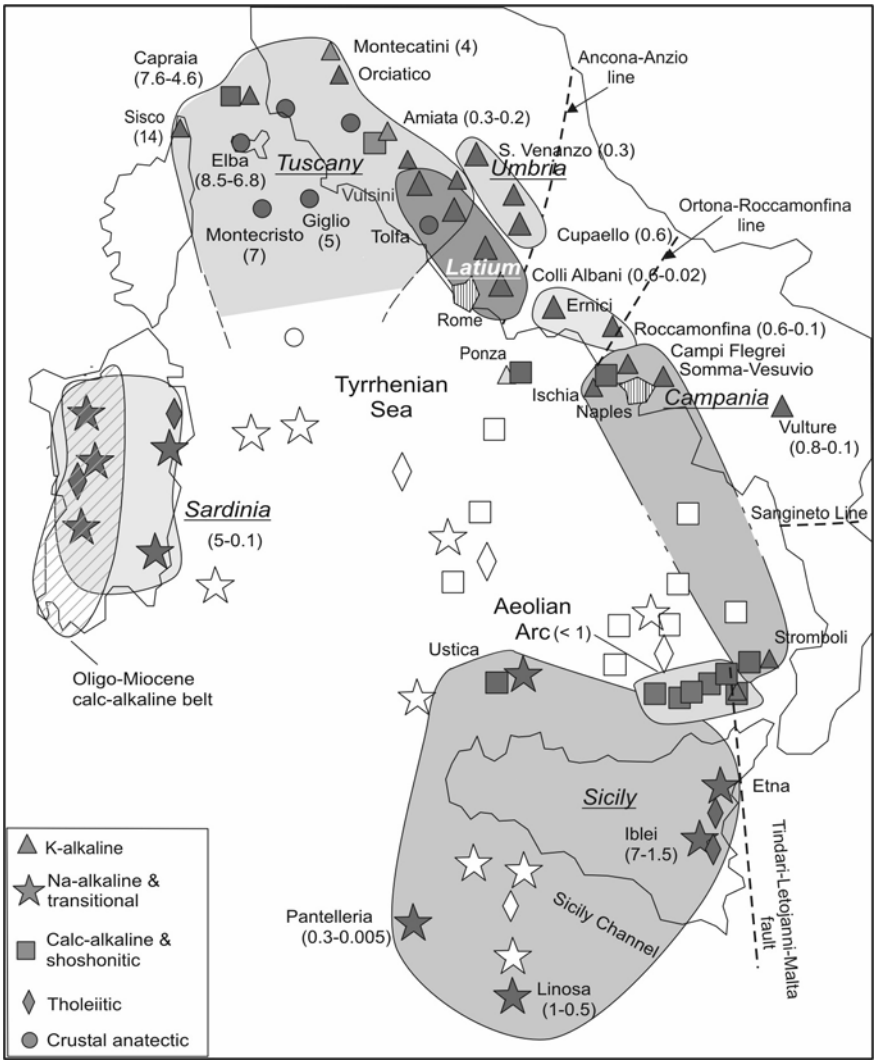

Fig. 10.1. Distribution of magmatic provinces in Italy. Open symbols indicate seamounts. Ages (in Ma) for some volcanoes are given in parentheses.

The rocks with orogenic geochemical signatures are found along the Italian peninsula and in the Aeolian arc, whereas magmas with anorogenic compositions occur in Sicily, in the Sicily Channel and in Sardinia. The volcanism located in the Tyrrhenian Sea basin is made up of both orogenic- and anorogenic-type rocks.

Detailed studies on major element, trace element and isotopic variations of mafic rocks have shown that the broad groups of orogenic and anorogenic magmas display strong internal compositional variations, and these have been interpreted as evidence for compositionally different mantle sources or/and different petrogenetic processes (e.g. Peccerillo 2002). Based on these studies, several distinct magmatic provinces have been recognised (Fig. 10.1). Some of these provinces are bounded by tectonic lines of lithospheric importance and are characterised by a distinct structure of the crust-upper mantle system (e.g. Moho depth, mechanical characteristics of the upper mantle, occurrence of deep or shallow seismicity, etc.; Peccerillo and Panza 1999; Peccerillo and Turco 2004). Therefore, geophysical evidence supports the subdivision into various provinces, which has been based on petrological and geochemical data. Moho depths, distribution of seismicity, and some of the most significant structural characteristics of the circum-Tyrrhenian area are shown in Fig. 10.2. Variation of S-wave velocities for the upper mantle beneath some volcanic areas is reported in Fig. 10.3.

The *Tuscany Magmatic Province* represents the northernmost sector of Italian Plio-Quaternary volcanism. It consists of an association of various types of mafic and felsic rocks, whose ages (14 to 0.1 Ma) decrease eastward from Corsica to the Tuscan archipelago and to the mainland of southern Tuscany. Mafic rocks range from calc-alkaline to potassic and ultrapotassic (lamproitic) and most of them have high Mg#, Ni and Cr contents that are within the compositional range of mantle-equilibrated magmas. Their incompatible trace element abundances (Th, U, K, Rb, LREE) are variable and increase from calc-alkaline rocks to lamproites. However, the incompatible trace element patterns of all mafic rocks (normalised to primitive mantle) show similar features, i.e. strong fractionation and negative anomalies of Ta, Nb, Hf, Zr, Ti, Sr and Ba. These patterns resemble closely those of some upper crustal rocks, such as granites, pelites and their metamorphic equivalents. Isotope signatures are closer to those of up-

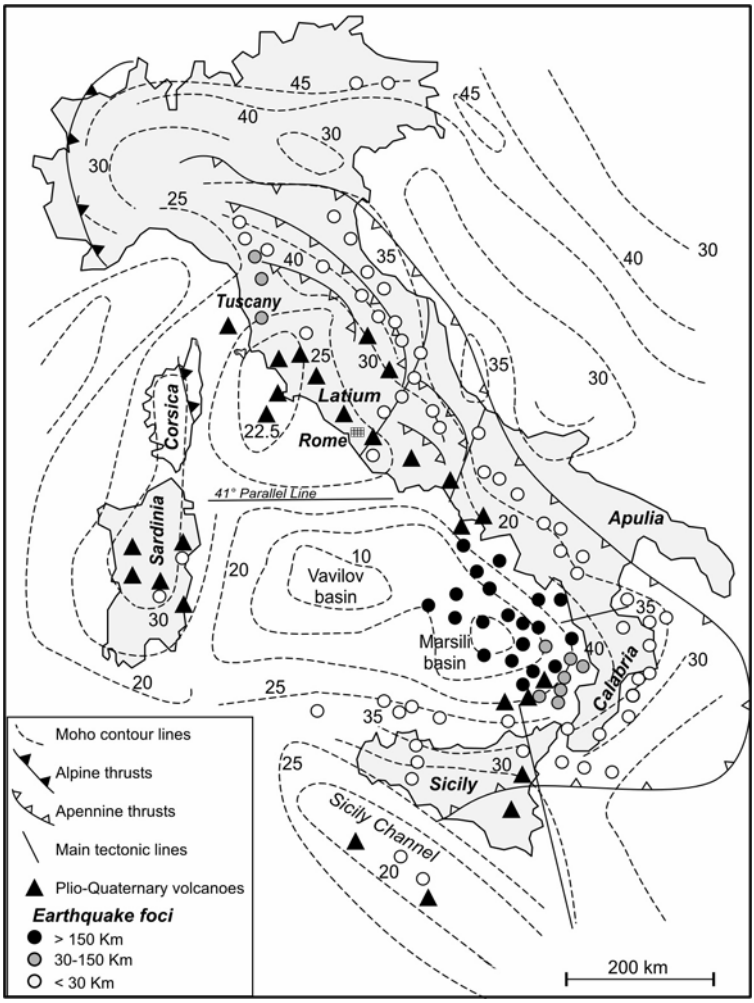

Fig. 10.2. Sketch map showing Moho depth, distribution of earthquakes hypocentres and main structural features in Italy. Simplified after Boccaletti et al. (1984) and Locardi and Nicolich (1988).

per crustal rocks than to mantle values (e.g. $^{87}Sr/^{86}Sr$ ~ 0.709-0.717; $^{143}Nd/^{144}Nd$ ~ 0.5121-0.5230). Overall these data have been interpreted as evidence that the mantle source of mafic magmatism in Tuscany was affected by bulk contamination of metapelites. A similar, though older, association of calc-alkaline to lamproitic rocks is found in the Western Alps (30 Ma) and in SE Spain (23-6 Ma). Felsic rocks in Tuscany include various types of granitoids (granodiorites, monzogranites, granites, leucograni-

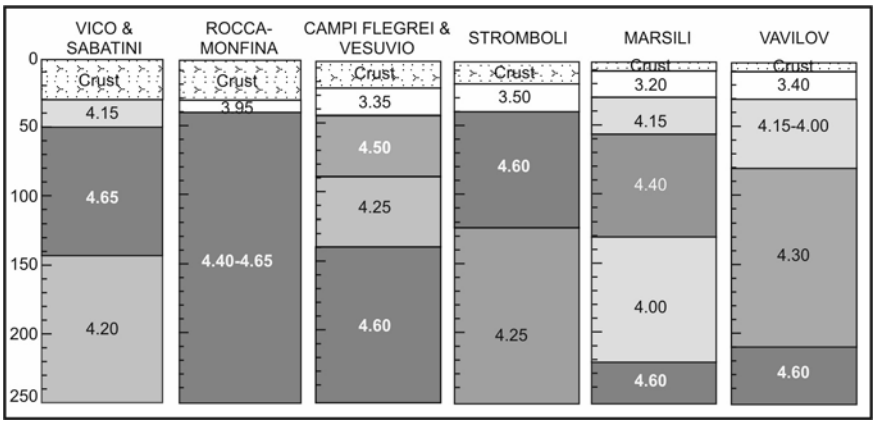

Fig. 10.3. Sketch of S-wave velocities (km/s) beneath some Italian volcanic areas. Simplified after Panza et al. (2003, 2004).

tes, etc.) and some lavas (rhyolites, rhyodacites, etc.); pyroclastic rocks are restricted to a few centres. Acid intrusive and effusive rocks have a crustal anatectic origin, and their genesis is likely related to an increase in temperature during mafic magma emplacement into the crust. However, pure crustal melts are rare, and most acid rocks are hybrids between crustal anatectic and mantle-derived magmas. In general terms, there is clear evidence of extensive mixing-mingling between various types of mafic magmas, and between these and silicic melts. The Tuscany Province developed in a zone of thinned continental crust and high regional heat flow (more than 100 mW/m^2 in southern Tuscany), with the Moho reaching a minimum depth of about 20-22 km. A seismic discontinuity (generally referred to as a second Moho) has been found at a depth of about 60 km and is believed to represent old subducted crust (Finetti et al. 2001). East of the volcanic province, beneath then Apennine chain, there is a vertical layer of rigid material (with an S-wave velocity of about 4.7 km/s, referred to as a lithospheric root). This body cuts the asthenosphere (S-wave velocity about 4.2 km/s) and has been interpreted as a relict slab from the Adriatic plate (e.g. Panza et al. 2003).

The *Roman Province* (0.8 to 0.02 Ma) consists of the large volcanic complexes and stratovolcanoes of Monti Vulsini, Vico, Monti Sabatini and Colli Albani (Alban Hills), which erupted about 900 km^3 of prevailingly pyroclastic material and minor lavas. Compositionally, the rocks belong to the Roman-type potassic series (KS) (nearly saturated trachybasalts, shoshonites, latites and trachytes) and high-potassium series (HKS) (undersaturated leucitites, leucite tephrites, phonotephrites, tephriphonolites and phonolites). Some melilite-bearing rocks also occur. The Roman volcanoes

are superimposed upon the Tuscany magmatic rocks in the north, and there is evidence of hybridisation between these two provinces (Conticelli and Peccerillo 1992). Volcanism has been prevailingly explosive, with phonolitic and trachytic pyroclastic rocks predominating over mafic lavas and scoriae. There is ample petrological and geochemical evidence that felsic magmas were generated predominantly by fractional crystallisation (some 50-60%) starting from the associated mafic lavas. This means that the amount of potassic mafic melts generated in the upper mantle beneath the Roman Province is enormous. The KS rocks have lower incompatible element concentrations than HKS, but radiogenic isotope ratios show similar ranges. They are intermediate between mantle and crust, although they are less similar to upper crust than the volcanic rocks from Tuscany (e.g. $^{87}Sr/^{86}Sr$ is typically around 0.709-0.711). The Roman mafic rocks also have incompatible trace element patterns that are similar to those of Tuscany rocks, but the former display higher LILE/HFSE ratios and distinct variation trends of incompatible trace element ratios. These characteristics have led to the suggestion that both Roman and Tuscany magmas were generated by melting of phlogopite-bearing sources that were enriched in incompatible elements by addition of upper crustal material. However, the nature of the crustal component added to the mantle differed in the two regions, being metapelitic in Tuscany and marly in the Roman Province. High LILE vs. HFSE contents in the Roman Province rocks probably mean that elemental fractionation occurred either during mantle contamination or during magma genesis. Low HFSE contents of Roman rocks have been interpreted to suggest a MORB-like composition for the mantle source prior to metasomatism (e.g. Serri 1990). The Roman Province developed in a zone of NW-SE trending normal faults cutting the allochthonous terranes of Tuscany and Umbria. Crustal thickness is around 25 km. Regional heat flow is high (up to 350 mW/m^2 beneath volcanic areas; Barberi et al. 1994a). The southern border is sharp and is marked by the so-called Ancona-Anzio line, a tectonic structure which is believed to cross the Italian peninsula in a NE-SW direction, dividing the northern Apennines from the Abruzzi-Latium sequences of central Apennines (Fig. 10.1, 10.2; Locardi 1988).

The *Intra-Apennine Province* consists of a few monogenetic centres that exhibit similar trace element and isotopic signatures to those from the Roman Province, suggesting a similar style of contamination of mantle sources. However, petrological characteristics are different, with the Intra-Apennine Province consisting only of rocks that have low Al_2O_3 and Na_2O combined with high CaO, K_2O/Na_2O and a strong degree of silica undersaturation, i.e. rocks of the kamafugitic ultrapotassic association. This has been interpreted as evidence that the Intra-Apennine magmas were gener-

ated from a mantle source with a different modal mineralogy and at a higher pressure than for the Roman Province. Some intra-Apennine pyroclastic rocks consist of a mixture of silicate and carbonate material, and have been suggested to represent carbonatitic magmas, an hypothesis which has been argued to conflict with many geochemical and isotopic data (Peccerillo 1998; 2004). The Intra-Apennine Province is characterised by rather thick crust (Moho at about 35-40 km) and lithosphere (e.g. Locardi and Nicolich 1988; Scarascia et al. 1994), by low heat flow and negative gravity anomalies. Extension is less intense than in the Roman Province and volcanic rocks are emplaced along faults bordering small subsiding basins. High-rigidity body cuts the asthenosphere reaching a depth of about 150 km beneath the Intra-Apennine Province (Panza et al. 2003).

The *Campania Province* is formed by Somma-Vesuvio, Campi Flegrei and Ischia-Procida volcanoes. Some of the Pontine Islands (Ventotene and the younger Ponza) may also belong to this province. Rock compositions mostly belong to KS and HKS. However, some mafic rocks with potassium contents falling in the field of calc-alkaline basalts are present as xenoliths and lavas at Procida and Ventotene. Moreover, Pliocene calc-alkaline lavas have been found in borehole cuttings a few km north of Campi Flegrei. All mafic rocks of the province have lower Sr and higher Nd and Pb isotopic ratios (e.g. $^{87}Sr/^{86}Sr \sim 0.706$-$0.707$) than rocks of the Tuscany and Roman provinces; some trace element ratios are also distinct. This has been interpreted as evidence of a distinct mantle source, with a distinct evolutionary history. By contrast, Campanian mafic rocks have several trace element and isotope ratios that resemble the rocks from Stromboli, in the eastern Aeolian arc. This has led to the suggestion that the Campanian volcanoes do not represent the southern end of the Roman Province but form a separate magmatic province, which probably includes the eastern Aeolian arc. Isotope compositions of Campanian volcanoes fall between upper mantle and crustal values, but are closer to mantle signatures than observed in the Roman and Tuscany provinces. Campanian volcanoes have higher HFSE concentrations and lower LILE/HFSE ratios than Roman and other Italian "orogenic" volcanoes, approaching intraplate compositions. Collectively, these features have been interpreted as evidence for an OIB-type pre-metasomatic mantle source (Beccaluva et al. 1991). Contamination of this source was provided by moderate amounts of subduction material, containing some sedimentary components. The Campania Province develops south of the so-called Ortona-Roccamonfina line, at the intersection between NW-SE and NE-SW trending faults. The area is characterised by high heath flow and by positive gravity anomalies. There is a thin low S-wave velocity layer (about $V_S = 3.3$ km/s) beneath

the Moho below Vesuvio and Campi Flegrei (Fig. 10.3), which becomes thicker beneath Ischia, where the Moho also becomes shallower.

The *Ernici-Roccamonfina Province* consists of the close association of KS and HKS rocks, with some lavas showing potassium concentrations falling in the field of calc-alkaline basalts. KS rocks have lower potassium, incompatible element contents and $^{87}Sr/^{86}Sr$ than HKS volcanics, and resemble very closely the KS rocks from the Campanian volcanoes. In contrast, HKS rocks have petrological, geochemical and isotopic signatures that resemble Roman HKS rocks. The coexistence of Roman- and Campanian-type rocks has led to the suggestion that the mantle source beneath the Ernici-Roccamonfina province includes both Roman-type and Campanian-type compositions (Peccerillo 2002). The Ernici-Roccamonfina Province occurs in an area affected by Plio-Quaternary extensional tectonics, with NW-SE normal faults and NE-SW transtensional faults. It is bounded by the Ancona-Anzio line in the north and by the Ortona-Roccamonfina line in the south. There is a very thin (about 10 km) low velocity layer (V_S = 3.95 km/s) beneath the Moho, which overlies a thick, high rigidity layer with an S-wave velocity of 4.65 km/s (Panza et al. 2003, 2004) continuing to more than 250 km depth. Tomographic images also suggest distinct mechanical characteristics for the upper mantle beneath Ernici-Roccamonfina area relative to the adjoining volcanic provinces (Lucente and Speranza 2001).

Mount Vulture shows several peculiar characteristics that make it unique among Italian volcanoes. Vulture rocks (mostly basanite and trachyphonolite with minor foidite, tephrite, phono-tephrite and melilitite) are rich in both Na_2O and K_2O, and contain haüyne as the main feldspathoid. Some pyroclastic rocks rich in carbonates have been suggested to represent carbonatitic magmas. Geochemical signatures are characterised by very high Th and Light Rare Earth Element contents. HFSE contents are also high, but LILE/HFSE ratios are still comparable to those of arc rocks. Patterns of incompatible elements are fractionated, and show negative spikes of HFSE as well as relative depletions in Rb and K. This latter feature is typical of some intraplate OIB-type alkaline rocks and is not unexpected, given the geodynamic position of this volcano which is situated east of the Apennine chain on the margin of the Apulia foreland. In contrast, the arc-type LILE/HFSE ratios represent a main problem for this volcano. The Moho is about 35 km deep beneath Mount Vulture and there is a thick, rigid layer with an S-wave velocity of 4.1-4.7 extending from near the Moho down to 160 km.

The *Aeolian arc* is formed by calc-alkaline, high-K calc-alkaline and shoshonitic rocks, with some slightly undersaturated potassic alkaline lavas similar to the KS rocks from central Italy. Three sectors have been

distinguished on the basis of volcanological, petrological and geochemical data. The western sector mainly contains island-arc-type mafic to intermediate calc-alkaline rocks with relatively unradiogenic Sr isotopic compositions ($^{87}Sr/^{86}Sr \sim 0.7035$ to 0.7045). The central islands (Vulcano and Lipari) are large stratovolcanoes with calderas, developed along the Tindari-Letojanni-Malta strike-slip fault. Rocks display similar isotopic signatures to some of the western volcanoes, but petrochemical affinity of rocks ranges from calc-alkaline to shoshonitic and potassic alkaline. Moreover, the degree of rock evolution in this sector is more variable and abundant rhyolites occur. The eastern sector (Panarea and Stromboli) resembles rocks from the Campania province, although Panarea has intermediate compositions between western islands and Stromboli. The eastern arc is associated with deep seismicity, defining a steep Benioff zone that extends almost to Campania (Fig. 10.2). Active volcanism is restricted to the central and eastern arc, i.e. along and east of the Tindari-Letojanni fault. The Aeolian arc has developed over continental crust that is about 20 km thick.

The *Sicily Province* includes a large number of volcanoes, i.e. Etna, Iblei, Ustica and Sicily Channel islands (Linosa and Pantelleria) and seamounts. Rock compositions range from tholeiitic to Na-alkaline and nephelinitic. Trace element contents are variable, but all rock types show compositional signatures typical of intraplate magmas. Some arc-like signatures (e.g. relatively low TiO_2), however, have been detected at Ustica and Etna. Radiogenic isotopes cover a wide range of values, defining a linear trend between HIMU and DMM mantle compositions. Sicilian volcanoes developed in different structural contexts. Etna is on the Tindari-Letojanni lineament, the Iblei volcanoes developed along a NE-SW fault zone, whereas Pantelleria and Linosa developed on NW to SE-trending grabens.

The *Sardinia Province* contains a wide variety of rocks, ranging from subalkaline to Na alkaline and nephelinitic, and from mafic to felsic. Most rocks have relatively unradiogenic Sr and Pb isotopic signatures, resembling EM1 mantle compositions. A few outcrops from southern Sardinia have isotopic and trace element signatures very close to the rocks of the Sicily Province. Plio-Quaternary volcanism in Sardinia overlies Oligocene-Miocene arc-type tholeiitic to calc-alkaline volcanism.

The *Tyrrhenian Sea* basin contains a large range of magmas, including MORB- and arc-type volcanoes. The age of rocks with island-arc geochemical signatures becomes younger going from Sardinia to south-eastern Tyrrhenian Sea. The coexistence of contrasting types of magmas on the Tyrrhenian Sea floor indicates tapping of various types of sources. The central Tyrrhenian Sea crust is oceanic in nature, and shows a minimum

thickness of about 10 km. Seismic studies suggest a stratified upper mantle with rather low S-wave velocities (Fig. 10.3).

10.3. Petrogenetic Constraints for Italian Plio-Quaternary Magmatism

Experimental studies demonstrate that the major element composition of primary magmas (i.e. those not modified by evolutionary processes) depend on the compositions and on the modal proportions of the mineral phases that enter into the liquid during partial melting. Magma compositions do not change significantly at various degrees of partial melting, providing that phase compositions and their proportions remain constant (e.g. during eutectic melting of minerals with constant compositions). Phase diagrams at different P-T-P_{fluid} conditions are the main tools for understanding how various minerals behave, i.e. when they melt and in what proportions, and what types of magmas they give.

Trace elements behave differently from major elements during magmatic processes. For equilibrium batch melting, abundance of any trace element in the magma depends on its concentration in the source rock, on its partitioning relationship between residual solid and liquid phases (i.e. the concentration ratio between the residual minerals and in the coexisting liquid), and on the degree of partial melting. For highly incompatible elements, which have a strong tendency to partition into the liquid phase rather than remain in the solid, the concentration in the melt for a given starting composition depends only on the degree of partial melting. Consequently, the ratios of highly incompatible trace elements do not change significantly during anatexis and, to a first approximation, are independent of the degree of partial melting. Therefore, these ratios reflect closely those of the source. The same is true for isotopic ratios of several elements (e.g. Sr, Nd, Pb, Hf), which do not fractionate during partial melting under equilibrium conditions.

Obviously, natural systems behave in a much more complex way than outlined above. However, this short and simplistic summary of igneous petrology and geochemistry has been drawn not only for the benefit of non-petrologists but also as a reminder that integrated major element, trace element and isotopic studies furnish complementary information and are necessary for unravelling complex magmatic regions, such as Italy. Selective investigation based on a single type of data (i.e. only major elements or trace elements or isotopes), which has been common in past studies of

Italian magmatism, is inadequate to explain the complexity of Italian rocks and may lead to incorrect conclusions.

As for most igneous rocks worldwide, very few if any of the oucropping magmas in the circum-Tyrrhenian area represent primary mantle-equilibrated melts, and most have suffered some type of petrogenetic evolution. Discussion in previous chapters has shown that a combination of processes, including fractional crystallisation, assimilation, and mixing, has been in operation within the magmatic plumbing system beneath most Italian volcanoes. However, numerous detailed studies on individual volcanoes have shown that these processes did not significantly affect incompatible trace element ratios and radiogenic isotopic compositions of the rocks in most cases, especially for mafic magmas. Therefore, the variations in trace element and radiogenic isotope ratios observed for mafic rocks through Italy can be assumed to reflect the compositions of their mantle sources.

As discussed in previous chapters, the petrological variability of Plio-Quaternary volcanism in Italy requires a number of different mantle sources with differing modal mineralogy, as well as variable physical-chemical conditions of melting. The potassium-rich nature of the magmatism in the Italian peninsula and, to a lesser extent, in the Aeolian arc suggests a derivation by melting of phlogopite-rich mantle sources. However, this mineral is relatively uncommon in mantle mineral assemblages, and its presence is evidence of enrichment processes. The high LIL element abundances and the anomalous isotopic compositions of most Italian volcanics point to the same conclusion. All of these rocks are characterised by high ratios of LILE/HFSE, which are typical of island arc volcanics. Therefore, most authors suggest a subduction-related origin for the mantle compositional anomalies (e.g. Cox et al. 1976; Di Girolamo 1978; Peccerillo 1985). However, this conclusion is not unanimously accepted, and there are alternative hypotheses that invoke, for example, deep mantle fluids as contaminants (e.g. Locardi 1988).

The tholeiitic to Na-alkaline nature of rocks in the Sicily and Sardinia provinces, and their relative deficiency in potassium with respect to sodium, suggest a magma source which contained amphibole and little or no phlogopite (e.g. Beccaluva et al. 1998). Their trace element geochemistry is characterised by a relative depletion in some LILE and a variable enrichment in some HFSE, such as Ta and Nb. Their source region has not been affected by recent subduction processes, although they could have suffered such a process some time in the past and remained isolated for a long period of time before being involved in melting (e.g. Lustrino et al. 2004a).

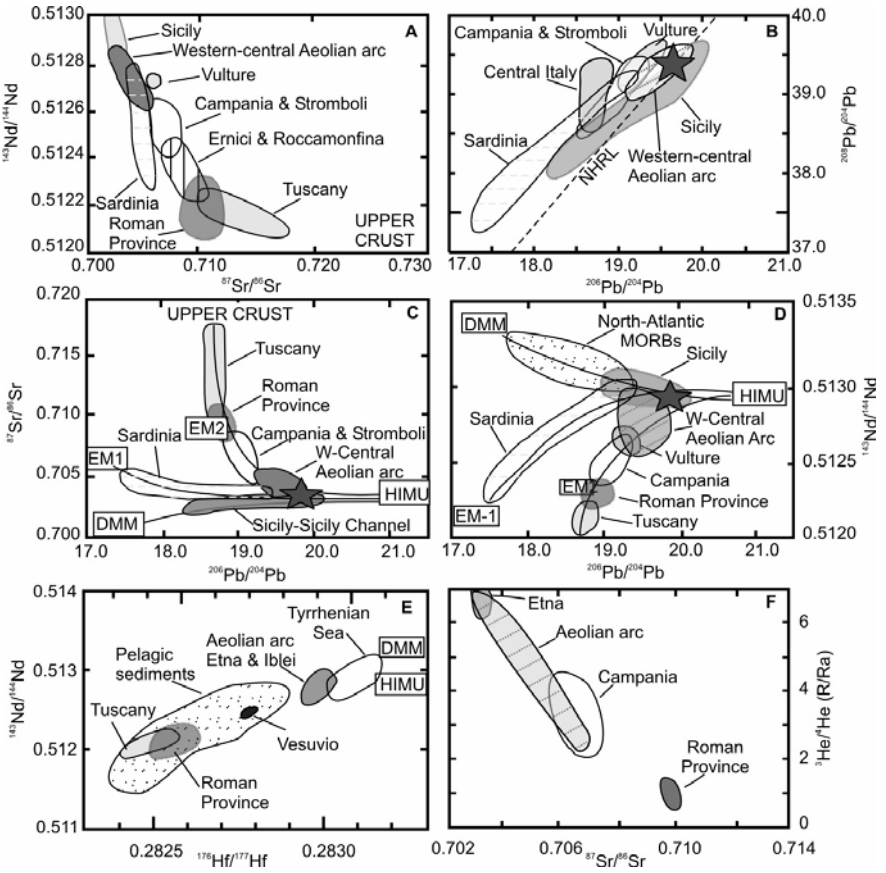

Fig. 10.4. Sr-Nd-Pb-Hf-He isotope diagrams for Italian Plio-Quaternary mafic rocks (MgO > 4 wt %) and for the main worldwide mantle compositions HIMU, DMM, EM1 and EM2. Star represents the composition of European Asthenospheric Reservoir.

The Italian Plio-Quaternary volcanics define trends in Sr-Nd-Pb-Hf-He isotopic space (Fig. 10.4), which have been highlighted by a number of au thors and have been interpreted as evidence for interaction between different types of mantle rocks (HIMU, EM1, DMM), and between these rocks and the continental crust (e.g. Vollmer 1976; Vollmer and Hawkesworth 1980; Sano et al. 1989; D'Antonio et al. 1996; Ayuso et al. 1998; Civetta et al. 1998; Gasperini et al. 2002; Peccerillo 2003; Martelli et al. 2004). Trends connecting mantle values to those typical of the crust have been observed in the "orogenic" rocks cropping out in the Aeolian arc and along the Italian peninsula, and have been interpreted as evidence for a role of both mantle and crustal reservoirs in magma genesis. Accord-

ing to this hypothesis, the increase of Sr isotopic ratios and the parallel decrease of Nd and Pb isotopic compositions from south to north along the Italian Peninsula suggest an increasing contribution from crustal components going northward. This cannot depend on increasing amounts of crustal assimilation of the upwelling magmas in shallow level magma chambers (magma contamination), but instead requires variable degrees of mantle contamination by crustal components. Trends of $^{87}Sr/^{86}Sr$ vs. $\delta^{18}O$ for mafic rocks along the Italian peninsula are considered as the most compelling evidence in favour of mantle contamination as a first-order process responsible for isotopic variations (e.g. Ellam and Harmon 1990). Sr and O-isotope ratios plot along upward concave trends, which are typical of mantle contamination (Fig. 10.5). However, single volcanoes define vertical trends, suggesting that magma contamination played an important role at the local scale (Turi et al. 1991; Harmon and Hoefs 1995; Barnekov 2000; Dallai et al. 2004). Very significant crustal contamination likely occurred for the Intra-Apennine centres, where a potassic magma with a Sr isotope composition similar to Roman Province magmas was contaminated

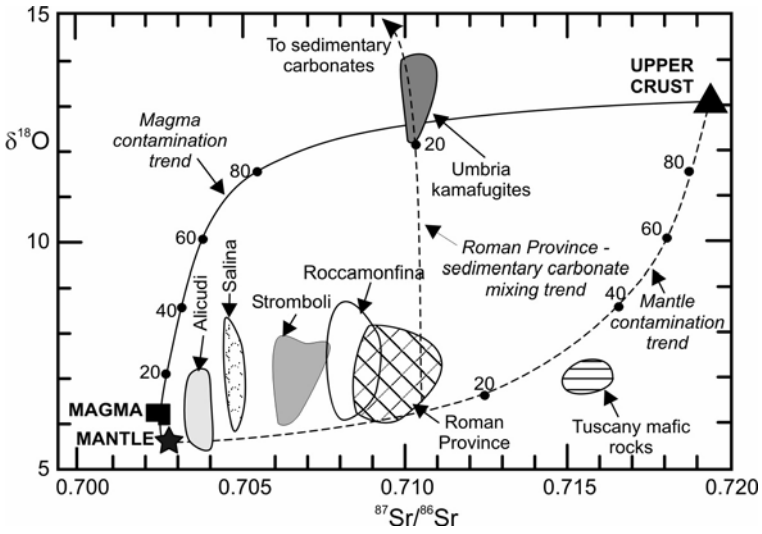

Fig. 10.5. Models showing Sr-O isotope variation during mixing between upper crustal rocks (full triangle), mantle peridotite (star) and mantle-derived basaltic magma (full square). Solid line represents the trend of magma contamination by upper crust. Dotted line is mantle contamination trend. Dashed line represents contamination trend of Roman Province magmas by sedimentary carbonates. Numbers along the lines indicate amounts of crustal end-member. For discussion, see text.

by carbonate sediments (see Chap. 3). Mantle contamination in the Italian area has been suggested as related to recent introduction of upper crust by subduction processes (e.g. Peccerillo 2002). Alternative hypotheses suggest that anomalous radiogenic isotope compositions may depend on aging of mantle material which had variable Rb/Sr, Sm/Nd, U/Pb, and Th/Pb, and remained isolated for long times to develop distinct Sr, Nd and Pb iso topic signatures (e.g. Castorina et al. 2000).

10.4. Geodynamic Evolution of the Western Mediterranean and Tyrrhenian Sea

Most authors agree that the complex magmatism in the Tyrrhenian Sea region cannot be related to a single type of geodynamic setting, but is the result of a long and complex evolution of the area, including several cycles of rifting and subduction over the last 300 Ma (e.g. Lustrino 2000; Peccerillo and Lustrino 2005). Therefore, an overview of the geodynamic evolution of the Western Mediterranean area is given here in order to provide a framework for understanding the magmatism.

Hercynian (Variscan) orogenesis occurred during Carboniferous to Permian time by the consumption of a ca. 3000-km-wide oceanic basin, along with several/numerous smaller basins separating Gondwana from Laurussia (central Europe). Plate convergence and continent-continent collision generated extensive mantle contamination and subduction-related magmatism, which is recorded by the intrusive calc-alkaline to shoshonitic complexes occurring in several places around the Tyrrhenian Sea (e.g. Corsica-Sardinia, Calabria and the Alps; Lustrino 2000 and references therein). According to some authors (e.g. Lustrino et al. 2004a,b), strong crustal thickening occurred during Hercynian collision, and this generated post-collisional delamination of a dense mafic lower crustal keel into the upper mantle, which underwent partial melting and further modified the mantle composition. After Hercynian orogenesis a rifting phase occurred in this area. This produced extensive mantle melting, extraction of basaltic magmas and the formation of the so-called Ligurian-Piemontese oceanic basin during Middle-Late Jurassic break-up of Pangea. Beginning in the early Cretaceous (~ 120 Ma), a new compressive phase took place, marking the start of Alpine orogenesis. The Ligurian-Piemontese basin was consumed during this phase of convergence between the African and the European cratons (e.g. Boccaletti et al. 1971; Dercourt et al. 1986; Boccaletti et al. 1990a,b). This process is responsible for the main structural

features across a very large area between Africa and Eurasia, including the Alps and Apennine chains.

Most authors agree that Ligurian-Piemontese oceanic crust was completely consumed during the Oligocene, whereas in some sectors there was still oceanic crust available for subduction (e.g. Panza and Mueller 1979; Keller et al. 1994; Doglioni et al. 1999). Therefore, whereas continent-continent collision between Europe and Africa brought about formation of the Betic chain and the Alps, in other places ocean-continent style convergence continued (e.g. along the Balearic and Sardinian margins; Monaco and Tortorici 1995; Carminati et al. 1998; Doglioni et al. 1999).

Oligocene to Middle Miocene evolution of the western Mediterranean was dominated by the opening of the Ligurian-Provençal, Algerian, and Valencia basins, and was accompanied by separation of the Corsica-Sardinia block from Provence as the former rotated counter-clockwise some 40-60°. Contemporaneously, the location of calc-alkaline magmatism migrated from Provence to Sardinia, where it extensively developed from about 32 to 15 Ma (Dostal et al. 1982; Morra et al. 1994, 1997; Lustrino et al. 2004a). The opening of Western Mediterranean basins generated breakup of the Alpine foreland and of the pre-existing Alpine-Betic collission zone (Doglioni et al. 1997).

The Tyrrhenian Sea opened between Early Miocene and Quaternary (about 15 to 0 Ma), following the formation of the Ligurian-Provençal and Alboran basins (Carminati et al. 1998). Magmatic activity shifted eastward during Tyrrhenian Sea opening, parallel to the migration of rifting (Savelli and Gasparotto 1994). At the same time, compression occurred in the Apennine front, with a progressive migration of the thrust belt-foredeep system towards the present-day Padanian-Adriatic-Ionian foreland (Doglioni 1991; Keller et al. 1994; Faccenna et al. 1997; Turco and Zuppetta 1998; Doglioni et al. 1999; Sartori 2003). In other words, there was a wave of compression migrating eastward, which was followed by distension and magmatism migrating in the same direction. During Tyrrhenian Sea opening, there was rifting and intraplate magmatism in Sardinia. Hercynian and Alpine blocks were detached from Sardinia and Corsica and were carried to the east. The Calabria-Peloritani block and most of the Tuscany-Latium terranes represent fragments of Hercynian and Alpine orogens drifted eastward to their present position during the Tyrrhenian Sea opening (Doglioni et al. 1998).

Formation of the Tyrrhenian Sea, and the associated counter-clockwise rotation of the Italian peninsula, resulted in longitudinal stretching of the Apennine chain and produced several arc sectors separated by important transverse tectonic lines. The main tectonic lineaments crossing the Apennine chain include the Ancona-Anzio line, the Ortona-Roccamonfina line,

the Sangineto fault and the Tindari-Letojanni fault (e.g. Locardi 1988; Turco and Zuppetta 1998; Fig. 10.1, 10.2). These structures separate crustal blocks characterised by different drifting velocity and variable styles of tectonic evolution, as also indicated by paleomagnetic data (Meloni et al. 1997; Turco and Zuppetta 1998). Strike-slip and extensional tectonics affected the African foreland where intraplate magmatism occurred, starting in the Miocene.

In conclusion, the overall evolution of the Western Mediterranean Sea area during the last 30-40 Ma can be summarised as follows:

1. Contraction of the Ligure-Piemontese oceanic basin and continent-continent collision between Adriatic and Europe during the Cretaceous to form the Alps and the Betic Cordillera;
2. Continuing convergence between Africa and Europe and formation of the Oligocene Ligurian and Provençal Basins, rotation of Sardinia-Corsica block and contemporaneous migration of calc-alkaline magmatism toward the east;
3. Development of extensive calc-alkaline magmatism in Sardinia between 32 and 15 Ma;
4. Opening of the Tyrrhenian Sea basin from about 15 Ma to present time, eastward migration of the Apennine compression, followed by rifting and magmatism migrating in the same direction;
5. Segmentation of the Apennine chain during rotation, development of different arc segments and of contrasting types of orogenic magmatism along different sectors;
6. Plio-Pleistocene rifting and intraplate magmatism in Sardinia;
7. Extensional and strike-slip faulting in Sicily and the Sicily Channel, with formation of tholeiitic to Na-alkaline volcanism.

10.5. Relationship between Petrogenesis and Geodynamics

Numerous hypotheses have been proposed to explain the relationship between magma genesis and the geodynamic evolution of the Tyrrhenian Sea and adjoining regions. In broad terms, three general classes of hypotheses can be recognised:

1. Lithospheric stretching, passive upwelling of asthenosphere and variable degrees of decompression melting at various mantle levels in an intracontinental rifting setting;
2. Upwelling of deep-rooted mantle plumes that impinge upon the lithosphere, cause opening of the Tyrrhenian basins and trigger magmatism;

3. Subduction-related processes, which generate differing styles of mantle contamination of sub-arc mantle, back-arc opening of the Tyrrhenian Sea and generation of variable types of magmas.

10.5.1. Passive-rifting-related Hypotheses

The hypothesis that circum-Tyrrhenian magmatism is related to intracontinental rifting, as in the East African Rift, is of old vintage (Marinelli 1967 1975). It basically stems from the occurrence of abundant K-alkaline and ultra-alkaline magmatism, which is believed to be typical of rift zones. According to Lavecchia and Stoppa (1990, 1996) the magmatism in Italy, the Apennine chain and the Tyrrhenian Sea basin are related to asymmetric passive rifting mechanisms, stretching of the lithosphere, upwelling of the asthenosphere and decompression melting in the mantle. According to this view, subduction can be present, but has little effect on magmatism. Stretching is related to external forces acting laterally along the plates. Therefore, there are no active mantle upwelling or deep mantle plumes. Evidence in favour of this hypothesis is the low amount of N-S shortening (about 100 km) compared to large W-E extension in the western Mediterranean area (800 km) in the last 23 Ma (Gueguen et al. 1998 and references therein). This requires that the compressive movements between Africa and Europe were minor compared to W-E extensional movements over this time period. According to Boccaletti et al. (1984), tensional fissures and extensional basins in the western Mediterranean area may have developed as a consequence of non-parallel convergence of rigid African and European plates. Many other authors also suggest that the Tyrrhenian Sea opening and rotation of southern Apennines are effects of block extrusion processes during oblique collision between Africa and Europe (e.g. Mantovani et al. 2002 and references therein).

According to passive rift hypotheses, the variable composition of the magmatism in the Tyrrhenian Sea area is the result of melting mantle sources of differing composition. Magmatism in Sicily, Sardinia and the western Tyrrhenian Sea would be derived from mantle material unaffected by metasomatism (Lavecchia and Stoppa 1990, 1996). Melting of amphibole-bearing peridotite at pressure within the stability field of spinel would produce Na-alkaline rocks. Increasing degrees of partial melting of somewhat lower pressure would be responsible for tholeiitic magma genesis. In contrast, lower degrees of partial melting in a metasomatised phlogopite-bearing mantle at pressure exceeding about 2.5 GPa would generate potassic alkaline magmas. The metasomatism responsible for anomalies in the source of potassic magmas is not related to subduction processes, but to

upwelling of deep mantle fluids with anomalous geochemical and isotopic compositions. Magmas from non-metasomatic sources would be generated at shallower levels than those from metasomatic sources. Melting processes for all types of magmas would occur in the thermal boundary layer at the base of the lithosphere. Therefore, the asymmetric distribution of Na-alkaline and K-alkaline magmatism in the Tyrrhenian Sea would be related to the variable thickness of the lithosphere, which increases eastward (Lavecchia and Stoppa 1990, 1996).

The explanation that the variable petrological and geochemical characteristics of magmas depend on the intensity of source metasomatism, on the degree of partial melting and on the depth of magma genesis is shared by other hypotheses. However, the rift-related model outlined above leaves a large number of problems unresolved, especially with regard to the origin of the metasomatising agents of potassic magma sources. The contention that the unusual compositions of potassic magmas depend on metasomatic fluids of deeper mantle origin does not solve the problem, since the reasons for the particular composition of the metasomatising fluid(s) remains unknown. The close similarity between trace element and geochemical signatures between potassic mafic magmas and upper crust (e.g. in Tuscany) requires that fluids producing metasomatism in the mantle had a composition similar to the upper crust. Therefore, models invoking a deep mantle origin for the metasomatising agents of potassic magma source regions should also try to explain why these fluids have trace element and isotopic signatures similar to the upper crust.

10.5.2. Plume-related Hypotheses

A plume-related origin for the Italian Plio-Quaternary volcanism was first advocated by Vollmer (1976). He suggested that smooth hyperbolic trends in plots of Sr vs. Pb isotopes were generated by two-end-member mixing between a mantle plume and upper crust. A decrease in age of the volcanism from Tuscany to southern Italy was suggested to represent the trace of a fixed hotspot beneath the rotating Italian peninsula. A role for an ascending mantle plume has been successively proposed by various authors (e.g. Locardi and Nicolich 1988; Ayuso et al. 1998; Gasperini et al. 2002; Bell et al. 2004).

Locardi and Nicolich (1988) suggested an active mechanism of formation of the Tyrrhenian basin and associated magmatism by upwelling of soft, low-density mantle beneath the Tyrrhenian Sea. However, the plume-like body in this model does not come from the deep mantle but rather from the asthenosphere; the decrease in density necessary to generate man-

tle upwelling is ascribed to fluids ascending from the deep mantle. This body was hypothesised to be mobile and to move eastward, explaining migration of magmatism with time.

Ayuso et al. (1998) invoked the presence of a plume beneath Campania to explain the high contents of HFSE and the low LILE/HFSE at Somma-Vesuvio. Gasperini et al. (2000, 2002) have recently suggested that a plume is rising beneath the southern Tyrrhenian Sea. However, in their model only Mt. Etna-Iblei-Ustica and Sardinia rocks are of plume origin; the rest of the circum-Tyrrhenian magmatism represents mixtures of plume material and subducted upper crustal components. According to this hypothesis, plume emplacement into the shallow mantle is favoured by a slab window that has opened beneath southern Italy as a result of differential rates of subduction between the northern and southern Apennines.

Finally, a more extreme hypothesis is that most, if not all of the magmatism in the Tyrrhenian area reflects a plume body extending from France and the Western Alps to Corsica-Sardinia and southern Italy (Bell et al. 2004). Following the idea of previous authors (e.g. Granet et al. 1995), this model postulates the occurrence of an asymmetric plume head at a depth of 670 to 410 km. It is suggested that the plume began its activity as early as 60-70 Ma ago, but has not yet reached sufficiently shallow depths to yield large quantities of melts. This would explain the absence of voluminous flood basalts in Italy. The volume excess resulting from the presence of the plume head in the transition zone would lead to lithospheric stretching, opening of the Western Mediterranean basins and to eastward rift-push of the lithosphere to generate the Apennine-Maghrebide chain. The geochemical and isotopic variations in Italian magmatism are attributed to chemical and isotopic heterogeneity in a plume head that had entrained upper mantle material during upwelling.

In summary, the following lines of evidence are generally invoked in favour of the plume hypothesis:

1. Smooth trends of Sr-Nd-Pb-Hf-He isotopes connecting different mantle compositions (Fig. 10.4). These are suggested to derive from mixing among different mantle end-members (HIMU or FOZO, EM1 and EM2), which occur worldwide and are believed to represent deep mantle plumes by several authors (e.g. Hofmann 1997);
2. The positive trend of $^{87}Sr/^{86}Sr$ vs. Rb/Sr displayed by Italian volcanic rocks. If interpreted as an isochron, this trend yields an age of ~1-2 Ga, supporting long term residence of high Rb/Sr material in the mantle and successive emplacement at shallow depth as a plume (Castorina et al. 2000);
3. The isotopic similarity of some Italian volcanoes, such as Mt. Etna and Iblei, with Na-alkaline and tholeiitic rocks from central and west-

ern Europe. This is consistent with the idea that magmas derived from a wide European Asthenospheric Reservoir (Fig. 10.4), which has been interpreted as a mantle plume head within the upper mantle (e.g. Granet et al. 1995; Hoernle et al. 1995);

4. The predominance in central Italy of ultrapotassic rocks, possibly associated with carbonatites, and the absence of calc-alkaline activity. A similar association occurs in the Toro-Ankole igneous province (western branch of the East Africa Rift; Bailey and Collier 2000), classically believed to have developed above mantle plumes.

Several objections have been raised to these arguments (e.g. Peccerillo and Lustrino 2005). It has been argued that compositions of mantle end-members, such as HIMU, EM1, EM2, are related to the recycling of different types of crustal materials into the mantle. However, age and extent of mantle contamination by crustal material may vary extensively. Therefore, the above mantle end-members do not necessarily represent plumes but may simply derive from patches of variably contaminated peridotite irregularly distributed within the mantle (see Meibom and Anderson 2003). Moreover, the isotopic trends defined by mafic rocks in Italy are not smooth, if examined in detail, but exhibit several sub-trends which suggest multiple mantle metasomatic events (Peccerillo 1999). This is shown, for instance by the Aeolian and Campania provinces, which show several irregularities in the isotopic trends, suggesting more complex processes than simple two-end-member mixing (see Chaps. 6, 7). In general terms, the strong regionality of the magmatism observed along the Italian peninsula and the strong lithospheric control evidenced by geochemical and structu-

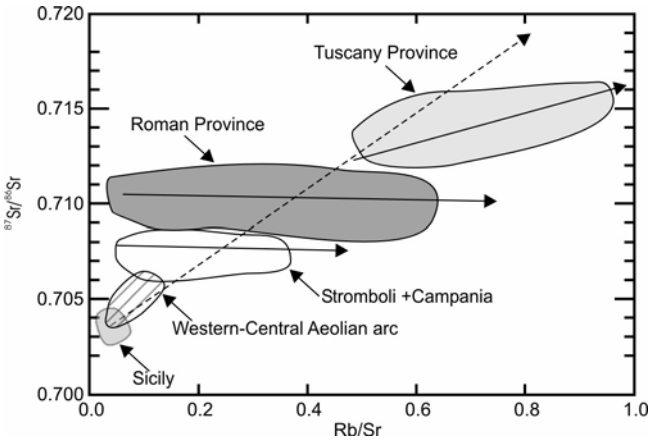

Fig. 10.6. $^{87}Sr/^{86}Sr$ vs. Rb/Sr ratios for mafic rocks (MgO > 4 wt %) along the Italian peninsula. Note that, whereas the Italian volcanics define a steep positive correlation, the single volcanic provinces show either flat or less steep trends.

ral changes between adjoining provinces do not support a deep plume mechanism, which should be independent of shallow features.

The positive trend of $^{87}Sr/^{86}Sr$ vs. Rb/Sr is observed only if the whole spectrum Italian magmatism is considered. When single magmatic provinces are taken in isolation, trends become flat or less steep (Fig. 10.6). This seems to favour distinct and young metasomatic events for the various magmatic provinces.

The Italian ultrapotassic rocks have compositions that are different from East Africa volcanic rocks, as observed previously, and there are strong doubts as to the carbonatitic nature of carbonate-rich pyroclastic rocks from central Italy (see Chap. 3). Moreover, there is ample evidence for calc-alkaline activity coeval with or slightly older than potassic magmatism along the Italian peninsula. Calc-alkaline rocks are found in the Campanian Plain (2Ma), in Tuscany (Capraia, 7.6 Ma) and as pyroclastic deposits with an age of about 2 Ma or less, often containing orthopyroxene, occurring in several places along the Apennines (Bigazzi et al. 2000; Bizzarri et al. 2003).

Other geochemical characteristics of Italian volcanism are also not easily explained by the plume hypotheses. For example, deep mantle plumes are commonly associated with high $^{3}He/^{4}He$ ratios (e.g. Farley and Neroda 1998). However, measurements carried out on fluid inclusions in olivine phenocrysts from mafic Italian rocks have yielded low He isotopic ratios with $R/R_A < 7.5$ (e.g. Sano et al. 1989; Graham et al. 1993; Marti et al. 1994; Di Liberto 2003; Martelli et al. 2004), which are much lower than compositions found for plume-related magmas.

Finally, the Tyrrhenian Sea (i.e. the focus of the mantle plume ascent) has a considerable depth (3700 m) and magmatism is not particularly voluminous. These characteristics do not fit a plume hypothesis. The suggestion that lack of magmatism is related to the great depth of the plume head is reasonable. However, the idea that such a deep body would be able to induce basin opening of the order of several hundred km, and to generate a collisional chain, is difficult to accept and needs much further refinement to avoid scepticism.

10.5.3. Subduction-related Hypotheses

Several authors explain the origin of the wide compositional variation of the Plio-Quaternary magmatism in Italy as a function of shallow level mantle heterogeneities, partially generated during the convergence between Africa and Europe, and partially inherited from older melting and contamination events (e.g. Cox et al. 1976; Di Girolamo et al. 1976; Pec-

cerillo 1985 1999; Rogers et al. 1985; Beccaluva et al. 1991; Serri et al. 1993; Doglioni et al. 1999; Lustrino et al. 2004a,b; Peccerillo and Lustrino 2005).

Rocks with island-arc geochemical signatures occurring along the Italian peninsula and in the southern Tyrrhenian Sea area would be directly related to subduction processes, and have been suggested to be generated by melting of mantle sources metasomatised by material (fluids, oceanic-type crust, sediments, etc.) introduced into the mantle wedge during recent (i.e. Cenozoic to Quaternary) subduction. Magma generation would not necessarily coeval with subduction and metasomatism; it may post-date these processes, and can be triggered by changes in the thermal regimes in the upper mantle (e.g. Peccerillo 1990; Tamburelli et al. 2001).

By contrast, magmas from the Sicily and Sardinia provinces, and some Tyrrhenian seamounts which lack evident arc-type geochemical signatures, would be generated by melting of mantle sources which were not contaminated by recent subduction. These would represent lithosphere-asthenosphere reservoirs, which melted during passive upwelling in zone of extensional tectonic regimes (e.g. along strike-slip faults or in back-arc areas) between converging European and African plates.

There are several versions of the subduction-related hypotheses for orogenic Italian magmatism, with important differences for various aspects, such as the nature of the downgoing crust, the role of older mantle contamination events, the causes of back-arc basin opening, etc. (e.g. Peccerillo 1985; Beccaluva et al. 1991; Serri et al. 1993; Gvirtzman and Nur 1999). However, all of the subduction-related models agree that post-Oligocene subduction of the Adriatic and Ionian plates beneath the southern European margin has been characterised by eastward migration of the subduction zone (Fig. 10.7). One consequence of this migration is that the age and nature of the magmatism vary, the latter being dependent on the different types of downgoing crust. For example, the calc-alkaline volcanism of Provence, Valencia basin, Sardinia (32 to 15 Ma) and of the southern Tyrrhenian Sea is interpreted as the consequence of subducting oceanic-type or thinned continetal crust. In contrast, the volcanism in central Italy is related to subduction of a continental-type Adriatic plate (Peccerillo 1985; Beccaluva et al. 1991; Serri et al. 1993). The introduction of continental-type crust in the north also explains the isotopic signatures of the potassic magmatism in central Italy the scarcity of calc-alkaline magmatism, which is so abundant in the southern Tyrrhenian Sea (e.g. Peccerillo 1985). Note that, although there is still debate on the role of aqueous fluids in determining various types of mafic magmas in the upper mantle, aqueous conditions favour the generation of oversaturated magmas and increase the degree of partial melting within the upper mantle, thus reducing

the amount of ultrapotassic melts which need low degrees of partial melting to be formed (e.g. Wendlandt and Eggler 1980a,b; Ulmer 2001). However, it has also been suggested that magmatism in the Tuscany Province may be due to an older contamination event, which probably occurred during Alpine collision (see Chap. 2), rather than the more recent subduction of the Adriatic plate beneath the Apennines (Peccerillo 1999).

In summary, subduction-related hypotheses explain the petrological and geochemical variation of the magmatism along the Italian peninsula as a result of the different nature, intensity and age of mantle contamination events (Peccerillo 1999). The magmatism in Tuscany is the result of mantle contamination during Alpine collision phases, which brought upper crustal material (metapelites or metagranites) into the mantle wedge beneath the African margin. Mantle melting was a younger event, which occurred during backarc opening behind the westerly dipping subduction zone of the Adriatic plate (see Chap. 2, Fig. 2.12). The magmas of the Roman Province were generated in a mantle source that was contaminated by upper crustal material (e.g. marls) coming from the subducting Adriatic plate. The superimposition of the Roman over the Tuscany Province suggests that the Roman magma sources also suffered the Alpine contamination event that affected Tuscany. Therefore, the Roman Province experienced two superimposed contamination events, which may explain the large volumes of potassic magmas in this area (see Chap. 4, Fig. 4.22). Finally, the Campanian and Aeolian arc volcanoes are basically related to subduction of the oceanic or thinned continental Ionian plate (Panza and Pontevivo 2004), which generated a much less intense contamination of the mantle wedge than in the case of the continental-type Adriatic lithosphere (see Chap. 6, Fig. 6.26; Peccerillo 1999, 2002).

Evidence in favour of subduction-related hypotheses for the magmatism along the Italian peninsula and in the southern Tyrrhenian Sea includes:

1. Abundant arc-type Plio-Quaternary calc-alkaline magmatism occurring in the Aeolian arc and seamounts, along the Tyrrhenian Sea floor and in some places along the Italian peninsula (e.g. Tuscany, Campania);
2. Crustal-like geochemical and isotopic signatures for most rocks along the Italian peninsula (Fig. 10.4), requiring crustal contamination of their mantle sources, a process that can be only accomplished by subduction processes;
3. Occurrence of an active seismic zone beneath the eastern Aeolian arc, defined by deep focus earthquakes extending to a depth of about 500 km until the Campania area (Fig. 10.2);
4. Occurrence of a vertical rigid body cutting the asthenosphere beneath the Apennine chain, interpreted as a remnant of a young subduction zone;

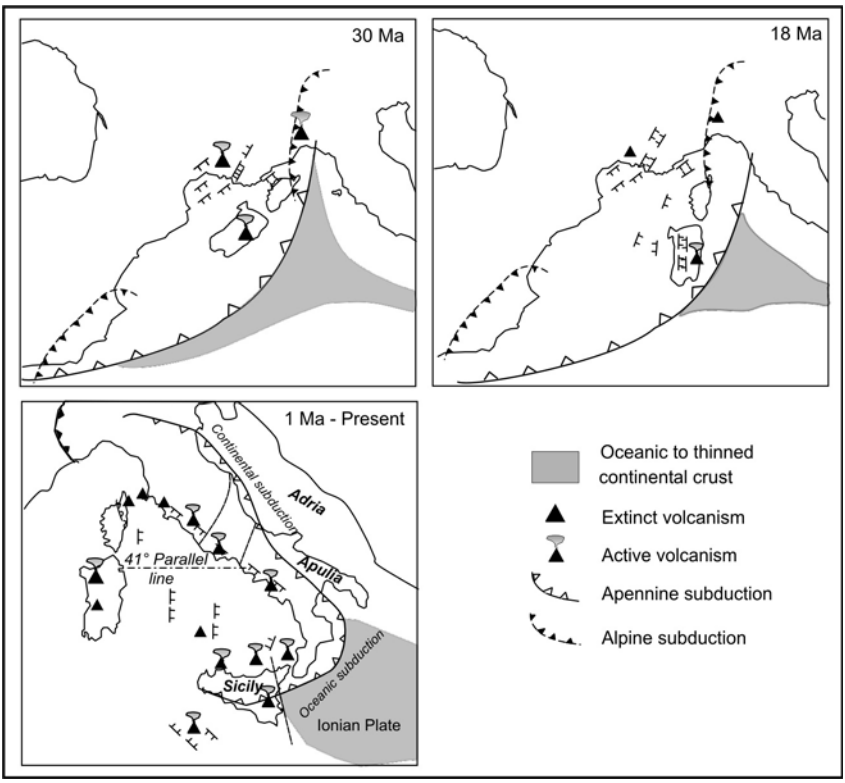

Fig. 10.7. Schematic evolution model of the Western Mediterranean and Tyrrhenian Sea from Oligocene to Present. Simplified after Carminati et al. (1998) and Cavazza and Wezel (2003). For discussion, see text.

5. Occurrence of a belt of cold mantle rimming the Apennine chain revealed by tomographic studies, which suggests recent immersion of cold material into the upper mantle (Wortel and Spakman 2000; Piromalli and Morelli 2003).

Although subduction-related hypotheses provide a satisfactory explanation for several features of orogenic magmatism in Italy, they leave several problems unresolved. For instance, the large volume of potassic magmatism in the Roman Province is uncommon for subduction-related volcanic settings. The isotopic trends, basically connecting discrete compositions, are also a problem. For instance, it is not clear why there is no trend connecting EM1 or DMM with upper crustal material, but only one main trend exists between the latter and HIMU-type rocks. In other words, it is not clear why crustal contamination prevailingly, or exclusively, affected HIMU-type mantle sources. Finally, the very narrow Pb isotopic composition of potassic rocks in central Italy is also a problem. Crustal rocks have

variable Pb isotope compositions. If Pb isotope ratios of potassium-rich rocks in Central Italy are related to mantle contamination by upper crustal material, the reason for the limited variations in Pb-isotope ratios in the Roman and Tuscany provinces is hard to understand.

10.6. Conclusions

Plio-Quaternary magmatism in Italy shows strong compositional complexities, which have made the Italian volcanoes much studied but not yet fully understood geological objects. The wide petrological, geochemical and isotopic variations observed cover almost completely the compositions of magmatic rocks occurring worldwide. Therefore, understanding the origin and geodynamic significance of volcanism in Italy is more than regional in interest and is a challenge and an opportunity for igneous petrology and geochemistry, in general.

Various hypotheses have been proposed to explain the compositional variations and peculiarities of this magmatism. From the discussion above, it can be concluded that each class of hypotheses is able to explain some but not all of the characteristics of various volcanoes.

Most probably, there are seeds of truth in all of the hypotheses. Future research will bring a better refinement of individual models and possibly to the rejection of some others. A satisfactory explanation of the petrogenesis of the recent Italian magmatism may well arise from some combination of the various models. Whatever the case, investigations into the complexity of Italian magmatism will certainly contribute to a better understanding of magmatism and geodynamics at a global scale[1].

[1] Chapter 10 has been written in collaboration with Pamela Kempton, NERC, UK

Appendix: Classification and Petrogenesis of K-rich Rocks

Classification and Nomenclature

Potassium-rich rocks are found in several tectonic environments, including continental cratons, active subduction zones and post-collisional settings (e.g. Müller and Grove 2000). They are limited in abundance over a global scale, but are widespread in Italy. Potassium-rich rocks cover a very wide range of petrological and geochemical compositions, from alkaline to transitional, from strongly undersaturated to oversaturated in silica, from ultrabasic and basic to intermediate. Mineralogical composition is even more variable, being dependent not only on the chemical composition of magmas but also on the pressure-temperature conditions of crystallisation (Yoder 1986). This makes rocks with similar major and trace element compositions display sometimes different mineralogical compositions (*heteromorsphism*).

In order to overcome this problem, it is appropriate to classify potassic rocks on the basis of chemical parameters. The K_2O vs. SiO_2 of Peccerillo and Taylor (1976; Fig. A.1) is useful to classify rocks from arc environments, including the mildly potassic shoshonites. The TAS diagram of Le Maitre (1989) is also useful for naming potassic and ultrapotassic rocks (Fig. A.2). In this book, nomenclature will follow, as close as possible, these diagrams. However, the extreme compositional variability which pertains to all the major petrological parameters in addition to silica and alkalis, makes K_2O vs. SiO_2 and TAS diagrams insufficient to express petrochemical affinities and variability of potassium-rich magmas.

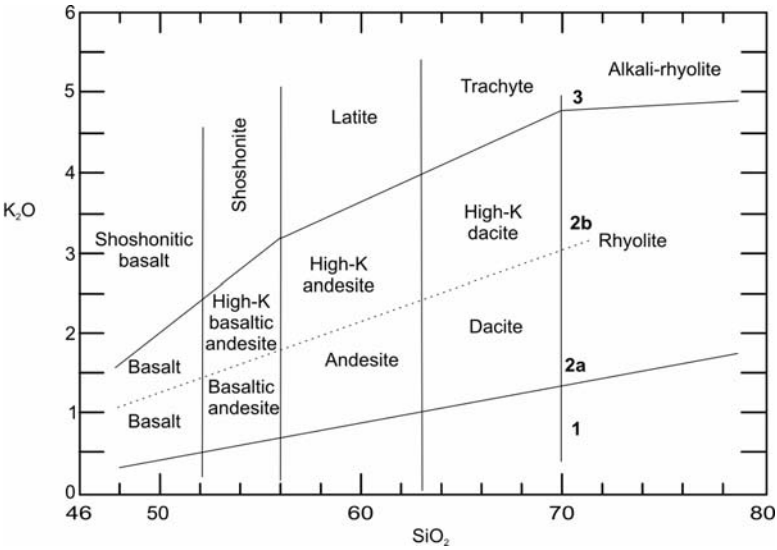

Fig. A.1. K_2O vs. SiO_2 classification grids for arc rocks. 1: arc tholeiitic series; 2a: calc-alkaline series; 2b: high-K calc-alkaline series; Field 3: shoshonitic series. Modified from Peccerillo and Taylor (1976).

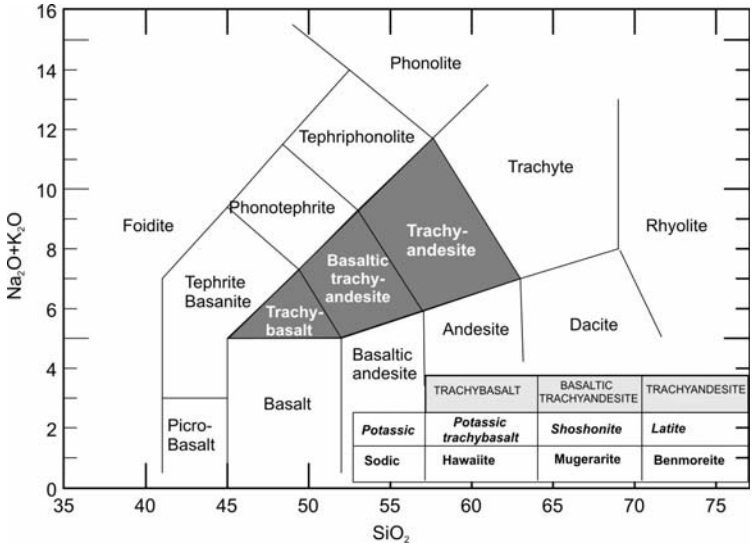

Fig. A.2. Total alkali vs. silica (TAS) classification diagram of volcanic rocks (modified from Le Maitre 1989). Rocks falling in the shaded area may be subdivided as shown in the inset table, on the basis of their sodic (Na_2O-2.0 ≥ K_2O) or potassic (Na_2O-2.0 ≤ K_2O) affinity.

In general, *potassic rocks* are defined as those that have K_2O higher about 2 wt % and K_2O/Na_2O = 1.0-2.5 at a MgO > 3-4 wt % and SiO_2 < 55-57 wt %. *Ultrapotassic rocks* have K_2O > 3 wt % and K_2O/Na_2O > 2.5-3.0 at a MgO > 3-4 wt % and SiO_2 < 55-57 wt % (see Chap. 1, Fig. 1.3). The restriction in the MgO and SiO_2 contents is required to exclude silicic rocks (e.g. dacite, rhyolite) whose high K_2O and K_2O/Na_2O ratios relate to magma evolutionary processes and do not denote a potassic nature for their parental melts. The terms *potassic* or *potassium-rich* are loosely used to indicate both potassic and ultrapotassic rocks.

Although there is a continuum in K_2O enrichment in potassium-rich rocks, the following groups can be distinguished (e.g. Peccerillo and Taylor 1976; Morrison 1980; Foley et al. 1987): 1 - Shoshonites; 2 - Roman-type potassic series (KS); 3 - Roman-type high potassic series (HKS); 4 - Lamproites; 5 - Kamafugites. An additional group could be represented by Group-2 micaceous kimberlites, which have K_2O contents and K_2O/Na_2O ratios comparable to those of some potassic rocks.

Shoshonites are slightly silica-oversaturated to undersaturated rocks. They have K_2O around 1.5-2.5 wt % (Peccerillo and Taylor 1976) and K_2O/Na_2O around unity in the mafic compositions. According to Morrison (1980), the shoshonitic suite should include only those rocks associated with calc-alkaline volcanics along active plate margins. However, Joplin (1968), who coined the term "shoshonitic suite", also included in this group moderately K-rich rocks occurring in some intraplate environments, where they represent the potassic equivalents of Na-transitional rocks. The shoshonitic suite includes mafic to silicic rocks. These fall in the shoshonitic basalts, shoshonite, latite, trachyte fields on the K_2O vs. SiO_2 diagram and in the K-trachybasalt, shoshonite, latite, trachyte fields of the TAS diagram. Some K-rich alkaline rhyolites may also belong to this suite.

Roman-type potassic series (KS) has slightly higher K_2O% (about 2.5-3.0 in the mafic range) and K_2O/Na_2O (1.5-2.5) than shoshonites. KS rocks are saturated to slightly undersaturated in silica. The entire rock suite includes trachybasalts, shoshonite, latite and trachyte.

Roman-type high-potassium series (HKS) rocks are ultrapotassic (K_2O > 3 wt %, K_2O/Na_2O > 2.5 in the mafic rocks) undersaturated in silica, rich in Al_2O_3 (12-20 wt % ca) and depleted in TiO_2 (generally < 1.2 wt %). The mafic types have high CaO, typically around 10-13 wt % and Na_2O around 2-3 wt %. HKS consists of the well known leucitite, leucite-tephrite, to leucite-phonolite series widely occurring in several Italian volcanoes. Compositions of these rocks fall in the foidite, basanite-tephrite, phonotephrite, tephriphonolite and phonolite fields in the TAS diagram.

Lamproites are ultrapotassic, slightly undersaturated to oversaturated in silica and typically have low Al_2O_3 (< 10-11 wt %), Na_2O (< 1.5-2 wt %) and CaO (< 6-7 wt %) in the mafic compositions. SiO_2 is variable, from less than 45% to about 60 wt%. This variation does not seem to depend on magma evolution processes but probably reflects different pressure of genesis in the upper mantle. In fact, Mg# is generally high to very high in most low-silica and high-silica lamproites, sometimes reaching 75-80. The mineralogy of lamproites consists of highly magnesian olivine, Al-poor diopsidic pyroxene, phlogopite, sanidine, K-richterite, leucite and several uncommon phases such as perovskite [$(Ca,Na,Fe^{2+},Ce)(Ti,Nb)O_3$], jeppeite [$(K,Ba)_2(Ti,Fe^{3+})_6O_{13}$], wadeite ($K_4Zr_2Si_6O_{18}$), shcherbakovite [$(Ba,K)(K,Na)Na(Ti,Fe,Nb,Zr)_2Si_4O_{14}$] priderite [$(K,Ba)(TiFe^{3+})_8O_{16}$] and armacolite [$(Mg,Fe)Ti_2O_5$]. Lamproitic rocks take special names, which are not reported on the TAS diagram.

Kamafugites owe their name to the katungite-mafurite-ugandite series of eastern Africa. They are ultrapotassic and share with lamproites low Al_2O_3 and Na_2O and high MgO abundances. However, they are rich in CaO (up to 18 wt %) and strongly undersaturated in silica. Typical minerals include melilite, leucite, kalsilite, Mg-rich olivine, diopside, monticellite, phlogopite and perovskite. Most kamafugites fall in the foidite field in the TAS diagram, but special names are often used in the nomenclature of kamafugites.

8.1. Petrogenesis of Potassium-rich Magmas

The genesis of potassic and ultrapotassic magmas has been a much debated issue since early times of igneous petrology (see Peccerillo 1992 for a review). Modern hypotheses suggest genesis by various degrees of partial melting in anomalous mantle sources, heterogeneously enriched in incompatible elements and with variable isotopic signatures. High potassium contents require that one or more minerals rich in this element, such as phlogopite or K-richterite, is present in the mantle and melts preferentially during magma formation (e.g. Edgar et al. 1976; Gupta and Fyfe 2003). These are not normal mantle phases and their occurrence suggests metasomatic enrichment in potassium. This can be accomplished by several processes such as addition to the lithospheric mantle of fluids or melts coming from the deep mantle (e.g. from the asthenosphere), addition of crustal material from subducting slabs, etc. The variable isotopic and trace element compositions of world-wide potassic and ultrapotassic magmas

suggest that different amounts and types of metasomatising agents acted on the sources of potassic magmas in various areas.

The variable concentrations in potassic magmas of some major oxides such as CaO, Na_2O, Al_2O_3, require that the peridotite contained different amounts of phases that hosted these elements. Therefore, the low CaO and Al_2O_3 contents of lamproites indicate that clinopyroxene was scarce or absent in the source of these magmas. In contrast, the high concentrations of these oxides in Roman-type KS and HKS rocks and in kamafugites suggest that clinopyroxene was the main phase of the mantle sources of these magmas. In summary, lamproites are believed to derive from a peridotite which contained phlogopite- and/or K-richterite but was depleted in clinopyroxene (i.e. phlogopite-bearing harzburgite), whereas Roman-type rocks and kamafugites derive from cpx-bearing rocks such as phlogopite-lherzolite, to phlogopite-pyroxenite. The scarcity of clinopyroxene in the mantle source of lamproites can be related to old, pre-enrichment melting events and extraction of basaltic magmas, which had generated preferential melting and removal of clinopyroxene. Clinopyroxene-rich mineralogy of the mantle sources of kamafugites and Roman-type KS and HKS are most likely related to metasomatic events by Ca-rich melts (e.g. carbonatites) or by carbonate-rich sediments.

References

Abbate E, Bortolotti V, Passerini P, Sagri M (1970) Introduction to the geology of Northern Apennines. Sedim Geol 4:521-558

Accordi B, Carbone F (eds) (1986) Lithofacies map of the Latium-Abruzzi and neighboring areas. Quad Ric Sci CNR Rome, 114, 5:223 pp

Albini A, Cristofoloni R, Di Girolamo P, Stanzione D (1980) Rare-earth and other trace-element distributions in the calc-alkaline volcanic rocks from deep boreholes in the Phlegrean Fields, Campania (south Italy). Chem Geol 28:123-133

Allan TD, Morelli C (1971) A geophysical study of the Mediterranean Sea. Boll Geofis Teor Appl 13:100-142

Appleton JD (1972) Petrogenesis of potassium-rich lavas from the Roccamonfina Volcano, Roman Region, Italy. J Petrol 13:425-456

Araña V, Barberi F, Santacroce R (1974) Some data on the comendite type-area of S. Pietro and S. Antioco islands, Sardinia. Bull Volcanol 38:725-736

Argnani A, Savelli C (1999) Cenozoic volcanism and tectonics in the southern Tyrrhenian Sea: space-time distribution and geodynamic significance. Geodynamics 27:409-432

Armienti P, Barberi F, Bizouard H, Clocchiatti R, Innocenti F, Metrich N, Rosi M, Sbrana A (1983) The Phlegraean Fields: magma evolution within a shallow chamber. J Volcanol Geotherm Res 17:289-311

Armienti P, Barberi F, Innocenti F, Pompilio M, Romano R, Villari L (1984) Compositional variation in the 1983 and other recent Etnean lavas: insights on the shallow feeding system. Bull Volcanol 47:995-1007

Armienti P, D'Orazio M, Innocenti F, Tonarini S, Villari L (1996) October 1995 - February 1996 Mt. Etna explosive activity: trace element and isotopic constraints on the feeding system. Acta Vulcanol 8:1-6

Armienti P, Pareschi MT, Pompilio M (1997) Lava textures and time scales of magma storage at Mt. Etna (Italy). Acta Vulcanol 9:1-5

Armienti P, Tonarini S, D'Orazio M, Innocenti F (2004) Genesis and evolution of Mt. Etna alkaline lavas: petrological and Sr-Nd-B isotope constraints. Per Mineral 73:29-52

Auger M, Gasparini P, Virieux J, Zollo A (2001) Seismic evidence of an extended magmatic sill under Mt. Vesuvius. Science 294:1510-1512

Aurisicchio C, Federico M, Gianfagna A (1988) Clinopyroxene chemistry of the High-Potassium Suite from the Alban Hills, Italy. Mineral Petrol 39:1-19

Ayuso RA, De Vivo B, Rolandi G, Seal II RR, Paone A (1998) Geochemical and isotopic (Nd-Pb-Sr-O) variations bearing on the genesis of volcanic rocks from Vesuvius, Italy. J Volcanol Geotherm Res 82:53-78

Bailey DK, Collier JD (2000) Carbonatite-melilitite association in the Italian collision zone and the Uganda rifted craton: significant common factors. Mineral Mag 64:675-682

Barberi F, Innocenti F, Mazzuoli R (1967a) Contributo alla conoscenza chimico-petrografica e magmatologica delle rocce intrusive, vulcaniche e filoniane del Campigliese (Toscana). Mem Soc Geol It 6:643-681

Barberi F, Borsi S, Ferrara G, Innocenti F (1967b) Contributo alla conoscenza vulcanologica e magmatologica delle Isole dell'Archipelago Pontino. Mem Soc Geol It 6:581-606

Barberi F, Innocenti F, Ricci CA (1971) La Toscana Meridionale. Il magmatismo. Rend Soc It Mineral Petrol 27:169-210

Barberi F, Civetta L, Gasparini P, Innocenti F, Scandone R, Villari L (1974) Evolution of a section of Africa-Europe plate boundary: paleomagnetic and volcanological evidence from Sicily. Earth Planet Sci Lett 22:123-132

Barberi F, Bizouard H, Capaldi G, Ferrara G, Gasparini P, Innocenti F, Joron JL, Lambert B, Treuil M, Allegre C (1978) Age and nature of basalts from the Tyrrhenian Abyssal Plain. In: Hsu K, Montadert L, et al. (eds) Init Rep Deep Sea Drilling Project. Washington, 42: pp 509-514

Barberi F, Buonasorte G, Cioni R, Fiordelisi A, Foresi L, Iaccarino S, Laurenzi MA, Sbrana A, Vernia L, Villa IM (1994a) Plio-Pleistocene geological evolution of the geothermal area of Tuscany and Latium. Mem Descr Carta Geol It 49:77-134

Barberi F, Gandino A, Gioncada A, La Torre P, Sbrana A, Zenucchini C (1994b) The deep structure of the Eolian arc (Filicudi-Panarea-Vulcano sector) in light of gravity, magnetic and volcanological data. J Volcanol Geotherm Res 61:189-206

Barbieri M, Di Girolamo P, Locardi E, Lombardi G, Stanzione D (1979) Petrology of the calc-alkaline volcanics of the Parete-2 well (Campania, Italy). Per Mineral 48:53-74

Barbieri M, Gasparotto G, Lucchini F, Savelli C, Vigliotti L (1986) Contributo allo studio del magmatismo del Mar Tirreno: l'intrusione granitica tardo-Miocenica del monte submarino Vercelli. Mem Soc Geol It 36:41-54

Barbieri M, Peccerillo A, Poli G, Tolomeo L (1988) Major, trace element and Sr isotopic composition of lavas from Vico volcano (Central Italy) and their evolution in an open system. Contrib Mineral Petrol 99:485-497

Barbieri M, Barbieri M, D'Orefice M, Graciotti R, Stoppa F (2002) Il vulcanismo monogenico medio-pleistocenico della Conca di Carsoli (L'Aquila). Geol Rom 36:13-31

Barchi M, Landuzzi A, Minelli G, Pialli G (2001) Outhern Northern Apennines. In: Vai GB, Martini PI (eds) Anatomy of an Orogen. The Apennines and the adjacent Mediterranean basins. Kluwer, Dordrecht, pp 215-254

Barker DS (1987) Rhyolites contaminated with metapelite and gabbro, Lipari, Aeolian Islands, Italy: products of lower crustal fusion or of assimilation plus fractional crystallization? Contrib Mineral Petrol 97:460-472

Barnekow P (2000) Volcanic rocks from central Italy: an Oxygen isotopic micro-analytical and geochemical study. PhD Thesis, University of Gottingen, 99 pp

Bartolini C, Bernini M, et al. (1982) Carta neotettonica dell'Appennino settentrionale. Note illustrative. Boll Soc Geol It 101:523-549

Barton M, Varekamp JC, Van Bergen MJ (1982) Complex zoning of clinopyroxenes in the lavas of Vulsini, Latium, Italy: evidence for magma mixing. J Volcanol Geotherm Res 14:361-388

Basilone P, Civetta L (1975) Datazione K/Ar dell'attivita vulcanica dei Monti Ernici (Latina). Rend Soc It Mineral Petrol 31:175-179

Beccaluva L, Deriu M, Gallo F, Vernia L (1973) Le vulcaniti post-elveziane del Montiferro occidentale (Sardegna centro-occidentale). Mem Soc Geol It 12:131-156

Beccaluva L, Macciotta G, Venturelli G (1975) Dati geochimici e petrografici sulle vulcaniti Plio-Quaternarie della Sardegna centro-occidentale. Boll Soc Geol It 94:1437-1457

Beccaluva L, Macciotta G, Venturelli G (1976) Le vulcaniti Plio-Quaternarie del Logudoro. Boll Soc Geol It 95:339-350

Beccaluva L, Deriu M, Macciotta G, Savelli C, Venturelli G (1977) Geochronology and magmatic character of the Pliocene-Pleistocene volcanism in Sardinia. Bull Volcanol 40:1-16

Beccaluva L, Colantoni P, Di Girolamo P, Savelli C (1981) Upper-Miocene submarine volcanism in the Strait of Sicily (Banco Senza Nome). Bull Volcanol 44:573-581

Beccaluva L, Rossi PL, Serri G (1982) Neogene to recent volcanism of the Southern Tyrrhenian-Sicilian area: implications for the geodynamic evolution of the Calabrian Arc. Earth Evol Sci 3:222-238

Beccaluva L, Morlotti E, Torelli L (1984) Notes of the geology of the Elimi Chain area (southwestern margin of the Tyrrhenian Sea). Mem Soc Geol It 27:213-232

Beccaluva L, Civetta L, Macciotta G, Ricci CA (1985a) Geochronology in Sardinia: results and problems. Rend Soc It Mineral Petrol 40:57-72

Beccaluva L, Gabbianelli G, Lucchini F, Rossi PL, Savelli C (1985b) Petrology and K/Ar ages of volcanics dredged from the Eolian seamounts: implications for geodynamic evolution of the southern Tyrrhenian basin. Earth Planet Sci Lett 74:187-208

Beccaluva L, Brotzu P, Macciotta G, Morbidelli L, Serri G, Traversa G (1989) Cainozoic tectono-magmatic evolution and inferred mantle sources in the Sardo-Tyrrhenian area. In: Boriani A, Bonafede M, Piccardo GB, Vai GB (eds) The Lithosphere in Italy. Atti Conv Lincei, Rome, 80:229-248

Beccaluva L, Bonatti E, Dupuy C, Ferrara G, Innocenti F, Lucchini F, Macera P, Petrini R, Rossi PL, Serri G, Seyler M, Siena F (1990) Geochemistry and mineralogy of the volcanic rocks from ODP sites 650, 651, 655, and 654 in the

Tyrrhenian Sea. In: Kastens KA, Mascle J, et al. (eds) Proc Ocean Drilling Program, Scientific Results, 107: pp 49-74

Beccaluva L, Di Girolamo P, Serri G (1991) Petrogenesis and tectonic setting of the Roman volcanic province, Italy. Lithos 26:191-221

Beccaluva L, Siena F, Coltorti M, Di Grande A, Lo Giudice A, Macciotta G, Tassinari R, Vaccaro C (1998) Nephelinitic to tholeiitic magma generation in a transtensional tectonic setting: an integrated model for the Iblean volcanism, Sicily. J Petrol 39:1547-1576

Beccaluva L, Bianchini G, Coltorti M, Perkins WT, Siena F, Vaccaro C, Wilson M (2001) Multistage evolution of the European lithospheric mantle: new evidence from Sardinian peridotite xenoliths. Contrib Mineral Petrol 142:284-297

Beccaluva L, Coltorti M, Di Girolamo P, Melluso L, Milani L, Morra V, Siena F (2002) Petrogenesis and evolution of Mt. Vulture alkaline volcanism (Southern Italy). Mineral Petrol 74:277-297

Becker H, Jochum KP, Carlson RW (2000) Trace element fractionation during dehydration of eclogites from high-pressure terranes and the implications for element fluxes in subduction zones. Chem Geol 163:65-99

Behncke B (2001) Volcanism in the Southern Apennines and Sicily. In: Vai GB, Martini PI (eds) Anatomy of an Orogen. The Apennines and the adjacent Mediterranean basins. Kluwer, Dordrecht, pp 105-120

Belkin HE, De Vivo B (1993) Fluid inclusion studies of ejected nodules from plinian eruptions of Mt. Somma–Vesuvius. J Volcanol Geotherm Res 58:98-100

Belkin HE, Kilburn CRJ, De Vivo B (1993) Sampling and major element chemistry of the recent (AD 1631-1944) Vesuvius activity. J Volcanol Geotherm Res 58:273-290

Belkin HE, De Vivo B, Roedder E, Cortini M (1985) Fluid inclusion geobarometry from ejected Mt. Somma-Vesuvius nodules. Am Mineral 70:288-303

Bell K, Castorina F, Lavecchia G, Rosatelli G, Stoppa F (2004) Is there a mantle plume below Italy? EOS 85:541-547

Bergen van MJ (1985) Common trace element characteristics of crustal- and mantle-derived K-rich magmas from Monte Amiata (central Italy). Chem Geol 48:125-135

Bergen van MJ, Barton M (1984) Complex interaction of aluminous metasedimentary xenoliths and siliceous magma: an example from Mt. Amiata (Central Italy). Contrib Mineral Petrol 86:374-385

Bergen van MJ, Ghezzo C, Ricci CA (1983) Minette inclusions in the rhyodacitic lavas of Mt. Amiata (central Italy): mineralogical and chemical evidence of mixing between Tuscan- and Roman-type magmas. J Volcanol Geotherm Res 19:1-35

Bertagnini A, Sbrana A (1986) Il vulcano di Vico: stratigrafia del complesso vulcanico e sequenze eruttive delle formazioni piroclastiche. Mem Soc Geol It 35:699-713

Bertagnini A, De Rita D, Landi P (1995) Mafic inclusions in the silica-rich rocks of the Tolfa-Ceriti-Manziana volcanic district (Tuscan Province, Central Italy): chemistry and mineralogy. Mineral Petrol 54:261-276

Bertagnini A, Metrich N, Landi P, Rosi M (2003) Stromboli volcano (Aeolian Archipelago, Italy): an open window on the deep-feeding system of a steady state basaltic volcano. J Geophys Res 108, B7, 2336, doi:10.1029/2002JB002146

Bertrand H, Boivin P, Robin C (1990) Petrology and geochemistry of basalts from the Vavilov Basin (Tyrrhenian Sea), Ocean Drilling Program LEG 107, Holes 651A and 655B. In: Kastens KA, Mascle J, et al. (eds) Proc Ocean Drilling Program, Scientific Results, 107: pp 75-89

Bianchini G, Clocchiatti R, Coltorti M, Joron JL, Vaccaro C (1998) Petrogenesis of mafic lavas from the northernmost sector of the Iblean district (Sicily). Eur J Mineral 10:301-315

Bigazzi G, Bonadonna FP, Centamore E, Leone G, Mozzi M, Nisio S, Zanchetta G (2000) New radiometric dating of volcanic ash layers in Periadriatic foredeep basin system, Italy. Palaeogeogr Palaeoclimatol Palaeoecol 155:327-340

Bindi L, Tasselli F, Olmi F, Peccerillo A, Menchetti S (2002) Crystal chemistry of clinopyroxenes from Linosa volcano: implications for modelling magmatic plumbing system. Mineral Mag 66:953-968

Bizzarri R, Ambrosetti P, Argenti P, Gatta GD, Baldanza A (2003) L'affioramento del Caio (Lago di Corbara, Orvieto, Italia Centrale) nell'ambito dell'evoluzione paleogeografica Plio-Pelistocenica della Valle del Tevere: evidenze sedimentologiche e stratigrafiche. Il Quaternario 16: 241-255

Boccaletti M, Guazzone G (1974) Remnant arcs and marginal basins in the Cainozoic development of the Mediterranean. Nature 252:18-21

Boccaletti M, Elter P, Guazzone G (1971) Plate tectonics model for the development of Western Alps and Northern Apennines. Nature 234:108-111

Boccaletti M, Nicolich R, Tortorici L (1984) The Calabrian arc and the Ionian Sea in the dynamic evolution of the central Mediterranean. Mar Geol 55:219-245

Boccaletti M, Nicolich R, Tortorici L (l990a) New data and hypothesis on the development of the Tyrrhenian Basin. Palaeogeogr Palaeoclimatol Palaeoecol 77:15-40

Boccaletti M, Ciaranfi N, Cosentino D, Deiana G, Gelati R, Lentini F, Massari F, Moratti G, Pescatore T, Ricci Lucchi F, Tortorici L (1990b) Palinspastic restoration and paleogeographic reconstruction of the peri-Tyrrhenian area during the Neogene. Palaeogeogr Palaeoclimatol Palaeoecol 77:41-50

Boenzi F, La Volpe L, Rapisardi L (1987) Evoluzione geomorfologica del complesso vulcanico del Monte Vulture (Basilicata). Boll Soc Geol It 106:673-682

Bonardi G, Cavazza W, Perrone V, Rossi S (2001) Calabria-Peloritani terrane and northern Ionian Sea. In: Vai GB, Martini PI (eds) Anatomy of an orogen. The Apennines and the Adjoining Mediterranean Basins. Kluwer, Dordercht, pp 287-306

Bonatti E, Seyler M, Channell J, Geraudeau J, Mascle G (1990) Peridotites drilled from the Tyrrhenian Sea, ODP LEG 107. In: Kastens KA, Mascle J, et al. (eds) Proc Ocean Drilling Program, Scientific Results, 107: pp 37-47

Borelli E, Groppelli G, Aldighieri B, Battaglia A, Gamba A, Gasparon M, Malara F, Pasquaré G, Serri G, Testa B, Wijbrans J (2003) Evoluzione geologica dell'Isola di Capraia (Arcipelago Toscano) nel quadro della geodinamica del Tirreno settentrionale. In: Capozzi R (ed), Geology of the Tyrrhenian Sea and Apennines. Geoacta 2:19-22

Borgia A, Ferrari L, Pasquarè G (1992) Role of gravitational spreading in the tectonic and volcanic evolution of Etna, Italy. Nature 357:231-235

Bosi C, Locardi E (1992) Vulcanismo meso-pleistocenico nell'Appennino laziale-abruzzese. Studi Geol Camerti, Spec Issue CROP 11: pp 319-325

Bosi C, Cittadini A Della Casa G, Messina P, Palieri L (1991) Dati preliminari su alcune successioni tufitiche pleistoceniche dell'Appennino abruzzese. Studi Geol Camerti, Spec Issue CROP 11: pp 313-318

Bousquet JC, Lanzafame G (2004) The tectonics and geodynamics of Mt. Etna: Synthesis and interpretation of geological and geophysical data. In: Bonaccorso A, Calvari S, Coltelli M, Del Negro C, Falsaperla S (eds) Mt. Etna: Volcano Laboratory. Am Geophys Un Mon 143, pp 29-47

Branca S, Del Carlo P (2004) Eruptions of Mt. Etna during the past 3,200 years: a revised compilation integrating historical and stratigraphic records. In: Bonaccorso A, Calvari S, Coltelli M, Del Negro C, Falsaperla S (eds) Mt. Etna: Volcano Laboratory. Am Geophys Un Mon 143, pp 1-27

Branca S, Coltelli M, Groppelli G (2004) Geological evolution of Etna volcano. In: Bonaccorso A, Calvari S, Coltelli M, Del Negro C, Falsaperla S (eds) Mt. Etna: Volcano Laboratory. Am Geophys Un Mon 143, pp 49-63

Brocchini D, La Volpe L, Laurenzi MA, Principe C (1994) Storia evolutiva del Monte Vulture. Plinius 12:22-25

Brocchini D, Di Battistini G, Laurenzi MA, Vernia L, Bargossi GM (2000) New $^{40}Ar/^{39}Ar$ datings on the southeastern sector of the Vulsinian volcanic district (Central Italy). Boll Soc Geol It 119:113-120

Brocchini D, Principe C, Castradori D, Laurenzi MA, Gorla L (2001) Quaternary evolution of the southern sector of the Campanian Plain and early Somma-Vesuvius activity: insights from the Trecase 1 well. Mineral Petrol 73:67-91

Brooks CK, Printzlau I (1978) Magma mixing in mafic alkaline volcanic rocks: the evidence from relict phenocryst phases and other inclusions. J Volcanol Geotherm Res 4:315-331

Brozzetti F, Stoppa F (1995) Le piroclastiti medio-pleistoceniche di Massa Martana-Acquasparta (Umbria): caratteri strutturali e vulcanologici. Il Quaternario 8:95-110

Bruno PP, Di Fiore V, Ventura G (2000) Seismic study of the "41st Parallel" fault system offshore the Campanian-Latial continental margin, Italy. Tectonophysics 324:37-55

Buonasorte G, Fiordelisi A, Pandeli E, Rossi U, Sollevanti F (1987) Stratigraphic correlations and structural setting of the pre-neoautochthonous sedimentary sequences of Northen Latium. Per Mineral 56:111-122

Cadoppi P (1990) Geologia del basamento cristallino nel settore settentrionale del massiccio Dora Maira, Alpi occidentali. PhD Thesis, University of Tourin, Italy, 208 pp

Cadoux A, Pinti DL, Aznar C, Chiesa S, Gillot PY (2005) New chronological and geochemical constraints on the genesis and evolution of Ponza and Palmarola volcanic islands (Tyrrhenian Sea, Italy). Lithos, 81:121-151

Calanchi N, Colantoni P, Gabbianelli G, Rossi PL, Serri G (1984) Physiography of Anchise Seamount and of the submarine part of Ustica (south Tyrrhenian): petrochemistry of dredged volcanic rocks and geochemical characteristics of their mantle sources. Miner Petrogr Acta 28:215-141

Calanchi N, Colantoni P, Rossi PL, Saitta M, Serri G (1989) The Strait of Sicily continental rift systems: physiography and petrochemistry of the submarine volcanic centres. Mar Geol 87:55-83

Calanchi N, De Rosa R, Mazzuoli R, Rossi L, Santacroce R, Ventura G (1993) Silicic magma entering a basaltic magma chamber: eruptive dynamics and magma mixing an example from Salina (Aeolian Islands, Southern Thyrrenian Sea). Bull Volcanol 55:504-522

Calanchi N, Romagnoli C, Rossi PL (1995) Morphostructural and some petrochemical data from the submerged area around Alicudi and Filicudi volcanic islands (Aeolian Arc, southern Tyrrhenian Sea). Mar Geol 123:215-238

Calanchi N, Tranne CA, Lucchini F, Rossi PL, Villa IM (1999) Explanatory notes to the geological map (1:10,000) of Panarea and Basiluzzo islands (Aeolian Arc, Italy). Acta Vulcanol 11:223-243

Calanchi N, Lucchi F, Pirazzoli PA, Romagnoli C, Tranne CA, Radtke U, Reyss JL, Rossi PL (2002a) Late Quaternary relative sea-level changes and vertical movements at Lipari (Aeolian Islands). J Quater Sci 17:459-467

Calanchi N, Peccerillo A, Tranne C, Lucchini F, Rossi PM, Kempton P, Barbieri M, Wu TW (2002b) Petrology and geochemistry of the Island of Panarea: implications for mantle evolution beneath the Aeolian island arc (Southern Tyrrhenian Sea, Italy). J Volcanol Geotherm Res 115:367-395

Calcagnile G, Panza GF (1981) The main characteristics of the lithosphere-asthenosphere system in Italy and surrounding regions. Pure Appl Geophys 119:865-879

Calcagnile G, D'Ingeo F, Farrugia P, Panza GF (1982) The lithosphere in the central-eastern Mediterranean area. Pure Appl Geophys 120:389-406

Calvari S, Coltelli M, Neri M, Pompilio M, Scribano V (1994) The 1991-1993 Etna eruption: chronology and lava flow-field evolution. Acta Vulcanol 4:1-14

Carmignani L, Carosi R, Di Pisa A, Gattiglio M, Musumeci C, Oggiano G, Pertusati P C (1994a) The Hercynian chain in Sardinia (Italy). Geodyn Acta 7:31-47

Carmignani L, Barca S, Disperati L, Fantozzi P, Funedda A, Oggiano G, Pasci S (1994b) Tertiary compression and extension in the Sardinian basement. Boll Geofis Teor Appl 36:5-62

Carmignani L, Decandia FA, Disperati L, Fantozzi PL, Lazzarotto A, Liotta D, Oggiano G (1995) Relationships between the Tertiary structural evolution of

the Sardinia-Corsica-Provençal domain and the northern Apennines. Terra Nova 7:128-137
Carmignani L, Decandia FA, Disperati L, Fantozzi PL, Kligfield R, Lazzarotto A, Liotta D, Meccheri M (2001) Inner Northen Apennines. In: Vai GB, Martini PI (eds) Anatomy of an Orogen. The Apennines and the adjacent Mediterranean basins. Kluwer, Dordrecht, pp 197-213
Carminati E, Wortel MJR, Spakman W, Sabadini R (1998) The role of slab detachment processes in the opening of the western-central Mediterranean basins: some geological and geophysical evidence. Earth Planet Sci Lett 160:651-665
Carter SR, Civetta L (1977) Genetic implications of the isotope and trace element variations in the eastern Sicilian volcanics. Earth Planet Sci Lett 36:168-180
Carveni P, Grasso MF, Romano R, Tricomi S (1991a) Vulcanismo del margine settentrionale ibleo. Mem Soc Geol It 47:417-429
Carveni P, Romano R, Capodicasa A, Tricomi S (1991b) Geologia dell'area vulcanica di Capo Passero (Sicilia sud-orientale). Mem Soc Geol It 47:431-447
Castellarin A, Colacicchi R, Praturlon A, Cantelli C (1982) The Jurassic-Lower Pliocene history of the Ancona-Anzio line (Central Italy). Mem Soc Geol It 24:243-260
Castorina F, Stoppa F, Cundari A, Barbieri M (2000) An enriched mantle source for Italy's melilitite-carbonatite association as inferred by its Nd-Sr isotope signature. Mineral Mag 64:625-639
Catalano R, Doglioni C, Merlini S (2001) On the Mesozoic Ionian basin. Geophys J Int 144:49-64
Cavarretta G, Lombardi G (1990) Origin of sulfur in the Quaternary perpotassic melts of Italy: evidence from haüyne sulfur isotope data. Chem Geol 82:15-20
Cavazza W, Wezel FC (2003) The Mediterranean region. A geological primer. Episodes 26:160-168
Cellai D, Conticelli S, Menchetti S (1994) Crystal-chemistry of clinopyroxenes from potassic and ultrapotassic rocks in central Italy: implications for their genesis. Contrib Mineral Petrol 116:301-315
Cello G, Mazzoli S (1999) Apennine tectonics in southern Italy. A review. J Geodyn 27:191-211
Chester DK, Duncan AN, Guest JE, Kilburn CRJ (1985) Mount Etna: The anatomy of a volcano. Cambridge University Press, Cambridge, 404 pp
Chiesa S, Floris B, Gillot PY, Prosperi L, Vezzoli L (1995) Il Vulcano di Roccamonfina. In: Lazio Meridionale. ENEA, Rome, pp 128-150
Chiesa S, Poli S (1988) Island of Ischia. Petrology. In: Vezzoli L (ed) Island of Ischia. Quad Ric Sci CNR Rome 114, 10: pp 72-93
Chopin C (1984) Very-high-pressure metamorphism in western Alps: implications for subduction of continental crust. Phil Trans R Soc London A321:183-197
Ciarapica G, Passeri L (1998) Evoluzione paleogeografica degli Appennini. Atti Tic Sci Terra 40:233-290
Cigolini C (1999) "High pressure" dunitic ejecta of kimberlitic affinity in recent pyroclastic deposits from Mount Vesuvius: inference on their genesis and evolution. Atti Acc Sc Fis, Torino, 133:149-158

Cinque A, Civetta L, Orsi G, Peccerillo A (1988) Geology and geochemistry of the island of Ustica (Southern Tyrrhenian Sea). Rend Soc It Mineral Petrol 43:987-1002

Cioni R, Clocchiatti R, Di Paola GM, Santacroce R, Tonarini S (1982) Miocene calc-alkaline heritage in the Pliocene post-collisional volcanism of Monte Arci (Sardinia, Italy). J Volcanol Geotherm Res 14:133-167

Cioni R, Laurenzi MA, Sbrana A, Villa IM (1993) $^{40}Ar/^{39}Ar$ chronostratigraphy of the initial activity of the Sabatini volcanic complex (Italy). Boll Soc Geol It 112:251-263

Cioni R, Civetta L, Marianelli P, Metrich N, Santacroce R, Sbrana A, (1995) Compositional layering and syneruptive mixing of a periodically refilled shallow magma chamber: the AD 79 Plinian eruption of Vesuvius. J Petrol 36:739-776

Cioni R, Marianelli P, Santacroce R (1997) Thermal and compositional evolution of the shallow magma chambers of Vesuvius: Evidence from pyroxene phenocrysts and melt inclusions. J Geophys Res 103:18277-18294

Civetta L, Santacroce R (1992) Steady state magma supply in the last 3400 years of Vesuvius activity. Acta Vulcanol 2:147-159

Civetta L, Orsi G, Scandone P, Pece R (1978) Eastwards migration of the Tuscan anatectic magmatism due to anticlockwise rotation of the Apennines. Nature 276:604-606

Civetta L, Innocenti, F, Manetti P, Peccerillo A, Poli G (1981) Geochemical characteristics of potassic volcanics from Mt. Ernici (Southern, Latium, Italy). Contrib Mineral Petrol 78:37-47

Civetta L, Cornette Y, Crisci G, Gillot PY, Orsi G, Requejo CS (1984) Geology, geochronology and chemical evolution of the island of Pantelleria. Geol Mag 121:541-562

Civetta L, Cornette Y, Gillot PY, Orsi G (1988) The eruptive history of Pantelleria (Sicily Channel) in the last 50 ka. Bull Volcan 50:47-57

Civetta L, Galati R, Santacroce R (1991a) Magma mixing and convective compositional layering within the Vesuvius magma chamber. Bull Volcanol 53:287-300

Civetta L, Carluccio E, Innocenti F, Sbrana A, Taddeucci G (1991b) Magma chamber evolution under the Phlegraean Field during the last 10 ka: trace element and isotope data. Eur J Mineral 3:415 428

Civetta L, Gallo G, Orsi G (1991c) Sr- and Nd-isotope and trace-element constraints on the chemical evolution of the magmatic system of Ischia (Italy) in the last 55 ka. J Volcanol Geotherm Res 46:213-230

Civetta L, D'Antonio M, Orsi G, Tilton GR (1998) The geochemistry of volcanic rocks from Pantelleria Island, Sicily Channel: petrogenesis and characteristics of the mantle source region. J Petrol 39:1453-1491

Civetta L, D'Antonio M, De Lorenzo S, Di Renzo V, Gasparini P (2004) Thermal and geochemical constraints on the 'deep' magmatic structure of Mt. Vesuvius. J Volcanol Geotherm Res 133:1-12

Clausen C, Holm PM (1990) Origin of acid volcanics of the Tolfa district, Tuscan Province, central Italy: an elemental and Sr-isotopic study. Contrib Mineral Petrol 105:403-411

Clocchiatti R, Joron JL, Treuil M (1988) The role of selective alkali contamination in the evolution of recent historic lavas of Mt. Etna. J Volcanol Geotherm Res 34:241-249

Clocchiatti R, Weisz J, Mosbah M, Tanguy JC (1992) Coexistence de «verres» alkalins et tholéiitiques saturés en CO_2 dans les olivines des hyaloclastites d'Aci Castello (Etna, Sicile, Italie). Arguments en faveur d'un manteau anormal et d'un réservoir profond. Acta Vulcanol 2:161-173

Clocchiatti R, Schiano P, Ottolini L, Bottazzi P (1998) Earlier alkaline and transitional pulsation of Mt Etna volcano. Earth Planet Sci Lett 163:399-407

Colantoni P, Fabbri A, Gallignani P, Sartori R (1981) Lithologic and stratigraphic map of the Italian seas. Litografia Artistica Cartografica, Firenze

Cole PD, Guest JE, Duncan AM, Chester DK, Bianchi R (1992) Post-collapse volcanic history of calderas on a composite volcano: an example from Roccamonfina volcano, southern Italy. Bull Volcanol 54:253-266

Condomines M, Allegre CJ (1980) Age and magmatic evolution of Stromboli volcano from ^{230}Th-^{238}U disequilibrium data. Nature 288:354-357

Condomines M, Tanguy JC, Kieffer G, Allegre CJ (1982) Magmatic evolution of a volcano studied by ^{230}Th/^{238}U disequilibrium and trace elements systematics: The Etna case. Geochim Cosmochim Acta 46:1397-1416

Condomines M, Tanguy JC, Michaud V (1995) Magma dynamics at Mt Etna: constraints from U-Th-Ra-Pb radioactive disequilibria and Sr isotopes in historical lavas. Earth Planet Sci Lett 132:25-41

Conte AM, Dolfi D (2002) Petrological and geochemical characteristics of Plio-Pleistocene volcanics from Ponza Island (Tyrrhenian Sea, Italy). Mineral Petrol 74:75-94

Conticelli S (1989) Genesi del magmatismo alcalino-potassico dell'Italia centrale: evidenze petrologiche, geochimiche e petrologico-sperimentali. PhD Thesis, University of Florence, 369 pp

Conticelli S (1998) The effect of crustal contamination on ultrapotassic magmas with lamproitic affinity: mineralogical, geochemical and isotope data from the Torre Alfina lavas and xenoliths, Central Italy. Chem Geol 149:51-81

Conticelli S, Peccerillo A (1990) Petrological significance of high-pressure ultramafic xenoliths from ultrapotassic rocks of Central Italy. Lithos 24:305-322

Conticelli S, Peccerillo A (1992) Petrology and geochemistry of potassic and ultrapotassic volcanism in Central Italy: petrogenesis and inferences on the evolution of the mantle sources. Lithos 28:221-240

Conticelli S, Francalanci L, Manetti P, Peccerillo A (1987) Evolution of Latera volcano, Vulsinian district (Central Italy): stratigraphical and petrological data. Per Mineral 56:175-199

Conticelli S, Francalanci L, Santo AP (1991) Petrology of the final stage Latera lavas: Mineralogical, Geochemical and Sr- isotopic data and their bearing on

the genesis of some potassic magmas in Central Italy. J Volcanol Geotherm Res 46:187--212
Conticelli S, Manetti P, Menichetti S (1992) Mineralogy, geochemistry and Sr isotopes in orendites from South Tuscany: constraints on their genesis and evolution. Eur J Mineral 4:1359-1375
Conticelli S, Francalanci L, Manetti P, Cioni R, Sbrana A (1997) Petrology and geochemistry of the ultrapotassic rocks from the Sabatini volcanic district, central Italy: the role of evolutionary processes in the genesis of variably enriched alkaline magmas. J Volcanol Geotherm Res 75:107-136
Conticelli S, Bortolotti V, Principi G, Laurenzi M, Vaggelli G, D'Antonio M (2001) Petrology, mineralogy and geochemistry of a mafic dyke from Monte Castello, Elba Island, Italy. Ofioliti 26:249-262
Conticelli S, D'Antonio M, Pinarelli L, Civetta L (2002) Source contamination and mantle heterogeneity in the genesis of Italian potassic and ultrapotassic volcanic rocks: Sr-Nd-Pb isotope data from Roman Province and Southern Tuscany. Mineral Petrol 74:189-222
Conticelli S, Melluso L, Perini G, Avanzinelli R, Boari E (2004) Petrologic, geochemical and isotopic characteristics of potassic and ultrapotassic magmatism in central-southern Italy: inferences on its genesis and on the nature of mantle sources. Per Mineral 73:135-164
Corsaro RA, Cristofolini R (1996) Origin and differentiation of recent basaltic magmas from Mount Etna. Mineral Petrol 57:1-21
Corsaro RA, Cristofolini R (1997) Geology, geochemistry and mineral chemistry of tholeiitic to transitional Etnean magmas. Acta Vulcanol 9:55-66
Corsaro RA, Cristofolini R (2000) Subaqueous volcanism in the Etnaean area: evidence for hydromagmatic activity and regional uplift inferred from the Castle Rock of Acicastello. J Volcanol Geotherm Res 95:29-225
Corsaro RA, Pompilio M (2004) Dynamics of magmas at Mount Etna. In: Bonaccorso A, Calvari S, Coltelli M, Del Negro C, Falsaperla S (eds) Mt. Etna: Volcano Laboratory. Am Geophys Un Mon 143, pp 91-110
Cortini M (1981) Aeolian Island Arc (South Tyrrhenian Sea) magma heterogeneities in historical lavas: Sr and Pb isotopic evidence. Bull Volcanol 44:711-722
Cortini M, Hermes OD (1981) Sr isotopic evidence for a multi-source origin of the potassic magmas in the Neapolitan area (south Italy) Contrib Mineral Petrol 77:47-55
Cortini M, Scandone R (1982) The feeding system of Vesuvius between 1754 and 1944. J Volcanol Geotherm Res 12:393-400
Cox HG, Hawkesworth CJ, O'Nions RK, Appleton JD (1976) Isotopic evidence for the derivation of some Roman Region volcanics from anomalously enriched mantle. Contrib Mineral Petrol 56:173-180
Crisci GM, De Francesco AM, Mazzuoli R, Poli G, Stanzione D (1989) Geochemistry of recent volcanics of Ischia Island, Italy: evidences for fractional crystallisation and magma mixing. Chem Geol 78:15-33

Crisci GM, De Rosa R, Esperança S, Mazzuoli R, Sonnino M (1991) Temporal evolution of a three component system: the Island of Lipari (Aeolian Arc, southern Italy). Bull Volcanol 53:207-221

Cristiani C, Mazzuoli R (2003) Monte Amiata volcanic products and their inclusions. Per Mineral 72:169-181

Cundari A (1975) Mineral chemistry and petrogenetic aspects of the Vico lavas, Roman Volcanic Region, Italy. Contrib Mineral Petrol 53:129-144

Cundari A (1979) Petrogenesis of leucite-bearing lavas in the Roman volcanic region, Italy. The Sabatini Lavas. Contrib Mineral Petrol 70:9-21

Cundari A, Ferguson AK (1991) Petrogenetic relationships between melilitite and lamproite in the Roman Comagmatic Region: the lavas of San Venanzo and Cupaello. Contrib Mineral Petrol 107:343-357

Cundari A, Mattias PP (1974) Evolution of the of the Vico lavas, Roman Volcanic Region, Italy. Bull Volcanol 38:98-114

Dallai L, Freda C, Gaeta M (2004) Oxygen isotope geochemistry of pyroclastic clinopyroxene monitors carbonate contributions to Roman-type ultrapotassic magmas. Contrib Mineral Petrol 148:247-263

Daly RA (1918) Genesis of alkaline rocks. J Geol 26:97-134

D'Antonio M, Di Girolamo P (1994) Petrological and geochemical study of mafic shoshonitic volcanics from Procida-Vivara and Ventotene islands (Campanian Region, South Italy). Acta Vulcanol 5:69-80

D'Antonio M, Tilton GR, Civetta L (1996) Petrogenesis of Italian alkaline lavas deduced from Pb-Sr-Nd isotope relationships. In: Basu A, Hart SR (eds) Isotopic Studies of Crust-Mantle Evolution. Am Geophys Un Mon 95: pp 253-267

D'Antonio M, Civetta L, Orsi G, Pappalardo L, Piochi M, Carandente A, De Vita S, Di Vito MA, Isaia R (1999a) The present state of the magmatic system of the Campi Flegrei caldera based on the reconstruction of its behaviour in the past 12 ka. J Volcanol Geotherm Res 91:247-268

D'Antonio M, Civetta L, Di Girolamo P (1999b) Mantle source heterogeneity in the Campanian region (south Italy) as inferred from geochemical and isotopic features of mafic volcanic rocks with shoshonitic affinity. Mineral Petrol 67:163-192

De Astis G, La Volpe L, Peccerillo A, Civetta L (1997) Volcanological and petrological evolution of Vulcano island (Aeolian arc, southern Tyrrhenian Sea). J Geophys Res 102:8021-8050

De Astis G, Peccerillo A, Kempton PD, La Volpe L, Wu TW (2000) Transition from calc-alkaline to potassium-rich magmatism in subduction environments: geochemical and Sr, Nd, Pb isotopic constraints from the island of Vulcano (Aeolian arc). Contrib Mineral Petrol 139:684-703

De Astis G, Kempton PD, Peccerillo A, Wu TW (2005) Geochemical and Sr-Nd-Pb isotope composition of Vulture and Campanian Province volcanics (southern Italy): implications for mantle evolution and geodynamics. Submitted for publication

De Fino M, La Volpe L, Peccerillo A, Piccarreta G, Poli G (1986) Petrogenesis of Monte Vulture volcano, Italy: inferences from mineral chemistry, major and trace element data. Contrib Mineral Petrol 92:135-145

De Rita D, Funiciello R, Rossi U, Sposato A (1983) Structure and evolution of the Sacrofano-Baccano caldera, Sabatini Volcanic Complex, Rome. J Volcanol Geotherm Res 17:219-236

De Rita D, Funiciello R, Pantosti D, Salvini F, Sposato A, Velona M (1986) Geological and structural characteristics of the Pontine islands (Italy) and implications with the evolution of the Tyrrhenian margin. Mem Soc Geol It 36:55-65

De Rita D, Funiciello R, Corda L, Sposato A, Rossi U (1993) Volcanic Units. In: Di Filippo M (ed), Sabatini Volcanic Complex. Quad Ric Sci CNR Rome, 114, 11: pp 33-79

De Rita D, Faccenna C, Funiciello R, Rosa C (1995) Stratigraphy and volcanotectonics. In: Trigila R (ed) The volcano of the Alban Hills. University La Sapienza, Rome, pp 33-71

De Rosa R, Gouillou H, Mazzuoli R, Ventura G (2003) New unspiked K-Ar ages of volcanic rocks of the central and western sector of the Aeolian Islands: reconstruction of the volcanic stages. J Volcanol Geotherm Res 120:161-178

De Vita S, Laurenzi MA, Orsi G, Voltaggio M (1998) Application of $^{40}Ar/^{39}Ar$ and ^{230}Th dating methods to the chronostratigraphy of Quaternary basaltic volcanic areas: the Ustica Island case history. Quat Intern 47/48:117-127

De Vita S, Orsi G, Civetta L, D'Antonio M, et al. (1999) The Agnano-Monte Spina eruption (4.1 ka) in the resurgent, nested CampiFlegrei caldera (Italy). J Volcanol Geotherm Res 91:269-301

De Vivo B, Rolandi G, Gans PB, Calvert A, Bohrson WA, Spera FJ, Belkin HE (2001) New constraints on the pyroclastic eruptive history of the Campanian volcanic Plain (Italy). Mineral Petrol 73:47-65

Decandia FA, Lazzarotto A, Liotta D, Cernobori L, Nicolich R (1998) The CROP 03 traverse: insights on post-collisional evolution of Northern Apennines. Mem Soc Geol It 52:427-439

Del Moro A, Gioncada A, Pinarelli L, Sbrana A, Joron JL (1998) Sr, Nd, Pb isotope evidence for open system evolution at Vulcano, Aeolian Arc, Italy. Lithos 43:81-106

Della Vedova B, Bellani S, Pelli G, Squarci P (2001) Deep temperatures and surface heath distribution. In: Vai GB, Martini PI (eds) Anatomy of an Orogen. The Apennines and the adjacent Mediterranean basins. Kluwer, Dordrecht, pp 65-76

Della Vedova B, Marson I, Panza G, Suhadolc P (1991) Upper mantle properties of the Tuscan-Tyrrhenian area: a key for understanding the recent tectonic evolution of the Italian region. Tectonophysics 195:311-318

Della Ventura G, William CT, Cabella R, Oberti R, Caprilli E, Bellatreccia F (1999) Britholite-hellandite intergrowths and associated REE-minerals from the alkali syenitic ejecta of the Vico volcanic complex (Latium, Italy): petrological implications bearing on REE mobility in volcanic systems. Eur J Mineral 11:843-854

Dercourt J, Zonenshain LP, Ricou LE, et al. (1986) Geological evolution of the Tethys belt from the Atlantic to the Pamirs since the Lias. Tectonophysics 123:241-315

Di Battistini G, Montanini A, Zerbi M (1990) Geochemistry of volcanic rocks from southeastern Montiferro. Neues Jahrb Mineral Abh 162:35-67

Di Battistini G, Montanini A, Vemia L, Bargossi GM, Castorina F (1998) Petrology and geochemistry of ultrapotassic rocks from the Montefiascone volcanic complex (Central Italy): magmatic evolution and petrogenesis. Lithos 43:169-195

Di Battistini G, Montanini A, Vernia L, Venturelli G, Tonarini S (2001) Petrology of melilite-bearing rocks from the Montefiascone Volcanic complex (Roman Magmatic Province): new insights into the ultrapotassic volcanism of Central Italy. Lithos 59:1-24

Di Filippo M (ed) (1993) Sabatini Volcanic Complex. Quad Ric Sci CNR Rome, 114, 11:109 pp

Di Girolamo P (1978) Geotectonic settings of Miocene Quaternary volcanism in and around the eastern Tyrrhenian Sea border (Italy) as deduced from major element geochemistry. Bull Volcanol 41:229-250

Di Girolamo P, Stanzione D (1973) Lineamenti geologici e petrologici dell'isola di Procida. Rend Soc It Mineral Petrol 29:81-125

Di Girolamo P, Nardi G, Rolandi G, Stanzione D (1976) Occurrence of calc-alkaline two-pyroxene andesites from deep bore-holes in the Phlegraean Fields. Petrographic and petrochemical data. Rend Accad Sci Fis Mat Napoli 43:1-29

Di Grande A, Mazzoleni P, Lo Giudice A, Beccaluva L, Macciotta G, Siena F (2002) Subaerial Plio-Pleistocene volcanism in the geo-petrographic and structural context of the north-central Iblean region (Sicily). Per Mineral 71:159-189

Di Liberto V (2003) Mantle-crust interaction under the Aeolian arc (Italy): inferences from He and Sr isotopes. PhD Thesis, University of Palermo, 73 pp

Di Sabatino B, Della Ventura GC (1982) Genesi ipoabissale di fusi legati al vulcanismo alcalino-potassico. II. Studio petrografico e petrologico degli inclusi termometamorfici delle vulcaniti cimine ed ipotesi genetiche. Per Mineral 51:311-359

Dietrich V, Emmermann R, Keller J, Puchelt H (1977) Tholeiitic basalts from the Tyrrhenian Sea floor. Earth Planet Sci Lett 36:285-296

Dini A, Innocenti F, Rocchi S, Tonarini S, Westerman S (2002) The magmatic evolution of the late Miocene laccolith-pluton-dyke granitic complex of Elba Island, Italy. Geol Mag 139:257-273

Doglioni C (1991) A proposal for the kinematic modelling of W-dipping subduction: possible applications to the Tyrrhenian-Appennines system. Terra Nova 3:423-434

Doglioni C, Gueguen E, Sabat F, Fernandez M (1997) The western Mediterranean extensional basins and the Alpine Orogen. Terra Nova 9:109-112

Doglioni C, Mongelli F, Pialli G (1998) Boudinage of the Alpine belt in the Apenninic back-arc. Mem Soc Geol It 52:457-468

Doglioni C, Harabaglia P, Merlini S, Mongelli F, Peccerillo A, Piromallo C (1999) Orogens and slabs vs. their direction of subduction. Earth Sci Review 45:167-208

Doglioni C, Innocenti F, Mariotti G (2001) Why Mt. Etna?. Terra Nova 13:25-31

Doglioni C, Innocenti F, Morellato C, Procaccianti D, Scrocca D (2004) On the Tyrrhenian Sea opening. Mem Descr Carta Geol It 64:147-164

Dolfi D, Trigila R (1978) Clinopyroxenes from potassic lavas of Central Italy Quaternary volcanism. Progr Exp Petrol, NERC, UK, Rep n 4, pp 18-22

D'Orazio M, Tonarini S, Innocenti F, Pompilio M (1997) Northern Valle del Bove volcanic succession (Mt. Etna, Sicily): petrography, geochemistry and Sr-Nd isotope data. Acta Vulcanol 9:73-86

D'Orazio M, Innocenti F, Petrini R, Serri G (1994) Il vulcano di Radicofani nel quadro del magmatismo neogenico-quaternario dell'Appennino Settentrionale. Studi Geol Camerti, 1994, 1: 79-92

D'Orazio M, Laurenzi MA, Villa IM (1991) $^{40}Ar/^{39}Ar$ dating of a shoshonitic lava flow of the Radicofani volcanic center (Southern Tuscany). Acta Vulcanol, 1, 63-67

Dostal J, Coulon C, Dupuy C (1982) Cainozoic andesitic rocks of Sardinia (Italy). In: Thorpe RS (ed) Andesites: Orogenic andesites and related rocks. Wiley, New York, pp 353-370

Downes H (2001) Formation and modification of the shallow sub-continental lithospheric mantle: a review of geochemical evidence from ultramafic xenolith suites and tectonically emplaced ultramafic massifs of Western and Central Europe. J Petrol 42:233-250

Downes H, Thirlwall MF, Trayhorn SC (2001) Miocene subduction-related magmatism in southern Sardinia: Sr-Nd and oxygen isotopic evidence for mantle source enrichment. J Volcanol Geotherm Res 106:1-21

Dupuy C, Dostal J, Girod M, Liotard JM (1981) Origin of volcanic rocks from Stromboli (Italy). J Volcanol Geotherm Res 10:49-65

Edgar AD (1987) The genesis of alkaline magmas with emphases on their source region: inferences from experimental studies. In: Fitton JG, Upton BGJ (eds) Alkaline igneous rocks. Geol Soc Sp Publ 30: pp 205-220

Edgar AD, Green DH, Hibberson WO (1976) Experimental petrology of highly potassic magmas. J Petrol 17:339-356

Ellam RM, Harmon RS (1990) Oxygen isotope constraints on the crustal contributions to the subduction-related magmatism of the Aeolian islands, southern Italy. J Volcanol Geotherm Res 44:105-122

Ellam RM, Menzies MA, Hawkesworth CJ, Leeman WP, Rosi M, Serri G (1988) The transition from calcalkaline to potassic orogenic magmatism in the Aeolian Islands, Southern Italy. Bull Volcanol 50:386-398

Ellam RM, Hawkesworth CJ, Menzies MA, Rogers NW (1989) The volcanism of southern Italy: role of subduction and the relationships between potassic and sodic alkaline magmatism. J Geophys Res 94:4589-4601

Esperança S, Crisci GM (1995) The island of Pantelleria: a case for the development of DMM-HIMU isotopic compositions in a long-lived extensional setting. Earth Planet Sci Lett 136:167-182

Esperança S, Crisci GM, De Rosa R, Mazzuoli R (1992) The role of the crust in the magmatic evolution of the Island of Lipari (Aeolian Islands, Italy). Contrib Mineral Petrol 112:450-562

Faccenna C, Mattei M, Funicello R, Jolivet L (1997) Styles of back-arc extension in the Central Mediterranean. Terra Nova 9:126-130

Faccenna C, Piromallo C, Crespo-Blanc A, Jolivet L, Rossetti F (2004) Lateral slab deformation and the origin of the western Mediterranean arcs. Tectonics, 23, doi:10.1029/2002TC001488

Faraone D (2002) I vulcani e l'uomo. Miti, Leggende e Storia. Liguori, Napoli, 341 pp

Falsaperla S, Lanzafame G, Longo V, Spampinato S (1999) Regional stress field in the area of Stromboli (Italy): insights into structural data and crustal tectonic earthquakes. J Volcanol Geotherm Res 88:147-166

Farley KA, Neroda E (1998) Noble gases in the Earth's mantle. Ann Rev Earth Planet Sci 26:189-218

Federico M (1995) Mineralogy. In: Trigila R (ed) The volcano of the Alban Hills. University La Sapienza, Rome, pp 73-93

Federico M, Peccerillo A (2002) Mineral chemistry and petrogenesis of granular ejecta from the Alban Hills volcano (Central Italy). Mineral Petrol 74:223-252

Federico M, Peccerillo A, Barbieri M, Wu TW (1994) Mineralogical and geochemical study on granular xenoliths from the Alban Hills volcano (Central Italy): bearing on evolutionary processes in potassic magma chambers. Contrib Mineral Petrol 115:384-401

Feldstein SN, Halliday AN, Davies GR, Hall CM (1994) Isotope and chemical microsampling constraints on the history of a S-type rhyolite, San Vincenzo, Tuscany (Italy). Geochim Cosmochim Acta 58:943-958

Feraud G (1990) ^{39}Ar-^{40}Ar analysis on basaltic lava series of Vavilov Basin, Tyrhenian Sea (Ocean Drilling Program, LEG 107, Holes 655B and 651A). In: Kastens KA, Mascle J, et al. (eds) Proc Ocean Drilling Program, Scientific Results, 107: pp 93-97

Ferrara G, Tonarini S (1985) Radiometric geochronology in Tuscany: results and problems. Rend Soc It Mineral Petrol 40:111-124

Ferrara G, Laurenzi MA, Taylor HP, Tonarini S, Turi B (1985) Oxygen and strontium isotopic studies of K-rich volcanic rocks from the Alban Hills, Italy. Earth Planet Sci Lett 75:13-28

Ferrara G, Preite-Martinez M, Taylor HP, Tonarini S, Turi B (1986) Evidence for crustal assimilation, mixing of magmas, and a ^{87}Sr-rich upper mantle. Contrib Mineral Petrol 92:269-280

Ferrara G, Petrini R, Serri G, Tonarini S (1989) Petrology and isotope-geochemistry of San Vincenzo rhyolites (Tuscany, Italy). Bull Volcanol 51:379-388

Ferrari L, Conticelli S, Burlamacchi L, Manetti P (1996) Volcanological evolution of the Monte Amiata, Southern Tuscany: new geological and petrochemical data. Acta Vulcanol 8:41-56

Finetti IR, Boccaletti M, Bonini M, Del Ben A, Geletti R, Pipan M, Sani F (2001) Crustal section based on CROP seismic data across the North Tyrrhenian-Northen Apennines-Adriatic Sea. Tectonophysics 43:135-163

Foley SF (1992) Vein-plus-wall-rock melting mechanisms in the lithosphere and the origin of potassic alkaline magmas. Lithos 28:435-453

Foley SF, Wheller GE (1990) Parallels in the origin of the geochemical signature of island-arc volcanics and continental potassic igneous rocks: The role of residual titanates. Chem Geol 85:1-18

Foley SF, Venturelli G, Green DH, Toscani L (1987) The ultrapotassic rocks: characteristics classification, and constraints for petrogenetic models. Earth Sci Rev 24:81-134

Fornaseri M (1985) Geochronology of volcanic rocks from Latium (Italy). Rend Soc It Mineral Petrol 40:73-106

Fornaseri M, Scherillo A, Ventriglia U (1963) La regione vulcanica dei Colli Albani. CNR, Rome, 561 pp

Foulger GR, Nathland JH, Presnall DC, Anderson DL (eds) (2005) Plates, plumes and paradigms. Geol Soc Am Spec Publ 388, in press.

Francalanci L, Manetti P, Peccerillo A (1989) Volcanological and magmatological evolution of Stromboli volcano (Aeolian Islands): the roles of fractional crystallization, magma mixing, crustal contamination, and source heterogeneity. Bull Volcanol 51:355-378

Francalanci L, Manetti P, Peccerillo A, Keller J (1993a) Magmatological evolution of the Stromboli volcano (Aeolian arc, Italy): inferences from major, trace element and Sr isotopic characteristics of lavas and pyroclastic rocks. Acta Vulcanol 3:127-151

Francalanci L, Taylor SR, McCulloch MT, Woodhead J (1993b) Geochemical and isotopic variations in the calc-alkaline rocks of Aeolian Arc (Southern Italy): constraints on the magma genesis. Contrib Mineral Petrol 113:300-313

Francalanci L, Avanzinelli R, Petrone CM, Santo A (2004) Petrochemical and magmatological characteristics of the Aeolian Arc volcanoes, southern Tyrrhenian Sea, Italy: inferences on shallow level processes and magma source variations. Per Mineral 73:75-104

Franceschini F, Innocenti F, Marsi A, Tamponi M, Serri G (2000) Petrography and chemistry of the buried Pliocene Castel di Pietra pluton (Southern Tuscany, Italy). Neues Jahrb Geol Palaeontol 215:17-46

Freda C, Gaeta M, Palladini DM, Trigila R (1997) The Villa Senni eruption (Alban Hills, central italy): the role of H_2O and CO_2 on the magma chamber evolution and on the eruptive scenario. J Volcanol Geotherm Res 78:103-120

Frey FA, Green DH, Roy SD (1978) Integrated models of basalt petrogenesis: a study of quartz tholeiites to olivine melilites from South-Eastern Australia utilizing geochemical and experimental petrological data. J Petrol 19:463 -513

Frezzotti ML, Peccerillo A (2004) Fluid inclusion and petrological studies elucidate reconstruction of magma conduits. Eos 85:157-163

Frezzotti ML, Peccerillo A, Bonelli R (2003) Magma ascent rates and depths of crustal magma reservoirs beneath the Aeolian volcanic arc (Italy): inferences from fluid and melt inclusions in xenoliths. In: De Vivo B, Bodnar RJ (eds) Melt Inclusions in Volcanic Systems: Methods, Applications and Problems. Elsevier, Amsterdam, pp 185-205

Frezzotti ML, Zanon V, Peccerillo A, Nikogossian I (2004b) Silica-rich melts in quartz xenoliths from Vulcano island and their bearing on processes of crustal anatexis and crust-magma interaction beneath the Aeolian Arc, southern Italy. J Petrol 45:3-26

Funiciello R, Parotto M (1978) Il substrato sedimentario nell'area dei Colli Albani: considerazioni geodinamiche e paleogeografiche sul margine tirrenico dell'Appennino centrale. Geol Rom 17:233-287

Funiciello R, Locardi E, Parotto M (1976) Lineamenti geologici dell'area Sabatina Orientale. Mem Soc Geol It 95:831-849

Fuster JM, Gastesi P, Sagredo J, Fermoso ML (1967) Las rocas lamproitica del SE de España. Estud Geol Madrid 23:53-69

Gabbianelli G, Gillot PY, Lanzafame G, Romagnoli C, Rossi PL (1990) Tectonic and volcanic evolution of Panarea (Aeolian Islands, Italy). Mar Geol 92:313-326

Gabbianelli G, Romagnoli C, Rossi PL, Calanchi N (1993) Marine geology of the Panarea-Stromboli area (Aeolian Archipelago, Southeastern Tyrrhenian sea). Acta Vulcanol 3:11-20

Gaeta M, Freda C, Christiensen JN, Dallai L, Marra F, Karner DB, Scarlato P (2005) Evolution of mantle source for ultrapotasic magmas of the Alban Hills Volcanic District (Central Italy). Lithos, submitted

Gallo F, Giammetti F, Venturelli G, Vernia L (1984) The kamafugitic rocks from San Venanzo and Cupaello, central Italy. Neues Jahrb Mineral Monatsh 1984:198-210

Gasperini D, Blichert-Toft J, Bosch D, Del Moro A, Macera P, Télouk P, Albaréde F (2000) Evidence from Sardinian basalt geochemistry for recycling of plume heads into the Earth's mantle. Nature 408:701-704

Gasperini D, Blichert Toft J, Bosch D, Del Moro A, Macera P, Albaréde F (2002) Upwelling of deep mantle material through a plate window: evidence from the geochemistry of Italian basaltic volcanics. J Geophys Res 107, B12, 2367, doi:10.1029/2001JB000418

Gertisser R, Keller J (2000) From basalt to dacite: origin and evolution of the calcalkaline series of Salina, Aeolian Arc, Italy. Contrib Mineral Petrol 139:607-626

Ghiara MR, Lirer L (1977) Mineralogy and geochemistry of the "low potassium" series of the Roccamonfina volcanic suite (Campania, South Italy). Bull Volcanol 40:39-56

Gianelli G, Laurenzi M (2001) Age and cooling rate of the geothermal system of Larderello. Trans Geotherm Resour Counc 25:731-735

Giannetti B (1964) Contributo alla conoscenza del vulcano di Roccamonfina. Le ultime manifestazioni eruttive della caldera. Boll Soc Geol It 83:87-133
Giannetti B, De Casa G (2000) Stratigraphy, chronology, and sedimentology of ignimbrites from the white trachytic tuff, Roccamonfina volcano, Italy. J Volcanol Geotherm Res 96:243-295
Giannetti B, Ellam R (1994) The primitive lavas of Rocccamonfina volcano, Roman region, Italy: new coinstraints on melting processes and source mineralogy. Contrib Mineral Petrol 116:21-31
Giannetti B, Luhr J L (1990) Phlogopite-clinopyroxenite nodules from the high-K magmas, Roccamonfina Volcano, Italy: evidence for a low-pressure metasomatic origin. Earth Planet Sci Lett 101:404-424
Giannetti B, Luhr JF (1983) The White Trachytic Tuff of Roccamonfina volcano (Roman Region, Italy). Contrib Mineral Petrol 84:235-252
Gill 1981 JB (1981) Orogenic andesites and plate tectonics. Springer, Berlin, 358 pp
Gillot PY (1987) Histoire volcanique des Iles Eoliennes: arc insulaire ou complexe orogénique anulaire? Doc Trav IGAL 11:35-42
Gillot PY, Chiesa S, Pasquare G, Vezzoli L (1982) <33000yr K/Ar dating of the volcano-tectonic horst of the Isle of Ischia, Gulf of Naples. Nature 299:242-245
Gillot PY, Keller J (1993) Radiochronological dating of Stromboli. Acta Vulcanol 3:69-77
Gillot PY, Kieffer G, Romano R (1994) The evolution of Mt. Etna in the light of potassium-argon dating. Acta Vulcanol 5:81-87
Gioncada A, Mazzuoli R, Bisson M, Pareschi MT (2003) Petrology of volcanic products younger than 42 ka on the Lipari-Vulcano complex (Aeolian Islands, Italy): an example of volcanism controlled by tectonics. J Volcanol Geotherm Res 122:191-220
Giraud A, Dupuy C, Dostal J (1986) Behaviour of trace elements during magmatic processes in the crust: application to silicic volcanic rocks of Tuscany. Chem Geol 57:269-288
Graham D, Allard P, Kilburn CRJ, Spera F, Lupton JE (1993) Helium isotopes in some historical lavas from Mount Vesuvius. J Volcanol Geotherm Res 58:359-366
Granet M, Wilson M, Achauer U (1995) Imaging a mantle plume beneath the French Massif Central. Earth Planet Sci Lett 136:281-296
Grasso M (2001) The Apenninic-Maghrebian orogen in Southern Italy, Sicily and adjacent areas. In: Vai GB, Martini PI (eds) Anatomy of an Orogen. The Apennines and adjacent Mediterranean basins. Kluwer, Dordrecht, pp 255-286
Grasso M, Lentini F, Nairn AEM, Vigliotti L (1983) A geological and paleomagnetic study of the Hyblean volcanic rocks, Sicily. Tectonophysics 98:271-295
Green DH, Falloon J (1998) Pyrolite: A Ringwood concept and its current expression In: Jackson I (ed) The Earth's Mantle: Composition, Structure and Evolution. Cambridge University Press, Cambridge, pp 311-378

Groppelli G, Pasquarè FA (2004) Nuovi contributi alla ricostruzione della stratigrafia vulcanica dell'area di Capo Passero, Sicilia sud-orientale, nel quadro del vulcanismo del Cretacico superiore del Plateau Ibleo. Boll Soc Geol It 123:275-289

Gueguen E, Doglioni C, Fernandez M (1997) Lithospheric boudinage in the Western Mediterranean back-arc basin. Terra Nova 9:184-187

Gueguen E, Doglioni C, Fernandez M (1998) On the post-25 Ma geodynamic evolution of the western Mediterranean. Tectonophysics 298:259-269

Guerrera F, Martin-Algarra A, Perrone V (1993) Late Oligocene-Miocene syn/late-orogenic successions in western and central Mediterranean chains from the Betic cordillera to the southern Apennines. Terra Nova 5:525-544

Guest JE, Duncan AM, Chester DK (1988) Monte Vulture Volcano (Basilicata, Italy): an analysis of morphology and volcaniclastic facies. Bull Volcanol 50:244-257

Gupta AK, Fyfe WS (2003) The young potassic rocks. Ane Books, New Delhi, 370 pp

Gvirtzman Z, Nur A (1999) The formation of Mount Etna as the consequence of slab rollback. Nature 401:782-785

Harlow GE, Davies R (2004) Status report on stability of K-rich phases in the upper mantle. Lithos 77:647-653

Harmon SR, Hoefs J (1995) Oxygen isotope heterogeneity of the mantle deduced from global $\delta^{18}O$ systematics of basalts from different geotectonic settings. Contrib Mineral Petrol 120:95-114

Hart SR (1988) Heterogeneous mantle domains: signatures, genesis and mixing chronologies. Earth Planet Sci Lett 90:273-296

Hart SR (1984) A large-scale isotopic anomaly in the Southern Hemisphere mantle. Nature 309:753-757

Hart SR, Hauri EH, Oschmann LA, Whitehead JA (1992) Mantle plumes and entrainment: isotopic evidence. Science 256:517-520

Hawkesworth CJ, Vollmer R (1979) Crustal contamination vs. enriched mantle: $^{143}Nd/^{144}Nd$ and $^{87}Sr/^{86}Sr$ evidence from the Italian volcanics. Contrib Mineral Petrol 69:151-165

Hirn A, Nicolich R, Gallart J, et al. (1997) Roots of Etna volcano in faults of great earthquakes. Earth Planet Sci Lett 148:171-191

Hoernle K, Zhang YS, Graham D (1995) Seismic and geochemical evidence for large-scale mantle upwelling beneath the eastern Atlantic and western and central Europe. Nature 374:34-112

Hoernle K, Behncke B, Schmincke H-U (1996) The geochemistry of basalt from the Iblean Hills (Sicily) and the Island of Linosa (Strait of Sicily): evidence for a plume from the lower mantle. Goldschmidt Conf, J Conf Abstr 1:264; www.the-conference.com/JConfAbs/1/264.html

Hofmann AW (1997) Mantle geochemistry: the message from oceanic volcanism. Nature 385:219-229

Holm PM (1982) Mineral chemistry of perpotassic lavas of the Vulsininan district, the Roman Province, Italy. Mneral Mag 46:379-386

Holm PM, Munksgaard NC (1982) Evidence for mantle metasomatism: an oxygen and strontium isotope study of the Vulsinian district, central Italy. Earth Planet Sci Lett 60:376-388

Holm PM, Munksgaard NC (1986) Reply to: a criticism of the Holm-Munksgaard oxygen and strontium isotope study of the Vulsinian District, Central Italy. Earth Planet Sci Lett 78:454-459

Holm PM, Lou S, Nielsen A (1982) The geochemistry and petrogenesis of the Vulsinian district, Roman Province, Central Italy. Contrib Mineral Petrol 80:367-378

Hornig-Kjarsgaard I, Keller J, Koberski U, Stadlbauer E, Francalanci L, Lenhart R (1993) Geology, stratigraphy and volcanological evolution of the island of Stromboli, Aeolian Arc, Italy. Acta Vulcanol 3:21-68

Innocenti F, Westerman DS, Rocchi S, Tonarini S (1997) The Montecristo monzogranite (Northern Tyrrhenian Sea, Italy): a collisional pluton in an extensional setting. Geol J 32:131-151

Ippolito F, D'Argenio B, Pescatore T, Scandone P (1975) Structural-stratigraphic units and tectonic framework of Southern Apennines. In: Squyres CH (ed) Geology of Italy. Petrol Expl Soc Libya, Tripoli, pp 317-328

Irvine TN, Baragar WRA (1971) A guide to chemical classification of common volcanic rocks. Can J Earth Sci 8:523-548

James DE (1981) The combined use of oxygen and radiogenic isotopes as indicators of crustal contamination. Ann Rev Earth Planet Sci 9:311-344

Jones AP, Kostoula T, Stoppa F, Wooley AR (2002) Petrography and mineral chemistry of mantle xenoliths in a carbonate-rich melilitic tuff from Vulture volcano, southern Italy. Mineral Mag 64:593-613

Joplin GA (1968) The shoshonite association – a review. J Geol Soc Australia 15:275-294

Joron JL, Metrich N, Rosi M, Santocroce R, Sbrana A (1987) Chemistry and petrography. In: Santacorce R (ed) Somma-Vesuvius. Quad Ric Sci CNR, Rome, 114, 8: pp 105-174

Kamenetsky V, Clocchiatti R (1996) Primitive magmatism of Mt. Etna: insights from mineralogy and melt inclusions. Earth Planet Sci Lett 142:553-572

Karner DB, Marra F, Renne PR (2001) The history of the Monti Sabatini and Alban Hills volcanoes: groundwork for assessing volcanic-tectonic hazards for Rome. J Volcanol Geotherm Res 107:185-219

Kastens K, Mascle J (1990) The geological evolution of the Tyrrhenian Sea: an introduction to the scientific results of the ODP LEG 107. In: Kastens KA, Mascle J, et al. (eds) Proc Ocean Drilling Program, Scientific Results, 107: pp 3-26

Kastens KA, Mascle J, et al. (1988) ODP Leg 107 in the Tyrrhenian Sea: insights into passive margin and back-arc basin evolution. Bull Geol Soc Am 100:1140-1156

Keller J (1980a) The Island of Salina. Rend Soc It Mineral Petrol 36:489-524

Keller J (1980b) The island of Vulcano. Rend Soc It Mineral Petrol 36:369-414

Keller J (1981) Alkalibasalts from the Tyrrhenian Sea Basin: magmatic and geodynamic significance. Bull Volcanol 44:327-337
Keller J (1982) The Mediterranean island arc. In: Thorpe RS (ed) Andesites: Orogenic andesites and related rocks. Wiley, Chichester, pp 307-325
Keller JVA, Minelli G, Pialli G (1994) Anatomy of late orogenic extension: the northern Apennines case. Tectonophysics 238:275-294
Kellogg JB, Jacobsen SB, O'Connel RJ (2002) Modeling the distribution of isotopic ratios in geochemical reservoirs. Earth Planet Sci Lett 204:183-202
Kreuzer H, Mohr M, Wendt I (1978) Potassium-argon age determination of basalt samples from LEG 42A, Hole 373A, Core 7. In: Hsu K, Montadert L, et al. (eds) Init Rep Deep Sea Drilling Project. Washington, 42: pp 531-537
La Volpe L, Patella D, Rapisardi L, Tramacere A (1984) The evolution of Monte Vulture volcano, Southern Italy: inferences from volcanological, geological and deep dipole electrical sounding data. J Volcanol Geotherm Res 22:147-162
La Volpe L, Principe C (1991) Comments on "Monte Vulture Volcano (Basilicata, Italy): an analysis of morphology and volcaniclastic facies" by Guest JE, Duncan AM, Chester DK. Bull Volcanol 52:222-227
Landi P (1987) Stratigraphy and petrochemical evolution of Latera Volcano (Central Italy). Per Mineral 56:210-224
Lanzafame G, Bousquet JC (1997) The Maltese escarpment and its extension from Etna to the Aeolian Islands (Sicily): importance and evolution of a lithospheric discontinuity. Acta Vulcanol 9:113-120
Lardini D, Nappi G (1987) I cicli eruttivi del complesso vulcanico Cimino. Rend Soc It Mineral Petrol 42:141-153
Laurenzi MA, Villa I, Stoppa F (1994) Eventi ignei monogenici e depositi piroclastici nel Distretto Ultra-alcalino Umbro-laziale (ULUD): revisione, aggiornamento e comparazione dei dati cronologici. Plinius 12:61-65
Laurenzi, MA, Villa IM (1987) $^{40}Ar/^{39}Ar$ chronostratigraphy of Vico ignimbrites. Per Mineral 56:285-293
Lavecchia G, Stoppa F (1990) The Tyrrhenian zone: a case of lithosphere extension control of intra-continental magmatism. Earth Planet Sci Lett 99:336-350
Lavecchia G, Stoppa F (1996) The tectonic significance of Italian magmatism: an alternative view to the popular interpretation. Terra Nova 8:435-446
Lavecchia G, Creati N, Boncio P (2002) The Intramontane Ultra-alkaline Province (IUP) of Italy: a brief review with considerations on the thickness of the underlying lithosphere. In: Barchi RM, Cirilli S, Minelli G (eds) Geological and geodynamic evolution of the Apennines. Boll Soc Geol It Spec Vol 1: pp 87-98
Le Maitre RW (ed) (1989) A Classification of igneous rocks and glossary of terms. Blackwell, Oxford, 193 pp
Locardi E (1965) Tipi ignimbritici di magmi mediterranei: le ignimbriti del vulcano di Vico. Atti Soc Tosc Sci Nat A72:55-174
Locardi E (1988) The origin of the Apenninic arc. Tectonophysics 146:105-123
Locardi E (1993) Dynamics of deep structures in the Tyrrhenian-Apennines area and its relation to neotectonics. Il Quaternario 6:59-66

Locardi E, Nicholich R (1988) Geodinamica del Tirreno e dell'Appennino centro-meridionale: la nuova carta della Moho. Mem Soc Geol It 41:121-140

Locardi E, Funiciello R, Lombardi G, Parotto M (1977) The main volcanic groups of Latium (Italy): relations between structural evolution and petrogenesis. Geol Rom 15:279-300

Longaretti G, Rocchi S (1990) Il magmatismo dell'avanpaese ibleo (Sicilia orientale) tra il Trias e il Quaternario: dati stratigrafici e petrologici di sottosuolo. Mem Soc Geol It 45:911-925

Longaretti G, Rocchi S Ferrari L (1991) Il magmatismo dell'avampaese Ibleo tra il Trias e il Quaternario: dati di sottosuolo della Piana di Catania dal Pleistocene al Miocene Medio. Mem Soc Geol It 47:537-555

Lowenstern JB, Mahood GA (1991) New data on magmatic H_2O contents of pantellerites, with implications for petrogenesis and eruptive dynamics at Pantelleria. Bull Volcanol 54:78-83

Luais B (1988) Mantle mixing and crustal contamination as the origin of the high-Sr radiogenic magmatism of Stromboli (Aeolian Arc). Earth Planet Sci Lett 88:93-106

Lucchi F (2000) Evoluzione dell'attività vulcanica e mobilità verticale delle Isole Eolie nel tardo Quaternario. PhD Thesis, University of Bologna, 186 pp

Lucente FP, Speranza F (2001) Belt bending driven by lateral bending of subducting lithospheric slab: geophysical evidences from the northern Apennines (Italy). Tectonophysics 337:53-64

Lucente FP, Chiarabba C, Cimini GB, Giardini D (1999) Tomographic constraints on the geodynamic evolution of the Italian region. J Geophys Res 104:20307-20327

Luhr JF, Giannetti B (1987) The Brown Leucitic Tuff of Roccamonfina Volcano (Roman Region, Italy). Contrib Mineral Petrol 95:420-436

Lustrino M (2000) Volcanic activity during the Neogene to Present evolution of the western Mediterranean area: a review. Ofioliti 25:87-101

Lustrino M, Dallai L (2003) On the origin of EM1 end-member. Neues Jahrb Mineral Abh 179:85-100

Lustrino M, Melluso L, Morra V, Secchi F (1996) Petrology of Plio-Quaternary volcanic rocks from central Sardinia. Per Mineral 65:275-287

Lustrino M, Melluso L, Morra V (2000) The role of lower continental crust and lithospheric mantle in the genesis of Plio-Pleistocene volcanic rocks from Sardinia (Italy). Earth Planet Sci Lett 180:259-270

Lustrino M, Melluso L, Morra V (2002) The transition from alkaline to tholeiitic magmas: a case study from the Orosei-Dorgali Pliocene volcanic district (NE Sardinia, Italy). Lithos 63:83-113

Lustrino M, Melluso L, Morra V, Dallai L, D'Amelio F, Petteruti Liebercknect AM (2003) Oxygen isotope composition of Plio-Quaternary volcanic rocks of Sardinia. Proc 4° Forum FIST, pp 231-232

Lustrino M, Morra V, Melluso L, Brotzu P, D'Amelio F, Fedele L, Lonis R, Franciosi L, Petteruti Liebercknect AM (2004a) The Cenozoic igneous activity in Sardinia. Per Mineral 73:105-134

Lustrino M, Brotzu P, Lonis R, Melluso L, Morra V (2004) European subcontinental mantle as revealed by Neogene volcanic rocks and mantle xenoliths of Sardinia. 32nd Int Geol Congr, Post-Congress Guide, P69, 42 pp

Maccarrone E (1963) Aspetti geochimico-petrografici di alcuni esemplari di andesite granato-cordieritifera dell'Isola di Lipari. Per Mineral 32:277-302

Maccioni L, Marchi M (1994) Eocene magmatic activity in Sardinia, Italy. New occurrence of alkaline lamprophyre. Mineral Petrogr Acta 37:199-210

Macdonald R (1974) Nomenclature and petrochemistry of the peralkaline oversaturated extrusive rocks. Bull Volcanol 38:498-516

Mahood GA, Hildreth W (1986) Geology of the peralkaline volcano at Pantelleria, Strait of Sicily. Bull Volcanol 48:143-172

Mahood GA, Baker D (1986) Experimental constraints on depths of fractionation of mildly alkalic basalts and associated felsic rocks: Pantelleria, Strait of Sicily. Contrib Mineral Petrol 93:251-264

Mantovani E, Albarello D, Tamburelli C, Babbucci D, Viti M (1997) Plate convergence, crustal delamination, extrusion tectonics and minimization of shortening work as main controlling factors of the recent Mediterranean deformation pattern. Ann Geophys 40:611-643

Mantovani E, Albarello D, Babbucci D, Tamburelli C, Viti M (2002) Trench-arc-backarc systems in the Mediterranean area: examples of extrusion tectonics. J Virtual Explorer 8:131-147

Marani MP, Trua T (2002) Thermal constriction and slab tearing at the origin of a superinflated spreading ridge: Marsili volcano (Tyrrhenian Sea). J Geophys Res 107, B2, 2188, doi:10.1029/2001JB000285

Marinelli G (1959) Le intrusioni terziarie dell'Isola d'Elba. Atti Soc Tosc Sci Nat A66:50-253

Marinelli G (1967) Genése des magmas du volcanisme Plio-Quaternaire des Apennines. Geol Rund 57:127-141

Marinelli G (1975) Magma evolution in Italy. In: Squyres CH (ed) Geology of Italy. Petrol Expl Soc Libya, Tripoli, pp 165-219

Marra F, Freda C, Scarlato P, Taddeucci J, Karner DB, Renne PR, Gaeta M, Palladino DM, Trigila R, Cavarretta G (2003) Post-caldera activity in the Alban Hills volcanic district (Italy): $^{40}Ar/^{39}Ar$ geochronology and insight into magma evolution. Bull Volcanol 65:227-247

Martelli M, Nuccio PM, Stuart FM, Burgess R, Ellam RM, Italiano F (2004) Helium-strontium isotope constraints on mantle evolution beneath the Roman Comagmatic Province, Italy. Earth Planet Sci Lett 224:295-308

Marty B, Trull T, Lussiez P, Basile I, Tanguy JC (1994) He, Ar, O, Sr and Nd isotope constraints on the origin and evolution of Mount Etna magmatism. Earth Planet Sci Lett 126:23-39

Mascle GH, Tricart P, Torelli L, Bouillin J-P, Rolfo F, Lapierre H, Monié P, Depardon S, Mascle J, Peis D (2001) Evolution of the Sardinia channel (western Mediterranean): new constraints from a diving survey on Cornacya seamount off SE Sardinia. Mar Geol 179:179-202

Matthews SJ, Marquillas RA, Kemp AJ, Grance FK, Gardeweg MC (1996) Active skarn formation beneath Lascar Volcano, northern Chile: a petrographic and geochemical study of xenoliths in eruption products. J Metam Geol 14:509-530

Mazzuoli R (1967) Le vulcaniti di Roccastrada (Grosseto). Atti Soc Tosc Sci Nat A84:315-373

Mazzuoli R, Pratesi M (1963) Rilevamento e studio chimico-petrografico delle rocce vulcaniche del Monte Amiata. Atti Soc Tosc Sci Nat A70:355-429

Mazzuoli R, Tortorici L, Ventura G (1995) Oblique rifting in Salina, Lipari and Vulcano Islands (Aeolian Islands, Southern Italy). Terra Nova 7:444-452

Meibom A, Anderson DL (2003) The statistical upper mantle assemblage. Earth Planet Sci Lett 217:123-139

Melluso L, Morra V, Di Girolamo P (1996) The Mt. Vulture volcanic complex (Italy): evidence for distinct parental magmas and for residual melts with melilite. Mineral Petrol 56:225-250

Melluso L, Conticelli S, D'Antonio M, Mirco NP, Saccani E (2003) Petrology and mineralogy of wollastonite- and melilite-bearing paralavas from the central Apennines, Italy. Am Mineral 88:1287-1299

Meloni A, Alfonsi L, Florindo F, Sagnotti L, Speranza F, Winkler A (1997) Neogene and Quaternari geodynamic evolution of the Italian peninsula: the contribution of paleomagnetic data. Ann Geophys 40:705-727

Melzer S, Foley SF (2000) Phase relations and fractionation sequences in potassic magma series modelled in the system $CaMgSi_2O_6$-$KAlSiO_4$-Mg_2SiO_4-F at 1 bar to 18 kbar. Contrib Mineral Petrol 138:186-197

Mercalli G. (1907) I vulcani attivi della Terra. Hoepli, Milano, 421 pp

Mercalli G, Silvestri O (1891) L'eruzione dell'Isola di Vulcano incominciata il 3 agosto 1888 e terminata il 22 marzo 1890. Ann Uff Centr Meteor Geodin It 10:71-281

Metrich N (1985) Mecanismes d'evolution a l'origine des magmas potassiques d'Italie centrale et meridionale. Exemples du Mt. Somme-Vesuve, des Champs Phlegreens et de l'Ile de Ventotene. PhD Thesis, University Paris-Sud, Orsay, 336 pp

Metrich N, Rutherford MJ (1998) Low pressure crystallization paths of H_2O-saturated basaltic-hawaiitic melts from Mt. Etna: implications for open-system degassing of basaltic volcanoes. Geochim Cosmochim Acta 62:1195-1205

Metrich N, Santacroce R, Savelli C (1988) Ventotene, a potassic Quaternary volcano in central Tyrrhenian Sea. Rend Soc It Mineral Petrol 43:1195-1213

Monaco C, Tortorici L (1995) Tectonic role of ophiolite-bearing terranes in the development of the southem Apennines orogenic belt. Terra Nova 70:153-160

Mongelli F, Zito G, Della Vedova B, Pellis G, Squarci P, Taffi L (1991) Geothermal regime of Italy and surrounding seas. In: Cermàk V, Rybach L (eds) Exploration of the Deep Continental Crust. Springer, Berlin, pp 380-394

Mongelli F, Zito G (1991) Flusso di calore nella regione Toscana. Studi Geol Camerti, Spec Issue CROP 03: pp 91-98

Montanini A, Barbieri M, Castorina F (1994) The role of fractional crystallization, crustal melting and magma mixing in the petrogenesis of rhyolites and mafic inclusion-bearing dacites from the Monte Arci volcanic complex (Sardinia, Italy). J Volcanol Geotherm Res 61:95-120

Montone P, Amato A, Chiarabba C, Buonasorte G, Fiordelisi A (1995) Evidence of active extension in Quaternary volcanoes of central Italy from breackouts analysis and seismiciy. Geophys Res Lett 22:1909-1912

Morelli C (1982) Le conoscenze geofisiche dell'Italia e dei mari antistanti. Mem Soc Geol It 24:521-530

Morra V, Secchi FA, Assorgia A (1994) Petrogenetic significance of peralkaline rocks from Cenozoic calc-alkaline volcanism from SW Sardinia, Italy. Chem Geol 118:109-142

Morra V, Secchi F A, Melluso L, Franciosi L (1997) High-Mg subduction-related Tertiary basalts in Sardinia, Italy. Lithos 40:69-91

Morris J, Ryan J, Leeman WP (1993) Be isotope and B-Be investigations of the historic eruptions of Mt. Vesuvius. J Volcanol Geotherm Res 58:345-358

Morrison GW (1980) Characteristics and tectonic setting of the shoshonite rock association. Lithos 13:97-108

Müller D, Groves DI (2000) Potassic igneous rocks and associated gold-copper mineralizations. Springer, Berlin, 252 pp

Murru M, Montuori C, Wyss M, Privitera E (1999) The locations of magma chambers at Mt. Etna, Italy, mapped by b-values. Geophys Res Lett 26:2553-2556

Nakai S, Wakita H, Nuccio M, Italiano F (1997) MORB-type neon in an enriched mantle beneath Etna, Sicily. Earth Planet Sci Lett 153:57-66

Nappi G, Renzulli A, Santi P (1987) An evolutionary model for the Paleo-Bolsena and Bolsena Volcanic Complexes: a structural and petrographic study. Per Mineral 56:241-267

Nappi G, Renzulli A, Santi P, Gillot PY (1995) Geological evolution and geochronology of the Vulsini volcanic district (Central Italy). Boll Soc Geol It 114:599-613

Nappi G, Antonelli F, Coltorti M, Milani A, Renzulli A, Siena F (1998) Volcanological and petrological evolution of the Eastern Vulsini District, Central Italy. J Volcanol Geotherm Res 87:211-132

Nazzareni S, Molin M, Peccerillo A, Zanazzi PF (2001) Volcanological implications of crystal chemical variations in clinopyroxenes from the Aeolian arc (Southern Tyrrhenian Sea, Italy). Bull Volcanol 63:73-82

Nicolich R (2001) Deep seismic transects. In: Vai GB, Martini PI (eds) Anatomy of an Orogen. The Apennines and adjacent Mediterranean basins. Kluwer, Dordrecht, pp 47-52

Ogniben L, Parotto M, Praturlon A (eds) (1975) Structural model of Italy. Quad Ric Sci CNR, Rome, 90:502 pp

Orsi G, Sheridan MF (1984) The Green Tuff of Pantelleria: rheoignimbrite or rheomorphic fall? Bull Volcanol 47:611-626

Orsi G, Civetta L, D'Antonio M, Di Girolamo P, Piochi M (1995) Step-filling and development of a three-layers magma chamber: the Neapolitan Yellow Tuff case history. J Volcanol Geotherm Res 67:291-312

Orsi G, De Vita S, Di Vito M (1996) The restless, resurgent Campi Flegrei nested caldera (Italy): constraints on its evolution and configuration. J Volcanol Geotherm Res 74:179-214

Palladino DM, Agosta E, Freda C, Spaziani S, Trigila R (1994) Geopetrographic and volcanologic study of southern Vulsini: the Valentano-Marta-La Rocca sector. Mem Descr Carta Geol It 49:255-276

Panza GF (1984) Structure of the lithosphere-asthenosphere system in the Mediterranean region. Ann Geophys 2:137-138

Panza GF, Mueller S (1979) The plate boundary between Eurasia and Africa in the Alpine area. Mem Soc Geol It 33:43-50

Panza GF, Pontevivo A (2004) The Calabrian Arc: a detailed structural model of the lithosphere-asthenosphere system. Rend Accad Naz Sci dei XL, Mem Sci Fis Nat 28:51-88

Panza GF, Pontevivo A, Chimera G, Raykova R, Aoudia A (2003) The lithosphere-asthenosphere: Italy and surroundings. Episodes 26:169-174

Panza GF, Pontevivo A, Sarao' A, Aoudia A, Peccerillo A (2004) Structure of the lithosphere-asthenosphere and volcanism in the Tyrrhenian Sea and surroundings. Mem Descr Carta Geol It 64:29-56

Pappalardo L, Civetta L, D'Antonio M, Deino A, Di Vito MA, Orsi G, Carandente A, De Vita S, Isaia R, Piochi M (1999) Chemical and isotopical evolution of the Phlegraean magmatic system before the Campanian Ignimbrite (37 ka) and the Neapolitan Yellow Tuff (12 ka) eruptions. J Volcanol Geotherm Res 91:141-166

Pappalardo L, Piochi M, D'Antonio M, Civetta L, Petrini R (2002) Evidence for multistage magmatic evolution during the past 60 kyr at Campi Flegrei (Italy) deduced from Sr, Nd, and Pb isotope data. J Petrol 43:1415-1434

Patacca E, Scandone P (2001) Late thrust propagation and sedimentary response in the thrust-belt-foredeep system of the southern Apennines (Pliocene-Pleistocene). In: Vai GB, Martini PI (eds) Anatomy of an Orogen. The Apennines and adjacent Mediterranean basins. Kluwer, Dordrecht, pp 401-440

Patacca E, Scandone P, Giunta G, Liguori V (1979) Mesozoic paleotectonic evolution of the Ragusa zone (Southern Sicily). Geol Rom 18:331-369

Patanè D, De Gori P, Chiarabba C, Bonaccorso A (2003) Magma ascent and the pressurization of Mount Etna's volcanic system. Science 299:2061-2063

Pearce JA (1982) Trace element characteristics of lavas from destructive plate boundaries. In: Thorpe RS (ed) Andesites: Orogenic andesites and related rocks. Wiley, Chichester, pp 525-548

Pearce JA, Parkinson IJ (1993) Trace element models for mantle melting: application to volcanic arc petrogenesis. Geol Soc London Spec Publ 76:373-403

Pearce JA, Peate DW (1995) Tectonic implications of the composition of volcanic arc magmas. Ann Rev Earth Planet Sci 23:251-285

Peccerillo A (1985) Roman Comagmatic Province (Central Italy): evidence for subduction-related magma genesis. Geology 13:103-106
Peccerillo A (1990) On the origin of italian potassic magmas: Comments. Chem Geol 85:183-196
Peccerillo A (1992) Potassic and ultrapotassic magmatism: compositional characteristics, genesis and geologic significance. Episodes, 15, 243-251
Peccerillo A (1995) Mafic calcalkaline to ultrapotassic magmas in central-southern Italy: constraints on evolutionary processes and implications for source composition and conditions of magma generation. Proc Intern Symp Upper Mantle, Sao Paulo. Acad Bras Sci 67:171-189
Peccerillo A (1998) Relationships between ultrapotassic and carbonate-rich volcanic rocks in central Italy: petrogenetic implications and geodynamic significance. Lithos 43:267-279
Peccerillo A (1999) Multiple mantle metasomatism in central-southern Italy: geochemical effects, timing and geodynamic implications. Geology 27:315-318
Peccerillo A (2001) Geochemical similarities between Vesuvius, Phlegraean Fields and Stromboli volcanoes: petrogenetic, geodynamic and volcanological implications. Miner Petrol 73:93-105
Peccerillo A (2002) Plio-Quaternary magmatism in central-southern Italy: a new classification scheme for volcanic provinces and its geodynamic implications. In: Barchi RM, Cirilli S, Minelli G (eds) Geological and geodynamic evolution of the Apennines. Boll Soc Geol It Spec Vol 1: pp 113-127
Peccerillo A (2003) Plio-Quaternary magmatism in Italy. Episodes 26:222-226
Peccerillo A (2004) Carbonate-rich pyroclastic rocks from central Apennines: carbonatites or carbonated rocks? A commentary. Per Mineral 73:165-175
Peccerillo A, Taylor SR (1976) Geochemistry of Eocene calc-alkaline volcanic rocks of the Kastamonu area, northern Turkey. Contrib Mineral Petrol 58:63-81
Peccerillo A, Manetti P (1985) The potassic alkaline volcanism of central southern Italy: A review of the data relevant to petrogenesis and geodinamic significance. Trans Geol Soc South Africa 88:379-394
Peccerillo A, Wu TW (1992) Evolution of calc-alkaline magmas in continental arc volcanoes: evidence from Alicudi, Aeolian Arc (Southern Tyrrhenian Sea, Italy). J Petrol 33:1295-1315
Peccerillo A, Panza GF (1999) Upper mantle domains beneath central-southern Italy: petrological, geochemical and geophysical constraints. Pure Appl Geophys 156:421-443
Peccerillo A, Turco E (2004) Petrological and geochemical variations of Plio-Quaternary volcanism in the Tyrrhenian Sea area: regional distribution of magma types, petrogenesis and geodynamic implications. Per Mineral 73:231-251
Peccerillo A, Lustrino M (2005) Compositional variations of the Plio-Quaternary magmatism in the circum-Tyrrhenian area: deep- vs. shallow-mantle processes. In: Foulger GR, Nathland JH, Presnall DC, Anderson DL (eds) Plates, plumes and paradigms. Geol Soc Am Spec Publ 388, in press

Peccerillo A, Poli G, Tolomeo L (1984) Genesis, evolution and tectonic significance of K-rich volcanics from the Alban Hills (Roman Comagmatic Region) as inferred from trace element geochemistry. Contrib Mineral Petrol 86:230-240

Peccerillo A, Conticelli S, Manetti P (1987) Petrological characteristics and the genesis of Recent magmatism of Southern Tuscany and Northern Latium. Per Mineral 56:157-172

Peccerillo A, Poli G, Serri G (1988) Petrogenesis of orenditic and kamafugitic rocks from Central Italy. Canad Mineral 26:45-65

Peccerillo A, Kempton PD, Harmon RS, Wu TW, Santo AP, Boyce AJ, Tripodo A (1993) Petrological and geochemical characteristics of the Alicudi Volcano, Aeolian Islands, Italy: implications for magma genesis and evolution. Acta Vulcanol 3:235-249

Peccerillo A, Barberio MR, Yirgu G, Ayalew D, Barbieri M, Wu TW (2003) Relationships between mafic and peralkaline acid magmatism in continental rift settings: a petrological, geochemical and isotopic study of the Gedemsa volcano, Central Ethiopian Rift. J Petrol 44:2003-2032

Peccerillo A, Dallai L, Frezzotti ML, Kempton PD (2004) Sr-Nd-Pb-O isotopic evidence for decreasing crustal contamination with ongoing magma evolution at Alicudi volcano (Aeolian arc, Italy): implications for style of magma-crust interaction and for mantle source compositions. Lithos, 78:217-233

Perini G, Conticelli S, Francalanci L, Davidson JP (2000) The relationship between potassic and calc-alkaline post-orogenic magmatism at Vico volcano, central Italy. J Volcanol Geotherm Res 95:247-272

Perini G, Tepley FG, Davidson JP, Conticelli S (2003) The origin of K-feldspar megacrysts hosted in alkaline potassic rocks from central Italy: a track for low-pressure processes in mafic magmas. Lithos 66:223-240

Perini G, Francalanci L, Davidson JP, Conticelli S (2004) The petrogenesis of Vico Volcano, Central Italy: an example of low scale mantle heterogeneity. J Petrol 45:139-182

Perrotta A, Scarpati C, Giacomelli L, Capozzi AR (1996) Proximal depositional facies from a caldera-forming eruption: the Parata Grande Tuff at Ventotene Island (Italy). J Volcanol Geotherm Res 71:207-228

Pichler H (1980) The Island of Lipari. Rend Soc It Mineral Petrol 36:415-440

Pinarelli L (1991) Geochemical and isotopic (Sr, Pb) evidence of crust-mantle interaction in silicicic melts. The Tolfa-Cerveteri-Manziana volcanic complex (Central Italy): a case history. Chem Geol 92:177-195

Pinarelli L, Poli G, Santo A (1989) Geochemical characterization of recent volcanism from the Tuscan Magmatic Province (Central Italy): the Roccastrada and San Vincenzo centers. Per Mineral 58:67-96

Piromallo C, Morelli A (2003) P wave tomography of the mantle under the Alpine-Mediterranean area. J Geophys Res, 108, B2, 2065, doi: 10.1029/2002JB001757

Plank T, Langmuir CH (1998) The chemical composition of subducting sediment and its consequences for the crust and mantle. Chem Geol 145:325-394

Poli G (1992) Geochemistry of Tuscan Archipelago granitoids, Central Italy: the role of hybridization processes in their genesis. J Geol 100:41-56
Poli G (2004) Genesis and evolution of Miocene-Quaternary intermediate-acid rocks from the Tuscan Magmatic Province. Per Mineral 73:187-214
Poli G, Perugini D (2003) The Island of Capraia. Per Mineral 72:195-201
Poli G, Frey FA, Ferrara G (1984) Geochemical characteristics of the south Tuscany (Italy) volcanic province, constraints on lava petrogenesis. Chem Geol 43:203-221
Poli G, Manetti P, Tommasini S (1989) A petrological review on Miocene-Pliocene intrusive rocks from Southern Tuscany and Tyrrhenian Sea (Italy). Per Mineral 58:109-126
Poli G, Peccerillo A, Donati C (2002) The Plio-Quaternary acid magmatism of Southern Tuscany. In: Barchi RM, Cirilli S, Minelli G (eds) Geological and geodynamic evolution of the Apennines. Boll Soc Geol It Spec Vol 1: pp 143-151
Poli G, Perugini D, Rocchi S, Dini A (eds) (2003) Miocene to Recent plutonism and volcanism in the Tuscan Magmatic Province. Per Mineral 72:244 pp
Poli S, Chiesa S, Gillot PY, Gregnanin A, Vezzoli L (1987) Chemistry versus time in the volcanic complex of Ischia (Gulf of Naples, Italy): evidence of successive magmatic cycles. Contrib Mineral Petrol 95:322-335
Presnall DC, Gudmundur H, Gudfinnsson H, Walter MJ (2002) Generation of mid-ocean redge basalts at pressures from 1 to 7 GPa. Geochim Cosmochim Acta 66:2073-2090
Principi G (1994) Stratigraphy and evolution of the Northern Apennine accretion wedge with particular regard to the ophiolitic sequences: a review. Boll Geofis Teor Appl 36:243-269
Prosperini N (1993) Petrologia e geochimica delle rocce dell'isola di Capraia (Arcipelago Toscano, Italia): un vulcano calcalcalino di origine complessa. BSc Thesis, University of Perugia, 149 pp
Puxeddu M (1971) Studio chimico-petrografico delle vulcaniti del M. Cimino (Viterbo). Atti Soc Tosc Sci Nat A78:329-394
Renzulli A, Upton BGJ, Nappi G (1995) Magma chamber processes preceding the Pitigliano Formation eruption (Latera volcanic complex, central Italy): evidence from cognate plutonic clasts. Acta Vulcanol 7:55-74
Renzulli A, Serri G, Santi P, Mattioli M, Holm PM (2001) Origin of high-silica rhyolites at Stromboli volcano (Aeolian Islands, Italy) inferred from crustal xenoliths. Bull Volcanol 7:400-419
Rittmann A (1930) Geologie der Insel Ischia, Zeitschr Vulkanol 6:265 pp
Rittmann A (1933) Die geologische bedingte evolution und differentiation des Somma-Vesuvius magmas. Zeitschr Vulkanol 15:8-94
Robin C, Colantoni P, Gennesseaux M, Rehault JP (1987) Vavilov seamount: a mildly alkaline quaternary volcano in the Tyrrhenian Basin. Mar Geol 78:125-136
Rocchi S, Westerman DS, Dini A, Innocenti F, Tonarini S (2002) Two-stage growth of laccoliths at Elba Island, Italy. Geology 30:983-986

Rogers NW, Hawkesworth CJ, Parker RJ, Marsh JS (1985) Geochemistry of potassic lavas from Vulsini, central Italy, and implications for mantle enrichment processes beneath the Roman region. Contrib Mineral Petrol 90:244-257

Rogers NW, De Mulder M, Hawkesworth CJ (1992) An enriched mantle source for potassic basanites: evidence from Karisimbi volcano, Virunga volcanic province, Rwanda. Contrib Mineral Petrol 111:543-556

Rolandi G, Petrosino P, Mc Geehin J (1998) The interplinian activity at Somma-Vesuvius in the last 3500 years. J Volcanol Geotherm Res 82:19-52

Romano R, Sturiale C (1971) L'isola di Ustica. Studio geovulcanologico e magmatologico. Riv Mineral Sicil 127-129:1-61

Rosi M (1980) The Island of Stromboli. Rend Soc It Mineral Petrol 36:345-368

Rosi M, Sbrana A (eds) (1987) The Phlegraean Fields. Quad Ric Sci CNR Rome, 114, 10:175 pp

Rosi M, Sbrana A, Vezzoli L (1988) Stratigrafia delle isole di Procida e Vivara. Boll Gruppo Naz Vulcanol 4:500-525

Rossi PL, Tranne CA, Calanchi N, Lanti E (1996) Geology, stratigraphy and volcanological evolution of the island of Linosa (Sicily Channel). Acta Vulcanol 8:73-90

Sabatini V (1900) I Vulcani dell'Italia Centrale e i loro prodotti. I: Vulcano Laziale. Tipografia Nazionale G Bertero, Roma 392 pp

Sahama TG (1974) Potassium-rich alkaline rocks In: Sorensen H (ed) The alkaline rocks. Wiley, London, pp 94-109

Sano Y, Wakita H, Italiano F, Nuccio M (1989) Helium isotopes and tectonics in Italy. Geophys Res Lett 16:511-514

Santacorce R (ed) (1987) Somma-Vesuvius. Quad Ric Sci CNR, Rome, 114, 8: 249 pp

Santacroce R, Bertagnini A, Civetta L, Landi P, Sbrana A (1993) Eruptive dynamics and petrogenetic processes in a very shallow magma reservoir: the 1906 eruption of Vesuvius. J Petrol 34:383-425

Santacroce R, Cristofolini R, La Volpe L, Orsi G, Rosi M (2003) Italian active volcanoes. Episodes 26:227-234

Santo AP (1998) Contribution of clinopyroxene EMP and SIMS data to the understanding of magmatic processes: an example from Filicudi Island (Aeolian Arc, Southern Tyrrhenian Sea). Neues Jahrb Mineral Abh 173:207-231

Santo AP, Chen Y, Clark AH, Farrar E, Tsegaye A (1995) $^{40}Ar/^{39}Ar$ ages of the Filicudi Island volcanics: implications for the volcanological history of the Aeolian Arc, Italy. Acta Vulcanol 7:3-18

Santo AP, Jacobsen SB, Baker J (2004) Evolution and genesis of calc-alkaline magmas at Filicudi volcano, Aeolian Arc (Southern Tyrrhenian Sea, Italy). Lithos 72:73-96

Sapienza G, Scribano V (2000) Distribution and representative whole-rock chemistry of deep-seated xenoliths from the Iblean Plateau, south-eastern Sicily, Italy. Per Mineral 69:185-204

Sartori R (1990) The main results of ODP Leg 107 in the frame of Neogene to Recent geology of peri-Tyrrhenian areas. In: Kastens KA, Mascle J, et al. (eds) Proc Ocean Drilling Program, Scientific Results, 107: pp 715-730

Sartori R (2001) Cordica-Sardinia block and the Tyrrhenian Sea. In: Vai GB, Martini Pi (eds): Anatomy of an Orogen. The Apennines and the adjacent Mediterranean basins. Kluwer, Dordrecht, pp 367-374

Sartori R (2003) The Thyrrhenian backarc basin and subduction of the Ionian lithosphere. Episodes 26:217-221

Savelli C (1967) The problem of rock assimilation by Somma-Vesuvius magma. Composition of Somma-Vesuvius lavas. Contrib Mineral Petrol 16:328-353

Savelli C (1988) Late Oligocene to Recent episodes of magmatism in and around the Tyrrhenian Sea: implications for the processes of opening in a young inter-arc basin of intra-orogenic (Mediterranean) type. Tectonophysics 146:163-181

Savelli C, Gasparotto G (1994) Calc-alkaline magmatism and rifting of the deep-water volcano of Marsili (Aeolian back-arc, Tyrrhenian Sea). Mar Geol 119:137-157

Savelli C, Lipparini E (1978) K/Ar determinations on basalt rocks from Hole 373A. In: Hsu K, Montaderd L, et al. (eds) Init Rep Deep Sea Drilling Project, Washington 81:537-538

Scambelluri M, Rampone E, Piccardo G (2001) Fluid and trace element cycling in subducted serpentinite: a trace element study of the Erro-Tobbio high-pressure ultramafites (Western Alps, NW Italy). J Petrol 42:55-67

Scarascia S, Lozej A, Cassinis R (1994) Crustal structure of Ligurian, Tyrrhenian and Ionian seas and adjacent onshore areas interpreted from wide-angle seismic profiles. Boll Geofis Teor Appl 36:1-19

Schiano P, Clocchiatti R, Ottolini L, Busà T (2001) Transition of Mount Etna lavas from a mantle-plume to an island-arc magmatic source. Nature 412:900-904

Schmincke H-U, Behncke B, Grasso M, Raffi S (1997) Evolution of the north-western Iblean Mountains, Sicily: uplift, Pliocene/Pleistocene sea-level changes, paleoenvironment, and volcanism. Geol Rund 86:637-669

Selli R, Lucchini F, Rossi PL, Savelli C, Del Monte M (1977) Dati geologici, petrochimici e radiometrici sui vulcani centro-tirrenici. Giorn Geol 42:221-246

Serri G (1990) Neogene-Quaternary magmatism of the Tyrrhenian region: characterization of the magma sources and geodynamic implications. Mem Geol Soc It 41:219-242

Serri G, Innocenti F, Manetti P (1993) Geochemical and petrological evidence of the subduction of delaminated Adriatic continental lithosphere in the genesis of the Neogene-Quaternary magmatism of central Italy. Tectonophysics 223:117-147

Sharygin VV, Stoppa F, Kolesov BA (1996) Zr-Ti disilicates from the Pian di Celle volcano, Umbria, Italy. Eur J Mineral 8:1199-1212

Shaw JE, Baker JA, Menzies MA, Thirlwall MF, Ibrahim KM (2003) Petrogenesis of the largest intraplate volcanic field on the Arabian plate (Jordan): a

mixed lithosphere-asthenosphere source activated by lithospheric extension. J Petrol 44:1657-1679
Sheridan MF, Frazzetta G, La Volpe L (1985) Eruptive histories of Lipari and Vulcano, Italy, during the past 22000 years. Geol Soc Am Spec Publ 212: pp 29-34
Signorelli S, Vaggelli G, Romano C (1999) Pre-eruptive volatile (H_2O, F, Cl and S) contents of phonolitic magmas feeding the 3550-year old Avellino eruption from Vesuvius, southern Italy. J Volcanol Geotherm Res 93:237-256
Sollevanti F (1983) Geologic, volcanologic and tectonic setting of the Vico-Cimini area, Italy. J Volcanol Getherm Res 17:203-217
Somma R, Ayuso RA, De Vivo B, Rolandi G (2001) Major, trace element and isotope geochemistry (Sr-Nd-Pb) of interplinian magmas from Mt. Somma-Vesuvius (Southern Italy). Mineral Petrol 73:121-143
Speranza F, Villa IM, Sagnotti L, Florindo F, Cosentino D, Cipollari P, Mattei M (2002) Age of the Corsica-Sardinia rotation and Liguro-Provençal basin spreading: new paleomagnetic and Ar/Ar evidence. Tectonophysics 347:231-251
Stoppa F (1988) L'euremite di Colle Fabbri (Spoleto): un litotipo ad affinità carbonatitica in Italia. Boll Soc Geol It 107:239-248
Stoppa F (1996) The San Venanzo maar and tuff ring: eruptive behaviour of a carbonatite-melilitite volcano. Bull Volcanol 57:563-577
Stoppa F, Lavecchia G (1992) Late Pleistocene ultra-alkaline magmatic activity in the Umbria-Latium region: an overview. J Volcanol Geotherm Res 52:277-293
Stoppa F, Lupini L (1993) Mineralogy and petrology of the Polino monticellite calciocarbonatite (Central Italy). Mineral Petrol 49:213-231
Stoppa F, Cundari A (1995) A new Italian carbonatite occurrence at Cupaello (Rieti) and its genetic significance. Contrib Mineral Petrol 122:275-288
Stoppa F, Principe C (1997) Eruption style and petrology of a new carbonatitic suite from the Mt. Vulture Southern Italy: the Monticchio Lake formation. J Volcanol Geotherm Res 78:251-265
Stoppa F, Woolley AR (1997) The Italian carbonatites: field occurrence, petrology and regional significance. Mineral Petrol 59:43-67
Stoppa F, Wooley AR, Cundari A (2002) Extension of the melilite-carbonatite province in the Apennines of Italy: the kamafugite of Grotta del Cervo. Mineral Mag 66:555-574
Sun SS, McDonough WF (1989) Chemical and isotopic systematics of oceanic basalts: implications for mantle composition and processes. In: Saunders AD, Norry MJ (eds) Magmatism in ocean basins. Geol Soc London Spec Publ 42: pp 313-345
Tait JA, Bachtadse V, Franke W, Soffel HC (1997) Geodynamic evolution of the European Variscan Fold Belt: paleomagnetic and geological constraints. Geol Rund 86:585-598
Tamburelli C, Babbucci D, Mantovani E (2001) Geodynamic implications of "subduction related" magmatism: insight from the Tyrrhenian-Apennine region. J Volcanol Geotherm Res 104:3-43

Tanguy JC (1978) Tholeiitic basalt magmatism of Mount Etna and its relations with the alkaline series. Contrib Mineral Petrol 66:51-67

Tanguy JC, Condomines M, Kieffer G (1997) Evolution of Mount Etna magma: constraints on the present feeding system and eruptive mechanism. J Volcanol Geotherm Res 75:221-250

Tappe S, Foley SF, Pearson DG (2003) The kamafugites of Uganda: a mineralogical and geochemical comparison with their Italian and Brasilian counterpart. Per Mineral 72:51-77

Taylor HP, Giannetti B, Turi B (1979) Oxygen isotope geochemistry of the potassic igneous rocks from the Roccamonfina volcano, Roman Comagmatic Region, Italy. Earth Planet Sci Lett 46:81-106

Taylor HP, Turi B, Cundari A (1984) $^{18}O/^{16}O$ and chemical relatioships in K-rich volcanic rocks from Australia, East Africa, Antarctica and San Venanzo-Cupaell, Italy. Earth Planet Sci Lett 69:263-276

Taylor SR, McLennan SM (1985) The continental crust: its composition and evolution. An examination of the geochemical record preserved in sedimentary rocks. Blackwell, Oxford, 312 pp

Tedesco D, Allard P, Sano Y, Wakita H, Pece R (1990) Helium-3 in subaerial and submarine fumaroles of Campi Flegrei caldera, Italy. Geochim Cosmochim Acta 54:1105-1116

Thompson RN (1977) Primary basalts and magma genesis. III. Alban Hills, Roman Comagmatic Province, Central Italy. Contrib Mineral Petrol 50:91-108

Tommasini S, Poli G, Halliday AN (1995) The role of sediment subduction and crustal growth in Hercynian plutonism: isotopic and trace elment evidence from the Sardinia-Corsica batholith. J Petrol 36:1305-1332

Tonarini S, Armienti P, D'orazio M, Innocenti F, Pompilio M, Petrini R (1995) Geochemical and isotopic monitoring of Mt. Etna 1989-93 eruptive activity: bearing on the shallow feeding system. J Volcanol Geotherm Res 64:95-115

Tonarini S, D'Orazio M, Armienti P, Innocenti F, Scribano V (1996) Geochemical features of eastern Sicily lithosphere as probed by Hyblean xenoliths and lavas. Eur J Mineral 8:1153-1173

Tonarini S, Leeman WP, Ferrara G (2001a) Boron isotopic variations in lavas of the Aeolian volcanic arc, South Italy. J Volcanol Geotherm Res 110:155-170

Tonarini S, Armienti P, D'Orazio M, Innocenti F (2001b) Subduction-like fluids in the genesis of Mt. Etna magmas: evidence from boron isotopes and fluid mobile elements. Earth Planet Sci Lett 192:471-483

Tonarini S, Leeman WP, Civetta L, D'Antonio M, Ferrara G, Necco A (2004) B/Nb and $\delta^{11}B$ systematics in the Phlegrean Fields District, Italy. J Volcanol Geotherm Res 133:123-139

Tranne CA, Calanchi N, Lucchi F, Rossi PL (2000) Geological sketch map of Lipari (Aeolian Islands, Italy). Dip Sci Terra, University of Bologna, Italy

Tranne CA, Lucchi F, Calanchi N, Rossi PL, Campanella T, Sardella A (2002) Geological map of Filicudi (Aeolian Islands), University of Bologna, LAC Florence

Treves B (1984) Orogenic belts as accretionary prisms: the example of the Northern Apennines. Ofioliti 9:577-618

Trigila R, De Benedetti A (1993) Petrogenesis of Vesuvius historical lavas constrained by Pearce element ratios analysis and experimental phase equilibria. J Volcanol Geotherm Res 58:315-343

Trigila R, Agosta E, Currado C, De Benedetti AA, Freda C, Gaeta M, Palladino DM, Rosa C (1995) Petrology. In: Trigila R (ed) The volcano of the Alban Hills. University La Sapienza, Rome, pp 95-165

Trua T, Esperança S, Mazzuoli R (1998) The evolution of the lithospheric mantle along the North African Plate: geochemical and isotopic evidence from the tholeiitic and alkaline volcanic rocks of the Hyblean Plateau, Italy. Contrib Mineral Petrol 131:307-322

Trua T, Serri G, Marani M, Renzulli A, Gamberi F (2002) Volcanological and petrological evolution of Marsili seamounts (southern Tyrrhenian Sea). J Volcanol Geotherm Res 114:441-464

Trua T, Serri G, Marani MP (2003) Lateral flow of African mantle below the nearby Tyrrhenian plate: geochemical evidence. Terra Nova 15:433-440

Trua T, Serri G, Marani MP, Rossi PL, Gamberi F, Renzulli A (2004) Mantle domains beneath the southern Tyrrhenian: constraints from recent seafloor sampling and dynamic implications. Per Mineral 73:53-73

Turbeville BN (1992a) $^{40}Ar/^{39}Ar$ ages and stratigraphy of the Latera caldera, Italy. Bull Volcanol 55:110-118

Turbeville BN (1992b) Relationships between chamber margin accumulates and pore liquids: evidence from arrested in situ processes in ejecta, Latera caldera, Italy. Contrib Mineral Petrol 110:429-441

Turbeville BN (1993) Petrology and petrogenesis of the Latera caldera, central Italy. J Petrol 34:77-123

Turco E, Zuppetta A (1998) A kinematic model for the Plio-Quaternary evolution of the Tyrrhenian-Apenninic system: implications for rifting processes and volcanism. J Volcanol Geotherm Res 82:1-18

Turi B, Taylor HP (1976) Oxygen isotope studies of potassic volcanic rocks of the Roman Province, central Italy. Contrib Mineral Petrol 55:1-31

Turi B, Taylor HP, Ferrara G (1991) Comparisons of $^{18}O/^{16}O$ and $^{87}Sr/^{86}Sr$ in volcanic rocks from the Pontine Islands, M. Ernici and Campania with other areas in Italy In: Taylor HP, O'Neil JR, Kaplan IR (eds) Stable Isotope Geochemistry: A Tribute to Samuel Epstein. Geochem Soc Spec Publ 3: pp 307-324

Turi B, Taylor HP, Ferrara G (1986) A criticism of the Holm-Munksgaard oxygen and strontium isotope study of the Vulsinian district, central Italy. Earth Planet Sci Lett 78:447-453

Ulmer P (2001) Partial melting in the mantle wedge – the role of H_2O in the genesis of mantle-derived "arc-related" magmas. Phys Earth Planet Intr 127: 215-232

Vaggelli G, Francalanci L, Ruggieri G, Testi S (2003) Persistent polybaric rests of calc-alkaline magmas at Stromboli volcano, Italy: pressure data from fluid inclusions in restitic quartzite nodules. Bull Volcanol 65:385-404

Vai GB, Martini PI (eds) (2001) Anatomy of an Orogen. The Apennines and adjacent Mediterranean basins. Kluwer, Dordrecht, 632 pp
Varekamp JC, Kalamarides R (1989) Hybridization processes in leucite tephrites from Vulsini, Italy, and the evolution of the Italian potassic suite. J Geophys Res 94:4603-4618
Vaselli O, Conticelli S (1990) Boron, cesium and lithium distribution in some alkaline potassic volcanics from central Italy. Mineral Petrogr Acta 33:189-204
Venturelli G, Capedri S, Di Battistini G, Crawford A, Kogarko LN, Celestini S (1984a) The ultrapotassic rocks from southereastern Spain. Lithos 17:37-54
Venturelli G, Thorpe RS, Dal Piaz GV, Del Moro A, Potts PJ (1984b) Petrogenesis of calc-alkaline, shoshonitic and associated ultrapotassic Oligocene volcanic rocks from the northwestern Alps, Italy. Contrib Mineral Petrol 86:209-220
Vezzoli L (ed) (1988a) Island of Ischia. Quad Ric Sci CNR Rome, 114, 10:133 pp
Vezzoli L (1988b) Attività esplosiva alcalino-potassica pleistocenica dell'isola di Ponza. Boll Gruppo Naz Vulcanol 4:584-599
Vezzoli L, Conticelli S, Innocenti F, Landi P, Manetti P, Palladino DM, Trigila L (1987) Stratigraphy of the Latera Volcanic Complex: proposal for a new nomenclature. Per Mineral 56:89-110
Villa IM (1993) Geochronology. In: Di Filippo M (ed), Sabatini Volcanic Complex. Quad Ric Sci 114, 11: pp 33-79
Villa IM, Giuliani O, De Grandis G, Cioni R (1989) Datazioni K/Ar dei vulcani di Tolfa e Manziana. Boll Gruppo Naz Vulcanol 2:1025-1026
Villa IM, Ruggieri G, Puxeddu M (2001) Geochronology of magmatic and hydrothermal micas from Larderello geothermal field. In: Cidu R (ed) Proc 10th Intern Symp Water-Rock Interaction. Balkema, 1: pp 1589-1592
Villari L (1980a) The Island of Alicudi. Rend Soc It Mineral Petrol 36:441-466
Villari L (1980b) The Island of Filicudi. Rend Soc It Mineral Petrol 36:467-488
Villemant B (1988) Trace element evolution in the Phlegrean Fields (Central Italy): fractional crystallization and selective enrichment. Contrib Mineral Petrol 98:169-183
Villemant B Palacin P (1987) Differentiation magmatique et mechanismes de concenntration del l'uranium: exemple du vulcanisme du Latium (Italie centrale). Bull Mineral 110:319-333
Villemant B, Flehoc C (1989) U-Th fractionation by fluids in K-rich magma genesis: the Vico volcano, Central Italy. Earth Planet Sci Lett 91:312-326
Vollmer R (1976) Rb-Sr and U-Th-Pb systematics of alkaline rocks: the alkaline rocks from Italy. Geochim Cosmochim Acta 40:283-295
Vollmer R (1977) Isotopic evidence for genetic relations between acid and alkaline rocks in Italy. Contrib Mineral Petrol 60:109-118
Vollmer R (1989) On the origin of the Italian potassic magmas. A discussion contribution. Chem Geol 74:229-239
Vollmer R, Hawkesworth CJ (1980) Lead isotopic composition of the potassic rocks from Roccamonfina (south Italy). Earth Planet Sci Lett 47:91-101
Voltaggio M, Barbieri M (1995) Geochronology. In: Trigila R (ed) The volcano of the Alban Hills. University La Sapienza, Rome, pp 167-192

Wagner C, Velde D (1986) The mineralogy of K-richterite-bearing lamproites. Am Mineral 71:17-37

Washington HS (1906) The Roman Comagmatic Region. Carnegie Inst Washington Publ 57: 199 pp

Washington HS (1909) The submarine eruptions of 1831 and 1891 near Pantelleria. Am J Sci 27:131-150

Wendlandt RF, Eggler DH (1980a) The origins of potassic magmas: 1. Melting relations in the systems $KAlSiO_4$ -Mg_2SiO_2 and $KAlSiO_4$ -MgO -SiO_2 -CO_2 to 30 kilobars. Am J Sci 280:385-420

Wendlandt RF, Eggler DH (1980b) The origins of potassic magmas: 2. Stability of phlogopite in natural spinel lherzolite an in the $KAlSiO_4$-MgO-SiO_2-H_2O-CO_2 at high pressures and high temperatures. Am J Sci 280:421-458

Westerman DS, Innocenti F, Tonarini S, Ferrara G (1993) The Pliocene intrusion of the Island of Giglio. Mem Soc Geol It 49:345-363

Wilson M (1989) Igneous petrogenesis. A global tectonic approach. Unwi Hyman, Boston, 466 pp

Wilson M, Downes H (1991) Tertiary-Quaternary extension-related alkaline magmatism in Western and Central Europe. J Petrol 32:811-849

Wilson M, Bianchini G (1999) Tertiary-Quaternary magmatism within the Mediterranean and surrounding regions. In: Durand B, Jolivet L, Horvath F, Sérrane M (eds) The Mediterranean basin: Tertiary extension within the Alpine Orogen. Geol Soc London Spec Publ 156:141-168

Wood DA (1979) A variably veined suboceanic upper mantle-Genetic significance for mid-ocean ridge basalts from geochemical evidence. Geology 7:499-503

Woolley AR, Kempe DRC (1989) Carbonatites: nomenclature, average chemical composition and element distribution. In: Bell K (ed) Carbonatites. Genesis and Evolution. Unwin-Hyman, Boston pp 1-14

Wortel MJR, Spakman W (2000) Subduction and slab detachment in the Mediterranean-Carpathian region. Science 290:1910-1917

Wyllie PJ, Tuttle OF (1960) The system CaO-CO_2-H_2O and the origin of carbonatites. J Petrol 1:1-46

Yoder HS (1986) Potassium-rich rocks: phase analysis and heterpmorphic relations. J Petrol 27:1215-1228

Zanon V, Frezzotti ML, Peccerillo A (2003) Magmatic feeding system and crustal magma accumulation beneath Vulcano Island (Italy): evidence from fluid inclusions in quartz xenoliths. J Geophys Res, 108, B6, 2298, doi:10.1029/2002JB002140

Zanon V, Nikogossian I (2004) Evidence of crustal melting events below the Island of Salina. Geol Mag 141: 524-540

Zeck HP (1998) Post collisional volcanism in a sinking slab setting – crustal anatectic origin of pyroxene-andesite magma, Caldear Volcanic Group, Neogene Alboràn volcanic province, southeastern Spain. Lithos 45:499-522

Zindler A, Hart SR (1986) Chemical geodynamics. Ann Rev Earth Planet Sci 14:493-571

Zitellini N, Trincardi F, Marani M, Fabbri A (1986) Neogene tectonics of the northern Tyrrhenian Sea. Giorn Geol 48:25-40

Zito G, Mongelli F, De Lorenzo S, Doglioni C (2003) Heat flow and geodynamics in the Tyrrhenian Sea. Terra Nova 15:425-432

Zollo A, Gasparini P, Virieux J, Biella G, Boschi E, Capitano P, De Franco R, Dell'Aversana P, De Matteis R, De Natale G, Jannaccone G, Guerra I, Le Meur H, Mirabile L (1998) An image of Mt. Vesuvius obtained by 2D seismic tomography. J Volcanol Geotherm Res 82:161-173

Subject Index